Meiotic recombination-based genome shuffling of *Saccharomyces cerevisiae* and characterization by genome sequencing and RNA-seq transcriptional expression profiling for improved tolerance to spent sulfite liquor

Dominic Pinel

A Thesis

In

The Department

Of

Biology

Presented in Partial Fulfillment of the Requirements

For the Degree of Doctor of Philosophy at

Concordia University

CONCORDIA UNIVERSITY

SCHOOL OF GRADUATE STUDIES

This is to certify that the thesis prepared

By: **Dominic Pinel**

Entitled:

Meiotic recombination-based genome shuffling of *Saccharomyces cerevisiae* and characterization by genome sequencing and RNA-seq transcriptional expression profiling for improved tolerance to spent sulfite liquor

and submitted in partial fulfillment of the requirements for the degree of

DOCTOR OF PHILOSOPHY (Biology

complies with the regulations of the University and meets the accepted standards with respect to originality and quality.

Signed by the final examining committee:

Dr. Joanne Turnbull	Chair
Dr. Shawn Mansfield	External Examiner
Dr. Paul Joyce	External to Program
Dr. Reginald Storms	Examiner
Dr. Malcolm Whiteway	Examiner
Dr. Vincent Martin	Thesis Supervisor

Approved by

Dr. S. Dayanandan
Chair of Department or Graduate Program Director

June 6/2013

Dr. B. Lewis
Dean of Faculty

ABSTRACT

Meiotic recombination-based genome shuffling of *Saccharomyces cerevisiae* and characterization by genome sequencing and RNA-seq transcriptional expression profiling for improved tolerance to spent sulfite liquor

Dominic Pinel Ph. D.

Concordia University, June, 2013.

Spent sulfite liquor (SSL) is a waste effluent from sulfite pulping that contains monomeric sugars that can be fermented to ethanol. However, the inhibitory substances found in this complex feedstock adversely affect yeasts used for the fermentation of the sugars in SSL. To overcome this limitation, evolutionary engineering of *Saccharomyces cerevisiae* was carried out using genome shuffling based on large-scale population recursive meiotic recombination. Populations of UV-induced yeast mutants more tolerant to hardwood spent sulfite liquor (HWSSL) were isolated and then recursively mated and enriched for more tolerant populations. After five rounds of genome shuffling, three strains were isolated that were able to grow on undiluted HWSSL and support efficient ethanol production from the sugars therein for prolonged fermentation of HWSSL. Analyses showed that greater HWSSL tolerance is associated with improved viability in the presence of salt, sorbitol, peroxide, and acetic acid. These results demonstrate that evolutionary engineering through genome shuffling will yield robust yeasts capable of fermenting the sugars present in HWSSL, which is a complex substrate containing multiple sources of inhibitors. The genome of R57, the most inhibitor-tolerant strain

generated in this study, was sequenced by massively parallel sequencing and twenty single nucleotide polymorphism mutations were located. Many of these mutations affect genes that correlate with known stress responses to the types of inhibition found in lignocellulosic hydrolysates. Cross-referencing the mutation findings with RNA-seq-derived differential gene expression analysis of R57 yields genes and biological processes that are likely playing determinant roles in the HWSSL tolerance trait of R57. The strongest findings support important roles for the following mutation-bearing proteins and biological processes: stress response transcriptional repressor, Nrg1p; NADPH-dependent glutamate dehydrogenase, Gdh1p, and a modified nitrogen usage and assimilation physiology including alterations to aromatic amino acid synthesis pathways and the associated Aro1p; protein homeostasis machinery including heat-shock 70-family proteins, especially Ssa1p, and Ubp7p and Art5p, which are related to ubiquitin-mediated proteolysis. Redox-associated metabolites NADPH, glutathione, mainly via GSH1 mutation, and iron are also implicated. Overall, these data provide important findings for understanding inhibition by multi-inhibitory lignocellulosic substrates; a meiotic recombination-mediated engineering strategy for generating inhibition-tolerant strains that may be unobtainable through classical evolutionary engineering; novel genetic targets for future rational biocatalyst design and inhibitor-tolerance studies; and a promising work-flow model for generating strains with desirable and complex phenotypic traits along with understanding of the genetic factors and biological processes involved in those traits.

Acknowledgement

None of this work would have been possible without the support and comradery of the fine people in the Martin lab both past and present, many thanks. I particularly thank Euan Burton, Corinne Cluis, Nicholas Gold and Andrew Wieczorek who will always be family to me and who made Montreal a home. I acknowledge and thank my excellent committee members Reginald Storms and Paul Joyce, and Hung Lee, who was a brilliant collaborator and knowledgeable resource. Finally, I acknowledge my supervisor Vincent Martin who never let me down, opened all the right doors at all the right times, kept faith in me further than anyone could ask, and, most importantly, taught me how to be a scientist.

Dedication

This work is dedicated to my family. Your support, patience and love have made the difference. To my wonderful and supportive Gaby, who has stuck with me through this process despite the unfathomable miscalculations, your love means everything. To Juniper, who was the only one that could unwaveringly make me smile. To Eleanor, my hope for the future. To brother Chris, who was always there to listen to the frustrations and successes. To my father, Leo, who has made every step in my life possible and who unfailingly picked me up after every misstep. To my grandmother, Mary, who passed on during the writing of this thesis and who instilled in me a wonder of living things. And finally, to my mother, Bonnie, who was always my ardent supporter until the end, no matter where I chose to go and what I chose to do, she made me believe it was possible.

Table of contents

List of tables

List of figures

List of abbreviations

HMF	5-hydroxymethyl-2-furaldehyde
ESR	environmental stress response
ROS	reactive oxygen species
HOG	high osmolarity glycerol
PDR	pleiotropic drug response
ABC	ATP-binding cassette
HSP	heat-shock protein
MAPK	mitogen activated protein kinase
STRE	stress response element
DCW	dry cell weight
FDM	furan-2,5-dimethanol
NADH	nicotinamide adenine dinucleotide
NADPH	nicotinamide adenine dinucleotide phosphate
SSL	spent sulfite liquor
SWSSL	softwood spent sulfite liquor
HWSSL	hardwood spent sulfite liquor
CRBF	cell recycle batch fermentation
GS	genome shuffling
CSI	classical strain improvement
MPS	massively parallel sequencing
bp	base pair
SNP	single nucleotide polymorphism

indel	insertion/deletion
Mb	megabase
CNV	copy number variation
SAM	sequence alignment map
BAM	binary SAM
ORF	open reading frame
SAGE	serial analysis of gene expression
RT-PCR	reverse transcription-polymerase chain reaction
RPKM	reads per kilobase of transcript per million mapped reads
GO	gene ontology
EUROSCARF	EUROpean *Saccharomyces Cerevisiae* ARchive for Functional analysis
YPD	yeast peptone dextrose
SD	synthetic defined
YNB	yeast nitrogen base without amino acids
PBS	phosphate buffered saline
CFU	colony forming units
GC	gas chromatography
WT	wild type
EMS	ethyl methane sulfate
PAGE	polyacrylamide gel electrophoresis
SIFT	sorting intolerant from tolerant
UTR	untranslated region
NBD	nucleotide-binding domain

SBD	substrate-binding domain
FDR	false discovery rate
SGD	*Saccharomyces* genome database
UBI	ubiquitin
UBL	ubiquitin-like
NRC	nitrogen catabolite repression
UPR	unfolded protein response
ETC	electron transport chain
ER	endoplasmic reticulum

Chapter 1

with excerpts from:

Pinel *et al.* 2011. *Saccharomyces cerevisiae* genome shuffling through recursive population mating leads to improved tolerance to spent sulfite liquor. Appl Environ Microbiol 77:4736-4743.

Pinel *et al*. 2011. 'Omics' technologies and systems biology for engineering *Saccharomyces cerevisiae* strains for lignocellulosic bioethanol production. Biofuels 2:659-675.

Pinel D, Martin VJJ. 2012. Meiotic recombination-based genome shuffling of *Saccharomyces cerevisiae* and *Schefferomyces stiptis* for increased inhibitor tolerance to lignocellulosic substrate toxicity, p. 233-250. In Patnaik R (ed.), Engineering complex phenotypes in industrial strains, 1 ed. John Wiley & Sons, Inc., Hoboken, New Jersey.

1 Introduction

1.1 Project goals, objectives and hypotheses

1.1.1 Goal 1

The first goal of this study (Chapter 2) is to generate a strain of *Saccharomyces cerevisiae* with enhanced tolerance to hardwood spent sulfite liquor, an inhibitor-rich biomass breakdown waste product, which contains sugars that can be fermented to ethanol. Because of the presence of multiple sources of inhibition within hardwood spent sulfite liquor it is hypothesized that a robust strain engineering methodology will be needed.

Therefore, the first objective of goal 1 is to develop and test a meiotic recombination-mediated genome shuffling methodology. The second objective of goal 1 is to implement the genome shuffling strategy in order to generate populations and strains of *S. cerevisiae* with enhanced tolerance to spent sulfite liquor. It is here hypothesized

that beneficial, tolerance-conferring mutations can be accumulated within a single strain. The third objective of goal 1 is to phenotypically characterize hardwood spent sulfite liquor-tolerant strains for growth and fermentation capabilities in hardwood spent sulfite liquor and investigate cross-tolerance to individual inhibitors. It is here hypothesized that tolerance to hardwood spent sulfite liquor will lead to increased survival and fermentative capabilities during hardwood spent sulfite liquor fermentation. It is further hypothesized that tolerance to the multi-inhibitory substrate will lead to cross-tolerance to single sources of inhibition generally found in lignocellulosic hydrolysates.

1.1.2 Goal 2

Once the evolved strains have been characterized phenotypically, the second goal of this study (Chapter 3) is to locate and describe the genetic changes that have taken place through genome shuffling for tolerance to spent sulfite liquor and to gain understanding of possible tolerance mechanisms to lignocellulosic substrates.

The objective of this portion of the study is to use massively parallel sequencing technology to sequence the genome of a highly-tolerant strain and locate variations that have been accumulated through genome shuffling. It is here hypothesized that novel mutations and combinations of mutations related to stress tolerance will be discovered and genetic determinants in hardwood spent sulfite liquor tolerance will be pinpointed.

1.1.3 Goal 3

The third goal of this study (Chapter 4) is to describe the physiology behind hard wood spent sulfite liquor tolerance by measuring transcriptional expression responses. The first objective of goal 3 will be to use RNA-seq technology to measure

transcriptional expression differences between the wild type parental *S. cerevisiae* with a hardwood spent sulfite liquor-tolerant mutant obtained through genome shuffling. The second objective of goal 3 is to measure the gene expression response of a tolerant mutant to hardwood spent sulfite liquor exposure. It is hypothesized that integration of the results obtained from pursuing these goals will yield a better understanding of the genetic determinants and biological processes involved in tolerance to multi-inhibitory lignocellulosic substrates.

1.2 Fermentation of lignocellulosic substrates to generate fuels or chemicals

With energy security, the rising demand and price for oil and gas derived energy, and climate change becoming omnipresent issues in society, producing alternative cleaner energy has become an important goal for governments, industry and academia alike (1). In this climate, opportunities exist for using lignocellulosic substrates as cleaner and renewable sources of sugars for fermentation to bio-derived products such as fuels and chemicals. The proposed merits of bio-derived fuels and chemicals from lignocellulosic substrates include reducing atmospheric carbon output, diminishing reliance on imports, and adding value to existing agricultural and forestry industries. Conversely, current starch-based ethanol production processes, which use food crops as feedstock, raise concerns about detrimentally affecting food supplies, and have at best a marginal to neutral carbon footprint, while currently relying heavily on governmental subsidies for industry viability (2). Using waste residues as fermentable sources of sugar alleviates some concerns that arise in existing starch-based biofuel production processes. For example, waste streams from the forestry industry exist as by-products of an existing process, and are therefore desirable as fermentation feedstocks to add value to active

industries and make full use of existing resources. However, the viability of the lignocelluloses-to-ethanol process will require extensive optimization in order to fulfill the unrealized promises of this technology.

One major barrier that exists in the fermentation of lignocellulose-derived sugars is that using plant biomass as a biofuel substrate is technically challenging due to its recalcitrant and variable nature. Plant material is broken down into the three major constituents of cellulose, hemicellulose, and lignin, composed of variable average amounts: 33-51% (w/w), 19-34%, and 21-32%, respectively (3, 4). Lignocellulosic bioconversion seeks to access the sugars contained in these polymers for microbial fermentation to fuels and commodity chemicals, with the most developed processes leading to ethanol production. Several pre-treatment practices have been developed like acid treatment, steam explosion and wet oxidation (5), with the aim of separating out lignin from hemicellulose, and at least partially disrupting the crystallinity of the cellulose. When biomass is broken down through such treatments a variety of inhibitory compounds derived mainly from lignin or the breakdown products of polysaccharides are also released (6). Inhibitors are generally separated into the groupings of furan aldehydes like 2-furaldehyde (furfural) and 5-hydroxymethyl-2-furaldehyde (HMF), organic acids like acetic, formic, and levulinic acids and phenolics like 4-hydroxybenzoic acid and vanillin (7). Other stressors are found in lignocellulosic hydrolysates, such as sulfites, high-dissolved solids (osmotic pressure), wood extractives, lignosulfonates, nutrient limitations, heat, and fermentation product toxicity including ethanol (8). The synergistic effects of multiple sources of inhibition has been demonstrated (6). Furthermore, it is likely that not all sources of inhibition have been accounted for in biomass hydrolysates

(9). All of these sources of stress combine to create a toxic environment for any microorganism that might be used for the bioconversion of the lignocelluloses-derived sugars.

1.3 The effects of common sources of inhibition

The inhibitory effects of the most common lignocellulosic hydrolysate inhibitors have been elucidated. Furan aldehydes tend to diminish overall biological activity, affect enzymes of central metabolism like pyruvate and alcohol dehydrogenases, damage DNA, inhibit protein and nucleotide biosynthesis and induce cellular reactive oxygen species (ROS) accumulation (10-13). ROS accumulation leads to cellular damage by oxidation of lipids, nucleic acids and protein (14). Organic acids lead to intracellular anion accumulation as undissociated acids diffuse across the plasma membrane and dissociate due to higher intracellular pH, leading to decreased cytosolic pH (7). Phenolic compounds are thought to diminish biological membrane integrity and destroy the electrochemical gradient across mitochondrial membranes (7, 15). Hyperosmotic pressure leads to water efflux, increased cytosolic ion concentration (especially Na^+), and cell shrinkage (16). Additionally, these types of chemical stressors damage protein conformation and lead to protein unfolding and aggregation, yielding a high level of toxicity (17). To circumvent costly detoxification of the substrate prior to fermentation, it is desirable to discover or develop effective fermentation biocatalysts that can survive and ferment lignocellulosic substrates despite their inhibitory effects (2, 18).

1.4 *Saccharomyces cerevisiae* as a lignocellulosic bioethanol biocatalyst

S. cerevisiae possesses the traits desirable for a biocatalyst of the first generation of bioethanol. It can remain productive under high sugar and ethanol concentrations, and is capable of a high-yielding, high-rate of fermentation, adding to its cost-effectiveness (19). Furthermore, *S. cerevisiae* is able to grow under strict anaerobic conditions and at low pH, which is important for reducing microbial contamination (20); and unlike bacteria, it is not susceptible to phage infection.

Though these traits are desirable for lignocellulosic biofuel biocatalysts as well, no one strain can yet fulfill all of the requirements to optimize bioethanol production from lignocellulose. Comparisons between the pros and cons of contending biocatalysts have been well-reviewed (21-24). The required level of ethanol production from lignocellulosics has been estimated at >90% of the theoretical yield (24). *S. cerevisiae* has proven to be a robust industrial ethanol producer on hexose sugars (1). However, to maintain a high level of ethanol production on lignocellulose-derived carbon sources will require the additional traits of robust tolerance to the fermentation inhibitors produced during the pre-treatment of lignocellulose, concurrent use of hexose and pentose sugars for fermentation under nutrient-limited conditions and, eventually, high levels of heterologous protein expression and secretion if enzymatic hydrolysis of the lignocelluloses feedstock is needed (23, 24). These attributes will allow for consolidated bioprocessing (CBP) of lignocellulose, or fermenting lignocellulosic material with a single biocatalyst in a single fermenter, the projected most cost-effective industrial biomass-to-ethanol scenario (1). A wide array of research has focused on addressing the shortcomings of *S. cerevisiae* in this regard, mainly individually (for recent reviews see

(7, 23, 25)). Though strides have been made in the laboratory towards developing a strain of *S. cerevisiae* with broadened inhibitor tolerance, sugar substrate utilization, and protein production and secretion, often the approach has been rigorously narrow and reductive by necessity. The development of a final industrial strain with all of the desired properties may be far from fruition. This limitation undoubtedly stems from the fact that each of the required phenotypic traits are multi-faceted problems, requiring an in-depth knowledge of the biocatalyst's overall biology including metabolic functioning, cell structure and productivity of the molecule of interest. Furthermore, by engineering non-native traits, the microorganism's biological systems could be perturbed in ways that are still poorly understood.

1.5 Cellular response to fermentation inhibition

1.5.1 Global stress responses

Of the contending fermentation organisms for lignocellulose-derived biofuels, *S. cerevisiae* is the least sensitive to the types of stress or inhibitors found in lignocellulosic substrates (26), and it therefore may have an inherent advantage for achieving the higher levels of tolerance desired of an optimal biocatalyst. To date, whole-cell analyses of *S. cerevisiae* stress responses and adaptation have primarily focused on single inhibitor molecules or source of stress in order to deconvolute complex data sets and link phenotypic behavior to specific genetic factors. However, oftentimes even a single stressor or inhibitor will induce a global cellular response, yielding an overwhelming amount of data that does not lend itself easily to strain development. This is due to the general differential regulation of a plethora of genes related to stress response in *S.*

cerevisiae. A large-scale microarray study of the expression of most of the *S. cerevisiae* genes was carried out in response to 10 different stress conditions, many of which are encountered during fermentation of lignocellulosics including: temperature shocks, hydrogen peroxide, superoxides, oxidation or reduction agents, osmotic shocks, nitrogen source depletion, amino acid starvation and progression into stationary phase (27). Here, it was found that a cluster of ~900 genes were typically differentially expressed and termed the environmental stress response (ESR). The ESR consists of genes belonging to a wide-ranging set of cellular processes including growth, RNA metabolism, energy generation, defense against ROS, protein folding and secretion and DNA damage repair, among others.

Similarly, another well-studied large-scale stress response is the high osmolarity glycerol (HOG) pathway, which is invoked under conditions of high osmotic stress and has been studied at the transcriptional level through induction by salt and sorbitol exposure (27). The HOG pathway results in a cell-wide response that includes reduced efflux and increased synthesis of glycerol, cell wall and cytoskeletal rearrangements, induction of sodium pump-encoding genes, and transient repression of protein synthesis (28, 29). The HOG pathway will be a contributing factor to stress responses in biomass hydrolysates due to their typically high dissolved solids content (30) and because higher ethanol titers rely on higher gravity fermentations (31). The HOG pathway also contains genes that are regulated in response to high ethanol titers (32) or are counterparts of the general stress response (33).

Additional multi-genic responses may also be related to tolerance to lignocellulosic substrate inhibitors. These include the pleiotropic drug response (PDR), which consists of a system of ATP-binding cassette (ABC) plasma membrane transporters that mediate the translocation of ions and a wide variety of toxic substrates across the membrane, regulate mitochondrial function and detoxify the vacuole (34). PDR genes have been linked to reducing acetic acid-associated acidity of the cytoplasm (35, 36) and furan aldehyde toxicity (reviewed in (37)). Additionally, the recently defined Haa1p regulon mediates acetic acid tolerance and is governed by Haa1p transcription factor, along with other co-regulators, and diminishes the lipophilicity of acetic and propionic acids (38). Another process of interest is unfolded protein toxicity-resistance, which is mediated by protein folding chaperones, mainly classified as heat-shock proteins (HSPs) (17), or by targeted degradation of damaged and misfolded proteins via the ubiquitin-directed proteasome pathway (39).

Multi-genic stress responses make it difficult to pinpoint precise factors involved with specific inhibitors or stressors for rational strain development. Also, because many genes display modified expression in a similar fashion to differing environmental perturbations (27), much of the differential regulation is a cellular all-purpose stress response tactic, not necessarily stream-lined to the needs of a robust lignocellulosic fermentation microorganism. Although ESRs are contingent upon regulation of the same gene cluster, they do differ with variable expression of genes within that cluster, depending on the stressor applied, indicative of a tailored response to a given condition, within the broader ESR response (33). For example, DNA damage elicits induction of a smaller subset of genes that are thought to aid in genome repair including *MAG1*,

encoding a 3-methyladenine DNA glycosylase (40), and *MEC1*, encoding a phospho-inositol kinase-related protein (41), that are not involved in cellular responses to all stressors (42). In this fashion, subsets of specific responses related to lignocellulosic fermentations are perhaps a starting point for engineering biocatalysts. Furthermore, as global stress responses tend to evoke a transient, large-scale shift in transcription (42), focus on sustained stress responses under steady-state conditions, beyond the initial pulse-induced response, may lead to more specific targets for strain engineering. Cross-referencing multiple '-omics' examinations may play a major role in biocatalyst engineering, as, for example, total mRNA levels do not necessarily reflect protein abundance (43) and affected pathways may rely heavily on intracellular/substrate metabolite concentrations. By applying multiple '-omics' studies, subsets of genes involved in broad stress responses can perhaps be deconstructed into usable categories that pertain to specific single sources of biocatalyst inhibition.

The regulators that control global stress responses might prove attractive targets for future strain development as well (44-46). Microarrays have already proven useful in differentiating between transcription factors that are active during different types of environmental stress. For example, Msn2p and Msn4p are positive transcription factors that respond to heat shock, starvation, osmotic and oxidative stress (46) by activating promoters for multi-stress response genes like *DDR2* (47). While Msn2p/Msn4p activate many of the same genes as the Yap1p transcription factor, Yap1p is more specifically involved in the induction of the osmotic stress response (33). Yap1p is part of the HOG pathway that also relies on Pbs2p (48) and is initiated by the mitogen activated protein kinase (MAPK) Hog1p, which in turn activates at least five transcription factors (49).

Msn2p/Msn4p have also been implicated in the response to cell wall damage in transcriptional studies (50-52), as part of the so-called compensatory mechanism to maintain cellular integrity, which also relies heavily on the Rlm1p transcription factor for the activation of compensatory genes (50, 51). As shown in the preceding examples, networks of transcription factors have been identified that may serve as specific control points for stress response manipulation. It is also possible to locate upstream regulatory stress response elements (STREs) comprised of short nucleotide consensus sequences (44, 45) affected by these transcription factors, which can be used to pinpoint genes involved in a specific response due to nucleotide homology (53) or can be engineered as stress-inducible response elements for genes of interest (44).

Since more than 100 inhibitors of ethanol fermentation have been identified from biomass hydrolysates (54), controlling the ESR through global regulators might be the only feasible approach to engineering the tolerance of *S. cerevisiae* to multiple inhibitors. Alper *et al*. demonstrated this potential by evolving ethanol tolerance in *S. cerevisiae* through mutation and selection of *SPT15*, a gene encoding a global transcription factor (55). Screening of wild-type cells harboring a library of randomly mutated *SPT15* was used to identify a strain with a 41 % increase in specific ethanol productivity (g/DCW h^{-1}) over the parent strain, using 10 % glucose (w/v) as substrate. This approach demonstrated the concept of engineering phenotypes through global transcriptional machinery manipulation and could potentially be used to evolve other multi-genic phenotypes such as (cross)tolerance to hydrolysate fermentation inhibitors.

1.5.2 Cellular response to specific lignocellulose hydrolysate inhibitors

Despite the overall complexity of stress tolerance in yeast, headway has been made in identifying specific genetic factors that respond to a single stressor. These studies can provide novel engineering targets or create understanding based on the mechanisms by which a mutant organism displays a desired trait.

1.5.2.1 Furan aldehydes

Furan aldehydes, like HMF and furfural are potent and abundant inhibitors found in lignocellulosic hydrolysates. Documentation of changes to *S. cerevisiae* gene and protein expression in response to HMF and furfural are consequently relatively well represented in the literature (56-60). Metabolic flux analysis of anaerobic and aerobic chemostat cultures of *S. cerevisiae* grown on glucose in the presence of furfural show that it is converted to furfuryl alcohol and furoic acid, respectively, and it has been surmised that prolonged fermentation of furfural-rich substrates relies on biocatalyst conversion of furfural to these less inhibitory compounds (61). The presence of increasing furfural levels in anaerobic cultures actually led to a 12 % increase in specific ethanol production rate and a 9 % increase in ethanol yield (61), showing that glucose fermentation and furfural conversion are complementary traits under certain conditions. Furthermore, it was also shown that anaerobic furfural conversion to produce furfuryl alcohol regenerated the NAD^+ cofactor normally supplied, in part, by glycerol formation and led to a nearly stoichiometric decrease in flux to glycerol (61), which may negatively affect stress responses like the HOG pathway when multi-inhibitory lignocellulose-derived substrates are fermented.

Proteomics analyses have shown that furfural does induce the HOG pathway, but also leads to the up-regulation of more specific factors, like 18 protein chaperones involved in the unfolded-protein response (UPR) (58). Sulfur amino acid synthesis is strongly down-regulated on furfural exposure and is required for adaptation to furfural (58), therefore up-regulation of this pathway may be a target for strain engineering. Specific enzymes involved in detoxification of furan compounds were identified through transcriptome monitoring as well. HMF is detoxified by yeast cells through reduction to furan-2,5-dimethanol (FDM) with the use of NAD(P)H cofactors. DNA microarray analysis has identified 15 gene products that can reduce HMF to FDM (60). *ADH6*, coding for an NADPH-dependent alcohol dehydrogenase, when up-regulated, provided greater *in vivo* HMF reduction potential (60). Liu *et al*. provided additional evidence to support the role of NADPH-dependent dehydrogenase using a furan inhibitor-tolerant strain of *S. cerevisiae* (59). This strain displayed higher transcript levels of 16 genes, 5 encoding enzymes with cofactor NAD(P)H regeneration activity (*ZWF1*, *GND1*, *GND2*, *ALD4* and *TDH1*) and 5 encoding aldehyde reducing enzymes (*ALD4*, *ALD6*, *ADH6*, *ADH7*, and *SFA1*) that can act on HMF and furfural.

Through a DNA microarray transcriptional study in the presence of furfural (56) it was observed that the mitochondria may play a major role in the effects resulting from exposure to furfural, as many mitochondria-related transcript levels were differentially expressed. The affected genes included: *MIS1* for tetrahydrofolate synthesis and redox balancing, *PUS2* involved in mitochondrial tRNA modification, along with several genes involved in stress response and translational control. As well, transcription of gene *SPE2*, which encodes *S*-adenosyl methionine decarboxylase for the synthesis of the

important polyamines (spermidine and spermine) and is required for many metabolic processes including usual cell growth and proliferation, was inhibited by furfural (62). Related to the HOG pathway, a glycerol biosynthesis pathway gene (*RHR2*) was also down-regulated in the presence of furfural, which corresponds to previous proteomics findings (57). Furthermore, *ECM38*, encoding a γ-glutamyl transpeptidase involved in the detoxification of electrophilic xenobiotics (63), was up-regulated, and three genes, *SRX1*, *CTA1*, and *GRX5*, involved in oxidative stress response were also up-regulated upon furfural exposure. In terms of lipid content, there is strong lipidomic evidence that increased levels of unsaturated phospholipids lead to greater furfural tolerance, due to higher membrane fluidity (64). Desirable engineering targets may therefore exist within lipid pathways in order to modify cell membrane constituents and achieve the optimal fluidity for the cell membrane under process conditions (64). It is clear that furan aldehyde tolerance affects cellular function on multiple levels and therefore engineering of this trait will be a complex problem, which must be reconciled with tolerance traits to other lignocellulosic hydrolysate inhibitors.

1.5.2.2 Acetic acid

Derived mainly from lignin and hemicellulose deacetylation (54), acetic acid is also a major inhibitor to fermentation in biomass hydrolysates. As with furans, acetic acid was also found to disrupt normal mitochondrial functioning, mainly by way of disrupting ribosomal mitochondrial expression, and resulted in down-regulation of 24 mitochondrial genes, including *ATP4* and *PPA2*, involved in energy generation (56). Because mitochondrial proteins are also involved in detoxification of acetic acid, for example, the acetyl-CoA hydrolase Ach1p (65), mitochondria localized proteins may

prove to be of special interest when engineering acetate tolerance. This is especially the case if one considers that cellular ATP is required for proton ATPases or the weak-acid efflux pump, Pdr12p, responsible for reducing acetic acid associated acidity of the cytoplasm (35, 36). Amino acid synthesis pathways were affected as well by the presence of high concentrations of acetic acid, of which the tryptophan biosynthetic pathway is of particular concern because its regulation is related to organic acid tolerance in *S. cerevisiae* (66, 67). Cellular lipid content is altered in response to acetic acid as well. It has been suggested that acetic acid-tolerant strains increase synthesis of more saturated phosphatidic acids as part of a signal event to impart tolerance. This change however, does not greatly affect the ratio of membrane lipid constituents (64). Overall, organic acids like acetic acid are a major concern in microbial sensitivity to biomass-derived substrates, due to their ability to affect intracellular pH, energy generation and membrane lipid constituents.

1.5.2.3 Phenolics

Phenol compounds, formed by the breakdown of lignin, also contribute to biocatalyst inhibition and can include compounds such as 4-hydroxybenzaldehyde, 4-hydroxybenzoic acid, syringaldehyde, syringic acid, vanillin, dihydroconiferyl alcohol and coniferyl aldehydes (7). Endo *et al.* discovered that a vanillin-tolerant strain of *S. cerevisiae* had relatively high levels of ergosterol content, which was concomitant with transcriptional up-regulation of five ergosterol biosynthesis genes, *ERG28*, *HMG1*, *MCR1*, *ERG5*, and *ERG7* (68). Ergosterol is an important component of yeast cellular membranes and increasing ergosterol content decreases membrane fluidity, which is believed to counterbalance the effect of fluidizing compounds like vanillin. A phenol-

tolerant strain was also shown to contain a higher ratio of longer versus shorter chain cellular phosphatidylinositol content, which is influenced by the cytidine diphosphate-diacylglycerol pathway that could potentially be engineered to up-regulate longer chain content (64). However, known stress response proteins could also play a major role in phenolic-compound tolerance. Exposure to coniferyl aldehyde, a common phenolic fermentation inhibitor, has been linked to up-regulation of the Yap1p transcription factor (discussed above as related to osmotic stress tolerance), along with Atr1p and Flr1p, which belong to the plasma membrane drug:H^+ antiporter superfamily and are Yap1p-inducible (69). While 11 and 7 genes were up-regulated at least 10-fold after 1 and 2 hours exposure to coniferyl aldehyde, respectively, deletion of *YAP1*, *ATR1*, and *FLR1* were the only modifications that led to coniferyl aldehyde sensitivity; deletion of *YAP1* conferred the most sensitivity, again outlining the important role of transcription factors in stress tolerance, and suggesting that osmotic stress and phenol tolerance could be controlled by transcription factor manipulation.

1.5.2.4 Osmotic stress

Cellular response to osmotic stress relies on the global HOG pathway, affecting hundreds of genes simultaneously (27). DNA microarray studies have started to elucidate the most highly differentially expressed genes in that pathway. Because global regulators of multi-genic stress response pathways can have widespread and pleiotropic effects (27), manipulation of these regulators may not be the most efficient means to attain a desired phenotype. For example, so-called translation-deactivated osmosense genes, that is, genes with products that are up-regulated at the transcriptional level, but down-regulated at the translational level, show that an entire stress response pathway is

not always needed for every stress condition and cells will counter-directionally regulate over-expressed genes to conform to what is needed at the protein level for an osmotic stress response. Therefore, manipulating individual genes of interest may make it possible to develop a strain tailored to a stressful environment like high osmolarity, mitigating to some extent the need for global compensatory mechanisms (70). For instance, microarray analysis has shown that the genes *GPD1* and *RHR2* for glycerol metabolism and *TPS1*, *TPS2*, *TPS3*, *ATH1* and *NTH1* for trehalose metabolism were highly up-regulated after exposure to high osmotic stress (71). Through comparative metabolomic analysis it was found that cellular glycerol content regulation was an important element for biocatalysts under industrial conditions, which corroborates the above observation (72). Therefore, up-regulation of single genes, such as those involved in glycerol metabolism may alleviate the burden of an energetically expensive global response to osmotic stress. The osmotic stress response is a good example of why researchers must be wary, however, of relying heavily on transcript profiles alone for strain engineering, as it has been demonstrated that increased transcript recruitment to ribosomes is a major source of translational regulation that is not reflected in transcript levels, in terms of HOG pathway control (70). As it stands, the HOG pathway and its constituents are the primary targets of interest for engineering osmotic pressure tolerance and the non-specific nature of this response suggests it is a pathway of interest for cross-tolerance to multiple sources of inhibition.

1.5.2.5 Ethanol tolerance and fermentation adaptation

While *S. cerevisiae* is relatively tolerant to ethanol, it is still sensitive to its effects. Ethanol can freely diffuse through cellular membranes, which results in inhibited

cell growth and viability (42, 73, 74). *S. cerevisiae*'s tolerance to ethanol has been studied at both the transcriptome and proteome levels (75-80). As with most stress responses, the cellular programming involved is highly complex, and correlates to cell size and cell cycle (76). In one study, not only was an expected global cellular stress response induced by ethanol stress, but up-regulation of tryptophan biosynthesis also led to increased ethanol tolerance, which was verified through inverse engineering (80). This finding correlates well, as mentioned above, with acetic acid tolerance (56). It was also shown through qRT-PCR that ethanol stress response is governed mainly by way of the transcription factors Msn4p/Msn2p, Yap1p, Hsf1p and Pdr1p/Pdr3p and many of the genes responding to ethanol stress contain binding motifs for these factors (81). The downstream effects of these factors include up-regulation of the glycogen and trehalose synthesis pathways, which is reconcilable with overcoming a high osmotic pressure challenge. A strong up-regulation of heat-shock proteins also serves to ensure proper protein folding during ethanol stress and could lead to cross-tolerance to multiple stressors.

Comparative analyses of genome sequences from robust industrial and laboratory strains of *S. cerevisiae* have yielded valuable insight into the genetic determinants of ethanol tolerance. For example, changes in gene copy number may have a beneficial effect on the industrially robust phenotype with respect to transmembrane transport and sugar and alcohol metabolism (82). More specific results were obtained using Illumina and 454 sequencing to compare an industrial bioethanol strain to the laboratory strain 288c. It was found that strain 288c bears a non-functional *HAP1* transcription factor coding gene (83), present in industrial strains, that is important for controlling

fermentation-associated genes (84) and ergosterol biosynthesis (85). Increased membrane ergosterol content, as outlined in the phenolics section above, typically decreases membrane fluidity (86) that is caused by exposure to ethanol (87). Ethanol-tolerant strains have high oleic acid (18:1) content, which also decreases membrane fluidity, further signifying that modifications in fatty acid synthesis may be important to stress tolerance (88).

Though the understanding of what makes a robust industrial strain is still fragmented, studies like those mentioned above already offer important targets for lignocellulosic-inhibitor tolerant strain development. However, many of these targets will require further testing to determine their importance towards conferring a tolerant phenotype or cross-tolerance to multiple inhibitors.

1.6 Spent sulfite liquor as an existing industrial inhibitory lignocellulosic substrate

Waste residues like effluents from the pulp and paper industry represent abundant, low-cost feedstocks for fermentation to renewable fuels such as ethanol, as they are rich in the carbohydrates that are the breakdown products of lignocellulose. However, pulping of lignocellulose also results in a number of the sources of fermentation inhibition discussed above being present in the wastewater (54, 89). Spent sulfite liquor (SSL), the effluent from pulp mills that utilize the acid sulfite process to obtain high-grade cellulose pulp, is used to produce ethanol and reduce the biological oxygen demand upon its disposal (8, 90). However, along with the fermentable sugars SSL contains, it can also prove highly inhibitory. While most lignocellulosic hydrolysates share common inhibitors, the distinct composition of SSL is likely to have a unique effect on SSL-

fermentation biocatalysts. The current study is based on yeast tolerance to SSL derived from the ammonium salt-based sulfite pulping process of hardwood. Hardwood SSL (HWSSL) contains sugars, lignosulfonates, the aforementioned inhibitors, residual pulping chemicals, ammonia, sulfite (91) and can contain heavy metal ions (iron, chromium, nickel and copper) that originate from the corrosion of pulping and bleaching equipment (92, 93). Some of the major constituents are approximated at the following levels (% w/v): 1.45 % hexose sugars, 1.7 % pentose sugars, 0.5 % furfural, 0.9 % acetic acid, 0.5-0.7 % sulfate, 1 % ammonia and 17 % lignosulfonate (94). However, the composition of SSL is highly variable depending on the type of wood being pulped (95). Softwood SSL (SWSSL) is a less problematic substrate due to higher hexose levels and lesser inhibition, while HWSSL contains more inhibitors and has lower concentrations of hexoses (96). *Saccharomyces cerevisiae* displays relatively high inhibitor tolerance and ethanol productivity on SSL and has been suggested as a suitable biocatalyst for SSL fermentation (26). However, more tolerant, efficient, fermentative strains are still required to make SSL fermentation a more viable process. A common practice in industrial plants that ferment SSL is to use cell recycle batch fermentation (CRBF) (96), which may adversely affect the viability of the yeast culture due to prolonged exposure to the inhibitors. Cell recycling leads to alternating exposure to HWSSL and SWSSL because SSL ethanol plants rely on the wood being processed. Sometimes, recycling in HWSSL leads to cell death or at least cultures that exhibit considerably reduced ethanol productivity on HWSSL and SWSSL (96). Therefore, yeast strains that are tolerant to HWSSL will maintain ethanol fermentation and reduce the need for population revival or replacement. Because detoxification of HWSSL prior to fermentation is not an

economically viable option, yeast strains fermenting HWSSL must not only display tolerance to simultaneous sources of inhibition, but must achieve this tolerance and maintain productivity under specific and restricted nutritional inputs.

1.7 Genome shuffling as a means to generate microbial strains displaying complex traits

Due to the complex nature of the inhibition in HWSSL, and the multiple cellular processes and genes likely involved in tolerance to the variety of inhibition sources present, rational microbial engineering of a strain to address these factors is presently implausible (60, 97). A handful of genetic targets that would make rational strain manipulation through classical molecular biology techniques plausible, like gene knock-outs or up-regulation, are difficult to pinpoint, and the desired traits may not be possible without addressing large-scale multi-genic cellular responses. Furthermore, using classical random mutation for strain development makes it difficult to affect a large number of mutations in a short amount of time, based on the sequential nature of mutational addition inherent in classical strain improvement schemata (98) (Fig. 1-1). Given the apparent complexity of developing lignocellulose-inhibitor tolerant traits, and the fact that the precise genetic factors involved in tolerance are largely unknown, genome shuffling (GS) is an attractive technology for developing strains that can ferment lignocellulosic substrates effectively.

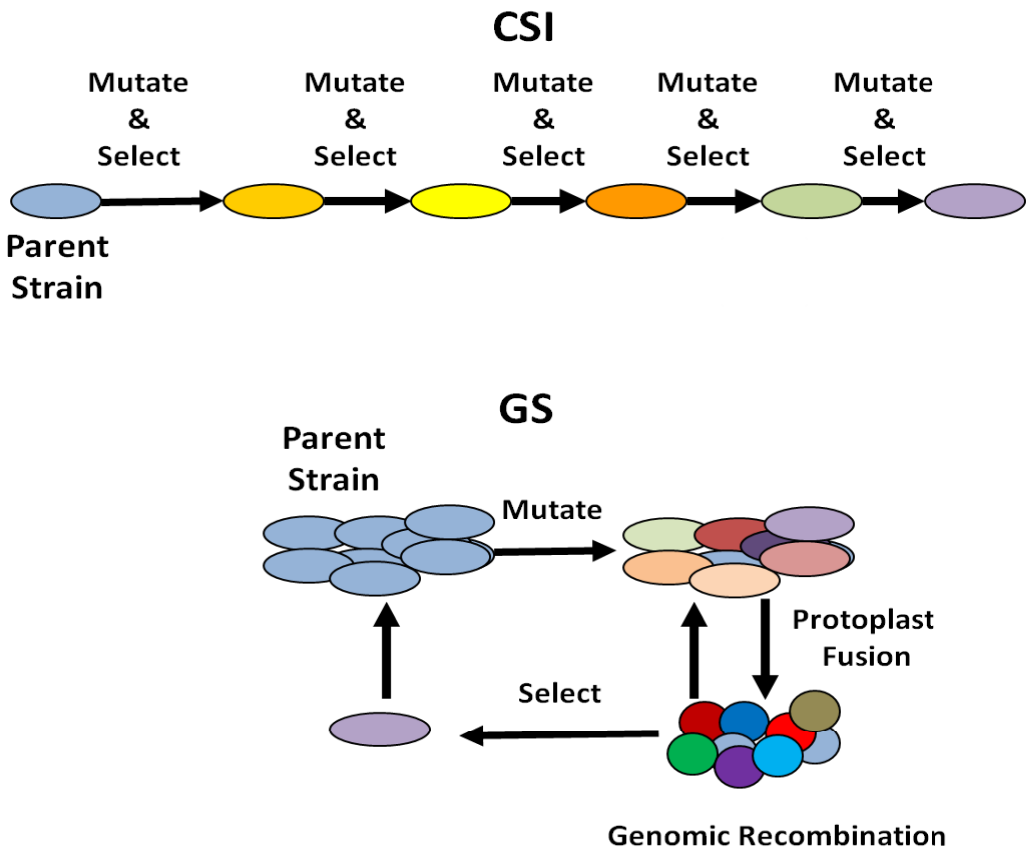

Figure 1-1. Schematic representation of classical strain improvement (CSI) vs protoplast fusion-mediated genome shuffling (GS). CSI follows a sequential process of mutation and selection of single strains, while GS utilizes recursive genomic recombination to accumulate mutations.

GS is an evolutionary engineering technology for recursive whole genome recombination to accelerate the accumulation of multiple useful mutations into one genome, or provide the ability to cross out deleterious mutations, to dramatically decrease the time and effort required for the engineering of complex phenotypic traits (99). This technology has been used successfully to shuffle the genomes of bacteria and eukaryotes for other specific traits such as improved antibiotic production (98), tolerance and degradation of pentachlorophenol (100), and tolerance to low pH (99, 101), high

temperatures or ethanol (102, 103).

GS has been predominantly employed through protoplast fusion, which requires the creation of mutant parental populations followed by protoplast generation, mutant population protoplast fusion and regeneration of the cell wall (98, 99, 104). Protoplast fusion-mediated GS has been attempted using *S. cerevisiae*. Shi *et al*. have reported protoplast fusion-based GS with *S. cerevisiae* in order to engineer the trait of enhanced ethanol and thermotolerance (103). In this study, a haploid *S. cerevisiae* population was made into a population of protoplasts by enzymatic digestion of the cell wall. Protoplast fusions were enacted by exposure to polyethylene glycol and fused protoplasts were regenerated on rich medium containing inhibitory levels of ethanol. This study reports protoplast preparation and regeneration rates of 100% and 75%, respectively, but does not address the level of protoplast fusion attained. Assuming fusion rates are high, protoplast fusions with fungi appears to be a strong option for GS, but will rely on the particular recombination attributes of the strain to be engineered. However, one unknown to protoplast fusion-based GS is the effect that the process of reiterative protoplast fusion and cellular regeneration may have on the stability of the final strain. Shi *et al*. report DNA levels at 5.089, 5.144, 6.289 and 7.477 mg/g of cells for the UV mutant population and rounds one, two and three of GS respectively (103). It is clear that the DNA content of strains resulting from protoplast fusion increases as GS is carried out. In the end, it is yet to be determined if such an increase will affect strain stability, though after 50 generations the thermotolerant phenotype was preserved in the strains obtained through this study. As a control, classical strain improvement was carried out alongside the GS for increased thermotolerance experiment. It was found that only slight

improvements to thermotolerance could be obtained by reiterative UV mutation and selection, again demonstrating the power of GS.

While GS has been predominantly employed through protoplast fusion (98, 99, 104), *S. cerevisiae* has a natural sexual cycle and therefore parasexual mating through protoplast fusion is not required (104). A recent study has shown GS of *S. cerevisiae* through recursive mating is possible (104), which can circumvent the low efficiency of protoplast fusion that can be encountered with protoplast fusion-based GS (105). The study by Hou showed that increased ethanol tolerance through recombination with the *S. cerevisiae* mating cycle, using a small population of starting mutants for each crossing, is suitable for evolutionary engineering for tolerance to a single source of inhibition (102). A similar study has recently produced *Scheffersomyces stipitis* strains that exhibited improved tolerance to HWSSL (106). While *S. stipitis* has pentose fermentation capabilities, its ability to tolerate and produce ethanol from undiluted HWSSL remains to be realized (106). However, that study supports the rationale behind the current study, that meiotic recombination-mediated GS could be used to evolve to tolerance to HWSSL. Differences between the *S. stipitis* HWSSL tolerance study and the following study will be discussed in more depth in Chapter 2.

1.8 Massively parallel DNA sequencing as a means to track random genomic changes

Reverse engineering of yeast strains based on non-targeted approaches of strain engineering, such as classical strain mutagenesis, evolutionary and GS-based strain engineering, can suffer from the inability to pinpoint the mutations that are responsible for a trait of interest. However, the rapidly evolving massively parallel sequencing

(MPS) technology has made it possible to efficiently track and identify genomic variation that has been exacted through non-targeted strain engineering approaches. Essentially, short DNA sequence reads can be aligned rapidly to a known genome sequence of high homology, which allows for an unparalleled depth of coverage that can make variation detectable at levels of ~100 % accuracy (107). This technology has already been used successfully to discover variation between yeast strains, like *S. stipitis* strains that differ in xylose metabolism abilities (107). Furthermore, MPS has been used in a limited number of cases to discover mutations involved in *S. cerevisiae* strains subjected to non-targeted evolution in a reverse engineering context (108-111). This subject will be explored more fully in Chapter 3.

1.8.1 MPS technology and detecting genome variations

MPS involves the digestion of genomic DNA into small fragments and the sequencing of millions of short segment DNA sequence reads in parallel (112, 113). These DNA sequence reads can be aligned upon a scaffold genome, or, if the reads are of sufficient length, can be used for *de novo* assembly of a genome, or large contiguous segments of a genome, and used for comparison between genetic backgrounds (113). The predominant, contending MPS technologies currently used in the scientific community all have attributes and shortfalls specific to the technology that make them desirable for use in differing applications. For example, of the three most mature and utilized MPS technologies, 454 sequencing generates a lower volume of reads, but the length of the reads are more amenable to *de novo* assembly; the SOLiD system generates high accuracy reads and high volume; while Illumina technology now generates relatively long reads, accompanied by a high-throughput and volume of data production,

allowing for adequate genome coverage depth for variant calling and making it arguably the most successful MPS technology thus far (114).

Variation between genomic DNA samples from different microbial strains can be discovered through MPS. By aligning DNA reads against a reference genome, variations such as single nucleotide polymorphisms (SNPs), insertions or deletions (indels) (113), or copy number variation (CNV) of segments of the genome (115) can be accessed to varying degrees of accuracy, depending on the sequencing technology employed and the depth of coverage (i.e. how many specific read bases can be aligned to a particular base position on the genome comparison scaffold). Once sequence data has been generated it must be processed and analyzed in order to elucidate existing variations within those data. Indeed, the major bottleneck to sequencing projects is currently not the sample generation and sequencing step, but the sophisticated computational analysis and interpretation of that data (116). Processing and analysis of MPS genome sequence data for variation can be broken down into 5 steps: quality assessment, alignment, variant identification, variant annotation and visualization (117). The most common raw read format FASTQ, which can be output or converted from existing MPS platforms, is a text-based DNA sequence read that carries associated quality scores derived from sequencing (117). Quality scores are a statistical measurement of the uncertainty associated with each base called in a DNA sequence read, typically reported using a phred scaling (113). These raw reads are subjected to quality assessment and manipulated to remove poor quality reads and sequence artifacts like base calling errors and adaptor contamination from the sequencing reaction by trimming, correcting or removing reads altogether from the higher-quality, alignable dataset (118). Alignment consists of matching these

sequence reads to a known genome using a hash data table or Burrows-Wheeler transform-based bioinformatics software program, like MAQ (119) or Bowtie (120), respectively. As part of the alignment process, the user must input a set of parameters by which a given read may be mapped to the genome, allowing for a small degree of variation between the backbone genome sequence and the aligning reads in order for variation discovery to take place. The most common mapping format output is the SAM/BAM (sequence alignment map/Binary SAM) format, which can be used as input by a variety of variation calling software. Variation identification calling is based on differences discovered between the aligned DNA reads and a known genome sequence, which requires adequate depth of coverage for reliable variation calling and relies on the quality scores of reads aligned at particular positions. SNP and indel calling are the most well established uses of MPS for variation discovery and generally require 20 to 40-fold coverage depth for accurate SNP calling (107, 113). However, heterozygous sequences may require higher coverage depth to discriminate between false positive variation calls arising from sequencing errors and a required lower threshold parameter for variation calling, given the need to account for a mixed population of alleles in the sequenced population. For example, a diploid heterozygous mutant would be expected to yield roughly 50 % of sequence reads that contain one of two accurate base calls per position and therefore the threshold for variation calling would be below 50 % of total reads yielding a particular base call. Typically, important parameters like required coverage depth and quality score of called variants and their surrounding bases can be manipulated using variant calling software. Variant calling software includes, for example, MAQ (119), CRISP (121), Dindel (122), SAMtools (123) and GATK (124). Such software

typically generate outputs in variant call format (VCF) (117), which includes the genomic position showing variant base calls, the bases of reads aligned at that position and the associated quality of those calls. CNV and structural variation are more difficult to identify because predictive algorithms often rely on divergence from a normal distribution of read depth mapping across the genome, which can be confounded by experimental biases like GC-rich/poor or repetitive regions receiving inordinate depth of coverage during mapping (125). However, programs like CNV-seq (126), which attempt to discover larger genomic changes based on depth of coverage changes between two different samples, have been used successfully to discover CNV in yeast (127). Once the variations have been compiled, they must be annotated to discover the nature of the mutation, which can include determining its location (intergenic, in an open-reading frame (ORF)), its potential effect at the protein level, or functions and associations of affected genes. Annotation can be done manually on a small scale, but as the use of MPS data becomes more common-place, computational methods are emerging to automate this process (128). Both methods make use of public databases and gene annotations in order to predict phenotypic linkage to the variation discovered within a given genome. Finally, once high quality variations of interest have been discovered, visualization tools can be used to attempt to effectively validate mutations. Visualization tools can be in the form of genome browsers or genome comparison software like Jbrowse (129), Apollo (130), or UCSD Genome Browser (131), which allow for variations to be viewed along with the DNA reads associated to a particular position (117). In this way, variation calls that are supported by reads that are mapped without many mismatches and by a large depth of read coverage can be preserved as reliable calls, whereas variation calls that are only

backed by a small fraction of reliable reads should be discarded. As the predictive reliability of variant calling software progresses, the need for the time-consuming process of manual curation by variant viewing should diminish, but as a verification process it is effective (117).

1.8.2 Bioinformatics resources for analyzing MPS genome sequence reads

Processing and variant-calling software for MPS-generated data is evolving at a rapid pace in order to make full use of the data as the technology platforms evolve. However, a consensus as to the proper set of bioinformatics tools that should be used for sequence analysis has not been accepted. Established, popular and emerging examples of currently available open source software along with their particularities have been recently described in comprehensive detail (117) and number in the hundreds. A few of the popular open-source choices for each step of mapping and variant calling with MPS genome sequence data are given above in their appropriate sections. Integrated bioinformatics workflow and pipeline resources are also emerging that allow a user to perform various analyses such as mapping, variation calling, annotation and visualization including Hugeseq (132), SIMPLEX (133), TREAT (134), and Galaxy (135). Similarly, commercial software packages are available such as CLC Genomics Workbench (www.clcbio.com), DNAnexus (dnanexus.com), Ingenuity Pathways Analysis (www.ingenuity.com), Partek Genomics Suite (www.partek.com) or SNP and Variation Suite (www.goldenhelix.com) that allow for integrated processing of genome sequencing and variant calling workflows. Although the wide array of bioinformatics software available is another non-trivial aspect of processing MPS-generated data, hopefully the

extensive current research into software analysis will translate into robust and accessible tools for biologists in the future.

1.9 RNA-seq transcriptomics as an MPS-based tool for gene expression analysis

While whole-genome sequencing approaches can discover the genomic variations associated with a trait of interest, they still cannot entirely explain the physiology behind that trait, especially if the effect of the mutations discovered are difficult to predict due to factors like location in an ambiguous, intergenic region or within a gene of unknown function. In order to understand an organism's response to environmental perturbations, measuring changes to gene expression can be particularly useful. Gene expression can be monitored by measuring changes in mRNA levels with response to stimuli or genetic changes. Several methods have been devised to profile mRNA transcript levels such as serial analysis of gene expression (SAGE), reverse transcription-polymerase chain reaction (RT-PCR), DNA chips or microarrays (136), and more recently, RNA-seq (137). Known as transcriptomics, these approaches are perhaps the '-omics' tools that have generated the most abundant information for understanding the *S. cerevisiae* system. Most of the existing transcriptomics data that exist for *S. cerevisiae* are based on data from experiments using microarrays, which continue to be a cost and labour effective means to assess transcription responses. DNA microarrays are a well-established technology for measuring changes in mRNA levels as they relate to different stress or growth conditions, and chemical inhibition or toxicity (138). As mentioned above, DNA microarrays have been used to understand the response of *S. cerevisiae* to stressors found in lignocellulosic substrates including oxidative stress and osmotic shock (27), furan aldehydes (59, 60) and acetic acid (139) and, in some instances, to generate reverse

engineering targets for improving tolerance based on that understanding (59). Though microarray experiments have proven productive, some shortcomings include the required foreknowledge and reliable annotation of expressed genes within the queried organism as well as the semi-quantitative nature of transcript levels, which are assessed based on comparative signals and not absolute mRNA levels. Furthermore, there is a limited detection range due to high background cross-hybridization levels and signal saturation (140). RNA-seq technology is emerging as a viable alternative to the above gene expression monitoring methods and as the technology matures it promises to replace microarrays as the method of choice for transcriptome analysis.

RNA-seq makes use of the same MPS technology described above. This method involves converting an RNA or mRNA sample to cDNA fragments, which are then sequenced according to the sequencing platform selected. RNA-seq data is analyzed in a similar fashion to MPS genome sequence data. Reads must be processed for quality, aligned to a known genome or transcriptome sequence file, and then reads mapping to a particular gene must be quantified and compared for differential expression analysis (141-144). RNA-seq has the advantage of allowing for assembly of transcripts *de novo*, especially when a larger read-yielding sequencing platform is employed (145), giving simultaneous transcriptional structure and gene expression level.

As with MPS technology, a variety of software tools are becoming available to carry out these steps. Read mappers can include Bowtie (146), BWA (147) and TopHat (148). Mapping output generally is followed by transcriptome reconstruction using software like Cufflinks (149) and Velvet (150) and expression quantification with

software like Cuffdiff (149) and Myrna (151). Analysis tools with integrated pipelines supporting these steps include Galaxy (135) and CLC Genomics Workbench.

RNA-seq transcript levels are quantified from the number of reads aligned to a specific gene (137, 144) and gene expression estimation requires normalization of read counts to account for gene length and the number of reads obtained per sequencing sample (152). In single-end reads these variables are accounted for by using the reads per kilobase of transcript per million mapped reads (RPKM) metric (144). While the dynamic range of detectable differential transcript level for expression arrays or tiling arrays requires at least two orders of magnitude of variation between compared samples, RNA-seq has sensitivity limited only by expression levels or sequencing depth (137). However, because of the youth and relatively high cost of RNA-seq, differential expression between samples is generally not built upon empirical estimations of variability by extensive biological replicates at high sequence depth, but analysis tools that attempt to model biological variability and assign significance to count variance (152-155). In actuality, parameters such as accepted differential gene expression thresholds and significance values must be varied according to the data set and the purpose of the experiment (141). Differences between technical RNA-seq replicates for differential expression using the Illumina platform have been demonstrated to have high reproducibility with significant variation between technical replicates being approximated at only ~0.5% of genes and to yield accurate differential expression calls, as verified by microarray (152). The study by Marioni *et al*. that demonstrated these results tested samples with 8.4-14.7 million reads per sequencing reaction (152). A similar finding by Nookaew *et al.* demonstrated a high level of agreement between RNA-seq biological

replicates (correlation ≥0.99) and a high level of consistency between RNA-seq and microarray expression analysis (correlation ≥0.91), using an average of 5.97 ± 1.2 million of 100 bp paired-end reads per sample for comparison (156). Although the technical aspects of what constitutes a reliable RNA-seq experiment are still being established, the technology can be used effectively to draw biological conclusions.

Once a differentially expressed data set has been established, it can be mined to ascertain affected biological processes of interest. In order to make sense of the data derived from differential expression analysis, a widely-used practice is to analyse the dataset for gene category over-representation (157). Such analysis is performed by grouping genes into categories based on common biological properties and testing for category over-representation within a set of differentially expressed genes. Gene ontology (GO) categories are used in this respect to assign known biological functions to genes using tools such as EasyGO (158), GOminer (159), GSEA (160), and DAVID (161) (see (161) for a comprehensive list). It has been shown that enrichment clustering by GO categories using RNA-seq can suffer from biases such as over-representation of categories containing longer genes due to the likelihood of significant differential expression identification from genes with more representative reads (157). Despite these concerns, it has been demonstrated in yeast that RNA-seq differential expression findings and GO category over-representation analyses largely agree with microarray data, and across biological and technical replicates (156). As RNA-seq technology grows with MPS technology, it is situated to become a valuable resource and may become a mainstay in reverse engineering workflows in order to narrow down or discover new genes and processes associated with a trait of interest.

1.10 Conclusions

One of the tenets of synthetic biology is to break down a cell into discreet parts of known function that can then be appropriated for rational biological design. However, when faced with a complex biological problem, such as tolerance to lignocellulosic substrate inhibition, the steps to take and parts to assemble to rationally design a suitable biocatalyst to ferment these substrates is not known. Strain development technologies like meiotic recombination-mediated GS of *S. cerevisiae* may allow for the efficient and effective evolution of *S. cerevisiae* to evolve complex traits of interest. In order to track changes to an evolved strain, to gain insight into the types of mutations accumulated through GS and to probe the physiology of tolerance to industrial lignocellulosic substrates like HWSSL, MPS technology is emerging as an invaluable tool. Through genome sequencing and RNA-seq technologies, it is possible to discover mutations caused by non-targeted strain evolution, novel avenues of research or to generate reverse engineering targets to inform future strain engineering studies. The following research makes use of these technologies to engineer and study HWSSL tolerance.

Chapter 2

based on:

Pinel *et al.* 2011. *Saccharomyces cerevisiae* genome shuffling through recursive population mating leads to improved tolerance to spent sulfite liquor. Appl Environ Microbiol 77:4736-4743.

Pinel *et al*. 2011. 'Omics' technologies and systems biology for engineering *Saccharomyces cerevisiae* strains for lignocellulosic bioethanol production. Biofuels 2:659-675.

Pinel D, Martin VJJ. 2012. Meiotic recombination-based genome shuffling of *Saccharomyces cerevisiae* and *Schefferomyces stiptis* for increased inhibitor tolerance to lignocellulosic substrate toxicity, p. 233-250. In Patnaik R (ed.), Engineering complex phenotypes in industrial strains, 1 ed. John Wiley & Sons, Inc., Hoboken, New Jersey

2.1 Introduction

The aim of the first portion of this study was to generate a strain of *S. cerevisiae* by evolutionary engineering for improved tolerance to the inhibitory conditions that accompany HWSSL fermentation. HWSSL was chosen for tolerance evolution because it is the least nutritious, most inhibitor-rich form of SSL and may therefore lead to more robust final strains. Because tolerance to lignocellulosic hydrolysate inhibitors, like those found in HWSSL, might be achieved by a variety of means, many genetic factors need to be addressed simultaneously to overcome inhibition (60, 97), which requires a robust strain improvement methodology. Therefore, a meiotic recombination-mediated genome shuffling method was developed to generate biocatalysts with increased HWSSL tolerance.

In order to test the methodology, pools of strains that are auxotrophic for differing markers were reiteratively mated, population-wise and assessed for loss of auxotrophy. The optimized meiotic recombination-mediated GS methodology was then used to evolve

increased HWSSL tolerance. Strains that showed the highest level of increased HWSSL tolerance were analyzed for growth and fermentation characteristics, as well as increased tolerance to single inhibitors commonly found in HWSSL. This study is the first instance described of sexual recombination GS of *S. cerevisiae* to evolve a phenotype tolerant of a lignocellulosic substrate with multiple sources of inhibition, which may be difficult to obtain through classical strain development techniques. This chapter presents a new strain of *S. cerevisiae* that is tolerant of prolonged exposure to undiluted HWSSL and can maintain ethanol production, concomitant with increased tolerance to salt, acetic acid, and peroxide.

2.2 Materials and Methods

2.2.1 Yeast strains and general maintenance

The *S. cerevisiae* CEN.PK strain set supplied by EUROSCARF was used for all experiments (162). Specific CEN.PK strains used for each experiment are listed in the appropriate section below. The *S. cerevisiae* strains of dry white wine yeast and Thermosacc were used for industrial strain comparisons and were kindly provided by Tembec Inc. and Lallemand, respectively. Yeast strains were grown in yeast peptone dextrose medium (YPD, 1% yeast extract, 2% peptone, 2% glucose, w/v), or minimal synthetic defined, SD, medium (0.67% yeast nitrogen base without amino acids (YNB), 2% glucose, w/v) and supplemented with the following nutrients, where required, for growth (% w/v): uracil- 0.002, L-tryptophan- 0.002, L-histidine- 0.002 and L-leucine- 0.006. Solid medium were prepared by adding 2% (w/v) agar to the liquid medium above. For long-term storage, strains were grown on YPD, combined with glycerol 15% (v/v) and stored at -80 °C.

2.2.2 Genome shuffling assessment with triple auxotrophic haploid *S. cerevisiae* strains

A meiotic recombination-based GS method was developed that consisted of mating mutant haploid populations to produce a diploid generation, presporulation and sporulation of diploids, followed by spore separation, and finally regeneration and germination of haploids for the next round of reiterative mating (Fig. 2-1). To test the ability to combine mutations into one strain via meiotic recombination-based GS, 8 triauxotrophic CEN.PK-derived *S. cerevisiae* strains of each mating type were used as parental strains, which require supplementation with 3 of the following 4 nutrients for growth: uracil, tryptophan, histidine, and/or leucine. They included 4 MATa strains: 113-1C (MATa, ura3-52, his3-11, LEU2, trp1-289, MAL2-8c, SUC2), 102-5B (MATa, ura3-52, his3-11, leu2-3/112, TRP1, MAL2-8c, SUC2), 113-6B (MATa, ura3-52, HIS3, leu2-3/112, trp1-289, MAL2-8c, SUC2), 113-5A (MATa, URA3, his3-11, leu2-3/112, trp1-289, MAL2-8c, SUC2); and 4 MATα strains: 110-4C (MATα, ura3-52, his3-11, LEU2, trp1-289, MAL2-8c, SUC2), 111-61A (MATα, ura3-52, his3-11, leu2-3/112, TRP1, MAL2-8c, SUC2), 113-7B (MATα, ura3-52, HIS3, leu2-3/112, trp1-289, MAL2-8c, SUC2), and 113-17D (MATα, URA3, his3-11, leu2-3/112, trp1-289, MAL2-8c, SUC2). Cultures were grown overnight in shake flasks containing SD medium and cell densities were normalized to the same optical density (OD600 nm of 5). For GS of triple auxotrophic strains, 100 μL of each of the 8 cultures were washed three times in PBS buffer, combined, mixed, and entirely spotted onto YPD agar for mating (163). After mating, two large loopfuls of the mated population were suspended in YPD, vortexed, and entirely spotted on presporulation medium (0.8% w/v yeast extract, 0.3% w/v

peptone, 10% Dextrose, 2% agar) (164). Two large loopfuls of the presporulated population were washed three times in PBS buffer, suspended in 200 µL PBS (cell density 1 x 10^9 CFU/mL) and entirely spotted on sporulation medium (1% w/v potassium acetate, 0.1% w/v yeast extract, 0.05% w/v dextrose, 2% w/v agar) (164) to induce sporulation of the diploid strains. To enrich for strains that had effectively mated and undergone meiotic recombination, the sporulated culture was treated with zymolyase to kill surviving vegetative cells and to break down the asci cell walls. Spores were then separated by sonication to optimize intergenic crosses in future matings (164). Induction of the mating cycle of the population was repeated a total of three times and a sample of the population (population size was ~3 x 10^6 CFU/mL) was tested at each successive round. Loss of auxotrophy was monitored between rounds of shuffling using plate counts on SD medium supplemented with all the possible combinations of uracil, tryptophan, leucine and histidine from supplementation with no nutrients to triple supplemented.

2.2.3 Creation of HWSSL tolerant mutant pools

For GS of HWSSL inhibitor-tolerant *S. cerevisiae* strains (Fig. 2-2), the haploid prototrophic strains CEN.PK-113 1A (MATα) and 113 7D (MATa) were used as the parental wild type (WT). Pools of mutants from each haploid mating type were first created by UV mutagenesis using a Stratalinker UV Crosslinker (Stratagene, La Jolla, CA). A lawn of each strain was plated onto YPD agar from an overnight culture grown on YPD at 30°C with shaking at 180 rpm. The cells were irradiated with 7,500-10,000 µJ of UV light (λ = 254 nm), resulting in a survival rate of ~30-40%, and the plates were incubated for 2 days in the dark at 30°C (modified from (164)). Mutants able to grow at

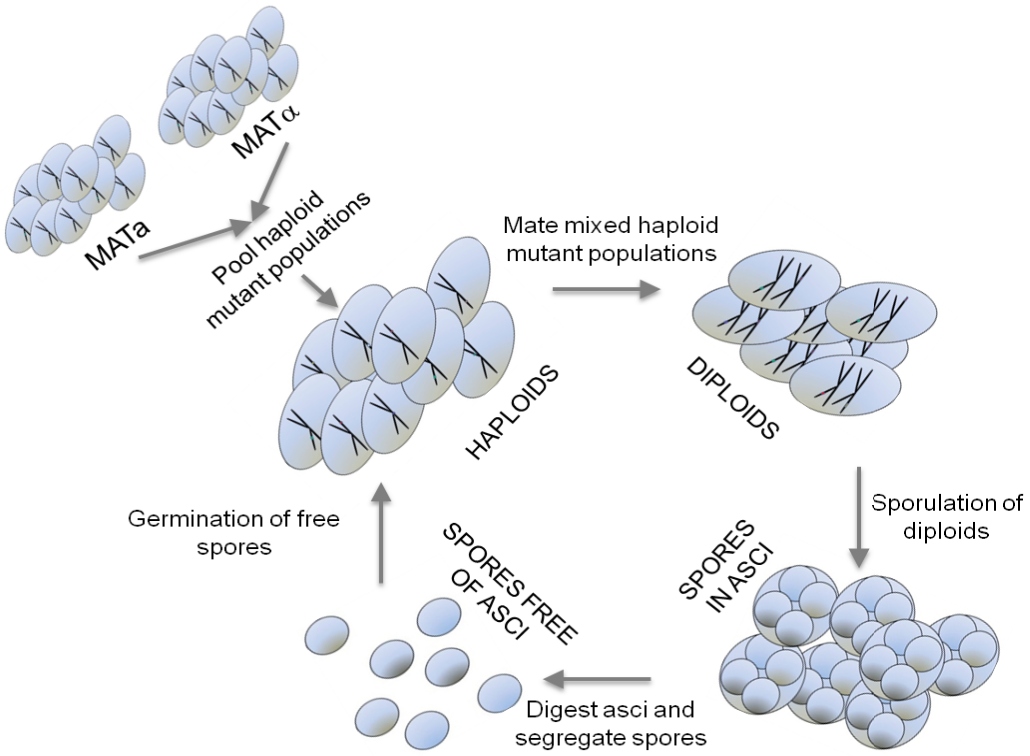

Figure 2-1. Schematic representation of meiotic recombination-based genome shuffling of *S. cerevisiae*. Firstly, haploid pools of each mating type (*MAT a* and *MAT α*) are mated on rich medium (YPD) to obtain the diploid generation. Diploids are sporulated on potassium acetate. Spores are segregated by enzymatic cell-wall degradation followed by sonication to generate a haploid generation. Haploids are germinated and mated on rich YPD medium and reiterative mating is carried out.

increased HWSSL concentrations were selected on HWSSL gradient agar plates. To create the agar plates with a gradient of growth inhibition, undiluted HWSSL agar (2%, w/v) was overlaid with inhibitor-free minimal medium to establish a gradient from higher to lower HWSSL concentration (165). HWSSL used for all experiments was kindly supplied by Tembec Inc. and adjusted to pH 5.5 with 10 M NaOH before use. HWSSL

contained an average, in (w/v): 0.076% arabinose, 2% xylose, 0.16% galactose, 0.24% glucose, 0.43% mannose.

2.2.4 GS for tolerance to HWSSL

The meiotic-recombination mediated GS methodology, described for the loss of auxotrophy experiment above, was modified to engineer HWSSL tolerance (Fig. 2-2). UV mutant populations that showed greater tolerance to growth inhibition on HWSSL gradient plates were scraped entirely and used as the parent populations for GS. To test if

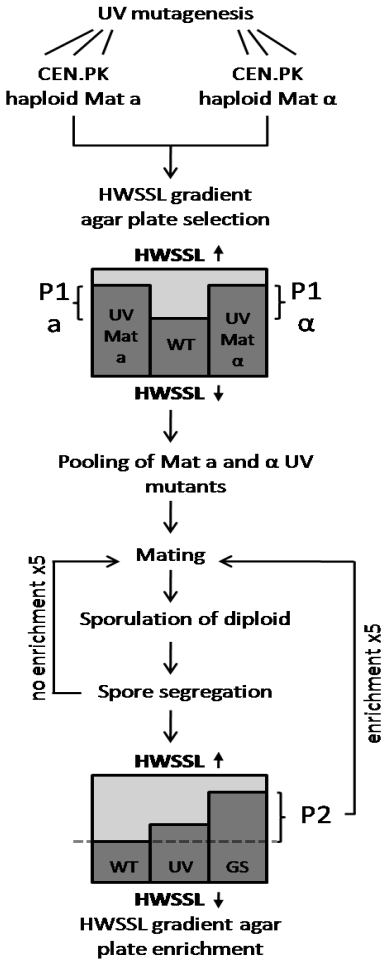

Figure 2-2. Schematic representation of genome shuffling by recursive mating for increased HWSSL tolerance. *S. cerevisiae* CEN.PK 113-1A (Mat α) and 7D (Mat a) were UV mutagenized (UV) and selected on HWSSL gradient agar plates for mixed mutant populations able to grow at higher HWSSL concentrations than the WT (P1). These populations were pooled and mated and subjected to 5 rounds of genome shuffling with or without enrichment. Genome shuffling entailed mating haploid strains, sporulation of diploid generation and spore segregation. Enrichment meant screening the shuffled populations (GS) for members that could colonize higher HWSSL concentrations than the WT on HWSSL gradient agar, and using them as the mating population (P2) for subsequent genome shuffling.

selecting for improved strains after each round of mating could augment strain evolution, populations were mated, followed either with or without enrichment of the parent

populations on gradient plates. Enrichment consisted of pre-growing selected UV mutants or shuffled populations in SD medium, and plating the entire portion of the shuffled population after each round of GS onto a HWSSL gradient plate and scraping the population growing at higher concentrations of HWSSL gradient agar for use as the subsequent parent population. GS without enrichment refers to populations that were recursively mated, without discarding members of that population that were able to colonize only a lower or similar concentration of HWSSL as the WT on HWSSL gradient plates, prior to mating. HWSSL tolerant, enriched and not enriched populations, were taken through the entire process of mating, sporulation, and spore segregation a total of 5 times. The entire HWSSL tolerant segregated spore population, obtained from sporulation plates, was pre-grown in SD medium for one day at 30°C with shaking at 180 rpm, so that each member of the population had equal opportunity to colonize higher concentrations of HWSSL when compared on HWSSL gradient agar plates. Population samples from every round of GS were compared on HWSSL gradient agar plates.

2.2.5 Growth and survival assessment of yeast mutant strains

To evaluate tolerance to HWSSL, colonies forming at the high inhibitor frontier of the HWSSL gradient plates were randomly selected and purified on YPD agar. These strains were subjected to a preliminary screen and final characterization in liquid culture with the following protocol: each streak-purified strain was grown in 50 mL SD medium in a 125 mL shake flask overnight at 30 ºC and 180 rpm, washed in PBS and inoculated at a low cell density of ~5 x 10^5 CFU/mL into 50 mL of HWSSL and cultured under semi-fermentative conditions (sealed 125 mL flasks shaken at 100 rpm) at 30 °C. The preliminary screen tested thirty strains from the initial parental UV mutant pool, as well

as 15 from rounds 1, 3 and 5 of the GS experiment with population enrichment. Cultures were sampled daily for viable plate counts on YPD agar over 3 days. The final characterization focused on strains, from the preliminary screen, showing increased growth tolerance to undiluted liquid HWSSL (Fig. 2-7). These were characterized more fully for survivability using YPD agar plate counts taken in triplicate from 3 independent cultures, with time points taken daily for 6 days. A control group of the two WT haploid strains of both mating types were subjected to the same regime of GS, for 5 rounds.

2.2.6 Fermentation of HWSSL

Strains selected from the survival assessment: R311, R57, R511, along with WT strains: haploids CEN.PK 113-1A, CEN.PK 113-7D, and the WT prototrophic diploid CEN.PK-122 were inoculated from YPD agar and grown individually in 100 mL SD medium for 1 day in 250 mL shake flasks at 30 ºC at 180 rpm. Cells from cultures were harvested at 1200 x g, washed 3 x in PBS and suspended in 50 mL undiluted HWSSL in 125-mL sealed shake flasks at an initial cell density of ~8 x 10^7 CFU/mL of each yeast strain for high-cell density fermentation and shaken at 180 rpm at 30 ºC. The yeast population was recycled into fresh HWSSL after 48, 120, 192, 264 and 336 h. Each of the HWSSL cultures was centrifuged at 3000 x g and suspended in 50 mL of fresh HWSSL for recycling. Samples of 1 mL were taken daily and centrifuged at 15000 x g to obtain supernatant that was frozen at -20 ºC for ethanol and sugar analyses. Fermentations were carried out in biological triplicates in separate shake flasks and reported with standard errors. Viability was measured daily with triplicate plate counts on YPD agar.

2.2.7 Ethanol and sugar analyses

Sugars in HWSSL were derivatized to aldonitrile acetates for GC analysis (166). Analysis of ethanol and derivatized sugar concentrations were done using an Equity-1 and Equity-1701 GC columns, respectively (30m x 0.32mm x 0.25µm, Supelco, Bellefont, PA) with a 6890N gas chromatogram, equipped with a flame ionization detector and a 7683B autosampler from Agilent Technologies (Mississauga, ON). Quantification of ethanol concentration was carried out with external ethanol standards. Sugar concentration was determined with an internal standard of ribose (0.6%, w/v) and external standards of xylose, arabinose, mannose, glucose and galactose. Detection limits for all compounds were below 0.01% (w/v) each, with a standard deviation of ~2% between injections.

2.2.8 Tolerance to selected inhibitors

To characterize their phenotypes, strains R311, R57, and R511 were compared to the WT diploid CEN.PK-122, in triplicate, on selected inhibitors. Starter cultures were incubated at 30 ºC in sealed 125 mL shake flasks, shaken at 100 rpm for 24 h in SD medium or in 100% HWSSL to allow for the full effects of exposure to SSL to be witnessed without a large population loss of the WT, which dies rapidly in the presence of HWSSL, before plating on inhibitor agar plates. The inhibitors tested included: 2-furaldehyde (0.05, 0.1, 0.2, 0.25, and 0.5%, w/v), HMF (0.05, 0.1, 0.2, 0.25, and 0.5%, w/v), acetic acid pH 5.5 (0.5, 1.0, 2, and 5%, w/v), acetic acid pH 3 (0.25, 0.5, and 1.0%, w/v), *p*-hydroxybenzoic acid (0.5%, w/v), ammonium sulfite (1, 2, and 5%, w/v), hydrogen peroxide (1, 2, 5, 20, 40, 60, 80, and 100, mM), sodium chloride (NaCl) (2, 5, and 7%, w/v), sorbitol (2 M) and ethanol (10, 12, and 13.5%, w/v). Inhibitors were

incorporated into Petri plates with SD medium and 1% (w/v) agar, and a dilution series of each strain was plated using 10, 100, 1000, and 10000 viable cells in 5 μL. These plates were sealed with parafilm and plastic wrap, incubated at 30 °C and viewed daily until a difference in growth patterns could be discerned. 2-Furaldehyde, HMF, acetic acid, *p*-hydroxybenzoic acid, ammonium sulfite, and hydrogen peroxide were obtained from Sigma (Oakville, ON).

2.3 Results

2.3.1 GS for reduced auxotrophy demonstrates the ability to combine mutations through reiterative poolwise meotic recombination

Initially, to test GS using a reiterative large scale population mating methodology, 8 *S. cerevisiae* strains of 4 Mat a and 4 Mat α mating type, each triauxotrophic for 3 of 4 possible leu, ura, trp, and his markers, were used as the parental mating pool (Fig. 2-3A). The proportion of auxotrophic individual strains in the population decreased with reiterative poolwise mating as the 4 WT alleles were combined into one genome. The ability to bring together prototrophic WT alleles was used as a surrogate assessment of the ability to bring together beneficial mutations on separate chromosomes. This test showed that double auxotrophy, or 2 beneficial mutations are incorporated into 1 strain to comprise ~35% of the second generation population, while just two rounds of GS without enrichment or selection yielded prototrophic strains, or strains containing 4 beneficial mutations, to comprise 0.024% of the third generation population and 0.84% of the fourth (Fig. 2-3A, Fig. 2-4). This trend suggests that a subset of the population can likely display the exponential addition of beneficial mutations if a starting mutant pool is large enough, reinforcing the importance of a large, diverse parent population bearing

heterogeneous mutations (Fig. 2-3B).

2.3.2 Meiotic recombination-based GS can be used to engineer HWSSL tolerant populations of *S. cerevisiae*.

The parent strains for HWSSL tolerance evolution were chosen from the CEN.PK strain family of *S. cerevisiae* because they are robust starting organisms, suitable for high ethanol productivity, and are amenable to genetic manipulation (162, 167). From this genetic background, haploid UV mutant populations were created that showed increased growth tolerance to HWSSL (Fig. 2-5A). These mutant populations of each mating type were used as the initial parent populations for 5 rounds of GS using the above methodology, with and without population enrichment between each round of mating. Regardless of the shuffling regime employed, every round of shuffling showed populations with higher tolerance than the previous round on HWSSL gradient agar plates (Fig. 2-6). However, enriching for tolerant populations between rounds of shuffling resulted in a more pronounced increase in tolerance (Fig. 2-6). This was demonstrated by HWSSL gradient agar plate screening where just two rounds of GS led to a without enrichment (Fig. 2-5B). It is hypothesized that enrichment increased the chances of mating two strains that harbored beneficial mutations while maintaining sufficient mutant population diversity to allow for continued evolution. HWSSL gradient agar plate screening revealed the evolutionary trend of the yeast populations toward greater HWSSL tolerance as GS progressed from the UV mutant populations through to round five, leading to populations containing strains with higher HWSSL tolerance than previous rounds (Fig. 2-5C and D). It is hypothesized that mutations from the preceding rounds of GS were incorporated through genomic recombination to

confer an overall more HWSSL tolerant trait to offspring in the subsequent rounds.

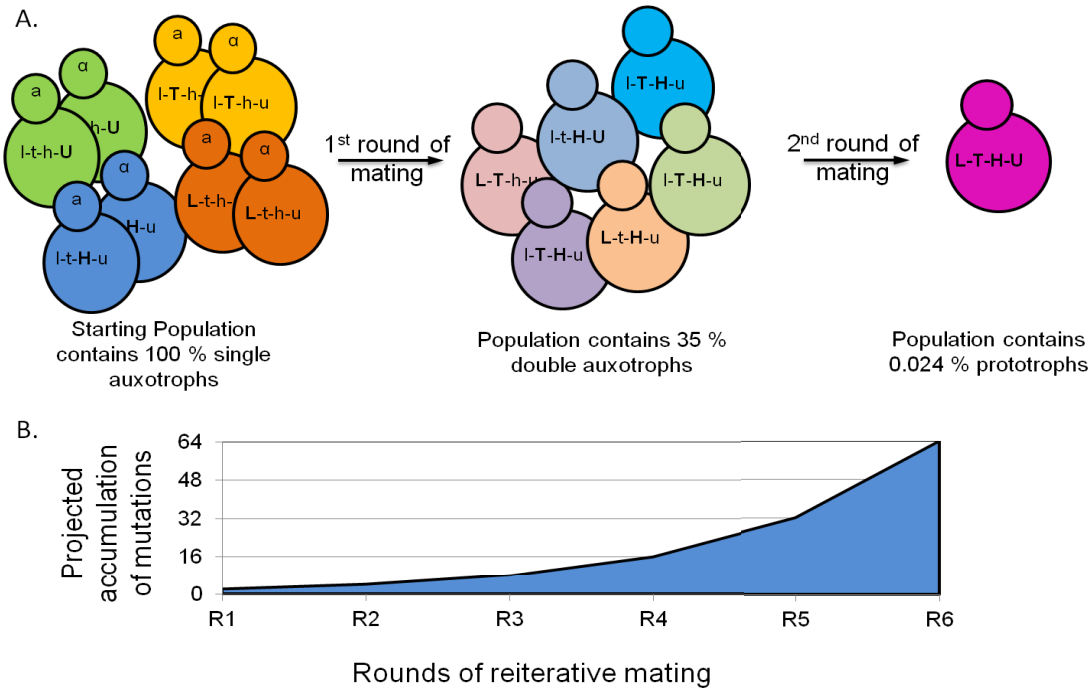

Figure 2-3. Testing of *S. cerevisiae* genome shuffling methodology using auxotrophic strains. (A.) A parental population of haploid strains, which were auxotrophic for 3 of 4 nutritional requirements were reiteratively mated using meiotic recombination-based GS. The auxotrophies were based on deletion in single-genes (depicted by lower-case letters: l for leucine, t for tryptophan, h for histidine, and u for uracil auxotrophies). WT alleles are depicted by corresponding upper-case letters. After 1 round of GS, 35 % of the population harboured 2 WT alleles and after 2 rounds 0.024 % of the screened population showed complete prototrophy, or 4 WT alleles. (B.) The graph depicts an extrapolation of the amount of beneficial mutations (y-axis) that are possible to accumulate through multiple rounds of meiotic recombination-mediated GS (R1-R6).

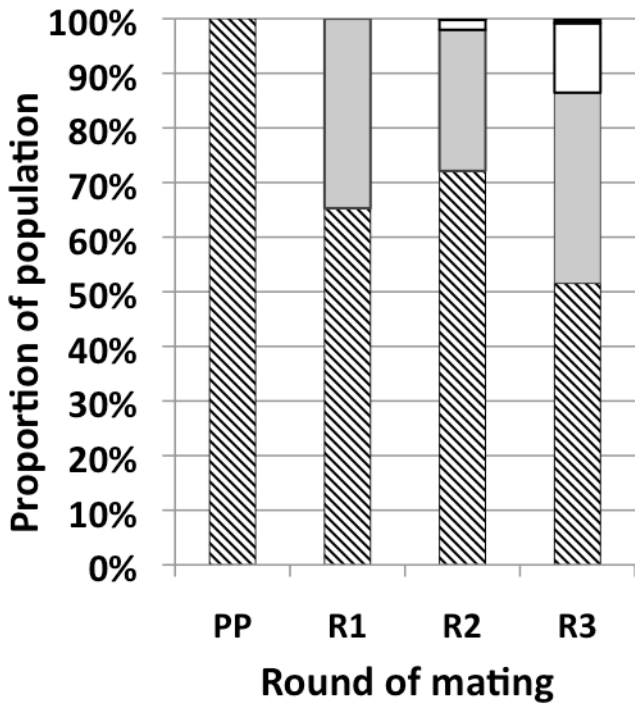

Figure 2-4. Proportion of auxotrophic mutants isolated after genome shuffling through reiterative mating. Figure shows the increase in diversity and loss of auxotrophy throughout population of genome shuffled triple auxotrophic strains of the parent population (PP) and 3 rounds (R1, R2 and R3 represent the three generations of evolved strains) of the reiterative mating methodology. Percentage of *S. cerevisiae* population, from bottom to top, that are quadruple or triple auxotrophs (☐), double auxotrophs (▩), single auxotrophs (☐), and prototrophs (■).

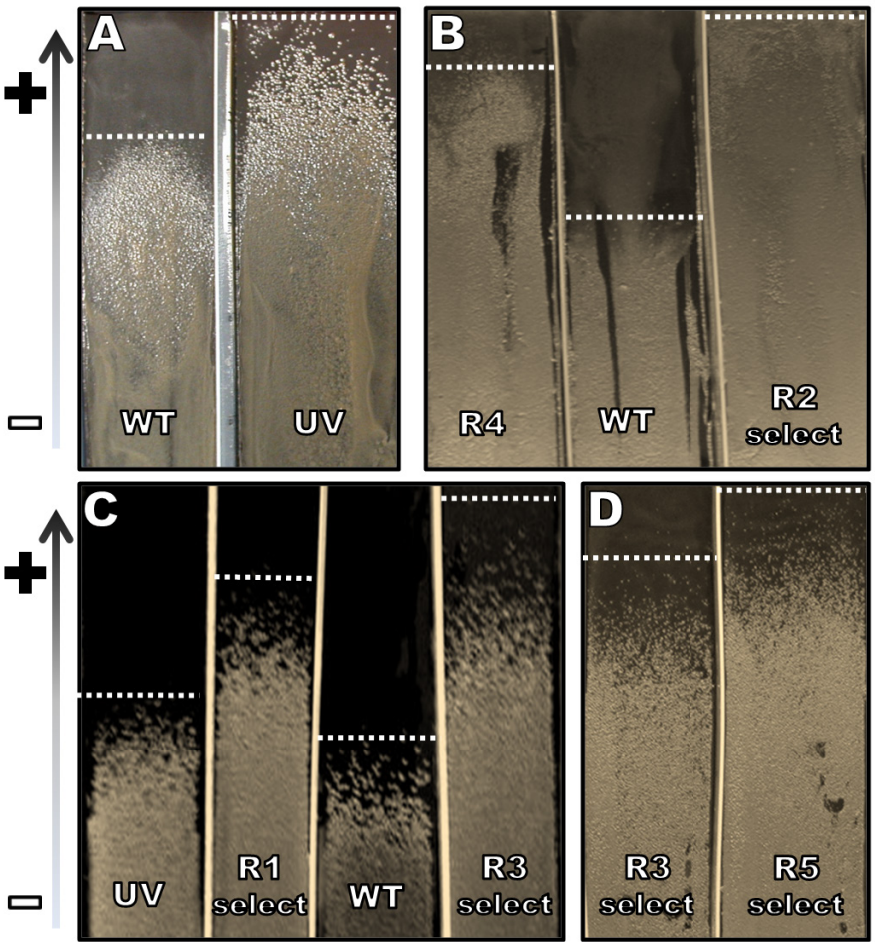

Figure 2-5. Gradient plates for comparison and selection of HWSSL mutant and evolved strains. Panels (A), (B), (C), and (D) all depict single HWSSL gradient agar plates of varying HWSSL concentrations, allowing for the resolution of the compared populations, separated by sterile plastic dividers. The white dashed lines indicate the SSL concentration at which colony growth was arrested. (A) Shows the comparison between a population of CEN.PK haploid mutants generated by UV mutagenesis (UV), indicative of the initial mutant population for GS, and the CEN.PK wild type 113-1A haploid strain (WT) (~30-60 % v/v HWSSL concentration plate). (B) Depicts populations from round 4 (R4) of the GS experiment without enrichment between crossings as compared to a population generated from just 2 rounds of GS with population enrichment between rounds of shuffling (R2 select) (~30-70 % v/v HWSSL concentration plate). (C) Shows the progress of the evolution of shuffled populations from the WT genome shuffled control (WT) to UV mutant (UV) through rounds 1 and 3 of GS with selection of enriched populations after each crossing (R1 select, R3 select, respectively) (~40-80 % v/v HWSSL concentration plate). (D) Shows the comparison of round 5 of GS with population enrichment (R5 select) and R3 select (~50-90 % v/v HWSSL concentration).

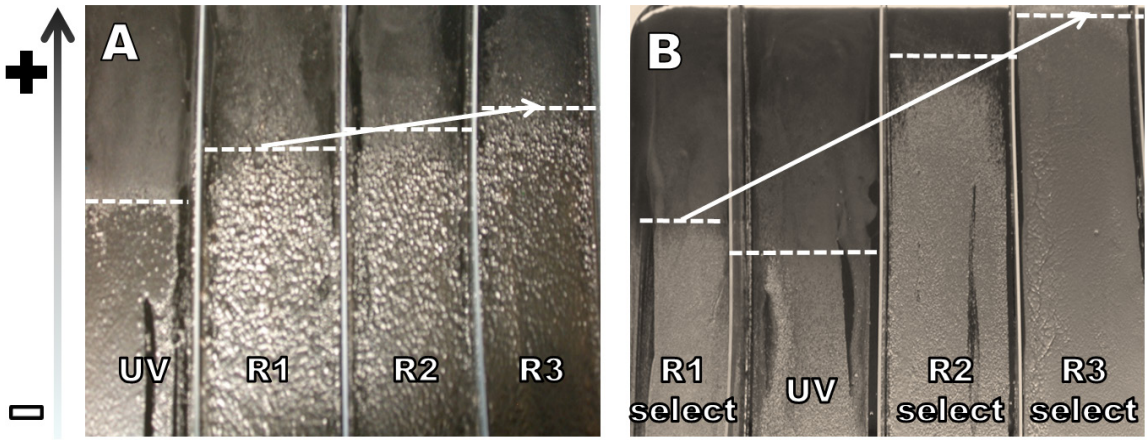

Figure 2-6. HWSSL gradient agar plates for comparison of HWSSL mutant and evolved strains with and without enrichment between shuffling rounds. Panels (A) and (B) depict single HWSSL gradient agar plates of 40-70 % v/v HWSSL concentrations, allowing for the resolution of the compared populations, separated by sterile plastic dividers. The white dashed lines indicate the SSL concentration at which colony growth was arrested. (A) Shows the comparison between a population of *S. cerevisiae* mutants generated by UV mutagenesis (UV), indicative of the initial mutant population for genome shuffling, and rounds 1, 2, and 3 of genome shuffling without enrichment between rounds (R1, R2, R3, respectively). (B) Shows the comparison between UV and rounds 1, 2, and 3 of genome shuffling with enrichment between rounds (R1 select, R2 select, R3 select, respectively). The white arrow shows the increasing frontier of growth towards higher concentrations of HWSSL.

2.3.3 Characterization of strains for enhanced viability and growth in HWSSL

HWSSL, when diluted 2-fold with sterile water, supported growth of WT *S. cerevisiae* (data not shown), showing it contains all the nutrients needed for growth, when inhibitors are present at lower concentrations. To test if HWSSL toxicity could be overcome by evolutionary engineering using serial transfer of cultures exposed to sub-lethal concentration of HWSSL, CEN.PK WT were repeatedly passed into diluted fresh liquid HWSSL shake flasks daily. This approach generated adapted populations that would grow more quickly in 2-fold and 1.75-fold water-diluted HWSSL, but would

succumb to toxicity at 1.5-fold diluted HWSSL (data not shown). This approach was abandoned when these populations showed less tolerance than the WT on higher concentrations of HWSSL, shown by gradient plate screening. To determine if it was possible to overcome these limitations using GS, strains that showed the greatest tolerance to undiluted HWSSL from intermittent rounds of GS were characterized for growth and survival in undiluted HWSSL. These included: M3, M23, and M29 from the UV mutant population, R12, R14, and R18 from the first round, R35, R311, R312, and R315 from the third round, and R56, R57, R510, and R511 from the fifth round of recursive mating and enrichment, respectively. As seen in Fig. 2-7, the UV M-series mutants performed similarly to the WT strains, which showed population survivability below 50% after 3 days in HWSSL, with the exception of strain M3, of which 71.7 ± 4.3 % of the starting population size still remained viable after 3 days. This shows that the starting UV mutant pools contained members like M3 that exhibited higher tolerance to undiluted liquid HWSSL. These results also show the diversity that existed within the parent UV populations, which is important for successful GS (99). As these UV mutants were genome shuffled, locating individual strains that displayed a more tolerant phenotype to undiluted HWSSL became more likely (Fig. 2-7). The yeast population from shuffling round 1 contained member strains R12 and R14 that retained over 50% population viability for at least 6 days. Likewise, the evolution progressed through subsequent rounds of shuffling with members from the shuffling round 3 population, R311 and R312, growing in HWSSL to an average population size of 186% and 161% of the original starting population after 6 days, respectively. In the final round 5 of shuffling, the tolerance of selected strains continued to increase and strains R57 and R511

showed significant growth, as reflected by an average viable population that was 326 % and 310 % the size of the starting inocula after 6 days, respectively. The final control population did not contain individuals that showed evolved tolerance to HWSSL, as displayed by all WT lanes of Fig. 2-5. This suggested that the evolved tolerance was a direct product of reiterative mutant mating and not a product of spontaneous mutation by

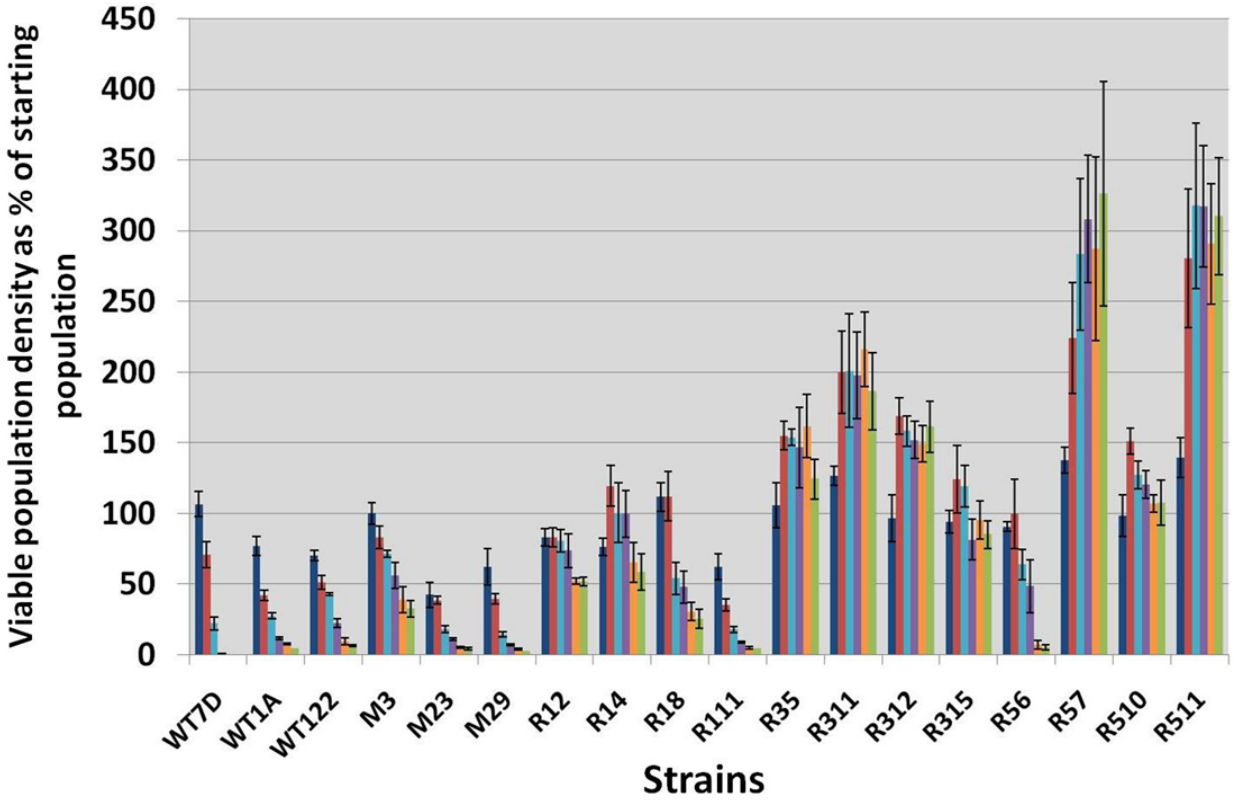

Figure 2-7. Survival and growth of individual strains taken from GS experiment for increased tolerance to HWSSL. The WT and most tolerant strains from gradient plate screens were selected for characterization which include: 3 WT strains, 2 haploids CEN.PK 113-7D and 1A (WT7D and WT1A) and the diploid CEN.PK 122 (WT122), 3 strains from the UV mutant parent population (M3, M23, and M29), 4 strains from the first round of GS (R12, R14, R18, R111), 4 from the third round (R35, R311, R312, R315), and 4 from the fifth round (R56, R57, R510, R511). Viable population densities, as a function of original population density starting at ~5 x 10^5 CFU/mL, were determined at 24 h ■, 48 h ■, 72 h ■, 96h ■, 120 h ■, and 144 h ■.

repeated exposure to HWSSL. The ability to locate increasingly tolerant individual strains progressed as further rounds of GS were carried out. Furthermore, the progressive increase in tolerance amongst the individual strains suggests that the shuffled populations contained more tolerant individuals with each round of population crossing by incorporating several mutations that conferred a more HWSSL-tolerant phenotype. Of the strains characterized for survival in HWSSL, R311, R57, and R511 were chosen for characterization of their fermentative abilities in HWSSL due to their increased relative tolerance.

2.3.4 Fermentation of the sugars in HWSSL to ethanol by *S. cerevisae* WT and evolved strains

It was important to verify that improved growth and survival of the evolved mutants in HWSSL did not come at the expense of ethanol productivity. Growth/survivability was chosen as a surrogate screen because resistance to SSL inhibition can relate to less inhibited ethanologenicity (168). Cultures were recycled repeatedly into fresh HWSSL to assess the effect of prolonged exposure to HWSSL on ethanol productivity at high cell density, to mimic cell recycle batch fermentation used in industry (Fig. 2-8). Previous research showed that *S. cerevisiae* strain Tembec T1, a SSL-fermenting strain adapted in and isolated from industrial SSL fermenters, only produces ethanol at approximately 62 % and 28 % w/v of the theoretical yield in 1 and 2 passes in HWSSL, respectively (96). As Fig. 2-8B shows, upon initial inoculation into HWSSL, the WT and selected evolved populations yielded comparable ethanol concentrations, about 0.35% (w/v), which is near the theoretical yield from the mannose and glucose present in HWSSL (Fig 2-8C and D). As expected, pentose sugars were not

consumed. Galactose was also left unconsumed, probably owing to a sensitivity of galactose transport and metabolism that occurs due to the presence of glucose (169), chemical perturbations like iron deficiency (170), pH below 6, or SSL exposure (96, 169), and is energetically unfavourable under anaerobic conditions. The amount of ethanol produced by each strain was paralleled by glucose and mannose consumption

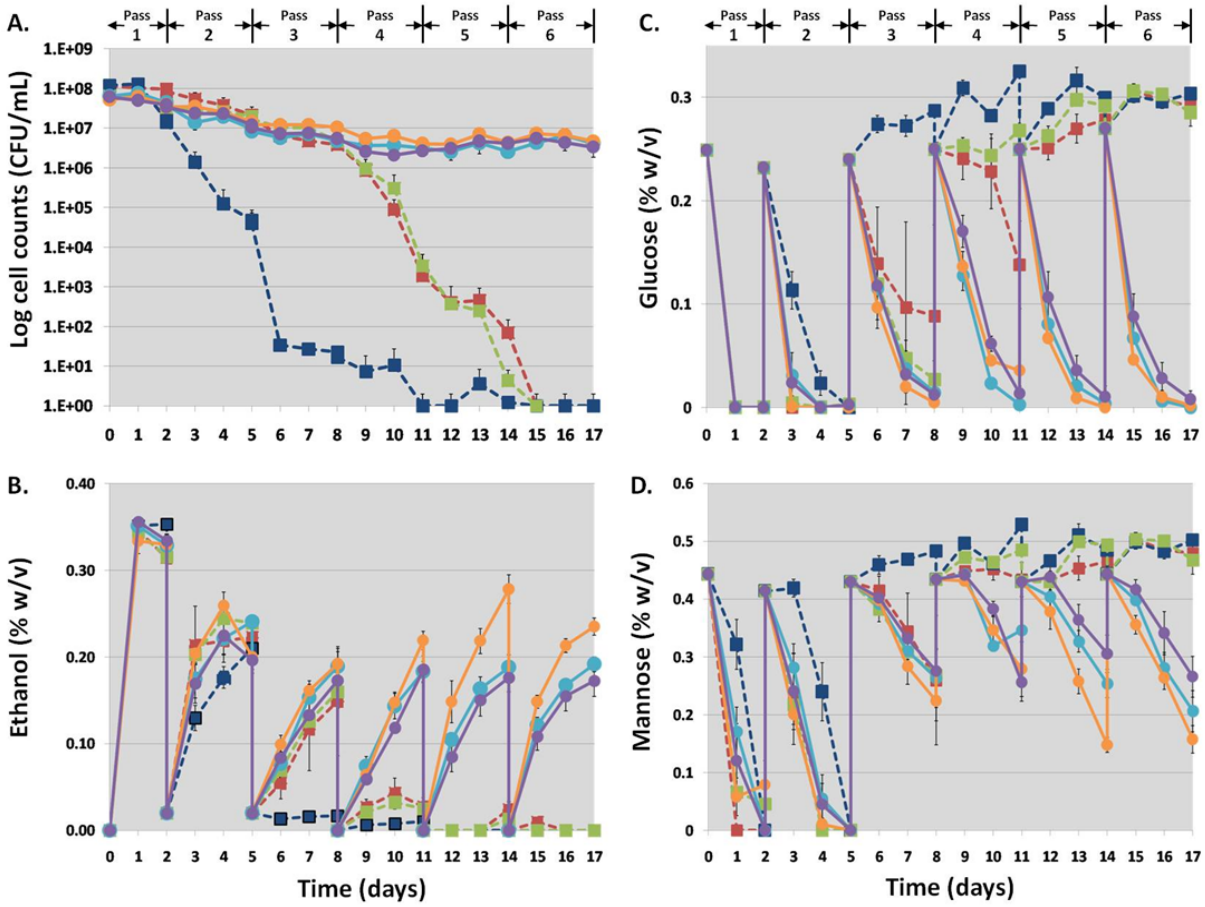

Figure 2-8. Survivability at high cell density (A), ethanol production (B), glucose (C) and mannose (D) consumption in undiluted liquid HWSSL by S. cerevisiae strains generated through GS. Symbols: R311 (●) from the third round of GS, R57 (●), and R511 (●) from the fifth round, the WT CEN.PK 113-1A (■) and 7D (■) haploids, and CEN.PK 122 (■) diploid. Strains were inoculated at high cell density into undiluted HWSSL in sealed shake flasks and ethanol production and sugar consumption were measured by GC. Survivability was monitored by daily plate counts. After 48, 120, 192, 264, 336 h each of the cultures was pelleted and re-suspended into fresh HWSSL (pass 1 - 6) and incubation continued.

and culture viability. Similarly to low cell density cultures (Fig 2-7), high cell density cultures revealed rapid cell death for WT strains, whereas mutant strains remained viable after repeated transfers in HWSSL. Mutant strains grown at low and high cell density cultures reached similar cell densities when at stationary phase. As exposure to HWSSL continued, all strains produced less ethanol after the first pass. For the WT strains, this may be largely due to an extensive population death (Fig. 2-8A). Liu *et al*. found that the SSL inhibitors 2-furaldehyde and HMF are reduced to furfuryl alcohol and furan-2,5-dimethanol (FDM), drawing away the co-factors NADH and NADPH, respectively (12, 171). This activity may, as a result, affect glycolysis and ethanol fermentation, but leads to a less toxic substrate, increasing population viability over time, which may explain reduced ethanol production by the mutant strains. Furthermore, reduced metabolic activity during exposure to HWSSL might be explained by changes to the environmental stress response (ESR). It has been demonstrated that a strain with a more active ESR would not only preserve cell viability when faced with, for example, high osmotic stress, but also leads to slower resource utilization (172).

By the third and fourth pass in HWSSL, all the WT strains succumbed to HWSSL toxicity, as shown by reduced population viability and negligible ethanol production and sugar consumption (Fig. 2-8). Cultures of the strains resulting from GS, R311, R57 and R511, however, were able to maintain their population viability, and ethanol productivity through 6 passes in HWSSL, with passes 2-6 yielding similar results using these strains. Strain R57 was the most productive, reaching approximately 80 and 65% (g ethanol/g

glucose and mannose) theoretical ethanol yield for passes 5 and 6, respectively. This finding suggests that these strains would be able to maintain ethanol productivity during prolonged exposure to SSL inhibitors in an industrial setting. Moreover, R57, when tested on HWSSL gradient agar plates, displayed higher tolerance than that of commonly used industrial fermentation strains (Fig. 2.9). Furthermore, the maintained level of ethanol production after multiple cell-recycle shake-flask fermentations suggests that the loss of productivity after prolonged exposure to HWSSL displayed by fermenter-adapted strains, like Tembec T1, has been overcome through GS-based evolutionary engineering (96).

2.3.5 Effect of single inhibitors on HWSSL tolerant strains

To assess if the HWSSL tolerant trait is concomitant with tolerance to multiple specific individual inhibitors found in HWSSL, strains R311, R57, and R511, the most HWSSL-tolerant strains identified in this study, were compared to the WT diploid CEN.PK 122, as the evolved strains were in the diploid state. These were compared on Petri plates each containing one of the inhibitors present in HWSSL (2-furaldehyde, *p*-hydroxybenzoic acid, HMF and acetic acid) as well as NaCl, sorbitol, hydrogen peroxide, ethanol, and ammonium sulfite to mimic osmotic stress, increased reactive oxygen species, high ethanol titers, and sulfite stress, respectively. Though not quantitative, these tests are able to illustrate qualitative differences between the evolved strains and the WT. Qualitative differences between phenotypes were deemed significant if divergence between the densities of the spotted cell concentrations were observable for two cell concentrations. Ethanol, 2-furaldehyde, *p*-hydroxybenzoic acid and ammonium sulfite

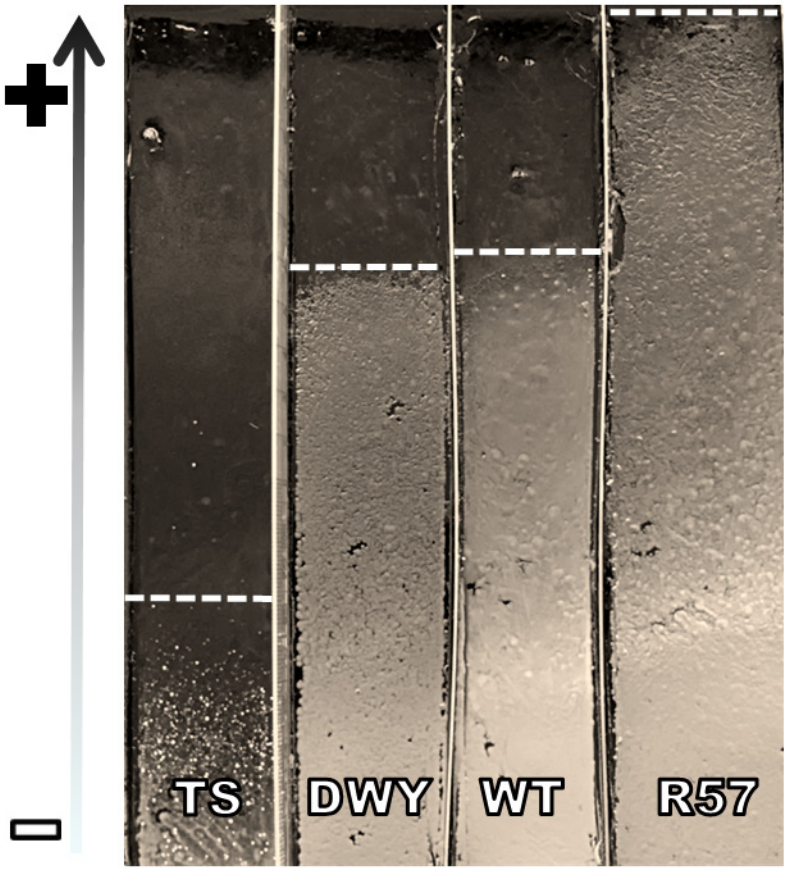

Figure 2-9. HWSSL gradient agar plate for comparison of robust strains. Genome-shuffling-generated HWSSL tolerant strain (R57) was compared to the wildtype parental CEN.PK 122 strain (WT), industrial fermentation strain Thermosacc (TS) and a dry wine yeast (DWY) currently used to ferment less inhibitory SSL, both obtained from Lallemand. The white dashed lines indicate the HWSSL concentration at which colony growth was arrested. The left arrow shows the increasing frontier of growth towards higher concentrations of HWSSL (~30-80 % HWSSL concentration).

revealed no noticeable difference between strains (data not shown). Pre-exposure to HWSSL or SD had no effect on the results of plating cells on single inhibitor plates, with the exception of cells grown on acetic acid (pH 3, 0.5% v/v and pH 5.5, 1% v/v) plates. All evolved strains showed a more tolerant phenotype on acetic acid dilution plates

compared to the WT when pre-grown on HWSSL (Fig. 2-10A, 2-10B). In contrast, all strains reacted similarly to acetic acid when pre-grown simply on minimal SD medium (data not shown). Strain R57 performed noticeably better than WT, R311, and R511 on NaCl at 3 and 7% (w/v) and sorbitol (2 M) (Fig. 2-10 D, E, F, respectively) under all pre-growth conditions. Strains R311 and R511 showed reduced tolerance to hydrogen peroxide, as shown on 1 mM H_2O_2 plates (Fig. 2-10F), while R57 exhibited greater tolerance. Overall, these data support the hypothesis that the HWSSL tolerance trait translates into simultaneous tolerance to multiple single sources of inhibition known to be present in the substrate, including acetic acid, osmotic pressure, HMF, and oxidative stress.

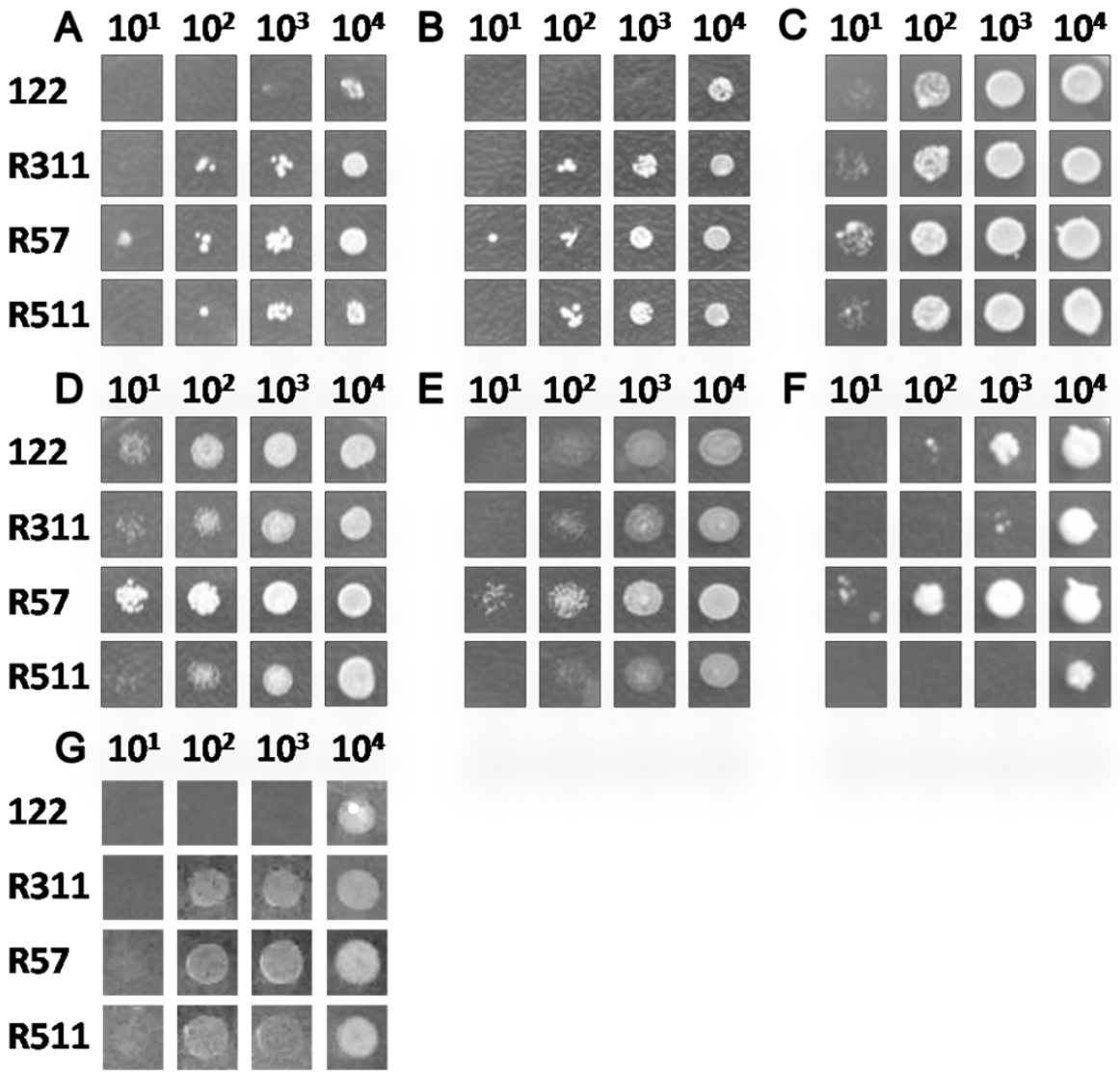

Figure 2-10. Yeast dilution plates with single inhibitors. All images show a dilution of viable yeast cells from left to right at cell counts of 10^1, 10^2, 10^3, and 10^4 cells, respectively. The strains used for comparison from top to bottom are CEN.PK 122 diploid WT, R311, R57, and R511, respectively. These images represent yeast dilutions from cultures pre-exposed to HWSSL. Panels show the results of plating on (A) 1% (w/v) acetic acid pH 5.5, (B) 0.5% (w/v) acetic acid pH 3, (C) 0.5% (w/v) HMF, (D) 3% (w/v) NaCl, (E) 7% (w/v) NaCl, (F) 1 mM H_2O_2 and (G) 2 M sorbitol.

2.4 Discussion

2.4.1 Meiotic recombination-mediated GS of *S. cerevisiae* can be used to accumulate beneficial mutations

A meiotic recombination-based GS methodology was successfully developed for *S. cerevisiae*. The methodology was tested using triauxotrophic parental strains of each mating type and it was demonstrated that WT alleles, which were counterparts to the auxotrophic markers and also present within the parental population, could be brought together into a single strain to attain completely prototrophic strains. If the WT alleles are treated as beneficial mutations, complete prototrophy is representative of the accumulation of four beneficial mutations within a single strain. Theoretically, it was hypothesized that because the alleles corresponding to auxotrophy, or lack thereof, were on different chromosomes, after two rounds of reiterative mating two WT alleles could be brought together during the first mating event and four during the second, a product of mating doubly auxotrophic strains. This was shown to be the case. Furthermore, no form of population enrichment or selection for decreased auxotrophy was used between rounds of GS, which could have led to more accelerated combination of the surrogate beneficial mutations. The findings in the reduced auxotrophy assessment did not adhere strictly to Mendelian genetic predictions. This was likely due to the different growth rates of strains bearing differing auxotrophies. Because growth occurred during germination and mating, strict Mendelian statistics no longer applied. However, if one extrapolates the findings of the mating for loss of auxotrophy experiment, with a large and diverse enough population or by enriching the mating population between rounds, beneficial mutations can be accumulated indefinitely at an exponential rate as rounds of reiterative mating

progress. If one contrasts this with classical strain improvement, which is sequentially subjecting a single strain to mutation for iterative improvement, as GS progresses it should greatly outpace the beneficial mutation accumulation possible in classical mutation-based strain development and generate a heterogeneous population of mutation combination. This methodology may serve as an efficient protocol to mediate population-wise mating with *S. cerevisiae.*

2.4.2 UV mutagenesis can be used to generate populations of mutants

UV mutagenesis was used in this study to cause mutation, with *S. cerevisiae* strains being exposed to UV dosages that led to a ~50 % death rate. It was hypothesized that this death rate would lead to a low amount of mutations per genome, in order to minimize the chance that other deleterious mutations would mask beneficial ones. It should be noted that other forms of mutagenesis have been applied to generate mutant pools for GS, such as chemical mutagenesis with ethyl methane sulfate (EMS) (173). The choice of mutagen will affect the types of mutations that can occur, though most GS reports have used mutagens that generate point mutations, such as with UV irradiation and EMS exposure. The mutagenesis step can also be carried out on haploid or diploid strains (104), or on protoplasts in the case of protoplast fusion-based GS (103). One *S. cerevisiae* GS project has reported starting with diploid strains and using a high dosage of EMS (leading to a ~90% death rate) to introduce mutation into the population (104). The rationale cited for using diploids as the initial population is that when using a higher dosage of mutagen, beneficial mutations might accompany detrimental ones, which could mask any favorable effects. These deadly mutations will be more likely accommodated by a strain if a second copy of the WT genome is present. In this study I chose to expose

haploids of each mating type to UV mutagenesis to generate initial mutant pools. This measure was taken in order to ensure that if a recessive beneficial mutation is generated it will not be masked by the presence of a WT allele. Transversely, if a diploid is used for the parental mutant population it would be more difficult to generate recessive beneficial mutations that would be selected through screening diploid mutant populations. In this case, the diploid parental mutant population would have to be sporulated in order to screen the haploid generation and obtain strains bearing recessive beneficial mutations. Furthermore, here a lower dosage of mutagen was used in order to minimize the chances of generating deleterious mutations that would accompany the beneficial ones. Since most mutations will either be deleterious or have no phenotypic effect, it remains to be shown whether a high rate of mutation, introducing more than one mutation into a parental strain at once, is of benefit.

2.4.3 Enrichment between rounds of GS can accelerate evolution of HWSSL tolerance

It was shown that if the shuffled populations are enriched for tolerant sub-populations between rounds, prior to the subsequent round of population mating, a more inhibitor-tolerant phenotype could be obtained with fewer rounds of GS. Specifically, 2 rounds of GS with enrichment between rounds led to populations that were more tolerant to HWSSL than 4 rounds of shuffling without enrichment. It is hypothesized that by limiting the amount of strains displaying WT-level tolerance to HWSSL, the chances of combining the genomes of strains harbouring beneficial mutations could be enhanced. This finding bolsters the theory that the utility of GS technology arises from the ability to bring together beneficial mutations and suggests that there exists a medium between GS

evolution with too few strains to adequately sample the combinatorial space of beneficial mutations and a large, dilute mutant pool that does not allow for accumulation of complementary mutations.

2.4.4 Meiotic recombination-based GS can be used to engineer HWSSL tolerant populations of yeasts

Shortly after the GS methodology described in this study was developed, a similar study was performed to produce *Scheffersomyces stipitis* strains that exhibited improved tolerance to HWSSL (106). At the onset of both studies, the WT strains would die off readily upon exposure to undiluted HWSSL. The tolerance of the WT *S. cerevisiae* and *S. stipitis* starting strains to HWSSL was assessed at approximately 60% (v/v) HWSSL diluted with water. Mutants of *S. cerevisiae* grew to approximately 70 % (v/v) HWSSL, and members of the final *S. stipitis* mutant population were able to grow at 75 % (v/v), though they underwent 3 rounds of sequential UV mutagenesis as opposed to 1 round for *S. cerevisiae* in this study (106). After 5 rounds of GS and selection it was found that a small number of *S. cerevisiae* genome shuffled strains could grow and ferment undiluted HWSSL, while *S. stipitis* genome shuffled strains could grow in 85 % (v/v) HWSSL. The *S. stipitis* study was able to produce a strain that could produce ethanol from HWSSL glucose alone to levels between 0.15 and 0.18 % (w/v) for a single 48 hour period in undiluted HWSSL, while the WT control was unable to ferment any of the sugars in HWSSL (106). These results, along with those of the current study show that using a surrogate screen of growth and viability on increased concentrations of inhibitory substrate is an appropriate screen for GS projects that aim to produce higher ethanol titres in the presence of lignocellulosic hydrolysate inhibitors.

There were important differences in how this study and the *S. stipitis* study were performed. A brief comparison can be seen in Table 2-1. One major difference was the size of the initial UV mutant population. The *S. stipitis* study used only six to eight individual colonies for meiotic recombination for each round of shuffling, while the current study used the entire population that displayed more tolerance to the WT, though the extent of the population diversity was not assessed. The tolerance to HWSSL displayed by *S. cerevisiae* grew from approximately 70 % (v/v) to 100 % (v/v) from UV mutant populations to round 5 of GS. The tolerance of *S. stipitis* increased from approximately 75 % (v/v) to 85 % (v/v) from UV mutant populations to round 3 of GS. Notably, 2 additional rounds of GS did not lead to a significant increase in tolerance in *S. stipitis*, while the evolution of *S. cerevisiae* progressed throughout all 5 rounds. This observation may stem from the fact that larger, more diverse populations were used for GS of *S. cerevisiae*, increasing the chance of bringing together synergistic mutations. Inversely, the smaller sample of tolerant individual strains used in the GS of *S. stipitis* may have exhausted the number of mutations existing in the initial mutant pool that were available for recombination, or minimized the possibility of combining rarer, synergistically beneficial mutations. Alternatively, it is possible that *S. cerevisiae* is naturally more genetically predisposed to inhibitor tolerance. Finally, the poor mating efficiency of *S. stipitis* (Table 2-1), as shown through a mating for loss of auxotrophy assessment, may have played a role in the stagnation of population evolution.

Though the tolerance attained by *S. cerevisiae* outpaced that attained by *S. stipitis* under the conditions described, it is important to note that *S. stipitis* has the added advantage of being able to utilize pentose sugars found in HWSSL (95). However, in

Table 2-1. Comparison of GS in *S. cerevisiae* and *S. stipitis* for HWSSL tolerance

Organism	*S. stipitis*	*S. cerevisiae*
Mating efficiency	0.05 %	<35 %
Possible size of mutant mating pools	6-8 individual colonies	10^7 individual colonies
Level of HWSSL concentration tolerated after GS	85 % v/v	100 %
Rounds of GS that led to increased tolerance	3	5
Increased ethanol production from HWSSL	Yes	Yes
Displayed cross-tolerance to multiple individual inhibitors	Yes	Yes

undiluted HWSSL the most tolerant *S. stipitis* strains isolated in the Bajwa *et al*. study were unable to use the xylose present (174). Ultimately, the adverse effects of HWSSL toxicity on pentose fermentation with *S. stipitis* may prove to be a formidable barrier to overcome. However, further GS with more diverse populations could perhaps diverse populations could perhaps yield *S. stipitis* strains that can tolerate undiluted HWSSL and still make use of the pentose sugars found therein. Furthermore, the low recombination efficiency of *S. stipits* (Table 2-1) suggests that future GS projects involving *S. stipitis* might benefit from protoplast-fusion-based GS in order to accelerate strain evolution. To make full use of the HWSSL substrate, the ability to ferment pentose sugars would have to be engineered into *S. cerevisiae* for xylose utilization in particular, which has been

shown to be a viable option (91). The tolerant strains produced in this study could act as background strains for rationally engineering a pentose-fermenting, HWSSL-tolerant *S. cerevisiae* strain, and further genome shuffled for strain optimization. In this way, rational strain engineering and GS may be complementary technologies for evolving complex phenotypes.

2.4.5 GS-evolved HWSSL tolerant strains display cross-tolerance to individual sources of inhibition

Many of the sources of inhibition present in HWSSL that have been accounted for are found in other lignocellulosic hydrolysates (175) and are therefore highly relevant to the biomass-to-biofuel industry. It was hypothesized at the outset of this study that in order to engineer a strain for tolerance to a complex substrate with multiple sources of inhibition, one would need to simultaneously address tolerance to multiple inhibitory compounds. The other side of this hypothesis is that if one were to randomly evolve a strain for tolerance to a substrate with multiple sources of inhibition, it should display cross-tolerance traits to some of the known sources of inhibition within that substrate. R57 is the most productive, viable strain identified in this study on HWSSL and displays a simultaneous increase in tolerance to salt or osmotic stress, acetic acid, peroxide and, marginally, to HMF. Strains R311 and R511 showed only increased tolerance to acetic acid, but to a lesser extent than R57. Similarly, *S. stipitis* GS-evolved for HWSSL tolerance show increased tolerance to the individual inhibitors acetic acid, furfural, and HMF (106). These findings suggest that tolerance to multiple sources of HWSSL inhibition may be related to overall ethanol productivity and viability in HWSSL and bolsters the hypothesis that the GS methodology we have employed can bring together

many diverse mutations into a single strain, produce multi-faceted phenotypes and address complex strain engineering requirements.

The pronounced tolerance of R311, R57, and R511 to acetic acid suggests a particularly important role for this inhibitor. These strains displayed increased acetic acid tolerance only after HWSSL pre-exposure. The reason for the different response to acetic acid due to pre-growth on SD or HWSSL is not known, but it is hypothesized that exposure to HWSSL elicits a tolerance response in the mutant strains. It was recently shown that evolutionarily engineered strains of *S. cerevisiae*, adapted to increased acetic acid concentrations, demonstrated strongly inducible rather than constitutive acetic acid tolerance (176). It was hypothesized that this might arise because acetic acid occurs in the natural *S. cerevisiae* environment and the native inducible acetic acid tolerance mechanisms, like the acetate-induced *HAA1* regulon, may be affected (38, 177). Additionally, tolerance to osmotic stress or high salt content, shown by R57, is expected to be beneficial to HWSSL tolerance since the amount of osmotic stress exerted by forms of SSL has been approximated to be as high as 200 g/L NaCl (26). High osmotic stress and acid effects may be related because high osmolarity can lead to a loss of water by the cell, increasing solute concentrations and lowering pH (178). The hydrogen peroxide tolerance of R57 is likely a beneficial trait due to an overall increase in intracellular ROS caused by SSL toxicity (7). The above findings also demonstrate the heterogeneity that can exist phenotypically within a GS-evolved population, most easily shown by the increase in peroxide tolerance shown by R57 and apparent decrease by R311 and R511. This suggests that within a given population the ways that a single strain can arrive at a phenotype of interest are by multiple paths, in turn suggesting that the strains will

harbour differing mutations and/or combinations thereof. Overall, cross-tolerance to HWSSL and these individual inhibitors validates the impetus placed on these inhibitors in current inhibition-related studies, which tend to examine the effects of single inhibitors as surrogate methods for studying the effects of inhibitory lignocellulosic substrates.

2.5 Conclusions

Meiosis-mediated GS of *S. cerevisiae* is a viable technology for engineering complex phenotypes. As demonstrated through the methodology developed in the loss of auxotrophy experiment described above, it is possible to combine separate genetic elements through poolwise reiterative mating to attain single strains with desirable accumulated genes. When random mutagenesis is applied to create pools of mutants with enhanced traits of interest, it is possible to use this methodology to evolve populations and individual strains to increase the specified trait to the desired point, in this case tolerance to undiluted HWSSL. As a counterpart to GS technologies based on protoplast fusion in bacteria, or spheroplast fusion in yeast, described in Chapter 1, these findings support the use of meiotic-recombination based GS technology in yeast strain engineering as an efficient means to evolve complex traits. This is especially true when a high-throughput screen is available and is particularly applicable to enhanced microbial tolerance to toxic substrates, where screening of large populations for growth can be applied.

This portion of the study demonstrates the utility of using GS technology to develop strains that are tolerant of lignocellulosic substrate inhibitors. As research and interest into biofuels progress, such methods may become commonplace for developing strains that are fine-tuned to fermenting specific substrates, or creating organisms that

display traits of cross-tolerance to specific inhibitors or a multitude of similar lignocellulosic substrates.

One traditional drawback of evolutionary engineering, such as GS, is that the exact genetic changes that accumulated in the evolution of a strain are difficult to ascertain. As high-throughput '-omics' technologies become more common and accessible and the price of DNA sequencing continues to diminish, the genetic changes that accompany the traits which are evolved in random strain development can be accessed in order to understand complex trait evolution and inform more rational approaches to strain design. By comparing the genomes of parental strains with final mutant strains at single nucleotide resolution, it is possible to identify the mutations that have taken place, the genes that have been targeted by mutation and selection, and subsequently, important genetic factors involved in a phenotype of interest. Therefore, to make the HWSSL tolerant phenotype to genotype connection, strain R57 was selected for further study due to its high level of tolerance, ethanol productivity on HWSSL and demonstrated co-tolerance to individual sources of inhibition. Whole-genome sequencing of strain R57 will be the subject of Chapter 2.

Chapter 3

3.1 Introduction

The principal behind GS is that complex phenotypic traits are difficult and time-consuming to generate by traditional strain improvement technologies (discussed more fully in Chapters 1 and 2). Furthermore, rational genetic engineering of productive, lignocellulosic hydrolysate inhibitor-resistant strains suffers from a lack of knowledge as to the precise genetic factors involved in tolerance (60, 97). This chapter describes the discovery and analysis of mutations that were accumulated in GS-engineered strain R57, the most productive and HWSSL-tolerant strain derived from the first part of this study described in Chapter 2. Full genome sequencing and comparison of R57 and the reference WT genomes allowed for differences arising in the genome of the GS engineered HWSSL-tolerant strain to be discovered. Analysis with current bioinformatics resources and comparison to known modes of lignocellulosic hydrolysate inhibitor tolerance are used to generate plausible targets for future strain development studies.

3.2 Materials and Methods

3.2.1 Genome sequencing of WT and GS-evolved R57 strains

Genomic DNA of WT haploid CEN.PK 113-7D and the CEN.PK-derived R57 diploid yeast strains were isolated from overnight cultures grown in YPD using the DNeasy blood and tissue kit (Qiagen, Toronto, Ontario, Canada). DNA samples were prepared and sequenced at the Michael Smith Genome Sciences Centre using the Illumina 1G Genome Analyzer according to manufacturer's specifications. Briefly, 3 µg

of DNA was sheared by sonication for a total of 50 minutes using a Bioruptor UCD-200 and separated on an 8 % (w/v) polyacrylamide gel. A DNA fraction of 350-450 bp was excised and eluted from the gel slice overnight at 4°C in 300 µl of elution buffer (5:1, LoTE buffer (3 mM Tris-HCl, pH 7.5, 0.2 mM EDTA)-7.5 M ammonium acetate), and was purified using a Spin-X Filter Tube (Fisher Scientific) and ethanol precipitation. Fragments were end-repaired with 1 unit of T4 DNA polymerase for 30 minutes at 20 ˚C. A single deoxyadenine nucleotide was added to the DNA fragment ends using 1 unit of Klenow fragment and deoxyadenosine-5'-triphosphate (dATP) incubated for 30 minutes at 20 ˚C and ligated to Illumina adapters. The adapter-ligated products were purified on Qiaquick spin columns (Qiagen) and PCR-amplified with Phusion DNA Polymerase in 10 cycles using Illumina's primer set. PCR products of ~200 bp were purified by polyacrylamide gel electrophoresis using an 8% (w/v) gel. The DNA quality was assessed and quantified using an Agilent DNA 1000 series II assay and Nanodrop 7500 spectrophotometer (Nanodrop, USA) followed by its dilution to 10 nM concentration. The final concentration was double checked and determined by Quant-iT dsDNA HS Assay Kit using Qubit fluorometer (Invitrogen). The amplified library was loaded onto the cluster generation station for single molecule bridge amplification on slides containing attached primers. The slide with amplified clusters was then subjected to step-wise sequencing using four-color labeled nucleotides on the Illumina 1G sequencing system for 50 cycles. Two lanes were sequenced for the WT strain and four for strain R57.

3.2.2 Sequencing alignment and mutation calling

Sequencing reads were aligned to the WT CEN.PK reference genome obtained from Nijkamp *et al*. (127) and cross-referenced with read alignments obtained in our laboratory using our WT CEN.PK consensus sequence that was created using the S288c genome sequence as an alignment backbone. Alignments were performed both with Bowtie using standard parameters (179) and CLC Genomics Workbench version 5.1 with default parameters and ignoring non-specific matches. SNP and insertion-deletion (indel) calling were both performed with Maq version 0.7.1 (119) and CLC Genomics Workbench for verification and visualization. In order to eliminate false positives from mutation calling, the DNA sequencing reads obtained from WT were subjected to the same variation calling protocol as strain R57. Variations that were called when CEN.PK-7D Illumina reads were aligned onto the CEN.PK-7D consensus genome sequence, and those that corresponded to variations called for R57 reads aligned onto the CEN.PK-7D consensus sequence were discarded as false positives. These false positives derive from sequence-specific miscall errors that are known to arise when using the Illumina platform (180) or due to alignments in non-specific regions of the genome or to areas of low complexity (181). Coverage requirements for SNP calling for WT reads was also lowered to $\leq$ 5-fold in order to ensure that SNPs that may result due to misalignment could be easily identified. These miscalls were edited out of the final mutation list by manual inspection. Maq SNP analysis was performed using the cns2snp command and SNPs were called if the region upon which they were mapped returned a genome copy score = 1 and carried a phred-like quality score $\geq$ 40. SNP analysis was corroborated with CLC Genomics workbench SNP Detection function with a quality score of $\geq$ 40 for the central

base and ≥ 30 for the surrounding bases. The threshold for variation at a specific base in the genome needed for SNP calling was lowered to ≥ 10% of reads yielding an aberrant base call for the CEN.PK-7D read alignment from ≥ 35% for R57 SNP calling in order to maintain stringency on positive variation calling. Therefore, if an SNP was called for more than 35% of the reads in R57, but was also called for 10% or more of the reads for the WT control it was discarded as a false SNP call. Indel analysis was also performed with Maq using the Indelpe command and verified with CLC Genomics Workbench, both under standard parameters and compared to WT reads for control, as described above. Copy number variation was assessed using CNV-seq (126) to compare WT to R57 reads with a log2 threshold of 0.75, below the level used to detect reliable CNVs in CEN.PK (127). The mutations identified were verified by Sanger sequencing and compared to the other Mat parental WT, CEN.PK 113-1A, to ensure the mutations were not present in either of the WT parental haploid strains. Locations of mutations were assessed using the CEN.PK consensus sequence as a guide Mutations in ORFs were examined by translating DNA sequences into their corresponding protein sequences using ExPASy translate (182) and performing a BLAST comparison using the BLAST2Seq software program hosted by NCBI.

3.2.3 Protein impact assessment of ORF-located mutations

Mutational impact assessment was done with the SIFT (Sorting Intolerant From Tolerant) program (183-187) using recommended best practices (184). Briefly, homologous proteins of appropriate homology (< 90 % identity) were chosen for comparison of the degree of conservation of the amino acid position in question for up to

100 homologous proteins. Amino acid substitutions were predicted as damaging if the SIFT score was <= 0.05, and tolerated if the score is > 0.05.

3.2.4 Interaction assessment of discovered mutations

Functional interaction was carried out on the 16 non-ambiguous genes affected by mutations through analysis with the BiNGO version 2.44 (188) software plugin for the Cytoscape 2.8 network analysis software program (189-191). Mutant genes were annotated with the complete BiNGO Gene Ontology (GO) file to visualize the full range of known functional relationships between the genes of interest (Fig. 3-1) or the GOSlim yeast annotation file for broader visualization of affected functional categories. Protein-protein, genetic, co-expression, co-localization, predicted functional relationship, and shared protein domain interactions between products of the genes affected by mutation were explored using the GeneMANIA version 3.2 (192, 193) software plugin for the Cytoscape 2.8 (189-191). The 20 most related genes as determined by GeneMANIA were included within the interaction network to explore non-direct interrelationships. Weighting for the GeneMANIA generated interaction map (Fig. 3-2) was based on GO molecular functional relationships, while evidence scoring was based on assigned relevance of the sources used to generate interactivity by the software. All annotations of genes are based on the *Saccharomyces* Genome Database (SGD) unless otherwise referenced.

3.3 Results

3.3.1 Whole-genome sequencing of GS evolved strain R57 reveals SNP mutations

Complete genome sequencing was carried out on the CEN.PK-derived, HWSSL-tolerant, GS-engineered R57 *S. cerevisiae* strain in order to elucidate the genetic changes that are associated with tolerance to HWSSL. Both the parental haploid CEN.PK 113-7D and mutant diploid R57 were sequenced and compared at ~100-fold and ~350-fold coverage per nucleotide (Table 3-1, 3-2), respectively, in order to discover what changes had been exacted through GS evolution. This depth of coverage was more than sufficient to allow for meaningful mutation prediction (107). The relative levels of sequence read coverage per chromosome between the strains is similar and indicates the absence of aneuploidy (Table 3-2). Indel and CNV analysis returned no detectable differences between the WT and R57 after visual inspection (data not shown). All of the mutations returned from the mutation analysis were single nucleotide

Table 3-1. Summary mapping report for strain R57 and the WT aligned on the WT backbone sequence.

	R57 read mapping		WT read mapping	
	Read count	**Total bases**	**Read count**	**Total bases**
Total reads	1.07E+08	5.33E+09	3.33E+07	1.67E+09
Matched	8.68E+07	4.34E+09	2.64E+07	1.32E+09
Not matched	1.98E+07	9.89E+08	6.87E+06	3.43E+08

Table 3-2. Mapping report per chromosome for strain R57 and the WT aligned on the WT backbone sequence

Chromosome mapped	Consensus length	Total read count	Average coverage R57	Total read count	Average coverage WT
0	5.51E+04	1.30E+07	9.99E+03	6.08E+06	4.58E+03
1	1.78E+05	1.23E+06	2.75E+02	4.11E+05	9.18E+01
2	7.81E+05	5.76E+06	3.56E+02	1.58E+06	9.75E+01
3	2.90E+05	2.06E+06	3.34E+02	6.12E+05	9.93E+01
4	1.42E+06	1.00E+07	3.44E+02	2.69E+06	9.00E+01
5	4.15E+05	3.04E+06	3.58E+02	8.89E+05	1.05E+02
6	2.38E+05	1.79E+06	3.61E+02	5.37E+05	1.08E+02
7	1.05E+06	7.95E+06	3.66E+02	2.13E+06	9.79E+01
8	2.69E+05	1.91E+06	3.43E+02	5.37E+05	9.64E+01
9	2.79E+05	1.96E+06	3.20E+02	5.63E+05	9.17E+01
10	6.90E+05	5.08E+06	3.48E+02	1.38E+06	9.43E+01
11	2.53E+05	1.80E+06	3.53E+02	4.89E+05	9.57E+01
12	4.78E+05	4.08E+06	3.89E+02	1.22E+06	1.17E+02
13	8.98E+05	6.53E+06	3.51E+02	1.76E+06	9.47E+01
14	7.34E+05	5.38E+06	3.45E+02	1.49E+06	9.54E+01
15	1.05E+06	7.64E+06	3.52E+02	2.05E+06	9.40E+01
16	8.94E+05	7.10E+06	3.74E+02	2.02E+06	1.06E+02
Average coverage			3.48E+02		9.84E+01

polymorphisms (SNPs). Using the SNP detection software alone yielded hundreds of SNP mutations, however sequencing of the WT for comparison revealed that many of the SNPs discovered were false positives that arose from sequencing specific errors or from mapping highly redundant and non-complex regions of the genome. The initial mutation analysis was performed on my own assembly of the CEN.PK 113-7D genome sequence, assembled by mapping 36-bp trimmed Illumina reads on the S288c reference genome as a backbone and mutations were verified by Sanger sequencing. Subsequently, when the CEN.PK 113-7D genome project sequence was made available (GenBank BioProject PRJNA52955), consisting of the *de novo* assembly and scaffolding of both 454 and

Illumina sequencing reads, the mutation analysis was performed using this version of the genome as a backbone upon which to align R57 sequence reads. It is noteworthy that this analysis yielded the same mutation calls as the original mutation assessment, signifying that useful mutation information can be derived from scaffolding of short sequence reads to a WT consensus sequence built upon a relatively closely related reference genome, without the added costs of longer DNA reads for a more reliable genome assembly. However, some false positives were eliminated by Sanger sequencing that were not called using the more complete CEN.PK genome scaffold. For example, there is a 20 bp duplication directly upstream of *IGD1* in CEN.PK (127) that is not apparent when Illumina reads are aligned on an S288c background for consensus generation, which led to a false SNP call. Using a highly reliable mapping scaffold genome sequence, comparing R57 mutation calls to the variation calls in the WT and filtering by visual inspection yielded true mutation calls as verified by Sanger sequencing.

3.3.2 R57 mutations mainly affect ORFs

Twenty SNP mutations were found to affect 16 genes. These included 16 SNPs affecting 12 ORFs, 14 of which led to missense mutations with the remaining 2 leading to silent mutations (Table 3-3). The 4 mutations not found within ORFs were discovered within close proximity of known ORFs, 2 within 50 bps 3' of an ORF and 2 within 200 bps 5' of an ORF. The non-ORF mutations are all located in 5' or 3' untranslated regions (UTRs) (194, 195). An ambiguous heterogeneous mutation lies 43 bps 3' of *BCS1*, required for complex III assembly of the electron transport chain (ETC), but is not found in the 3' UTR (194). This mutation is predicted to be part of the 5' UTR of *YDR374C* (195), a utative protein of unknown function, and in the 3' UTR of *WIP1*, a kinetochore

Table 3-3. SNP mutations discovered in HWSSL tolerant strain R57**Affected gene**	**Affected region**	**AA change**	**Affected gene function**	**Genotype**	**Sift score**
YAL005C/*SSA1*	ORF	Q31K of 642	ATP-ase, protein folding, heat shock, HSP70	Hetero	0
YDR043C/*NRG1*	ORF	P46Q of 231	Transcriptional repressor: glucose repression, stress tolerance	Homo	0
YDR103W/*STE5*	ORF	S171F of 917	Pheromone-response scaffold protein, forms MAPK cascade complex	Hetero	0
YDR103W/*STE5*	ORF	Silent		Hetero	-
YDR127W/*ARO1*	ORF	S428F of 1589	Catalyzes steps 2-6 in the biosynthesis of chorismate leading to aromatic amino acid synthesis	Hetero	0
YDR127W/*ARO1*	ORF	Silent		Hetero	-
YDR141C/*DOP1*	ORF	N14Y of 1698	Endosome to Golgi transport, ER organization, establishing cell polarity and morphogenesis	Hetero	0.05
YGR068C/*ART5*	ORF	L152I of 586	Regulates the endocytosis and turnover of cell-surface proteins by targeted ubiquitination	Hetero	0.17
YGR178C/*PBP1*	190 bp 5' (UTR)	-	Controlling mRNA poly(A), stress granule formation and translation control	Hetero	-
YGR289C/*MAL11*	ORF	P104S of 616	General alpha-glucoside symporter, with high affinity for trehalose	Hetero	0
YGR289C/*MAL11*	ORF	M161K of 616		Hetero	0.02
YIL156W/*UBP7*	ORF	N822K of 1071	Ubiquitin-specific protease	Homo	0.33
YJL101C/*GSH1*	72 bp 5' (UTR)	-	glutamylcysteine synthetase, glutathione biosynthesis, redox homeostasis	Hetero	-
YKR010C/*TOF2*	ORF	S714L of 771	Required for rDNA silencing and stimulates Cdc14p for mitotic rDNA separation	Hetero	0.27
YNL058C	ORF	K3E of 316	Unknown	Hetero	0.42
YOR073W/*SGO1*	ORF	S192Y of 590	Chromosomal segregation and stability	Hetero	0.03
YOR310C/*NOP58*	25 bp 3' (UTR)	-	Pre-rRNA processing and rRNA synthesis	Hetero	-
YOR375C/*GDH1*	ORF	S16F of 454	Glutamate synthesis from ammonia	Hetero	0
YOR375C/*GDH1*	ORF	F23C of 454		Hetero	0
YOR383C/*FIT3*	42 bp 3'	-	Iron transport	Hetero	-

(UTR)

localized protein of unknown function (194), and is not included in Table 3-3 due to the ambiguity of the affected gene. This mutation's close proximity to 3 genes may have pleiotropic effects, but the relationship to HWSSL tolerance and this particular mutation, if one exists, is difficult to reconcile with what is known of these three genes.

3.3.3 ORF mutations in R57 are predicted to lead to a phenotype

Phenotypic prediction of altered primary protein structure was carried out using the SIFT algorithm (183, 184, 186) (Table 3-3). Using this prediction software, 10 of the 14 missense mutations are expected to lead to a phenotype, with 4 predicted to be tolerated by the protein in question. All but two of the mutations are heterozygous (Table 3-3) and therefore are expected to have a dominant effect if they contribute to the R57 phenotype. The two homozygous mutations are located within *NRG1* and *UBP7*. Homozygous mutations suggest that they have been enriched for through HWSSL screening at a high enough population density that they were

able to mate with the opposite mating type during GS evolution and may therefore be important to the HWSSL-tolerance trait. Alternatively, if asci were not fully disrupted during the spore separation step of GS, there is a higher likelihood that homozygous diploid mutations might occur through mating events between haploid sister cells of opposite mating type despite visual screening for separated spores in the final population (Chapter 2). For the transcription factor Nrg1p, the P46Q mutation is predicted to not be tolerated with a SIFT score of 0.00. In fact, of the 42 homologous proteins selected by the SIFT-BLink algorithm for tolerance prediction that are represented by an amino acid at position 46 (i.e. are not gapped or missing this segment of the Nrg1p consensus

protein) a proline is 100% conserved, suggesting it is correlated with overall gene function and that substitution here will result in a profound phenotypic effect. *UBP7* bears an N822K mutation that is tolerated by SIFT prediction and therefore likely has a less profound effect on Ubp7p function. Of other particular note in the mutation analysis are genes that bear more than one mutation, which suggests that the affected gene is of particular importance to HWSSL tolerance, as they are likely present due to a phenotypic effect that has been selected by screening mutant strains for increased tolerance on HWSSL. However, 2 genes (*STE5* and *ARO1*) carry one missense mutation along with a silent mutation. It is possible the silent mutations are non-random and may lead to a phenotypic effect, for example through preferred codon usage (196) or altered transcript stability (197), or these mutations may be present simply due to genetic linkage to the productive missense mutation. This is especially plausible in the case of the *ARO1* gene, which contains 2 directly adjacent mutations at nucleotides 1293-4, yielding a CC to TT mutation of the ORF (5'-3'). The mutation is located on the same allele in R57, as shown by pileup viewing of R57 Illumina DNA sequence reads, leading to one missense mutation, S428F, that is strongly predicted as having a phenotypic effect (Table 3-3). Only the mutation at nucleotide 1293 leads to an amino acid change, while both mutations are likely the result of one mutation event, at the C-C pyrimidine dimer, a site where C-T transitions are more likely (198).

Conversely, multiple mutations that affect both WT alleles should not have been enriched due to genetic linkage and may therefore have an even greater effect on phenotype. Two missense mutations affect both *GDH1* and *MAL11*. Gdh1p bears 2 mutations in R57, S16F and F23C. Visual inspection of the pileup of read alignments

performed using CLC Genomics Workbench confirms that the two mutations are consistently located on differing reads that span the two loci, which shows they comprise 2 alleles, and no DNA sequencing reads spanning this portion of the gene contain the WT allelic sequence. The close proximity of these two mutations suggests a targeted region of *GDH1* that bears further investigation. The R57 *MAL11* gene contains two missense mutations (leading to P104S and M161K mutations of Mal11p) that, due to their proximity from each other, cannot be prescribed to one or two alleles by Illumina sequencing. However, preliminary cloning experiments of the mutant gene from R57 followed by Sanger sequencing of plasmids bearing the R57 *MAL11*, shows that the two mutations are not located on the same allele (data not shown).

3.3.4 Genes bearing mutations accumulated in strain R57 are related to a broad spectrum of biological processes

In order to examine any common functions that exist among the mutated genes accumulated in R57, interaction networks were generated using the 16 genes affected by non-ambiguous mutations. The small dataset does not allow for meaningful functional enrichment analysis, but it does allow for a topography of affected biological functions to be generated and known interactions to be identified. The first network was generated based on known biological processes associated with the mutated genes (Fig. 3-1) and the second based on physical, genetic and co-expression interactions generated from current knowledge of *S. cerevisiae* (Fig. 3-2). Using known GO categories, functionally-associated biological processes, an intricate interaction network was built between the genes affected by mutation (Fig. 3-1) consisting of 408 discreet biological processes; the main biological processes affected by mutation were summarized using the GOSlim yeast

functional categories, which yields 27 broader functional categories (Fig. 3-1). Although the possible phenotypic effects of any one mutated gene cannot be discounted at this point, the functional categories that represent several mutated genes suggest possible rational reverse engineering gene targets that are counterparts of cellular processes that have been principally affected by GS evolution. Fourteen of the identified biological processes are affected by more than one of the mutated R57 genes. Using this information, along with known function of the mutated genes (Table 3-3) several subsets of affected processes are discernible including: *ARO1*, *GDH1* and *GSH1* as constituents of modified amino acid-related metabolic processes; *SGO1* and *TOF2* as constituents of a modified cell cycle; *SSA1, UBP7* and *ART5* as part of the protein homeostasis machinery (either in protein folding, breakdown, or membrane-protein endocytosis, respectively); global stress response mechanisms via *GSH1*-mediated redox homeostasis, *SSA1*-mediated protein folding, *NRG1*-mediated transcription of stress response genes, or *PBP1*-mediated stress granule formation; and regulatory mechanisms and machinery associated with translation/transcription where *NRG1* (199), *SSA1* (200), *PBP1* (201), *NOP58* are implicated.

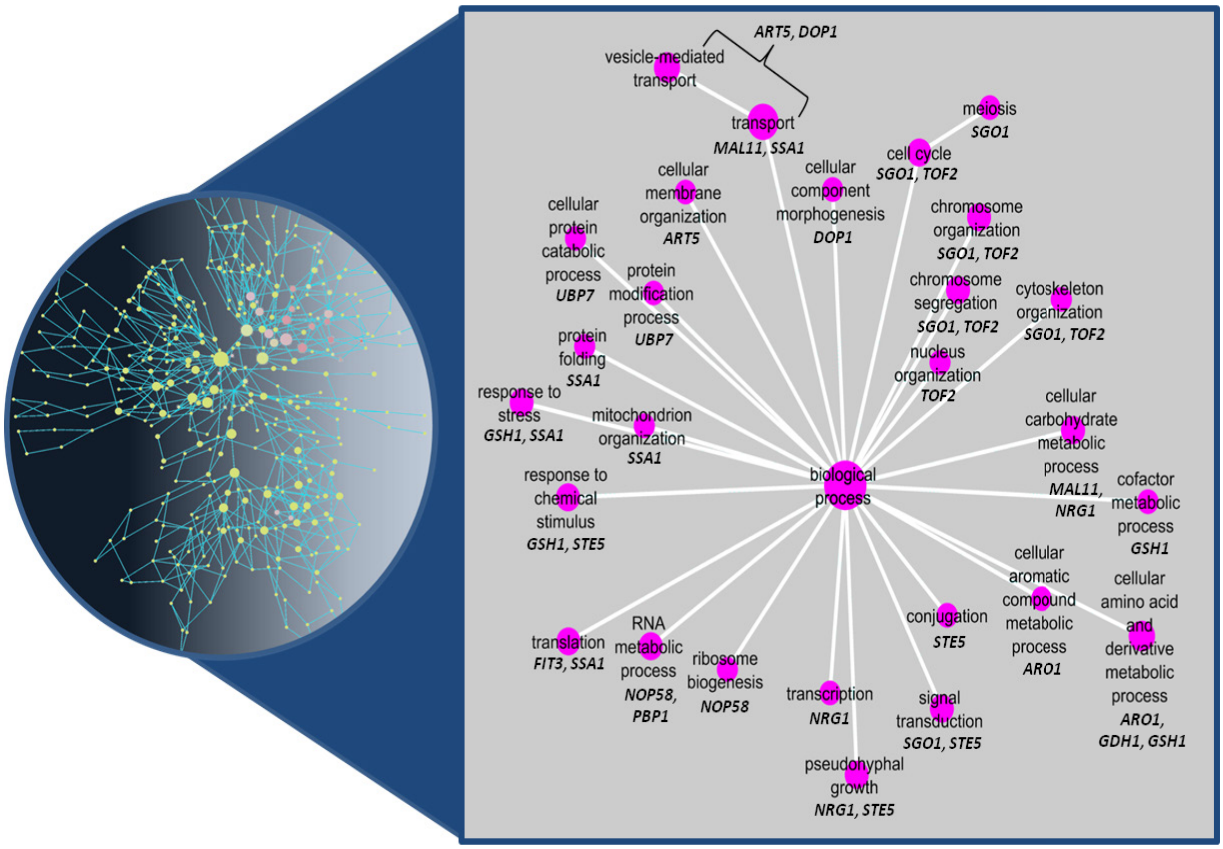

Figure 3-1. Ontology categories associated with R57 genes affected by mutation. Using the full gene ontology set for yeast, a vast interaction network can be generated of biological processes potentially affected by mutation (left) and summarized using the GOSlim Yeast ontology categories (right). Genes affected by mutation (bold, Table 3-3) are listed under their associated ontology category (purple node).

Furthermore, the products of genes showing mutation in R57 comprise a network of interaction through analysis of co-expression, genetic and protein-protein interactions (Fig. 3-2). Within the list of mutated genes, hubs of extensive interactivity indicate gene targets that have an increased likelihood for pleiotropic effects and a higher degree of interconnectivity to other R57 genes affected by mutation. In engineering complex microbial traits, modifying targets that have the potential to affect broad change within a cell, for example by engineering modified

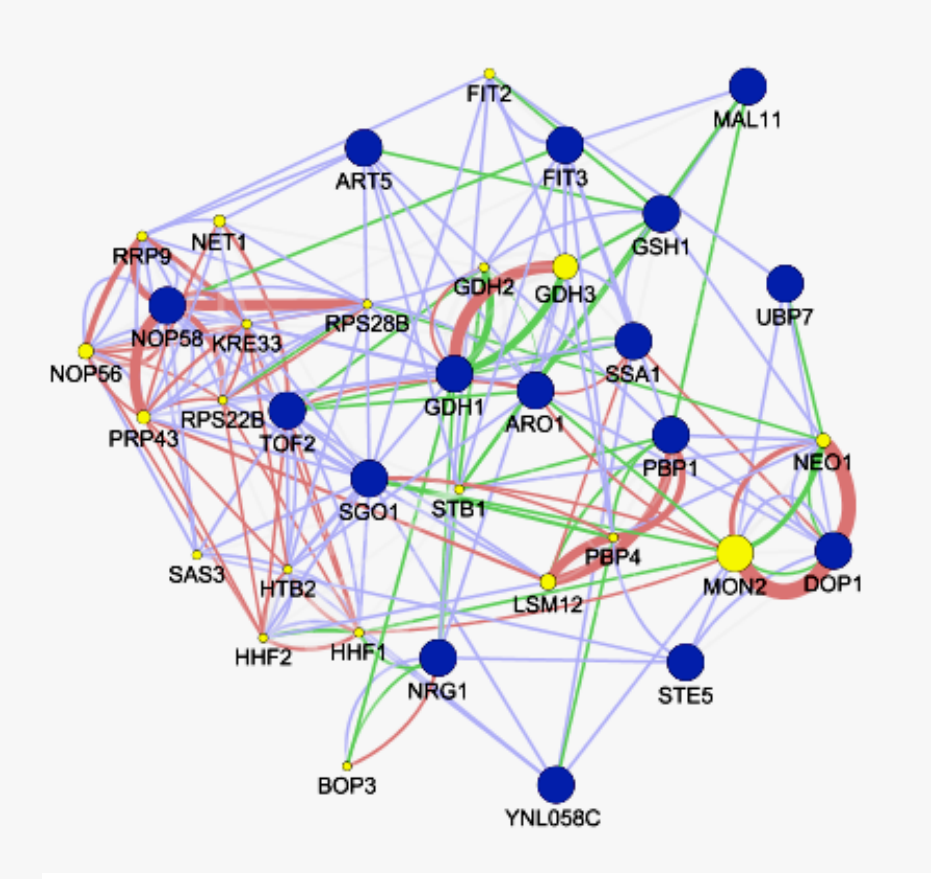

Figure 3-2. Interaction map of genes affected by mutation in R57. Interaction maps were generated through GeneMANIA, drawing from extensive source annotations built into the software. Blue nodes are the genes affected by mutation in R57 (uniform size), while the yellow nodes are the top 20 interacting genes as determined by GeneMANIA (larger size equals a higher degree of interaction within the network). The edges connecting the nodes represent protein-protein (red lines), genetic (green lines) and co-expression (light-blue lines) interactions. Thicker lines represent a higher confidence of interaction.

transcription factors (55), is a plausible means by which to reprogram cellular metabolism to influence multigenic traits. In keeping with GS theory, accumulated mutations have the potential to act additively and therefore known interactors represent attractive targets for future study. The genes and their products that are known to have the highest degree of interaction occupy a more central position on the interaction

network. Based on protein-protein, genetic and co-expression interactions, especially among the mutated R57 genes, these include: *ARO1*, *GDH1* and *SSA1* (Fig. 3-2). Furthermore, genes that show high levels of co-expression may signify a combined effect amongst mutations. For example, *TOF2* and *SGO1* show a high degree of co-expression and are scored as the most similarly expressed genes by meta-analysis of reported microarray expression data by the SPELL (Serial Pattern of Expression Levels Locator) (202) program hosted by the SGD. Also from this interaction network, a list of highly related genes was included in order to assess secondary effects that may be arising from mutation. The most affected nodes of interaction include the genes *MON2, NEO1,* which associate predominately with *DOP1* and affect endocytosis and the vacuole; *GDH3,* highly related to *GDH1*; *LSM12*, the product of which physically interacts with Pbp1p and likely binds RNA; and *NOP56*, which is highly associated with Nop58p and its interactors. In general, the ontology and interaction assessment of the mutant genes offers a rational priority to investigation and a means to access possible novel gene targets associated with the HWSSL phenotype that are not directly mutated.

3.4 Discussion

3.4.1 Whole genome sequencing GS-evolved strain R57

Whole genome sequencing of HWSSL-tolerant strain R57 led to the discovery of 20 SNP mutations within its genome. SNP mutations were predominantly expected due to the observation that UV mutagenesis, the method by which mutation was originally introduced into R57, generally leads to point mutations (198). Of the few existing reports on genome sequencing of randomly evolved strains for reverse engineering target

generation, a small number of mutations are often discovered (108, 110, 111, 203). Sequencing of 3 lines of yeast after 300 generations of evolution for saline stress yielded one mutation of interest (108). Sequencing of strains adapted for glucose limitation after ~100, 200 and 400 generations yielded 17 mutation calls, with only 1-2 adaptive mutations per clone (110). Using chemical mutagenesis to generate yeasts with increased lifespan, followed by genome sequencing led to the discovery of 4 missense and 13 total mutations and yielded one target that explained the enhanced trait (111). In contrast, it was shown that just ~400 generations of adaptation for increased galactose utilization led to 40, 44, and 334 mutations called in 3 evolved strains (109), which seems relatively high based on the $\sim 1.2 \times 10^{7}$ bp size of the *S. cerevisiae* genome and a natural mutation rate of $\sim 5 \times 10^{-10}$ bp^{-1} $generation^{-1}$, suggesting that the evolutionary pressure alone resulted in the accumulation of over 330 mutations for at least one of the sequenced strains (204). However, this study explains that sequencing coverage increased from 16 and 17-fold coverage to 55-fold for the strain with the largest amount of reported mutations. In our hands, a large coverage resulted in many miscalls or alignment errors within the dataset, presumably by increasing the likelihood of sequencing errors being called as mutations (180). In the current study, these false mutation calls were only controlled for by sequencing and analyzing the WT strain in parallel. In keeping with the theory behind GS, our study was expected to reveal a relatively larger amount of combined productive mutations within the R57 genome than would have been attainable by other random evolutionary methods in the short time-frame used for strain development. In the case of R57, the discovery of 14 missense mutations within a single strain supports the heretofore untested assertion that strain development by GS occurs by

the accumulation of beneficial mutations. This supports one premise of this study: that as a random evolutionary strain development scheme by which to locate genetic determinants in a trait of interest, GS followed by sequencing may be significantly informative and allow for the exploration of combinations of productive mutations, a possibility that seems less likely with strains obtained by non-recombinative evolution alone. Of course, more mutations to analyze from a strain of interest may lead to more false positive results being examined, even though selection between shuffling rounds is hypothesized to minimize this potential complication. In this respect, working with a well-known organism and mining known functional and interaction data can narrow the focus of engineering targets, which will be the concentration of the remainder of the discussion.

3.4.2 Genes related to amino acid metabolic processes are mutated in R57

Three genes (*GDH1*, *GSH1*, and *ARO1*) associated with amino acid-related metabolic processes harbor mutations in R57. The mutations in both *GDH1* copies of R57 are predicted to affect protein function, as shown by SIFT analysis that yields a score of 0 each (Table 3-3) and are therefore regarded as highly non-tolerated. The presence of mutation in both *GDH1* alleles and their close proximity (7 amino acids apart) suggests a deterministic role for *GDH1* in HWSSL tolerance and this area of the gene in particular. *GDH1* encodes an NADPH-dependent glutamate dehydrogenase that catalyzes the reductive amination of α–ketoglutarate by ammonia to yield glutamate, a reaction that is responsible for incorporation of 80 % of the cellular nitrogen in *S. cerevisiae* when ammonia is present (205). The highly related *GDH2*, encoding an NADH-dependent glutamate dehydrogenase and *GDH3*, an NADPH-dependent glutamate dehydrogenase

that is a paralog of *GDH1*, are hubs of interaction within the set of mutated genes (Fig. 3-2) indicating extensive association with other mutated genes and further suggesting an integral role for glutamate dehydrogenases in the HWSSL-tolerant phenotype. *GDH1* has been recognized as a determinant of resistance to acetic acid (206, 207). Likewise, recent proteomics research using a strain that is tolerant of furfural, phenol and acetic acid showed a downregulated nitrogen assimilation machinery, including Gdh1p; it is believed this occurs in order to slow growth and allow stress tolerance mechanisms to protect the cell more effectively (206). It has also been shown that deletion of *GDH1* enhances available cytosolic NADPH for other NADPH-requiring enzymes (208). NADPH is required for detoxification of inhibitors like the furan aldehydes by providing reduction potential to enzymes like Adh6p, capable of reducing and detoxifying HMF and furfural (60). However, impairment to Gdh1p could affect ammonia utilization, requiring alternative pathways for nitrogen assimilation. The central role of glutamate in amino acid production and nitrogen assimilation and the potential for Gdh1p activity to influence cellular co-factor pools makes it an attractive target to address in generating HWSSL tolerance, outlined by the fact that both R57 alleles bear a significant mutation.

As the major route for glutamate production in the cell, *GDH1* functionally relates to *GSH1*, which, in R57, bears a mutation 72 bp upstream of the ORF in the 5' UTR (194). *GSH1* encodes for an ATP-dependent gamma glutamylcysteine synthetase that catalyzes the first step in glutathione biosynthesis. Glutathione is comprised of glycine, cysteine and glutamate and is a major redox buffer of the cell, cycling between its reduced and oxidized form, relying on NADP(H) for recycling. It has been shown to protect against ROS damage and impart hydrogen peroxide tolerance (209). Moreover,

hydrogen peroxide induces *GSH1* transcription, but relies on the presence of intercellular amino acid pools, namely glutamate, glutamine, and lysine (210). Therefore, modified glutamate assimilation via *GDH1* mutation and the 5' UTR mutation in *GSH1*, which, if it has an effect would likely be seen in expression levels, both potentially affect intercellular glutamate pools and concomitant expression of *GSH1*. Engineering *GSH1* for increased activity has already been suggested as a means to mediate ROS-induced furaldehyde damage by upregulating cellular glutathione content (211). However, glutathione synthesis requires ATP and often valuable nitrogen and sulfur compounds. Yeast can act to catabolize glutathione for these resources when they are limiting (212), which suggests that cellular glutathione content may be modulated as a function of both stress tolerance and nutrient requirements. Glutathione has been implicated in protein homeostasis as well. For example, it can disulfide bond with exposed sulfydryl groups of proteins and thereby protect against unwanted disulfide bonding within proteins exposed to oxidizing conditions (213). Loss of cellular glutathione leads to activation of HSPs, including Ssa1p, with which Gsh1p has been shown to interact (214, 215) (Fig. 3-2). Gsh1p also genetically interacts with *ARO1* and *ART5* that bear mutations in R57, which, coupled with the interplay between *GSH1* expression and Gdh1p function, supports an important role for *GSH1* in HWSSL tolerance. Furthermore, because *GSH1* plays a pivotal role in glutathione production, which in turn can have an impact on signaling events that pervade the cell on a global scale (reviewed in (213)), a mutation that might affect *GSH1* expression level, like that found in R57, could influence HWSSL tolerance either through affecting oxidative stress tolerance, influencing protein folding machinery or affecting amino acid usage.

The remaining gene carrying a mutation in R57 related to amino acid metabolic processes is *ARO1* (Fig. 3-1). Aro1p catalyzes steps 2-6 of the chorismate pathway leading to synthesis of aromatic amino acids (216), and the domain in question catalyzes step 2, the condensation of 5-enolpyruvylshikimate-3-phosphate from shikimate-3-phosphate and phosphoenolpyruvate. *ARO1* occupies a central position in the interaction network between mutated genes, genetically interacting with *TOF2* and with Aro1p physically interacting with Gdh1p, Ssa1p and Pbp1p (Fig. 3-2). *ARO1* mutation might therefore be acting in concert with one or all of these evolved alleles. Aromatic amino acid synthesis and tryptophan synthesis in particular are pathways that are generally upregulated leading to tolerance of acetic acid (207). Additionally, mutants auxotrophic for aromatic amino acid synthesis are consistently more sensitive to acetic acid than prototrophic *S. cerevisiae* strains (66). It has been shown that weak acids inhibit yeast growth by reducing uptake of aromatic amino acids, which is likely a result of pronounced inhibition of Tat2p amino acid permease (66). It was further shown that deletion of *ARO1* leads to sensitivity to osmotic and ethanol stress (217). The integral roles of Aro1p in the pathway towards aromatic amino acid synthesis make it an attractive target for control and the traits of osmotic pressure and acetic acid tolerance previously demonstrated by R57 (218) suggests that this mutation is a likely candidate for influencing the HWSSL-tolerance trait. Overall, amino acid generation and usage alteration via *GDH1*, *GSH1*, and *ARO1* manipulation is a viable scheme for further strain development programs and the mutations collected in R57 bear further investigation from that standpoint.

3.4.3 Genes related to protein homeostasis machinery show mutation accumulation in R57

Protein damage and aggregation is likely a major source of toxicity in cells exposed to lignocellulosic hydrolysates and has at least been partially shown to arise due to ROS damage arising from furan aldehyde exposure (13). Mutations in R57 genes directly related to protein homeostasis include *SSA1*, *UBP7* and *ART5*. The most studied stress response protein from this group is Ssa1p, which bears a Q31K mutation in R57. It is probable that the longer-chained, more positively charged lysine residue has an important effect on Ssa1p structure and is indeed shown to be a highly conserved residue by SIFT prediction (Table 3-3). *SSA1* encodes a member of the heat shock 70, Hsp70, family of proteins, which consists of highly-conserved, broad-specificity, essential protein chaperones that assist in protein folding and protect cells by decreasing the aggregation of proteins that have denatured due to stress (for reviews see (219, 220)). Hsp70s also aid in cross-membrane polypeptide translocation, for example into the vacuole for degradation or the endoplasmic reticulum for secretion (221, 222)). More specifically, the Ssa family of Hsp70s consists of 4 (Ssa1-4p) highly homologous proteins, with Ssa1p sharing 99%, 84%, and 85% amino acid identity with Ssa2-4 respectively (223). Expression of any one of these proteins is enough to support vegetative growth, signifying a certain level of functional redundancy, but even between the highly homologous Ssa1p and Ssa2p they do, in some instances, serve different purposes, as, for example, only Ssa1p is able to mediate degradation of protein fructose-1,6-bisphosphatase (224, 225). Additionally, Ssa1p is known to play regulatory roles in translation initiation (200) and its presence represses activity of Hsf1p (226), a

transcription factor that regulates transcription of genes, including Hsps, involved in detoxification, protein folding, cell wall organization, carbohydrate metabolism and energy generation (227, 228). A recently discovered form of regulation involving Ssa1p, shows that the protein is sensitive to modification by thiol-reactive compounds, which then fails to repress Hsf1p and its downstream effects (229) thereby providing a means to activate an Hsf1p-induced stress response coupled to the redox state of the cell. In this respect, a functional relationship can be drawn between Ssa1p and Gdh1p, in terms of NADPH generation, and Gsh1p, as a means to produce glutathione, as players in intercellular redox homeostasis.

Furthermore, precedence has been established that single amino acid changes in Ssa1p, even between residues with similar physical properties, is enough to switch its functional specificities to that of other Hsp70 proteins if it occurs in a functional domain, while maintaining overall function (225). The structure of Hsp70s is that of two distinct modules: the nucleotide-binding domain (NBD), responsible for binding and hydrolyzing ATP, and the substrate-binding domain (SBD), which is known to bind short hydrophobic segments of incompletely folded or unfolded polypeptides, in order to prevent adverse aggregation (219). When ATP is bound to an Hsp70, a peptide substrate can be exchanged freely with the environment and ATP hydrolysis traps hydrophobic peptides within the SBD and releases them upon ADP/ATP nucleotide exchange (230). In this way, the NBD governs the well-known protein folding activity of Hsp70s. The Q31K mutation occurs in the NBD of Ssa1p and when DnaK, the *Escherichia coli* Hsp70 homolog is used as a structural reference, this mutation is shown to lie adjacent to the ATP binding pocket (231). Although the Q31K mutation has not been studied thus far,

this area of Ssa1p was shown to be of particular importance to protein function with 5 randomly obtained mutations between amino acids 17-34 having a dominant negative effect on [PSI+] prion propagation even in the presence of Ssa2p, abolishing or diminishing prion propagation while maintaining other cellular functions (231). Furthermore, Ssa1p bearing A17V or R34K mutations is able to reactivate unfolded luciferase at twice the rate of the WT (232), showing that mutations like Q31K, which likely affect the ATP binding and hydrolysis activity of the NBD, can also have a bearing on the ability of Ssa1p to refold certain substrates. The position of the Ssa1p mutation and the importance of the protein overall, especially as it relates to stress tolerance and its ability to orchestrate global changes, makes Ssa1p a likely candidate for involvement in the HWSSL-tolerant trait.

Refolding damaged proteins and preventing aggregation is not the only means by which the cell might maintain cellular protein integrity. The ultimate means by which a cell may regulate protein quality is through destruction of misfolded or damaged and potentially toxic polypeptides. In eukaryotes, this takes place largely through selective, energy-dependent labelling with ubiquitin leading to digestion to small peptides by the large proteolytic complex, the 26S proteasome (17). Hsp70s have been shown to play a role in this process, holding nascent peptides and leading to ubiquitination of certain proteins, presumably when the folding process is unsuccessful and quick peptide degradation is warranted (17). R57 mutant gene *UBP7* is known to encode a ubiquitin-specific protease that cleaves ubiquitin-protein fusions (233) and as such it is part of this ubiquitin-induced signalling machinery of the cell, which can also involve cell-cycle and apoptosis regulation, and DNA repair (234-236). Deubiquitinating enzymes act to

recover ubiquitin from ubiquitin-protein conjugates and may therefore have a direct bearing on cellular protein and ubiquitin homeostasis (236). Ubp10p, a similar yeast deubiquitinating enzyme has been demonstrated to influence RNA polymerase 1 stability and thereby acts as a key regulator of rRNA production and in turn ribosome biogenesis, one of the important and energy-expensive processes of the eukaryotic cell, thereby affecting cell growth (237) and demonstrating the potentially global influence a deubiquitinating enzyme can have. Furthermore, upregulation of *UBP13*, another yeast deubiquitinating enzyme, is beneficial to cells under cold-stress and suggests that altering ubiquitin-induced signalling may be a viable path towards other forms of stress tolerance (238). As one would expect, the cell's requirement for available ubiquitin increases during stress exposure (239). Relatedly, another role of ubiquitination is the internalization of cell-surface proteins (240-242). This function relates to Art5p, another R57 mutant protein, which belongs to the ART (arrestin-related trafficking) family of proteins that are believed to function as adaptors for Rsp5p, a ubiquitin ligase that promotes endocytosis of plasma membrane proteins, including transporters, targeting damaged or unneeded plasma membrane proteins for vacuolar degradation (243). Mutation of *ART5* may constitute a way for R57 to regulate destruction of proteins damaged by HWSSL stress or direct changes to the plasma membrane in order to respond more efficiently to the toxic HWSSL environment.

3.4.4 Genes that play a regulatory role in stress response are mutated in R57

Along with *SSA1* and *GSH1* discussed above, *PBP1* and *NRG1* are known regulators of stress response that are potentially having a major impact on the HWSSL tolerance trait. Although Nrg1p can mediate glucose repression (244) and negatively

regulate cellular processes like pseudohyphal filamentous growth (245), which is well known to be associated with cells under conditions of nitrogen stress, a recent large-scale study on transcription factors in *S. cerevisiae*, which included mining data from 1693 publicly available microarray gene expression data sets (199), found that the most significant transcriptional responses governed by Nrg1p were all related to a multitude of stressor exposures of varying length and intensity. Nrg1p represses genes by recruiting the Cyc8p-Tup1p transcriptional repressor complex to gene promoters where it disrupts transcription of a variety of genes (246). Zhu *et al*. found that one of the main functional gene categories affected by Nrg1p is related to peroxide tolerance, which is a specific tolerance trait of R57 (218). Nrg1p can also directly repress genes that are activated by the downstream action of protein kinase Snf1p (245), which stimulates upregulation of stress responsive genes (247); and the transcription activator Haa1p, which imparts acetic acid tolerance (139). Several mutants missing single genes from the Snf1p-pathway can affect tolerance to acetic acid (207). Additionally, Vyas *et al*. found that Nrg1p and closely related homolog Nrg2p regulate a set of stress-response genes and *Δnrg1Δnrg2* deletion mutants gain tolerance to oxidative stress and salt exposure (248), a trait that is also shared by R57 (218). It has further been shown that Nrg1p deletion leads to upregulation of Ena1p, the most important means of mediating the export of sodium and lithium from yeast (249-251) and that Nrg1p is a phosphorylation target of protein kinase Cdk2p, which is involved in controlling various important cellular functions including stress response (252, 253). Given the highly conserved nature of the mutated residue in Nrg1p, the likely result is a loss or reduction of function and a corresponding

derepression of Nrg1p governed genes, which will be explored more fully in the subsequent chapter.

Unlike *NRG1*, *PBP1* has the potential to affect stress response at the translation level. The R57 mutation that is believed to affect *PBP1* lies 190 bp 5' of the transcriptional start site and is part of the 5' UTR (195); therefore, any changes to *PBP1* function are likely a result of the expression level of the gene, and not gene function. Early studies of Pbp1p show that it plays a regulatory role in mRNA polyadenylation by interacting with Pab1p (poly(A)-binding protein) (254), which controls mRNA poly(A) tail length and plays a role in mediating translation activation (255). Pbp1p expression levels may therefore have a global impact on cellular function, but recent work has also demonstrated a more specific role Pbp1p plays in stress responses. Pbp1p has been shown as an important factor in stress granule formation, which are cytoplasmic RNA-protein granules containing non-translating mRNAs that tend to associate with ribosomal subunits and translation initiation factors (256, 257). Stress granules have been shown to form during heat shock (258), ethanol exposure (259) and glucose deprivation (260-262), but because stress responses tend to evoke transient translation initiation inhibition, stress granules are thought to accumulate under many stress conditions and contain differing constituents (260). Recently, stress granule formation resulting in bulk translation attenuation was shown to be induced by HMF and furfural (263). Pbp1p overexpression specifically was shown to induce stress granule formation and lead to the sequestration of the TORC1 complex into stress granules and to diminish TORC1 signalling (201). TORC1 is involved in the regulation of a variety of cellular processes including protein synthesis, transcriptional repression of genes induced by nutrient starvation, nutrient

permease sorting and turnover, cell cycling, ribosome biogenesis, meiosis and actin organization (reviewed in (264, 265)). Tor1p, a major component of the TORC1 complex is involved in signalling of acetic-acid induced apoptosis and *Δtor1* cells do not exhibit the decreased protein content seen with acetic acid treated WT cells (266) and show increased peroxide and hyperosmotic stress resistance (267). Due to the diverse and fundamental role that *PBP1* plays in yeast and its association with molecules known to influence resistance to lignocellulosic substrate inhibitors, it is an appropriate target for future reverse engineering studies, perhaps focussed on the modulation of its expression, due to the location of the R57 mutation.

3.4.5 Mutated R57 genes from a wide range of function are accumulated within the GS-evolved genome

Although it is tempting to disregard the lesser-studied mutated R57 genes in the interest of simplicity, the stringent selection used in engineering R57 suggests that some or all of these more difficultly reconciled genomic changes or those demonstrating lesser known interaction profiles may still be playing a determinant role in HWSSL tolerance. For example, Mal11p, which is mutated twice, in a heterozygous fashion, functions as a high-affinity α–glucoside transporter with broad substrate specificity (268-270). Although the effect of *MAL11* on tolerance to industrial processes has not been demonstrated, it is a common trend for non-S288c, industrial yeast strains to show a loss or reduction of *MAL11* genes (82, 271, 272). One possible link between Mal11p and the robust HWSSL/industrial fermentation phenotype is that it can also act as a high affinity trehalose-H^+ symporter (273, 274). Due to the role of cellular trehalose content in response to stressful environments like that of HWSSL (275-278) and the influence

proton transport might have on internal pH *in lieu* of the acetic acid content of HWSSL, it is plausible that Mal11p is playing a role in HWSSL tolerance as well. The other known transporter in R57 affected by mutation is iron transport facilitator Fit3p. Previous work has shown that 4 iron uptake transporter genes, including *FIT3* are required for acetic acid tolerance (207), while *FIT3* and another 3 iron transport genes were highly upregulated upon furfural challenge (279). Though the exact relationship between intracellular iron levels and lignocellulosic substrate inhibitors has not been resolved, it has been hypothesized that the demand for iron goes up with the upregulation of iron-sulfur enzymes, many of which are involved in oxidative stress responses (279) or that membrane damage could lead to iron leakage (7). Alternatively, with respect to HWSSL tolerance, the possibility of high heavy-metal content in the substrate could make modification to iron-uptake genes a useful strategy to exploit in order to optimize intracellular content.

Genes of relatively unknown function are of particular interest as well in that they are components of the precise impetus behind GS-evolution mediated strain development: that the mutations which might impart the trait of interest are not easily accessible. Little is known about *DOP1*, even though it encodes for an essential protein. In general, it is known to localize to the mitochondria and Golgi and is involved in endosome to Golgi transport and may have a function in endoplasmic reticulum (ER) organization, establishing cell polarity and morphogenesis (280-282). Recently, it was shown to interact with Neo1p and Mon2p, which figure prominently as highly interactive among the mutation-bearing proteins (Fig. 3-2). Neo1p is involved in the early secretory pathway and vacuolar biogenesis (283) and is a putative flippase that likely plays a role

in cell membrane phospholipid changes (284), while Mon2p plays a role in endocytosis and vacuole integrity (285, 286). The essentiality of Dop1p and the known toxic effects of furan inhibitors and phenols on the cell membrane and the vacuole (7) suggest that it may be playing a role in the HWSSL-tolerant phenotype and future reverse engineering studies may help to elucidate a more precise function for Dop1p. Similarly, the function of another R57-mutant protein, YNL058Cp, is largely unknown, but it may also affect the vacuole, where it is known to localize (282) and the cell surface. A recent study has shown that YNL058C is upregulated in response to cell wall damage as part of the yeast cell integrity MAPK pathway and to be regulated by Slt2p MAPK, a known regulator of cell wall integrity (287). Genes related to cell wall structure are affected by acetic acid exposure (207) and furan aldehydes are known to damage yeast cell walls (59). Therefore, genes related to cell wall integrity may be of particular importance to the R57 phenotype. In this way, although relatively unknown genes do not figure centrally within the interaction assessment, their investigation may reveal productive roles in lignocellulosic hydrolysate tolerance.

Mutations affecting the cell cycle are particularly difficult to reconcile with the HWSSL- tolerance phenotype. The affected genes include *SGO1*, involved in chromosomal segregation and stability, along with *TOF2* and *NOP58*. *TOF2* is involved in rDNA silencing and mitotic rDNA condensation, playing a regulatory role in mitotic exit (288). Any effect the *SGO1* and *TOF2* genes might exert on stress tolerances would most likely be manifested as an inadvertent overall effect on growth and replication of the cell. Similarly, the function of *NOP58* is related to more fundamental cellular processes. Specifically, *NOP58* is involved in pre-rRNA processing and rRNA synthesis. Cycling

cells must make ~2000 ribosomes per minute, while 80 % of produced RNA is ribosomal (289) and therefore even minimal changes to this machinery may have effects on the cell cycle and energy usage.

Finally, based on known function, some of the mutations found in R57 are likely less valuable as stress-tolerance determinant targets. For instance, *STE5* exhibits one missense and one silent mutation in R57 and does not interact extensively with other R57 mutant genes (Fig. 3-2) or share many functional relationships (Fig. 3-1). Ste5p is a pheromone response scaffold protein that mediates a mitogen-activated protein kinase (MAPK) cascade leading to phosphorylation of Fus3p and resulting in the haploid mating response (290). The R57 S171F mutation occurs NH_2-terminal-adjacent to a RING-H2 domain of Ste5p that is known to interact with Ste4p, the β-subunit of the heterotrimeric G protein, which binds Ste5p as part of a complex and is released upon pheromone binding leading to downstream activation of MAPK constituents Ste11p, Ste7p, and finally Fus3p (reviewed in (291)). Ste4p has been demonstrated as necessary for the proper functioning of the mating response (292, 293). Mutation in this area of the protein has led to hyperactivity of the mating response, imparting Ste4p independence (294), or an impaired mating response if mutation occurs within the RING-H2 domain itself (293). Ste5p interacts with and mediates activation of Ste7p and Ste11p, both of which have been implicated in stress response MAPK signalling cascades, such as the HOG-pathway (295), but existing evidence shows that cross-talk between these pathways is minimal (296). Furthermore, mutations in this domain of Ste5p do not seem to affect interaction with downstream constituents of the MAPK cascade (293, 294) and therefore any inadvertent stress tolerance arising from these interactions, though possible, seems

unlikely to explain the high level of HWSSL tolerance exhibited by R57. Indeed, any phenotypic response related to tolerance likely only manifested itself in the haploid strains that may have been exposed to HWSSL, as Ste5p is normally lowly expressed in diploid strains like R57 (297). Alternatively, because mating is essential to the GS method used to generate R57, a strain with a modified mating behaviour may have more tendency towards evolving fitness due either to an overactive mating response, which would increase the likelihood of accumulating beneficial mutations, or a repressed response that might decrease the chance of backcrossing out useful mutations that were acquired, but is likely not a target for investigation in stress tolerance.

3.5 Conclusions

GS followed by full genome sequencing at adequate depth of coverage is a viable option to discover a limited number of mutations that are likely linked to a phenotype of interest. The mutations discovered in R57 are found in ORF's, with the majority predicted to lead to some sort of phenotypic response, or UTRs with as yet unknown ramifications. Due to the high level of knowledge that exists for *S. cerevisiae*, plausible assertions can already be made as to novel avenues of microbial strain engineering from GS and sequencing alone, which may not be the case for less understood organisms without further study. Additionally, current bioinformatics analyses make it possible to prioritize the mutations based on known interactions within the set of mutations, phenotype prediction and known biological functions. Furthermore, the nature of mutation accumulation may provide insight into the importance of a given gene, if, for instance, it carries more than one mutation on separate chromosomes, is homozygous, or occurs in an area of a protein that has been demonstrated to affect function. These

analyses suggest possible determinant roles for many of the mutated genes discovered in this portion of the study. However, key genes including *NRG1*, *SSA1*, and *GDH1* are of primary interest due to their ability to influence cellular function in a widespread manner or their proven effect on resistance to the sources of stress found in HWSSL. Moreover, the nature of the mutations within these genes, either affecting an area of interest in the proteins, as with *SSA1*, or the fact that both gene copies are affected, as is the case with *NRG1* and *GDH1*, suggests that these particular mutations are present due to selective pressure. Furthermore, genes involved in multiple levels of regulation are affected by mutation in R57. For example, *SSA1* is involved in protein homeostasis and translation; *GSH1* and *GDH1* are major affectors of redox homeostasis or nitrogen assimilation; and *NRG1* and *PBP1,* which are involved in transcriptional/translational stress responses, respectively; modifying all of these genes has the potential for major downstream phenotypic changes like those exhibited by R57.

Of course, the validity of these assertions still warrants further investigation. As predictive software becomes more robust, discerning precise and affected biological modules under a given condition may become feasible, but at this point, with a small mutation data set, enriched affected function predictions are not meaningful. However, as a means to generate an overarching topography of the genomic changes as they relate to known biological function and to generate known complementary protein targets, current interaction software is useful. The impetus behind predictive software, rational strain design and studies like this one, which hope to inform strain design, presuppose a modular nature to the cell that can be treated as discreet parts with discreet functionalities. For example, discreet modules may include stress response elements that

can be pinpointed, manipulated and applied to engineering different strains or organisms. As the discussion of the *SSA1* and *NRG1* genes helps illustrate, genes involved in a specific trait likely cannot be regarded as single units of specific operation, even for those instances when the biochemical function of a protein is well-characterized. Likewise, mutations like those concerning *SGO1*, *TOF2*, and *NOP58*, which may affect the cell cycle or fundamental metabolic processes, are more difficult to treat as discreet stress response modules that can be appropriated and manipulated without affecting the system in unwanted ways. Strain engineering through GS is in many ways the antithesis to this type of modular thinking and it presumes that the cell can either not be completely broken down in this way or our knowledge is not robust enough to do so. In this way, although known stress response genes are attractive targets for future rational biocatalyst design, the mutations that potentially affect whole-cell physiology are perhaps more attractive targets to advance our knowledge of the types of changes evolution might introduce to establish a specific trait, which was ultimately one of the goals of sequencing the genome of R57. Several testing strategies might be attempted to elucidate mutations that have the most profound effect on tolerance. For example, the mutant versions of all genes might be substituted into the background strain CEN.PK and assessed for gain of HWSSL tolerance. Conversely, the mutated R57 genes could be replaced with WT alleles and assessed for loss of HWSSL tolerance. However, GS theory suggests that several or all of the mutations in R57, which are hypothesized to have accumulated progressively through reiterative recombination towards higher tolerance, are needed to fulfill the final HWSSL tolerance phenotype exhibited by R57; this makes either scenario, introducing gained or diminished tolerance, a vast undertaking given the

permutations involved in combining or reverting single or all of the mutations within a single host. Such an experiment could be further complicated if the order in which the mutations are combined within a final host affects the acquisition of HWSSL tolerance traits. This type of brute force cloning may be plausible for a smaller number of mutation targets. However, even if the final phenotype could be recovered or repressed successfully through such methods, it may not offer further insight into the physiological changes that accompany these mutations. Therefore, in order to gain understanding as to the mutations that are relevant to the HWSSL-tolerance trait, and to describe the expected physiological differences between R57 and the WT and the specific response of R57 to a HWSSL stress challenge, RNA-seq transcriptional expression analysis was employed. This will be the subject of Chapter 4.

Chapter 4

4.1 Introduction

Although genomic differences between the WT and GS-evolved R57 were discovered as outlined in Chapter 3, the physiological changes that give rise to the HWSSL-tolerance trait cannot be depicted through genome sequencing alone. To gain insight into the specific biological processes that are being affected, transcriptional analysis is uniquely suited to simultaneously examining the genome-wide reaction that accompanies a trait of interest. In order to study the specific transcriptional response of GS-evolved strain R57 to HWSSL exposure and to probe for transcriptional differences between R57 and the WT strains, RNA-seq expression analysis was performed and is the subject of this chapter.

The nature of at least some of the mutations discovered in R57 was hypothesized to have a direct impact on expression, possibly at the level of transcription. For instance, if the UTR mutations of *FIT3*, *GSH1*, *PBP1* and *NOP58* are expected to have an effect, they are likely impacting expression levels. Although productive UTR mutations may only be seen at the protein level, due to effects on translation like altered ribosome binding potential (298), changes to the UTR or coding sequence of a gene may also impact mRNA levels by, for example, altering decay rates due to changes in mRNA structure that influence stability (299). Furthermore, the mutation in the transcriptional repressor of stress response gene, *NRG1*, is likely to have an effect on the function of Nrg1p and thereby lead to downstream transcriptional changes. Beyond exploring these directly related transcriptional effects of mutation, the aim of the expression study is to further characterize phenotypic differences between the WT and R57 that may result

from mutation and to understand the physiology behind R57's phenotype. In cross-referencing the transcriptional response of R57 with the phenotypic and genome sequence data collected thus far, the mutations and biological processes of interest can be further narrowed if functional processes are affected both by mutation and differential gene expression in response to HWSSL. These data support many of the assertions generated by the mutation analysis and phenotypic characteristics of R57 described in the preceding chapters, and constitute the first description of the *S. cerevisiae* transcriptional response to lignocellulosic hydrolysate-inhibitor-rich medium by RNA-seq and one of the first yeast transcriptional profiles on a lignocellulosic substrate currently produced at industrial levels.

4.2 Materials and Methods

4.2.1 Growth conditions and RNA isolation

WT diploid strain CEN.PK-122 and HWSSL-tolerant R57 were used in RNA-seq experiments. Because the mutation to R57 resulted in a 'gain of function' phenotype (i.e. survival and growth on HWSSL), undiluted HWSSL exposure of the WT strain does not allow growth of the reference strain (Fig. 2-7). However, using the example of previous studies (300-302), in order to generate productive leads, I employed a three-way comparison of the strain R57 and its reference: firstly, the WT and R57 were compared under permissive conditions, secondly, R57 was exposed to a HWSSL challenge, and finally, general trends between the two data sets were assessed. As adaptation to lignocellulose-derived inhibitor stress likely manifests itself during lag phase (171), HWSSL-exposure experiments were performed at early and late lag phase. Strains were

inoculated from individual colonies isolated from frozen stocks on YPD agar medium and pre-grown overnight in test tubes containing 5 mL minimal synthetic defined (SD) medium at 200 rpm and 30 ºC. Fifty mL of SD were inoculated with ~1 x 10^6 cells from the pregrowth culture, cultured overnight under semi-fermentative conditions (sealed 125 mL flasks shaken at 100 rpm) at 30 °C to early stationary phase and normalized to an OD_{600} nm of 3. Biological replicate cell samples of these cultures were used as the permissive condition to compare transcriptional expression of the WT and R57 strains. HWSSL-exposed R57 cultures were generated by suspending SD-grown, PBS-washed R57 cells in 50 mL HWSSL at a cell density of ~5 x 10^5 CFU/mL and culturing under semi-fermentative conditions (sealed 125 mL flasks shaken at 100 rpm) and 30 °C for 2 and 24 hours, representing early and late lag phase respectively, due to the inhibitory nature of HWSSL (Fig. 2-7). For each sample, cells from 5 mL of culture were centrifuged at 1800 x g at 4 °C and frozen in liquid nitrogen until RNA isolation. RNA was extracted using the RNeasy Plant Minikit according to manufacturer's specifications for use with yeast (Qiagen, Toronto, Ontario, Canada) in which frozen cells were suspended in lysis buffer and disrupted with a mini bead beater (Precellys 24, Bertin Technologies) at 4 °C. RNA quality was verified using a Agilent 2100 Bioanalyzer according the manufacturer's specifications.

4.2.2 RNA-seq and differential expression analysis

RNA-seq was performed at the McGill/Genome Quebec Innovation Centre on an Illumina Genome Analyzer *IIx* for the R57 HWSSL-response time-course and in duplicate on the Illumina Genome Analyzer *IIx* and Illumina HiSeq 2000 for the WT vs

R57 permissive growth condition transcriptome analysis, both according to the manufacturer's specifications, similar to the process described for genome sequencing (Chapter 3.2.1). Sequencing libraries were generated using the TruSeq RNA kit (Illumina). Briefly, approximately 10 μg of total extracted RNA was used to isolate at least 100 ng of messenger RNA (mRNA) using oligo-dT beads. The mRNA enriched fraction was reversed transcribed to generate cDNA fragments that were sheared using a Covaris instrument to yield ~200 bp fragments. Following end-repair and 3' end adenylation steps, an index was ligated and a PCR step performed. The quality of the library was assessed on a DNA 1000 chip (Agilent) and quantified by PCR. Libraries were then subjected to 36 or 50 cycles of sequencing on the Illumina Genome Analyzer IIx and Illumina HiSeq 2000, respectively.

RNAseq differential transcription analysis was performed with CLC Genomics Workbench version 5.1 using standard parameters. The cDNA sequence reads from RNA-seq were trimmed to remove Illumina sequencing adaptors as well as unreliable read ends and alignments were performed using the CEN.PK 113-7D genome sequence and associated GTF file (127) as the backbone for alignment mapping and quantitation. Statistical analysis was performed using the package available with CLC software. Expression levels were calculated as RPKM values. Differential expression significance values were computed using Baggerly's test for WT vs R57 analysis, which is intended for samples with biological replicates (303), while Kal's test was used for the exposure to HWSSL analysis using strain R57 (304). The samples were then FDR-corrected in order to eliminate non-productive leads from the expression results. Gene transcripts showing differential expression with a corrected p-value of < 0.05 and a > 2-fold increase (unless

otherwise stated) were used for functional clustering and enrichment mapping of differentially expressed genes.

4.2.3 Bioinformatics analyses

Functional annotation clustering was executed with DAVID Bioinformatics Resources 6.7 (161). Clusters of up or down regulated genes with gene ontology (GO) term enrichment scores of ≥ 1.3 (equivalent to a non-log scale value of 0.05) are reported, unless stated otherwise. Enrichment maps of ontology categories from clustering were generated with the Enrichment Map 1.2 software plug-in (305, 306) (see Fig. 4.2 for details) for the Cytoscape 2.8 network analysis software program (189-191). All functional annotations presented were derived from SGD (307) or the DAVID server unless otherwise referenced. Transcription factor binding analysis was done through the YEASTRACT database (308-310).

4.3 Results

4.3.1 Coverage of RNA-seq reads

RNA-seq was performed with an average mappable read depth of ~ 17 millon mappable 36 bp reads per sample for the HWSSL time course. The WT vs R57 RNA-seq experiment resulted in an average of ~ 80 million mappable 36 and 50 bp reads per paired biological sample. Sequencing and mapping results are summarized in Table 4-1.

4.3.2 Growth and differential whole-genome expression profiling of non HWSSL-exposed WT vs R57 cells reveals significant phenotypic differences

In order to assess if the genetic changes of R57 functionally correspond with a specific differential transcriptional response by the mutant strain, RNA-seq was performed on

Table 4-1. Summary of sequence reads mapping for RNA-seq experiments

Sample	Uniquely mapped to gene	Non-specifically mapped	Fragments Mapped	% of total mapped to gene
CEN.PK 122 no HWSSL	11417881	1333605	12751486	100
CEN.PK 122 no HWSSL (b)	140812406	14275607	155088013	100
R57 no HWSSL	14316591	1584953	15901544	100
R57 no HWSSL (b)	135644842	15853016	151497858	100
R57 2 hrs HWSSL	15065307	2035530	17100837	100
R57 24 hrs HWSSL	8385600	7374215	15759815	100

cell cultures of WT and R57 in stationary phase under non-inhibitory growth conditions. Comparing R57 to the WT for growth in defined laboratory medium revealed a markedly reduced biomass yield for R57 (Fig 4-1). Furthermore, residual glucose remains in the medium of R57 well into stationary phase, while the WT has exhausted its carbon resources within 24 hours, even though both strains enter stationary phase at similar times. This finding shows that R57, even in an environment void of lignocellulosic substrate inhibitors, is reprogramming its metabolism and directing resources in ways divergent from the WT. Furthermore, the presence of residual glucose in the R57 culture medium suggests that another essential growth resource has become limiting. Finally, it is clear that R57 makes use of resources in a way that reduces the impetus on biomass generation, redirecting them to other processes and demonstrating a potential fitness trade-off that reduces growth in permissive environments, but preserves viability in the more toxic HWSSL environment (218). These phenotypic differences, even under growth-permissive environments were accompanied by significant mRNA expression differences. Transcriptional analysis of the two strains revealed that there were 148 differentially regulated genes (> 2-fold) between the WT background strain and the R57

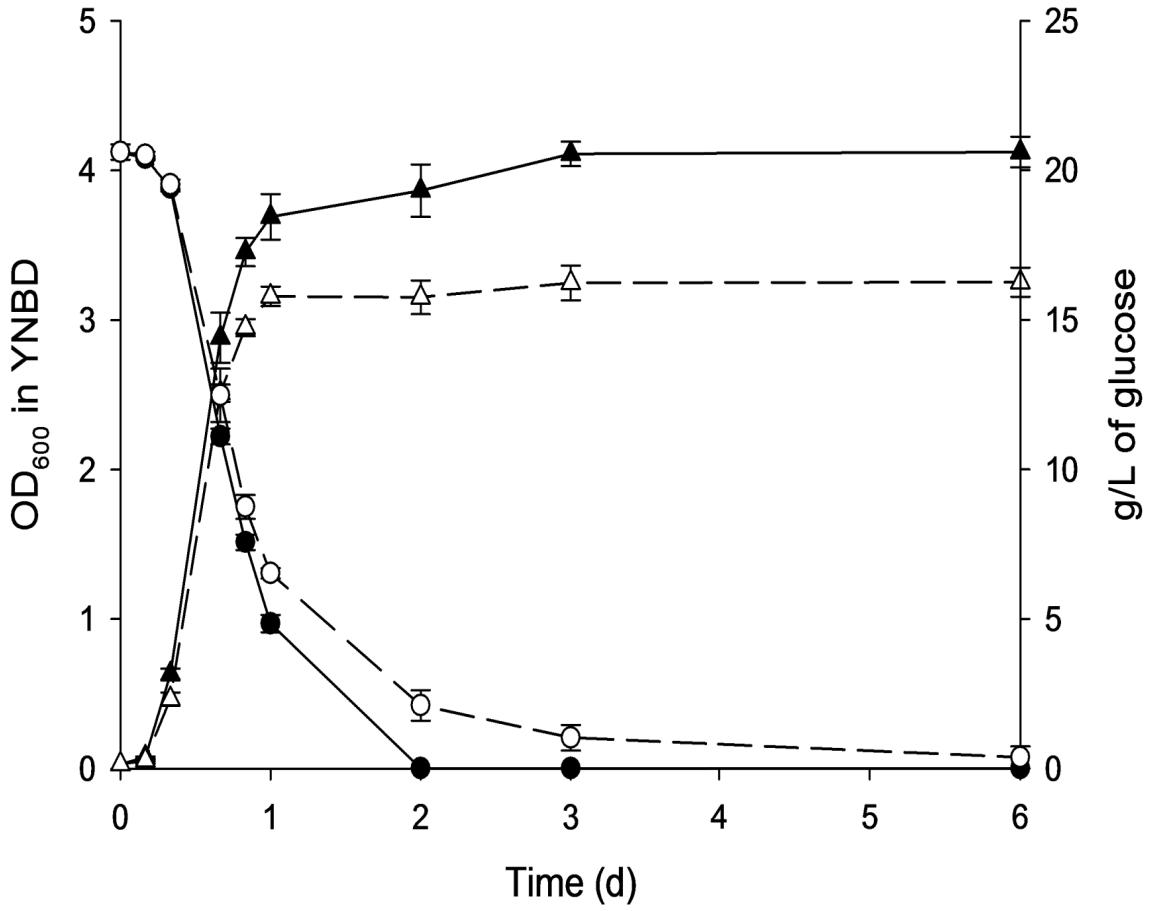

Figure 4-1. Cell growth and metabolic conversion profiles of S. cerevisiae WT and R57 mutant strains. Overnight YNBD cultures of WT (solid symbols) and R57 (open symbols) were inoculated into 50 mL of YNBD medium with an initial OD_{600} of 0.03 (0 h) and then cells were cultured at 200 rpm at 30 °C in 250-mL flasks. Cell growth (left y-axis, triangles) was monitored by measuring OD_{600} at 4, 8, 16, 20, 24, 48, 72 and 144 hours. Glucose (right y-axis, circles), concentration in the medium was determined by HPLC.

mutant. Functional clustering was carried out on the differentially expressed genes to discover enriched functional roles of gene products and biological pathways of interest (Fig. 4-2).

4.3.3 The expression of gene products involved in nitrogen usage, cell membrane composition and transport, metal-binding and NADH-generating alcohol biosynthesis are downregulated in HWSSL-tolerant strain R57

Only 18 genes were downregulated under inhibitor free conditions, resulting in 3 clusters of genes that are highly enriched (Fig. 4-2). The first major downregulated gene cluster contains 8 genes that are classified as integral to the membrane. This cluster contains 4 genes that encode transporters: *MEP3*, producing a low-affinity, high-capacity ammonia transporter that is normally induced upon exposure to ammonia; *CAN1*, which encodes a permease of arginine, a preferred nitrogen source that can readily be catabolised to glutamate (311); metal transporter-encoding *SMF2*; and the *PHO90* gene, encoding a low-affinity phosphate transporter. The remaining genes in the integral to membrane downregulated cluster are *AIM38*, encoding a cytochrome c oxidase subunit, and 4 genes related to the altered biosynthesis or manipulation of lipid membrane constituents: *CYB5*, cytochrome b5, involved in the sterol and lipid biosynthesis pathways; *ERG11*, part of the ergosterol biosynthesis pathway; *PLB3*, which leads to the hydrolysis of phosphatidylinositol and phosphatidylserine; and *SUR2* involved in sphingolipid biosynthesis. Due to the toxic environment of HWSSL and the membrane damaging potential of the various inhibitors like phenolics and organic acids (7), altered interaction with the environment via differential regulation of transporters and modifications to membrane composition are expected traits of R57. Differential regulation of genes encoding proteins that are involved in metal influx and usage are also traits that distinguish R57 from the WT in an inhibitor-free environment. As shown in the enrichment map (Fig. 4-2), there is extensive overlap between gene products that affect

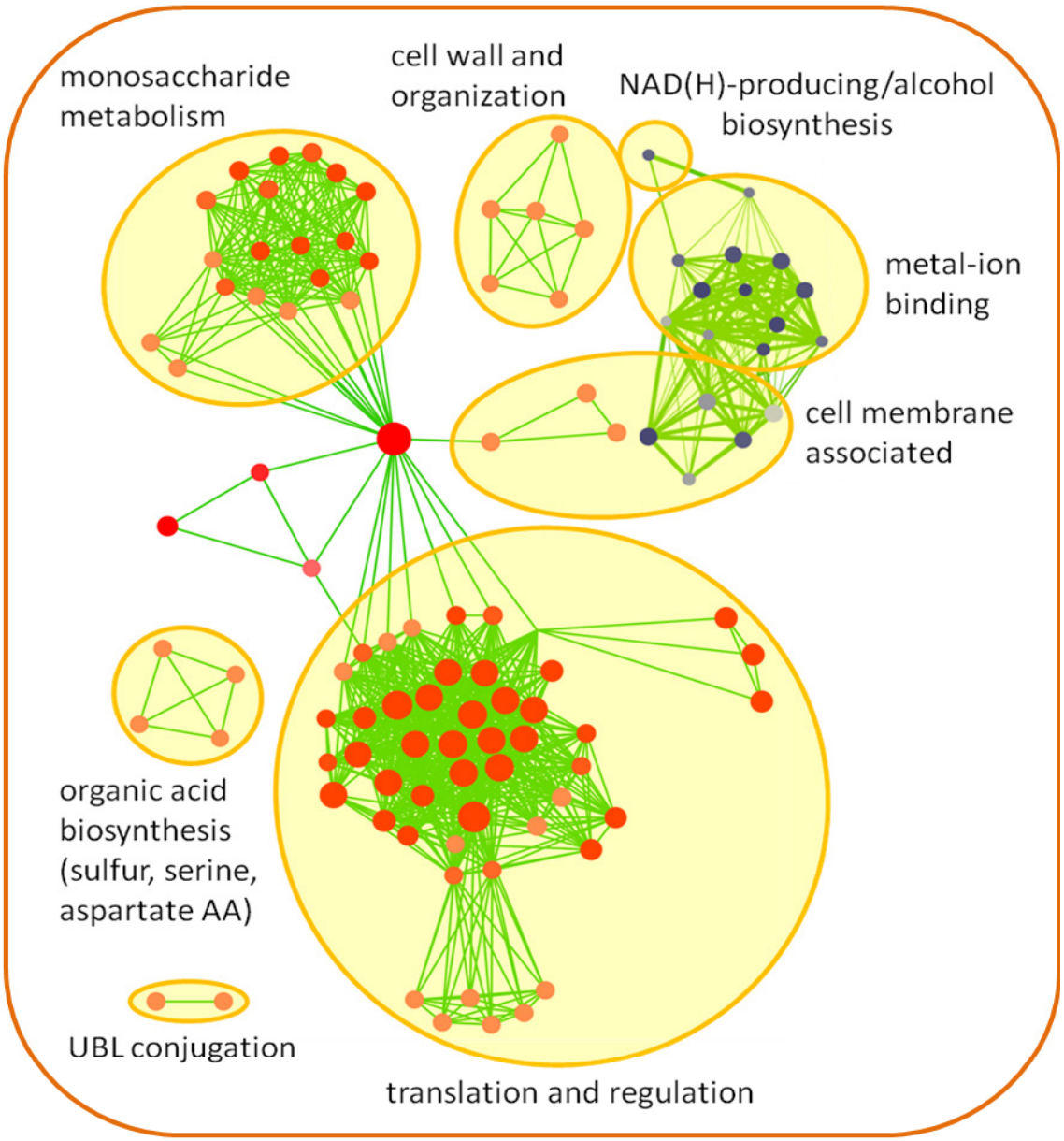

Figure 4-2. Enrichment map of differentially expressed genes between WT and R57 under non-HWSSL exposed conditions. Gene lists were compiled for significantly ($p < 0.05$) upregulated > 2-fold or significantly downregulated < 2-fold differentially expressed genes. Red colours represent upregulation, while blue colours represent downregulation. Darker shades represent a relatively higher confidence of enrichment score. Larger node sizes represent relatively larger numbers of differentially regulated genes associated with the given ontology category. Smaller distance between nodes denotes a higher degree of relationship between ontology categories, while thicker edge lines (green) denote a higher degree of similarity between category nodes in terms of the degree of overlap between the specific gene sets they are associated with.

the plasma membrane and those that bind metal. Eight metal-ion binding genes are downregulated, including 4 that encode iron-binding proteins and the aforementioned transporter Smf2p. One of these iron-binding proteins is Gzf3p, a negative regulator of nitrogen catabolite repression (NCR), which competes for DNA GATA-factor binding sites with Gat1p, a positive regulator of NCR-sensitive genes (312). This finding suggests a downstream upregulation of NCR-sensitive genes may be possible due to diminished Gzf3p content. Therefore, diminished expression of *GZF3* can result in the upregulation of genes involved in the metabolism of non-preferred nitrogen sources and, taken with the downregulation of *MEP3* expression, mentioned above, suggests that R57 is making use of nitrogen in divergent ways from the WT at this growth phase, even under conditions without inhibitors in the substrate. Overall, enrichment of genes related to known metal-requiring processes and transporters suggests that R57 is making use of metal resources differently than the WT as well and the diversity of metal-requiring cellular processes makes possible downstream effects extensive.

4.3.4 Functional clustering of upregulated genes in HWSSL-tolerant mutant R57 under non-stressed conditions reveals differential expression of primary metabolic systems, organic acid synthesis, ubiquitin-controlled products and cell wall affecters

Clustering of the 131 upregulated R57 genes as compared to the WT include the major cluster of translation-related genes, mainly associated with ribosome biogenesis and translation regulation (Fig. 4-2). Fifteen genes related to monosaccharide metabolism are also upregulated (Fig. 4-2), with 10 being part of the glycolytic/gluconeogenic pathways. These two findings suggest a more active metabolism in stationary phase and agree with growth differences between the WT and

R57 (Fig. 4-1). The residual carbon available in the substrate of R57 after extended growth in SD medium, once it has entered into stationary phase, that is not used for biomass generation, may be available for energy generation and protein production. The remaining 2 genes in the monosaccharide metabolism cluster are noteworthy as they include *GRE3*, encoding for a methylglyoxal reductase, that has been shown to reduce furan aldehyde inhibitors via NADH (313), and the R57 mutation-bearing transcription factor *NRG1*, discussed further below.

The ubiquitin-like (UBL) conjugation cluster (Fig. 4-2) contains genes that encode for proteins that are either post-translationally modified by a ubiquitin-like protein, or play a role in protein breakdown via ubiquitin-mediated proteolysis. The cluster consists of 7 ribosomal proteins including *RPL40B/UBI2* and *RPS31*/*UBI3*, which are 2 of the 3 genes (*RPL40A*/*UBI1* being the other) known to encode ribosomal proteins fused to the C terminus of ubiquitin, yielding the majority of free cellular ubiquitin under normal conditions (314). The non-ribosomal proteins include: histone-encoding *HTA2*; *RHR2*, involved in glycerol biosynthesis in response to osmotic stress, which is generally downregulated under stress-free environments; *PUN1*, which is induced by the HOG pathway, cell wall perturbations and metal-ion stress and is involved in cell wall patching; and *ENA5*, encoding a sodium ion pump similar to Ena1p, as discussed earlier (Chapter 1), which is upregulated 3.2-fold and is directly regulated by Nrg1p (315). This cluster consists of genes with divergent functionalities, but mainly involves genes related to ubiquitin generation, protein translation machinery or stress response mechanisms. Given that ubiquitin-like signalling machinery influences all of them, this regulatory

mechanism may be playing a determinant role in the HWSSL-tolerance phenotype by providing protein-level control beyond the differential expression response reported here.

Another major upregulated gene cluster in R57 contains 11 genes involved in organic acid synthesis, mainly involving amino acid biosynthesis (Fig. 4-2). Specifically upregulated genes include, *HOM2*, *MET16*, *MET17* and *MET3* that encode proteins that lead to the synthesis of the sulfur-containing amino acids cysteine and methionine. Furthermore, these 4 genes along with *HOM3*, *LYS9* and *LYS12* are upregulated as well and encode for proteins that lead to serine-family amino acid, including lysine, and aspartate-family amino acids, including glutamate, biosynthesis. Upregulated *BAT1* also provides a means to form glutamate from valine, leucine and isoleucine precursors. Again, a modified nitrogen metabolism seems likely in R57 based on the upregulation of amino acid biosynthetic pathways. The final genes in this cluster are *TPI1*, a hub of the glycolytic pathway, and *FEN1* and *SUR4*, which are both involved in sphingolipid biosynthesis. Sphingolipid metabolism has been linked to acetic acid tolerance (139) by affecting assembly of the vacuolar membrane H^+-ATPase and trafficking of plasma membrane nutrient transporters and H^+-ATPase Pma1p (316, 317).

Ten cell-wall associated genes that are upregulated in WT vs R57 and include those encoding Yps6p, Cis3p, Cwp1p, Ecm33p, Srl1p, Ccw12p and Utr2p, which can all be linked to maintaining cell wall stability and integrity. Furthermore, 5 cell membrane-associated genes are upregulated including *ECM33*, *YPS6*, *ENA5*, *PUN1* discussed above, along with *GAS1*, encoding for a membrane-anchored protein involved in cell wall biosynthesis. Functional enrichment of these two clusters in R57 demonstrates that cell-

surface rearrangements are taking place in accordance with predicted HWSSL-tolerance mechanisms (Chapter 1).

4.3.5 Highly upregulated R57 genes are associated with the cell wall, stress resistance or nitrogen usage

Of the upregulated genes between the WT and R57, there were 11 that were highly upregulated (> 5-fold). These include YLR012C, a gene of unknown function, which is upregulated 44-fold. *GAT3*, upregulated 23-fold, encodes a protein product that, like Gat1p, is annotated as a GATA-family zinc finger containing protein and is a likely transcription factor. The ability of the GATA factors to compete for cis-acting GATAAG promoter sequence elements is influenced by nitrogen source availability (312, 318). *GAT3*, therefore, may be viewed as an attractive reverse engineering target due to its probability of affecting transcriptional regulation and its possible involvement in modifying nitrogen usage. Furthermore, YLR012C and *GAT3* are adjacent on chromosome XII and code in opposite directions suggesting this region of the chromosome is being targeted for transcriptional upregulation and one or both of these genes may be fundamental to the HWSSL-tolerant phenotype. Additional highly-upregulated genes pertinent to the HWSSL-tolerance trait, based on known function, include: YOL014W, which has been related to acid resistance (319); cell wall stability and maintenance protein-encoding genes *YPS6*, *SLR1*, and *CWP1*, which has also been linked to propionic acid resistance and is known to be induced as part of the HOG response (320); *TDA6*, which is induced by DNA damage (321) and is a known target of acetic acid-induced activation by Haa1p (139); *RHR2*, mentioned above; and YIL029C, which is involved in pH acid resistance (319), with its deletion leading to glutathione

excretion (322). Finally, *NRG2* is upregulated ~ 5-fold. *NRG2* is paralogous to mutation-bearing *NRG1*, and is known to mediate similar responses like glucose repression, pseudohyphal growth, and stress resistance (245, 248, 315). Overall, the genes most upregulated in the R57 mutant are involved in cell wall composition and stability; acid pH resistance; osmotic pressure resistance; or are transcriptional regulators involved in nitrogen catabolism or stress resistance. Modification to all of these biological roles are expected counterparts of complex inhibitor-resistance traits and the high level of transcriptional upregulation displayed by these genes make them valuable targets for future study.

4.3.6 R57 transcriptional response to HWSSL exposure

In order to assess if any parallels exist between the function of R57 mutation-bearing genes and the transcriptional response of R57 when faced with a HWSSL challenge, cultures of cells were exposed to HWSSL for 0, 2 and 24 hours were also subjected to RNA-seq analysis.

4.3.7 Functional clustering of R57 genes after 2 hours of HWSSL exposure shows that central metabolic processes are downregulated

Clustering of the 401 downregulated genes reveals mainly changes in transcript levels of central carbon metabolism, mitochondrion, energy generation, storage carbohydrate biosynthesis, and membrane-associated proteins (Fig. 4-3). Although the decrease in central metabolism and energy generation and storage is expected based on similar 2-3 hour stress response studies performed by Gasch *et al*. (27), those studies, which defined the environmental stress response for *S. cerevisiae*, typically showed that

translation and transcription were similarly downregulated as an overall depression of metabolic and biosynthetic machinery in response to stress. However, as the protein biogenesis machinery is upregulated for this timepoint (Section 4.3.8), R57 cells are likely actively fulfilling protein biosynthesis requirements early on, despite the repression of energy generation abilities. Nevertheless, the repression of mitochondria-related/energy generation gene expression, coupled with the upregulation of storage carbohydrate biosynthesis genes suggests that R57 cells are entering into a state of resource preservation.

Another major downregulated cluster is comprised of genes encoding 147 membrane-targeted proteins, which supports the WT vs R57 RNA-seq findings that suggest cell-surface reconfiguration is indicative of the HWSSL-tolerance response given the altered expression response of R57 under non HWSSL-exposed conditions.

As expected with a HWSSL challenge, stress response-related genes are differentially expressed after 2 hours exposure in HWSSL. The 45 genes that cluster as related to stress response encode for proteins that have a wide variety of functional annotations including 34 related to heat response. Within the stress response cluster are 10 genes encoding proteins related to protein folding or refolding including *HSP10*, *HSP60*, *PHB2*, *AHA1*, *CPR6*, and *ERV2*, as well as 4 Hsp70s including *SSC1*, *SSC3*, *SSE1* and *SSA3*. Linked to the stress response, 51 macromolecular and vacuolar protein degradation-related genes are also overrepresented as downregulated. This finding along with the downregulation of genes related to protein re/folding demonstrates that the protein homeostasis machinery of the cell is affected by HWSSL exposure.

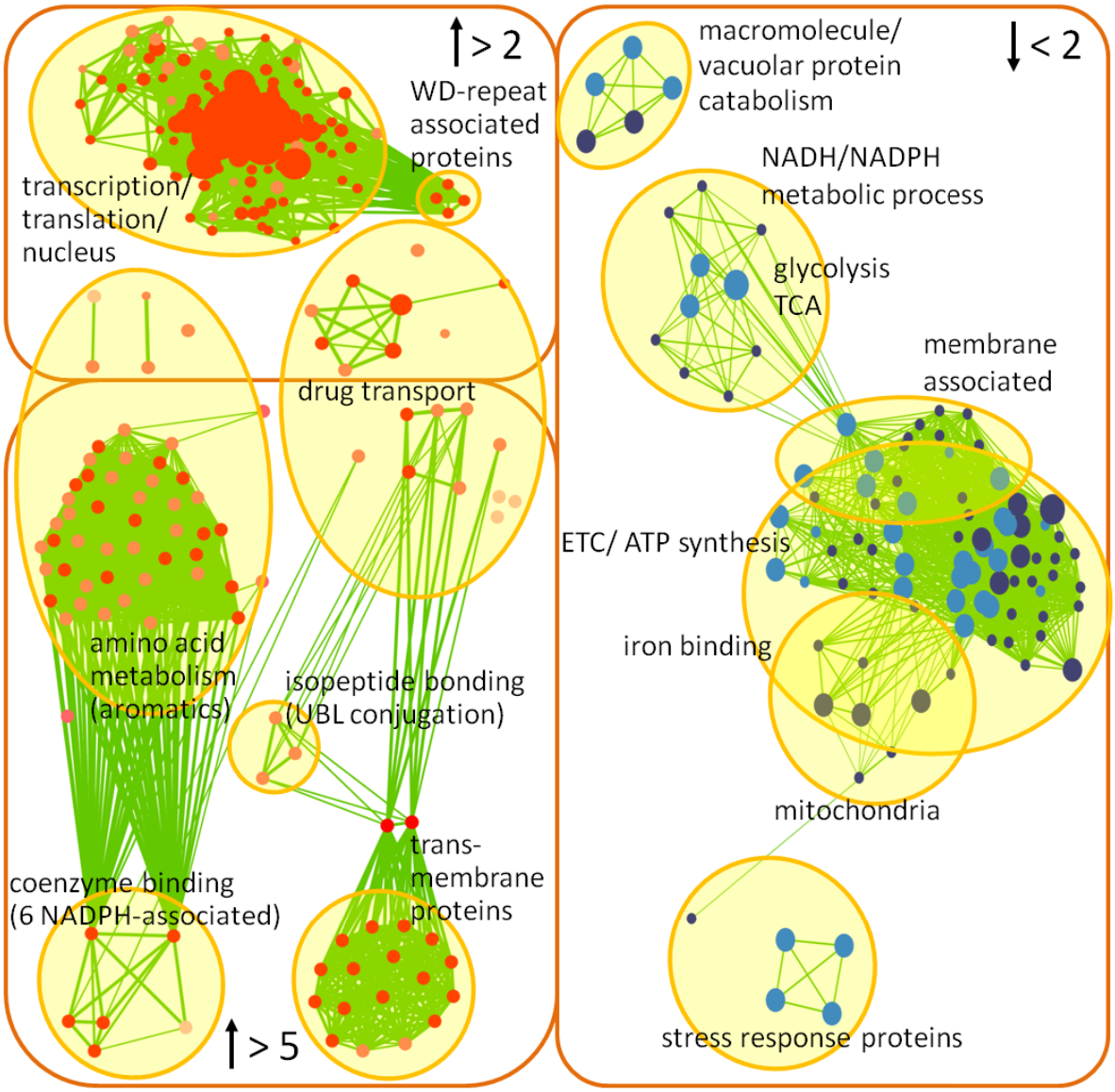

Figure 4-3. Enrichment map of differentially expressed genes between R57 under non-HWSSL exposed conditions and after 2 hours HWSSL exposure. Gene lists were compiled for significantly ($p < 0.05$) upregulated > 2-fold (top left panel) or > 5-fold (bottom left panel) or significantly downregulated < 2-fold (right panel) differentially expressed genes. Node and edge colours and sizes are represented as described for Fig. 4-2.

Genes related to NADH/NADPH-associated metabolic processes are downregulated (Fig. 4-3), including *SOL4* and *GLN2* from the oxidative branch of the pentose phosphate pathway and *UTR1* that is capable of phosphorylating NAD+/NADH to NADP+/NADPH. This finding again suggests that these key cofactors are being affected by HWSSL exposure and that NADPH generative processes are affected in particular.

Finally, fourteen genes encoding iron-binding proteins are also downregulated, including 10 from the ETC (Fig. 4-3). Mutation-bearing *FIT3*, encoding an iron-transporter, is included in this cluster, as well as thioredoxin-encoding *TRX2*, which is involved in protecting cells against oxidative and reductive stress. This finding further supports an important role for iron in modified HWSSL tolerance.

4.3.8 R57 genes showing increased expression after 2-hour exposure to HWSSL are associated with translation, transcription and amino acid catabolism

Over the first 2 hours of exposure to HWSSL the initial pulse differential transcriptional response of R57 involves the upregulation of 856 genes, mainly related to primary metabolic processes. Functional clustering of the upregulated genes results in 8 functional clusters bearing enrichment scores > 1.3 that are all related to translation (mainly comprised of genes related to ribosome biogenesis and rRNA processing), transcription (mainly comprised of genes related to RNA polymerase activity) and proteins that localize to the nucleus (Fig. 4-3). One of the two remaining upregulated clusters contain genes encoding proteins that have WD40 repeat domains, which tend to relate to fundamental metabolic processes like ribosome and chromatin assembly and cell cycle regulation.

Both anabolic and catabolic amino acid pathway genes also form enriched increased expression clusters (Fig. 4-3). Genes of particular note related to catabolism in this cluster are *PUT4*, required for high affinity proline transport; *UGA2*, a succinate semialdehyde dehydrogenase-encoding gene involved in gamma-aminobutyrate utilization as a nitrogen source; along with *AAT1*, an aspartate aminotransferase gene, and *ASP1*, an asparaginase gene, which can both lead to the formation of glutamate from aspartate. An additional gene, *CHA1*, encodes a serine/threonine deaminase that is required to use these amino acids as the sole source of nitrogen for *S. cerevisiae* leading to generation of ammonia and 2-oxobutanoate, a compound that can lead to ammonia reassimilation by generation of the compounds homoserine and O-succinyl-homoserine or biosynthesis of cystathione from cysteine and ammonia by way of *CYS3*, a gene that is upregulated 1.8-fold between the WT and R57 and a further 2.7-fold at this R57 timepoint. Additionally, anabolism-related genes that encode proteins belonging to the aromatic amino acid super-pathway are also upregulated and enriched at this timepoint. These include Trp3p and Trp4p, which catalyze consecutive steps in the anabolic tryptophan pathway, with Trp3p generating glutamate and pyruvate in catalyzing the reaction of chorismate to anthranilate. Similarly, Aro7p and Tyr1p, are also part of this cluster and catalyze consecutive steps in the tyrosine/phenylalanine branch of the aromatic amino acid synthesis pathway. The final genes in this cluster encode for Aat1p, mentioned above, and Aro9p, which catalyzes the final step in tyrosine and phenylalanine generation and is notable as being one of two enzymes in *S. cerevisiae* that catalyze these reactions, while the other Aro8p (not significantly upregulated at this timepoint) requires glutamate as a co-substrate. Enrichment of this cluster is of interest based on the

determinant role that has already been assigned to aromatic amino acid synthesis by acetic acid tolerance studies (66, 207) and demonstrates that R57 is exhibiting similar expression profiles. Furthermore, the differential expression of genes in this cluster again suggests an alternative route for nitrogen compound generation, particularly glutamate, and ammonia usage other than the expected route via Gdh1p (Chapter 3, section 3.4.2), even though HWSSL fermentation has only progressed for 2 hours and ammonia levels are expected to remain high.

Finally, 10 genes annotated as being involved in cellular drug response (Fig. 4-3) are also upregulated after 2 hours of exposure to HWSSL including: *PDR12*, *PDR5*, *TPO1*, *TPO2*, *TPO3*, *TPO4*, *QDR1*, *QDR2*, *AQR1* and *SNQ2*. All of these genes encode for proteins from the major facilitator family of multi-drug resistance proteins and are responsible for efflux of various compounds from the cell, conferring resistance to a multitude of toxicities. Pdr12p is known to

impart resistance to organic acids (36), while Pdr5p is exceptional for its ability to impart tolerance to a multitude of potentially toxic compounds, such as mutagens, fungicides and cations (323). Tpo1-4p are involved in the efflux of polyamines from the cell, while Tpo2p and Tpo3p can also provide protection against acetic, propionic, and benzoic acids (38). Like *TPO1-4*, *QDR2* encodes for a protein from the drug:H^+ antiporter-1 family. Qdr2p is known to impart quinidine tolerance, but it was recently shown to be involved in potassium uptake and to impart increased fitness under potassium limitation (324). *QDR2* overexpression can lead to the excretion of 18 different amino acids, either inadvertently or directly (324). In this way, many of the known constituents of the PDR

are linked to nitrogen metabolism in accompaniment to their roles in toxic compound efflux, a trait of interest in HWSSL tolerance.

4.3.9 Functional clustering of genes showing highly increased expression in R57 after 2 hours of HWSSL exposure support roles for the PDR, UBL-conjugation, NADPH-related processes and aromatic amino acid metabolism

When highly upregulated > 5-fold (115 gene transcripts) are clustered based on functional annotation (Fig. 4-3), 8 drug transport genes associated with the membrane and efflux of compounds from the cell are also enriched, including *PDR5*, *PDR12*, *QDR2* and *TPO1, TPO 2,* and *TPO4*, discussed above. The final two highly upregulated genes in this cluster are *PUN1*, discussed below, and *PUG1*, involved in heme efflux.

UBL conjugation and genes involved in isopeptide bonding are overrepresented with 8 being highly upregulated (Fig. 4-3). Two of these genes overlap with the drug response cluster, *PDR5* and *PDR12* being affected. This cluster also includes *GNP1*, upregulated 9-fold, which encodes for a permease involved primarily in the transport of glutamine, but is also known to transport leucine, serine, threonine, cysteine, methionine and asparagine and supports the theory that nitrogen assimilation is taking place via routes other than mutation-bearing Gdh1p. For example, the presence of glutamine makes it possible to generate glutamate via Glt1p (NADH-dependent glutamate synthase) (325). Another gene in this cluster that may be highly relevant to the HWSSL tolerant phenotype is *PUN1*, which is involved in maintaining cell wall integrity under stress conditions that induce cell wall damage and ion stress (282, 326-328), but is also involved in signalling due to nitrogen deprivation conditions (329). *PUN1* is upregulated 7-fold during the first 2 hours of exposure to HWSSL and also 2.5-fold between WT and

R57 under unstressed conditions. Xu *et al*. showed that Pun1p doubles in abundance in nitrogen stressed cells, and deleting *PUN1* abolishes filamentous growth in both haploids and diploids (329). Related to the filamentous growth trait is perhaps the most well-known regulator of pseudohyphal growth, Phd1p, a transcription factor which interacts with the same Cyc8p-Tup1p complex as Nrg1p (330, 331). The gene encoding this protein, *PHD1*, is also upregulated 2.3-fold in R57 at this timepoint. Pseudohyphal growth has long been known to accompany nitrogen limitation (332) and is yet another indicator that an early response of R57 to HWSSL is modified nitrogen metabolism towards a state of starvation and scavenging for non-preferred sources of nitrogen. Finally, *CDC20* is upregulated in this cluster; Cdc20p is known to direct ubiquitination of anaphase inhibitor proteins. Upregulation of this cluster of UBL-affected genes provides further evidence that the ubiquitination machinery of the cell, and proteins that are regulated by it, are playing roles in the HWSSL tolerance trait and that the nitrogen-usage-related genes contained here are possibly being subjected to expression regulation at the level of transcription and the protein level by a modified ubiquitination machinery.

There are also 9 proteins that cluster as involved in cofactor binding (Fig. 4-3), with 6 being NADPH-dependent. This cluster includes *GRE2*, coding for an NADPH-dependent methylglyoxal reductase, which has already been shown to detoxify furfural (333). Similarly, YKL071W, though below the threshold for this clustering experiment, is upregulated 3.5-fold after 2 hours HWSSL exposure and is induced by furfural stress and carries out NADPH-dependent reduction of the toxin (279). Included in this cluster is *FDH1*, upregulated 5-fold, which catalyzes formate detoxification to CO_2 via NAD(+) (175) and may therefore play an important role in protecting against the formic acid stress

that is often found in lignocellulosic hydrolysates, while providing NADH for detoxification reactions of furfural and HMF (37). This cluster is significant in that it provides further evidence that the NAD(P)H cofactor usage of R57 is affected by HWSSL exposure and that expression of known tolerance genes to furan aldehyde inhibitors are playing a role.

Finally, genes involved in amino acid metabolism cluster as highly upregulated as well over 2 hours HWSSL exposure by R57. Aromatic amino acid metabolism genes, discussed above as upregulated > 2-fold, are highly upregulated as well, along with amino acid catabolism genes, outlining the probable importance of this pathway in response to HWSSL.

4.3.10 Differential expression of R57 genes over 24 hours of HWSSL exposure are indicative of suppressed metabolism; cell surface changes including transport; and drug and stress responses

Over 24 hours of exposure to HWSSL, the vast majority of differentially regulated genes are downregulated (2737 genes), signifying a widespread decrease in transcription likely due to toxicity or poor nutrient availability and a general suppression of metabolism. However, 161 genes were significantly upregulated > 2-fold over 24 hours of exposure to HWSSL for R57 (Fig. 4-4). Functional clustering revealed that 49 genes encoding membrane proteins were upregulated including 13 associated with transmembrane transport comprised mainly of 4 sugar transporter genes and 7 organic acid transporters. The organic acid transport-associated genes include *ADY2* and *ATO3*, which are both believed to transport excess ammonia out of the cytosol as a part of a yeast acid-to-alkali transition system that accompanies a slow-growth trait and imparts the ability to shift

metabolism out of a stationary state to emerge from stressful conditions and survive for longer periods (334). This system is thought to operate as a long-range signal between yeast cells that helps mediate metabolic shifts between close cells to aid in overcoming stress challenges (334). Included in this cluster is *AQR1*, also upregulated over 2 hours HWSSL exposure, which confers resistance to acetic acid and is hypothesized to mediate acetate excretion (335), but was shown to be involved in homoserine, threonine, glutamate, aspartate and alanine excretion (336). The upregulation of these nitrogen compound excretion-related genes are indicative of exposure to excess nitrogen (337). However, 2 genes of this cluster also mediate uptake of amino acids. Namely, *PTR2* has been shown to encode a transporter of di-/tripeptides and *BAP3* encodes for an amino acid transporter of isoleucine, leucine, valine, cysteine, methionine, phenylalanine, tyrosine and tryptophan. In relation, 3 genes involved in aromatic amino acid catabolism to indole-3-ethanol are also enriched for increased expression (Fig. 4-4). Five genes related to amine transport show increased expression including *BAP3* and *AQR1*, as well as *TPO1, TPO2* and *TPO4*, mentioned earlier as highly expressed for 2 hours exposure to HWSSL and remain upregulated over 24 hours, which lead to the catalysis and excretion of various polyamines at acidic pH. Again, the response to nitrogen-containing compounds of R57 after HWSSL exposure seems nuanced, affected at the transcriptional level both at genes that would tend to suggest nitrogen intake, through amino acid and peptide uptake and degradation, and those that lead to nitrogen compound excretion. This finding further supports a primary role for nitrogen usage and amino acid metabolism as key determinants in the HWSSL-tolerance trait.

In addition to membrane-associated proteins, genes associated with the cell wall are also enriched as upregulated over 24 hours of exposure to HWSSL. These include *CWP1*, already shown as highly upregulated (13.6-fold) between the WT and R57, is upregulated here an additional 3.3-fold. In addition to the role *CWP1* plays in propionic acid resistance (319), it has been related to increased cell wall thickness (338) and copper resistance (339). This cluster also contains cell wall-maintenance associated gene YLR194C; *GAS1* (also upregulated between WT and R57, discussed above); along with 1 probable glucosidase and 2 probable glycosidase genes(*SCW10*, *CRH1* and *CRH2*, respectively), all three of which are involved in cell wall architecture. *YGP1*, encoding a secretory glycoprotein, is induced by nutrient deprivation and by acetic acid exposure as induced by Haa1p (139). Finally, *SSA2*, encoding an Hsp70 protein, included in this cluster due to its known association with the cell wall, is known for its protein folding activity and homology to *SSA1*, as discussed earlier (Chapter 3, section 3.4.3.).

SSA2 may also be grouped along with 14 stress response genes upregulated over 24 HWSSL exposure (Fig. 4-4). Other genes of particular note within this cluster include: *SSA4*, encoding another Hsp70 protein that is only transcribed under stress conditions and *MSN4*, which encodes for a stress response transcription factor that plays a role in regulating the response to various stressors including heat, osmotic, oxidative and organic acid pressures. The final upregulated cluster between 0 and 24 hours HWSSL exposure contains 6 genes that are associated with drug response. These also include the aforementioned *TPO1*, *AQR1*, *PDR5* and *QDR2* that were all highly upregulated after 2 hours exposure to HWSSL and also remain upregulated over 24 hours exposure. Additionally, *PDR16*, encoding for a phosphatidylinositol transfer protein is

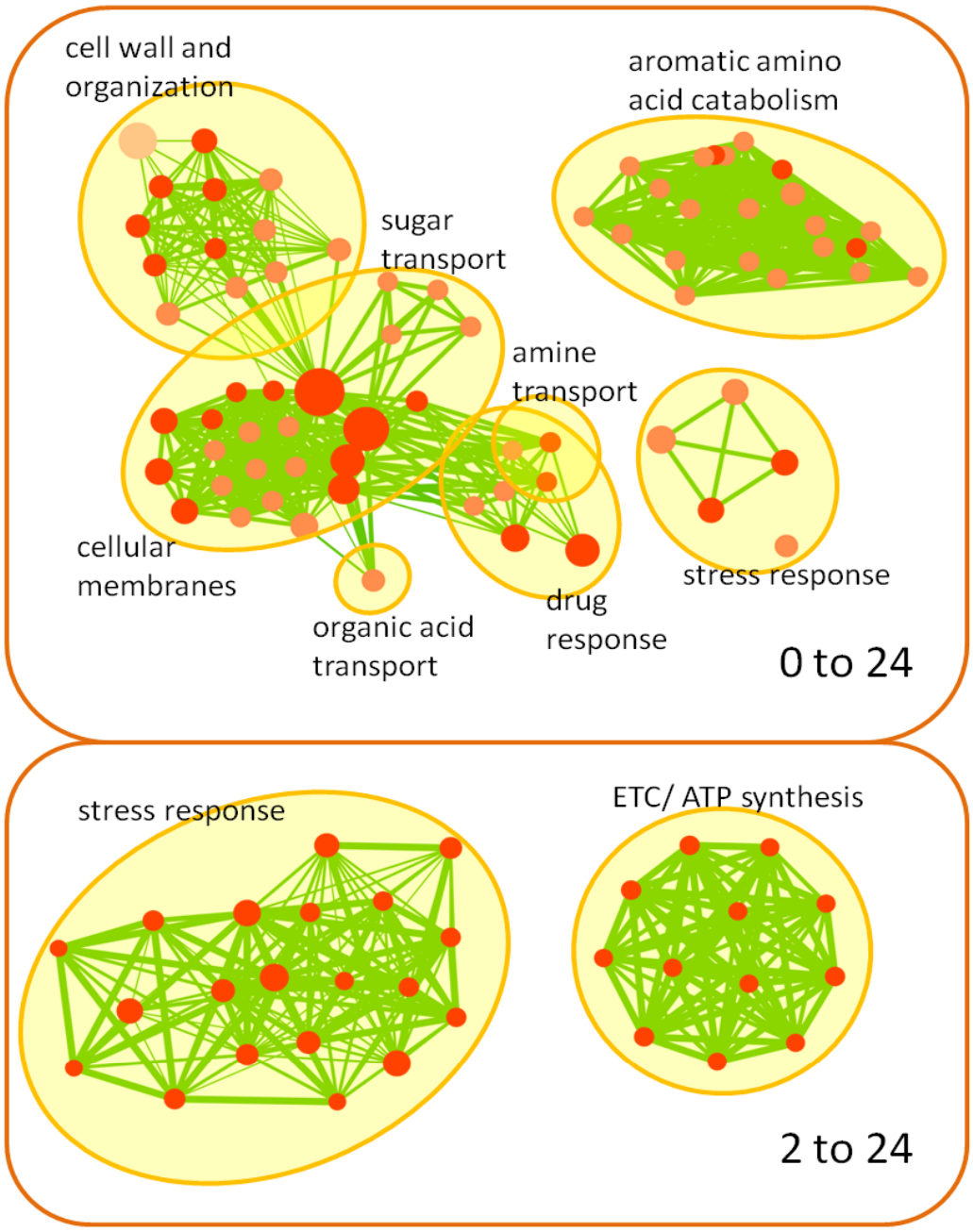

Figure 4-4. Enrichment map of differentially expressed genes between R57 under non-HWSSL exposed conditions and after 24 h HWSSL exposure and between 2 and 24 hours HWSSL exposure. Gene lists were compiled for significantly upregulated > 2-fold differentially expressed genes for 0 to 24 hours HWSSL exposure and significantly ($p < 0.05$) upregulated > 1-fold differentially expressed genes for 2 to 24 hours HWSSL exposure. Node and edge colours and sizes are represented as described for Fig. 4-2.

known to control levels of various lipids and may regulate lipid synthesis (340) is also represented, which correlates well with the differential expression of a relatively high number of membrane-associated genes. Therefore, drug response genes are not only highly upregulated over the first 2 hours HWSSL exposure, but also maintained at elevated levels over 24 hours exposure, supporting a role for this class of genes in HWSSL tolerance.

4.3.11 Differential expression analysis of 2 vs 24 hour HWSSL-exposed R57 cells reveals an integral role for Hsp70s and associated proteins

Environmental stress responses tend to be transient and expression levels often re-equilibrate after initial exposure to the stressor (27). Therefore, in order to assess any expression differences that might occur after the relatively short 2-hour exposure to HWSSL, an RNA-seq analysis on R57 was also carried out for differential expression between 2 and 24 hours exposure to HWSSL, which might constitute a sustained, specific response to HWSSL (Fig. 4-4). During this time, 4079 genes were significantly differentially expressed > 2-fold, with 4066 showing downregulation, indicative of a large-scale suppression of intracellular metabolism. The threshold was dropped from > 2-fold to > 1-fold significant expression increases for enrichment clustering due to the apparent global downregulation of mRNA expression, suggesting any significant increase in expression may be important to HWSSL tolerance. Only 48 genes showed a significant increase in expression or upregulation > 1-fold. These were clustered for functional enrichment analysis, revealing that 2 discreet functional groups were overrepresented. The most significant grouping, comprised of 3 major GO term clusters, share many of the same 18 genes and relate to stress response, protein folding and abiotic

stimulus. Twelve genes relate to protein folding and include 5 genes: *SSA1*, *SSA2*, *SSA4*, *SSE1*, *SSE2* that all encode Hsp70s with similar protein folding chaperone activities to *SSA1*, discussed previously. Transcripts of Hsp70 co-chaperones are also upregulated including *FES1*, encoding an Ssa1p nucleotide exchange factor and 3 genes encoding Hsp40 DNA J proteins: *YDJ1*, *SIS1* and *APJ1*. Hsp40 proteins stimulate the otherwise low level of ATPase activity of Hsp70 proteins, facilitating interaction with polypeptide substrates (341). Ydj1p is the regulating partner of Ssa1p, Ssa2p, and likely Ssa3p and Ssa4p (342) and when overexpressed, cures prion propagating cells (343, 344). Sis1p also stimulates Ssa1p activity (345). Apj1p has no known specific partner, but its overexpression also leads to reduced [PSI+] prion formation (344). Upregulation of Hsp70s and their co-chaperones points to an increased protein folding response and accelerated ATPase activity. Increased protein folding activity is also substantiated by upregulation of *CPR6*, encoding a peptidyl-prolyl cis-trans isomerase that accelerates folding. Other Hsps that are part of this cluster include *HSP26* and *HSP40*, which encode for small protein folding chaperones that prevent protein aggregation. *HSP26* is known to be upregulated, along with *SSA4*, in response to furan-aldehyde and acetic acid stress (139, 346). The tendency of harsh conditions to damage proteins and lead to aggregation (17) likely makes the role of these genes important for sustained tolerance. Other genes within this grouping that are functionally related to HWSSL-tolerance include: YJL144W, which shows induced expression under osmotic pressure and encodes for a hydrophilic protein that is essential in the desiccation-rehydration process (347); and *SPI1*, encoding a cell-wall protein involved in weak acid resistance that is controlled by transcription factors Msn2p, Msn4p and Haa1p (319, 348).

Finally, 4 genes that are part of the enriched oxidative phosphorylation cluster are also upregulated (Fig 4-4), which may signify a partial recovery from the metabolic suppression that accompanies exposure to lignocellulosic hydrolysate inhibitors as shown in the 2-hour HWSSL exposure expression data presented in this study.

4.3.12 Expression levels of mutated R57 genes are affected between the WT and R57 and during HWSSL exposure

The mutated genes accumulated in R57 were examined across each of the RNA-seq experiments described above. For the WT vs R57 under non-HWSSL exposed conditions, only *NRG1* was significantly differentially expressed and is discussed in more detail below. Upon exposure to HWSSL, 11 of the mutated genes show significant differential expression (Fig. 4-5). Four of the affected genes show downregulation between 0 and 2 hours HWSSL exposure and a further expression reduction from 2 to 24 hours, which includes *PBP1*, *FIT3*, *GSH1*, and *MAL11*. Of these 4 genes, *MAL11* shows the most marked decrease in expression of ~4 and 6.5-fold at 2 and 24 hours, respectively (discussed below). The decrease in expression shown by these genes due to HWSSL exposure suggests they are affected by the substrate directly or are being downregulated as part of the R57 HWSSL-tolerance response. Each of the genes, aside from *SSA1*, show a general downregulation between 2 and 24 hours, following the general trend of decreased expression for the majority of *S. cerevisiae* genes at this timepoint. *SSA1*, however, though showing slight downregulation over 2 hours, shows increased expression over 24 hours, similar to the other Hsp70 proteins and their co-regulator transcript levels at this timepoint, as discussed above. *GDH1* and *NOP58* show increased expression over 2 hours HWSSL exposure and return to unstressed expression levels

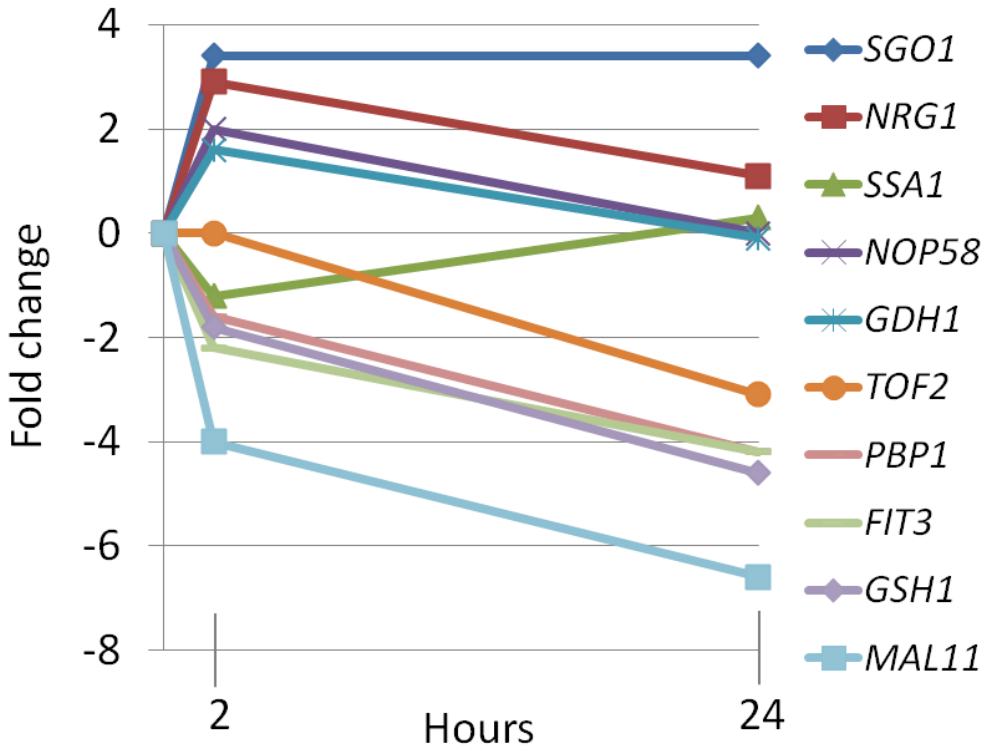

Figure 4-5. Differential expression of mutated R57 genes when exposed to HWSSL after 2 and 24 hours.

after 24 hours, which suggests they may be playing a role in early stress response, or their expressions are being influenced by another cue such as renewed nutrient availability. The known functions of *GDH1* and *NOP58* (Table 3-3) tend to bolster the hypothesis of a nutritional response given the role of both genes in nitrogen compound usage or rRNA synthesis, respectively. Expression of *NRG1* (discussed below) and *SGO1* are both highly increased after 2 hours HWSSL exposure and neither return to non HWSSL-exposed levels after 24 hours, suggesting more determinant roles in prolonged HWSSL tolerance, especially given the general decrease in expression levels across much of the genome over 24 hours exposure to HWSSL. Sgo1p's role in chromosome segregation and stability suggests that its increased expression may be a cell cycle effect. However, the expression of *SGO1* is downregulated when faced with osmotic (249) and

oxidative pressure (27) and responds with less extensive transcriptional changes of ~0.5-fold due to cell-cycle fluctuations on rich laboratory medium (349), suggesting *SGO1* may be involved in HWSSL tolerance, likely through preserving chromosome stability. Overall, the changes in expression of mutated genes tend to support roles for *NRG1*, *SSA1*, *SGO1*, *MAL11* in HWSSL-tolerance based on either their divergence from general trends of downregulation in R57 or the extremity of their differential expression response.

4.3.13 RNA-seq data support a determinant role for NRG1 in the phenotype of R57 and response to HWSSL

NRG1-regulated genes show a differential expression response in mutant R57 under non-stressed and HWSSL-exposed conditions. *NRG1*, which self-regulates its transcription (350-353), is upregulated 3-fold without exposure to HWSSL and 3-fold higher after 2 hours HWSSL exposure. The closely related transcription factor *NRG2* is similarly upregulated: 5.2-fold between WT and R57 and 1.8-fold after 2 hours HWSSL exposure. However, both return to near unstressed R57 levels after 24 hours, which may be due to the large-scale suppression of transcript levels seen at that timepoint, or may point to an early stress response role for this transcription factor. Although, it should be noted that the overall expression levels for both R57 HWSSL-exposed time points remain well above the WT expression level under non HWSSL-exposed conditions. Upregulation of *NRG1* and *NRG2* supports the hypothesis that the *NRG1* mutation is playing a significant role in the HWSSL phenotype either by being upregulated in order to compensate for a reduced Nrg1p function or is being caused by the *NRG1* mutation itself. *NRG1*, as mentioned previously, is responsible for recruiting the Tup1p-Cyc8p

complex in order to repress transcription of various genes. If the profound impact reported for this mutation by the SIFT algorithm is accurate (Table 3-3), a loss of functionality of Nrg1p may be a likely result. If that is the case then the transcription of genes that are repressed by Nrg1p would be expected to be upregulated transcriptionally. To test this theory further, differentially-expressed genes were analyzed from all RNA-seq experiments using the YEASTRACT database (308-310) in order to elucidate any trends in expression for Nrg1p-influenced genes. This analysis showed that 5.8 % of the yeast genome is predicted to be under the control of Nrg1p, while of the ≥ 2-fold constitutively upregulated genes 8.6 % are under control of Nrg1p as demonstrated by direct evidence, a figure which grows to 16.1 % after 24 h exposure to HWSSL. The percentages of genes showing decreased expression patterns are similar to the whole-genome level of 5.8%. Most strikingly, 4 of the 5 most highly upregulated genes between the WT and R57 without exposure to HWSSL are regulated by Nrg1p, as determined by direct evidence. These genes include *CWP1* (351), YLR012C (350-353), *GAT3* (351-353), *TDA6* (351), all mentioned above. *GAT3* (~23-fold upregulated) and YLR012C (~44-fold upregulated), flank each other and code in opposite directions on chromosome XII, sharing upstream regions. Since both genes are extremely upregulated under non-stressed conditions and share 5' regions it is likely that the transcription of these 2 genes is being controlled by the same factor, of which, Nrg1p seems a likely candidate. Altogether, increased expression in R57 of Nrg1p-governed genes supports the hypothesis of a decreased suppressive effect exerted by the mutated Nrg1p and, based on known functions of many of the affected genes, may partially explain the HWSSL-tolerance trait of R57.

4.3.14 Transcription of mutated Mal11p trehalose H^+-transporter is highly downregulated along with trehalose metabolism genes

During exposure to HWSSL, *MAL11* is significantly downregulated 4-fold over the first 2 hours of exposure and almost 6-fold over 24 hours. Between the WT and R57, *MAL11* is downregulated 8-fold, but gives a *p*-value of only 0.09 and is therefore not reported in the functional analysis. Closely related genes are also downregulated over 2 hour-HWSSL exposure including the maltose metabolism-related genes *MAL12*, *MAL32*, *MAL31*, which cluster also as part of oligosaccharide metabolic processes at an enrichment score of 1.2 along with *MAL11* and 2 other genes (*AMS1* and *SUC2*). Taken together with the presence of 2 mutations within *MAL11*, these results suggest a determinant role for *MAL* genes in HWSSL tolerance and for Mal11p in particular.

One possible role for the two *MAL11* mutations discovered in R57 is that they may be acting to affect the trehalose/proton symport activity of Mal11p (354). As mentioned, trehalose is a known osmotic stress protectant molecule and can affect protein folding machinery (275, 276) and therefore any process that affects cellular trehalose content is of interest to HWSSL tolerance. In order to assess the trehalose metabolism of R57, known trehalose metabolism genes were examined across RNA-seq experiments. Four genes involved in trehalose synthesis (*TPS1*, *TPS2*, *TPS3*, and *TSL1*) are all significantly downregulated in response to HWSSL exposure over 24 hours, with *TPS1* and *TPS3* being downregulated between 0 and 2 hours as well. Not unexpectedly, *NTH1*, the neutral trehalase of *S. cerevisiae* is also downregulated, either as a response to diminished cellular trehalose or due to the fact that the trehalose degradation and synthesis mechanisms are co-regulated by the presence of similar STREs in their

promoters (355-357). This trehalose degradation/biosynthetic gene expression co-regulation is a common occurrence under stress conditions and it is hypothesized that this pathway is tightly controlled post-transcriptionally (27). When these data are taken together trehalose may be regarded as a metabolite of interest in HWSSL tolerance, either in relation to Mal11p's transport specificity or in relation to a trehalose biosynthetic machinery that is affected by HWSSL exposure.

4.4 Discussion

The objectives of this portion of the study were to (a) describe the transcriptional differences that exist between WT and HWSSL-tolerant R57 under non HWSSL-exposed (permissive) conditions, (b) probe the expression response of R57 to HWSSL exposure, (c) assess the affects of mutations on gene expression, and (d) cross reference phenotypic characterization, mutation and gene expression analyses in order to narrow the possible genetic determinants of interest in HWSSL tolerance. By extension, the aim was to aid understanding of microbial tolerance to lignocellulosic hydrolysate-based inhibitory substrates and generate plausible avenues for future strain development. RNA-seq is a new technology and therefore best practices in using the technology are still being established. Therefore, in order to minimize false leads, the WT vs R57 expression analysis under permissive conditions was performed on biological replicates at high sequence depth. Furthermore, RNA-seq performed on strain R57 was analysed in order to minimize false leads by examining all of the differential expression profiles as enriched clusters of biological function with a focus on processes that are differentially expressed either in common between the WT and R57 and the R57 HWSSL-exposure

experiment, at multiple timepoints, or support the mutational analysis data based on known associated biological processes.

Expression analysis has been used successfully to elucidate rational engineering targets for strain development (358). Transcriptional analysis of R57 alone yielded far less precise reverse engineering targets than genome sequencing. This result was expected based on previous literature. For example, transcriptome-based analysis of glucose-limited, chemostat-evolved *S. cerevisiae* strains resulted in hundreds of genes displaying transcriptional changes (359, 360), while genome sequencing of a comparably evolved strain revealed only six mutations. Similarly, Hong *et al.* found that strains evolved for faster growth on galactose typically displayed differential regulation of hundreds of genes, while sequencing resulted in fewer than 20 mutations in 2 of the strains sequenced (109). Despite the less-easily interpretable nature of expression results, as a means to elucidate the productive mutations in the R57 background and to hone in on the pathways that have been affected, RNA-seq analysis revealed pathways and genes that were affected at the transcriptional level and support our genome sequence findings. Generally, trends within the expression analysis highlight chiefly impacted cellular processes, based on differential expression profiling between the WT and R57 and after exposure to HWSSL that include fundamental biological processes involving translation/transcription, central carbon metabolism and energy generation; protein homeostasis by way of ubiquitin-mediated degradation processes and protein re/folding mechanisms; cell surface rearrangements both at the cell membrane and cell wall; organic and amino acid metabolism and transport, with aromatic amino acid metabolic processes showing particular enrichment; NAD(P)H-related processes; and known stress response-

related gene transcripts. The following is an integrated discussion of the RNA-seq results presented above in the context of the known genetic and phenotypic particularities of R57 (Chapter 3).

4.4.1 Integrating RNA-seq data with mutation analysis supports a determinant role for stress response transcriptional repressor Nrg1p in the HWSSL-tolerance trait of R57

In Chapter 3, the transcriptional repressor Nrg1p was shown to bear a homozygous mutation that is strongly predicted to lead to a phenotype. It was hypothesized that this mutation may lead to a lost or protracted function causing a derepression of stress-tolerance factors, based on the tolerance traits of strain R57 and the predicted effect of the homozygous *NRG1* mutation. Nrg1p-controlled genes are highly upregulated under non-stressed conditions, which supports a decreased repression effect by the mutated Nrg1p and suggests that the homozygous mutation in *NRG1* is directly affecting the ability of Nrg1p to exact gene repression by some factor that may include protein stability, protracted DNA-binding affinity for upstream control elements or ability to recruit the Tup1p-Cyc8p repressor complex. Furthermore, *NRG1* and *NRG2*, which govern many of the same stress response genes (248), are both upregulated in the mutant strain under permissive growth conditions and after 2 hours HWSSL exposure. It is further hypothesized that this expression response may be a ramification of *NRG1* mutation, since Nrg1p normally represses both genes. Many of the genes that are upregulated between the WT and R57, which are controlled by Nrg1p, are reconcilable with the HWSSL-tolerance trait. For example, *TDA6* and *CWP1*, two of the most highly differentially expressed genes between the two strains, are known constituents of defined

stress responses. *TDA6* is a known target of acetic acid resistance (139), while CWP1 is related to cell wall thickness and propionic acid resistance, is a known constituent of the HOG pathway, and is highly upregulated between the WT and R57 and again after 2 hours of HWSSL exposure in R57. It is possible that expression changes such as these are able to enhance the stress response of R57 by maintaining a stress-tolerant physiology.

Additionally, the increased representation of Nrg1p-affected genes in the upregulated-gene transcriptional response to HWSSL exposure by R57 emphasizes the likely importance of Nrg1p-governed genes in the HWSSL-exposure response. Recently, a regulon for acetic acid tolerance, governed by transcriptional activator Haa1p, has been described, which is controlled also by Nrg1p and stress response transcriptional activator Msn4p (upregulated over 24 hours HWSSL exposure in R57) (139). Many of the genes highlighted as members of enriched clusters that show increased expression in R57 under permissive conditions and during HWSSL exposure are known constituents of this regulon including: *AQR1*, *HSP26*, *MSN4*, *PDR12*, *PDR16*, *SPI1*, *SUR2*, *SSE2*, *TDA6*, *TPO1*, *TPO2*, and *TPO3*. One proposed mode of Haa1p activation of stress-tolerance genes is by overriding the suppressive effects of Nrg1p (139). Genes like HAA1-dependent *TPO2* and *TPO3* have been shown to have a prominent effect on acetic acid tolerance (38) and *TPO3* expression is known to be regulated by Nrg1p (351). I hypothesize that the *NRG1* mutation may be precipitating the derepression of acetic acid or other stress tolerance genes. The acetic acid tolerance exhibited by R57 after pre-exposure to HWSSL (Chapter 1) parallels inducible acetic acid tolerance traits shown by acetic acid evolved strains (361). Because the acetic acid tolerance trait of R57 is only

apparent after HWSSL exposure, it is likely that specific acetic acid tolerance genes may require activation as well as derepression to confer tolerance, whereby Haa1p is likely playing a role by inducing expression of the aforementioned acetic acid regulon genes (38). It follows from this hypothesis that the effect of Haa1p induction of acetic acid-regulon gene expression may be more effective with a protracted Nrg1p-mediated gene repression.

Furthermore, many of the PDR-associated genes noted as upregulated (> 2-fold) and highly upregulated (> 5-fold) in R57 after 2 and 24 hours HWSSL exposure are members of this regulon (*AQR1*, *TPO1-3*, *PDR12*, *PDR16*). PDR-related genes are known to play diverse roles in the efflux of potentially toxic compounds from the cell. Upregulation of such a broad-acting stress response is expected in reaction to HWSSL exposure due to the diversity of sources of inhibition present in the substrate. The RNA-seq data presented above support a determinant role for genes classified as PDR-related and, integrated with mutational analysis of R57, suggest a link between influencing expression of the PDR by modification to *NRG1*. At the very least, engineering stress response through downstream expression changes to acetic acid tolerance genes and PDR-associated genes by way of *NRG1* alteration is strongly supported by this study and bears future investigation.

4.4.2 Differential expression of nitrogen usage-related genes support a pivotal role for mutated *GDH1* in the HWSSL tolerance trait of R57

As outlined in Chapter 3 (Table 3-3), Gdh1p is responsible for the majority of cellular nitrogen assimilation via ammonia. Mutation of *GDH1* suggests alternative

amino acid or glutamate synthesis or degradation pathways might be affected, as glutamate is a hub of amino acid synthesis and degradation. The RNA-seq data presented in this chapter further suggest that possible alternative glutamate biosynthesis or nitrogen usage routes are being affected. For example, constitutive expression differences between the WT and R57 show a 9-fold increase in glutamine permease *GLN1* expression, which makes glutamate synthesis from glutamine possible via Glt1p and a decrease in expression of *MEP3*, responsible for ammonia uptake upon ammonia exposure. Furthermore, expression is increased between the WT and R57 under permissive growth conditions of *BAT1*, *HOM3*, *LYS9* and *LYS12*, which can all participate in alternative glutamate biosynthesis pathways. Similarly, upon 2 hour HWSSL exposure, transcriptional expression of the genes encoding Aat1p, Asp1p and Trp3p are increased, all of which are known to participate in glutamate forming processes. These findings suggest that if the primary route of glutamate generation, via *GDH1*, is being disrupted by mutation, alternative glutamate biosynthesis pathways may be acting to fulfill glutamate requirements of the cell. Relatedly, genetic constituents of amino acid metabolism and transport are also enriched for differential expression in R57 both between the WT and R57 and through 2 and 24 hours HWSSL exposure. Therefore, processes related to cellular amino acid content in general are likely important factors in HWSSL tolerance and may be a result of the fundamental intermediary role glutamate plays in amino acid generation and breakdown. Additionally, because Nrg1p also governs pseudohyphal growth, which has a known relationship to nitrogen assimilation of non-preferred nitrogen sources, a functional link may exist between the mutations in *GDH1* and *NRG1* in R57. The high expression increase in R57 over the WT of *PUN1*

and *PHD1*, both important constituents of pseudohyphal growth, supports this possible connection. Additionally, *GAT3*, one of the most highly upregulated constitutive genes in R57 and controlled by Nrg1p, is structurally related to *GAT1* and contains the same zinc-finger binding domain by which *GAT1* mediates transcriptional activation of NCR-related genes. Gat3p, therefore, might also be involved in differentially regulating the nitrogen usage machinery of the cell. In support of this theory Gzf3p, a negative regulator of nitrogen catabolite repression (NCR) that also competes for DNA GATA-factor binding sites with Gat1p (312), is also downregulated between the WT and R57. Thus, though not readily apparent, the mutation-bearing R57 genes believed to have a phenotypic effect, like *NRG1* and *GDH1* may be linked in their functional repercussions.

In relation to stress tolerance, *GDH1* was recently shown to be downregulated in a mutant *S. cerevisiae* strain evolved for tolerance to furfural, phenol and acetic acid (206). The theory put forth by Ding *et al*. is that downregulation of *GDH1* will slow growth and allow the cell to respond to stress more efficiently, which is in keeping with the findings of Gasch *et al*. as a general feature of the ESR (27). Mutation in both alleles of *GDH1* in R57 may signify a loss of function mutation that has been introduced through GS evolution for tolerance to HWSSL, and may be acting to decrease efficiency of nitrogen assimilation and slow metabolism. This would be in keeping with the Ding *et al*. finding and the tenets of the ESR. The normal response to high levels of a preferred nitrogen source like ammonia may be accelerated growth, but the low carbon levels in the HWSSL substrate, coupled with other nutritional deficiencies known to be a factor in industrial-scale fermentations (362), could not only impair prolonged survival, but act in direct opposition to an efficient stress response. Nitrogen assimilation into amino acids

carries a metabolic cost both due to energy consumption and the carbon skeletons they incorporate (337). Ammonia assimilation by way of Gdh1p could act to exacerbate the low-level of available carbon and growth efficiency may impair tolerance to HWSSL by squandering resources needed for stress response. The marked decrease in biomass yield exhibited by R57 over the WT reference (Fig. 4-1) offers further evidence that metabolism has shifted to a state of decreased resource utilization efficiency. Because the SD growth substrate contains ammonia as the nitrogen source and R57 shows residual glucose available in the substrate well past stationary phase, reduced ammonia assimilation efficiency seems likely.

Furthermore, the yeast relationship with nitrogen is multifaceted as it is required for growth, but may also become toxic. Even though ammonia is a preferred nitrogen source, recent work by Hess *et al.* shows that ammonia may be toxic even at normal laboratory levels if potassium is limiting (337). Bayer *et al.* recently showed that by increasing expression variability of *GDH1* alone, one can tune the metabolism of a cell so that it responds more efficiently to limiting or toxic levels of ammonia (363). The high (1 % w/v) level of ammonia in the particular HWSSL we evolved tolerance to suggests that nitrogen is not a limiting nutrient. The ammonia levels reported by Hess *et al.* under which ammonia toxicity can be seen fall well below those found in HWSSL (337). That study also shows that amino acid secretion is one result of ammonia toxicity. Correspondingly, *QDR2*, upregulated after 2 hours and *AQR1* over 24 hours exposure by R57 to HWSSL, are both involved in amino acid excretion. Furthermore, genes related to ammonia excretion, *ADY2* and *ATO3*, are also upregulated over 24 hours HWSSL exposure by R57. These findings agree with the theory that R57 is responding to

HWSSL toxicity in a way that signifies modified nitrogen metabolism in an excess ammonia environment.

Taken together, our data point to modified nitrogen usage as a fundamental component of the R57 physiology in which non-preferred amino acid degradation and biosynthetic pathways, nitrogen secretion processes, and a modified response to the presence of ammonia may all be acting co-ordinately to increase HWSSL tolerance by attenuating nitrogen usage efficiency in order to shift available resources to other biological processes as a trade-off for stress tolerance. The known role of *GDH1* in orchestrating nitrogen metabolism and its proven ability to play a role in stress tolerance to the types of inhibitors found in HWSSL support future study of this gene as a target for rationally engineering microbial tolerance to lignocellulosic substrates by affecting nitrogen metabolism and, consequently, processes throughout the cell.

4.4.3 Genes related to protein homeostasis are affected by mutation and differential expression in strain R57

Two mutated genes are known to be directly associated with the ubiquitin-mediated protein degradation, including homozygous-mutation bearing *UBP7*, a deubiquitinase, and *ART5*. In relation, the RNA-seq data presented here show enrichment clustering for increased expression of genes that encode proteins which fall under the purview of the ubiquitin-mediated proteolytic machinery (UBL-conjugation) both between the WT and R57 and after 2 hours HWSSL exposure in R57. Many of the genes within these UBL-conjugated gene clusters are associated with diverse biological processes and are not known to play a direct role in the ubiquitination of proteins or

ubiquitin-mediated proteolysis. Rather, these genes encode proteins that are themselves known or expected to be regulated by this post-transcriptional control mechanism. The genes that encode ubiquitin-controlled proteins showing increased expression during HWSSL exposure come from a wide variety of biological processes but are mainly stress-tolerance related (*RHR2*, *PUN1*, *ENA5*, *PDR5*, *PDR12*), which therefore suggests that genes showing increased expression due to HWSSL exposure may be differentially controlled at the protein level by a modified ubiquitination machinery. Moreover, there is evidence of increased expression of genes directly related to the ubiquitin machinery in R57: *RPL40B/UBI2* and *RPS31*/*UBI3*, which encode ubiquitin fused to ribosomal proteins (314), show increased expression between the WT and R57 and Cdc20p, showing increased expression after 2 hours of HWSSL exposure in R57, is known to direct ubiquitination of anaphase inhibitor proteins. Ubiquitin is generated in *S. cerevisiae* as a fusion protein that is then cleaved to yield free ubiquitin by deubiquitinase enzymes, and it has been demonstrated that transcription of genes encoding ubiquitin are upregulated during stress exposure (364, 365). It has already been shown that mutations within a deubiquitinase enzyme, *UBP6*, can dramatically change steady-state ubiquitin levels within a cell (366), which is known to affect tolerance to a variety of stressors (367-369) and yeast prion toxicity (369). The important role that ubiquitin and ubiquitin-conjugation seems to be playing in the physiology of R57 suggests that UBP7 may be playing a similar role and is a likely determinant in HWSSL tolerance.

Ubiquitin-mediated protein degradation, however, is not the only protein homeostasis process affected in R57 by gene mutation and differential expression. The mutation in Hsp70 protein *SSA1* of R57 was hypothesized in Chapter 3 to be playing a

role in optimizing the protein folding machinery and decreasing harmful protein aggregation and prion formation in R57 due to HWSSL oxidative toxicity. The RNA-seq data support a role for Hsp70 proteins in HWSSL tolerance. Of the few transcripts that are upregulated between 2 and 24 hours HWSSL exposure in R57, Hsp70 proteins and their co-chaperones are prominently enriched (*SSA1*, *SSA2*, *SSA4*, *SSE1*, *SSE2, FES1*, *YDJ1*, *SIS1* and *APJ1*) along with 3 other protein folding chaperone genes. *SSA2* and *SSA4* also show increased expression between 0 and 24 hours HWSSL exposure in R57, while *SSA3, SSC1*, *SSC3*, *SSE1* are members of a decreased expression enrichment cluster for stress response over 0 to 2 hours HWSSL exposure. Only *SSE1* shows increased expression after initial decreased expression over the time-course. Taken together, these data suggest that specific Hsp70 protein expression is being modulated in R57 in response to HWSSL exposure and that Hsp70s, coupled with co-chaperones that act to increase their protein folding activity, may be important players in the HWSSL tolerance traits. Furthermore, both the location of the mutation in Ssa1p, and the transcriptional response of R57 at 24 hours HWSSL, namely increased expression of Hsp70s along with Hsp40s and Fes1p co-chaperones, may be acting to increase protein folding rates and decrease protein aggregation. Overall, changes to protein homeostasis accompany the HWSSL-tolerance trait of R57 and suggest that future strain engineering studies may benefit by addressing the cellular ubiquitin and protein folding machineries.

4.4.4 Strain R57 shows mutation and differential expression of genes related to metabolism and usage of oxidative stress tolerance-associated metabolites, iron, glutathione and NAD(P)H

One of the ways to engineer an organism to display a trait of interest is to manipulate the levels of key metabolites (370). Due to the presence of mutations in R57 genes *FIT3* (iron transporter), *GSH1* (leads to glutathione biosynthesis) and *GDH1* (NADPH-dependent) cellular processes that affect metabolism involving iron, glutathione and NAPDH were hypothesized to be playing a role in the R57 phenotype. As presented in the results section (Chapter 4, section 4.3), RNA-seq data of the WT vs R57 and R57 after HWSSL exposure also support important roles for these metabolites in the HWSSL tolerance trait.

The mutation in the 3' UTR of FIT3, coupled with its decreased expression upon HWSSL exposure, suggests that cellular iron content and iron-requiring proteins may be playing a role in HWSSL tolerance. Between the WT and R57 under permissive growth conditions, genes encoding metal-containing proteins cluster as enriched for decreased expression and include 4 iron-binding proteins including metal transporter *SMF2* (Fig. 4-2). Similarly, after 2 hours of exposure to HWSSL transcripts encoding 9 iron-binding proteins show decreased expression. The downregulation of genes leading to iron-transport and usage is in direct contrast to previous findings based on yeast exposure to single sources of inhibition like acetic acid and furfural, which show that iron transporter transcript levels are upregulated under those conditions (207, 279), or oxidative stress challenges, which are moderated by iron-sulfur proteins (279). However, the early transcriptional response of R57 to HWSSL suggests that iron-associated gene products

are being downregulated as a response to toxicity either because they are not needed to fulfill the HWSSL tolerance trait or are negatively impacted by inhibitor toxicity (Fig. 4-3). This may be a nutritional response, either because iron is not required by the ETC-associated genes or due to slowed central metabolism. Alternatively, because of the high heavy metal content that can be present in sulfite pulping waste (93, 371), it is plausible that the response of this cluster of genes is acting to maximize cellular resource usage while iron availability is not limiting or to decrease iron intake. This hypothesis is supported by the decreased expression of *FRE5* after 2 hours of exposure to HWSSL. *FRE5* encodes an $NADP^+$-dependent cell-surface metalloreductase, and its expression is induced by iron deprivation. Furthermore, *MRS3* is 1.7-fold upregulated after 2 hours HWSSL exposure, which although falls below the significance threshold for enrichment clustering, is predicted as significantly differentially expressed at this timepoint. *MRS3* encodes for a mitochondrial iron transporter that is generally upregulated under conditions of high-iron exposure in order to sequester iron in the mitochondria (372). The relationship between cellular iron content modulation and usage by R57 may stem from the role free iron can play in reactive oxygen species generation. Iron is able to participate in Fenton reactions that generate ROS and can lead to protein damage (372-374). As reported in Chapter 2, strain R57 shows tolerance to hydrogen peroxide and consequently modification to oxidative stress-response machinery is expected. Therefore, the decreased expression and mutation of known iron transporters may be playing a fundamental role in this aspect of R57's HWSSL tolerance trait.

Correspondingly, the redox state of the cell is linked to cellular glutathione content (209) and the mutation described in Chapter 3 to the 5' UTR of *GSH1*, a gene

which is integrally involved in glutathione biosynthesis, suggests further modulation in R57 of redox homeostasis mechanisms. *GSH1* itself is downregulated at both 2 and 24 hours of HWSSL exposure suggesting its expression is inhibited by HWSSL exposure. As outlined in Chapter 3, glutathione is comprised of glycine, cysteine and glutamate and its biosynthesis relies on intracellular pools of glutamate, glutamine, and lysine (210). Between the WT and R57, genes that lead to cysteine biosynthesis (*HOM2*, *MET16*, *MET17* and *MET3*), along with genes leading to glutamate and lysine biosynthesis (*HOM3*, *LYS9* and *LYS12*), are upregulated. This finding suggests that R57 has an upregulated pathway towards glutathione precursor generation as part of its physiology and constitutes a possible link to the *GSH1* mutation.

Another well known counterpart of a cell's redox state are the cofactors NADH and NADPH, which are responsible for providing reducing equivalents for a wide range of biological processes (375). It is well-documented that yeast detoxifies the furan aldehyde inhibitors found in HWSSL by way of NADH/NADPH requiring enzymes (37). The final aspect of Gdh1p, therefore, that warrants discussion is its NADPH cofactor requirement, which can be a viable engineering target for modulating intracellular NADPH levels (27). Differential expression analysis shows that NADH-requiring processes are enriched for increased expression in the WT under non-inhibitory conditions. Furthermore, NAD(P)H-associated processes are simultaneously enriched for decreased expression and highly increased expression after 2 hours HWSSL-exposure (Fig. 4-3), demonstrating the role of NAD(P)H-related processes in the R57 phenotype. Genes known to play a role in furan-aldehyde inhibitor detoxification via NADPH

include *GRE3*, upregulated between the WT vs R57, along with *GRE2* and YKL071W, upregulated after 2 hours HWSSL exposure in R57.

Overall, the potential modulation of metabolites like glutathione and NADPH via mutation or differential gene expression may have major effects on the redox state of the cell. This finding correlates well with the above findings regarding modification to protein homeostasis as a major determinant factor in the HWSSL tolerance trait of R57 in that changes to redox-state related metabolites may be acting to mitigate protein damage.

4.4.5 A determinant role in HWSSL tolerance for mutated transporter Mal11p is supported by RNA-seq expression analysis

The two mutations in *MAL11* and its extreme decrease in expression both between the WT and R57 and after HWSSL exposure suggest *MAL11* is involved in the HWSSL tolerance trait of R57. Decreased expression in R57 of other MAL-classified genes (*MAL12*, *MAL32*, *MAL31*) supports a role for MAL transporters in HWSSL tolerance. Significant polysaccharide content in HWSSL has not been reported. Therefore, it is plausible that the MAL genes affected by HWSSL evolution and differential expression upon HWSSL exposure may be explained simply by a low level of HWSSL polysaccharide content, which would render expression of *MAL* proteins a waste of cellular resources and may translate into a transcriptional signal for decreased expression, as MAL genes are known to be induced by the presence of maltose and reduced by the presence of glucose in the substrate (376), for example. The fact that Mal11p is a trehalose-proton symporter, coupled with the downregulation of the trehalose biosynthetic machinery over the timecourse at least suggests further investigation of

levels of this important metabolite upon exposure to HWSSL is warranted. Although trehalose is known to be a storage carbohydrate in *S. cerevisiae*, and therefore the differential expression of trehalose biosynthesis genes may be indicative of a lack of available carbon for storage processes, it is also an important factor in overcoming osmotic pressure challenges due to its unique propensity to displace the "water shell" around macromolecules, thereby minimizing the effects of desiccation (275) and is an effective stabilizer of proteins at physiological concentrations (276). If trehalose content is an important factor in HWSSL tolerance, as might be expected from its role in osmotic tolerance, then changes to the trehalose transport and generative abilities of the cell may be a logical outcome of evolution towards HWSSL tolerance. Furthermore, the presence of organic acids like acetic acid in HWSSL likely leads to acidification of the cell interior, which precipitates the arrest of cellular metabolism and dissipation of the electrochemical gradient of the plasma membrane. This can be alleviated by extrusion of protons from the cell (reviewed in (207)). Therefore, any transporter that relies on proton transport could be susceptible to malfunction, as it has been shown that sugar symporters are sensitive to a build up of internal proton concentrations and fail to mediate the influx of the target metabolite under such conditions (377). Mal11p transport activity has been shown to be highly pH sensitive (274), which is likely a result of this effect. Additionally, carbohydrate proton symporters can be involved in intracellular pH regulation by deacidification (378) and it is possible that protons exiting the cell via symporters could lose vital metabolites like trehalose. Alternatively, though elevated trehalose often leads to stress tolerance it can also have the opposite effect, leaving cells more prone to stress sensitivity or delayed stress recovery (277, 278, 379) and the

presence of trehalose is by no means a requirement of osmotic tolerance (380-382). Moreover, elevated cellular trehalose contents have been shown to interfere with the cell's protein refolding machinery, it is hypothesized, by the very same properties that make trehalose a protein stabilizer (379, 383), and might therefore be detrimental to stress tolerance under protein damaging conditions like those imparted by lignocellulosic hydrolysate inhibitors. Therefore, a Mal11p mutation, if it leads to loss of function, as may be expected by the nature of the mutations, together with its high degree of downregulation may have a two-fold protectant effect: firstly, by minimizing intracellular trehalose content, enabling protein-folding chaperone function, and secondly, by diminishing the import of protons that would further acidify the cell during polysaccharide transport. The known promiscuity of Mal11p for transport of multiple polysaccharides might make mutation within this particular *MAL* transporter particularly tell-tale (354, 384). That is, a plethora of polysaccharides existing within HWSSL, even at low concentration levels, might be imported by Mal11p and add to intracellular acidification. Though the role of *MAL11* in HWSSL tolerance remains unclear, the above data support further investigation.

4.4.6 Aromatic amino acid synthesis genes are affected by mutation and differential expression in R57

Mutation to *ARO1* and the known role of Aro1p in aromatic amino acid biosynthesis (Chapter 3, section 3.4.2) and acetic acid tolerance suggest a role for aromatic amino acid-related pathways in R57 HWSSL tolerance. The RNA-seq experiments presented in the results section highlight aromatic amino acid metabolism pathway genes as upregulated between 0 and 2 hours of HWSSL exposure as well as over

24 hours of HWSSL exposure. Directly downstream of *ARO1*, multiple genes related to tryptophan and tyrosine/phenylalanine biosynthesis demonstrate highly increased expression after 2 hours of HWSSL exposure, which is in keeping with the demonstrated transcriptional response of *S. cerevisiae* to acetic acid exposure (207). Over 24 hours, aromatic amino acid catabolism genes are enriched as a decreased expression cluster, adding to the evidence that aromatic amino acid metabolism is a biological pathway of interest in HWSSL tolerance.

4.4.7 Genes affecting the cell-surface are affected by mutation and differential expression

As pointed out in Chapter 1, the inhibitors present in HWSSL have the ability to affect the cell membrane and cell wall in detrimental ways (7). From the mutation data presented in Chapter 3, mutations were found in YNL058c, linked to cell wall integrity, Art5p, related to cell-surface protein turnover, and Nrg1p, which governs cell-surface-affecting genes, like the aforementioned, highly-upregulated, *CWP1*. Accordingly, enriched gene clusters for differential expression between WT and R57 were discovered through RNA-seq analyses that represent cell wall and organization genes, or cell-membrane associated genes. Similar enrichment is seen within the differentially expressed genes documented between 0 to 24 hours of HWSSL exposure. While most of the findings presented in this study tend to deal with preserving intracellular homeostasis, the burden on the intracellular environment is likely mediated, in part, at the cell surface as a first line of tolerance.

4.5 Conclusions

In order to probe for expression differences that could elucidate an underlying stress-response related physiology of GS-evolved HWSSL-tolerant strain R57, RNA-seq differential expression analysis was employed. The transcriptional differences under permissive conditions between the parental background WT and R57 imply a differing physiology based on changes to the cell-surface, metal-ion usage, amino acid biosynthesis, NADH and ubiquitin-related processes or fundamental processes like central carbon metabolism and translation. Furthermore, a major role for the mutated Nrg1p transcription factor in controlling differential expression of stress-tolerance related genes is apparent between the two strains under permissive conditions.

R57 exposure to HWSSL generated differential expression data that implicate major roles for the following in the R57 HWSSL response: nitrogen usage, aromatic amino acid metabolism and response to ammonia; protein homeostasis machinery based on ubiquitin-mediated degradation processes and re/folding mechanisms involving Hsp70s; oxidative stress response mechanisms mediated by iron, glutathione and NADPH; cell-membrane changes; the PDR; and a general repression of metabolism. To my knowledge, these data constitute the first description of a transcriptional response to HWSSL exposure and elucidate processes of interest in future lignocellulosic hydrolysate expression-response studies.

This portion of the study was productive, in a supporting role, to probe the transcriptional response of R57 to HWSSL-exposure and for differences between the WT and R57 that support the assertions generated by the genome resequencing and mutation

analysis of Chapter 3. Taken together, these data support important roles for many of the mutated genes discovered in R57, but implicate *NRG1*, as a modified regulator of stress response gene expression and *GDH1*, *UBP7*, *SSA1*, *ARO1*, *FIT3* and *MAL11* as components of predominant cellular processes in the modified R57 transcriptional landscape or pathways of interest in the R57 HWSSL-exposure response.

Chapter 5

5 General discussion and conclusions

In order to use biomass as feedstock for generating fuels or chemicals, biocatalysts that are tolerant of the various sources of inhibition associated with biomass-breakdown substrates are required. Meiotic recombination-mediated GS of *S. cerevisiae* was shown in this study to be a productive technology in generating tolerance to lignocellulosic substrate inhibition. This study further demonstrates that coupling this strain development technique with phenotypic characterization and MPS technology, like rapid genome sequencing and RNA-seq differential expression profiling, makes it possible to track the genetic and physiological factors involved in ligncellulosic substrate inhibition.

5.1 Challenges associated with GS, MPS and RNA-seq technologies

Several limitations of the technologies employed in this study were identified. Although strain development by GS is productive in engineering tolerance to specific sources of inhibition, this technology relies on a high-throughput screen, such as growth on inhibitory substrates using large populations of mutants, in order to be fully useful. Where a high-throughput screen may be more difficult to develop, as with increasing production titres of a compound that requires an involved isolation step, generating large populations of strains harbouring mutations for recombination and mutation accumulation may not be possible. Furthermore, the relative ease by which genetic recombination can be enacted will be a concern when using microorganisms that are not amenable to protoplast fusions, such as Gram-negative bacteria. Whole genome

sequencing using MPS technology is particularly useful in elucidating SNP mutations between a genomic DNA sample and a closely related scaffold genome sequence upon which to align MPS DNA sequence reads. However, when a closely related genome sequence is not available, one must be produced in order to make variation comparisons between strains, which adds to the difficulty of variation calling. Also, mapping of short DNA sequence reads allows for the discovery of SNP mutations, but detecting structural genomic variation using short reads is thus far not possible or unreliable. Emerging technologies like Pacific Biosciences SMRT platform is an indication that attaining large DNA reads at a low cost will be accessible in the near future. Longer, cheaper DNA reads should allow for accurate and cost-effective *de novo* genome assembly to provide easier access to more accurate DNA scaffolds for DNA sequence-read mapping and structural genome rearrangements. Finally, as best practices for RNA-seq experiments and data processing are still being established, the data generated by RNA-seq technology must be applied carefully when drawing biological conclusions, especially in cases where the data may not be supported by extensive genetic and phenotypic information. The process of drawing reliable biological conclusions using RNA-seq will become easier as MPS technology and analysis software advances. For example, as costs decrease and sequence read depth improves it is becoming increasingly possible for extensive sample multiplexing (385, 386), allowing for a variety of strains to be tested under multiple conditions, which should increase the sensitivity and reliability of differential gene expression analysis. Moreover, as the confounding variables such as 3'-end sequencing bias or overrepresentation of differential expression calls for longer

genes are accounted for in RNA-seq analysis software algorithms, the utility of RNA-seq will grow.

The design of the current study was intended to minimize the limitations of GS, genome sequencing by MPS and RNA-seq differential expression profiling in several ways. Firstly, an organism with a well-understood and easily-manipulated mating cycle was chosen for employing meiotic recombination-mediated GS under selective conditions that allowed for large populations of mutants to be compared. UV mutagenesis was chosen as the method to generate mutations as it predominantly leads to small SNP or indel mutations, which can be easily tracked by genome sequencing with MPS. MPS sequencing and variation discovery was aided by available, high-quality genome sequences of S. *cerevisiae*. Furthermore, a methodology was developed whereby the mutant strain of interest was sequenced in parallel with the WT parental strain for extensive comparison during variation calling, in order for sequence/technology-specific errors in DNA sequence read alignment to be controlled by systematic visualization and curation of variations in common between the WT and R57. Finally, RNA-seq differential gene expression analysis was utilized primarily in a supportive role to the phenotypic characterization and variation discovery analyses of R57, in conjunction with the relatively well-characterized information that exists on *S. cerevisiae* stress response mechanisms, in order to draw biological conclusions. Furthermore, the RNA-seq expression profiling was biologically replicated for the WT versus R57 comparison at high-read depth and multiple HWSSL-exposure timepoints were sampled to probe the R57 response to HWSSL. These differential gene expression datasets were cross-

referenced for existing commonalities in order to optimize the significance of the findings.

5.2 Summary of significant findings

By applying the GS methodology devised for this study it was possible to isolate *S. cerevisiae* strain R57 that shows simultaneous tolerance to HWSSL and common sources of stress found in biomass-derived substrates like acetic acid, osmotic pressure, HMF and hydrogen peroxide-induced stress. These results demonstrate the utility of employing GS-mediated engineering as a productive technology for inhibitor-tolerant strain development of *S. cerevisiae* and suggest that the findings of this study may be broadly applicable to understanding stress tolerance in multi-inhibitory lignocellulosic substrates. The genome sequencing and differential expression analysis portion of this study were intended to generate understanding of the tolerance trait of R57 to HWSSL and generate plausible and testable hypotheses as to the genetic determinants of HWSSL tolerance and the biological processes involved.

As the first description of the types of mutations that might accumulate through GS evolution, it is interesting to note that all of the mutations discovered and verified within R57 affect genes, either being located within the ORF or a UTR. If the accumulation of mutations occurred randomly, one might expect the mutations to be randomly dispersed across the yeast genome, of which ~30 % is non-coding (387). The majority of mutations accumulated in R57 are in genes associated with biological processes that are reconcilable with stress tolerance. These observations support the hypothesis that the R57 mutations were accumulated by the selection and use of mutated

strains showing enhanced HWSSL tolerance as mating pools for GS. Therefore, this study provides the first direct genetic evidence that productive mutations are assembled into a final strain by GS, though more extensive sequencing and mutation testing would have to be carried out to draw a concrete conclusion. The mutations were all SNP mutations, which could either be a result of the UV mutagenesis used to generate mutants, a higher likelihood that small nucleotide changes lead to HWSSL tolerance, or that sequencing by MPS using short reads can often only reliably elucidate variations of a few base pairs.

As was hypothesized at the onset of this study, the biological factors behind the HWSSL tolerant trait that was generated via GS strain engineering are complex, as a variety of genes and biological processes are implicated in the R57 HWSSL-tolerant phenotype. The most significant findings and hypotheses that are supported in this study are depicted in Figure 5-1.

Stress response transcriptional repressor Nrg1p was shown to bear a likely significant functional homozygous mutation. Genes known to be directly affected by Nrg1p show a differential expression response indicative of a decreased transcriptional suppression effect. The stress-inducible acetic acid tolerance trait of R57 and the known role of Nrg1p in the acetic-acid inducible Haa1p acetic acid tolerance regulon suggest an integral role for the *NRG1* mutation of R57 in its demonstrated acetic acid tolerance trait. The potential for transcription factors to have wide-spread phenotypic bearing on an organism support further study of *NRG1* and its ability to mediate stress response to various types of inhibitors found in HWSSL.

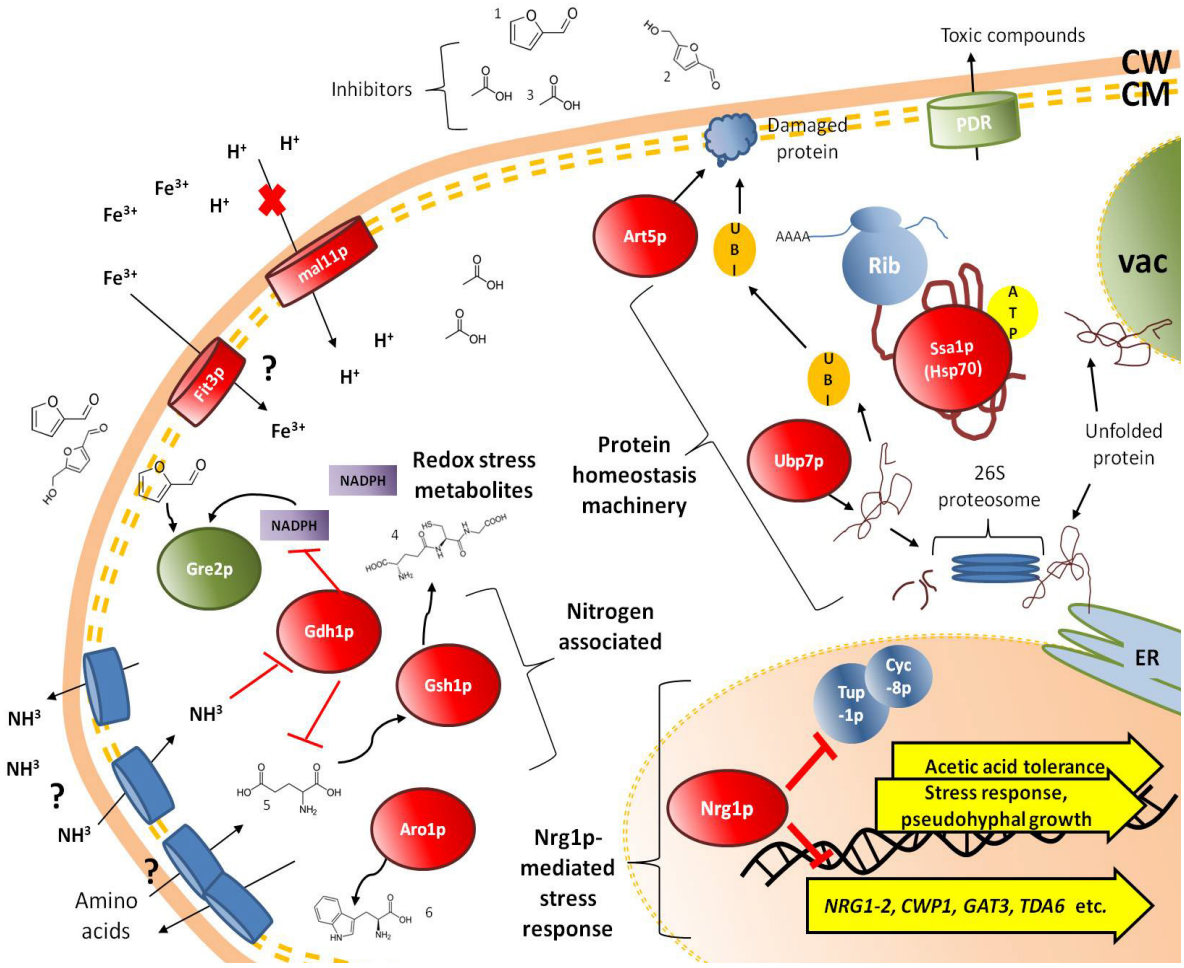

Figure 5-1. Summary of significant findings and hypotheses generated by phenotype, mutation and transcriptional analysis of strain R57. Proteins encoded by mutation-bearing R57 genes are depicted in red, proteins encoded by related over-expressed R57 genes are depicted in green. Chemical compounds are numbered as follows: 1. furfural, 2. HMF, 3. acetic acid, 4. glutamate, 5. glutathione, 6. tryptophan. UBI=ubiquitin, Rib=ribosome, vac=vacuole, ER=endoplasmic reticulum, PDR=pleiotropic drug response protein.

Another significant trend elucidated in this study is that nutrient usage, cell growth, and HWSSL stress tolerance are likely linked. This finding is in keeping with

known attributes of a diverse set of stress responses (27). Modifications in R57 to nitrogen assimilation and usage-related genes are likely playing a major role in this regard. The most significant finding related to nitrogen assimilation is the presence of two mutations, one in each copy, in NADPH-dependent Gdh1p, the main method of nitrogen assimilation via ammonia in yeast. Recent literature demonstrates the potential to affect fundamental yeast metabolism and stress tolerance by manipulation of Gdh1p (206). Overall, it is hypothesized that R57 has a modified nitrogen compound assimilation and usage machinery that may be causing a general metabolic inefficiency, resulting in a diminished growth efficiency that aids stress tolerance. Moreover, the NADPH cofactor requirement of Gdh1p is of particular note since it is required for the detoxification of furan aldehyde inhibitors, while genes that encode proteins known to be involved in detoxifying these compounds, *GRE3* and *GRE2*, show increased expression between the WT and R57 and after 2 hours HWSSL exposure in R57, respectively. Amino acid metabolism pathways show differential expression across RNA-seq experiments as well and support a prominent role for nitrogen-containing compounds in the R57 phenotype, which is reconcilable with mutations discovered in *GDH1*, *GSH1*, and *ARO1*. Modified amino acid metabolism, demonstrated by differential regulation of amino acid metabolism pathways across the differential expression experiments both between the WT and R57 and after HWSSL exposure, may be allowing R57 to reroute amino acids to compounds like glutathione, generated via Gsh1p. This hypothesis is supported by increased expression of 7 genes between the WT and R57 that are part of amino acid biosynthesis pathways leading to cysteine, glutamate, and lysine, which have all been shown to be required for glutathione synthesis (210). A role for aromatic amino

acid biosynthesis in HWSSL tolerance is also supported by this study, which is of interest due to the known effect of organic acids and ethanol exposure on tryptophan biosynthesis (66, 67). Aromatic amino acid metabolism pathways are affected by HWSSL exposure in R57 at the level of transcription and by mutation to Aro1p. Extensive differential expression of other genes related to nitrogen compound metabolism, like amino acid transporters, NCR-related control genes, or PDR-related genes supports a prominent role for modified nitrogen usage in the HWSSL tolerance trait, which was not hypothesized at the onset of this study and bears further investigation.

A modified protein homeostasis machinery in R57 is another major trend within the data presented herein, supported by phenotypic testing, mutation analysis and differential expression analysis. This may be taking place through a variety of processes that likely include modifications to: ROS tolerance-associated metabolites including iron, glutathione and NADPH, which relate to mutation-bearing *FIT3*, *GSH1* and *GDH1*; protein degradation machinery via ubiquitin-mediated proteolysis and mutation-bearing genes *UBP7* and *ART5*; and protein re/folding proteins, mainly mediated by the Hsp70 family of proteins and mutation-bearing Ssa1p. Protein damage is an expected ramification of stress exposure, especially in environments that cause oxidative damage like in substrates containing furan aldehyde inhibitors. The tolerance of R57 to peroxide and HWSSL suggests it is tolerant of the effects of oxidative damage caused by the presence of ROS. Engineering tolerance to lignocellulosic hydrolysate inhibitors via modifications to protein homeostasis machinery has, to my knowledge, not been attempted.

Based on known functions, other genes bearing mutations in R57 may be of interest for further study, though their role in HWSSL tolerance is less clear. These include the 2-mutation-bearing polysaccharide proton symporter Mal11p, which is also highly downregulated at the level of transcription in R57 and may be linked to intracellular trehalose levels or intracellular pH homeostasis. Modification to cell wall and cell membrane-associated processes is a pervasive trend in the transcriptional data gathered in this study with some genes, like NRG1p-controlled, stress-response related *CWP1* showing extensive upregulation both between the WT and R57 and after HWSSL exposure in R57. Therefore, cell-surface related R57 mutant-gene products, like Mal11p, iron-transporter Fit3p, cell-surface protein turnover mediator Art5p, and YNL058Cp, which has a largely unknown function but has been shown to be involved in mitigating cell wall damage, may prove to be useful targets in engineering stress tolerance. Also, Dop1p, which is essential and has known associations to ER organization, Golgi apparatus function and vacuolar biogenesis may be of interest and could be playing a role in protein and pH homeostasis due to the function of these organelles. Furthermore, a role for the mutation in the 5'UTR of *PBP1*, involved in stress granule formation, is supported by recent research showing that stress granules play a role in furan aldehyde tolerance (263), and Pbp1p may therefore be a productive and novel target in engineering stress tolerance. A role for R57-mutant gene *SGO1* in the HWSSL response is weakly supported by RNA-seq data with increased expression after 2 hours HWSSL exposure that does not significantly decrease over 24 hours exposure. *SGO1* is related to chromosome stability and is often tightly related in its expression to mutation-bearing *TOF2*. Tof2p and Nop58, also harboring a mutation, have corresponding roles in

ribosome synthesis. Although the stress-tolerance effect these mutations might contribute is unclear, their demonstrated interrelationship suggests that they may have been accumulated in complementary roles through GS strain engineering. Overall, what is clear from this study is that engineering tolerance to HWSSL via GS has likely resulted in multi-genic modifications, incorporating changes to multiple biological processes into a single phenotype that can withstand the complex toxic effects of lignocellulosic substrate inhibitors.

5.3 Future directions

As a workflow, meiotic recombination-mediated GS of *S. cerevisiae*, complemented with MPS genome sequencing and RNA-seq transcriptional profiling has been demonstrated in this study to be a productive means to engineer new strains with useful traits and study the changes that have been evolved, in order to gain biological insight into those traits. The most supported and plausible hypotheses to stem from these data are testable, but very extensive owing to the density of the data generated. Moreover, the precise physiology of R57 still remains largely unknown, while the impact of the variations discovered within its genome still bear further assessment.

A first logical step in further study of R57 would be to profile metabolites of interest both intracellularly and in the substrate including glutathione, NAD(P)H, iron, trehalose, ammonia and amino acids. These metabolite profiles may help to elucidate the following: the redox state of the cell upon HWSSL exposure and the mechanisms by which R57 mitigates oxidative damage; iron uptake and usage by R57 and its abundance in HWSSL; nitrogen compound assimilation and efflux by R57; and the trehalose content

of the cell and how it may relate to a role for Mal11p or effect protein homeostasis or osmotic stress protection in R57. Generating profiles for these metabolites in R57 would help us to understand tolerance to lignocellulosic substrate inhibition. In a similar fashion to the mutation analysis and RNA-seq work presented above, it would also aid in further prioritizing genes of interest for testing the contribution of the mutations in R57 to HWSSL tolerance.

Assuming not every mutation found in R57 is important for the HWSSL tolerance trait, or that there are some of lesser importance, quantitative trait loci (QTL) analysis could be performed. This would include, if possible, isolating a haploid progeny of R57 that maintained a high degree of HWSSL tolerance and crossing with a WT strain. Sampling of the offspring of that cross and genome sequencing the population or the specific mutation-regions of interest at high sequence depth would allow for the contributions of R57 mutations to HWSSL tolerance to be gauged (388). Transversely, populations of HWSSL-tolerant mutants generated throughout the GS engineering for HWSSL tolerance experiment could be sequenced to monitor the representation of mutations within the population of tolerant mutants as GS progressed. However, a statistical framework would have to be implemented to assess the significance of data generated through such an approach. Furthermore, the possibility of extra mutations not present in R57, but within the evolving populations, could confound these results. One drawback to this type of population sequencing approach is that any epistatic nature of the mutations cannot be ascertained.

Additionally, a rational cloning strategy based on the assertions generated in this study should be carried out. The preceding work allowed for the potentially most impactful HWSSL-tolerance-associated mutations in R57 to be discovered. Furthermore, mutations that are most likely to have complementary roles were described. Therefore, a systematic assembly of genes into single plasmids containing potentially complementary mutations could be introdnuced into the haploid background and tested for their effect on inhibitor tolerance, at least where the mutations are heterozygous in R57. Testing of homozygous mutations will require gene 'knock-outs' of the WT alleles and replacement with the mutant allele. Alternatively, the mutations found in R57 could be systematically replaced with WT alleles, although the diploid nature of R57 would make this a more involved process. While the cloning procedures involved in these types of experiments could be extensive in order to test permutations of mutations, the current study should serve as a way to prioritize mutations. Alternatively, automated or high-throughput cloning could make a brute force method of systematically re-introducing WT mutations into R57 or R57 mutant alleles back into the WT more feasible. A potentially useful workflow would incorporate GS, MPS of genomes of interest, followed by high-throughput cloning methods to generate and verify genes and mutations of interest.

Finally, the information generated in this study is highly applicable to an emerging lignocellulose-to-biofuels/biochemicals industry. Therefore, the strain development techniques and rational engineering targets developed above should be tested for cross-applicability to other lignocellulosic hydrolysates.

References

1. **Lynd L.** 1996. Overview and Evaluation of Fuel Ethanol from Cellulosic Biomass: Technology, Economics, the Environment, and Policy. Ann Rev Energy Environ **21:**403-465.
2. **Searchinger T, Heimlich R, Houghton RA, Dong FX, Elobeid A, Fabiosa J, Tokgoz S, Hayes D, Yu TH.** 2008. Use of US croplands for biofuels increases greenhouse gases through emissions from land-use change. Science **319:**1238-1240.
3. **Ingram LO, Aldrich HC, Borges AC, Causey TB, Martinez A, Morales F, Saleh A, Underwood SA, Yomano LP, York SW, Zaldivar J, Zhou S.** 1999. Enteric bacterial catalysts for fuel ethanol production. Biotechnol Prog **15:**855-866.
4. **van Maris AJ, Abbott DA, Bellissimi E, van den Brink J, Kuyper M, Luttik MA, Wisselink HW, Scheffers WA, van Dijken JP, Pronk JT.** 2006. Alcoholic fermentation of carbon sources in biomass hydrolysates by Saccharomyces cerevisiae: current status. Antonie Van Leeuwenhoek **90:**391-418.
5. **Sun Y, Cheng J.** 2002. Hydrolysis of lignocellulosic materials for ethanol production: a review. Bioresour Technol **83:**1-11.
6. **Palmqvist E, Hahn-Hägerdal B.** 2000. Fermentation of lignocellulosic hydrolysates. I: inhibition and detoxification. Biores Technol **74:**17-24.
7. **Almeida JRM, Modig T, Petersson A, Hahn-Hägerdal B, Lidén G, Gorwa-Grauslund MF.** 2007. Increased tolerance and conversion of inhibitors in

lignocellulosic hydrolysates by *Saccharomyces cerevisiae*. J Chem Technol Biotechnol **82:**340-349.

8. **Smith MT, Cameron DR, Duff SJB.** 1997. Comparison of industrial yeast strains for fermentation of spent sulphite pulping liquor fortified with wood hydrolysate. J Ind Microbiol Biotechnol **18:**18-21.

9. **Larsson S, Palmqvist E, Hahn-Hägerdal B, Tengborg C, Stenberg K, Zacchi G, Nilvebrant NO.** 1999. The generation of fermentation inhibitors during dilute acid hydrolysis of softwood. Enz Microb Technol **24:**151-159.

10. **Allen SA, Clark W, McCaffery JM, Cai Z, Lanctot A, Slininger PJ, Liu ZL, Gorsich SW.** 2010. Furfural induces reactive oxygen species accumulation and cellular damage in *Saccharomyces cerevisiae*. Biotechnol Biofuels **3:**2.

11. **Khan QA, Hadi SM.** 1994. Inactivation and repair of bacteriophage lambda by furfural. Biochem Mol Biol Int **32:**379-385.

12. **Liu ZL, Slininger PJ, Dien BS, Berhow MA, Kurtzman CP, Gorsich SW.** 2004. Adaptive response of yeasts to furfural and 5-hydroxymethylfurfural and new chemical evidence for HMF conversion to 2,5-bis-hydroxymethlfuran. J Ind Microbiol Biotechnol **31:**345-352.

13. **Modig T, Lidén G, Taherzadeh MJ.** 2002. Inhibition effects of furfural on alcohol dehydrogenase, aldehyde dehydrogenase and pyruvate dehydrogenase. Biochem J **363:**769-776.

14. **Moradas-Ferreira P, Costa V, Piper P, Mager W.** 1996. The molecular defences against reactive oxygen species in yeast. Mol Microbiol **19:**651-658.

15. **Terada H.** 1990. Uncouplers of oxidative phosphorylation. Environ Health Perspect **87:**213-218.

16. **Saito H, Posas F.** 2012. Response to hyperosmotic stress. Genetics **192:**289-318.

17. **Goldberg AL.** 2003. Protein degradation and protection against misfolded or damaged proteins. Nature **426:**895-899.

18. **Goldemberg J.** 2008. The Brazilian biofuels industry. Biotechnol Biofuels **1:**6.

19. **van Maris AJA, Abbott DA, Bellissimi E, van den Brink J, Kuyper M, Luttik MAH, Wisselink HW, Scheffers WA, van Dijken JP, Pronk JT.** 2006. Alcoholic fermentation of carbon sources in biomass hydrolysates by Saccharomyces cerevisiae: current status. Antonie Van Leeuwenhoek International Journal of General and Molecular Microbiology **90:**391-418.

20. **Thomas KC, Hynes SH, Ingledew WI.** 2001. Effect of lactobacilli on yeast growth, viability and batch and semi-continuous alcoholic fermentation of corn mash. J Appl Microbiol **90:**819-828.

21. **Dien BS, Cotta MA, Jeffries TW.** 2003. Bacteria engineered for fuel ethanol production: current status. Appl Microbiol Biotechnol **63:**258-266.

22. **Jarboe LR, Grabar TB, Yomano LP, Shanmugan KT, Ingram LO.** 2007. Development of ethanologenic bacteria. Adv Biochem Eng Biotechnol **108:**237-261.

23. **van Zyl WH, Lynd LR, Den Haan R, McBride JE.** 2007. Consolidated bioprocessing for bioethanol production using *Saccharomyces cerevisiae*. Adv Biochem Eng Biotechnol **108:**205-235.

24. **Zaldivar J, Nielsen J, Olsson L.** 2001. Fuel ethanol production from lignocellulose: a challenge for metabolic engineering and process integration. Appl Microbiol Biotechnol **56:**17-34.

25. **Hahn-Hägerdal B, Karhumaa K, Jeppsson M, Gorwa-Grauslund MF.** 2007. Metabolic engineering for pentose utilization in Saccharomyces cerevisiae. Adv Biochem Eng Biotechnol **108:**147-177.

26. **Olsson L, Hahn-Hägerdal B.** 1993. Fermentative performance of bacteria and yeasts in lignocellulose hydrolysates. Proc Biochem **28:**249-257.

27. **Gasch AP, Spellman PT, Kao CM, Carmel-Harel O, Eisen MB, Storz G, Botstein D, Brown PO.** 2000. Genomic expression programs in the response of yeast cells to environmental changes. Mol Biol Cell **11:**4241-4257.

28. **Dihazi H, Kessler R, Eschrich K.** 2004. High osmolarity glycerol (HOG) pathway-induced phosphorylation and activation of 6-phosphofructo-2-kinase are essential for glycerol accumulation and yeast cell proliferation under hyperosmotic stress. J Biol Chem **279:**23961-23968.

29. **Mager WH, Siderius M.** 2002. Novel insights into the osmotic stress response of yeast. FEMS Yeast Res **2:**251-257.

30. **Kumar P, Barrett DM, Delwiche MJ, Stroeve P.** 2009. Methods for pretreatment of lignocellulosic biomass for efficient hydrolysis and biofuel production. Ind Eng Chem Res **48:**3713–3729.

31. **Jorgensen H, Vibe-Pedersen J, Larsen J, Felby C.** 2007. Liquefaction of lignocellulose at high-solids concentrations. Biotechnol Bioeng **96:**862-870.

32. **van Voorst F, Houghton-Larsen J, Jonson L, Kielland-Brandt MC, Brandt A.** 2006. Genome-wide identification of genes required for growth of Saccharomyces cerevisiae under ethanol stress. Yeast **23:**351-359.

33. **Gasch AP, Spellman PT, Kao CM, Carmel-Harel O, Eisen MB, Storz G, Botstein D, Brown PO.** 2000. Genomic expression programs in the response of yeast cells to environmental changes. Mol Biol Cell **11:**4241-4257.

34. **Jungwirth H, Kuchler K.** 2006. Yeast ABC transporters-- a tale of sex, stress, drugs and aging. FEBS Lett **580:**1131-1138.

35. **Casey E, Sedlak M, Ho NW, Mosier NS.** 2010. Effect of acetic acid and pH on the cofermentation of glucose and xylose to ethanol by a genetically engineered strain of Saccharomyces cerevisiae. FEMS Yeast Res **10:**385-393.

36. **Piper P, Mahé Y, Thompson S, Pandjaitan R, Holyoak C, Egner R, Mühlbauer M, Coote P, Kuchler K.** 1998. The pdr12 ABC transporter is required for the development of weak organic acid resistance in yeast. Embo J **17:**4257-4265.

37. **Liu ZL.** 2011. Molecular mechanisms of yeast tolerance and in situ detoxification of lignocellulose hydrolysates. Appl Microbiol Biotechnol **90:**809-825.

38. **Fernandes AR, Mira NP, Vargas RC, Canelhas I, Sá-Correia I.** 2005. *Saccharomyces cerevisiae* adaptation to weak acids involves the transcription factor Haa1p and Haa1p-regulated genes. Biochem Biophys Res Commun **337:**95-103.

39. **Wang X, Xu H, Ha SW, Ju D, Xie Y.** 2010. Proteasomal degradation of Rpn4 in *Saccharomyces cerevisiae* is critical for cell viability under stressed conditions. Genetics **184:**335-342.

40. **Jelinsky SA, Samson LD.** 1999. Global response of Saccharomyces cerevisiae to an alkylating agent. Proc Natl Acad Sci U S A **96:**1486-1491.

41. **Gasch AP, Huang M, Metzner S, Botstein D, Elledge SJ, Brown PO.** 2001. Genomic expression responses to DNA-damaging agents and the regulatory role of the yeast ATR homolog Mec1p. Mol Biol Cell **12:**2987-3003.

42. **Gasch AP, Werner-Washburne M.** 2002. The genomics of yeast responses to environmental stress and starvation. Funct Integr Genomics **2:**181-192.

43. **Griffin TJ, Gygi SP, Ideker T, Rist B, Eng J, Hood L, Aebersold R.** 2002. Complementary profiling of gene expression at the transcriptome and proteome levels in Saccharomyces cerevisiae. Mol Cell Proteomics **1:**323-333.

44. **Kobayashi N, McEntee K.** 1993. Identification of cis and trans components of a novel heat shock stress regulatory pathway in Saccharomyces cerevisiae. Mol Cell Biol **13:**248-256.

45. **Marchler G, Schuller C, Adam G, Ruis H.** 1993. A Saccharomyces cerevisiae UAS element controlled by protein kinase A activates transcription in response to a variety of stress conditions. Embo J **12:**1997-2003.

46. **Martínez-Pastor MT, Marchler G, Schüller C, Marchler-Bauer A, Ruis H, Estruch F.** 1996. The Saccharomyces cerevisiae zinc finger proteins Msn2p and Msn4p are required for transcriptional induction through the stress response element (STRE). Embo J **15:**2227-2235.

47. **Kobayashi N, McClanahan TK, Simon JR, Treger JM, McEntee K.** 1996. Structure and functional analysis of the multistress response gene DDR2 from Saccharomyces cerevisiae. Biochem Biophys Res Commun **229:**540-547.

48. **Wojda I, Alonso-Monge R, Bebelman JP, Mager WH, Siderius M.** 2003. Response to high osmotic conditions and elevated temperature in Saccharomyces cerevisiae is controlled by intracellular glycerol and involves coordinate activity of MAP kinase pathways. Microbiology **149:**1193-1204.

49. **Hohmann S.** 2002. Osmotic stress signaling and osmoadaptation in yeasts. Microbiol Mol Biol Rev **66:**300-372.

50. **García R, Bermejo C, Grau C, Perez R, Rodriguez-Pena JM, Francois J, Nombela C, Arroyo J.** 2004. The global transcriptional response to transient cell wall damage in Saccharomyces cerevisiae and its regulation by the cell integrity signaling pathway. J Biol Chem **279:**15183-15195.

51. **García R, Rodríguez-Peña JM, Bermejo C, Nombela C, Arroyo J.** 2009. The high osmotic response and cell wall integrity pathways cooperate to regulate transcriptional responses to zymolyase-induced cell wall stress in Saccharomyces cerevisiae. J Biol Chem **284:**10901-10911.

52. **Lagorce A, Hauser NC, Labourdette D, Rodriguez C, Martin-Yken H, Arroyo J, Hoheisel JD, Francois J.** 2003. Genome-wide analysis of the response to cell wall mutations in the yeast Saccharomyces cerevisiae. J Biol Chem **278:**20345-20357.

53. **Moskvina E, Schüller C, Maurer CT, Mager WH, Ruis H.** 1998. A search in the genome of Saccharomyces cerevisiae for genes regulated via stress response elements. Yeast **14:**1041-1050.

54. **Klinke HB, Thomsen AB, Ahring BK.** 2004. Inhibition of ethanol-producing yeast and bacteria by degradation products produced during pre-treatment of biomass. Appl Microbiol Biotechnol **66:**10-26.

55. **Alper H, Moxley J, Nevoigt E, Fink GR, Stephanopoulos G.** 2006. Engineering yeast transcription machinery for improved ethanol tolerance and production. Science **314:**1565-1568.

56. **Li BZ, Yuan YJ.** 2010. Transcriptome shifts in response to furfural and acetic acid in Saccharomyces cerevisiae. Appl Microbiol Biotechnol **86:**1915-1924.

57. **Lin FM, Qiao B, Yuan YJ.** 2009. Comparative proteomic analysis of tolerance and adaptation of ethanologenic Saccharomyces cerevisiae to furfural, a lignocellulosic inhibitory compound. Appl Environ Microbiol **75:**3765-3776.

58. **Lin FM, Tan Y, Yuan YJ.** 2009. Temporal quantitative proteomics of Saccharomyces cerevisiae in response to a nonlethal concentration of furfural. Proteomics **9:**5471-5483.

59. **Liu ZL, Ma M, Song M.** 2009. Evolutionarily engineered ethanologenic yeast detoxifies lignocellulosic biomass conversion inhibitors by reprogrammed pathways. Mol Genet Genomics **282:**233-244.

60. **Petersson A, Almeida JRM, Modig T, Karhumaa K, Hahn-Hägerdal B, Gorwa-Grauslund MF, Lidén G.** 2006. A 5-hydroxymethyl furfural reducing

enzyme encoded by the *Saccharomyces cerevisiae* ADH6 gene conveys HMF tolerance. Yeast **23:**455-464.

61. **Horváth IS, Franzén CJ, Taherzadeh MJ, Niklasson C, Lidén G.** 2003. Effects of furfural on the respiratory metabolism of Saccharomyces cerevisiae in glucose-limited chemostats. Appl Environ Microbiol **69:**4076-4086.

62. **Coburn RF.** 2009. Polyamine effects on cell function: Possible central role of plasma membrane PI(4,5)P2. J Cell Physiol **221:**544-551.

63. **Ubiyvovk VM, Blazhenko OV, Gigot D, Penninckx M, Sibirny AA.** 2006. Role of gamma-glutamyltranspeptidase in detoxification of xenobiotics in the yeasts Hansenula polymorpha and Saccharomyces cerevisiae. Cell Biol Int **30:**665-671.

64. **Xia JM, Yuan YJ.** 2009. Comparative lipidomics of four strains of *Saccharomyces cerevisiae* reveals different responses to furfural, phenol, and acetic acid. J Agric Food Chem **57:**99-108.

65. **Fleck CB, Brock M.** 2009. Re-characterisation of Saccharomyces cerevisiae Ach1p: fungal CoA-transferases are involved in acetic acid detoxification. Fungal Genet Biol **46:**473-485.

66. **Bauer BE, Rossington D, Mollapour M, Mamnun Y, Kuchler K, Piper PW.** 2003. Weak organic acid stress inhibits aromatic amino acid uptake by yeast, causing a strong influence of amino acid auxotrophies on the phenotypes of membrane transporter mutants. Eur J Biochem **270:**3189-3195.

67. **Schüller C, Mamnun YM, Mollapour M, Krapf G, Schuster M, Bauer BE, Piper PW, Kuchler K.** 2004. Global phenotypic analysis and transcriptional

profiling defines the weak acid stress response regulon in Saccharomyces cerevisiae. Mol Biol Cell **15:**706-720.

68. **Endo A, Nakamura T, Shima J.** 2009. Involvement of ergosterol in tolerance to vanillin, a potential inhibitor of bioethanol fermentation, in Saccharomyces cerevisiae. FEMS Microbiol Lett **299:**95-99.

69. **Sundström L, Larsson S, Jönsson LJ.** 2009. Identification of Saccharomyces cerevisiae genes involved in the resistance to phenolic fermentation inhibitors. Appl Biochem Biotechnol **161:**106-115.

70. **Warringer J, Hult M, Regot S, Posas F, Sunnerhagen P.** 2010. The HOG Pathway Dictates the Short-term Translational Response after Hyperosmotic Shock. Mol Biol Cell **21:**3080-3092.

71. **Hirasawa T, Ashitani K, Yoshikawa K, Nagahisa K, Furusawa C, Katakura Y, Shimizu H, Shioya S.** 2006. Comparison of transcriptional responses to osmotic stresses induced by NaCl and sorbitol additions in Saccharomyces cerevisiae using DNA microarray. J Biosci Bioeng **102:**568-571.

72. **Ding MZ, Cheng JS, Xiao WH, Qiao B, Yuan YJ.** 2009. Comparative metabolomic analysis on industrial continuous and batch ethanol fermentation processes by GC-TOF-MS. Metabolomics **5:**229-238.

73. **Bai FW, Chen LJ, Zhang Z, Anderson WA, Moo-Young M.** 2004. Continuous ethanol production and evaluation of yeast cell lysis and viability loss under very high gravity medium conditions. J Biotechnol **110:**287-293.

74. **Pina C, Couto JA, Hogg T.** 2004. Inferring ethanol tolerance of Saccharomyces and non-Saccharomyces yeasts by progressive inactivation. Biotechnol Lett **26:**1521-1527.

75. **Alexandre H, Ansanay-Galeote V, Dequin S, Blondin B.** 2001. Global gene expression during short-term ethanol stress in Saccharomyces cerevisiae. FEBS Lett **498:**98-103.

76. **Dinh TN, Nagahisa K, Hirasawa T, Furusawa C, Shimizu H.** 2008. Adaptation of Saccharomyces cerevisiae cells to high ethanol concentration and changes in fatty acid composition of membrane and cell size. PLoS One **3:**e2623.

77. **Dinh TN, Nagahisa K, Yoshikawa K, Hirasawa T, Furusawa C, Shimizu H.** 2009. Analysis of adaptation to high ethanol concentration in Saccharomyces cerevisiae using DNA microarray. Bioprocess Biosyst Eng **32:**681-688.

78. **Ogawa Y, Nitta A, Uchiyama H, Imamura T, Shimoi H, Ito K.** 2000. Tolerance mechanism of the ethanol-tolerant mutant of sake yeast. J Biosci Bioeng **90:**313-320.

79. **Kolkman A, Olsthoorn MM, Heeremans CE, Heck AJ, Slijper M.** 2005. Comparative proteome analysis of Saccharomyces cerevisiae grown in chemostat cultures limited for glucose or ethanol. Mol Cell Proteomics **4:**1-11.

80. **Hirasawa T, Yoshikawa K, Nakakura Y, Nagahisa K, Furusawa C, Katakura Y, Shimizu H, Shioya S.** 2007. Identification of target genes conferring ethanol stress tolerance to Saccharomyces cerevisiae based on DNA microarray data analysis. J Biotechnol **131:**34-44.

81. **Ma M, Liu LZ.** 2010. Quantitative transcription dynamic analysis reveals candidate genes and key regulators for ethanol tolerance in Saccharomyces cerevisiae. BMC Microbiol **10:**169.

82. **Carreto L, Eiriz MF, Gomes AC, Pereira PM, Schuller D, Santos MA.** 2008. Comparative genomics of wild type yeast strains unveils important genome diversity. BMC Genomics **9:**524.

83. **Argueso JL, Carazzolle MF, Mieczkowski PA, Duarte FM, Netto OV, Missawa SK, Galzerani F, Costa GG, Vidal RO, Noronha MF, Dominska M, Andrietta MG, Andrietta SR, Cunha AF, Gomes LH, Tavares FC, Alcarde AR, Dietrich FS, McCusker JH, Petes TD, Pereira GA.** 2009. Genome structure of a *Saccharomyces cerevisiae* strain widely used in bioethanol production. Genome Res **19:**2258-2270.

84. **Mense SM, Zhang L.** 2006. Heme: a versatile signaling molecule controlling the activities of diverse regulators ranging from transcription factors to MAP kinases. Cell Res **16:**681-692.

85. **Tamura K, Gu Y, Wang Q, Yamada T, Ito K, Shimoi H.** 2004. A hap1 mutation in a laboratory strain of Saccharomyces cerevisiae results in decreased expression of ergosterol-related genes and cellular ergosterol content compared to sake yeast. J Biosci Bioeng **98:**159-166.

86. **Aguilera F, Peinado RA, Millán C, Ortega JM, Mauricio JC.** 2006. Relationship between ethanol tolerance, H+ -ATPase activity and the lipid composition of the plasma membrane in different wine yeast strains. Int J Food Microbiol **110:**34-42.

87. **Inoue T, Iefuji H, Fujii T, Soga H, Satoh K.** 2000. Cloning and characterization of a gene complementing the mutation of an ethanol-sensitive mutant of sake yeast. Biosci Biotechnol Biochem **64:**229-236.

88. **Yazawa H, Iwahashi H, Uemura H.** 2007. Disruption of URA7 and GAL6 improves the ethanol tolerance and fermentation capacity of Saccharomyces cerevisiae. Yeast **24:**551-560.

89. **Robinson J, Keating J, Saddler JN, Mansfield SD.** 2002. Concentrating dilute wood pre-hydrolysates to improve ethanol recovery. Abstracts of Papers of the Am Chem Soc **223:**U123-U123.

90. **Helle SS, Lin T, Duff SJB.** 2008. Optimization of spent sulfite liquor fermentation. Enz Micro Technol **42:**259-264.

91. **Helle SS, Murray A, Lam J, Cameron DR, Duff SJ.** 2004. Xylose fermentation by genetically modified *Saccharomyces cerevisiae* 259ST in spent sulfite liquor. Bioresour Technol **92:**163-171.

92. **Olsson L, HahnHagerdal B.** 1996. Fermentation of lignocellulosic hydrolysates for ethanol production. Enzyme Microb Tech **18:**312-331.

93. **Parajó JC, Domíngues H, Domínguez JM.** 1998. Biotechnological production of xylitol. Part 3: Operation in culturemedia made from lignocellulosehydrolysates. Bioresour Technol **66:**25-40.

94. **Helle S, Duff S.** 2004. Supplementing spent sulfite liquor with a lignocellulosic hydrolysate to increase pentose / hexose co-fermentation efficiency and ethanol yield. University of British Columbia.

95. **Nigam JN.** 2001. Ethanol production from hardwood spent sulfite liquor using an adapted strain of *Pichia stipitis*. J Ind Microbiol Biotechnol **26:**145-150.

96. **Keating JD, Panganiban C, Mansfield SD.** 2006. Tolerance and adaptation of ethanologenic yeasts to lignocellulosic inhibitory compounds. Biotechnol Bioeng **93:**1196-1206.

97. **Gorsich SW, Slininger PJ, Liu ZL.** 2005. Physiological responses to furfural and HMF and the link to other stress pathways. J Biotechnol **118:**S91-S91.

98. **Zhang YX, Perry K, Vinci VA, Powell K, Stemmer WPC, del Cardayre SB.** 2002. Genome shuffling leads to rapid phenotypic improvement in bacteria. Nature **415:**644-646.

99. **Patnaik R, Louie S, Gavrilovic V, Perry K, Stemmer WPC, Ryan CM, del Cardayre S.** 2002. Genome shuffling of *Lactobacillus* for improved acid tolerance. Nat Biotechnol **20:**707-712.

100. **Dai MH, Copley SD.** 2004. Genome shuffling improves degradation of the anthropogenic pesticide pentachlorophenol by *Sphingobium chlorophenolicum* ATCC 39723. Appl Environ Microbiol **70:**2391-2397.

101. **Wang YH, Li Y, Pei XL, Yu L, Feng Y.** 2007. Genome-shuffling improved acid tolerance and L-lactic acid volumetric productivity in *Lactobacillus rhamnosus*. J Biotechnol **129:**510-515.

102. **Hou L.** 2009. Improved production of ethanol by novel genome shuffling in *Saccharomyces cerevisiae*. Appl Biochem Biotechnol **160:**1084-1093.

103. **Shi DJ, Wang CL, Wang KM.** 2009. Genome shuffling to improve thermotolerance, ethanol tolerance and ethanol productivity of *Saccharomyces cerevisiae*. J Ind Microbiol Biotechnol **36:**139-147.

104. **Hou L.** 2009. Novel methods of genome shuffling in *Saccharomyces cerevisiae*. Biotechnol Lett **31:**671-677.

105. **Zhao K, Ping W, Zhang L, Liu J, Lin Y, Jin T, Zhou D.** 2008. Screening and breeding of high taxol producing fungi by genome shuffling. Sci China C Life Sci **51:**222-231.

106. **Bajwa PK, Pinel D, Martin VJ, Trevors JT, Lee H.** 2010. Strain improvement of the pentose-fermenting yeast *Pichia stipitis* by genome shuffling. J Microbiol Methods **81:**179-186.

107. **Smith DR, Quinlan AR, Peckham HE, Makowsky K, Tao W, Woolf B, Shen L, Donahue WF, Tusneem N, Stromberg MP, Stewart DA, Zhang L, Ranade SS, Warner JB, Lee CC, Coleman BE, Zhang Z, McLaughlin SF, Malek JA, Sorenson JM, Blanchard AP, Chapman J, Hillman D, Chen F, Rokhsar DS, McKernan KJ, Jeffries TW, Marth GT, Richardson PM.** 2008. Rapid whole-genome mutational profiling using next-generation sequencing technologies. Gen Res **18:**1638-1642.

108. **Dhar R, Sägesser R, Weikert C, Yuan J, Wagner A.** 2011. Adaptation of *Saccharomyces cerevisiae* to saline stress through laboratory evolution. J Evol Biol **24:**1135-1153.

109. **Hong KK, Vongsangnak W, Vemuri GN, Nielsen J.** 2011. Unravelling evolutionary strategies of yeast for improving galactose utilization through integrated systems level analysis. Proc Natl Acad Sci U S A **108:**12179-12184.

110. **Kvitek DJ, Sherlock G.** 2011. Reciprocal sign epistasis between frequently experimentally evolved adaptive mutations causes a rugged fitness landscape. PLoS Genet **7:**e1002056.

111. **Timmermann B, Jarolim S, Russmayer H, Kerick M, Michel S, Krüger A, Bluemlein K, Laun P, Grillari J, Lehrach H, Breitenbach M, Ralser M.** 2010. A new dominant peroxiredoxin allele identified by whole-genome re-sequencing of random mutagenized yeast causes oxidant-resistance and premature aging. Aging (Albany NY) **2:**475-486.

112. **Mardis ER.** 2008. Next-generation DNA sequencing methods. Annu Rev Genomics Hum Genet **9:**387-402.

113. **Nielsen R, Paul JS, Albrechtsen A, Song YS.** 2011. Genotype and SNP calling from next-generation sequencing data. Nat Rev Genet **12:**443-451.

114. **Stranneheim H, Lundeberg J.** 2012. Stepping stones in DNA sequencing. Biotechnol J **7:**1063-1073.

115. **Koboldt DC, Larson DE, Chen K, Ding L, Wilson RK.** 2012. Massively parallel sequencing approaches for characterization of structural variation. Methods Mol Biol **838:**369-384.

116. **Schadt EE, Linderman MD, Sorenson J, Lee L, Nolan GP.** 2010. Computational solutions to large-scale data management and analysis. Nat Rev Genet **11:**647-557.

117. **Pabinger S, Dander A, Fischer M, Snajder R, Sperk M, Efremova M, Krabichler B, Speicher MR, Zschocke J, Trajanoski Z.** 2013. A survey of tools for variant analysis of next-generation genome sequencing data. Brief Bioinform.

118. **Dai M, Thompson RC, Maher C, Contreras-Galindo R, Kaplan MH, Markovitz DM, Omenn G, Meng F.** 2010. NGSQC: cross-platform quality analysis pipeline for deep sequencing data. BMC Genomics **11 Suppl 4:**S7.

119. **Li H, Ruan J, Durbin R.** 2008. Mapping short DNA sequencing reads and calling variants using mapping quality scores. Genome Res **18:**1851-1858.

120. **Langmead B, Trapnell C, Pop M, Salzberg SL.** 2009. Ultrafast and memory-efficient alignment of short DNA sequences to the human genome. Genome Biol **10:**R25.

121. **Bansal V.** 2010. A statistical method for the detection of variants from next-generation resequencing of DNA pools. Bioinformatics **26:**i318-324.

122. **Albers CA, Lunter G, MacArthur DG, McVean G, Ouwehand WH, Durbin R.** 2011. Dindel: accurate indel calls from short-read data. Genome Res **21:**961-973.

123. **Li H, Handsaker B, Wysoker A, Fennell T, Ruan J, Homer N, Marth G, Abecasis G, Durbin R.** 2009. The Sequence Alignment/Map format and SAMtools. Bioinformatics **25:**2078-2079.

124. **DePristo MA, Banks E, Poplin R, Garimella KV, Maguire JR, Hartl C, Philippakis AA, del Angel G, Rivas MA, Hanna M, McKenna A, Fennell TJ, Kernytsky AM, Sivachenko AY, Cibulskis K, Gabriel SB, Altshuler D, Daly**

MJ. 2011. A framework for variation discovery and genotyping using next-generation DNA sequencing data. Nat Genet **43:**491-498.

125. **Szatkiewicz JP, Wang W, Sullivan PF, Sun W.** 2013. Improving detection of copy-number variation by simultaneous bias correction and read-depth segmentation. Nucleic Acids Res **41:**1519-1532.

126. **Xie C, Tammi MT.** 2009. CNV-seq, a new method to detect copy number variation using high-throughput sequencing. Bmc Bioinformatics **10**.

127. **Nijkamp JF, van den Broek M, Datema E, de Kok S, Bosman L, Luttik MA, Daran-Lapujade P, Vongsangnak W, Nielsen J, Heijne WH, Klaassen P, Paddon CJ, Platt D, Kötter P, van Ham RC, Reinders MJ, Pronk JT, de Ridder D, Daran JM.** 2012. De novo sequencing, assembly and analysis of the genome of the laboratory strain *Saccharomyces cerevisiae* CEN.PK113-7D, a model for modern industrial biotechnology. Microb Cell Fact **11:**36.

128. **Wang K, Li M, Hakonarson H.** 2010. ANNOVAR: functional annotation of genetic variants from high-throughput sequencing data. Nucleic Acids Res **38:**e164.

129. **Westesson O, Skinner M, Holmes I.** 2013. Visualizing next-generation sequencing data with JBrowse. Brief Bioinform **14:**172-177.

130. **Lee E, Harris N, Gibson M, Chetty R, Lewis S.** 2009. Apollo: a community resource for genome annotation editing. Bioinformatics **25:**1836-1837.

131. **Dreszer TR, Karolchik D, Zweig AS, Hinrichs AS, Raney BJ, Kuhn RM, Meyer LR, Wong M, Sloan CA, Rosenbloom KR, Roe G, Rhead B, Pohl A, Malladi VS, Li CH, Learned K, Kirkup V, Hsu F, Harte RA, Guruvadoo L,**

Goldman M, Giardine BM, Fujita PA, Diekhans M, Cline MS, Clawson H, Barber GP, Haussler D, James Kent W. 2012. The UCSC Genome Browser database: extensions and updates 2011. Nucleic Acids Res **40:**D918-923.

132. **Lam HY, Pan C, Clark MJ, Lacroute P, Chen R, Haraksingh R, O'Huallachain M, Gerstein MB, Kidd JM, Bustamante CD, Snyder M.** 2012. Detecting and annotating genetic variations using the HugeSeq pipeline. Nat Biotechnol **30:**226-229.

133. **Fischer M, Snajder R, Pabinger S, Dander A, Schossig A, Zschocke J, Trajanoski Z, Stocker G.** 2012. SIMPLEX: cloud-enabled pipeline for the comprehensive analysis of exome sequencing data. PLoS One **7:**e41948.

134. **Asmann YW, Middha S, Hossain A, Baheti S, Li Y, Chai HS, Sun Z, Duffy PH, Hadad AA, Nair A, Liu X, Zhang Y, Klee EW, Kalari KR, Kocher JP.** 2012. TREAT: a bioinformatics tool for variant annotations and visualizations in targeted and exome sequencing data. Bioinformatics **28:**277-278.

135. **Goecks J, Nekrutenko A, Taylor J.** 2010. Galaxy: a comprehensive approach for supporting accessible, reproducible, and transparent computational research in the life sciences. Genome Biol **11:**R86.

136. **Horak CE, Snyder M.** 2002. Global analysis of gene expression in yeast. Funct Integr Genomics **2:**171-180.

137. **Wilhelm BT, Landry JR.** 2009. RNA-Seq-quantitative measurement of expression through massively parallel RNA-sequencing. Methods **48:**249-257.

138. **Schena M, Shalon D, Davis RW, Brown PO.** 1995. Quantitative monitoring of gene expression patterns with a complementary DNA microarray. Science **270:**467-470.

139. **Mira NP, Becker JD, Sá-Correia I.** 2010. Genomic expression program involving the Haa1p-regulon in *Saccharomyces cerevisiae* response to acetic acid. OMICS **14:**587-601.

140. **Okoniewski MJ, Miller CJ.** 2006. Hybridization interactions between probesets in short oligo microarrays lead to spurious correlations. Bmc Bioinformatics **7:**276.

141. **Garber M, Grabherr MG, Guttman M, Trapnell C.** 2011. Computational methods for transcriptome annotation and quantification using RNA-seq. Nat Methods **8:**469-477.

142. **Wang ET, Sandberg R, Luo S, Khrebtukova I, Zhang L, Mayr C, Kingsmore SF, Schroth GP, Burge CB.** 2008. Alternative isoform regulation in human tissue transcriptomes. Nature **456:**470-476.

143. **Cloonan N, Forrest AR, Kolle G, Gardiner BB, Faulkner GJ, Brown MK, Taylor DF, Steptoe AL, Wani S, Bethel G, Robertson AJ, Perkins AC, Bruce SJ, Lee CC, Ranade SS, Peckham HE, Manning JM, McKernan KJ, Grimmond SM.** 2008. Stem cell transcriptome profiling via massive-scale mRNA sequencing. Nat Methods **5:**613-619.

144. **Mortazavi A, Williams BA, McCue K, Schaeffer L, Wold B.** 2008. Mapping and quantifying mammalian transcriptomes by RNA-Seq. Nat Methods **5:**621-628.

145. **Vera JC, Wheat CW, Fescemyer HW, Frilander MJ, Crawford DL, Hanski I, Marden JH.** 2008. Rapid transcriptome characterization for a nonmodel organism using 454 pyrosequencing. Mol Ecol **17:**1636-1647.

146. **Griffith M, Griffith OL, Mwenifumbo J, Goya R, Morrissy AS, Morin RD, Corbett R, Tang MJ, Hou YC, Pugh TJ, Robertson G, Chittaranjan S, Ally A, Asano JK, Chan SY, Li HI, McDonald H, Teague K, Zhao Y, Zeng T, Delaney A, Hirst M, Morin GB, Jones SJ, Tai IT, Marra MA.** 2010. Alternative expression analysis by RNA sequencing. Nat Methods **7:**843-847.

147. **Li H, Durbin R.** 2009. Fast and accurate short read alignment with Burrows-Wheeler transform. Bioinformatics **25:**1754-1760.

148. **De Bona F, Ossowski S, Schneeberger K, Ratsch G.** 2008. Optimal spliced alignments of short sequence reads. Bioinformatics **24:**i174-180.

149. **Trapnell C, Williams BA, Pertea G, Mortazavi A, Kwan G, van Baren MJ, Salzberg SL, Wold BJ, Pachter L.** 2010. Transcript assembly and quantification by RNA-Seq reveals unannotated transcripts and isoform switching during cell differentiation. Nat Biotechnol **28:**511-515.

150. **Lister R, Gregory BD, Ecker JR.** 2009. Next is now: new technologies for sequencing of genomes, transcriptomes, and beyond. Curr Opin Plant Biol **12:**107-118.

151. **Robinson MD, McCarthy DJ, Smyth GK.** 2010. edgeR: a Bioconductor package for differential expression analysis of digital gene expression data. Bioinformatics **26:**139-140.

152. **Marioni JC, Mason CE, Mane SM, Stephens M, Gilad Y.** 2008. RNA-seq: an assessment of technical reproducibility and comparison with gene expression arrays. Genome Res **18:**1509-1517.

153. **Robinson MD, Oshlack A.** 2010. A scaling normalization method for differential expression analysis of RNA-seq data. Genome Biol **11:**R25.

154. **Li J, Jiang H, Wong WH.** 2010. Modeling non-uniformity in short-read rates in RNA-Seq data. Genome Biol **11:**R50.

155. **Li B, Ruotti V, Stewart RM, Thomson JA, Dewey CN.** 2010. RNA-Seq gene expression estimation with read mapping uncertainty. Bioinformatics **26:**493-500.

156. **Nookaew I, Papini M, Pornputtapong N, Scalcinati G, Fagerberg L, Uhlen M, Nielsen J.** 2012. A comprehensive comparison of RNA-Seq-based transcriptome analysis from reads to differential gene expression and cross-comparison with microarrays: a case study in Saccharomyces cerevisiae. Nucleic Acids Res **40:**10084-10097.

157. **Young MD, Wakefield MJ, Smyth GK, Oshlack A.** 2010. Gene ontology analysis for RNA-seq: accounting for selection bias. Genome Biol **11:**R14.

158. **Zhou X, Su Z.** 2007. EasyGO: Gene Ontology-based annotation and functional enrichment analysis tool for agronomical species. BMC Genomics **8:**246.

159. **Zeeberg BR, Qin H, Narasimhan S, Sunshine M, Cao H, Kane DW, Reimers M, Stephens RM, Bryant D, Burt SK, Elnekave E, Hari DM, Wynn TA, Cunningham-Rundles C, Stewart DM, Nelson D, Weinstein JN.** 2005. High-Throughput GoMiner, an 'industrial-strength' integrative gene ontology tool for

interpretation of multiple-microarray experiments, with application to studies of Common Variable Immune Deficiency (CVID). Bmc Bioinformatics **6:**168.

160. **Subramanian A, Kuehn H, Gould J, Tamayo P, Mesirov JP.** 2007. GSEA-P: a desktop application for Gene Set Enrichment Analysis. Bioinformatics **23:**3251-3253.

161. **Huang da W, Sherman BT, Lempicki RA.** 2009. Systematic and integrative analysis of large gene lists using DAVID bioinformatics resources. Nat Protoc **4:**44-57.

162. **van Dijken JP, Bauer J, Brambilla L, Duboc P, Francois JM, Gancedo C, Giuseppin ML, Heijnen JJ, Hoare M, Lange HC, Madden EA, Niederberger P, Nielsen J, Parrou JL, Petit T, Porro D, Reuss M, van Riel N, Rizzi M, Steensma HY, Verrips CT, Vindelov J, Pronk JT.** 2000. An interlaboratory comparison of physiological and genetic properties of four *Saccharomyces cerevisiae* strains. Enz Microb Technol **26:**706-714.

163. **Sherman F.** 2002. Getting started with yeast. Guide to Yeast Genetics and Molecular and Cell Biology, Pt B **350:**3-41.

164. **Sherman F, Fink GR, Lawrence CW.** 1979. Methods in yeast genetics. Cold Spring Harbor, New York.

165. **Bajwa PK, Shireen T, D'Aoust F, Pinel D, Martin VJ, Trevors JT, Lee H.** 2009. Mutants of the pentose-fermenting yeast *Pichia stipitis* with improved tolerance to inhibitors in hardwood spent sulfite liquor. Biotechnol Bioeng **104:**892-900.

166. **McGinnis GD.** 1982. Preparation of aldononitrile acetates using N-methylimidazole as a catalyst and solvent. Carb Res **V.:**284.

167. **Tuite MF.** 1992. Strategies for the genetic manipulation of *Saccharomyces cerevisiae*. Crit Rev Biotechnol **12:**157-188.

168. **Martin C, Jonsson LJ.** 2003. Comparison of the resistance of industrial and laboratory strains of *Saccharomyces* and *Zygosaccharomyces* to lignocellulose-derived fermentation inhibitors. Enz Microb Technol **32:**386-395.

169. **Gancedo JM.** 1998. Yeast carbon catabolite repression. Microbiol Mol Biol Rev **62:**334-361.

170. **Shi X, Chabarek K, Budai A, Zhu Z.** 2003. Iron requirement for GAL gene induction in the yeast *Saccharomyces cerevisiae*. J Biol Chem **278:**43110-43113.

171. **Liu ZL.** 2006. Genomic adaptation of ethanologenic yeast to biomass conversion inhibitors. Appl Microbiol Biotechnol **73:**27-36.

172. **Gasch AP, Spellman PT, Kao CM, Carmel-Harel O, Eisen MB, Storz G, Botstein D, Brown PO.** 2000. Genomic expression programs in the response of yeast cells to environmental changes. Mol Biol Cell **11:**4241-4257.

173. **El-Gendy MM, El-Bondkly AM.** 2011. Genome shuffling of marine derived bacterium *Nocardia sp.* ALAA 2000 for improved ayamycin production. Antonie Van Leeuwenhoek **99:**773-780.

174. **Bajwa PK, Phaenark C, Grant N, Zhang X, Paice M, Martin VJ, Trevors JT, Lee H.** 2011. Ethanol production from selected lignocellulosic hydrolysates by genome shuffled strains of *Scheffersomyces stipitis*. Bioresour Technol **102:**9965-9969.

175. **Palmqvist E, Hahn-Hägerdal B.** 2000. Fermentation of lignocellulosic hydrolysates. II: inhibitors and mechanisms of inhibition. Biores Technol **74:**25-33.

176. **Wright J, Bellissimi E, de Hulster E, Wagner A, Pronk JT, van Maris AJ.** 2011. Batch and continuous culture-based selection strategies for acetic acid tolerance in xylose-fermenting *Saccharomyces cerevisiae*. FEMS Yeast Res **doi: 10.1111/j.1567-1364.2011.00719.x.:**1-8.

177. **Abbott DA, Suir E, van Maris AJ, Pronk JT.** 2008. Physiological and transcriptional responses to high concentrations of lactic acid in anaerobic chemostat cultures of *Saccharomyces cerevisiae*. Appl Environ Microbiol **74:**5759-5768.

178. **Attfield PV.** 1997. Stress tolerance: the key to effective strains of industrial baker's yeast. Nat Biotechnol **15:**1351-1357.

179. **Langmead B, Trapnell C, Pop M, Salzberg SL.** 2009. Ultrafast and memory-efficient alignment of short DNA sequences to the human genome. Genome Biology **10**.

180. **Nakamura K, Oshima T, Morimoto T, Ikeda S, Yoshikawa H, Shiwa Y, Ishikawa S, Linak MC, Hirai A, Takahashi H, Altaf-Ul-Amin M, Ogasawara N, Kanaya S.** 2011. Sequence-specific error profile of Illumina sequencers. Nucleic Acids Research **39:**e90.

181. **Oyola SO, Otto TD, Gu Y, Maslen G, Manske M, Campino S, Turner DJ, Macinnis B, Kwiatkowski DP, Swerdlow HP, Quail MA.** 2012. Optimizing

Illumina next-generation sequencing library preparation for extremely AT-biased genomes. BMC Genomics **13:**1.

182. **Artimo P, Jonnalagedda M, Arnold K, Baratin D, Csardi G, de Castro E, Duvaud S, Flegel V, Fortier A, Gasteiger E, Grosdidier A, Hernandez C, Ioannidis V, Kuznetsov D, Liechti R, Moretti S, Mostaguir K, Redaschi N, Rossier G, Xenarios I, Stockinger H.** 2012. ExPASy: SIB bioinformatics resource portal. Nucleic Acids Res **40:**W597-603.

183. **Sim NL, Kumar P, Hu J, Henikoff S, Schneider G, Ng PC.** 2012. SIFT web server: predicting effects of amino acid substitutions on proteins. Nucleic Acids Research **40:**W452-457.

184. **Kumar P, Henikoff S, Ng PC.** 2009. Predicting the effects of coding non-synonymous variants on protein function using the SIFT algorithm. Nat Protoc **4:**1073-1081.

185. **Ng PC, Henikoff S.** 2006. Predicting the effects of amino acid substitutions on protein function. Annu Rev Genomics Hum Genet **7:**61-80.

186. **Ng PC, Henikoff S.** 2003. SIFT: Predicting amino acid changes that affect protein function. Nucleic Acids Research **31:**3812-3814.

187. **Ng PC, Henikoff S.** 2001. Predicting deleterious amino acid substitutions. Genome Res **11:**863-874.

188. **Maere S, Heymans K, Kuiper M.** 2005. BiNGO: a Cytoscape plugin to assess overrepresentation of gene ontology categories in biological networks. Bioinformatics **21:**3448-3449.

189. **Smoot ME, Ono K, Ruscheinski J, Wang PL, Ideker T.** 2011. Cytoscape 2.8: new features for data integration and network visualization. Bioinformatics **27:**431-432.

190. **Shannon P, Markiel A, Ozier O, Baliga NS, Wang JT, Ramage D, Amin N, Schwikowski B, Ideker T.** 2003. Cytoscape: a software environment for integrated models of biomolecular interaction networks. Genome Res **13:**2498-2504.

191. **Cline MS, Smoot M, Cerami E, Kuchinsky A, Landys N, Workman C, Christmas R, Avila-Campilo I, Creech M, Gross B, Hanspers K, Isserlin R, Kelley R, Killcoyne S, Lotia S, Maere S, Morris J, Ono K, Pavlovic V, Pico AR, Vailaya A, Wang PL, Adler A, Conklin BR, Hood L, Kuiper M, Sander C, Schmulevich I, Schwikowski B, Warner GJ, Ideker T, Bader GD.** 2007. Integration of biological networks and gene expression data using Cytoscape. Nat Protoc **2:**2366-2382.

192. **Montojo J, Zuberi K, Rodriguez H, Kazi F, Wright G, Donaldson SL, Morris Q, Bader GD.** 2010. GeneMANIA Cytoscape plugin: fast gene function predictions on the desktop. Bioinformatics **26:**2927-2928.

193. **Warde-Farley D, Donaldson SL, Comes O, Zuberi K, Badrawi R, Chao P, Franz M, Grouios C, Kazi F, Lopes CT, Maitland A, Mostafavi S, Montojo J, Shao Q, Wright G, Bader GD, Morris Q.** 2010. The GeneMANIA prediction server: biological network integration for gene prioritization and predicting gene function. Nucleic Acids Res **38:**W214-220.

194. **Nagalakshmi U, Wang Z, Waern K, Shou C, Raha D, Gerstein M, Snyder M.** 2008. The transcriptional landscape of the yeast genome defined by RNA sequencing. Science **320:**1344-1349.

195. **Yassour M, Kaplan T, Fraser HB, Levin JZ, Pfiffner J, Adiconis X, Schroth G, Luo S, Khrebtukova I, Gnirke A, Nusbaum C, Thompson DA, Friedman N, Regev A.** 2009. Ab initio construction of a eukaryotic transcriptome by massively parallel mRNA sequencing. Proc Natl Acad Sci U S A **106:**3264-3269.

196. **Botzman M, Margalit H.** 2011. Variation in global codon usage bias among prokaryotic organisms is associated with their lifestyles. Genome Biol **12:**R109.

197. **Hunt R, Sauna ZE, Ambudkar SV, Gottesman MM, Kimchi-Sarfaty C.** 2009. Silent (synonymous) SNPs: should we care about them? Methods Mol Biol **578:**23-39.

198. **Miller JH.** 1985. Mutagenic specificity of ultraviolet light. J Mol Biol **182:**45-65.

199. **Zhu C, Byers KJ, McCord RP, Shi Z, Berger MF, Newburger DE, Saulrieta K, Smith Z, Shah MV, Radhakrishnan M, Philippakis AA, Hu Y, De Masi F, Pacek M, Rolfs A, Murthy T, Labaer J, Bulyk ML.** 2009. High-resolution DNA-binding specificity analysis of yeast transcription factors. Genome Res **19:**556-566.

200. **Horton LE, James P, Craig EA, Hensold JO.** 2001. The yeast hsp70 homologue Ssa is required for translation and interacts with Sis1 and Pab1 on translating ribosomes. J Biol Chem **276:**14426-14433.

201. **Takahara T, Maeda T.** 2012. Transient sequestration of TORC1 into stress granules during heat stress. Mol Cell **47:**242-252.

202. **Hibbs MA, Hess DC, Myers CL, Huttenhower C, Li K, Troyanskaya OG.** 2007. Exploring the functional landscape of gene expression: directed search of large microarray compendia. Bioinformatics **23:**2692-2699.

203. **de Kok S, Nijkamp JF, Oud B, Roque FC, de Ridder D, Daran JM, Pronk JT, van Maris AJ.** 2012. Laboratory evolution of new lactate transporter genes in a jen1Δ mutant of *Saccharomyces cerevisiae* and their identification as ADY2 alleles by whole-genome resequencing and transcriptome analysis. Fems Yeast Research.

204. **Lang GI, Murray AW.** 2008. Estimating the per-base-pair mutation rate in the yeast *Saccharomyces cerevisiae*. Genetics **178:**67-82.

205. **Magasanik B.** 2003. Ammonia assimilation by Saccharomyces cerevisiae. Eukaryot Cell **2:**827-829.

206. **Ding MZ, Wang X, Liu W, Cheng JS, Yang Y, Yuan YJ.** 2012. Proteomic research reveals the stress response and detoxification of yeast to combined inhibitors. PLoS One **7:**e43474.

207. **Mira NP, Palma M, Guerreiro JF, Sá-Correia I.** 2010. Genome-wide identification of *Saccharomyces cerevisiae* genes required for tolerance to acetic acid. Microb Cell Fact **9:**79.

208. **Asadollahi MA, Maury J, Patil KR, Schalk M, Clark A, Nielsen J.** 2009. Enhancing sesquiterpene production in *Saccharomyces cerevisiae* through in silico driven metabolic engineering. Metab Eng **11:**328-334.

209. **Grant CM.** 2001. Role of the glutathione/glutaredoxin and thioredoxin systems in yeast growth and response to stress conditions. Mol Microbiol **39:**533-541.

210. **Stephen DW, Jamieson DJ.** 1997. Amino acid-dependent regulation of the *Saccharomyces cerevisiae* GSH1 gene by hydrogen peroxide. Mol Microbiol **23:**203-210.

211. **Almeida JR, Bertilsson M, Gorwa-Grauslund MF, Gorsich S, Lidén G.** 2009. Metabolic effects of furaldehydes and impacts on biotechnological processes. Appl Microbiol Biotechnol **82:**625-638.

212. **Boer VM, de Winde JH, Pronk JT, Piper MD.** 2003. The genome-wide transcriptional responses of *Saccharomyces cerevisiae* grown on glucose in aerobic chemostat cultures limited for carbon, nitrogen, phosphorus, or sulfur. J Biol Chem **278:**3265-3274.

213. **Dalle-Donne I, Rossi R, Colombo G, Giustarini D, Milzani A.** 2009. Protein S-glutathionylation: a regulatory device from bacteria to humans. Trends Biochem Sci **34:**85-96.

214. **Liu H, Lightfoot R, Stevens JL.** 1996. Activation of heat shock factor by alkylating agents is triggered by glutathione depletion and oxidation of protein thiols. J Biol Chem **271:**4805-4812.

215. **Gavin AC, Aloy P, Grandi P, Krause R, Boesche M, Marzioch M, Rau C, Jensen LJ, Bastuck S, Dümpelfeld B, Edelmann A, Heurtier MA, Hoffman V, Hoefert C, Klein K, Hudak M, Michon AM, Schelder M, Schirle M, Remor M, Rudi T, Hooper S, Bauer A, Bouwmeester T, Casari G, Drewes G, Neubauer G, Rick JM, Kuster B, Bork P, Russell RB, Superti-Furga G.** 2006. Proteome survey reveals modularity of the yeast cell machinery. Nature **440:**631-636.

216. **Duncan K, Edwards RM, Coggins JR.** 1987. The pentafunctional arom enzyme of *Saccharomyces cerevisiae* is a mosaic of monofunctional domains. Biochem J **246:**375-386.

217. **Yoshikawa K, Tanaka T, Furusawa C, Nagahisa K, Hirasawa T, Shimizu H.** 2009. Comprehensive phenotypic analysis for identification of genes affecting growth under ethanol stress in *Saccharomyces cerevisiae*. Fems Yeast Research **9:**32-44.

218. **Pinel D, D'Aoust F, del Cardayre SB, Bajwa PK, Lee H, Martin VJJ.** 2011. *Saccharomyces cerevisiae* genome shuffling through recursive population mating leads to improved tolerance to spent sulfite liquor. Appl Environ Microbiol **77:**4736-4743.

219. **Wegele H, Müller L, Buchner J.** 2004. Hsp70 and Hsp90--a relay team for protein folding. Rev Physiol Biochem Pharmacol **151:**1-44.

220. **Verghese J, Abrams J, Wang Y, Morano KA.** 2012. Biology of the heat shock response and protein chaperones: budding yeast (*Saccharomyces cerevisiae*) as a model system. Microbiol Mol Biol Rev **76:**115-158.

221. **Becker J, Walter W, Yan W, Craig EA.** 1996. Functional interaction of cytosolic hsp70 and a DnaJ-related protein, Ydj1p, in protein translocation in vivo. Mol Cell Biol **16:**4378-4386.

222. **Brown CR, McCann JA, Chiang HL.** 2000. The heat shock protein Ssa2p is required for import of fructose-1, 6-bisphosphatase into Vid vesicles. J Cell Biol **150:**65-76.

223. **Boorstein WR, Ziegelhoffer T, Craig EA.** 1994. Molecular evolution of the HSP70 multigene family. J Mol Evol **38:**1-17.

224. **Juretschke J, Menssen R, Sickmann A, Wolf DH.** 2010. The Hsp70 chaperone Ssa1 is essential for catabolite induced degradation of the gluconeogenic enzyme fructose-1,6-bisphosphatase. Biochem Biophys Res Commun **397:**447-452.

225. **Sharma D, Masison DC.** 2011. Single methyl group determines prion propagation and protein degradation activities of yeast heat shock protein (Hsp)-70 chaperones Ssa1p and Ssa2p. Proc Natl Acad Sci U S A **108:**13665-13670.

226. **Marsh JA, Kalton HM, Gaber RF.** 1998. Cns1 is an essential protein associated with the hsp90 chaperone complex in *Saccharomyces cerevisiae* that can restore cyclophilin 40-dependent functions in cpr7Delta cells. Mol Cell Biol **18:**7353-7359.

227. **Hahn JS, Hu Z, Thiele DJ, Iyer VR.** 2004. Genome-wide analysis of the biology of stress responses through heat shock transcription factor. Mol Cell Biol **24:**5249-5256.

228. **Eastmond DL, Nelson HC.** 2006. Genome-wide analysis reveals new roles for the activation domains of the Saccharomyces cerevisiae heat shock transcription factor (Hsf1) during the transient heat shock response. J Biol Chem **281:**32909-32921.

229. **Wang Y, Gibney PA, West JD, Morano KA.** 2012. The yeast Hsp70 Ssa1 is a sensor for activation of the heat shock response by thiol-reactive compounds. Mol Biol Cell **23:**3290-3298.

230. **Mayer MP, Brehmer D, Gassler CS, Bukau B.** 2001. Hsp70 chaperone machines. Adv Protein Chem **59:**1-44.

231. **Jones GW, Masison DC.** 2003. *Saccharomyces cerevisiae* Hsp70 mutations affect [PSI+] prion propagation and cell growth differently and implicate Hsp40 and tetratricopeptide repeat cochaperones in impairment of [PSI+]. Genetics **163:**495-506.

232. **Loovers HM, Guinan E, Jones GW.** 2007. Importance of the Hsp70 ATPase domain in yeast prion propagation. Genetics **175:**621-630.

233. **Hochstrasser M.** 1996. Ubiquitin-dependent protein degradation. Annu Rev Genet **30:**405-439.

234. **Kimura Y, Tanaka K.** 2010. Regulatory mechanisms involved in the control of ubiquitin homeostasis. J Biochem **147:**793-798.

235. **Hershko A, Ciechanover A.** 1998. The ubiquitin system. Annu Rev Biochem **67:**425-479.

236. **Mukhopadhyay D, Riezman H.** 2007. Proteasome-independent functions of ubiquitin in endocytosis and signaling. Science **315:**201-205.

237. **Richardson LA, Reed BJ, Charette JM, Freed EF, Fredrickson EK, Locke MN, Baserga SJ, Gardner RG.** 2012. A conserved deubiquitinating enzyme controls cell growth by regulating RNA polymerase I stability. Cell Rep **2:**372-385.

238. **Hernández-López MJ, Garcia-Marqués S, Randez-Gil F, Prieto JA.** 2011. Multicopy suppression screening of *Saccharomyces cerevisiae* Identifies the

ubiquitination machinery as a main target for improving growth at low temperatures. Appl Environ Microbiol **77:**7517-7525.

239. **Finley D, Ozkaynak E, Varshavsky A.** 1987. The yeast polyubiquitin gene is essential for resistance to high temperatures, starvation, and other stresses. Cell **48:**1035-1046.

240. **Kolling R, Hollenberg CP.** 1994. The ABC-transporter Ste6 accumulates in the plasma membrane in a ubiquitinated form in endocytosis mutants. EMBO J **13:**3261-3271.

241. **Hein C, Springael JY, Volland C, Haguenauer-Tsapis R, Andre B.** 1995. NPl1, an essential yeast gene involved in induced degradation of Gap1 and Fur4 permeases, encodes the Rsp5 ubiquitin-protein ligase. Mol Microbiol **18:**77-87.

242. **Hicke L, Riezman H.** 1996. Ubiquitination of a yeast plasma membrane receptor signals its ligand-stimulated endocytosis. Cell **84:**277-287.

243. **Lin CH, MacGurn JA, Chu T, Stefan CJ, Emr SD.** 2008. Arrestin-related ubiquitin-ligase adaptors regulate endocytosis and protein turnover at the cell surface. Cell **135:**714-725.

244. **Zhou H, Winston F.** 2001. NRG1 is required for glucose repression of the SUC2 and GAL genes of *Saccharomyces cerevisiae*. BMC Genet **2:**1-5.

245. **Kuchin S, Vyas VK, Carlson M.** 2002. Snf1 protein kinase and the repressors Nrg1 and Nrg2 regulate FLO11, haploid invasive growth, and diploid pseudohyphal differentiation. Mol Cell Biol **22:**3994-4000.

246. **Park SH, Koh SS, Chun JH, Hwang HJ, Kang HS.** 1999. Nrg1 is a transcriptional repressor for glucose repression of STA1 gene expression in *Saccharomyces cerevisiae*. Mol Cell Biol **19:**2044-2050.

247. **Mayordomo I, Estruch F, Sanz P.** 2002. Convergence of the target of rapamycin and the Snf1 protein kinase pathways in the regulation of the subcellular localization of Msn2, a transcriptional activator of STRE (Stress Response Element)-regulated genes. J Biol Chem **277:**35650-35656.

248. **Vyas VK, Berkey CD, Miyao T, Carlson M.** 2005. Repressors Nrg1 and Nrg2 regulate a set of stress-responsive genes in *Saccharomyces cerevisiae*. Eukaryot Cell **4:**1882-1891.

249. **Causton HC, Ren B, Koh SS, Harbison CT, Kanin E, Jennings EG, Lee TI, True HL, Lander ES, Young RA.** 2001. Remodeling of yeast genome expression in response to environmental changes. Mol Biol Cell **12:**323-337.

250. **Lamb TM, Mitchell AP.** 2003. The transcription factor Rim101p governs ion tolerance and cell differentiation by direct repression of the regulatory genes NRG1 and SMP1 in *Saccharomyces cerevisiae*. Mol Cell Biol **23:**677-686.

251. **Platara M, Ruiz A, Serrano R, Palomino A, Moreno F, Arino J.** 2006. The transcriptional response of the yeast Na(+)-ATPase ENA1 gene to alkaline stress involves three main signaling pathways. J Biol Chem **281:**36632-36642.

252. **Berkey CD, Carlson M.** 2006. A specific catalytic subunit isoform of protein kinase CK2 is required for phosphorylation of the repressor Nrg1 in *Saccharomyces cerevisiae*. Curr Genet **50:**1-10.

253. **Olsten ME, Litchfield DW.** 2004. Order or chaos? An evaluation of the regulation of protein kinase CK2. Biochem Cell Biol **82:**681-693.

254. **Mangus DA, Amrani N, Jacobson A.** 1998. Pbp1p, a factor interacting with *Saccharomyces cerevisiae* poly(A)-binding protein, regulates polyadenylation. Mol Cell Biol **18:**7383-7396.

255. **Wyers F, Minet M, Dufour ME, Vo LT, Lacroute F.** 2000. Deletion of the PAT1 gene affects translation initiation and suppresses a PAB1 gene deletion in yeast. Mol Cell Biol **20:**3538-3549.

256. **Anderson P, Kedersha N.** 2009. RNA granules: post-transcriptional and epigenetic modulators of gene expression. Nat Rev Mol Cell Biol **10:**430-436.

257. **Buchan JR, Parker R.** 2009. Eukaryotic stress granules: the ins and outs of translation. Mol Cell **36:**932-941.

258. **Groušl T, Ivanov P, Frydlová I, Vašicová P, Janda F, Vojtová J, Malínská K, Malcová I, Nováková L, Janošková D, Valášek L, Hašek J.** 2009. Robust heat shock induces eIF2alpha-phosphorylation-independent assembly of stress granules containing eIF3 and 40S ribosomal subunits in budding yeast, *Saccharomyces cerevisiae*. Journal of Cell Science **122:**2078-2088.

259. **Kato K, Yamamoto Y, Izawa S.** 2011. Severe ethanol stress induces assembly of stress granules in *Saccharomyces cerevisiae*. Yeast **28:**339-347.

260. **Buchan JR, Muhlrad D, Parker R.** 2008. P bodies promote stress granule assembly in *Saccharomyces cerevisiae*. J Cell Biol **183:**441-455.

261. **Hoyle NP, Castelli LM, Campbell SG, Holmes LE, Ashe MP.** 2007. Stress-dependent relocalization of translationally primed mRNPs to cytoplasmic

granules that are kinetically and spatially distinct from P-bodies. J Cell Biol **179:**65-74.

262. **Brengues M, Parker R.** 2007. Accumulation of polyadenylated mRNA, Pab1p, eIF4E, and eIF4G with P-bodies in *Saccharomyces cerevisiae*. Mol Biol Cell **18:**2592-2602.

263. **Iwaki A, Kawai T, Yamamoto Y, Izawa S.** 2013. Biomass Conversion Inhibitors Furfural and 5-Hydroxymethylfurfural Induce Formation of Messenger RNP Granules and Attenuate Translation Activity in *Saccharomyces cerevisiae*. Appl Environ Microbiol **79:**1661-1667.

264. **Inoki K, Ouyang H, Li Y, Guan KL.** 2005. Signaling by target of rapamycin proteins in cell growth control. Microbiol Mol Biol Rev **69:**79-100.

265. **Martin DE, Hall MN.** 2005. The expanding TOR signaling network. Curr Opin Cell Biol **17:**158-166.

266. **Almeida B, Ohlmeier S, Almeida AJ, Madeo F, Leão C, Rodrigues F, Ludovico P.** 2009. Yeast protein expression profile during acetic acid-induced apoptosis indicates causal involvement of the TOR pathway. Proteomics **9:**720-732.

267. **Wei M, Fabrizio P, Madia F, Hu J, Ge H, Li LM, Longo VD.** 2009. Tor1/Sch9-regulated carbon source substitution is as effective as calorie restriction in life span extension. PLoS Genet **5:**e1000467.

268. **Teste MA, François JM, Parrou JL.** 2010. Characterization of a new multigene family encoding isomaltases in the yeast *Saccharomyces cerevisiae*, the IMA family. J Biol Chem **285:**26815-26824.

269. **Alves SL, Jr., Herberts RA, Hollatz C, Trichez D, Miletti LC, de Araujo PS, Stambuk BU.** 2008. Molecular analysis of maltotriose active transport and fermentation by Saccharomyces cerevisiae reveals a determinant role for the AGT1 permease. Appl Environ Microbiol **74:**1494-1501.

270. **Cheng Q, Michels CA.** 1991. MAL11 and MAL61 encode the inducible high-affinity maltose transporter of *Saccharomyces cerevisiae*. J Bacteriol **173:**1817-1820.

271. **Babrzadeh F, Jalili R, Wang C, Shokralla S, Pierce S, Robinson-Mosher A, Nyren P, Shafer RW, Basso LC, de Amorim HV, de Oliveira AJ, Davis RW, Ronaghi M, Gharizadeh B, Stambuk BU.** 2012. Whole-genome sequencing of the efficient industrial fuel-ethanol fermentative *Saccharomyces cerevisiae* strain CAT-1. Mol Genet Genomics **287:**485-494.

272. **Dunn B, Levine RP, Sherlock G.** 2005. Microarray karyotyping of commercial wine yeast strains reveals shared, as well as unique, genomic signatures. BMC Genomics **6:**53.

273. **Stambuk BU, Panek AD, Crowe JH, Crowe LM, de Araujo PS.** 1998. Expression of high-affinity trehalose-H+ symport in *Saccharomyces cerevisiae*. Biochim Biophys Acta **1379:**118-128.

274. **Jules M, Guillou V, Francois J, Parrou JL.** 2004. Two distinct pathways for trehalose assimilation in the yeast *Saccharomyces cerevisiae*. Appl Environ Microbiol **70:**2771-2778.

275. **Crowe JH.** 2007. Trehalose as a "chemical chaperone": fact and fantasy. Adv Exp Med Biol **594:**143-158.

276. **Hottiger T, De Virgilio C, Hall MN, Boller T, Wiemken A.** 1994. The role of trehalose synthesis for the acquisition of thermotolerance in yeast. II. Physiological concentrations of trehalose increase the thermal stability of proteins in vitro. Eur J Biochem **219:**187-193.

277. **Nwaka S, Kopp M, Holzer H.** 1995. Expression and function of the trehalase genes NTH1 and YBR0106 in *Saccharomyces cerevisiae*. J Biol Chem **270:**10193-10198.

278. **Nwaka S, Mechler B, Destruelle M, Holzer H.** 1995. Phenotypic features of trehalase mutants in *Saccharomyces cerevisiae*. FEBS Lett **360:**286-290.

279. **Heer D, Heine D, Sauer U.** 2009. Resistance of *Saccharomyces cerevisiae* to high concentrations of furfural is based on NADPH-dependent reduction by at least two oxireductases. Appl Environ Microbiol **75:**7631-7638.

280. **Pascon RC, Miller BL.** 2000. Morphogenesis in *Aspergillus nidulans* requires Dopey (DopA), a member of a novel family of leucine zipper-like proteins conserved from yeast to humans. Mol Microbiol **36:**1250-1264.

281. **Sickmann A, Reinders J, Wagner Y, Joppich C, Zahedi R, Meyer HE, Schonfisch B, Perschil I, Chacinska A, Guiard B, Rehling P, Pfanner N, Meisinger C.** 2003. The proteome of *Saccharomyces cerevisiae* mitochondria. Proc Natl Acad Sci U S A **100:**13207-13212.

282. **Huh WK, Falvo JV, Gerke LC, Carroll AS, Howson RW, Weissman JS, O'Shea EK.** 2003. Global analysis of protein localization in budding yeast. Nature **425:**686-691.

283. **Hua Z, Fatheddin P, Graham TR.** 2002. An essential subfamily of Drs2p-related P-type ATPases is required for protein trafficking between Golgi complex and endosomal/vacuolar system. Mol Biol Cell **13:**3162-3177.

284. **Paulusma CC, Oude Elferink RP.** 2005. The type 4 subfamily of P-type ATPases, putative aminophospholipid translocases with a role in human disease. Biochim Biophys Acta **1741:**11-24.

285. **Jochum A, Jackson D, Schwarz H, Pipkorn R, Singer-Krüger B.** 2002. Yeast Ysl2p, homologous to Sec7 domain guanine nucleotide exchange factors, functions in endocytosis and maintenance of vacuole integrity and interacts with the Arf-Like small GTPase Arl1p. Mol Cell Biol **22:**4914-4928.

286. **Barbosa S, Pratte D, Schwarz H, Pipkorn R, Singer-Krüger B.** 2010. Oligomeric Dop1p is part of the endosomal Neo1p-Ysl2p-Arl1p membrane remodeling complex. Traffic **11:**1092-1106.

287. **Arias P, Díez-Muñiz S, García R, Nombela C, Rodríguez-Peña JM, Arroyo J.** 2011. Genome-wide survey of yeast mutations leading to activation of the yeast cell integrity MAPK pathway: novel insights into diverse MAPK outcomes. BMC Genomics **12:**390.

288. **Waples WG, Chahwan C, Ciechonska M, Lavoie BD.** 2009. Putting the brake on FEAR: Tof2 promotes the biphasic release of Cdc14 phosphatase during mitotic exit. Mol Biol Cell **20:**245-255.

289. **Warner JR.** 1999. The economics of ribosome biosynthesis in yeast. Trends Biochem Sci **24:**437-440.

290. **Neiman AM, Herskowitz I.** 1994. Reconstitution of a Yeast Protein-Kinase Cascade in-Vitro - Activation of the Yeast Mek Homolog Ste7 by Ste11. Proc Natl Acad Sci U S A **91:**3398-3402.

291. **Elion EA.** 2001. The Ste5p scaffold. Journal of Cell Science **114:**3967-3978.

292. **Inouye C, Dhillon N, Durfee T, Zambryski PC, Thorner J.** 1997. Mutational analysis of STE5 in the yeast *Saccharomyces cerevisiae*: application of a differential interaction trap assay for examining protein-protein interactions. Genetics **147:**479-492.

293. **Inouye C, Dhillon N, Thorner J.** 1997. Ste5 RING-H2 domain: role in Ste4-promoted oligomerization for yeast pheromone signaling. Science **278:**103-106.

294. **Hasson MS, Blinder D, Thorner J, Jenness DD.** 1994. Mutational Activation of the Ste5 Gene-Product Bypasses the Requirement for G-Protein Beta-Subunit and Gamma-Subunit in the Yeast Pheromone Response Pathway. Molecular and Cellular Biology **14:**1054-1065.

295. **O'Rourke SM, Herskowitz I.** 1998. The Hog1 MAPK prevents cross talk between the HOG and pheromone response MAPK pathways in *Saccharomyces cerevisiae*. Gene Dev **12:**2874-2886.

296. **Saito H.** 2010. Regulation of cross-talk in yeast MAPK signaling pathways. Curr Opin Microbiol **13:**677-683.

297. **de Godoy LM, Olsen JV, Cox J, Nielsen ML, Hubner NC, Fröhlich F, Walther TC, Mann M.** 2008. Comprehensive mass-spectrometry-based proteome quantification of haploid versus diploid yeast. Nature **455:**1251-1254.

298. **Chatterjee S, Pal JK.** 2009. Role of 5'- and 3'-untranslated regions of mRNAs in human diseases. Biol Cell **101:**251-262.

299. **Fialcowitz EJ, Brewer BY, Keenan BP, Wilson GM.** 2005. A hairpin-like structure within an AU-rich mRNA-destabilizing element regulates trans-factor binding selectivity and mRNA decay kinetics. J Biol Chem **280:**22406-22417.

300. **van Maris AJ, Winkler AA, Kuyper M, de Laat WT, van Dijken JP, Pronk JT.** 2007. Development of efficient xylose fermentation in *Saccharomyces cerevisiae*: xylose isomerase as a key component. Adv Biochem Eng Biotechnol **108:**179-204.

301. **Wahlbom CF, Cordero Otero RR, van Zyl WH, Hahn-Hägerdal B, Jönsson LJ.** 2003. Molecular analysis of a *Saccharomyces cerevisiae* mutant with improved ability to utilize xylose shows enhanced expression of proteins involved in transport, initial xylose metabolism, and the pentose phosphate pathway. Appl Environ Microbiol **69:**740-746.

302. **Wisselink HW, Cipollina C, Oud B, Crimi B, Heijnen JJ, Pronk JT, van Maris AJ.** 2010. Metabolome, transcriptome and metabolic flux analysis of arabinose fermentation by engineered *Saccharomyces cerevisiae*. Metab Eng **12:**537-551.

303. **Baggerly KA, Deng L, Morris JS, Aldaz CM.** 2003. Differential expression in SAGE: accounting for normal between-library variation. Bioinformatics **19:**1477-1483.

304. **Kal AJ, van Zonneveld AJ, Benes V, van den Berg M, Koerkamp MG, Albermann K, Strack N, Ruijter JM, Richter A, Dujon B, Ansorge W, Tabak**

HF. 1999. Dynamics of gene expression revealed by comparison of serial analysis of gene expression transcript profiles from yeast grown on two different carbon sources. Mol Biol Cell **10:**1859-1872.

305. **Merico D, Isserlin R, Bader GD.** 2011. Visualizing gene-set enrichment results using the Cytoscape plug-in enrichment map. Methods Mol Biol **781:**257-277.

306. **Merico D, Isserlin R, Stueker O, Emili A, Bader GD.** 2010. Enrichment map: a network-based method for gene-set enrichment visualization and interpretation. PLoS One **5:**e13984.

307. **Cherry JM, Hong EL, Amundsen C, Balakrishnan R, Binkley G, Chan ET, Christie KR, Costanzo MC, Dwight SS, Engel SR, Fisk DG, Hirschman JE, Hitz BC, Karra K, Krieger CJ, Miyasato SR, Nash RS, Park J, Skrzypek MS, Simison M, Weng S, Wong ED.** 2012. *Saccharomyces* Genome Database: the genomics resource of budding yeast. Nucleic Acids Research **40:**D700-705.

308. **Abdulrehman D, Monteiro PT, Teixeira MC, Mira NP, Lourenco AB, dos Santos SC, Cabrito TR, Francisco AP, Madeira SC, Aires RS, Oliveira AL, Sa-Correia I, Freitas AT.** 2011. YEASTRACT: providing a programmatic access to curated transcriptional regulatory associations in *Saccharomyces cerevisiae* through a web services interface. Nucleic Acids Research **39:**D136-140.

309. **Monteiro PT, Mendes ND, Teixeira MC, d'Orey S, Tenreiro S, Mira NP, Pais H, Francisco AP, Carvalho AM, Lourenco AB, Sá-Correia I, Oliveira AL, Freitas AT.** 2008. YEASTRACT-DISCOVERER: new tools to improve the

analysis of transcriptional regulatory associations in *Saccharomyces cerevisiae*. Nucleic Acids Research **36:**D132-136.

310. **Teixeira MC, Monteiro P, Jain P, Tenreiro S, Fernandes AR, Mira NP, Alenquer M, Freitas AT, Oliveira AL, Sá-Correia I.** 2006. The YEASTRACT database: a tool for the analysis of transcription regulatory associations in *Saccharomyces cerevisiae*. Nucleic Acids Research **34:**D446-451.

311. **Ljungdahl PO, Daignan-Fornier B.** 2012. Regulation of Amino Acid, Nucleotide, and Phosphate Metabolism in *Saccharomyces cerevisiae*. Genetics **190:**885-929.

312. **Georis I, Feller A, Vierendeels F, Dubois E.** 2009. The yeast GATA factor Gat1 occupies a central position in nitrogen catabolite repression-sensitive gene activation. Mol Cell Biol **29:**3803-3815.

313. **Liu ZL, Blaschek HP.** 2010. Lignocellulosic biomass conversion to ethanol by *Saccharomyces*, p. 17-36. *In* Vertes A, Qureshi N, Yukawa H, Blaschek H (ed.), Biomass to biofuels: strategies for global industries. John Wiley & Sons, Ltd., West Sussex, U. K.

314. **Ozkaynak E, Finley D, Solomon MJ, Varshavsky A.** 1987. The yeast ubiquitin genes: a family of natural gene fusions. EMBO J **6:**1429-1439.

315. **Vyas VK, Kuchin S, Carlson M.** 2001. Interaction of the repressors Nrg1 and Nrg2 with the Snf1 protein kinase in *Saccharomyces cerevisiae*. Genetics **158:**563-572.

316. **Chung JH, Lester RL, Dickson RC.** 2003. Sphingolipid requirement for generation of a functional v1 component of the vacuolar ATPase. J Biol Chem **278:**28872-28881.

317. **Chung N, Mao C, Heitman J, Hannun YA, Obeid LM.** 2001. Phytosphingosine as a specific inhibitor of growth and nutrient import in *Saccharomyces cerevisiae*. J Biol Chem **276:**35614-35621.

318. **Georis I, Tate JJ, Cooper TG, Dubois E.** 2011. Nitrogen-responsive regulation of GATA protein family activators Gln3 and Gat1 occurs by two distinct pathways, one inhibited by rapamycin and the other by methionine sulfoximine. J Biol Chem **286:**44897-44912.

319. **Mira NP, Lourenco AB, Fernandes AR, Becker JD, Sá-Correia I.** 2009. The RIM101 pathway has a role in *Saccharomyces cerevisiae* adaptive response and resistance to propionic acid and other weak acids. Fems Yeast Research **9:**202-216.

320. **Kapteyn JC, ter Riet B, Vink E, Blad S, De Nobel H, Van Den Ende H, Klis FM.** 2001. Low external pH induces HOG1-dependent changes in the organization of the *Saccharomyces cerevisiae* cell wall. Mol Microbiol **39:**469-479.

321. **Dardalhon M, Lin W, Nicolas A, Averbeck D.** 2007. Specific transcriptional responses induced by 8-methoxypsoralen and UVA in yeast. Fems Yeast Research **7:**866-878.

322. **Perrone GG, Grant CM, Dawes IW.** 2005. Genetic and environmental factors influencing glutathione homeostasis in *Saccharomyces cerevisiae*. Mol Biol Cell **16:**218-230.

323. **Golin J, Ambudkar SV, May L.** 2007. The yeast Pdr5p multidrug transporter: how does it recognize so many substrates? Biochem Biophys Res Commun **356:**1-5.

324. **Vargas RC, García-Salcedo R, Tenreiro S, Teixeira MC, Fernandes AR, Ramos J, Sá-Correia I.** 2007. *Saccharomyces cerevisiae* multidrug resistance transporter Qdr2 is implicated in potassium uptake, providing a physiological advantage to quinidine-stressed cells. Eukaryot Cell **6:**134-142.

325. **Zhu X, Garrett J, Schreve J, Michaeli T.** 1996. GNP1, the high-affinity glutamine permease of *S. cerevisiae*. Curr Genet **30:**107-114.

326. **Alvarez FJ, Douglas LM, Rosebrock A, Konopka JB.** 2008. The Sur7 protein regulates plasma membrane organization and prevents intracellular cell wall growth in *Candida albicans*. Mol Biol Cell **19:**5214-5225.

327. **Mir SS, Fiedler D, Cashikar AG.** 2009. Ssd1 is required for thermotolerance and Hsp104-mediated protein disaggregation in *Saccharomyces cerevisiae*. Mol Cell Biol **29:**187-200.

328. **Rodríguez-Peña JM, Pérez-Díaz RM, Alvarez S, Bermejo C, García R, Santiago C, Nombela C, Arroyo J.** 2005. The 'yeast cell wall chip' - a tool to analyse the regulation of cell wall biogenesis in Saccharomyces cerevisiae. Microbiology **151:**2241-2249.

329. **Xu T, Shively CA, Jin R, Eckwahl MJ, Dobry CJ, Song Q, Kumar A.** 2010. A profile of differentially abundant proteins at the yeast cell periphery during pseudohyphal growth. J Biol Chem **285:**15476-15488.

330. **Gimeno CJ, Fink GR.** 1994. Induction of pseudohyphal growth by overexpression of PHD1, a *Saccharomyces cerevisiae* gene related to transcriptional regulators of fungal development. Mol Cell Biol **14:**2100-2012.

331. **Hanlon SE, Rizzo JM, Tatomer DC, Lieb JD, Buck MJ.** 2011. The stress response factors Yap6, Cin5, Phd1, and Skn7 direct targeting of the conserved co-repressor Tup1-Ssn6 in *S. cerevisiae*. PLoS One **6:**e19060.

332. **Gimeno CJ, Ljungdahl PO, Styles CA, Fink GR.** 1992. Unipolar cell divisions in the yeast *S. cerevisiae* lead to filamentous growth: regulation by starvation and RAS. Cell **68:**1077-1190.

333. **Moon J, Liu ZL.** 2012. Engineered NADH-dependent GRE2 from *Saccharomyces cerevisiae* by directed enzyme evolution enhances HMF reduction using additional cofactor NADPH. Enzyme Microb Technol **50:**115-120.

334. **Palková Z, Devaux F, Icicová M, Mináriková L, Le Crom S, Jacq C.** 2002. Ammonia pulses and metabolic oscillations guide yeast colony development. Mol Biol Cell **13:**3901-3914.

335. **Tenreiro S, Nunes PA, Viegas CA, Neves MS, Teixeira MC, Cabral MG, Sá-Correia I.** 2002. AQR1 gene (ORF YNL065w) encodes a plasma membrane transporter of the major facilitator superfamily that confers resistance to short-chain monocarboxylic acids and quinidine in *Saccharomyces cerevisiae*. Biochem Biophys Res Commun **292:**741-748.

336. **Velasco I, Tenreiro S, Calderon IL, Andre B.** 2004. *Saccharomyces cerevisiae* Aqr1 is an internal-membrane transporter involved in excretion of amino acids. Eukaryot Cell **3:**1492-1503.

337. **Hess DC, Lu W, Rabinowitz JD, Botstein D.** 2006. Ammonium toxicity and potassium limitation in yeast. PLoS Biol **4:**e351.

338. **Zhang M, Liang Y, Zhang X, Xu Y, Dai H, Xiao W.** 2008. Deletion of yeast CWP genes enhances cell permeability to genotoxic agents. Toxicol Sci **103:**68-76.

339. **van Bakel H, Strengman E, Wijmenga C, Holstege FC.** 2005. Gene expression profiling and phenotype analyses of *S. cerevisiae* in response to changing copper reveals six genes with new roles in copper and iron metabolism. Physiol Genomics **22:**356-367.

340. **Li X, Routt SM, Xie Z, Cui X, Fang M, Kearns MA, Bard M, Kirsch DR, Bankaitis VA.** 2000. Identification of a novel family of nonclassic yeast phosphatidylinositol transfer proteins whose function modulates phospholipase D activity and Sec14p-independent cell growth. Mol Biol Cell **11:**1989-2005.

341. **Qiu XB, Shao YM, Miao S, Wang L.** 2006. The diversity of the DnaJ/Hsp40 family, the crucial partners for Hsp70 chaperones. Cell Mol Life Sci **63:**2560-2570.

342. **Cyr DM, Douglas MG.** 1994. Differential regulation of Hsp70 subfamilies by the eukaryotic DnaJ homologue YDJ1. J Biol Chem **269:**9798-9804.

343. **Moriyama H, Edskes HK, Wickner RB.** 2000. [URE3] prion propagation in *Saccharomyces cerevisiae*: requirement for chaperone Hsp104 and curing by overexpressed chaperone Ydj1p. Mol Cell Biol **20:**8916-8922.

344. **Kryndushkin DS, Smirnov VN, Ter-Avanesyan MD, Kushnirov VV.** 2002. Increased expression of Hsp40 chaperones, transcriptional factors, and ribosomal protein Rpp0 can cure yeast prions. J Biol Chem **277:**23702-23708.

345. **Lu Z, Cyr DM.** 1998. Protein folding activity of Hsp70 is modified differentially by the hsp40 co-chaperones Sis1 and Ydj1. J Biol Chem **273:**27824-27830.

346. **Ma M, Liu ZL.** 2010. Comparative transcriptome profiling analyses during the lag phase uncover *YAP1*, *PDR1*, *PDR3*, *RPN4*, and *HSF1* as key regulatory genes in genomic adaptation to the lignocellulose derived inhibitor HMF for *Saccharomyces cerevisiae*. BMC Genomics **11:**660.

347. **Dang NX, Hincha DK.** 2011. Identification of two hydrophilins that contribute to the desiccation and freezing tolerance of yeast (*Saccharomyces cerevisiae*) cells. Cryobiology **62:**188-193.

348. **Simões T, Mira NP, Fernandes AR, Sá-Correia I.** 2006. The SPI1 gene, encoding a glycosylphosphatidylinositol-anchored cell wall protein, plays a prominent role in the development of yeast resistance to lipophilic weak-acid food preservatives. Appl Environ Microbiol **72:**7168-7175.

349. **Cho RJ, Campbell MJ, Winzeler EA, Steinmetz L, Conway A, Wodicka L, Wolfsberg TG, Gabrielian AE, Landsman D, Lockhart DJ, Davis RW.** 1998. A genome-wide transcriptional analysis of the mitotic cell cycle. Mol Cell **2:**65-73.

350. **Goh WS, Orlov Y, Li J, Clarke ND.** 2010. Blurring of high-resolution data shows that the effect of intrinsic nucleosome occupancy on transcription factor binding is mostly regional, not local. PLoS Comput Biol **6:**e1000649.

351. **Harbison CT, Gordon DB, Lee TI, Rinaldi NJ, Macisaac KD, Danford TW, Hannett NM, Tagne JB, Reynolds DB, Yoo J, Jennings EG, Zeitlinger J, Pokholok DK, Kellis M, Rolfe PA, Takusagawa KT, Lander ES, Gifford DK, Fraenkel E, Young RA.** 2004. Transcriptional regulatory code of a eukaryotic genome. Nature **431:**99-104.

352. **Lee TI, Rinaldi NJ, Robert F, Odom DT, Bar-Joseph Z, Gerber GK, Hannett NM, Harbison CT, Thompson CM, Simon I, Zeitlinger J, Jennings EG, Murray HL, Gordon DB, Ren B, Wyrick JJ, Tagne JB, Volkert TL, Fraenkel E, Gifford DK, Young RA.** 2002. Transcriptional regulatory networks in Saccharomyces cerevisiae. Science **298:**799-804.

353. **Workman CT, Mak HC, McCuine S, Tagne JB, Agarwal M, Ozier O, Begley TJ, Samson LD, Ideker T.** 2006. A systems approach to mapping DNA damage response pathways. Science **312:**1054-1059.

354. **Stambuk BU, de Araujo PS.** 2001. Kinetics of active alpha-glucoside transport in *Saccharomyces cerevisiae*. FEMS Yeast Res **1:**73-78.

355. **Treger JM, Schmitt AP, Simon JR, McEntee K.** 1998. Transcriptional factor mutations reveal regulatory complexities of heat shock and newly identified stress genes in *Saccharomyces cerevisiae*. J Biol Chem **273:**26875-26879.

356. **Zahringer H, Burgert M, Holzer H, Nwaka S.** 1997. Neutral trehalase Nth1p of Saccharomyces cerevisiae encoded by the NTH1 gene is a multiple stress responsive protein. FEBS Lett **412:**615-620.

357. **Winderickx J, de Winde JH, Crauwels M, Hino A, Hohmann S, Van Dijck P, Thevelein JM.** 1996. Regulation of genes encoding subunits of the trehalose synthase complex in Saccharomyces cerevisiae: novel variations of STRE-mediated transcription control? Mol Gen Genet **252:**470-482.

358. **Bro C, Knudsen S, Regenberg B, Olsson L, Nielsen J.** 2005. Improvement of galactose uptake in *Saccharomyces cerevisiae* through overexpression of phosphoglucomutase: example of transcript analysis as a tool in inverse metabolic engineering. Appl Environ Microbiol **71:**6465-6472.

359. **Ferea TL, Botstein D, Brown PO, Rosenzweig RF.** 1999. Systematic changes in gene expression patterns following adaptive evolution in yeast. Proc Natl Acad Sci U S A **96:**9721-9726.

360. **Jansen ML, Diderich JA, Mashego M, Hassane A, de Winde JH, Daran-Lapujade P, Pronk JT.** 2005. Prolonged selection in aerobic, glucose-limited chemostat cultures of *Saccharomyces cerevisiae* causes a partial loss of glycolytic capacity. Microbiology **151:**1657-1669.

361. **Wright J, Bellissimi E, de Hulster E, Wagner A, Pronk JT, van Maris AJ.** 2011. Batch and continuous culture-based selection strategies for acetic acid tolerance in xylose-fermenting *Saccharomyces cerevisiae*. FEMS Yeast Res **11:**299-306.

362. **Stambuk BU, Dunn B, Alves SL, Jr., Duval EH, Sherlock G.** 2009. Industrial fuel ethanol yeasts contain adaptive copy number changes in genes involved in vitamin B1 and B6 biosynthesis. Genome Res **19:**2271-2278.

363. **Bayer TS, Hoff KG, Beisel CL, Lee JJ, Smolke CD.** 2009. Synthetic control of a fitness tradeoff in yeast nitrogen metabolism. J Biol Eng **3:**1.

364. **Watt R, Piper PW.** 1997. UBI4, the polyubiquitin gene of *Saccharomyces cerevisiae*, is a heat shock gene that is also subject to catabolite derepression control. Mol Gen Genet **253:**439-447.

365. **Simon JR, Treger JM, McEntee K.** 1999. Multiple independent regulatory pathways control UBI4 expression after heat shock in Saccharomyces cerevisiae. Mol Microbiol **31:**823-832.

366. **Hanna J, Meides A, Zhang DP, Finley D.** 2007. A ubiquitin stress response induces altered proteasome composition. Cell **129:**747-759.

367. **Leggett DS, Hanna J, Borodovsky A, Crosas B, Schmidt M, Baker RT, Walz T, Ploegh H, Finley D.** 2002. Multiple associated proteins regulate proteasome structure and function. Mol Cell **10:**495-507.

368. **Hanna J, Leggett DS, Finley D.** 2003. Ubiquitin depletion as a key mediator of toxicity by translational inhibitors. Mol Cell Biol **23:**9251-9261.

369. **Chernova TA, Allen KD, Wesoloski LM, Shanks JR, Chernoff YO, Wilkinson KD.** 2003. Pleiotropic effects of Ubp6 loss on drug sensitivities and yeast prion are due to depletion of the free ubiquitin pool. J Biol Chem **278:**52102-52115.

370. **San KY, Bennett GN, Berríos-Rivera SJ, Vadali RV, Yang YT, Horton E, Rudolph FB, Sariyar B, Blackwood K.** 2002. Metabolic engineering through cofactor manipulation and its effects on metabolic flux redistribution in Escherichia coli. Metab Eng **4:**182-192.

371. **Olsson L, Hahn-Hägerdal B.** 1993. Fermentative Performance of Bacteria and Yeasts in Lignocellulose Hydrolysates. Process Biochemistry **28:**249-257.

372. **Lin H, Li L, Jia X, Ward DM, Kaplan J.** 2011. Genetic and biochemical analysis of high iron toxicity in yeast: iron toxicity is due to the accumulation of cytosolic iron and occurs under both aerobic and anaerobic conditions. J Biol Chem **286:**3851-3862.

373. **Valko M, Morris H, Cronin MT.** 2005. Metals, toxicity and oxidative stress. Curr Med Chem **12:**1161-1208.

374. **Touati D.** 2000. Iron and oxidative stress in bacteria. Arch Biochem Biophys **373:**1-6.

375. **Pollak N, Dölle C, Ziegler M.** 2007. The power to reduce: pyridine nucleotides--small molecules with a multitude of functions. Biochem J **402:**205-218.

376. **Lagunas R.** 1993. Sugar transport in *Saccharomyces cerevisiae*. FEMS Microbiol Rev **10:**229-242.

377. **Page MG, Rosenbusch JP, Yamato I.** 1988. The effects of pH on proton sugar symport activity of the lactose permease purified from *Escherichia coli*. J Biol Chem **263:**15897-15905.

378. **Vanderheyden N, Wong J, Docampo R.** 2000. A pyruvate-proton symport and an H+-ATPase regulate the intracellular pH of *Trypanosoma brucei* at different stages of its life cycle. Biochem J **346 Pt 1:**53-62.

379. **Singer MA, Lindquist S.** 1998. Thermotolerance in *Saccharomyces cerevisiae*: the Yin and Yang of trehalose. Trends Biotechnol **16:**460-468.

380. **Rep M, Krantz M, Thevelein JM, Hohmann S.** 2000. The transcriptional response of *Saccharomyces cerevisiae* to osmotic shock. Hot1p and Msn2p/Msn4p are required for the induction of subsets of high osmolarity glycerol pathway-dependent genes. J Biol Chem **275:**8290-8300.

381. **Parrou JL, Teste MA, François J.** 1997. Effects of various types of stress on the metabolism of reserve carbohydrates in *Saccharomyces cerevisiae*: genetic evidence for a stress-induced recycling of glycogen and trehalose. Microbiology **143 (Pt 6):**1891-1900.

382. **Parrou JL, Enjalbert B, Plourde L, Bauche A, Gonzalez B, François J.** 1999. Dynamic responses of reserve carbohydrate metabolism under carbon and nitrogen limitations in *Saccharomyces cerevisiae*. Yeast **15:**191-203.

383. **Estruch F.** 2000. Stress-controlled transcription factors, stress-induced genes and stress tolerance in budding yeast. FEMS Microbiol Rev **24:**469-486.

384. **Batista AS, Miletti LC, Stambuk BU.** 2004. Sucrose fermentation by *Saccharomyces cerevisiae* lacking hexose transport. J Mol Microbiol Biotechnol **8:**26-33.

385. **Wang L, Si Y, Dedow LK, Shao Y, Liu P, Brutnell TP.** 2011. A low-cost library construction protocol and data analysis pipeline for Illumina-based strand-specific multiplex RNA-seq. PLoS One **6:**e26426.

386. **Islam S, Kjallquist U, Moliner A, Zajac P, Fan JB, Lonnerberg P, Linnarsson S.** 2011. Characterization of the single-cell transcriptional landscape by highly multiplex RNA-seq. Genome Res **21:**1160-1167.

387. **Shabalina SA, Ogurtsov AY, Kondrashov VA, Kondrashov AS.** 2001. Selective constraint in intergenic regions of human and mouse genomes. Trends Genet **17:**373-376.

388. **Gibson DG, Young L, Chuang RY, Venter JC, Hutchison CA, 3rd, Smith HO.** 2009. Enzymatic assembly of DNA molecules up to several hundred kilobases. Nat Methods **6:**343-345.

Appendices

Appendix 1. Variation calls for the WT vs R57.

Mapping	Reference Position	Consensus Position	Variation Type	Reference	Variants	Allele Variations	Frequencies	Counts	Coverage	Affected gene
I mapping	124270	123585	SNP	G	2	T/G	51.5/48.5	224/211	435	*SSA1*
IV mapping	534017	533990	SNP	G	1	T	100	174	174	*NRG1*
IV mapping	649234	649203	SNP	C	2	C/T	56.0/44.0	154/121	275	*STE5*
IV mapping	651371	651340	SNP	T	2	C/T	51.2/48.8	132/126	258	*STE5*
IV mapping	696096	696065	SNP	C	2	C/T	58.8/41.2	224/157	381	*ARO1*
IV mapping	696097	696066	SNP	C	2	C/T	58.7/41.1	220/154	375	*ARO1*
IV mapping	730256	730226	SNP	T	2	T/A	54.2/45.8	156/132	288	*DOP1*
IV-1 mapping	420924	420925	SNP	T	2	T/A	57.2/42.8	210/157	367	*BCS1*
VII mapping	625487	625442	SNP	G	2	G/T	50.9/49.1	110/106	216	*ART5*
VII mapping	852174	852130	SNP	T	2	T/C	51.3/48.4	176/166	343	*PBP1*
VII-1 mapping	80669	80664	SNP	A	2	A/T	53.5/46.5	236/205	441	*MAL11*
VII-1 mapping	80841	80836	SNP	G	2	G/A	52.0/47.7	217/199	417	*MAL11*
IX mapping	50510	50435	SNP	T	1	A	99.7	376	377	*UBP7*
X mapping	234127	233952	SNP	A	2	T/A	51.4/48.6	199/188	387	*GSH1*
XI mapping	458903	458834	SNP	G	2	G/A	56.9/43.1	197/149	346	*TOF2*
XIV mapping	516499	516499	SNP	T	2	C/T	51.9/48.1	180/167	347	YNL058C
XV mapping	464829	464838	SNP	C	2	C/A	60.6/39.4	275/179	454	*SGO1*
XV-1 mapping	63293	63293	SNP	A	2	G/A	53.4/46.6	220/192	412	*GDH1*
XV-1 mapping	63314	63314	SNP	G	2	G/A	55.1/44.9	236/192	428	*GDH1*
XV-1 mapping	80716	80716	SNP	C	2	T/C	50.4/48.7	118/114	234	*FIT3*

Appendix 2. RNA-seq differential expression results.

RNA-seq results for differentially expressed genes between WT vs R57 without HWSSL exposure								
Gene ID	**Experiment - Fold Change**	**Baggerley's test: 122T0 vs R57T0 original values - FDR p-value correction**	**122T0 (a) Expression values (RPKM)**	**122T0 (b) Expression values (RPKM)**	**122T0 - Means**	**R57T0 (a) Expression values**	**R57T0 (b) Expression values**	**R57T0 - Means**
YPL054W	-4.01	0.00	122.31	81.78	102.04	26.52	24.34	25.43
YHR050W	-2.51	0.00	318.20	354.87	336.54	120.51	147.96	134.24
YJL198W	-2.49	0.01	35.24	36.71	35.97	20.53	8.38	14.46
YGL056C	-2.46	0.00	317.75	364.11	340.93	153.56	123.89	138.73
YJL153C	-2.46	0.00	2033.25	1944.92	1989.08	663.02	956.89	809.96
YPR138C	-2.38	0.00	71.49	77.68	74.58	30.07	32.56	31.32
YEL063C	-2.33	0.00	99.96	71.11	85.54	36.57	36.93	36.75
YDR297W	-2.31	0.00	276.12	311.05	293.59	140.93	113.80	127.36
YMR303C	-2.29	0.05	14.83	19.22	17.03	9.49	5.40	7.44
YNL111C	-2.27	0.04	186.44	108.46	147.45	80.73	49.06	64.90
YKL198C	-2.24	0.00	282.82	218.48	250.65	144.97	78.53	111.75
YOL011W	-2.19	0.00	139.11	109.53	124.32	77.62	36.15	56.89
YNR018W	-2.13	0.00	204.94	201.05	203.00	125.59	65.20	95.39
YOL126C	-2.11	0.00	191.91	203.35	197.63	99.71	87.95	93.83
YDR075W	-2.10	0.04	34.85	37.87	36.36	23.54	11.06	17.30
YLR091W	-2.03	0.00	36.19	39.06	37.62	17.61	19.44	18.52
YJL110C	-2.01	0.05	27.75	20.06	23.91	14.05	9.71	11.88
YHR007C	-1.99	0.00	234.23	260.18	247.20	139.43	109.31	124.37
YOL127W	1.95	0.00	139.11	118.32	128.72	285.56	215.73	250.64
YLR348C	1.96	0.01	25.97	28.46	27.21	47.18	59.29	53.24
YBL072C	1.96	0.00	177.91	113.24	145.58	319.75	251.80	285.78
YNL264C	1.99	0.01	23.68	31.62	27.65	60.68	49.45	55.06
YDR382W	2.00	0.00	115.63	75.81	95.72	218.50	163.95	191.22
YLR303W	2.00	0.00	153.97	94.09	124.03	284.95	211.82	248.38
YHR104W	2.01	0.00	411.48	329.88	370.68	711.31	781.83	746.57
YLR075W	2.02	0.01	310.04	243.97	277.00	669.00	451.92	560.46
YCL050C	2.03	0.00	39.05	39.17	39.11	80.66	78.30	79.48
YDR158W	2.03	0.00	47.42	42.06	44.74	97.71	84.29	91.00
YEL039C	2.03	0.00	3032.78	3405.22	3219.00	7395.29	5704.92	6550.11
YOL157C	2.04	0.00	52.37	34.08	43.22	97.39	78.65	88.02
YGR148C	2.05	0.00	92.50	64.58	78.54	186.11	136.11	161.11
YHR203C	2.05	0.01	94.98	66.77	80.88	194.34	137.69	166.02
YDL191W	2.06	0.04	181.04	119.30	150.17	372.12	246.85	309.49
YMR307W	2.08	0.00	50.69	48.97	49.83	111.29	95.79	103.54
YOR198C	2.08	0.02	19.76	17.25	18.50	36.23	40.92	38.57
YPR167C	2.09	0.04	18.66	13.22	15.94	38.08	28.64	33.36
YBR004C	2.09	0.02	32.34	37.12	34.73	85.54	59.87	72.71

YPL090C	2.09	0.00	126.40	102.53	114.47	271.80	207.62	239.71
YBR078W	2.11	0.00	95.57	65.89	80.73	159.95	180.84	170.39
YLR301W	2.14	0.02	31.05	17.76	24.41	57.33	46.96	52.14
YMR316W	2.14	0.01	58.18	57.02	57.60	145.55	100.59	123.07
YBL092W	2.14	0.00	139.28	110.73	125.01	312.03	222.46	267.25
YLR110C	2.16	0.00	665.61	545.65	605.63	1311.71	1304.11	1307.91
YAL038W	2.17	0.00	366.34	190.20	278.27	665.52	542.74	604.13
YLR179C	2.19	0.05	61.99	36.60	49.29	128.89	87.06	107.97
YLR441C	2.19	0.00	109.26	105.26	107.26	274.48	196.34	235.41
YCR012W	2.21	0.00	392.36	293.29	342.82	719.91	792.43	756.17
YNL162W	2.22	0.02	48.86	69.46	59.16	135.37	127.64	131.50
YER052C	2.22	0.01	16.44	18.44	17.44	40.57	37.01	38.79
YJR145C	2.24	0.00	72.14	66.09	69.11	156.98	152.97	154.97
YDR064W	2.24	0.00	89.08	68.24	78.66	184.39	168.77	176.58
YKL152C	2.25	0.00	371.35	280.89	326.12	709.59	758.55	734.07
YLR150W	2.29	0.00	80.14	65.39	72.76	194.17	139.67	166.92
YIL094C	2.30	0.00	29.23	27.87	28.55	66.04	65.23	65.63
YOR222W	2.31	0.01	21.47	15.42	18.44	49.00	36.10	42.55
YJL144W	2.31	0.01	848.95	336.69	592.82	1475.15	1261.81	1368.48
YGL123W	2.33	0.00	99.74	95.09	97.42	238.97	214.04	226.50
YLR454W	2.33	0.02	18.32	26.82	22.57	46.27	58.76	52.52
YGR185C	2.33	0.03	13.63	10.42	12.03	28.66	27.41	28.03
YER074W	2.33	0.00	81.50	60.67	71.08	179.41	152.09	165.75
YNL178W	2.33	0.00	84.71	84.37	84.54	225.02	169.46	197.24
YOL016C	2.35	0.00	180.42	142.45	161.44	378.49	379.72	379.11
YFR032C-A	2.37	0.01	64.92	84.15	74.53	210.67	142.06	176.37
YGR085C	2.37	0.00	43.32	59.09	51.20	128.41	114.01	121.21
YGR214W	2.38	0.00	51.25	41.39	46.32	114.42	105.89	110.16
YDR050C	2.38	0.00	277.36	175.88	226.62	507.89	571.89	539.89
YOR312C	2.38	0.00	85.07	55.34	70.20	190.24	144.30	167.27
YLR448W	2.39	0.05	52.58	27.32	39.95	114.52	76.31	95.42
YIL018W	2.39	0.00	104.87	75.29	90.08	236.92	193.48	215.20
YDR209C	2.39	0.00	61.37	49.45	55.41	142.33	122.48	132.41
YHR193C	2.40	0.01	54.67	38.53	46.60	134.04	90.03	112.04
YMR143W	2.41	0.00	87.14	53.05	70.09	195.07	142.77	168.92
YLR029C	2.41	0.05	74.47	126.35	100.41	232.84	251.18	242.01
YCR034W	2.41	0.04	9.99	9.18	9.58	20.00	26.23	23.11
YOL121C	2.42	0.00	38.22	45.67	41.94	116.52	86.89	101.70
YLR264W	2.43	0.00	38.83	39.48	39.15	110.98	79.40	95.19
YHR141C	2.44	0.00	67.92	47.16	57.54	156.53	124.02	140.27
YJR123W	2.44	0.00	170.72	121.60	146.16	399.77	313.33	356.55
YLR340W	2.45	0.00	93.96	62.00	77.98	221.41	161.25	191.33
YIL055C	2.45	0.00	19.61	16.07	17.84	47.43	40.12	43.78
YLR414C	2.45	0.00	60.20	61.86	61.03	165.32	134.34	149.83
YDR447C	2.46	0.00	43.70	56.76	50.23	121.80	125.14	123.47
YBR005W	2.46	0.00	59.85	59.84	59.85	171.42	123.47	147.45
YJR010W	2.52	0.00	24.10	15.87	19.98	55.19	45.54	50.36

YLR372W	2.53	0.00	13.60	13.23	13.41	30.35	37.40	33.88
YMR142C	2.55	0.04	89.14	54.38	71.76	225.55	140.09	182.82
YGR192C	2.56	0.00	889.26	452.80	671.03	1704.56	1728.25	1716.40
YBR181C	2.58	0.00	52.06	64.51	58.28	165.22	135.88	150.55
YNR034W	2.59	0.00	108.05	66.84	87.45	220.23	232.22	226.22
YKL060C	2.60	0.00	728.46	470.79	599.62	1615.96	1505.23	1560.60
YGL202W	2.61	0.00	23.01	20.65	21.83	53.68	60.29	56.98
YHR016C	2.62	0.00	190.40	152.62	171.51	417.50	482.46	449.98
YGR194C	2.63	0.00	55.98	24.23	40.10	119.53	91.29	105.41
YKL081W	2.63	0.00	17.66	25.16	21.41	52.99	59.57	56.28
YNL302C	2.63	0.00	60.57	50.18	55.37	144.42	147.30	145.86
YGL076C	2.65	0.00	72.13	52.72	62.43	165.30	165.28	165.29
YOR369C	2.67	0.00	119.99	107.26	113.63	354.76	251.61	303.18
YOR385W	2.67	0.00	13.74	12.84	13.29	37.67	33.37	35.52
YML063W	2.67	0.00	66.58	64.71	65.65	181.70	169.20	175.45
YHR021C	2.69	0.04	79.68	49.05	64.36	214.93	131.64	173.29
YLR406C	2.72	0.00	47.24	39.54	43.39	114.74	121.09	117.92
YKR094C	2.73	0.01	64.24	55.55	59.89	199.55	127.58	163.56
YPL131W	2.74	0.00	76.76	92.53	84.64	252.11	211.93	232.02
YOR096W	2.76	0.00	47.90	45.26	46.58	132.58	124.69	128.63
YER102W	2.79	0.00	81.41	47.08	64.25	212.96	145.83	179.40
YBR191W	2.80	0.00	55.04	43.97	49.51	144.26	132.64	138.45
YBR189W	2.80	0.00	59.62	51.88	55.75	164.49	147.47	155.98
YIL099W	2.83	0.04	11.45	6.44	8.95	30.30	20.29	25.30
YLR167W	2.83	0.01	186.91	130.08	158.50	551.87	346.14	449.01
YML026C	2.83	0.01	71.31	44.33	57.82	199.21	128.60	163.91
YHR208W	2.85	0.04	39.74	31.30	35.52	88.53	114.03	101.28
YGL031C	2.86	0.05	67.53	48.28	57.90	209.22	122.14	165.68
YOL120C	2.91	0.00	66.12	68.21	67.17	180.48	210.08	195.28
YGR137W	2.92	0.04	31.16	25.21	28.18	102.97	61.50	82.23
YBL003C	2.92	0.00	49.33	19.70	34.52	115.06	86.45	100.76
YLL045C	2.94	0.00	60.72	50.94	55.83	185.40	142.35	163.87
YDR043C	2.94	0.00	137.35	153.76	145.56	504.45	350.13	427.29
YMR116C	3.01	0.00	61.76	44.57	53.16	162.33	157.32	159.82
YHL015W	3.02	0.00	145.49	86.06	115.77	419.25	280.35	349.80
YFR031C-A	3.03	0.00	48.80	33.72	41.26	130.62	119.05	124.84
YDL082W	3.06	0.00	25.23	24.65	24.94	90.35	62.19	76.27
YKL120W	3.10	0.00	8.45	8.27	8.36	27.54	24.35	25.95
YGR034W	3.12	0.01	55.96	55.26	55.61	214.86	132.34	173.60
YNL301C	3.16	0.00	6.71	7.85	7.28	20.96	24.99	22.98
YDR038C	3.27	0.00	7.44	9.45	8.45	26.74	28.43	27.58
YJL177W	3.28	0.00	28.97	24.08	26.53	101.19	72.62	86.90
YGL259W	3.56	0.05	6.46	16.69	11.57	48.49	34.02	41.26
YFL034C-A	3.59	0.02	7.44	8.98	8.21	36.13	22.75	29.44
YGL253W	3.62	0.00	22.97	18.73	20.85	70.16	80.99	75.58
YNR050C	3.79	0.00	11.64	6.73	9.18	33.44	36.14	34.79
YLR061W	3.91	0.00	27.43	28.40	27.91	115.98	102.04	109.01

YER131W	3.99	0.01	45.09	25.49	35.29	176.78	104.66	140.72
YJL200C	4.09	0.00	7.64	6.36	7.00	28.98	28.25	28.61
YHR174W	4.26	0.01	198.32	156.01	177.17	648.49	860.60	754.55
YJR009C	4.30	0.00	155.12	107.55	131.33	582.29	548.37	565.33
YJL190C	4.61	0.00	35.52	24.66	30.09	142.26	135.16	138.71
YEL040W	4.80	0.00	7.32	3.23	5.27	23.52	27.13	25.32
YJL158C	4.90	0.00	19.26	6.53	12.90	73.18	53.11	63.15
YLR044C	5.06	0.02	163.01	95.02	129.01	848.31	457.02	652.66
YBR066C	5.16	0.00	8.04	12.03	10.04	57.29	46.34	51.82
YIL053W	6.47	0.00	21.97	24.88	23.43	172.63	130.68	151.65
YOR247W	6.49	0.00	27.63	12.42	20.02	130.84	128.91	129.87
YIL029C	7.85	0.04	0.73	1.31	1.02	8.06	7.94	8.00
YIR039C	10.31	0.00	22.79	16.32	19.55	234.37	168.89	201.63
YKL096W	13.64	0.00	4.68	8.16	6.42	99.05	76.07	87.56
YPR157W	14.66	0.00	1.01	3.59	2.30	27.59	39.79	33.69
YOL014W	16.85	0.00	2.72	1.99	2.36	47.46	31.95	39.70
YLR013W	23.30	0.00	1.47	0.58	1.02	23.77	23.94	23.85
YLR012C	44.42	0.05	1.31	2.02	1.66	55.55	92.26	73.90

RNA-seq results for differentially expressed genes between R57 before and after 2 hours HWSSL exposure

Gene ID	Fold Change	FDR p-value correction	R57 unexposed Expression values (RPKM)	R57 2 hr HWSSL exposure Expression values (RPKM)
YDL041W	-6.65	0.00	17.59	2.64
YBL075C	-5.51	0.00	2247.13	408.08
YDR343C	-5.40	0.00	10738.84	1987.56
YLR157W-D	-5.27	0.02	14.47	2.75
YMR323W	-5.03	0.00	2936.64	583.97
YOR393W	-4.93	0.00	174.59	35.38
YPR123C	-4.93	0.00	508.73	103.24
YDL085W	-4.86	0.00	381.78	78.54
YKL065W-A	-4.76	0.00	443.61	93.25
YPR184W	-4.68	0.00	479.62	102.56
YPL281C	-4.60	0.00	171.53	37.25
YPR124W	-4.59	0.00	466.01	101.63
YJR038C	-4.50	0.00	34.82	7.73
YGR290W	-4.47	0.00	371.09	82.97
YMR118C	-4.40	0.00	322.10	73.22
YMR206W	-4.39	0.00	574.66	130.80
YLR411W	-4.37	0.00	736.11	168.42
YDR453C	-4.32	0.00	607.59	140.70
YMR250W	-4.26	0.00	832.30	195.32

YEL041W	-4.25	0.00	167.45	39.38
YPL119C-A	-4.24	0.00	117.44	27.69
YJL020W-A	-4.20	0.00	349.29	83.18
YOR186C-A	-4.16	0.00	206.03	49.57
YJL137C	-4.15	0.00	514.59	124.12
YIL086C	-3.97	0.00	168.92	42.58
YGR289C	-3.96	0.00	632.57	159.63
YGR236C	-3.96	0.00	5361.99	1354.10
YML042W	-3.89	0.00	532.27	136.88
YOL081W	-3.82	0.00	82.69	21.67
YDL223C	-3.80	0.00	239.70	63.06
YPR160C-A	-3.75	0.00	464.92	124.13
YDL204W	-3.74	0.00	663.88	177.56
YKL026C	-3.73	0.00	1156.80	309.90
YFL030W	-3.72	0.00	704.46	189.57
YLR217W	-3.69	0.00	1163.41	315.12
YPL223C	-3.65	0.00	2810.19	769.08
YCR091W	-3.65	0.00	138.33	37.88
YOR391C	-3.58	0.00	445.58	124.57
YPL201C	-3.53	0.00	215.43	60.97
YJR120W	-3.51	0.00	1011.92	288.22
YPL171C	-3.49	0.00	620.35	177.52
YJL045W	-3.49	0.00	125.58	36.01
YMR081C	-3.41	0.00	334.28	97.92
YML128C	-3.41	0.00	1422.01	417.26
YLR216C	-3.38	0.00	1171.35	346.35
YIL155C	-3.38	0.00	624.35	184.82
YFL014W	-3.35	0.00	14566.91	4347.30
YOR186W	-3.35	0.00	121.15	36.16
YNL013C	-3.35	0.00	426.40	127.32
YPL186C	-3.33	0.00	579.18	173.90
YJL042W	-3.33	0.00	186.52	56.05
YGR174C	-3.33	0.00	640.27	192.53
YBL022C	-3.29	0.00	242.08	73.57
YNL014W	-3.25	0.00	221.72	68.25
YBL015W	-3.23	0.00	1568.63	484.90
YML030W	-3.23	0.00	651.54	201.50
YLR259C	-3.23	0.00	1799.94	556.80
YLR446W	-3.23	0.00	40.62	12.58
YMR031C	-3.21	0.00	403.80	125.73
YEL011W	-3.21	0.00	789.11	245.93
YFL051C	-3.20	0.00	76.82	23.97
YHR050W-A	-3.19	0.00	329.51	103.27
YOR031W	-3.19	0.00	6959.19	2181.46
YNL195C	-3.15	0.00	750.96	238.37
YGR256W	-3.15	0.00	679.98	215.88
YLR053C	-3.14	0.00	586.56	186.52

YDR070C	-3.14	0.00	2372.09	754.81
YKL187C	-3.13	0.00	464.07	148.36
YOR020C	-3.13	0.00	2754.29	880.61
YMR324C	-3.12	0.00	175.20	56.07
YML075C	-3.12	0.00	133.32	42.79
YNL200C	-3.09	0.00	673.93	218.20
YPR160W	-3.08	0.00	533.60	173.06
YDL199C	-3.08	0.00	101.34	32.89
YPL006W	-3.06	0.00	94.52	30.89
YJR045C	-3.04	0.00	2118.54	696.30
YGR292W	-3.02	0.00	364.42	120.82
YIL119C	-3.02	0.00	105.02	34.83
YHL045W	-3.01	0.00	44.45	14.79
YAL017W	-3.00	0.00	136.91	45.66
YPL262W	-2.99	0.00	688.20	230.12
YMR089C	-2.98	0.00	244.42	81.96
YBR241C	-2.98	0.00	329.61	110.54
YCR011C	-2.97	0.00	76.28	25.67
YGR201C	-2.97	0.00	1027.34	346.29
YMR271C	-2.96	0.00	700.77	236.81
YJR115W	-2.95	0.00	980.54	331.83
YLR203C	-2.94	0.00	397.80	135.51
YDR119W-A	-2.93	0.00	1734.87	591.17
YNL052W	-2.93	0.00	3940.37	1344.20
YGL156W	-2.93	0.00	299.80	102.33
YDL197C	-2.92	0.00	109.16	37.43
YNL115C	-2.90	0.00	330.29	113.99
YLR465C	-2.89	0.00	174.41	60.37
YHL032C	-2.89	0.00	240.83	83.43
YLR347W-A	-2.88	0.00	182.86	63.45
YMR107W	-2.88	0.00	2743.17	953.10
YIL125W	-2.86	0.00	685.99	239.51
YLR454W	-2.86	0.00	46.27	16.17
YIL136W	-2.86	0.00	1638.04	573.09
YPL189C-A	-2.86	0.00	1189.38	416.40
YGR226C	-2.84	0.00	65.58	23.11
YAL062W	-2.84	0.00	319.29	112.57
YGR183C	-2.83	0.00	5396.70	1904.42
YKL151C	-2.83	0.00	812.01	287.08
YCL048W-A	-2.83	0.00	64.72	22.90
YMR175W	-2.82	0.00	9128.04	3236.20
YOR384W	-2.80	0.00	92.05	32.93
YLR152C	-2.79	0.00	284.24	101.72
YAL054C	-2.79	0.00	552.10	197.79
YIR038C	-2.77	0.00	431.56	155.69
YHR054W-A	-2.77	0.00	4911.96	1772.29
YJR039W	-2.76	0.00	54.22	19.65

YLL041C	-2.76	0.00	1526.48	553.81
YBR200W-A	-2.75	0.00	48.79	17.72
YLR450W	-2.75	0.00	122.01	44.33
YBR026C	-2.74	0.00	192.46	70.19
YIR039C	-2.74	0.00	234.37	85.50
YPL196W	-2.74	0.00	297.83	108.70
YIL146C	-2.74	0.00	176.95	64.62
YHR052W-A	-2.73	0.00	4873.26	1786.39
YMR165C	-2.73	0.00	226.33	83.03
YKL147C	-2.71	0.00	186.73	68.79
YNL144W-A	-2.69	0.00	944.80	350.86
YOR215C	-2.69	0.00	534.76	198.69
YMR174C	-2.68	0.00	3381.31	1262.47
YCR021C	-2.67	0.00	13840.30	5175.80
YLR064W	-2.67	0.00	108.56	40.62
YDL130W-A	-2.67	0.00	1716.74	642.57
YKL038W	-2.67	0.00	133.83	50.12
YFL052W	-2.66	0.00	62.03	23.30
YOR227W	-2.66	0.00	112.85	42.44
YOR394W	-2.66	0.00	39.26	14.77
YPL282C	-2.66	0.00	42.69	16.07
YIL046W-A	-2.65	0.01	30.11	11.34
YHR053C	-2.65	0.00	5676.39	2139.11
YDL222C	-2.65	0.00	317.41	119.66
YIL045W	-2.65	0.00	325.17	122.63
YJL185C	-2.65	0.00	139.04	52.51
YLR437C-A	-2.65	0.00	151.98	57.45
YMR110C	-2.64	0.00	398.72	151.18
YJL067W	-2.63	0.00	998.67	379.18
YPL247C	-2.63	0.00	243.19	92.51
YML035C	-2.63	0.00	74.98	28.53
YOL037C	-2.62	0.00	125.24	47.74
YGL062W	-2.61	0.00	651.56	249.27
YJL066C	-2.61	0.00	909.09	347.93
YKR018C	-2.61	0.00	473.38	181.20
YMR280C	-2.61	0.00	105.25	40.32
YBR230W-A	-2.61	0.00	690.82	264.75
YHR055C	-2.60	0.00	5701.08	2193.50
YLR347C	-2.59	0.00	122.20	47.13
YFR017C	-2.59	0.00	1456.88	562.29
YDL169C	-2.59	0.00	514.23	198.49
YML034C-A	-2.58	0.00	107.18	41.48
YKL221W	-2.58	0.00	42.81	16.61
YHR102W	-2.57	0.00	128.64	50.04
YJL102W	-2.57	0.00	131.53	51.23
YGL227W	-2.57	0.00	100.29	39.07
YMR322C	-2.55	0.00	345.00	135.05

YPL106C	-2.55	0.00	544.39	213.46
YDL246C	-2.55	0.00	48.42	19.00
YML054C	-2.54	0.00	895.71	352.08
YOR007C	-2.53	0.00	1582.44	624.99
YNL274C	-2.53	0.00	584.14	230.85
YAL056W	-2.53	0.00	102.19	40.47
YPL119C	-2.53	0.00	230.18	91.15
YDR216W	-2.52	0.00	158.85	62.95
YPL203W	-2.51	0.00	420.51	167.45
YLR255C	-2.51	0.02	27.36	10.90
YOL052C-A	-2.50	0.00	3974.73	1590.50
YDR214W	-2.50	0.00	385.68	154.38
YKL148C	-2.49	0.00	973.36	390.70
YDL215C	-2.49	0.00	132.68	53.34
YOL060C	-2.49	0.00	248.35	99.86
YBR280C	-2.48	0.00	267.88	107.94
YLR312C	-2.48	0.00	320.79	129.41
YHR082C	-2.48	0.00	221.22	89.30
YER141W	-2.48	0.00	715.26	288.90
YMR090W	-2.45	0.00	1339.93	545.87
YLR149C	-2.45	0.00	325.36	132.61
YLL009C	-2.45	0.00	907.67	370.63
YDR231C	-2.44	0.00	548.79	225.01
YBR139W	-2.44	0.00	252.66	103.74
YMR086W	-2.43	0.00	111.79	46.02
YPR010C-A	-2.43	0.00	2021.29	832.83
YBR064W	-2.42	0.00	81.21	33.53
YGL093W	-2.42	0.00	120.52	49.77
YKR076W	-2.42	0.00	339.75	140.54
YHR008C	-2.41	0.00	1078.04	446.57
YDR150W	-2.41	0.00	91.89	38.14
YML087C	-2.41	0.00	142.78	59.35
YPL078C	-2.40	0.00	1519.30	633.38
YGR194C	-2.40	0.00	119.53	49.85
YJL005W	-2.40	0.00	82.88	34.57
YDL067C	-2.39	0.00	4005.20	1674.71
YNR007C	-2.39	0.00	606.15	253.52
YBL105C	-2.39	0.00	98.15	41.08
YMR114C	-2.39	0.00	363.52	152.19
YFL044C	-2.39	0.00	185.88	77.84
YIL097W	-2.39	0.00	110.89	46.45
YIR036C	-2.39	0.00	143.72	60.25
YDR298C	-2.38	0.00	665.09	279.48
YFL036W	-2.37	0.00	87.74	36.97
YLR356W	-2.37	0.00	402.10	169.52
YDR230W	-2.37	0.00	602.12	254.07
YDR022C	-2.36	0.00	120.03	50.76

YJL020C	-2.36	0.00	221.99	94.15
YIR006C	-2.36	0.00	98.23	41.71
YNL101W	-2.35	0.00	151.11	64.18
YHR188C	-2.35	0.00	166.26	70.79
YBL059C-A	-2.35	0.00	367.79	156.82
YBR212W	-2.34	0.00	207.69	88.80
YGR248W	-2.34	0.00	758.41	324.29
YPR038W	-2.34	0.00	117.74	50.35
YFR040W	-2.34	0.00	224.19	95.95
YPR061C	-2.33	0.00	331.44	142.45
YBR039W	-2.32	0.00	1119.27	481.43
YFL067W	-2.32	0.00	161.62	69.55
YKL146W	-2.32	0.00	306.99	132.20
YHR017W	-2.32	0.00	240.80	103.77
YLL040C	-2.32	0.02	31.59	13.64
YMR302C	-2.31	0.00	291.87	126.37
YDL096C	-2.31	0.00	93.27	40.42
YBR298C	-2.31	0.00	437.69	189.85
YDR403W	-2.31	0.00	57.66	25.01
YBR201C-A	-2.31	0.00	358.83	155.65
YDR124W	-2.30	0.01	46.31	20.09
YMR170C	-2.30	0.00	186.97	81.16
YPL185W	-2.30	0.00	91.79	39.87
YIL160C	-2.30	0.00	151.05	65.70
YIL030C	-2.30	0.00	72.72	31.65
YCL012C	-2.30	0.00	560.08	244.01
YIL115C	-2.29	0.03	31.55	13.76
YHR195W	-2.29	0.00	354.02	154.42
YDL004W	-2.29	0.00	1063.74	464.18
YLR038C	-2.29	0.00	1470.11	641.62
YDR504C	-2.29	0.00	85.81	37.46
YER119C	-2.29	0.00	150.75	65.86
YLR395C	-2.29	0.00	2110.30	922.06
YML110C	-2.29	0.00	423.06	184.92
YBR221C	-2.28	0.00	542.45	237.52
YLR247C	-2.28	0.00	67.13	29.41
YGR225W	-2.28	0.04	27.70	12.14
YER178W	-2.28	0.00	790.54	346.51
YHR199C	-2.28	0.00	852.04	373.67
YMR115W	-2.28	0.00	243.15	106.66
YBR090C	-2.28	0.00	414.99	182.09
YPL092W	-2.27	0.00	87.78	38.60
YBR179C	-2.27	0.00	130.01	57.25
YJR103W	-2.27	0.00	228.59	100.73
YLR070C	-2.27	0.00	51.20	22.60
YJR121W	-2.26	0.00	1991.95	879.89
YDL078C	-2.26	0.00	548.68	242.46

YDL185W	-2.26	0.00	289.19	127.99
YJR005C-A	-2.26	0.00	51.51	22.81
YFR015C	-2.26	0.00	153.80	68.13
YGR032W	-2.26	0.00	245.81	108.88
YBR059C	-2.26	0.00	111.96	49.60
YMR257C	-2.26	0.02	36.82	16.33
YLR164W	-2.25	0.01	42.30	18.80
YIL158W	-2.25	0.03	30.57	13.60
YDR293C	-2.25	0.00	278.71	124.04
YKR049C	-2.24	0.00	881.04	392.90
YPL271W	-2.24	0.00	3335.67	1487.91
YPL222W	-2.24	0.00	252.80	112.88
YPR127W	-2.24	0.00	518.42	231.54
YGL074C	-2.24	0.00	115.97	51.86
YNL321W	-2.23	0.00	75.46	33.77
YMR297W	-2.23	0.00	888.76	397.96
YBR235W	-2.23	0.01	46.71	20.92
YPL111W	-2.23	0.00	152.20	68.16
YLR248W	-2.23	0.00	492.56	220.99
YOR173W	-2.23	0.00	1059.54	475.58
YNL100W	-2.23	0.00	401.58	180.32
YMR306C-A	-2.23	0.01	47.41	21.29
YOL083C-A	-2.23	0.00	170.82	76.72
YPR049C	-2.22	0.00	75.42	33.91
YIL057C	-2.22	0.00	343.15	154.76
YCR033W	-2.21	0.00	78.76	35.57
YFL050C	-2.21	0.00	86.51	39.10
YBR286W	-2.21	0.00	517.94	234.23
YNL269W	-2.21	0.00	72.10	32.63
YJL057C	-2.21	0.00	130.89	59.29
YHR189W	-2.21	0.00	90.32	40.92
YGL150C	-2.21	0.01	47.92	21.72
YOL067C	-2.20	0.00	179.36	81.36
YDR494W	-2.20	0.00	254.56	115.55
YFL042C	-2.20	0.00	124.22	56.43
YKR058W	-2.20	0.00	167.26	76.01
YGL010W	-2.20	0.00	291.20	132.55
YIL087C	-2.20	0.00	326.11	148.54
YOR383C	-2.20	0.00	2395.33	1091.18
YJR077C	-2.19	0.00	1438.20	656.05
YMR256C	-2.19	0.00	2976.99	1359.02
YDL195W	-2.19	0.00	84.79	38.77
YNL271C	-2.18	0.00	54.26	24.88
YOL051W	-2.18	0.00	109.64	50.28
YNL073W	-2.18	0.00	220.59	101.18
YMR278W	-2.18	0.00	125.10	57.41
YDR031W	-2.18	0.00	265.64	122.07

YPL013C	-2.17	0.00	387.29	178.31
YDR457W	-2.17	0.02	38.55	17.76
YOL119C	-2.17	0.00	198.22	91.48
YLR438W	-2.16	0.00	188.81	87.46
YBL100C	-2.16	0.00	390.90	181.37
YBR299W	-2.15	0.00	119.79	55.78
YKR009C	-2.15	0.00	179.87	83.81
YNL144C	-2.15	0.00	230.98	107.64
YOL025W	-2.14	0.00	70.34	32.82
YPR185W	-2.14	0.01	47.23	22.05
YDL043C	-2.14	0.03	34.39	16.06
YLR299C-A	-2.14	0.00	294.82	137.70
YMR190C	-2.14	0.01	45.37	21.22
YLR036C	-2.14	0.03	35.55	16.63
YNL270C	-2.14	0.00	73.88	34.57
YAL016C-B	-2.14	0.00	153.16	71.68
YLR069C	-2.13	0.00	132.13	61.90
YMR160W	-2.13	0.01	45.62	21.38
YGR053C	-2.13	0.00	72.93	34.18
YGL014C-A	-2.13	0.01	46.19	21.66
YOL113W	-2.13	0.00	140.38	65.88
YNL071W	-2.13	0.00	425.93	200.37
YDR089W	-2.12	0.05	29.32	13.80
YGL094C	-2.12	0.01	50.23	23.65
YBL066C	-2.12	0.00	74.67	35.18
YLR295C	-2.12	0.00	998.48	470.93
YHR096C	-2.12	0.00	377.11	177.96
YKL087C	-2.12	0.00	402.94	190.24
YOL083W	-2.12	0.00	102.63	48.47
YEL070W	-2.12	0.00	141.74	67.00
YKL157W	-2.11	0.00	168.80	80.03
YHR078W	-2.11	0.00	103.67	49.21
YLR189C	-2.11	0.00	133.75	63.50
YNL242W	-2.10	0.02	39.67	18.86
YGR209C	-2.10	0.00	2144.55	1019.54
YMR219W	-2.10	0.02	37.83	18.00
YOL036W	-2.10	0.00	250.42	119.15
YJR049C	-2.10	0.00	209.78	100.03
YER079C-A	-2.10	0.00	99.43	47.44
YPR150W	-2.10	0.00	503.82	240.40
YMR275C	-2.10	0.00	79.21	37.81
YKR096W	-2.09	0.00	92.75	44.28
YFR024C-A	-2.09	0.00	300.81	143.73
YER133W	-2.09	0.00	532.16	254.46
YHL024W	-2.09	0.00	158.60	75.87
YDL126C	-2.09	0.00	848.42	406.10
YGR231C	-2.09	0.00	595.57	285.30

YIR037W	-2.09	0.00	750.43	359.54
YIL157C	-2.09	0.00	265.52	127.29
YHR198C	-2.09	0.00	123.82	59.38
YLR382C	-2.08	0.01	51.55	24.76
YNR033W	-2.08	0.00	110.34	53.03
YPR098C	-2.08	0.00	154.37	74.24
YPR037C	-2.08	0.00	115.98	55.81
YHR161C	-2.08	0.00	228.94	110.17
YMR069W	-2.07	0.05	29.98	14.45
YER182W	-2.07	0.00	355.85	171.61
YKL141W	-2.07	0.00	710.61	342.93
YIL033C	-2.07	0.00	490.83	236.90
YLL006W	-2.07	0.01	47.18	22.78
YLR163W-A	-2.07	0.00	168.80	81.56
YDR330W	-2.06	0.00	221.63	107.58
YAL008W	-2.06	0.00	208.46	101.28
YNR036C	-2.06	0.00	838.77	407.82
YIL162W	-2.06	0.00	430.02	209.15
YPL222C-A	-2.05	0.00	366.33	178.28
YCL049C	-2.05	0.00	263.94	128.66
YOR290C	-2.05	0.01	56.40	27.50
YDL149W	-2.05	0.00	61.27	29.90
YER084W	-2.05	0.00	103.67	50.62
YML091C	-2.05	0.00	96.43	47.12
YIL029W-A	-2.05	0.03	39.22	19.18
YGL173C	-2.04	0.00	106.87	52.28
YLR299W	-2.04	0.00	192.28	94.10
YGR110W	-2.04	0.00	220.81	108.08
YDR477W	-2.04	0.00	129.34	63.37
YDR204W	-2.04	0.00	167.95	82.32
YKR055W	-2.04	0.00	69.13	33.91
YLR206W	-2.03	0.00	327.31	161.08
YHR016C	-2.03	0.00	417.50	205.60
YOR124C	-2.03	0.01	57.54	28.34
YER004W	-2.03	0.00	811.12	399.76
YPR028W	-2.03	0.00	280.15	138.17
YLR267W	-2.03	0.00	110.24	54.38
YGL187C	-2.03	0.00	1222.67	603.13
YGL163C	-2.03	0.00	162.20	80.05
YLR178C	-2.03	0.00	1615.15	797.14
YBL001C	-2.03	0.00	395.89	195.48
YMR012W	-2.02	0.01	58.88	29.09
YOR211C	-2.02	0.00	74.87	37.02
YDL066W	-2.02	0.00	406.10	201.06
YKL064W	-2.01	0.00	145.18	72.12
YEL030W	-2.01	0.03	38.48	19.13
YLR290C	-2.01	0.00	102.32	50.97

YKL105C	-2.01	0.04	36.69	18.29
YMR317W	-2.00	0.04	36.27	18.09
YPR115W	-2.00	0.00	97.83	48.95
YBR214W	-2.00	0.00	433.46	217.07
YOL100W	-2.00	0.00	90.34	45.25
YDR442W	-2.00	0.00	65.93	33.03
YLR264W	2.00	0.00	110.98	221.58
YGR185C	2.00	0.01	28.66	57.24
YOR367W	2.00	0.00	51.83	103.67
YDL122W	2.00	0.00	50.02	100.16
YER187W	2.00	0.00	51.08	102.27
YOR167C	2.00	0.00	303.34	607.70
YGR113W	2.00	0.05	16.82	33.71
YIL114C	2.01	0.04	17.54	35.18
YBR181C	2.01	0.00	165.22	331.45
YIR012W	2.01	0.00	38.38	77.02
YKR095W-A	2.01	0.00	36.74	73.81
YEL016C	2.01	0.04	17.82	35.83
YML055W	2.01	0.01	25.30	50.85
YML053C	2.01	0.00	47.04	94.62
YDR226W	2.01	0.00	154.07	309.95
YAL003W	2.01	0.00	171.45	344.93
YKL006W	2.01	0.00	156.39	314.68
YKR069W	2.01	0.01	27.63	55.62
YPL149W	2.01	0.00	63.24	127.33
YHR013C	2.02	0.02	21.49	43.39
YKR025W	2.02	0.00	51.48	104.00
YER031C	2.02	0.00	51.94	105.03
YGR260W	2.02	0.00	33.89	68.57
YMR252C	2.03	0.00	90.22	182.79
YPL250C	2.03	0.00	84.00	170.31
YGL067W	2.03	0.03	19.17	38.93
YKR044W	2.03	0.02	21.39	43.51
YOR338W	2.03	0.00	102.74	209.06
YDR361C	2.04	0.00	42.96	87.44
YOL120C	2.04	0.00	180.48	367.43
YJL139C	2.04	0.01	25.07	51.07
YJL189W	2.04	0.00	253.97	517.67
YJR145C	2.04	0.00	156.98	320.51
YER046W	2.04	0.00	43.09	87.99
YOL022C	2.04	0.01	24.55	50.14
YOL085W-A	2.04	0.00	29.82	60.95
YOL125W	2.05	0.01	23.42	47.93
YDR041W	2.05	0.00	87.86	180.02
YDR412W	2.05	0.00	52.49	107.62
YER090C-A	2.05	0.01	27.25	55.88
YER145C	2.05	0.00	149.48	306.53

YJR061W	2.05	0.00	54.73	112.29
YOR253W	2.05	0.02	21.20	43.50
YKL036C	2.05	0.05	15.36	31.54
YGR095C	2.06	0.00	33.41	68.66
YDR280W	2.06	0.00	49.80	102.37
YLR017W	2.06	0.00	37.65	77.39
YER119C-A	2.06	0.05	15.05	30.97
YPL043W	2.06	0.04	15.83	32.59
YDL130W	2.06	0.00	243.71	501.88
YLR154W-B	2.06	0.00	6356.54	13099.48
YOR278W	2.06	0.03	18.15	37.43
YDR472W	2.06	0.02	19.26	39.74
YNL207W	2.06	0.00	30.07	62.05
YMR233W	2.06	0.01	22.72	46.88
YLR373C	2.06	0.01	23.63	48.80
YCL045C	2.07	0.02	20.74	42.85
YBR070C	2.07	0.04	15.77	32.60
YBR167C	2.07	0.00	31.07	64.28
YDR539W	2.07	0.02	20.71	42.85
YEL001C	2.07	0.00	64.93	134.46
YMR131C	2.07	0.03	18.46	38.26
YCL007C	2.07	0.00	39.68	82.28
YFL010W-A	2.08	0.00	191.97	398.87
YMR318C	2.08	0.00	71.19	147.95
YOL039W	2.08	0.00	184.55	383.65
YGL183C	2.08	0.00	51.64	107.56
YPL056C	2.08	0.00	71.93	149.82
YPR197C	2.08	0.05	14.38	29.96
YJL110C	2.08	0.05	14.05	29.27
YMR194W	2.08	0.00	132.00	275.01
YLR060W	2.09	0.02	19.03	39.70
YCR027C	2.09	0.00	28.55	59.59
YBR014C	2.09	0.00	49.12	102.53
YLR300W	2.09	0.00	181.00	377.82
YLR026C	2.09	0.00	48.56	101.41
YBL098W	2.09	0.01	22.92	47.86
YLR018C	2.09	0.00	31.23	65.23
YPR141C	2.09	0.02	19.07	39.84
YGR195W	2.09	0.01	23.25	48.61
YKL106W	2.09	0.05	13.82	28.89
YJL188C	2.09	0.00	160.58	335.91
YGR239C	2.09	0.00	27.27	57.06
YEL026W	2.09	0.00	51.99	108.82
YER035W	2.09	0.00	223.26	467.41
YPR063C	2.09	0.00	62.59	131.05
YBR191W	2.09	0.00	144.26	302.07
YGR080W	2.09	0.00	33.74	70.65

YPR065W	2.09	0.00	197.92	414.46
YER156C	2.09	0.00	39.45	82.63
YDL069C	2.10	0.05	14.40	30.26
YBR071W	2.10	0.00	102.93	216.53
YFL034C-A	2.11	0.00	36.13	76.07
YHR029C	2.11	0.01	25.01	52.66
YJR095W	2.11	0.00	65.29	137.65
YLR066W	2.11	0.02	18.58	39.20
YIL172C	2.11	0.01	21.32	45.06
YKL163W	2.11	0.00	1741.67	3682.36
YGR015C	2.12	0.01	21.03	44.49
YKL084W	2.12	0.01	20.78	43.98
YOL126C	2.12	0.00	99.71	211.06
YEL018W	2.12	0.00	37.81	80.06
YMR009W	2.12	0.00	359.39	761.28
YKL047W	2.12	0.02	19.34	40.98
YGL135W	2.12	0.00	209.82	444.74
YBR183W	2.12	0.00	253.13	537.30
YLR364W	2.13	0.00	25.92	55.11
YDL225W	2.13	0.00	26.51	56.39
YNL302C	2.13	0.00	144.42	307.57
YIL021W	2.13	0.00	41.14	87.62
YDR050C	2.13	0.00	507.89	1082.72
YJL168C	2.13	0.03	15.25	32.53
YOR225W	2.13	0.00	34.30	73.18
YPL067C	2.13	0.00	51.09	109.02
YNL152W	2.14	0.03	16.57	35.37
YML021C	2.14	0.00	35.81	76.51
YGR103W	2.14	0.01	21.58	46.16
YOL128C	2.14	0.01	23.42	50.13
YBR195C	2.14	0.02	16.85	36.08
YML115C	2.14	0.00	30.70	65.79
YPL128C	2.14	0.03	16.01	34.31
YBR096W	2.14	0.01	22.32	47.84
YLR262C	2.14	0.00	26.40	56.58
YIL060W	2.14	0.00	40.19	86.17
YLR210W	2.14	0.05	13.05	27.99
YDL226C	2.15	0.00	27.44	58.86
YBR107C	2.15	0.00	36.98	79.40
YNL124W	2.15	0.00	25.68	55.16
YGR241C	2.15	0.00	26.60	57.14
YDR045C	2.15	0.04	13.97	30.03
YLR006C	2.15	0.02	17.14	36.85
YGL099W	2.15	0.02	16.65	35.79
YBR119W	2.15	0.00	36.81	79.27
YLR197W	2.15	0.01	21.71	46.78
YNL020C	2.16	0.00	37.59	81.02

YJR105W	2.16	0.00	97.68	210.53
YGR148C	2.16	0.00	186.11	401.59
YHR170W	2.16	0.00	31.30	67.57
YKL042W	2.16	0.02	18.60	40.16
YDL111C	2.16	0.00	27.03	58.40
YJR025C	2.16	0.00	57.82	124.95
YDR120C	2.16	0.01	22.83	49.36
YNL253W	2.16	0.05	12.64	27.33
YER140W	2.16	0.03	15.66	33.88
YLR110C	2.16	0.00	1311.71	2839.03
YIL020C-A	2.16	0.00	46.38	100.39
YNL184C	2.17	0.04	14.04	30.40
YOR037W	2.17	0.01	21.02	45.52
YDL061C	2.17	0.00	203.74	441.48
YNR057C	2.17	0.04	13.83	29.98
YGR075C	2.18	0.01	19.58	42.67
YDL012C	2.18	0.00	181.87	396.34
YKL009W	2.18	0.00	28.48	62.10
YOR106W	2.18	0.00	46.94	102.40
YDR311W	2.18	0.03	15.16	33.07
YNL030W	2.18	0.00	640.76	1399.69
YDR354C-A	2.19	0.00	26.20	57.26
YBR061C	2.19	0.03	15.57	34.03
YDL153C	2.19	0.00	25.80	56.40
YDR013W	2.19	0.01	20.76	45.42
YHR127W	2.19	0.03	14.78	32.35
YGR126W	2.19	0.01	21.96	48.10
YLL053C	2.19	0.00	44.66	97.84
YJL169W	2.19	0.01	20.11	44.06
YPL205C	2.19	0.04	13.31	29.15
YHR041C	2.19	0.01	17.98	39.45
YOL101C	2.19	0.00	69.52	152.57
YML070W	2.20	0.00	196.76	431.93
YPL135C-A	2.20	0.00	795.85	1747.24
YBR162W-A	2.20	0.00	255.04	560.25
YAL009W	2.20	0.01	20.88	45.88
YNL029C	2.20	0.02	17.36	38.16
YMR211W	2.20	0.05	11.80	26.00
YLL008W	2.21	0.01	22.13	48.82
YJL196C	2.21	0.00	62.89	138.76
YKL211C	2.21	0.00	27.53	60.81
YLR287C	2.21	0.03	14.78	32.69
YML038C	2.21	0.00	25.55	56.54
YBL024W	2.22	0.05	12.15	26.92
YGR085C	2.22	0.00	128.41	284.81
YMR321C	2.22	0.01	18.98	42.11
YOR004W	2.22	0.02	15.54	34.47

YNL162W	2.22	0.00	135.37	300.40
YNL061W	2.22	0.01	20.79	46.16
YNL097C-B	2.22	0.05	11.76	26.15
YHR063C	2.22	0.01	20.41	45.40
YBR030W	2.23	0.05	12.21	27.18
YNR021W	2.24	0.05	11.39	25.46
YLR009W	2.24	0.00	45.80	102.53
YLR198C	2.24	0.00	34.24	76.67
YDR321W	2.24	0.01	18.55	41.59
YOR279C	2.24	0.01	19.95	44.75
R0020C	2.24	0.00	1517.02	3403.27
YOR137C	2.25	0.00	25.44	57.19
YDR005C	2.25	0.00	31.23	70.24
YLR023C	2.25	0.00	129.36	291.38
YHR180C-B	2.25	0.02	15.57	35.09
YKL208W	2.25	0.01	17.65	39.77
YBR055C	2.25	0.04	12.69	28.61
YKL018W	2.25	0.03	14.23	32.07
YPL177C	2.25	0.00	60.57	136.57
YKL001C	2.26	0.00	140.44	316.77
YBL103C	2.26	0.00	35.34	79.93
YDR398W	2.26	0.04	11.82	26.73
YLR243W	2.26	0.01	16.66	37.70
YFR041C	2.26	0.01	18.77	42.47
YMR217W	2.26	0.00	24.35	55.14
YBR171W	2.26	0.00	30.68	69.49
YJL015C	2.27	0.00	68.18	154.50
YJL016W	2.27	0.00	55.28	125.45
YDL098C	2.27	0.00	33.65	76.37
YDR075W	2.27	0.00	23.54	53.43
YGL070C	2.27	0.00	37.15	84.47
YDR064W	2.27	0.00	184.39	419.21
YDL151C	2.27	0.01	16.75	38.08
YNR054C	2.27	0.00	24.20	55.03
YIL122W	2.27	0.00	56.75	129.08
YGL253W	2.27	0.00	70.16	159.58
YKL119C	2.27	0.05	10.87	24.73
YOR281C	2.28	0.00	22.20	50.53
YKL128C	2.28	0.00	30.81	70.20
YMR037C	2.28	0.00	25.84	58.89
YDL014W	2.28	0.00	64.80	147.74
YML015C	2.28	0.01	17.58	40.11
YDR354W	2.28	0.01	17.55	40.06
YGL039W	2.29	0.00	22.16	50.66
YOR277C	2.29	0.00	104.81	239.58
YNL019C	2.29	0.00	26.63	60.87
YBR166C	2.29	0.01	18.32	41.91

YER073W	2.29	0.00	34.84	79.73
YIL059C	2.29	0.00	39.86	91.23
YBR031W	2.29	0.00	117.92	270.26
YKL044W	2.30	0.00	45.06	103.47
YBR012C	2.30	0.00	31.44	72.26
YFL010C	2.30	0.00	145.06	333.48
YNL292W	2.30	0.04	11.62	26.73
YNR019W	2.30	0.00	288.00	662.64
YER007C-A	2.30	0.00	25.57	58.91
YKL122C	2.30	0.00	25.08	57.78
YOR306C	2.30	0.00	23.65	54.52
YIL040W	2.31	0.01	15.68	36.18
YHR070C-A	2.31	0.00	20.20	46.67
YHR070W	2.31	0.03	13.12	30.33
YMR035W	2.31	0.00	37.10	85.85
YLR293C	2.31	0.00	162.08	375.14
YLR089C	2.32	0.00	130.55	302.90
YCR044C	2.32	0.05	10.72	24.88
YMR122W-A	2.32	0.00	992.63	2306.50
YHR169W	2.32	0.01	16.50	38.35
YKL043W	2.33	0.00	121.72	283.35
YPL077C	2.33	0.02	13.74	32.03
YMR048W	2.33	0.02	14.83	34.57
YMR192W	2.33	0.05	10.61	24.76
YDR308C	2.34	0.01	15.31	35.80
YGR122W	2.34	0.01	16.75	39.23
YDR047W	2.35	0.00	47.30	111.05
YLR146W-A	2.35	0.00	18.97	44.55
YLR388W	2.35	0.00	115.11	270.84
YMR221C	2.35	0.02	12.91	30.38
YER006W	2.36	0.00	32.51	76.66
YMR121C	2.36	0.00	76.69	180.85
YNL153C	2.36	0.00	35.80	84.42
YHR139C-A	2.36	0.00	19.55	46.11
YPL129W	2.36	0.00	50.31	118.70
YNL090W	2.36	0.04	11.08	26.16
YIR026C	2.36	0.04	10.85	25.63
YNR053C	2.36	0.01	16.18	38.26
YDR161W	2.36	0.00	29.17	68.98
YGL188C	2.37	0.00	26.38	62.51
YDR257C	2.37	0.02	14.27	33.83
YNR009W	2.37	0.01	15.01	35.63
YBR188C	2.37	0.00	19.33	45.90
YPR137W	2.38	0.01	17.20	40.85
YKL172W	2.38	0.00	35.61	84.57
YGL038C	2.38	0.00	25.36	60.26
YIR008C	2.38	0.04	10.74	25.53

YGR161W-C	2.38	0.00	307.45	731.48
YOR283W	2.38	0.00	56.53	134.59
YBR154C	2.38	0.00	24.94	59.47
YOR130C	2.39	0.01	17.81	42.51
YBL087C	2.39	0.00	102.53	245.21
YOL066C	2.40	0.05	9.77	23.41
YOL092W	2.40	0.03	10.92	26.18
YDR121W	2.40	0.00	43.63	104.59
YOR046C	2.40	0.00	25.91	62.23
YLL052C	2.40	0.00	46.96	112.79
YCR043C	2.40	0.00	44.05	105.84
YBL039C	2.40	0.05	9.25	22.25
YJR097W	2.40	0.00	26.66	64.11
YLR054C	2.41	0.01	16.86	40.57
YGL223C	2.41	0.03	11.89	28.63
YDR383C	2.41	0.03	11.58	27.89
YMR193C-A	2.41	0.05	9.59	23.12
YBL028C	2.42	0.00	34.28	82.89
YHR089C	2.42	0.00	48.34	116.95
YDL219W	2.42	0.03	10.83	26.20
YLR104W	2.42	0.00	31.76	76.94
YGR137W	2.42	0.00	102.97	249.50
YML066C	2.43	0.05	9.40	22.81
YAL061W	2.43	0.00	857.35	2080.21
YGR018C	2.43	0.00	90.52	219.73
YOR102W	2.43	0.00	59.30	144.11
YKL048C	2.43	0.02	12.20	29.65
YDL189W	2.43	0.03	11.31	27.49
YGL196W	2.44	0.00	42.71	104.00
YBR073W	2.44	0.04	10.32	25.16
YDR496C	2.44	0.05	9.41	22.96
YJL088W	2.45	0.00	27.27	66.81
YIL127C	2.45	0.00	31.80	77.97
YHR134W	2.45	0.00	26.32	64.61
YAL036C	2.46	0.00	19.55	47.99
YKL068W-A	2.46	0.00	124.45	305.71
YLL012W	2.46	0.02	12.31	30.26
YCL047C	2.46	0.01	14.08	34.69
YLR022C	2.47	0.00	20.88	51.49
YDR528W	2.47	0.04	9.99	24.64
YBR091C	2.47	0.00	36.97	91.26
YKR043C	2.47	0.00	63.12	155.94
YDR339C	2.47	0.00	45.23	111.93
YOR271C	2.48	0.00	22.50	55.68
YPL047W	2.48	0.00	47.79	118.32
YKR081C	2.48	0.00	25.94	64.24
YCL026C-B	2.48	0.00	176.88	438.07

YCR057C	2.48	0.05	8.71	21.58
YFL047W	2.48	0.02	11.20	27.75
YIL118W	2.48	0.00	41.02	101.75
YDL068W	2.48	0.00	16.77	41.64
YLR285W	2.48	0.00	20.96	52.08
YAL025C	2.49	0.01	15.50	38.54
YGR249W	2.49	0.00	45.09	112.13
YOL155W-A	2.49	0.00	18.63	46.35
YPL126W	2.49	0.03	10.73	26.73
YBR054W	2.50	0.00	990.88	2479.07
YPR167C	2.50	0.00	38.08	95.30
YOL135C	2.50	0.00	36.75	92.04
YOL157C	2.51	0.00	97.39	244.12
YMR316C-A	2.51	0.00	207.00	519.17
YDR524C-B	2.51	0.00	1362.55	3419.87
YBR178W	2.51	0.00	16.27	40.86
YNL166C	2.51	0.00	25.35	63.69
YML107C	2.52	0.05	8.70	21.88
YPR187W	2.52	0.00	47.84	120.33
YLR083C	2.52	0.00	16.95	42.66
YPL273W	2.52	0.01	13.63	34.32
YOR103C	2.52	0.00	44.32	111.60
YER131W	2.52	0.00	176.78	445.72
YML119W	2.53	0.00	63.94	161.65
YHL013C	2.53	0.00	22.80	57.65
YGR245C	2.53	0.02	11.19	28.30
YLR065C	2.54	0.01	12.67	32.13
YOR026W	2.54	0.01	12.14	30.78
YHR139C	2.54	0.00	74.87	189.97
YKL166C	2.54	0.00	22.33	56.67
YPL135W	2.54	0.00	714.11	1812.66
YFR032C-A	2.54	0.00	210.67	535.06
YBL005W	2.54	0.01	14.01	35.61
YOL102C	2.54	0.00	22.05	56.11
YGR166W	2.55	0.00	19.21	48.92
YDR147W	2.55	0.03	10.11	25.80
YEL040W	2.55	0.00	23.52	60.06
YPR016W-A	2.56	0.00	16.38	41.90
YNR020C	2.56	0.00	17.48	44.74
YGL246C	2.56	0.00	18.37	47.02
YBL002W	2.56	0.00	86.07	220.47
YOL019W	2.56	0.00	15.57	39.90
YOR254C	2.57	0.01	14.81	37.99
YNL301C	2.57	0.00	20.96	53.79
YOR218C	2.57	0.02	10.63	27.29
YGR242W	2.58	0.02	10.58	27.25
YKR091W	2.58	0.00	74.43	191.69

YNL119W	2.58	0.01	11.50	29.63
YGR065C	2.58	0.01	13.52	34.85
YOR238W	2.58	0.05	8.21	21.16
YCR020W-B	2.58	0.00	28.13	72.54
YML116W-A	2.58	0.00	36.94	95.34
YPL018W	2.58	0.00	54.22	139.98
YDR037W	2.58	0.00	16.01	41.32
YOR078W	2.58	0.00	34.51	89.12
YML102W	2.58	0.00	18.24	47.09
YIL079C	2.58	0.01	14.34	37.04
YPR156C	2.58	0.00	179.98	464.87
YHR069C-A	2.58	0.05	7.80	20.14
YHR040W	2.58	0.00	32.84	84.87
YDR537C	2.58	0.00	31.55	81.54
YKL154W	2.59	0.00	15.23	39.38
YMR016C	2.59	0.00	24.35	62.97
YDR083W	2.59	0.00	18.99	49.15
YML080W	2.59	0.01	13.40	34.71
YDL208W	2.59	0.00	51.27	132.85
YPL066W	2.59	0.00	24.98	64.77
YBR141W-A	2.59	0.00	24.89	64.57
YER034W	2.60	0.00	42.60	110.56
YER184C	2.60	0.04	8.67	22.56
YPL227C	2.60	0.03	9.64	25.08
YKL070W	2.60	0.00	26.02	67.76
YEL014C	2.61	0.00	18.70	48.73
YIL016W	2.61	0.00	15.72	41.06
YBL054W	2.61	0.00	19.05	49.77
YOR224C	2.62	0.00	32.23	84.33
YGR040W	2.62	0.01	14.09	36.87
YPL259C	2.62	0.00	29.59	77.48
YIL029C	2.62	0.04	8.06	21.13
YML011C	2.62	0.00	25.32	66.36
YAR033W	2.63	0.00	14.63	38.40
YNL027W	2.63	0.00	59.61	156.54
YJL171C	2.63	0.00	221.66	583.49
YPL267W	2.63	0.05	7.69	20.23
YGL061C	2.63	0.03	8.62	22.71
YMR238W	2.64	0.00	81.84	216.16
YEL059C-A	2.64	0.00	31.86	84.21
YGR017W	2.64	0.00	69.22	183.02
YHR072W-A	2.65	0.00	160.95	426.19
YGL210W	2.65	0.00	43.80	116.08
YLL055W	2.66	0.00	29.08	77.24
YDR242W	2.66	0.00	29.69	78.93
YGL078C	2.66	0.00	28.40	75.55
YBR159W	2.66	0.00	33.25	88.50

YAL012W	2.67	0.00	75.04	200.30
YNL158W	2.67	0.00	32.65	87.18
YGR187C	2.67	0.01	13.06	34.89
YML094C-A	2.69	0.03	8.45	22.69
YML093W	2.69	0.05	6.94	18.69
YMR014W	2.69	0.00	14.11	38.01
YDR351W	2.70	0.01	10.52	28.35
YGL247W	2.71	0.00	18.42	49.91
YCR024C-B	2.72	0.00	250.13	679.82
YOR226C	2.72	0.00	37.25	101.31
YKL052C	2.72	0.00	134.14	364.90
YOR108C-A	2.72	0.00	16.17	44.00
YDR538W	2.72	0.00	28.64	77.97
YML101C-A	2.73	0.00	14.44	39.35
YMR184W	2.73	0.00	33.92	92.47
YDR123C	2.73	0.00	34.91	95.35
YDR210W	2.73	0.00	233.62	638.37
YMR303C	2.74	0.02	9.49	25.97
YDR033W	2.74	0.00	125.06	343.27
YJR022W	2.76	0.01	11.05	30.48
YHR133C	2.76	0.00	17.37	47.93
YKL130C	2.76	0.00	20.62	56.90
YNR011C	2.76	0.05	6.84	18.87
YGR159C	2.76	0.00	24.14	66.65
YEL017C-A	2.76	0.00	532.63	1470.78
YDR184C	2.76	0.02	9.38	25.90
YGR035W-A	2.76	0.00	19.26	53.21
YOR361C	2.76	0.00	22.33	61.74
YPR171W	2.77	0.00	13.55	37.50
YOL052C	2.78	0.00	13.57	37.76
YGL041C-B	2.79	0.01	9.97	27.80
YOR299W	2.79	0.00	19.62	54.77
YCR007C	2.79	0.00	62.19	173.81
YOR288C	2.80	0.00	12.16	34.04
YIL104C	2.80	0.01	11.02	30.85
YKL053W	2.80	0.00	153.44	430.08
YGR049W	2.81	0.00	210.52	591.51
YBR164C	2.81	0.00	23.92	67.27
YGL225W	2.81	0.00	32.00	90.08
YDL161W	2.82	0.00	30.59	86.19
YGR173W	2.83	0.01	10.79	30.53
YDL150W	2.83	0.00	14.92	42.26
YJL011C	2.84	0.00	14.62	41.51
YDR252W	2.84	0.03	7.69	21.83
YHR196W	2.85	0.01	10.04	28.60
YDR043C	2.85	0.00	504.45	1439.74
YNL151C	2.86	0.00	31.11	88.88

YGR123C	2.86	0.01	9.01	25.79
YNR027W	2.87	0.01	10.94	31.38
YJL148W	2.87	0.00	19.89	57.06
YHR052W	2.87	0.00	14.90	42.76
YDL139C	2.88	0.00	23.68	68.22
YLR121C	2.88	0.00	169.92	490.02
YPR060C	2.88	0.01	11.17	32.23
YOR276W	2.89	0.00	55.25	159.43
YOL007C	2.90	0.05	5.95	17.21
YGR074W	2.90	0.00	40.50	117.35
YMR301C	2.90	0.01	9.95	28.86
YPR110C	2.91	0.00	34.50	100.25
YNL075W	2.91	0.00	22.62	65.78
YBR141C	2.91	0.01	10.17	29.58
YGL224C	2.91	0.00	13.65	39.75
YJL107C	2.92	0.00	63.43	185.48
YLR002C	2.93	0.00	11.96	35.05
YDR209C	2.93	0.00	142.33	417.11
YBR105C	2.93	0.00	311.55	913.93
YHR085W	2.94	0.00	11.58	33.98
YPL246C	2.94	0.00	20.09	59.00
YMR291W	2.94	0.00	47.78	140.50
YOR091W	2.94	0.00	24.05	70.81
YMR006C	2.94	0.00	23.81	70.11
YGL117W	2.94	0.00	34.44	101.42
YJR071W	2.95	0.02	8.01	23.61
YNL191W	2.95	0.00	66.99	197.64
YDR384C	2.95	0.00	13.06	38.56
YKL120W	2.95	0.00	27.54	81.33
YHL043W	2.96	0.00	19.74	58.36
YJL019W	2.96	0.01	10.56	31.22
YKR024C	2.96	0.02	7.82	23.17
YLR405W	2.97	0.00	13.84	41.05
YJL060W	2.98	0.00	30.57	91.07
YGL171W	2.98	0.02	7.35	21.91
YCR087C-A	2.99	0.00	18.78	56.07
YDR055W	2.99	0.00	810.89	2423.30
YDL209C	3.00	0.00	13.38	40.07
YEL045C	3.00	0.00	15.94	47.91
YGR081C	3.01	0.00	12.82	38.52
YGR073C	3.01	0.00	18.60	55.96
YLR435W	3.01	0.00	18.32	55.16
YLR196W	3.02	0.00	11.95	36.05
YPL239W	3.02	0.00	47.45	143.33
YIL056W	3.02	0.00	59.45	179.66
YGR120C	3.02	0.00	12.99	39.28
YHR062C	3.03	0.01	8.41	25.53

YLR276C	3.04	0.01	8.24	25.03
YMR198W	3.04	0.00	12.54	38.13
YOL016C	3.05	0.00	378.49	1153.22
YOL017W	3.06	0.03	6.16	18.81
YMR290C	3.06	0.00	13.30	40.76
YER126C	3.07	0.00	17.44	53.49
YGR078C	3.07	0.00	14.04	43.08
YGR176W	3.07	0.05	5.42	16.64
YOR058C	3.07	0.00	29.12	89.39
YLR417W	3.07	0.00	15.19	46.65
YBR034C	3.07	0.00	25.65	78.75
YPR170C	3.08	0.00	14.60	44.90
YOL123W	3.08	0.00	25.86	79.61
YOR079C	3.10	0.02	6.94	21.54
YGR243W	3.11	0.00	752.22	2336.68
YEL019C	3.11	0.02	6.57	20.44
YKL051W	3.11	0.00	64.13	199.71
YER049W	3.12	0.00	24.02	74.92
YNL120C	3.12	0.01	7.63	23.82
YDR165W	3.13	0.03	5.75	18.00
YNL110C	3.14	0.00	33.58	105.31
YPL093W	3.14	0.00	15.43	48.40
YGR160W	3.14	0.00	12.84	40.32
YPL086C	3.14	0.00	11.76	36.92
YNL174W	3.14	0.00	11.52	36.23
YOR209C	3.15	0.00	62.64	197.14
YLR186W	3.16	0.00	25.77	81.36
YMR199W	3.16	0.02	7.05	22.27
YNL065W	3.16	0.00	15.96	50.51
YGR152C	3.18	0.01	8.98	28.56
YNL175C	3.18	0.00	15.72	49.99
YLR136C	3.19	0.00	40.02	127.52
YML094W	3.19	0.00	18.28	58.36
YOR287C	3.19	0.00	11.56	36.91
YLR409C	3.21	0.05	4.73	15.16
YDR101C	3.21	0.01	7.02	22.58
YOR028C	3.22	0.00	31.73	102.20
YPR186C	3.22	0.01	7.21	23.25
YDL085C-A	3.23	0.00	26.43	85.31
YCR016W	3.23	0.00	11.31	36.51
YBR175W	3.23	0.01	7.43	24.00
YLR285C-A	3.24	0.00	22.07	71.47
YBR254C	3.25	0.00	13.82	44.97
YGL169W	3.26	0.00	10.80	35.20
YHR148W	3.27	0.00	9.34	30.51
YAL059W	3.27	0.00	19.98	65.25
YMR049C	3.27	0.01	7.81	25.57

YIR034C	3.28	0.00	92.59	303.64
YPL108W	3.28	0.01	7.69	25.26
YPL175W	3.30	0.00	20.22	66.78
YKR026C	3.31	0.00	16.03	53.00
YJR043C	3.31	0.02	5.85	19.38
YOL020W	3.31	0.03	5.41	17.91
YML014W	3.31	0.00	11.83	39.19
YHR192W	3.32	0.00	9.39	31.16
YDR465C	3.33	0.00	12.59	41.96
YDL128W	3.33	0.00	120.53	401.91
YHL026C	3.34	0.00	20.56	68.65
YNR029C	3.35	0.00	13.16	44.15
YDR299W	3.36	0.01	7.56	25.39
YNL113W	3.36	0.00	34.01	114.23
YKR061W	3.36	0.00	24.51	82.36
YMR296C	3.36	0.00	26.96	90.66
Q0130	3.37	0.05	4.36	14.68
YOR179C	3.38	0.00	29.06	98.08
YKR060W	3.38	0.00	9.07	30.62
YAR029W	3.39	0.00	67.08	227.15
YJR063W	3.39	0.00	16.30	55.23
YOL011W	3.39	0.00	77.62	262.96
YDR087C	3.39	0.00	9.84	33.40
YIL120W	3.40	0.00	16.69	56.75
YGR052W	3.41	0.00	135.29	460.70
YPR146C	3.42	0.00	12.39	42.35
YDL235C	3.42	0.00	17.22	58.94
YGR158C	3.42	0.00	13.11	44.89
YNL182C	3.42	0.04	4.64	15.88
YDL121C	3.43	0.00	11.74	40.28
YER149C	3.44	0.00	19.62	67.41
YHR140W	3.44	0.00	23.76	81.79
YGR055W	3.44	0.00	28.18	97.02
YGR189C	3.45	0.00	116.04	400.28
YBR083W	3.46	0.00	15.75	54.43
YCR087W	3.46	0.00	16.70	57.80
YDR038C	3.46	0.00	26.74	92.61
YFL034C-B	3.46	0.02	5.82	20.17
YPR070W	3.47	0.01	7.43	25.75
YHR088W	3.48	0.00	18.98	66.05
YKR090W	3.49	0.00	10.64	37.14
YKL071W	3.49	0.00	25.53	89.19
YNL043C	3.50	0.00	139.49	487.85
YOR094W	3.50	0.00	14.47	50.64
YCR010C	3.50	0.00	88.57	310.02
YCR024C-A	3.50	0.00	1210.19	4238.37
YPL221W	3.52	0.00	116.14	408.26

YBR182C	3.53	0.00	65.02	229.22
YNL114C	3.53	0.00	23.67	83.47
YNL044W	3.53	0.00	112.63	397.88
YDR259C	3.54	0.00	8.46	29.95
YJL069C	3.54	0.00	11.24	39.84
YNL112W	3.55	0.00	9.43	33.46
YGL188C-A	3.56	0.00	10.26	36.50
YBL071C-B	3.56	0.05	3.81	13.59
YOL041C	3.56	0.00	14.76	52.63
YFR028C	3.57	0.00	10.63	37.96
YDR247W	3.57	0.00	151.41	540.97
YOL152W	3.58	0.00	17.79	63.62
YGR251W	3.58	0.00	22.13	79.26
YDR243C	3.59	0.00	10.32	37.07
YNL160W	3.59	0.00	1716.73	6171.24
YFR023W	3.60	0.02	4.76	17.14
YKL216W	3.60	0.00	32.81	118.25
YBL081W	3.61	0.01	6.53	23.56
YLR099W-A	3.62	0.00	54.79	198.24
YCR024C	3.63	0.00	18.03	65.36
YER148W-A	3.63	0.00	22.05	79.99
YMR017W	3.63	0.04	4.06	14.74
YFL053W	3.64	0.00	46.14	167.92
YPL001W	3.66	0.00	8.78	32.12
YJL122W	3.66	0.00	22.87	83.73
YPL211W	3.66	0.00	17.39	63.72
YPL024W	3.67	0.00	24.34	89.25
YMR132C	3.67	0.00	9.83	36.09
YLR328W	3.68	0.00	31.91	117.54
YJL108C	3.69	0.00	74.41	274.31
YMR316W	3.69	0.00	145.55	536.87
YKL045W	3.70	0.00	7.17	26.53
YER038C	3.71	0.00	31.24	115.78
YNL141W	3.71	0.00	8.43	31.25
YGR177C	3.73	0.05	3.48	12.98
YKR092C	3.75	0.00	19.42	72.80
YPL026C	3.76	0.00	91.23	342.64
YKL099C	3.76	0.00	18.54	69.66
YEL046C	3.76	0.00	90.39	340.16
YNR003W-A	3.77	0.00	10.80	40.76
YOR134W	3.80	0.00	54.30	206.28
YDR365C	3.81	0.00	9.40	35.79
YAL037C-A	3.81	0.00	6.76	25.78
YHL042W	3.82	0.00	15.83	60.41
YGR129W	3.83	0.00	9.90	37.90
YMR274C	3.83	0.05	3.32	12.71
YAL059C-A	3.86	0.00	12.19	47.00

YKL143W	3.86	0.00	17.21	66.42
YDL152W	3.86	0.04	3.44	13.26
YKL144C	3.90	0.00	7.77	30.29
YMR272C	3.90	0.00	605.68	2362.00
YMR007W	3.90	0.00	36.64	143.05
YMR093W	3.91	0.00	8.48	33.18
YLL011W	3.91	0.00	11.12	43.52
YLR154C-H	3.91	0.00	84.80	331.81
YJR112W	3.92	0.00	8.72	34.16
YLR120W-A	3.92	0.00	158.45	621.46
YCR005C	3.92	0.00	962.58	3775.36
YLR428C	3.94	0.03	3.83	15.09
YOL077C	3.95	0.00	17.01	67.15
YDR091C	3.96	0.00	15.52	61.52
YHR066W	3.96	0.00	8.45	33.49
YER065C	3.97	0.00	28.40	112.69
YDR297W	3.99	0.00	140.93	561.65
YDR449C	3.99	0.01	4.85	19.36
YMR010W	4.00	0.00	21.58	86.32
YER064C	4.01	0.00	12.01	48.15
YMR307C-A	4.01	0.00	110.94	444.72
YKL132C	4.03	0.00	15.81	63.72
YAR064W	4.05	0.05	2.93	11.89
YNR062C	4.09	0.02	3.90	15.93
YAR030C	4.12	0.00	38.43	158.33
YOL079W	4.13	0.00	8.51	35.17
YDL129W	4.13	0.00	23.98	99.13
YLR375W	4.14	0.00	275.01	1137.92
YIL058W	4.15	0.00	5.74	23.80
YLR374C	4.16	0.00	76.11	316.82
YOL124C	4.16	0.00	6.67	27.76
YLL028W	4.18	0.00	64.35	269.24
YKL055C	4.18	0.03	3.46	14.46
YKL162C-A	4.18	0.00	5.75	24.08
YLL035W	4.22	0.01	4.44	18.72
YMR272W-A	4.22	0.00	778.92	3287.00
YLR120C	4.23	0.00	82.67	349.56
YDR009W	4.24	0.00	8.97	38.09
YOR051C	4.26	0.00	31.22	133.09
YHR049C-A	4.27	0.00	23.93	102.19
YBR006W	4.29	0.00	126.07	540.77
YMR263W	4.34	0.00	25.94	112.51
YOR348C	4.35	0.00	17.56	76.32
YGL008C	4.38	0.00	390.92	1710.97
YNL192W	4.38	0.00	80.09	351.14
YOR049C	4.39	0.00	126.90	557.20
YBR021W	4.40	0.00	5.85	25.73

YNR038W	4.40	0.00	5.36	23.58
YPL088W	4.41	0.00	69.61	306.82
YDR300C	4.42	0.00	12.31	54.39
YPL102C	4.43	0.04	2.70	11.97
YLR194C	4.44	0.00	291.50	1293.52
YHR071C-A	4.45	0.04	2.74	12.21
YER137C	4.49	0.00	10.41	46.70
YLR363W-A	4.49	0.00	11.21	50.32
YKL096W	4.52	0.00	99.05	447.35
YJL033W	4.52	0.00	7.34	33.17
YDR011W	4.55	0.00	54.42	247.39
YKL149C	4.55	0.00	5.83	26.55
YOL149W	4.55	0.00	46.53	211.81
YHR030C	4.55	0.00	63.10	287.32
YLR180W	4.56	0.00	126.76	577.44
YMR307W	4.57	0.00	111.29	508.50
YDL039C	4.57	0.00	5.73	26.18
YOR047C	4.59	0.00	23.79	109.29
YIL117C	4.61	0.00	20.90	96.30
YDR072C	4.63	0.00	73.05	338.20
YPR036W-A	4.65	0.00	5137.00	23882.56
YOR272W	4.66	0.00	6.41	29.89
YLR154W-E	4.67	0.00	1061.37	4951.31
YOL080C	4.68	0.00	9.98	46.65
YMR254C	4.68	0.00	5.49	25.74
YGR213C	4.68	0.00	14.04	65.77
YLR179C	4.69	0.00	128.89	605.03
YPR144C	4.72	0.00	5.16	24.36
YKL131W	4.73	0.00	10.12	47.83
YLR112W	4.74	0.00	4.49	21.30
YOL014W	4.76	0.00	47.46	225.95
YOR274W	4.78	0.00	22.97	109.73
YGR283C	4.81	0.00	7.17	34.48
YHR049W	4.81	0.00	54.21	260.75
YCR072C	4.81	0.00	4.18	20.13
YDR095C	4.82	0.04	2.45	11.81
YLR415C	4.82	0.00	12.80	61.75
YKR093W	4.84	0.00	8.08	39.08
YDR044W	4.85	0.00	64.61	313.48
YGL007C-A	4.88	0.02	2.89	14.12
YPR112C	4.91	0.00	5.64	27.72
YKL062W	4.93	0.00	50.43	248.55
YNL210W	4.96	0.04	2.32	11.51
YDL236W	4.96	0.00	29.53	146.53
YJL214W	4.96	0.01	3.82	18.98
YER127W	4.96	0.00	11.24	55.81
YDR191W	4.97	0.01	3.79	18.81

YIR035C	4.98	0.00	180.28	897.64
YOR388C	4.98	0.00	48.76	243.01
YHR046C	4.99	0.00	16.57	82.64
YHR065C	5.02	0.00	5.68	28.50
YKL159C	5.04	0.00	53.39	269.31
YER037W	5.06	0.00	144.59	732.29
YDL148C	5.08	0.01	3.10	15.74
YDR042C	5.09	0.00	3.96	20.17
YAL037W	5.09	0.00	6.41	32.66
YNL262W	5.11	0.00	4.87	24.86
YDL023C	5.11	0.00	400.44	2047.05
YGR145W	5.13	0.00	7.40	37.97
YGR250C	5.16	0.00	200.11	1032.24
YDR222W	5.18	0.00	18.04	93.38
YKL078W	5.19	0.01	3.10	16.10
YMR315W-A	5.21	0.00	8.73	45.48
YLR099C	5.21	0.00	127.42	663.87
YBL043W	5.24	0.00	120.41	631.31
YOR269W	5.29	0.04	2.03	10.75
YBR005W	5.35	0.00	171.42	917.14
YAR028W	5.36	0.00	39.87	213.92
YPL025C	5.39	0.03	2.25	12.16
YGR140W	5.41	0.00	9.48	51.35
YHR137W	5.46	0.00	9.99	54.57
YGR146C-A	5.46	0.01	3.11	16.97
YJL160C	5.51	0.04	1.97	10.83
YGL134W	5.53	0.00	125.44	693.46
YLR329W	5.55	0.01	2.69	14.93
YDR320W-B	5.58	0.02	2.28	12.71
YNL231C	5.67	0.00	106.72	605.59
YNL162W-A	5.70	0.00	4.31	24.57
YOR050C	5.72	0.00	3.61	20.67
YGR164W	5.73	0.02	2.25	12.88
YDR344C	5.73	0.00	3.40	19.49
YGR036C	5.73	0.00	8.91	51.09
YGL162W	5.81	0.00	12.79	74.33
YJR094C	5.82	0.00	22.88	133.26
YFR022W	5.89	0.00	79.57	469.01
YOR344C	5.90	0.00	15.22	89.72
YBR018C	5.91	0.00	10.45	61.77
YDR509W	5.93	0.01	2.89	17.14
YGR161C	5.98	0.00	184.85	1105.59
YDR345C	6.00	0.00	1409.49	8458.56
YDL022W	6.13	0.00	508.71	3119.05
YGR051C	6.24	0.00	24.07	150.16
YLL056C	6.31	0.00	70.39	443.89
YNL036W	6.51	0.00	75.45	491.52

YGL116W	6.52	0.00	8.03	52.38
YOR062C	6.54	0.00	58.45	382.16
YGR139W	6.66	0.00	15.95	106.26
YPL144W	6.70	0.00	4.08	27.34
YCL064C	6.80	0.05	1.28	8.69
YOL010W	6.84	0.00	17.03	116.42
YGR050C	6.85	0.00	14.80	101.39
YER137W-A	6.87	0.00	5.75	39.56
YLR414C	6.90	0.00	165.32	1141.03
YDL241W	6.92	0.00	34.99	242.24
YNL024C	6.97	0.00	5.18	36.06
YER185W	6.99	0.00	7.72	53.99
YKR075C	7.01	0.00	185.67	1300.98
YPL014W	7.11	0.00	41.21	293.05
YBR131C-A	7.13	0.01	2.10	14.94
YOR273C	7.25	0.00	91.50	663.44
YDR380W	7.36	0.00	2.77	20.38
YOR385W	7.39	0.00	37.67	278.25
YKR075W-A	7.41	0.00	173.06	1282.37
YOR107W	7.72	0.00	46.39	358.03
YOR381W-A	7.81	0.01	1.87	14.62
YGL157W	8.07	0.00	49.82	402.11
YGL179C	8.20	0.00	27.31	224.00
YBR056C-B	8.21	0.00	277.26	2275.81
YMR195W	8.48	0.00	172.12	1459.02
YOR318C	8.52	0.02	1.23	10.51
YER130C	8.60	0.00	77.62	667.39
YPR145C-A	8.60	0.00	91.01	782.90
YMR102C	8.61	0.00	22.69	195.37
YGL209W	8.76	0.00	97.59	855.21
YPL068C	8.80	0.00	7.34	64.64
YGL158W	8.94	0.01	1.39	12.42
YJL218W	8.98	0.00	5.32	47.79
YBR056W-A	9.04	0.00	318.82	2881.65
YDR508C	9.20	0.00	7.80	71.72
YOL136C	9.30	0.00	52.14	485.10
YCR022C	9.69	0.00	3.46	33.56
YOL013W-A	9.92	0.02	0.98	9.75
YLR346C	10.14	0.00	83.85	849.82
YJL136W-A	10.23	0.05	0.75	7.66
YHR092C	10.30	0.00	42.98	442.88
YHR137C-A	10.38	0.00	4.15	43.12
YGR035C	10.43	0.00	82.95	864.82
YLR044C	10.80	0.00	848.31	9158.23
YPR116W	10.84	0.00	2.19	23.70
YPR157W	10.98	0.00	27.59	302.88
YOL150C	11.28	0.00	299.32	3377.03

YBL070C	11.55	0.00	15.28	176.52
YOL151W	11.56	0.00	290.97	3363.40
YIL121W	11.64	0.00	29.11	338.80
YOR153W	12.14	0.00	49.04	595.12
YLR134W	12.35	0.00	65.19	805.09
YDR046C	12.59	0.00	12.68	159.64
YBL069W	12.83	0.00	34.90	447.69
YJL216C	13.29	0.00	5.47	72.74
YER062C	13.54	0.00	146.24	1979.66
YGR138C	13.60	0.00	183.68	2497.51
YMR011W	13.73	0.00	41.15	564.88
YMR242W-A	13.95	0.02	0.70	9.75
YCR102W-A	14.41	0.02	0.64	9.16
YPL058C	14.85	0.00	30.20	448.41
YDR536W	15.18	0.00	48.88	742.14
YHR094C	17.17	0.00	141.05	2421.54

RNA-seq results for differentially expressed genes between R57 before and after 24 hours HWSSL exposure

Gene ID	Fold Change	FDR p-value correction	Expression values for R57 before exposure to HWSSL (RPKM)	Expression values for R57 after 24 hrs HWSSL exposure (RPKM)
YBR196C-B	-15.86	0.02	9.58	0.60
YLR411W	-15.57	0.00	736.11	47.28
YMR323W	-14.64	0.00	2936.64	200.55
YBL075C	-14.51	0.00	2247.13	154.89
YMR118C	-13.82	0.00	322.10	23.30
YDR453C	-13.35	0.00	607.59	45.52
YOR393W	-12.38	0.00	174.59	14.10
YPR123C	-12.15	0.00	508.73	41.86
YDL085W	-12.03	0.00	381.78	31.73
YMR324C	-11.98	0.00	175.20	14.62
YBR027C	-11.89	0.03	9.06	0.76
YDL223C	-11.84	0.00	239.70	20.24
YML042W	-11.46	0.00	532.27	46.46
YEL030C-A	-11.19	0.00	15.77	1.41
YNL332W	-10.87	0.00	19.55	1.80
YDR343C	-10.80	0.00	10738.84	994.65
YMR250W	-10.78	0.00	832.30	77.24
YPL119C-A	-10.62	0.00	117.44	11.06
YPR124W	-10.51	0.00	466.01	44.33
YPL281C	-10.42	0.00	171.53	16.47

YGR290W	-10.35	0.00	371.09	35.87
YEL041W	-10.25	0.00	167.45	16.33
YJL020W-A	-10.22	0.00	349.29	34.19
YJL137C	-10.20	0.00	514.59	50.46
YFL066C	-10.12	0.05	7.63	0.75
YML075C	-10.11	0.00	133.32	13.19
YOR384W	-10.05	0.00	92.05	9.16
YNL014W	-9.99	0.00	221.72	22.18
YGL239C	-9.98	0.00	30.15	3.02
YDL199C	-9.93	0.00	101.34	10.21
YPR184W	-9.75	0.00	479.62	49.21
YLR053C	-9.72	0.00	586.56	60.35
YAL017W	-9.67	0.00	136.91	14.15
YCR091W	-9.66	0.00	138.33	14.32
YLL006W	-9.62	0.00	47.18	4.90
YLR454W	-9.55	0.00	46.27	4.84
YJR120W	-9.55	0.00	1011.92	105.93
YLR465C	-9.44	0.00	174.41	18.48
YJL045W	-9.36	0.00	125.58	13.42
YGR236C	-9.35	0.00	5361.99	573.72
YPL223C	-9.30	0.00	2810.19	302.12
YJL042W	-9.19	0.00	186.52	20.30
YBL022C	-9.12	0.00	242.08	26.54
YOR391C	-9.00	0.00	445.58	49.50
YNL115C	-9.00	0.00	330.29	36.69
YML128C	-8.96	0.00	1422.01	158.71
YOR186W	-8.93	0.00	121.15	13.57
YNL013C	-8.76	0.00	426.40	48.68
YHL045W	-8.71	0.00	44.45	5.11
YMR271C	-8.69	0.00	700.77	80.61
YLR446W	-8.68	0.00	40.62	4.68
YPL006W	-8.68	0.00	94.52	10.89
YDL204W	-8.64	0.00	663.88	76.87
YOR215C	-8.63	0.00	534.76	61.97
YKL026C	-8.63	0.00	1156.80	134.08
YOR186C-A	-8.52	0.00	206.03	24.17
YMR206W	-8.50	0.00	574.66	67.63
YML054C	-8.45	0.00	895.71	106.04
YBR026C	-8.44	0.00	192.46	22.82
YIL086C	-8.31	0.00	168.92	20.33
YFL030W	-8.31	0.00	704.46	84.82
YML030W	-8.26	0.00	651.54	78.92
YKL065W-A	-8.26	0.00	443.61	53.73
YDL130W-A	-8.19	0.00	1716.74	209.56
YMR165C	-8.11	0.00	226.33	27.92
YMR031C	-8.08	0.00	403.80	49.97
YMR089C	-8.08	0.00	244.42	30.27

YKR018C	-8.00	0.00	473.38	59.14
YGR174C	-8.00	0.00	640.27	80.03
YMR160W	-7.97	0.00	45.62	5.72
YBR280C	-7.94	0.00	267.88	33.75
YOL081W	-7.93	0.00	82.69	10.43
YNL250W	-7.83	0.00	16.78	2.14
YKL221W	-7.80	0.00	42.81	5.49
YOR227W	-7.79	0.00	112.85	14.49
YMR086W	-7.75	0.00	111.79	14.42
YDR216W	-7.74	0.00	158.85	20.53
YJR039W	-7.71	0.00	54.22	7.03
YIL029W-A	-7.66	0.00	39.22	5.12
YJR038C	-7.66	0.00	34.82	4.54
YKL038W	-7.61	0.00	133.83	17.59
YBL015W	-7.60	0.00	1568.63	206.37
YOR394C-A	-7.60	0.05	8.61	1.13
YIR033W	-7.60	0.00	133.43	17.56
YLR087C	-7.58	0.01	13.44	1.77
YKR076W	-7.57	0.00	339.75	44.87
YDR124W	-7.57	0.00	46.31	6.12
YFL044C	-7.56	0.00	185.88	24.58
YOR386W	-7.50	0.00	38.96	5.19
YIL146C	-7.49	0.00	176.95	23.63
YER021W	-7.48	0.00	406.73	54.37
YLR450W	-7.48	0.00	122.01	16.32
YGL156W	-7.46	0.00	299.80	40.21
YMR302C	-7.45	0.00	291.87	39.19
YGR201C	-7.44	0.00	1027.34	138.04
YCL048W-A	-7.42	0.00	64.72	8.72
YGL074C	-7.38	0.00	115.97	15.72
YPL171C	-7.36	0.00	620.35	84.23
YGR053C	-7.36	0.00	72.93	9.91
YHR202W	-7.35	0.00	94.56	12.87
YGL227W	-7.32	0.00	100.29	13.70
YPL186C	-7.32	0.00	579.18	79.12
YNL237W	-7.30	0.00	103.67	14.21
YAL054C	-7.29	0.00	552.10	75.78
YFL014W	-7.26	0.00	14566.91	2007.21
YLR347W-A	-7.26	0.00	182.86	25.20
YPL196W	-7.23	0.00	297.83	41.22
YNL195C	-7.22	0.00	750.96	104.06
YKL151C	-7.21	0.00	812.01	112.70
YKL187C	-7.20	0.00	464.07	64.44
YMR107W	-7.19	0.00	2743.17	381.26
YGL150C	-7.18	0.00	47.92	6.67
YDL215C	-7.18	0.00	132.68	18.48
YAL056W	-7.18	0.00	102.19	14.24

YBL105C	-7.18	0.00	98.15	13.68
YDL214C	-7.08	0.00	116.73	16.50
YDL149W	-7.07	0.00	61.27	8.67
YMR322C	-7.06	0.00	345.00	48.88
YPR160C-A	-7.05	0.00	464.92	65.90
YJL057C	-7.05	0.00	130.89	18.55
YBR200W-A	-7.05	0.00	48.79	6.92
YDL041W	-7.01	0.00	17.59	2.51
YGR194C	-6.99	0.00	119.53	17.10
YLR047C	-6.99	0.00	46.04	6.59
YHR199C-A	-6.99	0.00	201.69	28.87
YPL185W	-6.99	0.00	91.79	13.14
YKR031C	-6.98	0.00	24.65	3.53
YMR280C	-6.95	0.00	105.25	15.15
YDR371C-A	-6.94	0.02	12.58	1.81
YCR011C	-6.94	0.00	76.28	11.00
YMR219W	-6.93	0.00	37.83	5.46
YNL269W	-6.92	0.00	72.10	10.42
YIR038C	-6.92	0.00	431.56	62.37
YIL125W	-6.91	0.00	685.99	99.23
YOL025W	-6.91	0.00	70.34	10.18
YOL083W	-6.91	0.00	102.63	14.85
YMR114C	-6.91	0.00	363.52	52.62
YJL020C	-6.91	0.00	221.99	32.15
YER079C-A	-6.90	0.00	99.43	14.41
YOL100W	-6.90	0.00	90.34	13.10
YIL097W	-6.90	0.00	110.89	16.08
YIL030C	-6.89	0.00	72.72	10.56
YNL101W	-6.88	0.00	151.11	21.95
YGR256W	-6.88	0.00	679.98	98.85
YMR175W	-6.87	0.00	9128.04	1328.27
YMR304W	-6.85	0.00	71.81	10.48
YDL222C	-6.85	0.00	317.41	46.33
YFL042C	-6.84	0.00	124.22	18.17
YMR058W	-6.83	0.00	218.01	31.91
YMR115W	-6.80	0.00	243.15	35.77
YJL005W	-6.79	0.00	82.88	12.21
YBL059C-A	-6.76	0.00	367.79	54.42
YLR205C	-6.74	0.00	507.78	75.29
YDL169C	-6.73	0.00	514.23	76.39
YOL119C	-6.71	0.00	198.22	29.54
YJL102W	-6.70	0.00	131.53	19.63
YBR241C	-6.68	0.00	329.61	49.31
YJL225W-A	-6.67	0.00	45.57	6.83
YFL036W	-6.65	0.00	87.74	13.19
YDR270W	-6.65	0.00	98.83	14.86

YLL009C	-6.60	0.00	907.67	137.48
YGL062W	-6.60	0.00	651.56	98.76
YLR152C	-6.59	0.00	284.24	43.11
YDR070C	-6.59	0.00	2372.09	360.01
YNR007C	-6.58	0.00	606.15	92.08
YHR188C	-6.57	0.00	166.26	25.30
YPR049C	-6.57	0.00	75.42	11.48
YPL123C	-6.55	0.00	80.28	12.25
YJR033C	-6.55	0.00	22.75	3.47
YDR443C	-6.54	0.00	22.50	3.44
YDL042C	-6.52	0.00	23.27	3.57
YGL094C	-6.51	0.00	50.23	7.71
YKL105C	-6.51	0.00	36.69	5.64
YMR278W	-6.49	0.00	125.10	19.28
YOR124C	-6.48	0.00	57.54	8.87
YAR066W	-6.48	0.04	10.07	1.56
YNL271C	-6.47	0.00	54.26	8.39
YDR403W	-6.45	0.00	57.66	8.94
YPL203W	-6.44	0.00	420.51	65.28
YHR050W-A	-6.43	0.00	329.51	51.21
YIR037W	-6.43	0.00	750.43	116.72
YGL240W	-6.42	0.00	24.89	3.88
YAL016C-B	-6.41	0.00	153.16	23.88
YPL282C	-6.40	0.00	42.69	6.67
YHR017W	-6.40	0.00	240.80	37.64
YOR394W	-6.38	0.00	39.26	6.15
YJR098C	-6.38	0.00	57.27	8.98
YLR203C	-6.37	0.00	397.80	62.48
YAL062W	-6.37	0.00	319.29	50.15
YOR191W	-6.36	0.00	44.40	6.98
YDL067C	-6.34	0.00	4005.20	631.35
YLR206W	-6.34	0.00	327.31	51.64
YPL119C	-6.33	0.00	230.18	36.38
YOL051W	-6.31	0.00	109.64	17.38
YPL092W	-6.31	0.00	87.78	13.92
YCR093W	-6.30	0.00	21.99	3.49
YER080W	-6.30	0.00	148.91	23.64
YLR189C	-6.28	0.00	133.75	21.31
YIR039C	-6.28	0.00	234.37	37.35
YKL147C	-6.27	0.00	186.73	29.78
YBR230W-A	-6.27	0.00	690.82	110.17
YHR102W	-6.27	0.00	128.64	20.52
YOL098C	-6.26	0.00	53.74	8.58
YKR096W	-6.26	0.00	92.75	14.82
YNL052W	-6.26	0.00	3940.37	629.72
YJL185C	-6.25	0.00	139.04	22.23

YFR024C-A	-6.25	0.00	300.81	48.14
YAL048C	-6.24	0.00	27.89	4.47
YLL041C	-6.24	0.00	1526.48	244.54
YOL131W	-6.24	0.00	134.43	21.54
YBR255C-A	-6.24	0.00	224.70	36.01
YLL015W	-6.23	0.00	53.41	8.57
YLR382C	-6.23	0.00	51.55	8.27
YIL045W	-6.23	0.00	325.17	52.23
YBR235W	-6.22	0.00	46.71	7.51
YLR149C	-6.22	0.00	325.36	52.31
YDL197C	-6.21	0.00	109.16	17.57
YKL220C	-6.20	0.03	12.16	1.96
YLR247C	-6.20	0.00	67.13	10.83
YBR059C	-6.20	0.00	111.96	18.06
YIL115C	-6.19	0.00	31.55	5.10
YEL030W	-6.18	0.00	38.48	6.23
YEL065W	-6.18	0.00	21.60	3.50
YIL155C	-6.17	0.00	624.35	101.23
YOR192C	-6.17	0.01	14.78	2.40
YGL173C	-6.16	0.00	106.87	17.36
YAL001C	-6.15	0.00	34.83	5.67
YLR290C	-6.14	0.00	102.32	16.66
YBL066C	-6.13	0.00	74.67	12.19
YMR012W	-6.11	0.00	58.88	9.63
YBR221C	-6.11	0.00	542.45	88.75
YLR255C	-6.11	0.00	27.36	4.48
YIL017C	-6.10	0.00	73.10	11.97
YLR371W	-6.09	0.00	35.90	5.89
YFR040W	-6.09	0.00	224.19	36.84
YJL077W-A	-6.09	0.00	221.91	36.47
YIL137C	-6.08	0.00	45.51	7.48
YMR306C-A	-6.07	0.00	47.41	7.81
YFL007W	-6.07	0.00	58.45	9.63
YLR312C	-6.06	0.00	320.79	52.90
YMR257C	-6.06	0.00	36.82	6.07
YIL136W	-6.06	0.00	1638.04	270.34
YGL192W	-6.06	0.00	59.89	9.89
YBR212W	-6.05	0.00	207.69	34.35
YLR115W	-6.04	0.00	29.71	4.92
YGL059W	-6.03	0.00	76.78	12.72
YOL060C	-6.03	0.00	248.35	41.16
YPR151C	-6.03	0.00	402.13	66.72
YJR005C-A	-6.02	0.00	51.51	8.55
YDR457W	-6.02	0.00	38.55	6.40
YPR115W	-6.02	0.00	97.83	16.25
YLR266C	-6.01	0.00	39.86	6.63
YOL099C	-6.00	0.00	219.72	36.63

YHR109W	-6.00	0.00	21.21	3.54
YMR190C	-6.00	0.00	45.37	7.57
YBR179C	-5.99	0.00	130.01	21.69
YJR149W	-5.99	0.00	72.57	12.12
YPL262W	-5.97	0.00	688.20	115.23
YJR049C	-5.97	0.00	209.78	35.13
YLR345W	-5.96	0.00	299.23	50.22
YBR140C	-5.95	0.00	21.21	3.56
YGL093W	-5.95	0.00	120.52	20.25
YFL067W	-5.95	0.00	161.62	27.16
YDR168W	-5.95	0.00	213.72	35.92
YDR269C	-5.95	0.00	64.05	10.77
YPR150W	-5.94	0.00	503.82	84.85
YKL121W	-5.93	0.00	37.65	6.35
YIR006C	-5.93	0.00	98.23	16.57
YLR422W	-5.91	0.00	28.60	4.84
YPR097W	-5.90	0.00	38.37	6.50
YHR080C	-5.89	0.00	63.70	10.81
YDL091C	-5.89	0.00	90.15	15.31
YJR151C	-5.88	0.03	11.78	2.00
YDL043C	-5.87	0.00	34.39	5.86
YPL111W	-5.86	0.00	152.20	25.96
YOL117W	-5.86	0.01	17.07	2.91
YAL047W-A	-5.85	0.04	11.24	1.92
YML035C	-5.84	0.00	74.98	12.83
YGL141W	-5.82	0.00	72.53	12.47
YLR038C	-5.82	0.00	1470.11	252.80
YLR386W	-5.81	0.00	34.88	6.00
YPL257W	-5.80	0.00	20.85	3.60
YDL147W	-5.80	0.00	581.63	100.35
YLR347C	-5.79	0.00	122.20	21.10
YHR195W	-5.79	0.00	354.02	61.15
YLL005C	-5.79	0.00	24.51	4.24
YLR425W	-5.78	0.00	21.20	3.67
YCL012C	-5.78	0.00	560.08	96.98
YHR008C	-5.77	0.00	1078.04	186.74
YDR504C	-5.77	0.00	85.81	14.87
YHR082C	-5.77	0.00	221.22	38.34
YGR289C	-5.76	0.00	632.57	109.73
YMR090W	-5.76	0.00	1339.93	232.57
YHL032C	-5.75	0.00	240.83	41.85
YNL200C	-5.75	0.00	673.93	117.14
YOR354C	-5.75	0.00	90.50	15.75
YNL242W	-5.75	0.00	39.67	6.90
YPL201C	-5.75	0.00	215.43	37.49
YFR010W	-5.74	0.00	158.94	27.71
YDR128W	-5.73	0.00	32.71	5.71

YCR033W	-5.73	0.00	78.76	13.76
YBL100C	-5.72	0.00	390.90	68.29
YOL067C	-5.72	0.00	179.36	31.37
YMR174C	-5.71	0.00	3381.31	591.92
YDR494W	-5.70	0.00	254.56	44.64
YLL040C	-5.70	0.00	31.59	5.54
YJR150C	-5.70	0.03	12.90	2.26
YPL166W	-5.70	0.00	81.11	14.23
YKL157W	-5.70	0.00	168.80	29.63
YMR086C-A	-5.69	0.00	108.71	19.09
YOR211C	-5.69	0.00	74.87	13.17
YBR117C	-5.68	0.00	348.68	61.34
YBL113C	-5.67	0.00	37.83	6.67
YOL075C	-5.66	0.01	17.74	3.14
YDR330W	-5.66	0.00	221.63	39.18
YMR152W	-5.65	0.00	138.49	24.50
YPR185W	-5.65	0.00	47.23	8.36
YKL146W	-5.64	0.00	306.99	54.42
YMR110C	-5.64	0.00	398.72	70.75
YLR356W	-5.63	0.00	402.10	71.36
YEL011W	-5.63	0.00	789.11	140.20
YGR231C	-5.63	0.00	595.57	105.82
YDL132W	-5.62	0.00	76.94	13.69
YDR028C	-5.61	0.00	195.72	34.88
YLR389C	-5.60	0.00	53.81	9.61
YJR066W	-5.59	0.00	20.18	3.61
YER008C	-5.58	0.00	30.65	5.49
YKR049C	-5.57	0.00	881.04	158.16
YOR290C	-5.57	0.00	56.40	10.13
YGR226C	-5.57	0.00	65.58	11.78
YPL222W	-5.56	0.00	252.80	45.43
YPR140W	-5.56	0.00	121.82	21.93
YKR015C	-5.55	0.00	21.26	3.83
YFL055W	-5.54	0.00	33.97	6.13
YLR035C	-5.54	0.00	46.11	8.33
YMR317W	-5.53	0.00	36.27	6.56
YBR024W	-5.53	0.00	134.66	24.37
YNL270C	-5.52	0.00	73.88	13.38
YDL094C	-5.52	0.00	30.21	5.47
YDR442W	-5.52	0.00	65.93	11.95
YKL134C	-5.52	0.00	37.59	6.81
YOR377W	-5.51	0.00	100.39	18.22
YMR275C	-5.50	0.00	79.21	14.40
YER141W	-5.50	0.00	715.26	130.16
YDL027C	-5.49	0.00	93.26	16.98
YLR241W	-5.49	0.00	85.72	15.61
YGR225W	-5.48	0.00	27.70	5.06

YOL087C	-5.48	0.00	54.24	9.90
YGR111W	-5.48	0.00	140.36	25.63
YDR031W	-5.47	0.00	265.64	48.54
YKL141W	-5.47	0.00	710.61	129.88
YER142C	-5.47	0.00	235.31	43.01
YJR161C	-5.46	0.00	36.41	6.66
YMR170C	-5.45	0.00	186.97	34.29
YOR008W-B	-5.45	0.02	13.56	2.49
YNL274C	-5.45	0.00	584.14	107.20
YDR420W	-5.45	0.01	16.54	3.04
YIL075C	-5.44	0.00	387.38	71.26
YDR271C	-5.43	0.00	139.97	25.76
YDL194W	-5.43	0.00	67.74	12.48
YEL012W	-5.43	0.00	1022.75	188.52
YBR139W	-5.42	0.00	252.66	46.58
YLR299W	-5.42	0.00	192.28	35.49
YLR069C	-5.42	0.00	132.13	24.40
YGL104C	-5.41	0.00	36.63	6.78
YHR189W	-5.40	0.00	90.32	16.72
YJL205C	-5.40	0.00	207.29	38.38
YGR209C	-5.40	0.00	2144.55	397.23
YER133W	-5.39	0.00	532.16	98.79
YFR016C	-5.38	0.00	56.11	10.42
YBR064W	-5.38	0.00	81.21	15.09
YJL066C	-5.38	0.00	909.09	168.96
YBR300C	-5.38	0.00	40.41	7.52
YNR051C	-5.37	0.00	83.28	15.49
YKL150W	-5.37	0.00	1062.30	197.76
YDR099W	-5.37	0.00	881.57	164.11
YGL055W	-5.37	0.00	5512.85	1026.42
YOR014W	-5.37	0.00	173.45	32.31
YGL014C-A	-5.36	0.00	46.19	8.62
YEL077C	-5.35	0.00	33.85	6.32
YDR230W	-5.35	0.00	602.12	112.50
YCL057W	-5.35	0.00	149.88	28.03
YHR096C	-5.34	0.00	377.11	70.59
YMR159C	-5.34	0.00	30.68	5.74
YIL072W	-5.34	0.00	21.07	3.94
YGR274C	-5.33	0.00	59.90	11.24
YJL206C	-5.33	0.00	22.87	4.29
YNL054W	-5.33	0.00	41.46	7.78
YBL113W-A	-5.33	0.00	63.67	11.95
YLR133W	-5.32	0.00	119.27	22.42
YMR100W	-5.30	0.00	90.70	17.10
YER178W	-5.30	0.00	790.54	149.06
YGR032W	-5.30	0.00	245.81	46.37

YDR014W-A	-5.30	0.00	47.45	8.95
YDR293C	-5.29	0.00	278.71	52.67
YIL115W-A	-5.29	0.00	120.03	22.69
YJR126C	-5.29	0.00	94.61	17.89
YER182W	-5.28	0.00	355.85	67.34
YDR104C	-5.28	0.03	13.36	2.53
YGL160W	-5.28	0.00	61.42	11.63
YLR267W	-5.26	0.00	110.24	20.97
YOL004W	-5.25	0.00	60.66	11.55
YJL067W	-5.24	0.00	998.67	190.54
YGL136C	-5.24	0.00	71.12	13.57
YDR204W	-5.23	0.00	167.95	32.10
YAL031C	-5.22	0.00	63.85	12.23
YPL194W	-5.22	0.00	26.30	5.04
YKR016W	-5.21	0.00	200.21	38.39
YPR081C	-5.21	0.00	29.56	5.67
YGR258C	-5.21	0.00	56.49	10.84
YDR436W	-5.21	0.00	108.17	20.76
YER033C	-5.20	0.00	68.82	13.24
YHR028C	-5.20	0.00	149.14	28.69
YGL180W	-5.19	0.00	96.83	18.65
YLR295C	-5.19	0.00	998.48	192.39
YOL050C	-5.18	0.00	150.46	29.06
YDR015C	-5.18	0.00	49.26	9.52
YOR055W	-5.18	0.00	135.89	26.26
YMR158W-B	-5.18	0.00	27.62	5.34
YJL095W	-5.17	0.01	18.43	3.56
YDL231C	-5.17	0.00	40.53	7.83
YOL063C	-5.17	0.00	31.97	6.18
YEL025C	-5.16	0.01	17.54	3.40
YNR033W	-5.16	0.00	110.34	21.39
YAL016C-A	-5.15	0.00	124.38	24.17
YER162C	-5.15	0.00	139.38	27.09
YLR163W-A	-5.14	0.00	168.80	32.84
YJR090C	-5.14	0.00	41.89	8.15
YJL101C	-5.14	0.00	252.47	49.15
YDL019C	-5.14	0.00	123.26	24.00
YDL185W	-5.12	0.00	289.19	56.45
YPL022W	-5.12	0.00	48.49	9.47
YDR477W	-5.11	0.00	129.34	25.29
YAL028W	-5.11	0.00	67.64	13.23
YIL087C	-5.10	0.00	326.11	63.99
YMR193W	-5.09	0.00	130.63	25.64
YGR218W	-5.09	0.00	125.19	24.58
YHR199C	-5.09	0.00	852.04	167.37
YJR035W	-5.09	0.00	27.24	5.36

YER155C	-5.08	0.00	28.62	5.63
YML091C	-5.08	0.00	96.43	18.97
YOL071W	-5.08	0.00	282.54	55.67
YKR050W	-5.06	0.00	30.52	6.04
YGL238W	-5.06	0.00	41.73	8.25
YFR019W	-5.04	0.01	20.17	4.00
YDR186C	-5.03	0.00	270.48	53.79
YNL118C	-5.02	0.00	76.25	15.18
YIL129C	-5.02	0.00	22.69	4.52
YKR058W	-5.02	0.00	167.26	33.32
YML110C	-5.02	0.00	423.06	84.33
YDR282C	-5.02	0.00	62.63	12.49
YML013W	-5.01	0.00	93.06	18.58
YNL127W	-5.01	0.00	48.49	9.69
YAL008W	-5.00	0.00	208.46	41.66
YLR248W	-5.00	0.00	492.56	98.55
YGR183C	-4.99	0.00	5396.70	1080.59
YKL171W	-4.99	0.00	147.41	29.55
YNL100W	-4.99	0.00	401.58	80.55
YNL321W	-4.98	0.00	75.46	15.15
YOR031W	-4.98	0.00	6959.19	1398.37
YLR165C	-4.98	0.00	38.80	7.80
YPL195W	-4.98	0.00	39.70	7.98
YLR309C	-4.97	0.00	45.21	9.09
YDR515W	-4.97	0.00	56.34	11.33
YJL197W	-4.97	0.01	21.20	4.26
YER172C	-4.97	0.03	13.59	2.74
YPR193C	-4.97	0.00	64.22	12.93
YDR358W	-4.97	0.00	130.81	26.34
YKR095W	-4.96	0.00	32.57	6.56
YBL001C	-4.96	0.00	395.89	79.77
YPL268W	-4.96	0.00	39.64	8.00
YLR199C	-4.96	0.00	72.27	14.58
YKL020C	-4.95	0.00	101.85	20.56
YDR298C	-4.95	0.00	665.09	134.45
YKL197C	-4.94	0.00	22.43	4.54
YPL214C	-4.94	0.00	67.81	13.72
YDR125C	-4.94	0.00	30.38	6.15
YDR335W	-4.94	0.00	97.49	19.74
YDR079W	-4.94	0.00	331.84	67.23
YOL096C	-4.93	0.00	62.02	12.57
YLL025W	-4.93	0.00	36.73	7.45
YOL083C-A	-4.93	0.00	170.82	34.65
YNL073W	-4.93	0.00	220.59	44.76
YHR161C	-4.93	0.00	228.94	46.48
YNL137C	-4.93	0.00	135.63	27.54
YDR089W	-4.92	0.00	29.32	5.96

YML029W	-4.92	0.00	29.28	5.95
YPL013C	-4.92	0.00	387.29	78.71
YER115C	-4.92	0.00	120.32	24.46
YDR231C	-4.91	0.00	548.79	111.71
YGL217C	-4.91	0.01	19.12	3.90
YKL168C	-4.91	0.00	32.35	6.59
YPR098C	-4.91	0.00	154.37	31.47
YLR395C	-4.90	0.00	2110.30	430.25
YLR440C	-4.90	0.00	31.27	6.38
YLR102C	-4.90	0.00	111.12	22.66
YFL041W	-4.90	0.00	150.10	30.62
YLR430W	-4.90	0.02	15.33	3.13
YDL195W	-4.89	0.00	84.79	17.33
YBR286W	-4.89	0.00	517.94	105.95
YOR082C	-4.89	0.00	26.29	5.38
YOL113W	-4.89	0.00	140.38	28.73
YLR207W	-4.88	0.00	43.71	8.95
YER129W	-4.88	0.00	34.94	7.16
YBR039W	-4.88	0.00	1119.27	229.47
YGR101W	-4.87	0.00	109.64	22.49
YFL025C	-4.87	0.01	20.51	4.21
YPR095C	-4.87	0.00	24.19	4.96
YGR157W	-4.87	0.00	204.76	42.06
YHR103W	-4.87	0.00	121.06	24.87
YGR127W	-4.87	0.00	275.52	56.63
YPL167C	-4.86	0.04	12.72	2.61
YCR097W	-4.86	0.00	85.00	17.49
YPR061C	-4.86	0.00	331.44	68.21
YJR036C	-4.86	0.00	28.31	5.83
YIL162W	-4.86	0.00	430.02	88.53
YCL052C	-4.86	0.00	229.03	47.17
YDR456W	-4.85	0.00	83.72	17.25
YLR125W	-4.85	0.00	49.42	10.19
YMR029C	-4.85	0.00	60.09	12.39
YAR019C	-4.85	0.00	41.02	8.46
YNL267W	-4.85	0.00	41.49	8.56
YGR088W	-4.84	0.00	666.59	137.69
YOR117W	-4.83	0.00	402.38	83.24
YML007W	-4.83	0.00	274.18	56.73
YPL247C	-4.83	0.00	243.19	50.33
YPL109C	-4.83	0.02	15.99	3.31
YAL031W-A	-4.82	0.00	106.85	22.18
YBR137W	-4.81	0.00	218.59	45.47
YKL195W	-4.80	0.00	363.94	75.76
YMR201C	-4.80	0.00	141.16	29.40
YBL017C	-4.80	0.00	56.28	11.73
YPR010C-A	-4.80	0.00	2021.29	421.28

YAL016W	-4.80	0.00	187.64	39.11
YGR292W	-4.80	0.00	364.42	76.00
YHR106W	-4.79	0.00	144.48	30.15
YPR020W	-4.79	0.00	345.70	72.20
YMR098C	-4.79	0.00	72.97	15.25
YHR198C	-4.78	0.00	123.82	25.88
YDR287W	-4.78	0.00	168.84	35.30
YLR240W	-4.78	0.00	35.54	7.44
YBL047C	-4.77	0.00	91.96	19.27
YOR007C	-4.77	0.00	1582.44	331.59
YML087C	-4.77	0.00	142.78	29.94
YGL013C	-4.76	0.00	55.40	11.63
YHR078W	-4.76	0.00	103.67	21.80
YLR178C	-4.75	0.00	1615.15	339.76
YIL177W-A	-4.75	0.00	45.57	9.59
YMR004W	-4.75	0.00	131.30	27.64
YOL036W	-4.75	0.00	250.42	52.71
YOR081C	-4.75	0.00	31.75	6.68
YLR070C	-4.75	0.00	51.20	10.78
YDR150W	-4.74	0.00	91.89	19.37
YDL140C	-4.74	0.00	104.00	21.96
YDR310C	-4.74	0.00	34.96	7.38
YGL163C	-4.73	0.00	162.20	34.26
YCR032W	-4.73	0.02	15.01	3.17
YBL107C	-4.73	0.00	228.14	48.21
YFR010W-A	-4.73	0.00	190.66	40.29
YDR381C-A	-4.73	0.00	236.60	50.03
YDL100C	-4.73	0.00	313.02	66.19
YDR203W	-4.73	0.00	85.83	18.16
YJR091C	-4.72	0.00	129.31	27.37
YHR211W	-4.72	0.01	19.13	4.05
YCL057C-A	-4.72	0.00	857.53	181.72
YKL210W	-4.72	0.00	116.65	24.72
YLR427W	-4.72	0.00	102.62	21.75
YJL129C	-4.72	0.00	43.99	9.33
YFL061W	-4.72	0.00	23.84	5.05
YHR193C-A	-4.71	0.00	35.89	7.61
YGL048C	-4.71	0.00	646.79	137.27
YOL065C	-4.71	0.00	31.31	6.65
YJR135W-A	-4.71	0.00	122.20	25.96
YJR077C	-4.70	0.00	1438.20	305.74
YMR075W	-4.70	0.00	37.58	8.00
YDR022C	-4.70	0.00	120.03	25.55
YNL026W	-4.70	0.00	43.22	9.20
YLR013W	-4.69	0.00	23.77	5.06
YGR132C	-4.69	0.00	636.88	135.94
YHR027C	-4.68	0.00	283.08	60.45

YJL092W	-4.68	0.00	37.48	8.01
YPL190C	-4.68	0.00	207.98	44.46
YLL013C	-4.68	0.00	60.36	12.91
YDL078C	-4.67	0.00	548.68	117.37
YER079W	-4.67	0.00	298.94	63.95
YPR091C	-4.67	0.00	58.78	12.59
YNL071W	-4.67	0.00	425.93	91.26
YLR324W	-4.67	0.00	199.46	42.75
YOR120W	-4.67	0.00	421.52	90.35
YAL049C	-4.67	0.00	190.95	40.93
YMR176W	-4.66	0.00	31.00	6.65
YLR201C	-4.66	0.00	101.20	21.72
YPL078C	-4.66	0.00	1519.30	326.24
YJL031C	-4.66	0.00	97.27	20.89
YIL157C	-4.65	0.00	265.52	57.04
YGL073W	-4.65	0.00	153.87	33.07
YLL032C	-4.65	0.01	20.12	4.33
YIL033C	-4.65	0.00	490.83	105.55
YKL050C	-4.65	0.01	20.12	4.33
YMR297W	-4.64	0.00	888.76	191.35
YHR171W	-4.64	0.00	49.96	10.76
YHR016C	-4.64	0.00	417.50	89.92
YOL164W-A	-4.64	0.00	30.58	6.59
YLR362W	-4.64	0.00	88.55	19.09
YOR185C	-4.64	0.00	442.58	95.42
YDL089W	-4.63	0.00	72.96	15.74
YER143W	-4.63	0.00	226.19	48.81
YER119C	-4.63	0.00	150.75	32.55
YLR090W	-4.63	0.00	140.72	30.39
YDR463W	-4.63	0.00	298.11	64.39
YDL097C	-4.63	0.00	620.77	134.10
YDR316W	-4.63	0.00	90.42	19.54
YOR371C	-4.63	0.02	17.11	3.70
YMR196W	-4.63	0.00	181.42	39.21
YCL041C	-4.63	0.02	16.01	3.46
YHL024W	-4.62	0.00	158.60	34.30
YMR261C	-4.61	0.00	82.90	17.96
YDL126C	-4.61	0.00	848.42	183.91
YDL190C	-4.61	0.00	37.31	8.09
YBR274W	-4.61	0.00	48.16	10.46
YDR262W	-4.60	0.00	781.06	169.67
YOR165W	-4.60	0.00	61.00	13.26
YMR075C-A	-4.60	0.00	62.20	13.52
YBR218C	-4.59	0.00	73.24	15.94
YLR305C	-4.59	0.03	13.79	3.00
YCL004W	-4.59	0.00	38.67	8.43
YKL148C	-4.59	0.00	973.36	212.14

YAL064W-B	-4.59	0.00	41.26	8.99
YNR060W	-4.59	0.00	24.25	5.29
YNL331C	-4.59	0.00	42.70	9.31
YPR028W	-4.58	0.00	280.15	61.12
YBR225W	-4.58	0.00	69.08	15.07
YOR173W	-4.58	0.00	1059.54	231.29
YHR051W	-4.58	0.00	947.67	207.11
YDR159W	-4.57	0.01	18.05	3.95
YER078C	-4.57	0.00	71.20	15.57
YER114C	-4.57	0.00	52.36	11.46
YHR021W-A	-4.57	0.03	14.62	3.20
YPR092W	-4.57	0.01	21.78	4.77
YLR390W	-4.56	0.00	167.33	36.69
YDR059C	-4.56	0.00	425.86	93.40
YJL164C	-4.55	0.00	181.29	39.80
YKL140W	-4.55	0.00	36.31	7.97
YDR357C	-4.55	0.00	96.29	21.15
YDL058W	-4.55	0.03	14.14	3.11
YKL064W	-4.55	0.00	145.18	31.92
YCR049C	-4.55	0.00	84.55	18.60
YPL084W	-4.55	0.00	65.19	14.34
YML034W	-4.55	0.00	172.24	37.89
YDL095W	-4.54	0.00	151.58	33.36
YIL031W	-4.54	0.00	58.35	12.85
YJL068C	-4.54	0.00	224.16	49.42
YJR057W	-4.53	0.00	117.37	25.93
YNL045W	-4.53	0.00	40.74	9.00
YMR213W	-4.52	0.00	90.20	19.93
YPR160W	-4.52	0.00	533.60	117.96
YLR097C	-4.52	0.00	81.18	17.96
YPL150W	-4.52	0.00	55.19	12.22
YHR158C	-4.52	0.00	26.90	5.95
YDR255C	-4.52	0.00	112.06	24.81
YFR052W	-4.52	0.00	281.66	62.38
YNL315C	-4.51	0.00	141.28	31.30
YML004C	-4.51	0.00	1114.34	247.08
YDR426C	-4.51	0.00	77.19	17.12
YGR112W	-4.51	0.00	53.05	11.77
YGR276C	-4.50	0.00	75.49	16.76
YMR272W-B	-4.50	0.00	63.47	14.10
YEL013W	-4.50	0.00	51.27	11.40
YGR043C	-4.50	0.00	1037.32	230.70
YLR289W	-4.50	0.00	34.59	7.69
YPR127W	-4.49	0.00	518.42	115.35
YMR067C	-4.49	0.00	80.68	17.96
YML034C-A	-4.49	0.00	107.18	23.85

YDR422C	-4.49	0.00	58.11	12.93
YDR511W	-4.49	0.00	195.70	43.56
YER087W	-4.49	0.00	25.69	5.72
YEL005C	-4.49	0.00	46.29	10.31
YHL030W	-4.49	0.01	23.06	5.14
YJR034W	-4.49	0.00	127.12	28.33
YFR034C	-4.49	0.00	196.70	43.86
YBR128C	-4.48	0.01	23.09	5.15
YJR121W	-4.48	0.00	1991.95	444.33
YDR119W-A	-4.48	0.00	1734.87	387.03
YML086C	-4.48	0.00	63.64	14.21
YKR067W	-4.48	0.00	89.88	20.07
YJL046W	-4.47	0.00	54.71	12.23
YKL068W	-4.47	0.00	43.65	9.76
YOR018W	-4.47	0.00	32.72	7.32
YPR022C	-4.47	0.00	43.68	9.77
YNL085W	-4.47	0.00	43.89	9.82
YNR045W	-4.47	0.00	129.58	29.01
YDL245C	-4.46	0.00	25.43	5.70
YHL038C	-4.45	0.00	26.58	5.97
YDR314C	-4.45	0.03	14.25	3.20
YOR048C	-4.44	0.00	95.22	21.42
YJR152W	-4.44	0.00	26.94	6.07
YKR055W	-4.44	0.00	69.13	15.57
YML076C	-4.44	0.00	38.84	8.75
YEL052W	-4.44	0.00	100.99	22.77
YBL099W	-4.44	0.00	693.95	156.46
YDR178W	-4.43	0.00	1061.25	239.52
YAR007C	-4.43	0.00	69.73	15.74
YGR270W	-4.43	0.00	79.60	17.98
YOR366W	-4.43	0.05	11.90	2.69
YGR184C	-4.42	0.00	58.13	13.14
YBR063C	-4.42	0.00	123.70	27.99
YOR245C	-4.42	0.00	142.98	32.36
YCL049C	-4.42	0.00	263.94	59.74
YGL197W	-4.42	0.00	45.59	10.32
YOR175C	-4.42	0.00	75.80	17.16
YER093C	-4.42	0.00	24.16	5.47
YPR108W	-4.42	0.00	231.80	52.48
YLR157W-D	-4.41	0.03	14.47	3.28
YMR155W	-4.41	0.00	69.66	15.79
YGL121C	-4.41	0.00	1438.81	326.42
YHR155W	-4.41	0.03	15.47	3.51
YML078W	-4.41	0.00	508.25	115.35
YPL271W	-4.40	0.00	3335.67	757.74
YGL233W	-4.40	0.01	21.56	4.90

YDR112W	-4.40	0.01	22.59	5.13
YMR319C	-4.40	0.00	146.55	33.31
YFL050C	-4.40	0.00	86.51	19.67
YOR231C-A	-4.40	0.00	54.13	12.31
YPL217C	-4.39	0.00	34.36	7.82
YFL027C	-4.39	0.03	14.35	3.27
YDR030C	-4.39	0.00	65.00	14.81
YDR427W	-4.39	0.00	158.71	36.18
YGL140C	-4.39	0.00	42.96	9.80
YBL064C	-4.38	0.00	1078.44	245.98
YMR316C-B	-4.38	0.00	70.21	16.02
YMR284W	-4.38	0.00	24.75	5.65
YEL039C	-4.38	0.00	7395.29	1687.80
YMR140W	-4.38	0.00	160.55	36.65
YFL004W	-4.38	0.00	68.27	15.59
YGL107C	-4.37	0.00	63.76	14.58
YMR258C	-4.37	0.00	58.76	13.44
YJL077W-B	-4.37	0.00	226.77	51.92
YBL058W	-4.37	0.00	464.48	106.35
YLR423C	-4.37	0.00	36.01	8.25
YHR194W	-4.36	0.00	40.73	9.34
YNR022C	-4.36	0.00	209.47	48.04
YDR227W	-4.36	0.02	16.49	3.78
YKR014C	-4.36	0.00	745.01	170.92
YMR119W	-4.36	0.00	39.68	9.10
YOR098C	-4.35	0.00	92.86	21.33
YDL007W	-4.35	0.00	475.82	109.33
YER101C	-4.35	0.00	74.32	17.08
YIL046W-A	-4.35	0.00	30.11	6.92
YHR147C	-4.35	0.00	132.21	30.40
YOR350C	-4.35	0.00	28.67	6.59
YAR042W	-4.34	0.00	75.74	17.45
YLL054C	-4.34	0.02	17.29	3.98
YFL033C	-4.34	0.02	16.26	3.75
YPR172W	-4.33	0.00	126.71	29.25
YPR202W	-4.33	0.01	20.70	4.78
YGL259W	-4.32	0.00	48.49	11.21
YKL176C	-4.32	0.00	73.58	17.02
YER134C	-4.32	0.00	162.90	37.69
YBR272C	-4.32	0.00	64.02	14.82
YLR270W	-4.32	0.00	523.52	121.24
YIL014W	-4.31	0.00	27.04	6.27
YHR215W	-4.31	0.03	15.01	3.48
YHL021C	-4.31	0.00	853.70	198.07
YBR062C	-4.31	0.00	218.43	50.72
YGL084C	-4.31	0.00	40.43	9.39
YOR118W	-4.30	0.00	57.68	13.41

YAL035W	-4.30	0.00	107.38	24.97
YMR063W	-4.30	0.01	23.50	5.46
YHR074W	-4.30	0.00	81.91	19.05
YNL023C	-4.29	0.00	65.99	15.37
YDR197W	-4.29	0.00	39.34	9.17
YGR186W	-4.29	0.00	176.64	41.15
YDR495C	-4.29	0.01	23.05	5.37
YPR083W	-4.29	0.00	28.48	6.64
YDL066W	-4.29	0.00	406.10	94.66
YHR190W	-4.28	0.00	378.55	88.36
YPR101W	-4.28	0.00	166.75	38.94
YOR261C	-4.28	0.00	296.87	69.38
YNL211C	-4.27	0.00	66.50	15.56
YNL287W	-4.27	0.00	80.36	18.80
YMR097C	-4.27	0.00	116.66	27.30
YDL243C	-4.27	0.00	47.07	11.02
YOR059C	-4.27	0.00	228.45	53.56
YLR383W	-4.27	0.03	15.45	3.62
YMR244C-A	-4.26	0.00	349.57	81.98
YLR001C	-4.26	0.00	65.29	15.32
YOR329C	-4.26	0.00	79.72	18.70
YDL056W	-4.26	0.01	22.70	5.33
YPR001W	-4.26	0.00	28.67	6.73
YPR026W	-4.25	0.00	117.89	27.71
YBL007C	-4.25	0.00	95.89	22.56
YLL048C	-4.25	0.01	19.73	4.65
YJL056C	-4.24	0.00	54.92	12.94
YDL054C	-4.24	0.00	162.32	38.26
YIR002C	-4.24	0.00	45.38	10.70
YBR226C	-4.24	0.00	89.66	21.15
YDR505C	-4.24	0.00	152.31	35.95
YGL139W	-4.24	0.00	46.65	11.01
YPL249C	-4.24	0.00	38.04	8.98
YIL143C	-4.23	0.00	182.92	43.20
YIL159W	-4.23	0.04	13.79	3.26
YJL047C	-4.23	0.02	18.58	4.39
YLL001W	-4.23	0.00	78.43	18.56
YFR011C	-4.22	0.00	118.05	27.95
YOR160W	-4.22	0.02	18.33	4.35
YNL171C	-4.22	0.00	39.88	9.46
YOR382W	-4.22	0.00	1823.86	432.63
YKL005C	-4.22	0.00	84.52	20.05
YKL222C	-4.21	0.02	18.56	4.40
YKL182W	-4.21	0.00	169.17	40.15
YHR205W	-4.21	0.00	134.36	31.89
YOR330C	-4.21	0.00	28.40	6.74
YEL053C	-4.21	0.02	16.99	4.03

YDR425W	-4.21	0.00	41.66	9.90
YPL040C	-4.21	0.00	27.15	6.45
YFR050C	-4.21	0.00	515.58	122.55
YIL156W	-4.21	0.01	21.16	5.03
YGR100W	-4.20	0.00	46.53	11.08
YPL140C	-4.20	0.00	90.05	21.44
YMR286W	-4.19	0.00	490.08	116.94
YLL003W	-4.19	0.00	33.09	7.91
YMR182W-A	-4.18	0.00	137.34	32.82
YKL196C	-4.18	0.00	573.18	137.01
YOR383C	-4.18	0.00	2395.33	573.03
YML010W	-4.18	0.00	114.78	27.47
YER175C	-4.18	0.00	87.48	20.94
YMR081C	-4.18	0.00	334.28	80.05
YJL141C	-4.18	0.00	279.49	66.93
YDR513W	-4.17	0.00	515.03	123.53
YIL005W	-4.17	0.00	71.82	17.23
YIL156W-A	-4.17	0.00	94.02	22.57
YDL004W	-4.17	0.00	1063.74	255.39
YLR394W	-4.16	0.00	42.49	10.20
YDR160W	-4.16	0.00	37.77	9.08
YER014W	-4.16	0.00	58.85	14.14
YPL270W	-4.16	0.00	99.61	23.94
YGR248W	-4.16	0.00	758.41	182.43
YKL213C	-4.16	0.00	81.04	19.50
YBR204C	-4.16	0.00	199.42	47.98
YBR046C	-4.15	0.00	238.72	57.45
YDL176W	-4.15	0.00	60.58	14.59
YLR127C	-4.15	0.01	24.57	5.92
YGL228W	-4.15	0.00	216.66	52.22
YIR003W	-4.15	0.00	120.01	28.93
YNL088W	-4.14	0.01	23.25	5.61
YOR075W	-4.14	0.00	120.76	29.14
YLR398C	-4.14	0.01	23.81	5.75
YJR155W	-4.14	0.00	203.97	49.25
YDR196C	-4.14	0.00	111.39	26.92
YKL016C	-4.14	0.00	786.39	190.12
YMR208W	-4.14	0.00	74.27	17.96
YLR176C	-4.13	0.00	30.75	7.45
YNL294C	-4.12	0.00	142.61	34.58
YDL210W	-4.12	0.01	23.93	5.81
YLR071C	-4.12	0.00	37.43	9.08
YIL147C	-4.12	0.01	21.41	5.20
YNL139C	-4.12	0.00	28.90	7.01
YER088C	-4.12	0.00	301.06	73.10
YNL091W	-4.11	0.00	74.59	18.13

YDR237W	-4.11	0.00	109.18	26.56
YMR256C	-4.11	0.00	2976.99	724.68
YGL218W	-4.10	0.00	202.38	49.32
YNL015W	-4.10	0.00	2200.22	536.29
YPR042C	-4.10	0.01	24.49	5.98
YNL012W	-4.09	0.00	36.58	8.94
YLL049W	-4.09	0.00	69.76	17.04
YGR293C	-4.09	0.02	17.42	4.26
YLR119W	-4.09	0.00	50.54	12.35
YBL063W	-4.09	0.04	14.78	3.61
YJL077C	-4.09	0.00	114.66	28.04
YOL037C	-4.09	0.00	125.24	30.65
YCR068W	-4.08	0.00	96.00	23.51
YDR530C	-4.08	0.00	162.68	39.84
YJR103W	-4.08	0.00	228.59	56.00
YGR193C	-4.08	0.00	117.56	28.82
YDR288W	-4.08	0.00	82.26	20.18
YDR430C	-4.08	0.00	35.28	8.65
YMR168C	-4.07	0.00	29.71	7.29
YAR035C-A	-4.07	0.00	89.28	21.93
YJL212C	-4.07	0.00	37.55	9.23
YJR115W	-4.07	0.00	980.54	241.00
YKR009C	-4.07	0.00	179.87	44.23
YCL014W	-4.06	0.01	21.85	5.37
YDR111C	-4.06	0.00	38.75	9.53
YKL054C	-4.06	0.00	215.41	53.01
YOR328W	-4.06	0.00	48.70	11.99
YMR287C	-4.06	0.02	19.04	4.69
YDR369C	-4.06	0.02	18.07	4.45
YBR047W	-4.05	0.01	21.44	5.29
YER151C	-4.05	0.00	122.38	30.19
YKL053C-A	-4.05	0.00	403.10	99.43
YBR269C	-4.05	0.00	584.08	144.10
YDR466W	-4.05	0.00	35.19	8.68
YNL252C	-4.05	0.00	116.93	28.88
YCL025C	-4.05	0.00	77.63	19.18
YEL031W	-4.05	0.00	78.95	19.52
YBR123C	-4.05	0.00	38.70	9.57
YGL206C	-4.04	0.00	47.94	11.88
YKL015W	-4.03	0.00	44.64	11.07
YDL028C	-4.03	0.00	55.95	13.88
YMR279C	-4.03	0.03	16.55	4.11
YDL142C	-4.03	0.00	32.99	8.19
YPL015C	-4.03	0.00	243.35	60.44
YIL070C	-4.02	0.00	180.73	44.92
YBR298C	-4.02	0.00	437.69	108.78
YLR164W	-4.02	0.00	42.30	10.51

YLR096W	-4.02	0.00	29.71	7.39
YMR167W	-4.02	0.00	29.48	7.33
YOR119C	-4.02	0.00	91.41	22.76
YNR016C	-4.01	0.00	128.51	32.02
YLR421C	-4.01	0.00	708.58	176.62
YKL117W	-4.01	0.00	939.54	234.51
YGL187C	-4.01	0.00	1222.67	305.20
YCR037C	-4.00	0.01	22.55	5.63
YMR133W	-4.00	0.00	37.67	9.42
YML117W	-3.99	0.00	249.61	62.48
YIL093C	-3.99	0.00	105.52	26.42
YGR178C	-3.99	0.00	144.07	36.10
YJL163C	-3.99	0.00	141.99	35.61
YGL142C	-3.99	0.00	40.87	10.25
YHR132W-A	-3.99	0.00	384.63	96.46
YPR155C	-3.99	0.02	17.77	4.46
YOR256C	-3.99	0.00	71.30	17.89
YJL032W	-3.98	0.00	120.38	30.22
YGL258W-A	-3.98	0.00	61.54	15.46
YKR088C	-3.98	0.00	84.41	21.21
YDR187C	-3.98	0.00	199.45	50.13
YFL051C	-3.98	0.00	76.82	19.31
YGR092W	-3.97	0.00	61.42	15.47
YCR030C	-3.97	0.00	56.97	14.35
YHL034C	-3.97	0.00	544.24	137.16
YOL035C	-3.96	0.00	425.89	107.43
YDR264C	-3.96	0.00	122.05	30.80
YOR259C	-3.96	0.00	399.96	100.97
YKL142W	-3.96	0.00	832.01	210.07
YNL240C	-3.96	0.00	184.10	46.51
YBR255W	-3.96	0.00	41.41	10.47
YIL024C	-3.95	0.00	122.35	30.95
YER017C	-3.95	0.00	183.19	46.38
YBL020W	-3.94	0.00	48.01	12.18
YHR159W	-3.94	0.00	53.67	13.61
YKR074W	-3.94	0.00	90.84	23.05
YMR047C	-3.94	0.00	38.37	9.74
YDR455C	-3.94	0.00	28.29	7.19
YER058W	-3.93	0.00	181.87	46.22
YGL219C	-3.93	0.00	251.46	63.91
YJR001W	-3.93	0.00	58.37	14.84
YPL045W	-3.93	0.01	20.20	5.14
YOR171C	-3.93	0.00	104.21	26.50
YKR046C	-3.93	0.00	1357.16	345.27
YOR020W-A	-3.92	0.00	752.57	191.75
YKL034W	-3.92	0.00	71.97	18.36

YNR047W	-3.92	0.00	113.63	29.01
YOL143C	-3.92	0.00	392.24	100.16
YPL189C-A	-3.92	0.00	1189.38	303.78
YDR272W	-3.92	0.00	370.08	94.53
YNL176C	-3.91	0.00	121.00	30.91
YBR260C	-3.91	0.00	59.15	15.13
YML079W	-3.91	0.00	74.92	19.16
YOR149C	-3.91	0.01	22.71	5.81
YPL152W	-3.91	0.00	81.92	20.97
YGR233C	-3.90	0.02	18.70	4.79
YJR117W	-3.90	0.00	116.22	29.77
YDL246C	-3.90	0.00	48.42	12.41
YJL008C	-3.90	0.00	165.12	42.34
YIL158W	-3.90	0.00	30.57	7.84
YBR149W	-3.90	0.00	392.09	100.60
YDR394W	-3.90	0.00	330.22	84.75
YLR064W	-3.90	0.00	108.56	27.87
YDR065W	-3.89	0.01	22.05	5.66
YDL188C	-3.89	0.00	72.31	18.58
YER169W	-3.89	0.00	82.82	21.28
YDR467C	-3.89	0.00	79.23	20.37
YOR363C	-3.89	0.00	29.94	7.70
YKR021W	-3.89	0.00	31.24	8.04
YGL095C	-3.89	0.00	58.86	15.15
YDR485C	-3.88	0.00	82.16	21.15
YHR131C	-3.88	0.00	85.52	22.02
YDR029W	-3.88	0.00	38.33	9.87
YMR164C	-3.88	0.01	23.70	6.10
YGL207W	-3.88	0.00	80.53	20.76
YMR056C	-3.88	0.00	129.63	33.43
YDL096C	-3.88	0.00	93.27	24.06
YOR054C	-3.88	0.00	205.87	53.11
YOR114W	-3.87	0.01	21.10	5.45
YJL131C	-3.87	0.00	99.12	25.59
YNL333W	-3.87	0.00	29.31	7.57
YNL097C	-3.87	0.00	164.47	42.49
YGL190C	-3.87	0.00	88.34	22.84
YBR170C	-3.87	0.00	121.59	31.45
YML068W	-3.86	0.00	55.85	14.46
YOR132W	-3.86	0.00	125.01	32.38
YKR106W	-3.86	0.01	21.34	5.53
YMR030W	-3.86	0.00	159.36	41.29
YOR336W	-3.86	0.01	20.67	5.36
YER075C	-3.86	0.01	26.26	6.81
YLR384C	-3.86	0.01	24.72	6.41
YJR045C	-3.86	0.00	2118.54	549.44
YJL154C	-3.86	0.00	75.60	19.61

YGR087C	-3.85	0.00	28.32	7.35
YLR036C	-3.85	0.00	35.55	9.23
YBR216C	-3.85	0.01	25.47	6.61
YDL093W	-3.85	0.01	23.41	6.08
YEL057C	-3.85	0.05	14.60	3.80
YLR437C-A	-3.85	0.00	151.98	39.52
YLR228C	-3.84	0.00	28.11	7.32
YLR032W	-3.84	0.03	16.73	4.36
YOR378W	-3.84	0.00	45.34	11.81
YJR142W	-3.84	0.00	70.53	18.38
YGR130C	-3.84	0.00	184.91	48.20
YKL010C	-3.84	0.00	82.61	21.54
YBR201C-A	-3.83	0.00	358.83	93.62
YCL022C	-3.83	0.01	21.21	5.53
YHR152W	-3.83	0.00	89.87	23.46
YOR289W	-3.83	0.00	245.31	64.04
YER139C	-3.83	0.00	36.75	9.60
YPL222C-A	-3.83	0.00	366.33	95.69
YOL023W	-3.83	0.00	55.70	14.56
YJL036W	-3.83	0.00	203.25	53.13
YDR379C-A	-3.82	0.00	292.16	76.41
YOR034C	-3.82	0.00	38.49	10.07
YPL248C	-3.82	0.00	35.29	9.23
YDR069C	-3.82	0.00	42.13	11.02
YBR043C	-3.82	0.00	41.71	10.91
YEL043W	-3.82	0.00	56.07	14.68
YJR072C	-3.82	0.00	166.23	43.51
YLR163C	-3.82	0.00	156.56	40.98
YOR015W	-3.82	0.00	143.42	37.54
YDR137W	-3.82	0.03	17.52	4.59
YMR139W	-3.82	0.00	138.49	36.26
YPL165C	-3.82	0.00	94.33	24.71
YCR026C	-3.82	0.00	102.75	26.93
YIL108W	-3.81	0.00	115.82	30.38
YDR367W	-3.81	0.00	40.32	10.58
YGL124C	-3.81	0.03	17.13	4.49
YER125W	-3.81	0.00	129.60	34.00
YBL080C	-3.81	0.01	21.27	5.58
YGR068W-A	-3.81	0.00	32.75	8.59
YKL067W	-3.81	0.00	1196.76	313.97
YJR080C	-3.81	0.00	104.71	27.47
YLR173W	-3.81	0.00	86.81	22.78
YBR237W	-3.81	0.00	47.87	12.57
YLR361C-A	-3.80	0.00	348.74	91.65
YJL090C	-3.80	0.02	18.30	4.81
YNL183C	-3.80	0.00	53.29	14.01

YML099C	-3.80	0.00	31.76	8.35
YHR075C	-3.80	0.00	49.66	13.08
YNL293W	-3.80	0.00	79.39	20.92
YHL034W-A	-3.79	0.00	646.70	170.44
YML002W	-3.79	0.00	36.41	9.60
YDL026W	-3.79	0.00	70.95	18.71
YMR068W	-3.79	0.00	149.88	39.53
YLR299C-A	-3.79	0.00	294.82	77.78
YDR202C	-3.79	0.00	105.88	27.94
YOR231W	-3.79	0.00	71.78	18.95
YPR089W	-3.79	0.00	29.92	7.90
YKL094W	-3.79	0.00	600.36	158.56
YPL028W	-3.78	0.00	248.19	65.57
YDR018C	-3.78	0.00	110.62	29.25
YKR040C	-3.78	0.03	18.09	4.78
YPL083C	-3.78	0.00	27.32	7.23
YGL011C	-3.78	0.00	800.71	211.93
YFL034W	-3.78	0.00	34.74	9.20
YNL094W	-3.77	0.00	159.00	42.12
YHR001W	-3.77	0.00	62.50	16.56
YGR097W	-3.77	0.00	79.66	21.11
YDR512C	-3.77	0.00	131.57	34.88
YKL093W	-3.77	0.00	161.22	42.74
YEL050C	-3.77	0.00	112.79	29.90
YBL019W	-3.77	0.00	27.56	7.31
YER030W	-3.77	0.00	325.73	86.39
YMR314W	-3.77	0.00	567.68	150.58
YCR017C	-3.77	0.00	86.42	22.92
YBR299W	-3.77	0.00	119.79	31.78
YDR326C	-3.77	0.03	17.39	4.62
YGL132W	-3.77	0.01	24.89	6.61
YGL260W	-3.77	0.04	15.52	4.12
YOR150W	-3.77	0.00	228.28	60.62
YDR177W	-3.76	0.00	199.43	52.98
YHR164C	-3.76	0.02	19.19	5.10
YOL138C	-3.76	0.02	19.04	5.06
YDL057W	-3.76	0.00	36.76	9.77
YDR529C	-3.76	0.00	3468.28	922.54
YIL088C	-3.76	0.00	112.84	30.02
YDR356W	-3.76	0.04	16.15	4.30
YIL066C	-3.76	0.03	16.43	4.38
YOR083W	-3.74	0.00	67.07	17.94
YMR225C	-3.74	0.00	199.67	53.41
YOR321W	-3.74	0.01	21.91	5.86
YGL254W	-3.74	0.00	57.16	15.30
YLR393W	-3.73	0.00	53.60	14.35
YIL098C	-3.73	0.00	118.38	31.73

YHR165C	-3.73	0.02	18.65	5.00
YBL016W	-3.73	0.00	28.96	7.77
YMR157C	-3.73	0.00	126.27	33.87
YGL159W	-3.73	0.00	29.10	7.81
YOR121C	-3.72	0.00	385.34	103.47
YKR002W	-3.72	0.00	121.94	32.75
YHR024C	-3.72	0.00	97.65	26.23
YDR017C	-3.72	0.00	43.82	11.77
YKR011C	-3.72	0.00	169.89	45.65
YMR150C	-3.72	0.00	90.65	24.36
YPL105C	-3.72	0.00	102.44	27.55
YNL241C	-3.72	0.00	870.56	234.12
YER166W	-3.72	0.00	46.93	12.62
YPL085W	-3.72	0.03	18.08	4.86
YKL133C	-3.72	0.00	82.00	22.06
YOL130W	-3.72	0.00	126.77	34.11
YNL131W	-3.71	0.00	316.76	85.29
YDR347W	-3.71	0.00	237.55	63.98
YJL059W	-3.71	0.01	26.29	7.08
YLL023C	-3.71	0.00	302.61	81.66
YNL051W	-3.71	0.00	34.14	9.21
YKL023W	-3.71	0.00	240.46	64.90
YBR122C	-3.71	0.00	333.28	89.95
YCR067C	-3.70	0.02	18.82	5.08
YOR142W	-3.70	0.00	300.14	81.01
YDR490C	-3.70	0.00	71.61	19.33
YBL059W	-3.70	0.00	61.37	16.57
YJR050W	-3.70	0.00	137.05	37.01
YHR004C	-3.70	0.00	60.26	16.28
YGR253C	-3.70	0.00	490.49	132.50
YBR229C	-3.70	0.04	16.07	4.34
YMR325W	-3.70	0.00	28.17	7.61
YGL131C	-3.70	0.04	16.38	4.43
YLR182W	-3.69	0.00	39.66	10.73
YMR273C	-3.69	0.00	31.12	8.43
YCL021W-A	-3.69	0.00	33.44	9.06
YJL062W-A	-3.69	0.00	688.59	186.67
YMR173W-A	-3.69	0.00	409.59	111.06
YDL181W	-3.69	0.00	737.34	199.95
YBR125C	-3.69	0.00	45.33	12.29
YPL120W	-3.69	0.00	28.78	7.81
YFL018C	-3.68	0.00	379.54	103.00
YOL082W	-3.68	0.00	118.01	32.03
YPL184C	-3.68	0.00	57.55	15.63
YIL126W	-3.68	0.00	37.39	10.16
YJR085C	-3.68	0.00	625.71	170.00

YPL096W	-3.68	0.00	43.19	11.74
YHR104W	-3.68	0.00	711.31	193.32
YAL030W	-3.68	0.00	391.71	106.47
YMR169C	-3.68	0.00	880.05	239.21
YPR191W	-3.68	0.00	1203.15	327.06
YDR363W	-3.67	0.00	44.68	12.17
YPR038W	-3.67	0.00	117.74	32.08
YLR369W	-3.67	0.00	73.15	19.93
YJL049W	-3.67	0.00	28.91	7.88
YIR036C	-3.67	0.00	143.72	39.18
YDR181C	-3.67	0.00	32.84	8.95
YMR064W	-3.67	0.00	79.97	21.80
YML032C	-3.67	0.00	109.30	29.80
YJL197C-A	-3.67	0.04	16.50	4.50
YHR200W	-3.67	0.00	607.60	165.75
YNR036C	-3.66	0.00	838.77	229.09
YML048W	-3.66	0.00	444.93	121.56
YCR077C	-3.66	0.00	58.26	15.92
YPL164C	-3.66	0.00	81.59	22.30
YKL107W	-3.66	0.00	64.37	17.60
YFR049W	-3.65	0.00	540.96	148.06
YHL010C	-3.65	0.00	35.34	9.67
YLR193C	-3.65	0.00	342.90	93.86
YER012W	-3.65	0.00	317.49	86.94
YLR424W	-3.65	0.04	16.23	4.44
YKR072C	-3.65	0.00	327.28	89.64
YOR065W	-3.65	0.00	982.73	269.16
YLR144C	-3.65	0.00	29.99	8.22
YDL035C	-3.65	0.00	56.28	15.43
YOR228C	-3.65	0.00	46.84	12.84
YHR113W	-3.64	0.00	124.92	34.29
YBL078C	-3.64	0.00	1067.66	293.06
YFR029W	-3.64	0.00	82.37	22.61
YCL042W	-3.64	0.01	27.60	7.58
YOL073C	-3.64	0.00	115.13	31.63
YLR109W	-3.64	0.00	6077.65	1669.96
YJR079W	-3.64	0.00	80.42	22.11
YLR034C	-3.64	0.00	78.85	21.69
YMR158C-A	-3.63	0.00	50.13	13.79
YDR274C	-3.63	0.00	192.72	53.05
YPL117C	-3.63	0.00	343.23	94.56
YCL035C	-3.63	0.00	1278.70	352.32
YIL083C	-3.63	0.00	98.11	27.05
YDR464C-A	-3.62	0.00	38.93	10.74
YDL160C	-3.62	0.00	69.34	19.15
YJL041W	-3.62	0.00	51.49	14.22
YNL186W	-3.62	0.00	77.72	21.47

YMR027W	-3.62	0.00	226.89	62.69
YDL086W	-3.62	0.00	241.60	66.77
YJL100W	-3.62	0.00	116.81	32.28
YGR167W	-3.62	0.00	684.50	189.18
YHR033W	-3.62	0.00	266.18	73.58
YHR038W	-3.62	0.00	29.13	8.06
YDR479C	-3.61	0.00	115.42	31.94
YOR053W	-3.61	0.00	655.53	181.45
YPL118W	-3.61	0.00	166.97	46.23
YBR251W	-3.61	0.00	87.05	24.10
YGR286C	-3.61	0.00	99.13	27.45
YGR246C	-3.61	0.00	52.70	14.60
YFR006W	-3.61	0.00	63.40	17.56
YOL068C	-3.61	0.00	150.35	41.67
YKL091C	-3.60	0.00	139.73	38.77
YER087C-A	-3.60	0.00	41.01	11.38
YDR014W	-3.60	0.03	17.40	4.83
YNL005C	-3.60	0.00	248.67	69.08
YDR239C	-3.60	0.00	41.71	11.60
YLR253W	-3.60	0.00	79.95	22.23
YJR159W	-3.59	0.01	22.72	6.32
YBR044C	-3.59	0.00	33.29	9.27
YEL037C	-3.59	0.00	522.43	145.41
YBR114W	-3.59	0.00	214.39	59.68
YPR100W	-3.59	0.00	427.87	119.25
YGL133W	-3.58	0.01	27.87	7.77
YNL310C	-3.58	0.00	100.02	27.92
YGR238C	-3.58	0.00	49.64	13.87
YBL106C	-3.58	0.05	15.34	4.29
YBR147W	-3.58	0.00	102.13	28.56
YDL158C	-3.57	0.00	85.88	24.03
YDL099W	-3.57	0.00	103.89	29.07
YPR177C	-3.57	0.00	40.23	11.26
YFR047C	-3.57	0.00	342.90	95.96
YJL070C	-3.57	0.02	22.26	6.23
YGL215W	-3.57	0.00	142.20	39.83
YBR094W	-3.57	0.03	18.82	5.27
YDL022C-A	-3.57	0.01	22.73	6.37
YKL138C	-3.57	0.00	180.56	50.63
YBR090C	-3.56	0.00	414.99	116.59
YEL020W-A	-3.56	0.00	435.44	122.34
YER116C	-3.56	0.00	166.94	46.92
YEL050W-A	-3.56	0.00	131.67	37.01
YOR125C	-3.56	0.00	70.41	19.80
YGL113W	-3.56	0.04	16.64	4.68
YER014C-A	-3.55	0.00	73.23	20.60
YLR080W	-3.55	0.00	56.24	15.83

YOR187W	-3.55	0.00	695.73	195.81
YJR108W	-3.55	0.00	32.12	9.04
YML057W	-3.55	0.00	136.31	38.39
YGR234W	-3.55	0.00	562.63	158.53
YML049C	-3.55	0.02	20.61	5.81
YDR329C	-3.55	0.00	249.37	70.30
YCL033C	-3.55	0.00	138.05	38.92
YIR036W-A	-3.55	0.00	61.01	17.20
YLR130C	-3.55	0.00	84.74	23.90
YMR158W	-3.54	0.00	111.40	31.46
YCL051W	-3.54	0.00	63.35	17.89
YIL036W	-3.54	0.00	124.85	35.29
YGL010W	-3.54	0.00	291.20	82.31
YER027C	-3.54	0.00	158.02	44.68
YML057C-A	-3.54	0.00	67.89	19.20
YHR052W-A	-3.53	0.00	4873.26	1380.66
YPR180W	-3.53	0.00	45.48	12.88
YMR203W	-3.53	0.00	193.90	54.95
YBR056W	-3.53	0.00	185.53	52.58
YKL204W	-3.53	0.00	70.60	20.01
YMR069W	-3.52	0.00	29.98	8.50
YJR051W	-3.52	0.00	72.87	20.69
YPL132W	-3.52	0.00	89.28	25.37
YCR083W	-3.52	0.00	393.70	111.87
YGL040C	-3.52	0.00	232.17	65.98
YDR346C	-3.51	0.00	342.01	97.33
YDR251W	-3.51	0.00	140.51	39.99
YJL161W	-3.51	0.00	72.27	20.57
YHR054W-A	-3.51	0.00	4911.96	1397.91
YEL020C-B	-3.51	0.00	231.86	66.02
YJL081C	-3.51	0.00	49.71	14.16
YKL006C-A	-3.51	0.00	234.01	66.69
YBR126C	-3.51	0.00	1034.97	295.09
YLR077W	-3.51	0.00	44.83	12.78
YNR032C-A	-3.51	0.00	190.36	54.31
YHR114W	-3.50	0.00	47.35	13.51
YPL031C	-3.50	0.00	149.68	42.72
YNL216W	-3.50	0.00	71.01	20.28
YKL124W	-3.50	0.00	70.33	20.09
YAL044W-A	-3.50	0.00	150.70	43.06
YDL141W	-3.50	0.02	22.60	6.46
YBL045C	-3.50	0.00	811.86	232.06
YJL112W	-3.50	0.00	57.73	16.51
YDR470C	-3.50	0.02	21.75	6.22
YLR131C	-3.50	0.01	25.12	7.19
YKR052C	-3.49	0.00	113.82	32.59

YFL056C	-3.49	0.00	81.78	23.43
YLR269C	-3.49	0.00	61.81	17.72
YJL001W	-3.49	0.00	343.84	98.61
YPL074W	-3.49	0.00	41.51	11.91
YBR214W	-3.48	0.00	433.46	124.38
YDL115C	-3.48	0.00	259.01	74.33
YHR057C	-3.48	0.00	387.40	111.20
YOR109W	-3.48	0.01	25.20	7.23
YMR187C	-3.48	0.01	25.91	7.44
YLR079W	-3.48	0.00	225.29	64.71
YJL054W	-3.48	0.00	134.48	38.64
YOR064C	-3.48	0.00	209.05	60.09
YJR133W	-3.48	0.00	191.96	55.19
YKL025C	-3.47	0.00	53.61	15.43
YGR206W	-3.47	0.00	64.12	18.46
YER004W	-3.47	0.00	811.12	233.66
YDR464W	-3.47	0.01	28.10	8.10
YER007W	-3.47	0.02	20.64	5.95
YOR068C	-3.47	0.02	22.97	6.62
YDR337W	-3.47	0.00	97.36	28.08
YLR447C	-3.47	0.00	263.24	75.92
YAR018C	-3.47	0.01	24.71	7.13
YDL107W	-3.46	0.00	44.96	12.98
YDR421W	-3.46	0.01	23.19	6.69
YBR133C	-3.46	0.00	42.63	12.31
YPR054W	-3.46	0.01	26.73	7.72
YDL086C-A	-3.46	0.00	311.54	90.00
YPL035C	-3.46	0.00	71.92	20.79
YML129C	-3.46	0.00	1081.77	312.79
YOR151C	-3.46	0.00	77.91	22.53
YGL112C	-3.46	0.00	60.82	17.59
YGL014W	-3.45	0.00	57.86	16.75
YPR111W	-3.45	0.00	62.59	18.12
YCR048W	-3.45	0.00	143.37	41.51
YER136W	-3.45	0.00	155.08	44.92
YOR097C	-3.45	0.00	182.11	52.76
YNL272C	-3.45	0.02	22.48	6.51
YOR147W	-3.45	0.00	116.22	33.68
YGR008C	-3.45	0.00	3723.65	1079.94
YMR294W	-3.45	0.00	45.23	13.12
YNL259C	-3.45	0.00	289.51	84.03
YPR076W	-3.44	0.00	238.97	69.37
YGL047W	-3.44	0.00	72.49	21.05
YER074W-A	-3.44	0.00	271.05	78.70
YLR227C	-3.44	0.00	49.69	14.43
YNL295W	-3.44	0.00	105.25	30.58
YGR102C	-3.44	0.00	502.87	146.10

YNR031C	-3.44	0.01	23.72	6.89
YKL087C	-3.44	0.00	402.94	117.22
YDL032W	-3.44	0.02	20.96	6.10
YNL305C	-3.44	0.00	665.73	193.76
YNL219C	-3.43	0.00	55.65	16.21
YDR085C	-3.43	0.00	125.30	36.51
YOR086C	-3.43	0.01	27.16	7.93
YFR020W	-3.42	0.00	361.85	105.66
YDL174C	-3.42	0.00	324.95	94.89
YDR220C	-3.42	0.01	24.38	7.12
YBR205W	-3.42	0.00	91.66	26.79
YEL074W	-3.42	0.00	93.50	27.33
YHR045W	-3.42	0.00	32.25	9.43
YBL090W	-3.42	0.00	163.81	47.89
YIL107C	-3.42	0.00	84.15	24.62
YDR176W	-3.42	0.00	37.00	10.83
YDL183C	-3.42	0.00	89.79	26.29
YGL005C	-3.42	0.00	122.03	35.73
YNL070W	-3.41	0.00	159.79	46.81
YNL134C	-3.41	0.00	757.59	221.94
YNL117W	-3.41	0.00	99.64	29.19
YHR042W	-3.41	0.00	178.51	52.33
YBR089C-A	-3.41	0.00	430.57	126.27
YGR165W	-3.41	0.00	70.04	20.54
YDL034W	-3.41	0.01	25.70	7.54
YCR082W	-3.41	0.00	499.20	146.58
YOR041C	-3.40	0.00	139.02	40.83
YER024W	-3.40	0.00	99.05	29.09
YNL202W	-3.40	0.00	238.67	70.17
YDR377W	-3.40	0.00	981.74	288.65
YDR296W	-3.40	0.00	217.38	63.92
YDR068W	-3.40	0.00	102.92	30.26
YLR092W	-3.40	0.00	53.74	15.80
YFR004W	-3.40	0.00	414.81	122.01
YDR363W-A	-3.40	0.00	582.05	171.32
YOL013C	-3.39	0.00	91.29	26.90
YNR034W	-3.39	0.00	220.23	64.90
YGL114W	-3.39	0.00	54.17	15.97
YPL219W	-3.39	0.00	47.15	13.90
YFL029C	-3.39	0.00	43.34	12.78
YDL237W	-3.39	0.00	87.66	25.86
YBR262C	-3.39	0.00	387.31	114.25
YDR304C	-3.39	0.00	165.84	48.95
YPR168W	-3.39	0.03	19.50	5.76
YIL105C	-3.39	0.00	123.33	36.42
YML012C-A	-3.39	0.00	107.97	31.89

YDR306C	-3.38	0.00	84.24	24.90
YFR003C	-3.38	0.00	134.78	39.86
YPL004C	-3.38	0.00	808.95	239.28
YCR021C	-3.38	0.00	13840.30	4094.69
YMR267W	-3.38	0.03	19.08	5.64
YHR110W	-3.38	0.00	176.75	52.33
YOL164W	-3.38	0.00	45.49	13.47
YJL084C	-3.38	0.00	55.72	16.50
YLR310C	-3.38	0.02	23.26	6.89
YNR005C	-3.37	0.00	45.96	13.63
YLR239C	-3.37	0.00	36.19	10.74
YIL112W	-3.37	0.00	79.81	23.69
YLR387C	-3.37	0.00	174.86	51.92
YJR130C	-3.37	0.00	60.43	17.95
YDR416W	-3.37	0.04	18.38	5.46
YDR166C	-3.37	0.01	25.92	7.70
YOR141C	-3.36	0.00	64.60	19.21
YBR239C	-3.36	0.00	43.74	13.01
YCR076C	-3.36	0.00	101.97	30.34
YHR119W	-3.36	0.01	24.24	7.22
YBR276C	-3.36	0.01	29.52	8.80
YFR033C	-3.36	0.00	4380.56	1305.06
YDR057W	-3.36	0.00	61.57	18.35
YJL210W	-3.35	0.00	126.24	37.64
YER015W	-3.35	0.00	60.55	18.06
YGR197C	-3.35	0.00	73.02	21.81
YFR045W	-3.35	0.00	49.57	14.81
YAL021C	-3.35	0.00	38.25	11.43
YMR022W	-3.35	0.00	516.99	154.55
YGL164C	-3.34	0.00	36.51	10.94
YDR199W	-3.34	0.00	116.32	34.85
YBR223C	-3.34	0.00	40.16	12.03
YJR116W	-3.34	0.00	63.79	19.11
YLR279W	-3.34	0.01	26.61	7.97
YNL144W-A	-3.34	0.00	944.80	283.27
YBL041W	-3.33	0.00	475.90	142.72
YBR293W	-3.33	0.05	16.02	4.81
YFR008W	-3.33	0.00	69.50	20.87
YKR083C	-3.33	0.00	39.42	11.84
YDR481C	-3.33	0.00	368.78	110.75
YDR390C	-3.33	0.02	24.09	7.24
YHR186C	-3.33	0.05	16.71	5.02
YDR175C	-3.33	0.00	134.75	40.52
YFR017C	-3.32	0.00	1456.88	438.23
YLR217W	-3.32	0.00	1163.41	349.97
YBL049W	-3.32	0.00	632.19	190.21
YLR335W	-3.32	0.00	80.53	24.23

YJR037W	-3.32	0.04	18.67	5.62
YLR294C	-3.32	0.00	76.04	22.88
YOR152C	-3.32	0.00	161.34	48.56
YML065W	-3.32	0.01	24.95	7.51
YOL033W	-3.32	0.04	18.31	5.51
YER060W-A	-3.32	0.00	32.53	9.80
YHR191C	-3.32	0.00	93.24	28.10
YNR073C	-3.32	0.00	81.35	24.51
YLR219W	-3.32	0.00	146.10	44.04
YDL040C	-3.32	0.02	23.88	7.20
YBR111W-A	-3.31	0.00	103.30	31.18
YPL034W	-3.31	0.00	48.11	14.53
YGL051W	-3.31	0.02	23.82	7.20
YDR238C	-3.31	0.00	60.48	18.28
YBR127C	-3.30	0.00	368.30	111.47
YHR009C	-3.30	0.00	274.59	83.11
YKL088W	-3.30	0.00	169.46	51.32
YMR237W	-3.30	0.00	47.74	14.47
YFL005W	-3.30	0.00	298.42	90.48
YIL065C	-3.30	0.00	410.51	124.46
YBR283C	-3.30	0.00	117.06	35.50
YDR170C	-3.30	0.02	22.93	6.96
YLR004C	-3.30	0.04	18.76	5.69
YBR037C	-3.30	0.00	134.48	40.80
YDR322C-A	-3.30	0.00	1030.61	312.68
YDR462W	-3.30	0.00	283.56	86.03
YPR088C	-3.30	0.00	135.56	41.13
YDR409W	-3.29	0.01	28.03	8.51
YLR108C	-3.29	0.00	61.08	18.54
YML050W	-3.29	0.00	55.16	16.74
YLR304C	-3.29	0.00	744.23	225.93
YDR080W	-3.29	0.05	17.25	5.24
YPL104W	-3.29	0.01	25.03	7.61
YLR438W	-3.29	0.00	188.81	57.38
YDR320C	-3.29	0.02	23.41	7.11
YOL043C	-3.29	0.00	44.57	13.55
YNL121C	-3.29	0.00	86.87	26.42
YGL081W	-3.28	0.02	21.42	6.52
YER112W	-3.28	0.00	127.33	38.81
YGR232W	-3.28	0.00	179.96	54.86
YOR030W	-3.28	0.00	48.21	14.70
YBR193C	-3.28	0.00	62.23	18.98
YGR110W	-3.28	0.00	220.81	67.34
YOR168W	-3.28	0.00	40.84	12.46
YHR214W-A	-3.28	0.00	36.36	11.10
YKL193C	-3.28	0.00	91.58	27.95

YJL176C	-3.28	0.01	30.20	9.22
YPL046C	-3.28	0.00	65.82	20.09
YAL045C	-3.27	0.00	106.24	32.44
YJL098W	-3.27	0.00	33.61	10.27
YGR013W	-3.27	0.00	90.43	27.62
YDR452W	-3.27	0.00	66.05	20.18
YBR270C	-3.27	0.02	22.69	6.93
YNL055C	-3.27	0.00	1566.42	479.10
YPL133C	-3.27	0.00	94.21	28.82
YJR132W	-3.27	0.05	16.55	5.06
YNL155W	-3.27	0.00	308.26	94.29
YDR122W	-3.27	0.00	62.69	19.18
YDR423C	-3.26	0.00	106.75	32.71
YDR116C	-3.26	0.00	129.59	39.71
YGL072C	-3.26	0.00	221.85	68.04
YBR273C	-3.26	0.00	162.52	49.85
YDR419W	-3.26	0.01	26.03	7.99
YNL165W	-3.26	0.00	68.09	20.89
YLR259C	-3.26	0.00	1799.94	552.47
YOR270C	-3.26	0.00	75.62	23.21
YOR042W	-3.26	0.00	247.48	75.98
YIL050W	-3.26	0.00	149.74	46.00
YER071C	-3.25	0.00	55.79	17.15
YMR141C	-3.25	0.00	152.23	46.82
YBR263W	-3.25	0.00	213.85	65.78
YLR451W	-3.25	0.02	23.09	7.11
YKL039W	-3.25	0.00	148.66	45.77
YEL060C	-3.25	0.00	2763.40	851.09
YOR326W	-3.25	0.03	20.58	6.34
YNL039W	-3.25	0.00	119.75	36.90
YNL284C	-3.24	0.00	144.46	44.53
YOR040W	-3.24	0.00	189.39	58.42
YKL145W	-3.24	0.00	354.93	109.51
YMR313C	-3.24	0.00	99.20	30.62
YFR015C	-3.24	0.00	153.80	47.49
YGL122C	-3.24	0.00	451.29	139.41
YOR020C	-3.24	0.00	2754.29	850.98
YDR313C	-3.24	0.00	267.62	82.69
YNL329C	-3.24	0.04	19.05	5.89
YPL193W	-3.23	0.01	27.93	8.64
YDR486C	-3.23	0.00	163.23	50.49
YER005W	-3.23	0.00	67.37	20.85
YHR044C	-3.23	0.00	44.81	13.87
YHR012W	-3.23	0.00	107.63	33.33
YNL181W	-3.23	0.00	39.00	12.08
YJL123C	-3.23	0.00	94.35	29.23
YJR114W	-3.23	0.00	292.35	90.58

YER133W-A	-3.23	0.00	175.97	54.55
YOR113W	-3.23	0.00	37.73	11.70
YNL189W	-3.22	0.00	81.65	25.32
YPL091W	-3.22	0.00	152.67	47.37
YMR178W	-3.22	0.00	173.87	53.99
YDR359C	-3.22	0.03	19.75	6.13
YGL056C	-3.22	0.00	153.56	47.71
YPL147W	-3.22	0.00	58.05	18.04
YBR086C	-3.22	0.00	96.13	29.88
YMR020W	-3.22	0.00	180.51	56.14
YPR099C	-3.21	0.00	373.09	116.06
YPR032W	-3.21	0.04	18.14	5.65
YJL127C	-3.21	0.01	25.44	7.92
YGL208W	-3.21	0.00	134.59	41.89
YLR117C	-3.21	0.00	101.12	31.48
YKL198C	-3.21	0.00	144.97	45.14
YCR081C-A	-3.21	0.04	18.04	5.62
YDR322W	-3.21	0.00	83.91	26.15
YPL100W	-3.21	0.00	59.26	18.47
YNL194C	-3.21	0.00	726.53	226.50
YPR037C	-3.21	0.00	115.98	36.18
YDR208W	-3.20	0.00	91.67	28.61
YJL094C	-3.20	0.00	95.46	29.79
YNL215W	-3.20	0.00	190.36	59.43
YPL010W	-3.20	0.00	105.14	32.84
YDR362C	-3.20	0.00	69.52	21.72
YGL161C	-3.20	0.00	83.58	26.12
YER054C	-3.20	0.00	264.22	82.56
YIL105W-A	-3.20	0.00	201.60	63.00
YLR049C	-3.20	0.00	47.59	14.89
YMR311C	-3.20	0.00	924.44	289.31
YDL200C	-3.19	0.00	56.12	17.57
YHR055C	-3.19	0.00	5701.08	1784.86
YOR157C	-3.19	0.00	242.35	75.88
YER084W	-3.19	0.00	103.67	32.46
YDR328C	-3.19	0.00	562.44	176.15
YKL192C	-3.19	0.00	476.31	149.23
YMR099C	-3.19	0.00	122.61	38.47
YBR215W	-3.19	0.01	31.01	9.73
YMR015C	-3.19	0.00	44.37	13.93
YCL028W	-3.18	0.00	149.11	46.83
YDR435C	-3.18	0.00	148.71	46.74
YJL103C	-3.18	0.00	60.65	19.07
YOL111C	-3.18	0.00	211.10	66.43
YGL226W	-3.18	0.00	139.81	44.01
YBR025C	-3.18	0.00	251.23	79.09
YMR276W	-3.18	0.00	507.08	159.65

YBR120C	-3.18	0.00	123.20	38.80
YGL018C	-3.17	0.00	82.72	26.07
YBR015C	-3.17	0.00	80.24	25.29
YOR022C	-3.17	0.02	24.74	7.80
YLR361C	-3.17	0.00	37.18	11.73
YNL203C	-3.17	0.00	166.67	52.57
YDR461C-A	-3.17	0.00	237.57	74.94
YGL226C-A	-3.17	0.00	104.81	33.06
YLR234W	-3.17	0.01	26.51	8.37
YHR037W	-3.17	0.00	196.45	62.02
YKL135C	-3.17	0.00	49.45	15.62
YGR077C	-3.16	0.01	27.68	8.75
YJR002W	-3.16	0.00	73.79	23.32
YOR325W	-3.16	0.01	30.91	9.77
YNL097W-A	-3.16	0.00	284.20	89.89
YHR032W	-3.16	0.00	80.61	25.51
YJL211C	-3.16	0.00	105.09	33.30
YGR026W	-3.16	0.00	66.49	21.08
YBR256C	-3.15	0.00	184.80	58.59
YDR444W	-3.15	0.00	38.97	12.36
YDL025C	-3.15	0.00	164.83	52.28
YDR212W	-3.15	0.00	104.18	33.05
YPR024W	-3.15	0.00	184.99	58.70
YPR199C	-3.15	0.00	64.17	20.36
YGR070W	-3.15	0.00	58.92	18.70
YPR075C	-3.15	0.00	578.53	183.62
YDL178W	-3.15	0.00	68.49	21.75
YKR098C	-3.15	0.00	74.36	23.63
YMR188C	-3.15	0.00	213.67	67.90
YER153C	-3.15	0.00	38.88	12.36
YMR053C	-3.15	0.00	48.62	15.46
YBL086C	-3.14	0.00	205.90	65.54
YKL073W	-3.14	0.01	28.85	9.18
YOR017W	-3.14	0.01	29.68	9.45
YOR322C	-3.14	0.00	95.42	30.40
YCL001W-B	-3.14	0.01	28.11	8.96
YPL039W	-3.14	0.00	108.45	34.56
YGL110C	-3.14	0.02	25.26	8.05
YGR141W	-3.13	0.00	173.12	55.23
YBR186W	-3.13	0.04	19.48	6.21
YKR089C	-3.13	0.00	102.81	32.81
YKL137W	-3.13	0.00	149.73	47.78
YJL155C	-3.13	0.00	266.59	85.07
YDR254W	-3.13	0.00	43.02	13.73
YHR059W	-3.13	0.00	72.33	23.09
YML120C	-3.13	0.00	759.58	242.58
YDR411C	-3.13	0.00	115.60	36.92

YDL090C	-3.13	0.00	40.61	12.97
YEL034W	-3.13	0.00	2186.85	698.65
YPR002W	-3.13	0.00	59.16	18.90
YBR132C	-3.13	0.00	138.27	44.18
YDR286C	-3.13	0.00	109.37	34.94
YIL055C	-3.13	0.00	47.43	15.16
YLR223C	-3.13	0.01	29.86	9.54
YLR151C	-3.13	0.00	70.45	22.52
YMR072W	-3.12	0.00	220.56	70.58
YKL004W	-3.12	0.00	178.39	57.09
YKL184W	-3.12	0.00	97.23	31.11
YER048C	-3.12	0.00	257.59	82.45
YGR131W	-3.12	0.00	44.92	14.38
YNR068C	-3.12	0.00	35.32	11.31
YLR114C	-3.12	0.00	71.98	23.06
YKL100C	-3.12	0.00	109.34	35.04
YKR048C	-3.12	0.00	566.99	181.70
YPL138C	-3.12	0.00	82.19	26.35
YMR166C	-3.12	0.00	42.55	13.64
YNL223W	-3.12	0.00	84.48	27.09
YER066W	-3.12	0.00	53.19	17.06
YHR053C	-3.12	0.00	5676.39	1820.34
YDR145W	-3.12	0.00	98.56	31.61
YMR245W	-3.12	0.00	215.29	69.07
YIL119C	-3.12	0.00	105.02	33.70
YOR123C	-3.12	0.00	141.60	45.44
YDL070W	-3.12	0.00	259.88	83.41
YEL024W	-3.12	0.00	1280.25	410.97
YGL085W	-3.11	0.01	28.51	9.15
YDL230W	-3.11	0.00	168.95	54.26
YPL023C	-3.11	0.00	115.36	37.06
YER180C-A	-3.11	0.00	60.45	19.43
YNL040W	-3.11	0.01	32.25	10.37
YDR173C	-3.11	0.00	80.55	25.90
YAL026C-A	-3.11	0.00	36.47	11.73
YDR127W	-3.11	0.00	38.11	12.27
YNL156C	-3.10	0.00	385.78	124.30
YGR223C	-3.10	0.00	142.53	45.93
YDR200C	-3.10	0.00	48.82	15.73
YFL013C	-3.10	0.00	83.76	27.01
YLR455W	-3.10	0.00	85.57	27.60
YDL248W	-3.10	0.00	291.23	93.97
YPL072W	-3.10	0.05	18.61	6.01
YMR129W	-3.10	0.03	21.15	6.83
YLR370C	-3.10	0.00	279.42	90.28
YBL050W	-3.09	0.00	303.06	97.96
YLL019C	-3.09	0.00	269.39	87.13

YDL021W	-3.09	0.00	54.49	17.63
YEL070W	-3.09	0.00	141.74	45.88
YNL104C	-3.09	0.00	232.24	75.19
YFR007W	-3.09	0.01	33.40	10.81
YAR023C	-3.09	0.01	28.30	9.17
YDR206W	-3.09	0.02	26.34	8.53
YJL111W	-3.09	0.00	132.43	42.92
YLR190W	-3.09	0.01	32.89	10.66
YMR135C	-3.08	0.00	552.38	179.23
YDR067C	-3.08	0.00	63.45	20.59
YKR047W	-3.08	0.00	592.08	192.22
YDL079C	-3.08	0.00	124.65	40.49
YGL203C	-3.08	0.00	65.44	21.27
YGL115W	-3.08	0.00	93.45	30.38
YMR191W	-3.08	0.00	536.95	174.58
YPR086W	-3.07	0.00	321.40	104.53
YNL136W	-3.07	0.00	77.21	25.12
YDL006W	-3.07	0.00	103.92	33.83
YOR257W	-3.07	0.00	347.30	113.07
YML099W-A	-3.07	0.00	65.55	21.34
YIL089W	-3.07	0.00	35.31	11.50
YBR284W	-3.07	0.00	45.65	14.87
YDR148C	-3.07	0.00	581.12	189.26
YNL116W	-3.07	0.00	120.80	39.35
YOR232W	-3.07	0.00	241.30	78.60
YDR338C	-3.07	0.00	47.10	15.35
YBR010W	-3.07	0.00	641.57	209.04
YKR029C	-3.07	0.01	27.85	9.08
YLR214W	-3.06	0.04	20.47	6.68
YLR278C	-3.06	0.00	38.57	12.59
YCL043C	-3.06	0.00	754.92	246.69
YGR076C	-3.06	0.00	56.12	18.34
YDR290W	-3.06	0.04	20.58	6.73
YOR317W	-3.06	0.00	475.05	155.39
YNL334C	-3.05	0.02	24.63	8.06
YGL252C	-3.05	0.00	153.32	50.20
YKL170W	-3.05	0.00	165.44	54.17
YLL021W	-3.05	0.03	22.23	7.28
YOL101C	-3.05	0.00	69.52	22.77
YBR008C	-3.05	0.01	32.57	10.67
YGL154C	-3.05	0.00	80.62	26.42
YGL146C	-3.05	0.00	61.41	20.13
YMR105W-A	-3.05	0.02	25.80	8.46
YDR006C	-3.05	0.00	76.37	25.04
YER010C	-3.05	0.00	103.74	34.02
YCR046C	-3.05	0.00	306.54	100.65

YHR213W-B	-3.04	0.00	63.10	20.73
YOR045W	-3.04	0.00	376.65	123.83
YFL052W	-3.04	0.00	62.03	20.42
YNL084C	-3.04	0.00	80.20	26.41
YDR188W	-3.03	0.00	252.89	83.33
YOL077W-A	-3.03	0.00	719.10	236.95
YOL018C	-3.03	0.00	49.35	16.26
YBR201W	-3.03	0.00	45.68	15.06
YPR067W	-3.03	0.00	105.15	34.68
YPR082C	-3.03	0.00	108.60	35.84
YGL041W-A	-3.03	0.00	131.05	43.26
YNL103W-A	-3.03	0.00	38.43	12.69
YDR142C	-3.03	0.00	80.34	26.55
YPL260W	-3.03	0.00	332.09	109.78
YKR017C	-3.02	0.01	31.18	10.31
YDR248C	-3.02	0.00	222.59	73.59
YMR227C	-3.02	0.00	80.09	26.48
YJR065C	-3.02	0.00	189.27	62.61
YDR164C	-3.02	0.05	19.40	6.42
YGL082W	-3.02	0.00	73.64	24.36
YDR376W	-3.02	0.00	37.89	12.54
YJR005W	-3.02	0.00	58.40	19.34
YPL099C	-3.02	0.00	120.28	39.87
YML025C	-3.02	0.00	245.85	81.51
YOR392W	-3.01	0.01	31.02	10.29
YOL009C	-3.01	0.00	45.47	15.09
YBR029C	-3.01	0.00	101.70	33.76
YMR269W	-3.01	0.00	60.71	20.15
YIL109C	-3.01	0.00	89.86	29.84
YNL266W	-3.01	0.00	77.26	25.68
YNL144C	-3.01	0.00	230.98	76.81
YCR008W	-3.01	0.00	236.07	78.51
YDL065C	-3.01	0.00	182.24	60.62
YJL132W	-3.01	0.02	25.65	8.53
YKR073C	-3.01	0.05	18.42	6.13
YGR220C	-3.00	0.00	162.19	53.97
YBR173C	-3.00	0.00	364.24	121.23
YGR244C	-3.00	0.00	272.17	90.63
YDR224C	-3.00	0.00	466.25	155.27
YKL085W	-3.00	0.00	1309.68	436.40
YIL048W	-3.00	0.02	27.82	9.27
YDL024C	-3.00	0.00	63.60	21.20
YLR028C	-3.00	0.00	260.68	86.89
YNR002C	-3.00	0.00	391.25	130.42
YDR364C	-3.00	0.00	62.06	20.69
YFL059W	-3.00	0.02	25.45	8.49

YGR099W	-3.00	0.00	55.49	18.51
YMR074C	-3.00	0.00	246.67	82.29
YKL162C	-3.00	0.00	47.18	15.75
YDR392W	-3.00	0.00	82.30	27.47
YPL019C	-2.99	0.00	50.30	16.80
YER165W	-2.99	0.00	227.83	76.11
YLR098C	-2.99	0.02	26.32	8.80
YMR298W	-2.99	0.00	158.81	53.09
YLR410W	-2.99	0.00	37.01	12.37
YJL117W	-2.99	0.00	160.58	53.69
YJL128C	-2.99	0.00	84.54	28.30
YDR492W	-2.99	0.00	358.54	120.03
YJR118C	-2.99	0.02	25.38	8.50
YJR107W	-2.98	0.00	67.54	22.63
YOR172W	-2.98	0.00	44.91	15.05
YPL009C	-2.98	0.00	44.81	15.02
YER121W	-2.98	0.00	117.94	39.54
YPL206C	-2.98	0.00	263.53	88.41
YGR003W	-2.98	0.01	29.77	9.99
YDR458C	-2.98	0.03	23.14	7.77
YDL205C	-2.98	0.00	47.04	15.80
YOR389W	-2.98	0.00	171.15	57.53
YER094C	-2.98	0.00	695.52	233.79
YHR039C	-2.97	0.00	38.71	13.02
YBL008W	-2.97	0.05	18.89	6.36
YGL002W	-2.97	0.00	127.03	42.79
YJR008W	-2.96	0.00	755.82	255.00
YHL029C	-2.96	0.00	37.33	12.60
YHR135C	-2.96	0.00	164.20	55.45
YIL057C	-2.96	0.00	343.15	115.88
YOL003C	-2.96	0.02	24.94	8.43
YOL108C	-2.96	0.00	275.13	92.95
YGR162W	-2.96	0.00	49.98	16.89
YGR143W	-2.96	0.00	135.82	45.92
YGL221C	-2.96	0.00	108.44	36.67
YBR221W-A	-2.96	0.00	223.40	75.54
YLR420W	-2.96	0.00	72.13	24.40
YIL009W	-2.96	0.01	30.13	10.20
YER180C	-2.95	0.00	50.37	17.05
YML081C-A	-2.95	0.00	1619.69	548.51
YOR069W	-2.95	0.01	30.58	10.36
YGL100W	-2.95	0.00	74.21	25.14
YAR014C	-2.95	0.00	40.45	13.70
YDR232W	-2.95	0.00	333.18	113.00
YDR214W	-2.95	0.00	385.68	130.88
YKR001C	-2.95	0.00	88.46	30.03

YDR077W	-2.94	0.00	6796.06	2307.69
YNL146C-A	-2.94	0.00	60.31	20.50
YDR473C	-2.94	0.00	65.88	22.41
YHR073W	-2.94	0.00	39.46	13.43
YPL277C	-2.94	0.00	61.00	20.76
YHR056C	-2.94	0.00	46.86	15.96
YGL087C	-2.94	0.00	246.99	84.14
YMR172C-A	-2.94	0.00	88.27	30.07
YOL028C	-2.93	0.00	43.88	14.96
YCR073W-A	-2.93	0.00	232.84	79.38
YOR352W	-2.93	0.00	59.78	20.41
YHR180W	-2.93	0.00	65.70	22.44
YJR089W	-2.93	0.05	19.71	6.73
YPL122C	-2.92	0.01	31.89	10.90
YLL029W	-2.92	0.00	256.77	87.82
YJL002C	-2.92	0.00	79.72	27.27
YHL002C-A	-2.92	0.00	89.38	30.62
YJL156C	-2.92	0.01	36.23	12.42
YGR269W	-2.92	0.05	19.81	6.79
YNR064C	-2.92	0.02	25.64	8.79
YDR327W	-2.92	0.00	589.45	202.19
YPL231W	-2.91	0.00	289.00	99.17
YJR113C	-2.91	0.00	343.93	118.04
YBL101C	-2.91	0.00	97.82	33.58
YIL131C	-2.91	0.00	39.50	13.56
YDR058C	-2.91	0.02	26.35	9.06
YNL177C	-2.91	0.00	190.76	65.57
YDR468C	-2.91	0.00	82.82	28.48
YOR023C	-2.91	0.00	337.62	116.12
YGL216W	-2.91	0.00	47.83	16.45
YDR349C	-2.91	0.00	131.08	45.10
YNL275W	-2.91	0.00	42.18	14.52
YOR285W	-2.90	0.00	2916.16	1004.51
YOR032W-A	-2.90	0.02	25.66	8.84
YJR106W	-2.90	0.02	27.05	9.32
YLR360W	-2.90	0.00	59.12	20.38
YNL025C	-2.90	0.00	38.82	13.38
YFR048W	-2.90	0.01	32.09	11.07
YFL057C	-2.90	0.00	74.53	25.71
YDR082W	-2.90	0.01	37.39	12.90
YKL194C	-2.90	0.02	25.81	8.91
YOR362C	-2.89	0.00	377.97	130.56
YOR370C	-2.89	0.00	98.15	33.93
YOR156C	-2.89	0.03	24.48	8.47
YPL180W	-2.89	0.00	50.91	17.61
YJR109C	-2.89	0.00	39.40	13.63

YJR064W	-2.89	0.00	136.24	47.15
YIL034C	-2.89	0.00	129.85	44.95
YOR170W	-2.89	0.00	140.78	48.73
YCR069W	-2.88	0.00	201.80	69.95
YGR022C	-2.88	0.00	355.98	123.44
YGR215W	-2.88	0.00	153.72	53.35
YMR113W	-2.88	0.01	36.73	12.75
YBR268W	-2.88	0.00	252.34	87.60
YHR214W	-2.88	0.00	51.07	17.73
YGR207C	-2.88	0.00	62.73	21.80
YDR105C	-2.88	0.00	87.56	30.43
YOR163W	-2.88	0.00	142.97	49.69
YFL046W	-2.88	0.00	50.89	17.69
YDR391C	-2.88	0.00	130.27	45.30
YBR003W	-2.88	0.00	80.97	28.16
YCL039W	-2.88	0.00	68.56	23.84
YOR316C	-2.87	0.00	143.02	49.75
YGL129C	-2.87	0.00	70.74	24.62
YPR031W	-2.87	0.04	21.41	7.46
YOR324C	-2.87	0.00	50.13	17.47
YGR266W	-2.87	0.02	27.83	9.70
YCL044C	-2.87	0.00	74.42	25.96
YOR372C	-2.86	0.00	40.72	14.21
YOR320C	-2.86	0.00	50.36	17.58
YHR132C	-2.86	0.00	176.11	61.49
YHR005C-A	-2.86	0.00	266.04	92.93
YKR051W	-2.86	0.00	49.83	17.42
YLR312W-A	-2.86	0.00	95.98	33.56
YBR065C	-2.86	0.00	78.22	27.35
YNL265C	-2.86	0.00	60.08	21.01
YNL322C	-2.86	0.00	438.54	153.58
YMR080C	-2.86	0.01	35.97	12.60
YCR050C	-2.85	0.00	199.85	70.02
YKL003C	-2.85	0.00	193.90	67.94
YBR053C	-2.85	0.00	131.15	45.95
YLR132C	-2.85	0.01	35.87	12.57
YJL076W	-2.85	0.01	36.83	12.92
YKL007W	-2.85	0.00	148.06	51.97
YJR122W	-2.85	0.01	35.44	12.44
YER138W-A	-2.85	0.00	147.93	51.97
YDL029W	-2.85	0.00	117.59	41.33
YBR045C	-2.84	0.01	31.87	11.20
YJL093C	-2.84	0.00	68.64	24.15
YOR193W	-2.84	0.02	28.52	10.04
YJR148W	-2.84	0.00	169.87	59.81
YJL014W	-2.84	0.00	173.97	61.28
YLR271W	-2.84	0.05	20.73	7.31

YDR334W	-2.84	0.01	37.32	13.15
YMR283C	-2.83	0.01	35.11	12.39
YCR088W	-2.83	0.00	96.96	34.21
YGL201C	-2.83	0.01	31.92	11.26
YDL088C	-2.83	0.00	95.46	33.71
YER186C	-2.83	0.00	79.41	28.04
YDR135C	-2.83	0.04	22.22	7.85
YML005W	-2.83	0.00	68.09	24.07
YHL019C	-2.83	0.00	50.50	17.87
YLR258W	-2.82	0.00	443.86	157.13
YDR510C-A	-2.82	0.00	654.13	231.57
YGL186C	-2.82	0.00	71.27	25.24
YOR090C	-2.82	0.01	35.23	12.48
YGR182C	-2.82	0.00	263.63	93.39
YDL137W	-2.82	0.00	628.87	222.78
YGR135W	-2.82	0.00	309.58	109.76
YPL048W	-2.82	0.00	369.51	131.02
YLR015W	-2.82	0.00	47.27	16.76
YLR439W	-2.82	0.00	84.96	30.14
YPR019W	-2.82	0.00	49.33	17.50
YLR358C	-2.82	0.00	113.17	40.16
YOR131C	-2.82	0.00	88.16	31.29
YJR125C	-2.82	0.00	136.02	48.30
YLR338W	-2.81	0.00	61.20	21.74
YNR043W	-2.81	0.00	121.92	43.31
YMR077C	-2.81	0.00	83.57	29.73
YPR147C	-2.81	0.00	59.04	21.01
YGL191W	-2.81	0.00	2327.30	829.60
YCR071C	-2.80	0.00	210.62	75.11
YHL036W	-2.80	0.00	72.20	25.75
YPR047W	-2.80	0.05	21.81	7.79
YGR146C	-2.80	0.00	136.95	48.89
YDR424C	-2.80	0.00	131.86	47.08
YHR101C	-2.80	0.02	30.82	11.02
YPR181C	-2.80	0.00	107.43	38.42
YJR099W	-2.80	0.00	50.15	17.94
YCL008C	-2.79	0.00	53.11	19.01
YBR146W	-2.79	0.00	187.61	67.17
YLR153C	-2.79	0.00	159.52	57.11
YOL045W	-2.79	0.00	53.70	19.23
YPL137C	-2.79	0.03	25.36	9.09
YPL098C	-2.79	0.00	264.24	94.81
YDR079C-A	-2.79	0.00	72.65	26.08
YHR086W	-2.79	0.00	41.04	14.73
YGR021W	-2.78	0.00	130.96	47.03
YDL206W	-2.78	0.01	35.41	12.72
YIL138C	-2.78	0.00	122.41	44.00

YJL063C	-2.78	0.00	187.61	67.43
YPR133W-A	-2.78	0.00	340.33	122.34
YJR102C	-2.78	0.01	31.29	11.25
YHR098C	-2.78	0.01	37.06	13.33
YCL017C	-2.78	0.00	137.43	49.48
YGR227W	-2.78	0.03	24.55	8.85
YBR109C	-2.77	0.00	505.36	182.21
YDL143W	-2.77	0.00	124.51	44.90
YJR131W	-2.77	0.02	29.42	10.61
YIL084C	-2.77	0.01	39.50	14.25
YLR181C	-2.77	0.00	55.60	20.06
YER174C	-2.77	0.02	30.37	10.96
YLR287C-A	-2.77	0.00	1228.59	443.51
YNL083W	-2.77	0.00	61.79	22.30
YER105C	-2.77	0.03	26.26	9.48
YBR199W	-2.77	0.00	198.13	71.55
YKR019C	-2.77	0.01	33.93	12.26
YOL069W	-2.77	0.01	33.39	12.07
YCR096C	-2.76	0.00	112.50	40.72
YOR178C	-2.76	0.00	216.88	78.50
YNL336W	-2.76	0.00	77.21	27.96
YAL044C	-2.76	0.00	251.55	91.16
YBR017C	-2.76	0.04	23.04	8.35
YMR194C-B	-2.76	0.00	241.92	87.75
YBR185C	-2.76	0.00	74.61	27.06
YOR374W	-2.76	0.00	887.71	322.10
YFL019C	-2.75	0.05	22.21	8.07
YML009C	-2.75	0.00	381.75	138.82
YGL071W	-2.75	0.00	61.61	22.41
YLR399C	-2.75	0.00	137.98	50.18
YCL055W	-2.75	0.05	22.15	8.06
YLR459W	-2.75	0.00	42.83	15.58
YDR246W	-2.75	0.00	260.79	94.89
YHR168W	-2.75	0.01	34.05	12.39
YFR014C	-2.75	0.00	103.59	37.71
YOR035C	-2.75	0.00	73.29	26.69
YPL094C	-2.75	0.00	98.18	35.76
YJL140W	-2.74	0.00	166.28	60.59
YFR043C	-2.74	0.03	27.30	9.95
YJL172W	-2.74	0.00	93.40	34.05
YNL306W	-2.74	0.00	230.78	84.22
YHR112C	-2.74	0.00	160.67	58.65
YHL019W-A	-2.74	0.00	80.14	29.27
YBL067C	-2.74	0.02	29.96	10.94
YDR265W	-2.74	0.00	80.69	29.47
YHR073C-B	-2.74	0.00	135.09	49.35
YGL143C	-2.74	0.01	39.85	14.56

YOR070C	-2.74	0.00	57.40	20.99
YLR431C	-2.74	0.02	29.69	10.85
YNL048W	-2.73	0.04	23.06	8.44
YJR082C	-2.73	0.00	154.64	56.59
YHL002W	-2.73	0.00	115.82	42.40
YML031W	-2.73	0.00	50.01	18.31
YJR100C	-2.73	0.00	64.61	23.67
YJR096W	-2.73	0.00	1322.03	484.53
YOR033C	-2.73	0.00	44.82	16.43
YKL072W	-2.73	0.02	28.86	10.59
YDR182W	-2.72	0.00	77.54	28.46
YGL066W	-2.72	0.01	35.11	12.89
YLR118C	-2.72	0.00	109.13	40.08
YKL032C	-2.72	0.00	255.79	93.94
YHR115C	-2.72	0.00	87.42	32.11
YJR127C	-2.72	0.00	73.13	26.86
YOL110W	-2.72	0.00	184.35	67.72
YPR084W	-2.72	0.00	54.63	20.09
YNL280C	-2.72	0.00	45.46	16.72
YOL122C	-2.72	0.00	45.38	16.71
YPR129W	-2.72	0.00	119.31	43.93
YPR106W	-2.72	0.00	90.93	33.49
YDL005C	-2.72	0.00	121.50	44.75
YCL056C	-2.71	0.00	116.81	43.03
YOR331C	-2.71	0.00	512.45	188.88
YMR092C	-2.71	0.00	63.67	23.49
YOR258W	-2.71	0.02	29.71	10.96
YKL169C	-2.71	0.00	189.81	70.06
YDR027C	-2.71	0.01	38.89	14.35
YLR399W-A	-2.71	0.00	122.78	45.32
YPR085C	-2.71	0.00	63.60	23.49
YLR204W	-2.71	0.00	335.96	124.07
YNL212W	-2.71	0.00	77.05	28.47
YKL058W	-2.71	0.00	429.98	158.89
YOL038W	-2.71	0.00	297.99	110.15
YCR028C	-2.70	0.01	40.45	14.97
YAL051W	-2.70	0.00	52.91	19.60
YNL103W	-2.70	0.00	108.80	40.32
YKR006C	-2.70	0.00	97.53	36.16
YNR042W	-2.70	0.00	68.60	25.44
YOR003W	-2.70	0.00	54.53	20.22
YKL202W	-2.69	0.00	364.03	135.19
YDL182W	-2.69	0.00	323.18	120.05
YBR151W	-2.69	0.00	696.72	258.81
YDR387C	-2.69	0.01	36.76	13.66
YBL030C	-2.69	0.00	1079.07	400.94
YMR084W	-2.69	0.00	174.23	64.74

YCR079W	-2.69	0.00	75.81	28.17
YCL010C	-2.69	0.00	49.91	18.55
YFL009W	-2.69	0.00	58.51	21.75
YNL214W	-2.69	0.00	45.80	17.03
YDR532C	-2.69	0.00	57.18	21.26
YDR219C	-2.69	0.00	85.33	31.73
YJR104C	-2.69	0.00	5151.32	1915.31
YOR005C	-2.69	0.01	33.41	12.42
YCR047W-A	-2.69	0.00	353.63	131.50
YPL207W	-2.69	0.00	66.20	24.62
YDL159W	-2.69	0.00	72.84	27.09
YJL009W	-2.69	0.00	188.28	70.05
YBR057C	-2.69	0.00	64.26	23.92
YMR137C	-2.69	0.05	21.88	8.15
YDR207C	-2.69	0.01	36.72	13.67
YGR048W	-2.69	0.00	164.28	61.17
YLR010C	-2.68	0.03	27.86	10.38
YOL084W	-2.68	0.00	245.76	91.60
YDL113C	-2.68	0.00	98.11	36.59
YDR088C	-2.68	0.00	70.11	26.18
YER163C	-2.68	0.00	302.11	112.83
YFL024C	-2.68	0.00	43.81	16.38
YIL042C	-2.67	0.00	67.29	25.17
YLR352W	-2.67	0.04	25.40	9.50
YPL236C	-2.67	0.01	36.70	13.73
YKL136W	-2.67	0.00	107.02	40.08
YPL127C	-2.67	0.00	235.52	88.20
YOR116C	-2.67	0.02	30.03	11.25
YIL144W	-2.67	0.00	48.38	18.12
YCL002C	-2.67	0.00	43.83	16.42
YBR230C	-2.67	0.00	808.99	303.16
YKL022C	-2.67	0.00	48.03	18.01
YBR223W-A	-2.67	0.00	59.22	22.21
YDR493W	-2.67	0.00	57.31	21.49
YPL168W	-2.67	0.00	67.12	25.17
YJR073C	-2.67	0.00	1354.45	508.23
YLR256W	-2.66	0.00	72.13	27.08
YKR087C	-2.66	0.00	50.47	18.95
YJL024C	-2.66	0.00	89.55	33.62
YKR100C	-2.66	0.00	121.18	45.51
YLR138W	-2.66	0.00	85.02	31.94
YMR299C	-2.66	0.00	66.17	24.87
YMR251W	-2.66	0.01	36.96	13.89
YHL040C	-2.66	0.00	53.94	20.28
YDR115W	-2.66	0.00	240.28	90.39
YDL203C	-2.66	0.01	39.00	14.68

YAR002C-A	-2.66	0.00	76.61	28.84
YDR510W	-2.66	0.00	612.43	230.59
YIR001C	-2.65	0.00	74.50	28.06
YGL108C	-2.65	0.00	68.09	25.65
YNR008W	-2.65	0.02	32.90	12.40
YLR078C	-2.65	0.00	87.96	33.15
YNL072W	-2.65	0.04	24.23	9.13
YOR169C	-2.65	0.00	63.70	24.02
YPR104C	-2.65	0.03	26.91	10.16
YOR353C	-2.65	0.00	49.18	18.59
YOL052C-A	-2.64	0.00	3974.73	1502.73
YOL027C	-2.64	0.00	144.51	54.65
YEL034C-A	-2.64	0.00	1616.50	611.38
YJL174W	-2.64	0.00	392.53	148.51
YNL314W	-2.64	0.00	51.10	19.33
YPR166C	-2.64	0.00	99.75	37.74
YLR135W	-2.64	0.02	32.88	12.45
YPR149W	-2.64	0.00	1136.06	430.43
YLR368W	-2.64	0.00	45.18	17.13
YLR254C	-2.64	0.00	112.64	42.75
YGR116W	-2.63	0.02	30.92	11.74
YER057C	-2.63	0.00	156.41	59.39
YLR357W	-2.63	0.01	41.92	15.92
YMR226C	-2.63	0.00	331.64	125.96
YLR216C	-2.63	0.00	1171.35	445.02
YMR246W	-2.63	0.00	271.79	103.41
YGR023W	-2.63	0.00	279.35	106.29
YLR209C	-2.63	0.00	72.49	27.59
YJL096W	-2.63	0.00	128.62	48.96
YDR460W	-2.63	0.00	104.23	39.67
YMR124W	-2.63	0.00	60.20	22.92
YOL053W	-2.63	0.00	68.87	26.22
YJR141W	-2.62	0.03	27.59	10.51
YML130C	-2.62	0.00	217.58	82.95
YDR379W	-2.62	0.04	26.13	9.97
YPL136W	-2.62	0.01	40.56	15.48
YER051W	-2.62	0.00	60.59	23.12
YGR060W	-2.62	0.00	219.70	83.85
YEL063C	-2.62	0.01	36.57	13.96
YIL124W	-2.62	0.00	69.36	26.47
YPL020C	-2.62	0.00	56.65	21.63
YBR108W	-2.62	0.00	118.87	45.38
YGR219W	-2.62	0.00	234.63	89.61
YPR011C	-2.62	0.00	72.31	27.62
YML058W	-2.62	0.00	1339.99	511.85
YPR030W	-2.62	0.00	137.49	52.54
YKL138C-A	-2.62	0.00	140.75	53.78

YMR111C	-2.62	0.00	48.17	18.41
YFR009W	-2.62	0.04	24.69	9.44
YHR116W	-2.62	0.00	139.43	53.29
YDR221W	-2.62	0.04	25.11	9.60
YKL139W	-2.62	0.00	51.87	19.83
YDR117C	-2.62	0.01	34.89	13.34
YDR292C	-2.61	0.01	38.86	14.86
YLR281C	-2.61	0.03	28.35	10.85
YMR040W	-2.61	0.00	136.45	52.29
YNR055C	-2.61	0.00	72.28	27.71
YOR071C	-2.60	0.01	35.14	13.49
YDR491C	-2.60	0.00	94.71	36.37
YGR028W	-2.60	0.00	111.51	42.83
YGR275W	-2.60	0.00	155.09	59.57
YLR208W	-2.60	0.00	123.87	47.62
YDR004W	-2.60	0.01	40.42	15.55
YOL042W	-2.60	0.01	35.19	13.54
YMR096W	-2.60	0.00	370.36	142.52
YGR082W	-2.60	0.00	102.99	39.66
YLR008C	-2.60	0.00	120.56	46.43
YHL009C	-2.59	0.00	55.03	21.21
YNL122C	-2.59	0.00	98.31	37.93
YKL079W	-2.59	0.00	57.56	22.21
YGR006W	-2.59	0.01	36.10	13.93
YNL239W	-2.59	0.00	73.71	28.45
YBR217W	-2.59	0.01	41.03	15.83
YPL076W	-2.59	0.05	24.17	9.33
YNL307C	-2.59	0.00	78.89	30.49
YHR180W-A	-2.59	0.01	36.77	14.22
YGR042W	-2.59	0.00	71.60	27.68
YPR130C	-2.59	0.00	170.47	65.94
YMR210W	-2.58	0.00	130.99	50.72
YML085C	-2.58	0.00	184.26	71.43
YER122C	-2.58	0.00	127.56	49.45
YNL238W	-2.58	0.01	40.92	15.88
YAL027W	-2.58	0.01	43.04	16.71
YIR025W	-2.58	0.00	90.04	34.96
YOR304W	-2.57	0.05	24.78	9.62
YHR176W	-2.57	0.00	60.56	23.54
YGL054C	-2.57	0.00	113.11	43.98
YIL142W	-2.57	0.00	179.45	69.78
YOR332W	-2.57	0.00	646.61	251.73
YNL130C	-2.57	0.00	56.87	22.17
YGR280C	-2.56	0.00	112.29	43.78
YDR375C	-2.56	0.00	63.94	24.95
YOR335C	-2.56	0.00	70.84	27.68

YMR304C-A	-2.56	0.05	25.44	9.94
YGL111W	-2.56	0.00	71.02	27.76
YNL161W	-2.56	0.00	59.40	23.22
YNL323W	-2.56	0.00	72.84	28.49
YOL155C	-2.56	0.00	754.75	295.33
YML009C-A	-2.56	0.00	186.93	73.15
YLL060C	-2.55	0.00	72.74	28.47
YGR005C	-2.55	0.00	139.57	54.64
YOR089C	-2.55	0.00	538.76	211.01
YPR134W	-2.55	0.01	39.74	15.57
YMR085W	-2.55	0.00	265.88	104.19
YPR109W	-2.55	0.00	87.05	34.13
YOR139C	-2.55	0.00	129.29	50.70
YPL124W	-2.55	0.05	24.18	9.49
YDR155C	-2.55	0.00	2825.80	1109.96
YGR255C	-2.54	0.00	68.04	26.75
YKL109W	-2.54	0.00	664.00	261.17
YPL107W	-2.54	0.00	88.73	34.91
YNL308C	-2.54	0.00	80.45	31.65
YOR002W	-2.54	0.03	30.08	11.84
YBR009C	-2.54	0.00	1169.25	460.23
YNR041C	-2.54	0.00	64.24	25.29
YFL002C	-2.54	0.02	32.19	12.68
YAL014C	-2.54	0.00	124.30	48.99
YDR034C	-2.54	0.02	34.80	13.72
YBR207W	-2.54	0.00	187.76	74.03
YGL041C	-2.53	0.00	138.72	54.74
YDR439W	-2.53	0.01	36.80	14.53
YBR161W	-2.53	0.02	34.81	13.75
YGL181W	-2.53	0.00	200.33	79.12
YGL128C	-2.53	0.01	45.62	18.02
YHR121W	-2.53	0.00	72.59	28.69
YLR354C	-2.53	0.00	452.75	178.96
YPR148C	-2.53	0.00	221.59	87.66
YKL095W	-2.53	0.00	47.71	18.88
YBR036C	-2.52	0.00	298.16	118.11
YLR246W	-2.52	0.00	71.91	28.49
YLR088W	-2.52	0.05	24.81	9.84
YPR056W	-2.52	0.01	45.63	18.09
YKL167C	-2.52	0.00	159.95	63.45
YMR083W	-2.52	0.00	868.93	344.71
YOR192C-C	-2.52	0.00	159.21	63.18
YPL183W-A	-2.52	0.00	141.16	56.03
YGL019W	-2.52	0.00	132.46	52.61
YKL188C	-2.52	0.03	30.41	12.09
YOL001W	-2.52	0.02	32.94	13.09
YBL084C	-2.52	0.00	49.77	19.79

YBR035C	-2.52	0.00	342.17	136.05
YKL125W	-2.51	0.01	41.46	16.50
YJR112W-A	-2.51	0.00	120.25	47.88
YFL013W-A	-2.51	0.00	119.52	47.59
YBR222C	-2.51	0.00	339.83	135.42
YOR001W	-2.51	0.03	31.44	12.53
YLL050C	-2.51	0.00	367.57	146.59
YHR182C-A	-2.51	0.00	279.14	111.38
YLR433C	-2.50	0.05	26.11	10.42
YML081W	-2.50	0.01	39.98	15.96
YGR010W	-2.50	0.00	57.91	23.13
YER025W	-2.50	0.00	134.15	53.60
YLR226W	-2.50	0.00	55.32	22.11
YDR225W	-2.50	0.00	1041.18	416.50
YML028W	-2.50	0.00	703.36	281.83
YEL075W-A	-2.50	0.00	85.90	34.42
YGR133W	-2.49	0.00	110.96	44.49
YBL102W	-2.49	0.00	127.71	51.21
YLR046C	-2.49	0.02	36.59	14.67
YCR039C	-2.49	0.00	88.22	35.39
YOR133W	-2.49	0.00	306.43	122.92
YOL062C	-2.49	0.00	63.87	25.62
YGL255W	-2.49	0.00	96.53	38.77
YMR172W	-2.49	0.01	38.63	15.54
YPR103W	-2.48	0.00	233.35	93.93
YIL041W	-2.48	0.00	213.66	86.03
YLR457C	-2.48	0.04	28.56	11.50
YMR060C	-2.48	0.04	28.50	11.48
YIR014W	-2.48	0.01	42.96	17.32
YBR111C	-2.48	0.00	229.05	92.35
YGL152C	-2.48	0.00	106.57	43.05
YOR158W	-2.47	0.00	124.53	50.32
YLR245C	-2.47	0.00	73.88	29.88
YER144C	-2.47	0.00	56.83	22.99
YHR138C	-2.47	0.00	1800.94	728.69
YIL022W	-2.47	0.00	262.85	106.44
YKR065C	-2.47	0.00	86.50	35.04
YKL019W	-2.47	0.00	63.55	25.75
YNL011C	-2.47	0.01	41.50	16.83
YHL004W	-2.47	0.00	83.85	34.00
YDL247W-A	-2.46	0.00	145.90	59.22
YHR007C	-2.46	0.00	139.43	56.64
YIL111W	-2.46	0.00	394.56	160.30
YDR524C	-2.46	0.01	50.00	20.32
YDL052C	-2.46	0.00	82.68	33.60
YBL056W	-2.46	0.00	186.83	75.94
YLR025W	-2.46	0.00	292.95	119.09

YDL045C	-2.46	0.00	57.77	23.49
YIL038C	-2.46	0.04	29.33	11.93
YGL176C	-2.46	0.02	35.88	14.60
YDR090C	-2.46	0.00	118.16	48.08
YCL034W	-2.46	0.00	202.83	82.58
YDR258C	-2.46	0.00	522.12	212.58
YHR032C-A	-2.46	0.00	116.86	47.59
YDL224C	-2.46	0.04	29.64	12.07
YER050C	-2.45	0.00	321.22	130.86
YMR264W	-2.45	0.00	127.42	51.94
YGL222C	-2.45	0.00	62.17	25.36
YJR074W	-2.45	0.00	111.03	45.30
YBL026W	-2.45	0.00	104.16	42.52
YKL201C	-2.45	0.00	102.07	41.67
YBL089W	-2.45	0.03	31.08	12.69
YBR200W	-2.45	0.00	62.77	25.67
YFR025C	-2.44	0.03	32.32	13.22
YGR174W-A	-2.44	0.05	26.75	10.94
YCR028C-A	-2.44	0.00	112.52	46.03
YPL274W	-2.44	0.01	48.02	19.68
YOR244W	-2.44	0.00	96.16	39.41
YBR197C	-2.44	0.00	52.50	21.54
YGL029W	-2.44	0.01	41.75	17.13
YOR219C	-2.44	0.05	26.54	10.89
YIR015W	-2.43	0.00	61.01	25.09
YNL159C	-2.43	0.00	106.19	43.69
YDL120W	-2.43	0.00	189.98	78.20
YJL146W	-2.43	0.02	34.52	14.22
YER053C	-2.43	0.00	295.77	121.85
YKL002W	-2.43	0.00	252.36	104.03
YDR054C	-2.43	0.00	464.64	191.57
YFR021W	-2.42	0.00	57.53	23.73
YPR023C	-2.42	0.00	320.22	132.11
YBL051C	-2.42	0.02	38.01	15.68
YFL045C	-2.42	0.00	142.87	58.97
YER029C	-2.42	0.00	96.94	40.05
YDR205W	-2.42	0.05	26.46	10.94
YOR122C	-2.42	0.00	762.90	315.60
YLR072W	-2.41	0.01	43.34	17.95
YJL055W	-2.41	0.00	348.18	144.27
YLR005W	-2.41	0.00	71.69	29.71
YGR235C	-2.41	0.00	262.92	109.01
YNR061C	-2.41	0.00	70.70	29.32
YGL090W	-2.41	0.01	43.02	17.84
YGL091C	-2.41	0.00	141.96	58.89
YLR403W	-2.41	0.00	67.82	28.14

YNL098C	-2.41	0.00	242.01	100.58
YER099C	-2.41	0.00	147.06	61.13
YNL227C	-2.41	0.02	37.88	15.75
YJL121C	-2.41	0.00	97.27	40.44
YKL206C	-2.40	0.01	50.29	20.91
YML020W	-2.40	0.01	44.41	18.48
YMR189W	-2.40	0.04	30.68	12.77
YKR101W	-2.40	0.04	29.16	12.14
YGR295C	-2.40	0.00	238.60	99.44
YGR149W	-2.40	0.00	204.10	85.09
YJR068W	-2.40	0.00	56.43	23.54
YAL060W	-2.40	0.00	942.59	393.47
YDL134C	-2.40	0.00	168.15	70.20
YDL159C-B	-2.39	0.00	117.60	49.11
YMR073C	-2.39	0.00	83.23	34.76
YDR393W	-2.39	0.03	33.12	13.84
YNL317W	-2.39	0.01	50.83	21.24
YIL113W	-2.39	0.00	73.27	30.62
YLL051C	-2.39	0.00	61.53	25.72
YIL152W	-2.39	0.00	79.76	33.34
YNL079C	-2.39	0.00	279.74	116.96
YOR111W	-2.39	0.01	52.09	21.79
YHR002W	-2.39	0.00	81.21	33.97
YJL075C	-2.39	0.00	60.02	25.11
YIL006W	-2.39	0.03	32.17	13.46
YKL061W	-2.39	0.00	235.73	98.70
YNL187W	-2.39	0.04	29.63	12.41
YOR381W	-2.39	0.05	27.79	11.64
YDR429C	-2.38	0.00	178.98	75.07
YBR203W	-2.38	0.00	108.21	45.39
YNL123W	-2.38	0.01	51.73	21.70
YPL059W	-2.38	0.00	164.23	68.92
YGR288W	-2.38	0.01	45.60	19.14
YNL111C	-2.38	0.00	80.73	33.91
YER147C	-2.38	0.01	48.73	20.47
YOR376W-A	-2.38	0.01	53.21	22.37
YOL049W	-2.38	0.02	37.58	15.82
YNL167C	-2.37	0.03	34.87	14.69
YNR025C	-2.37	0.00	53.98	22.74
YGR007W	-2.37	0.00	151.72	63.91
YER089C	-2.37	0.00	127.17	53.58
YGL098W	-2.37	0.00	85.30	35.94
YGL172W	-2.37	0.00	82.52	34.79
YIL142C-A	-2.37	0.00	80.45	33.92
YJL217W	-2.37	0.00	363.00	153.16
YNL335W	-2.37	0.03	34.60	14.60

YNL081C	-2.37	0.00	269.02	113.54
YDR001C	-2.37	0.00	396.31	167.29
YFL062W	-2.37	0.05	28.74	12.13
YIL135C	-2.37	0.00	138.68	58.56
YHR146W	-2.37	0.00	254.65	107.57
YOR138C	-2.37	0.00	73.31	30.97
YOR159C	-2.37	0.00	131.73	55.66
YDL001W	-2.37	0.02	38.08	16.10
YML092C	-2.37	0.00	216.05	91.34
YNL230C	-2.36	0.03	36.19	15.31
YLR330W	-2.36	0.00	158.12	66.88
YDR480W	-2.36	0.00	56.16	23.76
YDR445C	-2.36	0.04	31.60	13.37
YBR242W	-2.36	0.00	82.36	34.87
YBL091C	-2.36	0.00	143.36	60.70
YDL106C	-2.36	0.00	77.34	32.75
YJR139C	-2.36	0.00	151.34	64.10
YNR023W	-2.36	0.04	30.46	12.91
YDL002C	-2.36	0.00	66.48	28.20
YFL054C	-2.36	0.00	259.52	110.13
YBR152W	-2.36	0.04	31.23	13.26
YIL043C	-2.36	0.00	205.06	87.05
YFL049W	-2.36	0.01	49.18	20.88
YHR001W-A	-2.36	0.00	1436.99	610.12
YKR066C	-2.35	0.00	1115.00	473.50
YDR348C	-2.35	0.00	108.04	45.90
YPR094W	-2.35	0.00	59.01	25.07
YBR172C	-2.35	0.01	43.74	18.58
YOR307C	-2.35	0.02	37.58	15.98
YGL167C	-2.35	0.00	62.86	26.73
YPL116W	-2.35	0.05	29.28	12.45
YHR072W	-2.35	0.05	29.95	12.74
YGR106C	-2.35	0.00	104.18	44.37
YDR320C-A	-2.35	0.00	110.84	47.23
YDR179C	-2.35	0.04	32.28	13.75
YDR519W	-2.35	0.00	99.26	42.30
YOL054W	-2.35	0.00	94.25	40.17
YGR125W	-2.34	0.03	33.86	14.44
YKR070W	-2.34	0.01	46.20	19.71
YGR154C	-2.34	0.02	39.69	16.94
YNL010W	-2.34	0.00	146.39	62.49
YLR007W	-2.34	0.00	132.31	56.49
YAL043C	-2.34	0.04	32.32	13.80
YEL006W	-2.34	0.00	58.89	25.18
YGL079W	-2.34	0.05	28.91	12.36
YGL053W	-2.34	0.00	121.72	52.08

YIL051C	-2.34	0.00	259.59	111.11
YNR035C	-2.34	0.00	113.49	48.59
YMR026C	-2.33	0.03	35.43	15.18
YJL156W-A	-2.33	0.01	43.34	18.58
YBR231C	-2.33	0.00	102.88	44.11
YDR319C	-2.33	0.00	59.91	25.69
YFL028C	-2.33	0.01	48.65	20.86
YLR260W	-2.33	0.01	47.74	20.47
YGL244W	-2.33	0.00	59.51	25.54
YNL244C	-2.33	0.00	801.57	344.04
YML052W	-2.33	0.00	83.71	35.95
YJR059W	-2.33	0.00	114.97	49.40
YDR516C	-2.33	0.00	324.27	139.36
YDR268W	-2.33	0.05	29.90	12.86
YLR268W	-2.32	0.00	85.99	36.99
YMR054W	-2.32	0.00	71.07	30.57
YGR019W	-2.32	0.00	249.55	107.46
YNL245C	-2.32	0.00	141.61	60.98
YHR213W-A	-2.32	0.01	44.07	18.98
YEL020C	-2.32	0.01	52.61	22.66
YHL030W-A	-2.32	0.00	83.85	36.12
YLL018C	-2.32	0.00	132.76	57.20
YDL025W-A	-2.32	0.00	419.25	180.69
YCR004C	-2.32	0.00	396.93	171.08
YMR277W	-2.32	0.04	32.26	13.91
YOL029C	-2.32	0.01	47.84	20.63
YLR220W	-2.32	0.00	142.91	61.62
YOR358W	-2.32	0.00	161.06	69.46
YJR044C	-2.32	0.01	49.36	21.30
YKR085C	-2.32	0.00	98.18	42.41
YHR077C	-2.31	0.04	31.79	13.74
YDR289C	-2.31	0.00	71.22	30.80
YHR156C	-2.31	0.02	38.85	16.81
YLR191W	-2.31	0.00	97.50	42.19
YBL029W	-2.31	0.00	62.33	26.99
YBR113W	-2.31	0.03	35.81	15.50
YLR116W	-2.31	0.00	96.46	41.77
YKR063C	-2.31	0.05	30.92	13.41
YMR021C	-2.30	0.00	102.96	44.68
YGL212W	-2.30	0.05	29.82	12.94
YHL014C	-2.30	0.02	41.15	17.87
YNL147W	-2.30	0.00	153.60	66.73
YGR267C	-2.30	0.00	230.93	100.47
YDR139C	-2.30	0.00	172.54	75.11
YHR071W	-2.30	0.00	350.62	152.65
YPR072W	-2.30	0.01	53.06	23.11

YML074C	-2.29	0.00	164.34	71.62
YGR155W	-2.29	0.00	139.72	60.91
YDR026C	-2.29	0.05	31.68	13.82
YFL038C	-2.29	0.00	636.36	277.62
YGL185C	-2.29	0.02	40.44	17.64
YBL011W	-2.29	0.00	59.60	26.02
YPL080C	-2.29	0.05	31.54	13.78
YCR023C	-2.29	0.00	158.76	69.40
YGL153W	-2.29	0.00	80.36	35.13
YDR368W	-2.29	0.00	178.68	78.12
YGL077C	-2.29	0.00	60.29	26.36
YBL094C	-2.29	0.00	396.77	173.59
YHR034C	-2.28	0.02	42.84	18.76
YJL003W	-2.28	0.00	99.00	43.37
YGR204W	-2.28	0.00	138.17	60.59
YDR172W	-2.28	0.00	86.08	37.77
YLR251W	-2.28	0.01	52.09	22.86
YMR061W	-2.28	0.02	40.44	17.75
YNL197C	-2.28	0.03	37.55	16.49
YMR241W	-2.28	0.00	186.53	81.92
YIL165C	-2.28	0.01	48.56	21.33
YOR357C	-2.28	0.00	84.49	37.11
YNL199C	-2.28	0.01	54.89	24.12
YIR029W	-2.28	0.01	46.31	20.35
YFR018C	-2.27	0.00	73.89	32.48
YGR037C	-2.27	0.00	543.35	238.91
YPR178W	-2.27	0.01	51.28	22.56
YIL164C	-2.27	0.02	45.17	19.88
YLR327C	-2.27	0.00	9895.66	4358.05
YIL090W	-2.27	0.03	38.94	17.15
YER098W	-2.27	0.00	91.01	40.12
YLR337C	-2.27	0.00	84.80	37.39
YML016C	-2.27	0.02	45.40	20.02
YAL055W	-2.27	0.00	66.25	29.21
YNL149C	-2.26	0.00	378.93	167.42
YGL125W	-2.26	0.01	56.82	25.13
YJL116C	-2.26	0.00	120.75	53.44
YJL013C	-2.26	0.02	40.91	18.12
YMR135W-A	-2.26	0.01	48.28	21.39
YLR085C	-2.26	0.03	38.82	17.20
YBR118W	-2.26	0.00	3664.48	1623.82
YJR015W	-2.26	0.01	55.01	24.38
YBR103W	-2.26	0.02	42.20	18.70
YLR288C	-2.25	0.04	33.32	14.78
YDR483W	-2.25	0.00	272.70	121.03
YEL002C	-2.25	0.01	47.18	20.95

YOR008C	-2.25	0.00	173.67	77.18
YIL145C	-2.25	0.00	97.17	43.19
YGL101W	-2.25	0.00	74.24	33.00
YBR145W	-2.25	0.00	72.30	32.15
YNL220W	-2.25	0.00	100.71	44.79
YER028C	-2.25	0.03	37.20	16.55
YDL193W	-2.25	0.00	80.28	35.72
YGL250W	-2.25	0.01	55.35	24.65
YGL068W	-2.25	0.00	138.57	61.72
YPL063W	-2.24	0.00	81.70	36.40
YKL075C	-2.24	0.02	43.13	19.23
YDR517W	-2.24	0.00	185.57	82.73
YML116W	-2.24	0.01	50.19	22.40
YDR096W	-2.24	0.00	95.04	42.44
YBR049C	-2.24	0.03	37.89	16.93
YML062C	-2.24	0.04	35.04	15.66
YNL133C	-2.24	0.00	108.79	48.62
YCL011C	-2.24	0.00	150.65	67.36
YPR073C	-2.24	0.01	60.43	27.03
YBL038W	-2.23	0.00	165.09	73.89
YPL159C	-2.23	0.00	260.30	116.75
YDR229W	-2.23	0.05	33.01	14.81
YGR086C	-2.23	0.00	709.45	318.44
YIL068W-A	-2.23	0.04	35.70	16.03
YJL023C	-2.23	0.01	49.82	22.37
YOL103W	-2.23	0.01	53.26	23.92
YDL072C	-2.23	0.00	296.35	133.13
YBL025W	-2.22	0.00	92.46	41.58
YNL213C	-2.22	0.00	157.07	70.63
YPL145C	-2.22	0.01	56.96	25.62
YGR262C	-2.22	0.00	65.13	29.30
YKL012W	-2.22	0.00	65.90	29.66
YEL009C	-2.22	0.00	877.67	395.19
YOR262W	-2.22	0.00	113.85	51.30
YPL134C	-2.22	0.00	97.60	44.00
YPL096C-A	-2.22	0.01	54.38	24.52
YPR053C	-2.22	0.00	86.33	38.96
YPR005C	-2.22	0.00	129.75	58.58
YBR234C	-2.21	0.00	74.92	33.84
YKL018C-A	-2.21	0.00	108.17	48.86
YMR105C	-2.21	0.00	420.94	190.17
YMR071C	-2.21	0.00	192.78	87.12
YBL039W-B	-2.21	0.05	33.54	15.16
YBL021C	-2.21	0.00	109.73	49.60
YER152W-A	-2.21	0.00	117.79	53.27
YJR021C	-2.21	0.00	122.18	55.26
YCL030C	-2.21	0.00	149.80	67.76

YNL268W	-2.21	0.00	149.61	67.74
YOR027W	-2.21	0.00	921.35	417.28
YMR028W	-2.21	0.05	32.44	14.70
YNR006W	-2.21	0.00	87.95	39.86
YPL182C	-2.21	0.00	112.67	51.06
YJL078C	-2.21	0.00	183.15	83.02
YLL026W	-2.21	0.00	1607.43	728.78
YBL029C-A	-2.21	0.00	176.75	80.15
YIL007C	-2.21	0.00	84.42	38.28
YNL286W	-2.20	0.05	34.38	15.60
YOL044W	-2.20	0.00	69.11	31.40
YKR022C	-2.20	0.01	58.21	26.45
YGR009C	-2.20	0.00	163.94	74.51
YGR281W	-2.20	0.00	73.07	33.23
YKR062W	-2.20	0.00	158.08	71.94
YJR048W	-2.20	0.00	653.45	297.46
YML098W	-2.20	0.00	158.71	72.27
YER083C	-2.20	0.00	76.96	35.05
YOR044W	-2.19	0.00	148.86	67.87
YIL004C	-2.19	0.00	116.10	52.95
YGR270C-A	-2.19	0.05	33.02	15.07
YLR262C-A	-2.19	0.00	212.53	96.97
YNL285W	-2.19	0.00	97.54	44.52
YCR095C	-2.19	0.03	41.98	19.17
YOL026C	-2.19	0.00	141.77	64.75
YDR366C	-2.19	0.00	553.85	253.01
YER066C-A	-2.19	0.00	232.84	106.39
YLL018C-A	-2.19	0.00	139.33	63.67
YNL056W	-2.19	0.00	204.86	93.68
YDR476C	-2.19	0.00	236.36	108.10
YLL019W-A	-2.19	0.00	210.30	96.20
YDR469W	-2.19	0.00	66.70	30.52
YKL104C	-2.18	0.00	177.16	81.10
YBL048W	-2.18	0.00	65.31	29.90
YOR221C	-2.18	0.00	78.39	35.92
YKL041W	-2.18	0.00	184.10	84.42
YBR041W	-2.18	0.03	39.92	18.31
YPR059C	-2.18	0.03	39.32	18.04
YIL160C	-2.18	0.00	151.05	69.32
YOR335W-A	-2.18	0.00	146.74	67.37
YER161C	-2.18	0.00	192.49	88.40
YDR275W	-2.18	0.00	215.57	99.03
YGL069C	-2.18	0.00	116.71	53.63
YOR115C	-2.18	0.02	47.22	21.70
YNL143C	-2.18	0.01	55.85	25.67
YLR094C	-2.18	0.00	214.96	98.82

YCL067C	-2.17	0.00	79.78	36.69
YPL224C	-2.17	0.00	85.41	39.29
YMR024W	-2.17	0.00	79.83	36.73
YJL133C-A	-2.17	0.00	1637.86	754.66
YDL165W	-2.17	0.01	51.64	23.79
YOR194C	-2.16	0.00	166.68	77.01
YMR262W	-2.16	0.03	40.52	18.73
YNR024W	-2.16	0.04	37.44	17.31
YHR209W	-2.16	0.00	121.04	55.99
YOR260W	-2.16	0.03	40.19	18.59
YJR075W	-2.16	0.00	90.92	42.09
YHR206W	-2.16	0.00	86.81	40.20
YGL022W	-2.16	0.00	108.08	50.07
YPR107C	-2.16	0.00	67.50	31.27
YPL218W	-2.16	0.00	241.89	112.07
YNL206C	-2.16	0.01	63.07	29.22
YDL074C	-2.16	0.02	46.20	21.42
YBL095W	-2.16	0.00	271.12	125.73
YKL065C	-2.16	0.00	402.74	186.78
YOL086W-A	-2.15	0.00	152.73	70.89
YIL027C	-2.15	0.04	38.82	18.02
YDR003W-A	-2.15	0.00	198.89	92.34
YGR061C	-2.15	0.04	38.98	18.10
YPR062W	-2.15	0.00	678.05	315.00
YNL150W	-2.15	0.00	371.16	172.47
YCL058W-A	-2.15	0.00	106.47	49.54
YMR243C	-2.15	0.00	137.08	63.83
YDR100W	-2.15	0.04	39.74	18.51
YJR144W	-2.14	0.02	51.24	23.89
YPR133C	-2.14	0.00	146.63	68.44
YNR032W	-2.14	0.01	53.12	24.82
YDR051C	-2.14	0.00	86.98	40.66
YDR129C	-2.14	0.00	401.61	187.86
YJL151C	-2.13	0.00	1094.58	512.83
YHR058C	-2.13	0.03	41.78	19.58
YGL168W	-2.13	0.00	143.53	67.26
YKL100W-A	-2.13	0.00	127.87	59.93
YDR167W	-2.13	0.00	136.81	64.17
YPL188W	-2.13	0.04	39.75	18.65
YOR039W	-2.13	0.00	135.57	63.62
YGL026C	-2.13	0.00	99.19	46.63
YNL074C	-2.13	0.00	229.29	107.81
YHL031C	-2.13	0.00	83.94	39.47
YBL076C	-2.12	0.01	57.30	26.99
YHR050W	-2.12	0.00	120.51	56.76
YLR230W	-2.12	0.00	118.79	55.99

YGL242C	-2.12	0.03	46.07	21.73
YHR183W	-2.12	0.00	435.72	205.68
YPL154C	-2.12	0.00	610.28	288.25
YDL053C	-2.12	0.00	192.04	90.74
YML126C	-2.11	0.00	92.97	43.98
YGL137W	-2.11	0.02	47.70	22.58
YPL101W	-2.11	0.01	62.57	29.62
YPL181W	-2.11	0.00	192.75	91.36
YBL046W	-2.11	0.00	80.34	38.09
YBR052C	-2.11	0.00	331.03	156.98
YKL175W	-2.11	0.00	118.66	56.32
YBL036C	-2.11	0.00	89.62	42.55
YLR326W	-2.10	0.00	82.89	39.41
YDR340W	-2.10	0.00	313.19	148.89
YKL156W	-2.10	0.00	400.81	190.61
YDR194C	-2.10	0.01	65.00	30.92
YHR087W	-2.10	0.00	2091.74	995.03
YER002W	-2.10	0.00	206.19	98.10
YGL049C	-2.10	0.01	61.31	29.22
YER067W	-2.10	0.00	1596.63	761.43
YPR065W	-2.10	0.00	197.92	94.40
YDR273W	-2.09	0.02	48.28	23.06
YLR379W	-2.09	0.03	47.46	22.67
YDR533C	-2.09	0.00	215.88	103.18
YMR186W	-2.09	0.00	592.59	283.35
YIL077C	-2.09	0.00	233.33	111.68
YNL125C	-2.09	0.00	123.60	59.18
YDR092W	-2.09	0.00	180.36	86.39
YJL134W	-2.09	0.00	77.00	36.89
YEL027W	-2.09	0.00	362.09	173.54
YJL053W	-2.08	0.01	60.46	29.00
YJL152W	-2.08	0.00	900.51	432.01
YDR152W	-2.08	0.00	117.03	56.22
YOL070C	-2.08	0.04	42.34	20.35
YDR032C	-2.08	0.00	377.01	181.22
YGR057C	-2.08	0.00	97.74	47.00
YNL185C	-2.08	0.00	137.11	65.98
YML053C	-2.08	0.03	47.04	22.64
YNL173C	-2.08	0.00	189.69	91.40
YNL330C	-2.08	0.00	77.67	37.43
YGL044C	-2.07	0.03	45.95	22.15
YPR176C	-2.07	0.00	74.14	35.75
YJR014W	-2.07	0.00	144.73	69.83
YPL240C	-2.07	0.00	2075.83	1001.57
YER088C-A	-2.07	0.04	41.73	20.17
YPL215W	-2.07	0.00	85.28	41.23
YIL023C	-2.07	0.00	86.99	42.12

YGL036W	-2.06	0.00	81.20	39.35
YDL084W	-2.06	0.00	98.86	47.93
YGR084C	-2.06	0.05	40.01	19.41
R0040C	-2.06	0.00	2866.12	1391.61
YIL154C	-2.06	0.00	194.40	94.42
YKL059C	-2.06	0.01	70.05	34.02
YGR038W	-2.06	0.01	60.07	29.21
YNL168C	-2.06	0.03	49.34	24.00
YJL178C	-2.06	0.01	69.36	33.75
YMR180C	-2.06	0.02	57.01	27.74
YFR030W	-2.05	0.02	55.14	26.85
YDL202W	-2.05	0.04	43.60	21.24
YBL096C	-2.05	0.01	71.23	34.70
YAL039C	-2.05	0.00	383.38	186.83
YOR135C	-2.05	0.00	179.28	87.39
YML100W	-2.05	0.00	140.94	68.71
YJL167W	-2.05	0.00	155.82	75.98
YNL108C	-2.05	0.02	57.78	28.18
YMR046W-A	-2.05	0.00	250.09	121.99
YDL046W	-2.05	0.00	638.03	311.55
YNL290W	-2.05	0.02	55.76	27.23
YNL086W	-2.05	0.02	51.29	25.05
YPR012W	-2.05	0.01	63.13	30.86
YNL135C	-2.04	0.00	447.14	218.68
YOR140W	-2.04	0.00	94.37	46.22
YJL127C-B	-2.04	0.00	149.90	73.43
YER048W-A	-2.04	0.00	274.05	134.25
YJL202C	-2.04	0.03	50.60	24.80
YGL001C	-2.04	0.00	106.61	52.27
YGL109W	-2.04	0.00	77.06	37.80
YOR155C	-2.04	0.02	52.38	25.70
YCR047C	-2.04	0.00	297.35	146.06
YPL202C	-2.03	0.01	77.57	38.19
YDR074W	-2.03	0.00	241.06	118.89
YEL071W	-2.03	0.00	841.61	415.44
YNL099C	-2.03	0.00	111.13	54.87
YJL026C-A	-2.03	0.00	120.39	59.45
YNL312W	-2.02	0.00	84.38	41.68
YKL160W	-2.02	0.00	202.88	100.25
YDR405W	-2.02	0.00	217.33	107.52
YDR333C	-2.02	0.02	57.68	28.54
YOR265W	-2.02	0.05	41.14	20.36
YFR044C	-2.02	0.00	84.76	41.95
YPL106C	-2.02	0.00	544.39	269.75
YNL031C	-2.02	0.00	968.25	479.83
YGR094W	-2.02	0.05	41.41	20.54

YIR004W	-2.01	0.00	96.82	48.07
YER019C-A	-2.01	0.00	292.29	145.20
YOR251C	-2.01	0.02	53.68	26.70
YCR084C	-2.01	0.00	86.43	43.01
YFR001W	-2.01	0.04	45.20	22.49
YHR100C	-2.01	0.05	41.59	20.70
YOL158C	-2.01	0.00	89.03	44.32
YNR034W-A	-2.01	0.00	3563.81	1775.82
YNL107W	-2.01	0.02	61.87	30.84
YBR267W	-2.01	0.02	54.27	27.06
YMR134W	-2.01	0.00	257.89	128.59
YNL234W	-2.00	0.03	49.63	24.77
YER042W	-2.00	0.00	233.64	116.62
YDR385W	-2.00	0.00	160.74	80.36
YLR200W	-2.00	0.01	62.89	31.45
YGL245W	-2.00	0.01	73.00	36.51
YIL156W-B	-2.00	0.00	170.25	85.18
YML131W	-2.00	0.00	711.75	356.15
YDR465C	2.00	0.04	12.59	25.20
YLR134W	2.01	0.00	65.19	130.84
YLR180W	2.01	0.00	126.76	255.03
YLR099C	2.01	0.00	127.42	256.49
YBR083W	2.02	0.02	15.75	31.79
YHR049W	2.03	0.00	54.21	109.92
YPL250C	2.04	0.00	84.00	171.37
YMR305C	2.05	0.00	111.15	227.45
YNL043C	2.06	0.00	139.49	287.02
YHL015W-A	2.06	0.01	16.47	33.99
YGL179C	2.07	0.00	27.31	56.67
YNR003W-A	2.08	0.04	10.80	22.43
YER064C	2.09	0.03	12.01	25.08
YER127W	2.09	0.04	11.24	23.51
YDR384C	2.10	0.02	13.06	27.43
YDR448W	2.11	0.04	10.51	22.12
YER035W	2.14	0.00	223.26	478.21
YPL239W	2.14	0.00	47.45	101.65
YDL129W	2.15	0.00	23.98	51.65
YFR022W	2.16	0.00	79.57	171.51
YOL047C	2.16	0.00	23.37	50.42
YHR088W	2.16	0.00	18.98	41.09
YML101C-A	2.18	0.01	14.44	31.53
YKR061W	2.19	0.00	24.51	53.57
YFL053W	2.19	0.00	46.14	101.00
YDR046C	2.19	0.02	12.68	27.83
YLL056C	2.21	0.00	70.39	155.27
YOR338W	2.22	0.00	102.74	227.60

YHR094C	2.22	0.00	141.05	313.52
YOL080C	2.23	0.03	9.98	22.24
YKR092C	2.24	0.00	19.42	43.44
YNL231C	2.27	0.00	106.72	242.27
YDR213W	2.27	0.00	22.89	52.00
YLR375W	2.27	0.00	275.01	625.18
YLL024C	2.29	0.00	198.52	454.02
YKR097W	2.35	0.00	72.95	171.32
YMR307W	2.40	0.00	111.29	266.88
YDR345C	2.41	0.00	1409.49	3400.44
YGL134W	2.41	0.00	125.44	302.69
YAL037C-A	2.42	0.05	6.76	16.37
YGR036C	2.42	0.02	8.91	21.59
YJR094C	2.43	0.00	22.88	55.54
YKL062W	2.43	0.00	50.43	122.55
YPR078C	2.44	0.04	7.19	17.58
YGL209W	2.44	0.00	97.59	238.57
YER130C	2.46	0.00	77.62	191.02
YBR018C	2.47	0.01	10.45	25.82
YLR179C	2.48	0.00	128.89	320.19
YOR274W	2.50	0.00	22.97	57.34
YMR238W	2.51	0.00	81.84	205.06
YMR307C-A	2.51	0.00	110.94	278.54
YEL040W	2.53	0.00	23.52	59.43
YBR182C	2.55	0.00	65.02	165.61
YDR297W	2.55	0.00	140.93	359.69
YPR174C	2.59	0.05	6.04	15.62
YGR140W	2.59	0.01	9.48	24.60
YPR145C-A	2.60	0.00	91.01	236.41
YKR091W	2.60	0.00	74.43	193.61
YGR250C	2.61	0.00	200.11	521.68
YNL141W	2.61	0.01	8.43	22.00
YOR049C	2.62	0.00	126.90	332.04
YKL159C	2.64	0.00	53.39	141.07
YLR415C	2.65	0.00	12.80	33.88
YPL088W	2.66	0.00	69.61	185.30
YOL124C	2.72	0.02	6.67	18.13
YOL136C	2.74	0.00	52.14	142.95
YGR211W	2.77	0.00	82.51	228.79
YDR259C	2.77	0.01	8.46	23.46
YMR195W	2.78	0.00	172.12	478.21
YIR035C	2.80	0.00	180.28	503.89
YAR028W	2.80	0.00	39.87	111.60
YBR157C	2.80	0.05	4.83	13.55
YNL160W	2.82	0.00	1716.73	4839.01
YMR315W-A	2.83	0.01	8.73	24.68

YBR034C	2.84	0.00	25.65	72.91
YOL010W	2.88	0.00	17.03	49.03
YNL065W	2.89	0.00	15.96	46.09
YLR112W	2.89	0.05	4.49	12.99
YNL112W	2.90	0.00	9.43	27.30
YER103W	2.95	0.00	376.96	1113.53
YDR072C	2.96	0.00	73.05	216.24
YDR044W	3.00	0.00	64.61	193.96
YNR009W	3.07	0.00	15.01	46.11
YLL028W	3.08	0.00	64.35	198.10
YBL043W	3.10	0.00	120.41	373.01
YDL241W	3.13	0.00	34.99	109.68
YLR194C	3.17	0.00	291.50	923.01
YGR139W	3.18	0.00	15.95	50.72
YGR159C	3.18	0.00	24.14	76.86
YPL068C	3.19	0.00	7.34	23.45
YGR161C	3.21	0.00	184.85	592.86
YGR189C	3.21	0.00	116.04	372.60
YKR075W-A	3.25	0.00	173.06	562.85
YKR075C	3.29	0.00	185.67	610.70
YCR022C	3.29	0.05	3.46	11.40
YNL036W	3.31	0.00	75.45	249.43
YDR210W	3.34	0.00	233.62	780.08
YKL096W	3.34	0.00	99.05	331.01
YPR009W	3.38	0.00	6.62	22.41
YHR030C	3.39	0.00	63.10	214.17
YPL144W	3.41	0.03	4.08	13.91
YOR344C	3.43	0.00	15.22	52.15
YMR244W	3.44	0.03	3.77	12.95
YJL088W	3.46	0.00	27.27	94.27
YOR153W	3.46	0.00	49.04	169.86
YNL162W-A	3.50	0.02	4.31	15.07
YOR273C	3.52	0.00	91.50	322.36
YLR044C	3.53	0.00	848.31	2993.48
YCR010C	3.53	0.00	88.57	312.79
YPR157W	3.54	0.00	27.59	97.80
YOL014W	3.69	0.00	47.46	174.96
YBR005W	3.71	0.00	171.42	636.30
YHR137W	3.73	0.00	9.99	37.28
YDR209C	3.76	0.00	142.33	535.67
YGR160W	3.93	0.00	12.84	50.49
YLR346C	3.95	0.00	83.85	331.57
YBR056C-B	3.96	0.00	277.26	1098.25
YBL070C	3.97	0.00	15.28	60.69
YKR093W	4.10	0.00	8.08	33.10
YPL025C	4.29	0.04	2.25	9.67
YLR414C	4.29	0.00	165.32	709.84

YNL024C	4.32	0.00	5.18	22.35
YNL210W	4.34	0.04	2.32	10.07
YIL121W	4.45	0.00	29.11	129.55
YOR107W	4.64	0.00	46.39	215.40
YLR154C-H	4.69	0.00	84.80	398.02
YPL014W	4.77	0.00	41.21	196.61
YGR138C	4.79	0.00	183.68	879.94
YGR283C	4.90	0.00	7.17	35.13
YGL188C-A	5.09	0.00	10.26	52.20
YBR019C	5.14	0.00	3.44	17.71
YDR380W	5.15	0.01	2.77	14.27
YMR102C	5.16	0.00	22.69	117.03
YLR162W-A	5.27	0.00	29.95	157.79
YGR152C	5.28	0.00	8.98	47.42
YER062C	5.38	0.00	146.24	786.37
YBR056W-A	5.89	0.00	318.82	1876.43
YBL069W	6.08	0.00	34.90	212.05
YHR092C	6.13	0.00	42.98	263.49
YBR296C	6.39	0.00	6.12	39.14
Q0130	6.56	0.00	4.36	28.57
YGL162W	6.95	0.00	12.79	88.83
YGR035C	7.06	0.00	82.95	585.72
YLR154W-E	7.24	0.00	1061.37	7679.93
YIL117C	7.65	0.00	20.90	159.79
YDL039C	8.05	0.00	5.73	46.08
YHR137C-A	9.29	0.00	4.15	38.60
YLR154W-C	9.67	0.00	14632.21	141560.21
YGL158W	9.79	0.00	1.39	13.61
YLR162W	9.89	0.00	2180.79	21561.59
YJL216C	10.57	0.00	5.47	57.89
YLR154W-B	12.02	0.00	6356.54	76420.29
YMR011W	12.23	0.00	41.15	503.13
YLR154W-A	12.25	0.00	12968.92	158912.75
YBR072C-A	12.51	0.00	1.94	24.28
YJL218W	14.39	0.00	5.32	76.55
YLR154W-F	14.72	0.00	3108.22	45756.92
Q0275	15.28	0.01	0.54	8.30
Q0250	59.53	0.00	0.17	9.90
Q0045	71.23	0.00	0.20	13.96

RNA-seq results for differentially expressed genes between R57 before and after 24 hours HWSSL exposure				
Gene ID	Fold Change	FDR p-value correction	Expression values for R57 after 2 hrs HWSSL exposure	Expression values for R57 after 24 hrs HWSSL exposure
YDR536W	-14.56	0.00	742.14	50.98
YBR196C-B	-11.98	0.04	7.24	0.60
YDR320W-B	-9.22	0.01	12.71	1.38
YPL058C	-8.70	0.00	448.41	51.55
YDL022W	-7.86	0.00	3119.05	396.74
YOR199W	-7.74	0.05	7.44	0.96
YHR094C	-7.72	0.00	2421.54	313.52
YLL020C	-7.37	0.03	9.17	1.24
YDR523C	-7.34	0.05	7.90	1.08
YCR102W-A	-7.14	0.04	9.16	1.28
YOL150C	-6.90	0.00	3377.03	489.32
YGL239C	-6.82	0.00	20.61	3.02
YDL023C	-6.80	0.00	2047.05	301.25
YOL101C	-6.70	0.00	152.57	22.77
YOL151W	-6.64	0.00	3363.40	506.33
YEL030C-A	-6.45	0.04	9.10	1.41
YOR381W-A	-6.45	0.01	14.62	2.27
YGL007C-A	-6.45	0.01	14.12	2.19
YKR040C	-6.18	0.00	29.59	4.78
YLR134W	-6.15	0.00	805.09	130.84
YOR348C	-5.98	0.00	76.32	12.76
YLR108C	-5.88	0.00	108.93	18.54
YDR508C	-5.86	0.00	71.72	12.23
YDR271C	-5.86	0.00	150.91	25.76
YOL164W-A	-5.82	0.00	38.35	6.59
YDR046C	-5.74	0.00	159.64	27.83
YAR064W	-5.62	0.03	11.89	2.12
YOR349W	-5.59	0.01	14.92	2.67
YDR270W	-5.58	0.00	82.95	14.86
YOL152W	-5.54	0.00	63.62	11.48
YDR269C	-5.43	0.00	58.48	10.77
YIR040C	-5.43	0.05	9.31	1.71
YKL165C-A	-5.41	0.03	11.75	2.17
YBR221W-A	-5.30	0.00	400.43	75.54
YBR131C-A	-5.30	0.01	14.94	2.82
YGL157W	-5.29	0.00	402.11	75.97
YDR371C-A	-5.22	0.05	9.47	1.81

YAR035C-A	-5.20	0.00	114.07	21.93
YMR246W	-5.20	0.00	537.31	103.41
YGL116W	-5.18	0.00	52.38	10.11
YNL332W	-5.18	0.05	9.32	1.80
YER006C-A	-5.16	0.04	10.30	2.00
YNR060W	-5.12	0.00	27.07	5.29
YCL027W	-5.06	0.03	12.31	2.43
YGL188C	-5.04	0.00	62.51	12.40
YBR047W	-4.96	0.00	26.25	5.29
YOL013W-A	-4.92	0.05	9.75	1.98
YGR050C	-4.88	0.00	101.39	20.80
YJL087C	-4.87	0.04	10.83	2.22
YNR062C	-4.84	0.01	15.93	3.29
YGR171C	-4.84	0.04	11.20	2.31
YHR046C	-4.82	0.00	82.64	17.15
YMR058W	-4.78	0.00	152.57	31.91
YDR492W	-4.76	0.00	571.48	120.03
YGR242W	-4.74	0.00	27.25	5.75
YLR136C	-4.74	0.00	127.52	26.92
YPR070W	-4.73	0.00	25.75	5.45
YML116W-A	-4.69	0.00	95.34	20.31
YNL324W	-4.67	0.05	10.48	2.24
YDR137W	-4.67	0.01	21.40	4.59
YLL006W	-4.65	0.00	22.78	4.90
YDR242W	-4.64	0.00	78.93	17.00
YDR534C	-4.63	0.01	19.79	4.28
YFL027C	-4.61	0.02	15.07	3.27
YLR146W-A	-4.58	0.00	44.55	9.74
YER174C	-4.57	0.00	50.12	10.96
YKL050C	-4.55	0.01	19.70	4.33
YNL237W	-4.54	0.00	64.49	14.21
YFR005C	-4.53	0.02	15.37	3.39
YER139C	-4.53	0.00	43.45	9.60
YKR064W	-4.52	0.01	18.27	4.04
YDR491C	-4.52	0.00	164.50	36.37
YEL065W	-4.49	0.02	15.71	3.50
YGL053W	-4.49	0.00	233.66	52.08
YOL038C-A	-4.45	0.01	17.66	3.97
YGL085W	-4.45	0.00	40.69	9.15
YGR049W	-4.43	0.00	591.51	133.66
YBR021W	-4.41	0.00	25.73	5.84
YGL240W	-4.41	0.01	17.08	3.88
YPR065W	-4.39	0.00	414.46	94.40
YJL025W	-4.38	0.03	14.04	3.20
YLR089C	-4.36	0.00	302.90	69.55
YLL047W	-4.35	0.03	12.94	2.97

YKL076C	-4.33	0.01	21.47	4.96
YJL085W	-4.33	0.04	12.18	2.81
YOR034C-A	-4.32	0.02	14.68	3.39
YEL019C	-4.32	0.01	20.44	4.74
YPR048W	-4.31	0.03	13.74	3.19
YPR202W	-4.30	0.01	20.55	4.78
YDR263C	-4.28	0.00	29.80	6.97
YBR054W	-4.27	0.00	2479.07	580.70
YGL136C	-4.25	0.00	57.63	13.57
YCR066W	-4.25	0.02	16.38	3.86
YGR261C	-4.23	0.01	21.87	5.17
YDR320C	-4.22	0.00	30.04	7.11
YJL205C	-4.21	0.00	161.71	38.38
YNL298W	-4.21	0.00	42.18	10.01
YPR155C	-4.21	0.01	18.77	4.46
YPR116W	-4.21	0.00	23.70	5.63
YKR082W	-4.21	0.04	12.83	3.05
YDL243C	-4.18	0.00	46.13	11.02
YGL051W	-4.18	0.00	30.11	7.20
YML053C	-4.18	0.00	94.62	22.64
YPL194W	-4.18	0.01	21.05	5.04
YOR282W	-4.18	0.04	12.39	2.97
YIL001W	-4.17	0.02	15.28	3.66
YOR022C	-4.16	0.00	32.48	7.80
YDR065W	-4.16	0.01	23.54	5.66
YLR211C	-4.15	0.00	24.39	5.87
YBR096W	-4.15	0.00	47.84	11.54
YOR149C	-4.14	0.00	24.05	5.81
YNL171C	-4.14	0.00	39.14	9.46
YBR281C	-4.14	0.01	17.92	4.33
YFR023W	-4.13	0.02	17.14	4.15
YCL055W	-4.13	0.00	33.24	8.06
YJL107C	-4.11	0.00	185.48	45.08
YGR068W-A	-4.11	0.00	35.33	8.59
YAR033W	-4.10	0.00	38.40	9.36
YML055W	-4.10	0.00	50.85	12.41
YPL274W	-4.10	0.00	80.62	19.68
YMR006C	-4.08	0.00	70.11	17.17
YIL176C	-4.08	0.03	14.98	3.67
YDL214C	-4.08	0.00	67.28	16.50
YJL206C	-4.06	0.02	17.41	4.29
YOL144W	-4.06	0.00	31.31	7.72
YMR130W	-4.05	0.00	40.46	9.98
YJL162C	-4.05	0.02	17.76	4.38
YJR159W	-4.05	0.00	25.59	6.32
YNL143C	-4.05	0.00	103.86	25.67

YGL113W	-4.04	0.01	18.91	4.68
YJL225W-A	-4.04	0.00	27.60	6.83
YFL003C	-4.04	0.04	12.93	3.20
YLR205C	-4.03	0.00	303.60	75.29
YOR333C	-4.03	0.05	11.64	2.89
YMR065W	-4.03	0.05	11.46	2.85
YGR055W	-4.02	0.00	97.02	24.13
YHR021W-A	-4.01	0.04	12.82	3.20
YHR005C	-4.01	0.01	18.63	4.65
YMR067C	-4.00	0.00	71.80	17.96
YDL148C	-4.00	0.02	15.74	3.94
YFL061W	-3.99	0.01	20.18	5.05
YOR385W	-3.99	0.00	278.25	69.78
YHL038C	-3.99	0.01	23.79	5.97
YHL030W	-3.98	0.01	20.45	5.14
YGL066W	-3.97	0.00	51.22	12.89
YGL179C	-3.95	0.00	224.00	56.67
YEL068C	-3.95	0.01	24.06	6.10
YPL259C	-3.94	0.00	77.48	19.68
YDR416W	-3.93	0.01	21.46	5.46
YDL142C	-3.93	0.00	32.19	8.19
YJL047C	-3.93	0.02	17.25	4.39
YPL109C	-3.93	0.04	13.00	3.31
YDR014W-A	-3.93	0.00	35.16	8.95
YMR244C-A	-3.92	0.00	321.53	81.98
YJR110W	-3.92	0.00	31.88	8.13
YMR132C	-3.92	0.00	36.09	9.21
YMR272W-B	-3.92	0.00	55.23	14.10
YDR509W	-3.92	0.02	17.14	4.38
YBR255C-A	-3.91	0.00	140.96	36.01
YBR081C	-3.91	0.04	12.91	3.30
YOL148C	-3.91	0.00	31.45	8.04
YGR278W	-3.91	0.02	17.87	4.57
YOR386W	-3.91	0.01	20.28	5.19
YJR149W	-3.90	0.00	47.26	12.12
YGL124C	-3.89	0.02	17.50	4.49
YGL242C	-3.89	0.00	84.50	21.73
YDR440W	-3.89	0.04	13.67	3.52
YHR199C-A	-3.88	0.00	111.95	28.87
YIR033W	-3.88	0.00	68.10	17.56
YJL029C	-3.88	0.02	17.93	4.63
YBL104C	-3.86	0.03	15.80	4.09
YJR136C	-3.86	0.01	19.54	5.06
YDL091C	-3.85	0.00	58.99	15.31
YML076C	-3.85	0.00	33.70	8.75

YHL044W	-3.85	0.01	19.99	5.20
YKL071W	-3.84	0.00	89.19	23.21
YPR081C	-3.84	0.01	21.79	5.67
YGL055W	-3.84	0.00	3940.63	1026.42
YMR324C	-3.83	0.00	56.07	14.62
YLR424W	-3.83	0.02	17.02	4.44
YCL047C	-3.83	0.00	34.69	9.06
YMR187C	-3.83	0.00	28.47	7.44
YDR325W	-3.83	0.04	13.43	3.51
YAL034C-B	-3.82	0.04	13.71	3.58
YLL033W	-3.82	0.02	16.45	4.30
YOR081C	-3.82	0.01	25.55	6.68
YGL110C	-3.82	0.00	30.78	8.05
YMR159C	-3.82	0.01	21.94	5.74
YNR061C	-3.82	0.00	111.99	29.32
YGL041C-B	-3.82	0.00	27.80	7.28
YJR161C	-3.82	0.01	25.43	6.66
YPL034W	-3.81	0.00	55.31	14.53
YLR047C	-3.81	0.01	25.08	6.59
YIR008C	-3.81	0.01	25.53	6.71
YPR179C	-3.80	0.01	21.54	5.67
YDR367W	-3.79	0.00	40.13	10.58
YOL065C	-3.79	0.01	25.21	6.65
YPL103C	-3.79	0.00	27.85	7.35
YER021W	-3.78	0.00	205.75	54.37
YHL029C	-3.78	0.00	47.64	12.60
YGR051C	-3.78	0.00	150.16	39.76
YPR180W	-3.77	0.00	48.62	12.88
YJL108C	-3.77	0.00	274.31	72.71
YGL223C	-3.77	0.00	28.63	7.59
YBL037W	-3.77	0.03	16.47	4.37
YOR245C	-3.77	0.00	121.84	32.36
YKR031C	-3.77	0.04	13.29	3.53
YIL029W-A	-3.75	0.02	19.18	5.12
YML126C	-3.74	0.00	164.65	43.98
YPR097W	-3.74	0.01	24.32	6.50
YBR201W	-3.74	0.00	56.36	15.06
YMR160W	-3.74	0.01	21.38	5.72
YNR024W	-3.73	0.00	64.63	17.31
YNL107W	-3.73	0.00	115.15	30.84
YGL119W	-3.73	0.01	22.48	6.03
YEL014C	-3.73	0.00	48.73	13.06
YGL192W	-3.73	0.00	36.88	9.89
YLR322W	-3.73	0.02	17.26	4.63
YPL096W	-3.72	0.00	43.64	11.74
YDR443C	-3.72	0.05	12.78	3.44
YLR287C	-3.72	0.00	32.69	8.79

YLR389C	-3.72	0.00	35.70	9.61
YLR241W	-3.72	0.00	58.00	15.61
YBR255W	-3.71	0.00	38.87	10.47
YIL072W	-3.71	0.04	14.64	3.94
YNL236W	-3.71	0.03	15.75	4.25
YDR531W	-3.70	0.00	44.23	11.95
YOL063C	-3.70	0.01	22.87	6.18
YBR271W	-3.70	0.00	42.65	11.53
YDL044C	-3.70	0.00	29.26	7.91
YKR078W	-3.69	0.03	15.07	4.08
YHR202W	-3.69	0.00	47.55	12.87
YNL216W	-3.69	0.00	74.86	20.28
YDR182W-A	-3.69	0.05	12.61	3.42
YDR461W	-3.69	0.00	27.39	7.43
YPL166W	-3.69	0.00	52.47	14.23
YLR315W	-3.69	0.02	18.73	5.08
YDL056W	-3.68	0.02	19.61	5.33
YJR062C	-3.68	0.00	28.90	7.85
YER037W	-3.67	0.00	732.29	199.29
YOR094W	-3.67	0.00	50.64	13.79
YJL197W	-3.66	0.03	15.62	4.26
YGL104C	-3.66	0.01	24.82	6.78
YGR069W	-3.66	0.01	26.28	7.18
YBL048W	-3.66	0.00	109.46	29.90
YOR356W	-3.65	0.00	49.29	13.49
YGR003W	-3.65	0.00	36.50	9.99
YMR158W-B	-3.65	0.02	19.49	5.34
YKL121W	-3.65	0.01	23.17	6.35
YBR302C	-3.65	0.04	15.03	4.12
YCR042C	-3.65	0.02	19.12	5.24
YDR369C	-3.65	0.03	16.23	4.45
YDR058C	-3.63	0.00	32.90	9.06
YJL084C	-3.63	0.00	59.97	16.50
YBR222C	-3.63	0.00	491.75	135.42
YFR043C	-3.63	0.00	36.12	9.95
YAR029W	-3.63	0.00	227.15	62.61
YOR350C	-3.62	0.01	23.90	6.59
YER007W	-3.62	0.01	21.52	5.95
YGL084C	-3.61	0.00	33.91	9.39
YPL208W	-3.61	0.01	21.06	5.83
YJR003C	-3.61	0.04	14.39	3.99
YDL027C	-3.61	0.00	61.30	16.98
YGR146C-A	-3.61	0.03	16.97	4.70
YOL123W	-3.61	0.00	79.61	22.06
YAL048C	-3.61	0.03	16.11	4.47
YLL008W	-3.61	0.00	48.82	13.54

YDL220C	-3.60	0.04	14.92	4.14
YCR019W	-3.60	0.00	47.34	13.13
YHL040C	-3.60	0.00	73.03	20.28
YFR006W	-3.60	0.00	63.17	17.56
YOR384W	-3.59	0.00	32.93	9.16
YOR055W	-3.59	0.00	94.37	26.26
YJR134C	-3.59	0.01	22.22	6.18
YIL038C	-3.59	0.00	42.85	11.93
YDR011W	-3.59	0.00	247.39	68.87
YFR048W	-3.59	0.00	39.75	11.07
YNR029C	-3.59	0.00	44.15	12.30
YHR075C	-3.59	0.00	46.96	13.08
YBL019W	-3.59	0.01	26.23	7.31
YJL010C	-3.59	0.01	22.41	6.25
YKR017C	-3.59	0.00	36.97	10.31
YLR035C	-3.59	0.00	29.85	8.33
YGL209W	-3.58	0.00	855.21	238.57
YDR539W	-3.58	0.00	42.85	11.96
YGR088W	-3.58	0.00	493.30	137.69
YBR061C	-3.57	0.00	34.03	9.52
YDR470C	-3.57	0.01	22.24	6.22
YEL005C	-3.57	0.00	36.85	10.31
YHR011W	-3.57	0.01	24.64	6.91
YKL125W	-3.56	0.00	58.82	16.50
YOL087C	-3.56	0.00	35.28	9.90
YMR268C	-3.56	0.01	21.33	5.99
YLR411W	-3.56	0.00	168.42	47.28
YDL245C	-3.56	0.02	20.28	5.70
YOR381W	-3.56	0.00	41.45	11.64
YNL188W	-3.56	0.04	14.91	4.19
YDR159W	-3.56	0.05	14.04	3.95
YLR097C	-3.56	0.00	63.90	17.96
YMR304W	-3.56	0.00	37.27	10.48
YOR069W	-3.56	0.00	36.82	10.36
YGR233C	-3.56	0.03	17.03	4.79
YBR109W-A	-3.55	0.05	14.03	3.95
YBR058C	-3.55	0.01	23.93	6.73
YDR515W	-3.55	0.00	40.20	11.33
YER075C	-3.54	0.01	24.13	6.81
YDR368W	-3.54	0.00	276.63	78.12
YPR089W	-3.54	0.00	27.96	7.90
YDR254W	-3.53	0.00	48.54	13.73
YER028C	-3.53	0.00	58.48	16.55
YOR154W	-3.53	0.00	36.83	10.43
YJL071W	-3.53	0.01	21.66	6.14
YNL262W	-3.53	0.01	24.86	7.05

YGR281W	-3.52	0.00	117.12	33.23
YDR164C	-3.52	0.01	22.61	6.42
YOR352W	-3.52	0.00	71.91	20.41
YCR020W-B	-3.52	0.00	72.54	20.62
YGR263C	-3.52	0.02	20.82	5.92
YPL268W	-3.52	0.01	28.12	8.00
YMR293C	-3.51	0.02	20.62	5.87
YGR091W	-3.51	0.01	23.12	6.58
YDR308C	-3.51	0.00	35.80	10.20
YHR060W	-3.51	0.00	29.77	8.48
YDR114C	-3.51	0.02	19.11	5.44
YMR294W	-3.51	0.00	46.02	13.12
YBR044C	-3.51	0.00	32.49	9.27
YOL043C	-3.51	0.00	47.48	13.55
YCR005C	-3.50	0.00	3775.36	1077.18
YOR153W	-3.50	0.00	595.12	169.86
YPR032W	-3.50	0.02	19.77	5.65
YPL045W	-3.50	0.03	17.98	5.14
YLR131C	-3.50	0.01	25.16	7.19
YDL231C	-3.50	0.01	27.40	7.83
YGR089W	-3.50	0.02	18.95	5.42
YPL022W	-3.50	0.00	33.12	9.47
YNR019W	-3.50	0.00	662.64	189.57
YER130C	-3.49	0.00	667.39	191.02
YDR401W	-3.49	0.04	14.93	4.28
YNL331C	-3.49	0.00	32.52	9.31
YML070W	-3.49	0.00	431.93	123.87
YGL065C	-3.49	0.03	17.56	5.04
YBR074W	-3.49	0.03	17.36	4.98
YJL031C	-3.48	0.00	72.80	20.89
YOR038C	-3.48	0.02	19.94	5.72
YDR056C	-3.48	0.00	286.14	82.14
YDL216C	-3.48	0.01	23.38	6.71
YGL024W	-3.48	0.00	41.42	11.90
YBR128C	-3.48	0.03	17.91	5.15
YKL015W	-3.47	0.00	38.45	11.07
YOR109W	-3.47	0.01	25.12	7.23
YER049W	-3.47	0.00	74.92	21.58
YFR002W	-3.47	0.00	29.96	8.64
YIL066W-A	-3.47	0.02	18.83	5.43
YGR286C	-3.47	0.00	95.18	27.45
YBR017C	-3.47	0.00	28.95	8.35
YIL035C	-3.47	0.00	63.86	18.43
YGL171W	-3.46	0.01	21.91	6.33
YHR196W	-3.46	0.01	28.60	8.26
YBL080C	-3.46	0.02	19.31	5.58
YLR269C	-3.46	0.00	61.31	17.72

YOR058C	-3.46	0.00	89.39	25.83
YBR152W	-3.46	0.00	45.86	13.26
YDL168W	-3.46	0.00	394.88	114.17
YMR137C	-3.46	0.01	28.18	8.15
YDL151C	-3.46	0.00	38.08	11.01
YDR464C-A	-3.46	0.00	37.13	10.74
YPL123C	-3.46	0.00	42.35	12.25
YDL107W	-3.46	0.00	44.85	12.98
YOL100W	-3.46	0.00	45.25	13.10
YOL149W	-3.45	0.00	211.81	61.36
YMR193W	-3.45	0.00	88.51	25.64
YOL145C	-3.45	0.02	18.55	5.38
YKR095W-A	-3.45	0.00	73.81	21.39
YGR053C	-3.45	0.00	34.18	9.91
YDL149W	-3.45	0.00	29.90	8.67
YDR224C	-3.45	0.00	535.45	155.27
YOR087W	-3.45	0.05	14.13	4.10
YHR033W	-3.45	0.00	253.63	73.58
YGR241C	-3.45	0.00	57.14	16.58
YLR309C	-3.45	0.00	31.33	9.09
YML105C	-3.45	0.00	46.81	13.59
YPR171W	-3.44	0.00	37.50	10.89
YGL108C	-3.44	0.00	88.34	25.65
YLR154C	-3.44	0.01	24.94	7.24
YOR057W	-3.44	0.00	64.92	18.85
YJL046W	-3.44	0.00	42.07	12.23
YHR040W	-3.44	0.00	84.87	24.67
YJR089W	-3.44	0.01	23.17	6.73
YLR199C	-3.44	0.00	50.17	14.58
YJL070C	-3.44	0.02	21.44	6.23
YLR352W	-3.44	0.00	32.66	9.50
YPL010W	-3.44	0.00	112.85	32.84
YCR037C	-3.44	0.02	19.34	5.63
YKL073W	-3.43	0.00	31.54	9.18
YDR426C	-3.43	0.00	58.79	17.12
YDL207W	-3.43	0.00	48.06	14.01
YML094W	-3.43	0.00	58.36	17.02
YIL150C	-3.43	0.04	16.22	4.73
YDR336W	-3.43	0.01	24.38	7.12
YMR212C	-3.42	0.05	13.69	4.00
YPL249C	-3.42	0.00	30.75	8.98
YDR282C	-3.42	0.00	42.74	12.49
YJR102C	-3.42	0.00	38.50	11.25
YBR215W	-3.42	0.00	33.26	9.73
YPL069C	-3.42	0.00	33.13	9.69
YEL033W	-3.42	0.00	118.21	34.60
YDR419W	-3.42	0.01	27.28	7.99

YOL098C	-3.41	0.00	29.26	8.58
YDR057W	-3.41	0.00	62.57	18.35
YGL243W	-3.41	0.03	17.79	5.22
YPR156C	-3.41	0.00	464.87	136.48
YOR068C	-3.40	0.01	22.54	6.62
YDR015C	-3.40	0.00	32.41	9.52
YLR014C	-3.40	0.05	14.32	4.21
YLR207W	-3.40	0.00	30.48	8.95
YGL029W	-3.40	0.00	58.32	17.13
YBR043C	-3.40	0.00	37.15	10.91
YMR167W	-3.40	0.01	24.96	7.33
YOL033W	-3.40	0.02	18.77	5.51
YKR106W	-3.40	0.02	18.80	5.53
YGL155W	-3.40	0.00	38.31	11.28
YEL053C	-3.40	0.05	13.70	4.03
YBR293W	-3.40	0.04	16.33	4.81
YDR421W	-3.40	0.01	22.73	6.69
YGR187C	-3.39	0.00	34.89	10.28
YOL136C	-3.39	0.00	485.10	142.95
YGL160W	-3.39	0.00	39.46	11.63
YDR320C-A	-3.39	0.00	160.21	47.23
YDR112W	-3.39	0.03	17.41	5.13
YER080W	-3.39	0.00	80.17	23.64
YNL272C	-3.39	0.01	22.08	6.51
YKR003W	-3.39	0.00	36.08	10.65
YER185W	-3.39	0.00	53.99	15.93
YNL049C	-3.39	0.01	25.49	7.52
YER093C	-3.39	0.03	18.53	5.47
YGL112C	-3.39	0.00	59.57	17.59
YPL115C	-3.39	0.01	22.13	6.54
YOL099C	-3.38	0.00	123.97	36.63
YMR173W	-3.38	0.00	400.47	118.42
YBR227C	-3.38	0.01	24.02	7.10
YPR177C	-3.38	0.00	38.04	11.26
YGR218W	-3.38	0.00	83.05	24.58
YER022W	-3.37	0.02	19.92	5.90
YML036W	-3.37	0.03	18.42	5.46
YAL001C	-3.37	0.02	19.11	5.67
YJR141W	-3.37	0.00	35.46	10.51
YNL304W	-3.37	0.01	24.72	7.34
YOR278W	-3.37	0.00	37.43	11.11
YJR142W	-3.37	0.00	61.89	18.38
YDL045C	-3.37	0.00	79.11	23.49
YML107C	-3.36	0.02	21.88	6.50
YHR182W	-3.36	0.02	19.72	5.87
YNL062C	-3.36	0.03	18.39	5.48
YOR168W	-3.36	0.00	41.82	12.46

YOR032W-A	-3.36	0.01	29.67	8.84
YMR287C	-3.36	0.04	15.73	4.69
YOR191W	-3.36	0.01	23.44	6.98
YBR274W	-3.35	0.00	35.07	10.46
YPR162C	-3.35	0.01	24.90	7.42
YHR119W	-3.35	0.01	24.22	7.22
YKL144C	-3.35	0.00	30.29	9.04
YMR087W	-3.35	0.00	32.83	9.80
YDR490C	-3.35	0.00	64.75	19.33
YER187W	-3.35	0.00	102.27	30.53
YGL075C	-3.35	0.00	30.85	9.21
YGL233W	-3.35	0.04	16.39	4.90
YMR224C	-3.35	0.03	17.66	5.28
YDR455C	-3.34	0.01	24.03	7.19
YPR168W	-3.34	0.02	19.25	5.76
YML057C-A	-3.34	0.00	64.17	19.20
YDL147W	-3.34	0.00	335.34	100.35
YIL095W	-3.34	0.01	22.57	6.75
YPL083C	-3.34	0.01	24.16	7.23
YPR151C	-3.34	0.00	222.89	66.72
YLR454W	-3.34	0.04	16.17	4.84
YJL209W	-3.34	0.01	26.84	8.04
YHR045W	-3.34	0.00	31.44	9.43
YDR091C	-3.34	0.00	61.52	18.44
YFL025C	-3.34	0.05	14.04	4.21
YHR073C-B	-3.34	0.00	164.60	49.35
YDR228C	-3.33	0.04	15.30	4.59
YDR422C	-3.33	0.00	43.12	12.93
YOR129C	-3.33	0.03	19.08	5.73
YNL088W	-3.33	0.03	18.69	5.61
YBR014C	-3.33	0.00	102.53	30.79
YJR065C	-3.33	0.00	208.44	62.61
YPR026W	-3.33	0.00	92.25	27.71
YML062C	-3.32	0.00	52.03	15.66
YBL113W-A	-3.32	0.00	39.71	11.95
YLR326W	-3.32	0.00	130.86	39.41
YIL137C	-3.32	0.01	24.84	7.48
YML054C	-3.32	0.00	352.08	106.04
YDR430C	-3.32	0.01	28.73	8.65
YDR004W	-3.32	0.00	51.63	15.55
YLR423C	-3.32	0.01	27.37	8.25
YER038C	-3.32	0.00	115.78	34.89
YDR512C	-3.32	0.00	115.71	34.88
YIL039W	-3.32	0.00	45.15	13.61
YGL180W	-3.32	0.00	61.84	18.65
YHR013C	-3.31	0.00	43.39	13.10

YNL054W	-3.31	0.01	25.78	7.78
YPR145C-A	-3.31	0.00	782.90	236.41
YJL112W	-3.31	0.00	54.66	16.51
YML132W	-3.31	0.05	14.93	4.51
YLR119W	-3.31	0.00	40.90	12.35
YJL090C	-3.31	0.04	15.93	4.81
YCL045C	-3.31	0.00	42.85	12.95
YOR308C	-3.31	0.02	22.01	6.65
YLR451W	-3.31	0.01	23.49	7.11
YMR066W	-3.31	0.03	18.28	5.53
YJR013W	-3.31	0.00	30.98	9.37
YFR045W	-3.30	0.00	48.92	14.81
YML003W	-3.30	0.03	18.96	5.74
YGR169C	-3.30	0.01	23.10	7.00
YLR127C	-3.30	0.02	19.54	5.92
YJR090C	-3.30	0.01	26.90	8.15
YGL074C	-3.30	0.00	51.86	15.72
YFR008W	-3.30	0.00	68.84	20.87
YMR219W	-3.30	0.03	18.00	5.46
YOR062C	-3.30	0.00	382.16	115.90
YFR010W	-3.30	0.00	91.34	27.71
YDL099W	-3.30	0.00	95.81	29.07
YOL131W	-3.30	0.00	70.99	21.54
YLR102C	-3.30	0.00	74.67	22.66
YFL007W	-3.29	0.00	31.72	9.63
YDR518W	-3.29	0.01	25.29	7.68
YDR049W	-3.29	0.00	46.31	14.07
YGR131W	-3.29	0.00	47.34	14.38
YER079C-A	-3.29	0.00	47.44	14.41
YGL164C	-3.29	0.00	35.98	10.94
YMR267W	-3.29	0.03	18.55	5.64
YDR067C	-3.29	0.00	67.66	20.59
YER129W	-3.29	0.01	23.53	7.16
YFR030W	-3.29	0.00	88.20	26.85
YGL257C	-3.29	0.04	16.28	4.96
YBR270C	-3.28	0.02	22.78	6.93
YDL141W	-3.28	0.02	21.21	6.46
YDR124W	-3.28	0.02	20.09	6.12
YLR371W	-3.28	0.03	19.35	5.89
YFL002C	-3.28	0.00	41.65	12.68
YCR016W	-3.28	0.00	36.51	11.12
YMR037C	-3.28	0.00	58.89	17.94
YDR255C	-3.28	0.00	81.43	24.81
YPL150W	-3.28	0.00	40.09	12.22
YNL325C	-3.28	0.05	14.51	4.42
YPR095C	-3.28	0.04	16.28	4.96
YPL219W	-3.28	0.00	45.59	13.90

YER087W	-3.28	0.03	18.75	5.72
YBR153W	-3.28	0.00	71.60	21.84
YOR037W	-3.28	0.00	45.52	13.89
YOR392W	-3.28	0.00	33.72	10.29
YCR094W	-3.28	0.01	25.46	7.77
YLR240W	-3.28	0.01	24.37	7.44
YEL020C	-3.27	0.00	74.18	22.66
YGR065C	-3.27	0.00	34.85	10.65
YNR005C	-3.27	0.00	44.62	13.63
YNL292W	-3.27	0.01	26.73	8.17
YHL002C-A	-3.27	0.00	100.21	30.62
YPR140W	-3.27	0.00	71.74	21.93
YKL173W	-3.27	0.01	25.93	7.92
YLR115W	-3.27	0.04	16.09	4.92
YNL254C	-3.27	0.02	22.89	7.00
YPL258C	-3.27	0.01	27.19	8.31
YGL095C	-3.27	0.00	49.54	15.15
YNL221C	-3.27	0.01	28.88	8.84
YLR465C	-3.27	0.00	60.37	18.48
YDR243C	-3.27	0.00	37.07	11.35
YDR028C	-3.27	0.00	113.94	34.88
YLR410W	-3.27	0.00	40.41	12.37
YDL028C	-3.26	0.00	45.30	13.88
YOL083W	-3.26	0.00	48.47	14.85
YIL017C	-3.26	0.00	39.07	11.97
YNL118C	-3.26	0.00	49.52	15.18
YBR111W-A	-3.26	0.00	101.68	31.18
YCL046W	-3.26	0.04	16.60	5.09
YML029W	-3.26	0.03	19.40	5.95
YAR018C	-3.26	0.01	23.25	7.13
YCL021W-A	-3.26	0.01	29.55	9.06
YJR044C	-3.26	0.00	69.40	21.30
YIL019W	-3.26	0.00	66.90	20.54
YBR123C	-3.26	0.00	31.16	9.57
YMR049C	-3.26	0.01	25.57	7.85
YHR091C	-3.26	0.00	40.10	12.32
YMR075W	-3.26	0.01	26.04	8.00
YPL278C	-3.26	0.00	74.30	22.83
YGL150C	-3.25	0.02	21.72	6.67
YPL104W	-3.25	0.01	24.76	7.61
YDR288W	-3.25	0.00	65.66	20.18
YDR332W	-3.25	0.01	24.44	7.51
YKL047W	-3.25	0.00	40.98	12.60
YGR119C	-3.25	0.00	50.89	15.65
YGR047C	-3.25	0.04	17.16	5.28
YOR114W	-3.25	0.03	17.71	5.45

YDR428C	-3.25	0.02	21.50	6.62
YNL146C-A	-3.25	0.00	66.57	20.50
YPL145C	-3.25	0.00	83.17	25.62
YCL025C	-3.25	0.00	62.26	19.18
YBR216C	-3.25	0.02	21.46	6.61
YKR036C	-3.24	0.01	25.58	7.88
YKL155C	-3.24	0.00	36.88	11.37
YJR083C	-3.24	0.02	21.69	6.69
YKL105C	-3.24	0.03	18.29	5.64
YML075C	-3.24	0.00	42.79	13.19
YKL021C	-3.24	0.00	52.66	16.24
YCR102C	-3.24	0.05	15.42	4.76
YLL015W	-3.24	0.01	27.78	8.57
YLR090W	-3.24	0.00	98.48	30.39
YDR181C	-3.24	0.01	29.00	8.95
YKL078W	-3.24	0.04	16.10	4.97
YLR409C	-3.24	0.05	15.16	4.68
YIL091C	-3.24	0.04	16.60	5.13
YGL141W	-3.24	0.00	40.35	12.47
YKR052C	-3.23	0.00	105.39	32.59
YLR369W	-3.23	0.00	64.43	19.93
YFR013W	-3.23	0.03	19.00	5.88
YBL067C	-3.23	0.00	35.36	10.94
YJR098C	-3.23	0.01	29.02	8.98
YPR134W	-3.23	0.00	50.29	15.57
YKL132C	-3.23	0.00	63.72	19.73
YNL035C	-3.23	0.01	25.39	7.86
YBR237W	-3.23	0.00	40.57	12.57
YJR126C	-3.23	0.00	57.76	17.89
YER008C	-3.23	0.03	17.71	5.49
YAL017W	-3.23	0.00	45.66	14.15
YCR067C	-3.23	0.04	16.38	5.08
YDR499W	-3.23	0.03	19.34	5.99
YJR127C	-3.23	0.00	86.65	26.86
YOL025W	-3.23	0.00	32.82	10.18
YJL077W-A	-3.23	0.00	117.63	36.47
YMR302C	-3.22	0.00	126.37	39.19
YDL199C	-3.22	0.00	32.89	10.21
YBL017C	-3.22	0.00	37.79	11.73
YNL249C	-3.22	0.03	17.95	5.57
YER134C	-3.22	0.00	121.42	37.69
YHR065C	-3.22	0.01	28.50	8.85
YDR176W	-3.22	0.00	34.88	10.83
YGR015C	-3.22	0.00	44.49	13.82
YPL195W	-3.22	0.01	25.68	7.98
YDR363W	-3.22	0.00	39.16	12.17
YNL059C	-3.22	0.01	29.96	9.32

YGL262W	-3.22	0.03	18.16	5.65
YHR038W	-3.22	0.01	25.91	8.06
YDL040C	-3.21	0.02	23.14	7.20
YOL029C	-3.21	0.00	66.29	20.63
YDR390C	-3.21	0.02	23.26	7.24
YPL072W	-3.21	0.03	19.30	6.01
YOL066C	-3.21	0.02	23.41	7.29
YJL011C	-3.21	0.00	41.51	12.93
YPL046C	-3.21	0.00	64.52	20.09
YPR001W	-3.21	0.02	21.61	6.73
YOL138C	-3.21	0.04	16.24	5.06
YKL214C	-3.21	0.00	38.60	12.03
YKL095W	-3.21	0.00	60.57	18.88
YJL099W	-3.21	0.01	24.71	7.70
YAR030C	-3.21	0.00	158.33	49.35
YKL075C	-3.21	0.00	61.67	19.23
YJR004C	-3.21	0.05	15.63	4.87
YML057W	-3.21	0.00	123.07	38.39
YOR215C	-3.21	0.00	198.69	61.97
YJL081C	-3.21	0.00	45.39	14.16
YPL214C	-3.21	0.00	43.99	13.72
YMR193C-A	-3.20	0.02	23.12	7.21
YDL094C	-3.20	0.04	17.54	5.47
YMR168C	-3.20	0.02	23.37	7.29
YBL113C	-3.20	0.02	21.36	6.67
YLR144C	-3.20	0.01	26.31	8.22
YOR112W	-3.20	0.03	19.11	5.97
YNL120C	-3.20	0.01	23.82	7.44
YNL030W	-3.20	0.00	1399.69	437.25
YPR055W	-3.20	0.03	18.80	5.87
YEL072W	-3.20	0.00	44.61	13.95
YJL013C	-3.20	0.00	57.95	18.12
YBR280C	-3.20	0.00	107.94	33.75
YPR105C	-3.20	0.03	18.75	5.86
YOR229W	-3.20	0.00	34.53	10.80
YIL068C	-3.20	0.03	18.62	5.83
YKL206C	-3.20	0.00	66.84	20.91
YCL029C	-3.20	0.01	28.51	8.92
YJL057C	-3.20	0.00	59.29	18.55
YDL026W	-3.20	0.00	59.79	18.71
YOR124C	-3.19	0.01	28.34	8.87
YGL013C	-3.19	0.00	37.16	11.63
YPL074W	-3.19	0.00	38.03	11.91
YMR284W	-3.19	0.03	18.04	5.65
YML127W	-3.19	0.00	58.61	18.35
YMR086W	-3.19	0.00	46.02	14.42
YHR047C	-3.19	0.02	21.74	6.81

YPR146C	-3.19	0.00	42.35	13.27
YOR379C	-3.19	0.01	24.49	7.67
YDR199W	-3.19	0.00	111.20	34.85
YDL150W	-3.19	0.00	42.26	13.25
YLR310C	-3.19	0.02	21.97	6.89
YPR147C	-3.19	0.00	66.98	21.01
YBR125C	-3.19	0.00	39.18	12.29
YNL048W	-3.19	0.01	26.88	8.44
YOR152C	-3.18	0.00	154.65	48.56
YML086C	-3.18	0.00	45.24	14.21
YPL217C	-3.18	0.01	24.91	7.82
YOL028C	-3.18	0.00	47.62	14.96
YOL084W	-3.18	0.00	291.40	91.60
YMR211W	-3.18	0.01	26.00	8.18
YGR170W	-3.18	0.05	16.00	5.03
YLR057W	-3.18	0.03	17.96	5.65
YDR456W	-3.18	0.00	54.82	17.25
YLR304C	-3.18	0.00	717.91	225.93
YBR006W	-3.18	0.00	540.77	170.23
YOL164W	-3.18	0.00	42.78	13.47
YKL072W	-3.18	0.00	33.62	10.59
YKR005C	-3.18	0.04	17.49	5.51
YFL004W	-3.18	0.00	49.49	15.59
YDR392W	-3.17	0.00	87.20	27.47
YNL045W	-3.17	0.01	28.57	9.00
YJL076W	-3.17	0.00	40.97	12.92
YBR055C	-3.17	0.01	28.61	9.02
YKR083C	-3.17	0.00	37.53	11.84
YJR005W	-3.17	0.00	61.31	19.34
YGR276C	-3.17	0.00	53.13	16.76
YPR083W	-3.17	0.02	21.04	6.64
YML093W	-3.17	0.03	18.69	5.90
YLR306W	-3.17	0.04	17.02	5.37
YJL041W	-3.17	0.00	45.04	14.22
YFL046W	-3.17	0.00	56.04	17.69
YHR004C	-3.17	0.00	51.54	16.28
YFL044C	-3.17	0.00	77.84	24.58
YOR048C	-3.17	0.00	67.83	21.42
YHR186C	-3.17	0.05	15.90	5.02
YOR250C	-3.16	0.00	35.27	11.14
YCR088W	-3.16	0.00	108.24	34.21
YKR029C	-3.16	0.01	28.75	9.08
YFL041W-A	-3.16	0.01	31.37	9.91
YML002W	-3.16	0.01	30.37	9.60
YFR016C	-3.16	0.00	32.97	10.42
YLR345W	-3.16	0.00	158.84	50.22
YPL085W	-3.16	0.05	15.38	4.86

YNL199C	-3.16	0.00	76.22	24.12
YLR149C-A	-3.16	0.05	16.13	5.11
YER155C	-3.16	0.04	17.78	5.63
YGR179C	-3.16	0.00	38.74	12.26
YNL260C	-3.16	0.00	52.70	16.69
YMR283C	-3.16	0.00	39.10	12.39
YER118C	-3.16	0.02	21.77	6.90
YKR063C	-3.15	0.00	42.32	13.41
YLR428C	-3.15	0.05	15.09	4.78
YGL210W	-3.15	0.00	116.08	36.80
YPR091C	-3.15	0.00	39.72	12.59
YMR309C	-3.15	0.01	25.85	8.19
YMR086C-A	-3.15	0.00	60.20	19.09
YPL035C	-3.15	0.00	65.53	20.79
YDR273W	-3.15	0.00	72.70	23.06
YDR305C	-3.15	0.02	23.25	7.37
YNR051C	-3.15	0.00	48.84	15.49
YHR044C	-3.15	0.00	43.72	13.87
YMR239C	-3.15	0.01	30.64	9.72
YGR043C	-3.15	0.00	726.52	230.70
YHL042W	-3.15	0.00	60.41	19.19
YMR007W	-3.15	0.00	143.05	45.47
YIL120W	-3.15	0.00	56.75	18.04
YGR165W	-3.15	0.00	64.62	20.54
YGR271C-A	-3.15	0.01	29.57	9.40
YPR108W	-3.15	0.00	165.09	52.48
YOL062C	-3.15	0.00	80.58	25.62
YLR002C	-3.14	0.00	35.05	11.15
YNR025C	-3.14	0.00	71.47	22.74
YOL003C	-3.14	0.01	26.49	8.43
YNL229C	-3.14	0.00	138.20	43.97
YMR118C	-3.14	0.00	73.22	23.30
YDL235C	-3.14	0.00	58.94	18.76
YOR001W	-3.14	0.00	39.38	12.53
YNL041C	-3.14	0.02	22.46	7.15
YGR058W	-3.14	0.00	80.46	25.62
YPL182C	-3.14	0.00	160.35	51.06
YMR308C	-3.14	0.01	24.68	7.86
YPL158C	-3.14	0.03	19.59	6.24
YDL237W	-3.14	0.00	81.16	25.86
YDR009W	-3.14	0.00	38.09	12.14
YFR050C	-3.14	0.00	384.44	122.55
YNL137C	-3.14	0.00	86.37	27.54
YLR394W	-3.14	0.01	32.00	10.20
YLR283W	-3.14	0.01	25.06	7.99
YCR020C-A	-3.13	0.00	94.61	30.18
YNL269W	-3.13	0.00	32.63	10.42

YKR076W	-3.13	0.00	140.54	44.87
YDR274C	-3.13	0.00	166.16	53.05
YFR003C	-3.13	0.00	124.83	39.86
YHL002W	-3.13	0.00	132.75	42.40
YPL248C	-3.13	0.01	28.91	9.23
YLR098C	-3.13	0.01	27.54	8.80
YCR030C	-3.13	0.00	44.89	14.35
YOL102C	-3.13	0.00	56.11	17.95
YOR345C	-3.13	0.05	15.83	5.06
YPL060W	-3.13	0.00	41.53	13.28
YHR066W	-3.13	0.00	33.49	10.72
YJR132W	-3.12	0.05	15.81	5.06
YKL168C	-3.12	0.03	20.59	6.59
YER128W	-3.12	0.00	48.25	15.45
YNL253W	-3.12	0.01	27.33	8.75
YDR030C	-3.12	0.00	46.21	14.81
YAL049C	-3.12	0.00	127.69	40.93
YLR206W	-3.12	0.00	161.08	51.64
YNL267W	-3.12	0.01	26.71	8.56
YGR052W	-3.12	0.00	460.70	147.77
YMR213W	-3.12	0.00	62.14	19.93
YNL266W	-3.12	0.00	80.06	25.68
YHR048W	-3.12	0.00	38.53	12.36
YKL068W	-3.12	0.01	30.42	9.76
YDR300C	-3.12	0.00	54.39	17.45
YNR039C	-3.12	0.00	46.54	14.94
YDL223C	-3.12	0.00	63.06	20.24
YDR081C	-3.11	0.01	29.03	9.32
YDR427W	-3.11	0.00	112.70	36.18
YNL151C	-3.11	0.00	88.88	28.54
YOR082C	-3.11	0.04	16.76	5.38
YNL311C	-3.11	0.04	17.32	5.56
YBL047C	-3.11	0.00	59.99	19.27
YAL002W	-3.11	0.05	15.59	5.01
YPR111W	-3.11	0.00	56.37	18.12
YPR031W	-3.11	0.02	23.19	7.46
YMR019W	-3.11	0.04	16.82	5.41
YER053C	-3.11	0.00	378.84	121.85
YHR080C	-3.11	0.00	33.61	10.81
YGR193C	-3.11	0.00	89.59	28.82
YNL183C	-3.11	0.00	43.54	14.01
YBR008C	-3.11	0.00	33.16	10.67
YHR101C	-3.11	0.00	34.23	11.02
YGL142C	-3.11	0.01	31.84	10.25
YNL115C	-3.11	0.00	113.99	36.69
YHL048C-A	-3.11	0.00	39.42	12.69
YDR080W	-3.11	0.05	16.27	5.24

YGR162W	-3.11	0.00	52.44	16.89
YDL225W	-3.10	0.00	56.39	18.16
YLR440C	-3.10	0.03	19.79	6.38
YFL042C	-3.10	0.00	56.43	18.17
YGR035W-A	-3.10	0.00	53.21	17.15
YOR030W	-3.10	0.00	45.62	14.70
YBL024W	-3.10	0.01	26.92	8.68
YLR433C	-3.10	0.01	32.33	10.42
YDR495C	-3.10	0.05	16.66	5.37
YOL096C	-3.10	0.00	38.98	12.57
YHR164C	-3.10	0.05	15.81	5.10
YJR100C	-3.10	0.00	73.39	23.67
YIL062C	-3.10	0.00	275.91	88.97
YPR193C	-3.10	0.00	40.10	12.93
YHL039W	-3.10	0.01	28.87	9.31
YDR489W	-3.10	0.03	19.56	6.31
YLR266C	-3.10	0.03	20.55	6.63
YDR239C	-3.10	0.00	35.94	11.60
YEL013W	-3.10	0.00	35.31	11.40
YBR063C	-3.10	0.00	86.73	27.99
YLR046C	-3.10	0.00	45.46	14.67
YDR379W	-3.10	0.01	30.88	9.97
YOL119C	-3.10	0.00	91.48	29.54
YDR240C	-3.10	0.00	39.06	12.61
YPR157W	-3.10	0.00	302.88	97.80
YKR023W	-3.10	0.00	35.64	11.51
YJR124C	-3.10	0.05	16.63	5.37
YNL211C	-3.10	0.00	48.17	15.56
YOR117W	-3.10	0.00	257.66	83.24
YIL014W	-3.09	0.03	19.40	6.27
YNL265C	-3.09	0.00	65.00	21.01
YMR028W	-3.09	0.00	45.46	14.70
YLR200W	-3.09	0.00	97.29	31.45
YGR004W	-3.09	0.01	32.92	10.64
YDL085C-A	-3.09	0.00	85.31	27.59
YLR214W	-3.09	0.03	20.66	6.68
YOR334W	-3.09	0.04	17.22	5.57
YPL029W	-3.09	0.03	20.02	6.48
YKR095W	-3.09	0.03	20.28	6.56
YER029C	-3.09	0.00	123.78	40.05
YFR046C	-3.09	0.00	35.22	11.39
YDR453C	-3.09	0.00	140.70	45.52
YLR053C	-3.09	0.00	186.52	60.35
YHR061C	-3.09	0.04	17.02	5.51
YMR273C	-3.09	0.01	26.05	8.43
YIL147C	-3.09	0.05	16.06	5.20

YGL099W	-3.09	0.00	35.79	11.58
YLR418C	-3.09	0.01	30.52	9.88
YOR377W	-3.09	0.00	56.29	18.22
YGR093W	-3.09	0.01	25.21	8.16
YDR003W-A	-3.09	0.00	285.25	92.34
YLR066W	-3.09	0.00	39.20	12.69
YGR122W	-3.09	0.00	39.23	12.70
YLR126C	-3.09	0.00	45.87	14.86
YKL182W	-3.09	0.00	123.95	40.15
YOR265W	-3.09	0.00	62.85	20.36
YML049C	-3.09	0.04	17.92	5.81
YPL183C	-3.08	0.02	22.84	7.40
YMR105W-A	-3.08	0.01	26.09	8.46
YNL252C	-3.08	0.00	89.03	28.88
YLR364W	-3.08	0.00	55.11	17.88
YIR037W	-3.08	0.00	359.54	116.72
YKL119C	-3.08	0.02	24.73	8.03
YOR161W-B	-3.08	0.00	101.05	32.82
YDL224C	-3.08	0.00	37.16	12.07
YLR336C	-3.08	0.02	23.87	7.76
YFR009W	-3.08	0.01	29.04	9.44
YDR168W	-3.08	0.00	110.53	35.92
YNL014W	-3.08	0.00	68.25	22.18
YBR026C	-3.08	0.00	70.19	22.82
YDL161W	-3.07	0.00	86.19	28.03
YIL016W	-3.07	0.00	41.06	13.35
YMR004W	-3.07	0.00	84.97	27.64
YBL008W	-3.07	0.03	19.56	6.36
YDR444W	-3.07	0.00	37.99	12.36
YLR297W	-3.07	0.00	744.75	242.26
YGL159W	-3.07	0.02	24.01	7.81
YGL212W	-3.07	0.00	39.78	12.94
YLR215C	-3.07	0.00	34.93	11.37
YGR246C	-3.07	0.00	44.86	14.60
YOR261C	-3.07	0.00	213.21	69.38
YEL030W	-3.07	0.03	19.13	6.23
YDR060W	-3.07	0.03	19.17	6.25
YER110C	-3.07	0.04	18.58	6.06
YDR216W	-3.07	0.00	62.95	20.53
YDL130W-A	-3.07	0.00	642.57	209.56
YGL094C	-3.07	0.02	23.65	7.71
YKR010C	-3.07	0.03	18.81	6.14
YDR335W	-3.06	0.00	60.48	19.74
YKR018C	-3.06	0.00	181.20	59.14
YPR068C	-3.06	0.03	20.78	6.78

YDR026C	-3.06	0.00	42.33	13.82
YDL183C	-3.06	0.00	80.52	26.29
YHR158C	-3.06	0.04	18.24	5.95
YAL035W	-3.06	0.00	76.45	24.97
YNL206C	-3.06	0.00	89.47	29.22
YGL232W	-3.06	0.02	23.66	7.73
YBR080C	-3.06	0.00	54.91	17.95
YLR044C	-3.06	0.00	9158.23	2993.48
YLR290C	-3.06	0.00	50.97	16.66
YGR258C	-3.06	0.01	33.17	10.84
YLR289W	-3.06	0.02	23.54	7.69
YJL180C	-3.06	0.01	25.59	8.37
YGL059W	-3.06	0.00	38.91	12.72
YKL134C	-3.06	0.03	20.83	6.81
YHR180C-B	-3.06	0.00	35.09	11.48
YER012W	-3.06	0.00	265.64	86.94
YLR384C	-3.06	0.03	19.58	6.41
YEL012W	-3.05	0.00	575.78	188.52
YJL073W	-3.05	0.02	23.90	7.83
YEL071W	-3.05	0.00	1268.45	415.44
YOR017W	-3.05	0.01	28.86	9.45
YJR057W	-3.05	0.00	79.14	25.93
YGR144W	-3.05	0.00	55.85	18.30
YMR195W	-3.05	0.00	1459.02	478.21
YBR225W	-3.05	0.00	45.97	15.07
YKR105C	-3.05	0.03	19.36	6.35
YLR460C	-3.05	0.00	38.98	12.79
YOR295W	-3.05	0.02	24.77	8.13
YER066W	-3.05	0.00	51.98	17.06
YJL147C	-3.05	0.02	22.55	7.40
YLR239C	-3.05	0.01	32.70	10.74
YGL071W	-3.05	0.00	68.24	22.41
YGR247W	-3.04	0.01	33.54	11.02
YHR191C	-3.04	0.00	85.53	28.10
YGR206W	-3.04	0.00	56.18	18.46
YLR319C	-3.04	0.04	18.85	6.19
YMR176W	-3.04	0.03	20.24	6.65
YML079W	-3.04	0.00	58.28	19.16
YPR136C	-3.04	0.02	22.57	7.42
YIL067C	-3.04	0.00	38.55	12.68
YBR228W	-3.04	0.00	41.73	13.73
YPR112C	-3.04	0.01	27.72	9.12
YMR154C	-3.04	0.04	17.22	5.67
YJL075C	-3.04	0.00	76.29	25.11
YHR129C	-3.04	0.02	24.20	7.97
YDL189W	-3.04	0.01	27.49	9.05
YGR100W	-3.04	0.01	33.63	11.08

YMR075C-A	-3.04	0.00	41.06	13.52
YPR117W	-3.04	0.02	21.94	7.23
YJR002W	-3.03	0.00	70.78	23.32
YPL185W	-3.03	0.00	39.87	13.14
YDR068W	-3.03	0.00	91.82	30.26
YBR246W	-3.03	0.01	31.75	10.47
YBR247C	-3.03	0.00	49.17	16.21
YML015C	-3.03	0.00	40.11	13.23
YPL100W	-3.03	0.00	56.01	18.47
YNR013C	-3.03	0.04	18.90	6.24
YIL031W	-3.03	0.00	38.95	12.85
YMR164C	-3.03	0.04	18.49	6.10
YLR165C	-3.03	0.02	23.62	7.80
YDR458C	-3.03	0.02	23.54	7.77
YER078C	-3.03	0.00	47.17	15.57
YLR041W	-3.03	0.02	25.14	8.30
YLR398C	-3.03	0.04	17.40	5.75
YKL221W	-3.03	0.05	16.61	5.49
YHR168W	-3.03	0.00	37.48	12.39
YOR228C	-3.03	0.00	38.86	12.84
YNL227C	-3.02	0.00	47.59	15.75
YER017C	-3.02	0.00	140.18	46.38
YHR192W	-3.02	0.01	31.16	10.31
YOR054C	-3.02	0.00	160.50	53.11
YGR037C	-3.02	0.00	721.88	238.91
YMR001C	-3.02	0.03	19.19	6.35
YGR184C	-3.02	0.00	39.69	13.14
YMR097C	-3.02	0.00	82.47	27.30
YIL071C	-3.02	0.01	28.43	9.41
YMR012W	-3.02	0.01	29.09	9.63
YKL212W	-3.02	0.00	59.57	19.73
YLR321C	-3.02	0.01	28.12	9.31
YGL042C	-3.02	0.00	142.75	47.28
YBL101C	-3.02	0.00	101.38	33.58
YPR022C	-3.02	0.01	29.48	9.77
YFL024C	-3.02	0.00	49.40	16.38
YLL031C	-3.02	0.04	17.48	5.80
YNL085W	-3.02	0.01	29.63	9.82
YML023C	-3.01	0.05	16.03	5.32
YDL247W-A	-3.01	0.00	178.55	59.22
YGL114W	-3.01	0.00	48.11	15.97
YFR029W	-3.01	0.00	68.15	22.61
YJR088C	-3.01	0.00	75.91	25.19
YKL126W	-3.01	0.00	121.53	40.34
YDL153C	-3.01	0.00	56.40	18.73
YNL139C	-3.01	0.03	21.13	7.01
YGL173C	-3.01	0.00	52.28	17.36

YPR115W	-3.01	0.00	48.95	16.25
YOR335W-A	-3.01	0.00	202.86	67.37
YGL254W	-3.01	0.00	46.07	15.30
YOL004W	-3.01	0.00	34.76	11.55
YKL005C	-3.01	0.00	60.34	20.05
YGR173W	-3.01	0.01	30.53	10.15
YBR172C	-3.01	0.00	55.90	18.58
YBL053W	-3.01	0.00	53.95	17.94
YOR216C	-3.01	0.03	19.41	6.45
YLR271W	-3.01	0.02	21.97	7.31
YDR189W	-3.01	0.00	42.05	13.98
YBR062C	-3.01	0.00	152.49	50.72
YPL246C	-3.01	0.00	59.00	19.62
YCR086W	-3.01	0.00	45.92	15.28
YHR073W	-3.00	0.00	40.35	13.43
YGL161C	-3.00	0.00	78.47	26.12
YOL137W	-3.00	0.02	25.52	8.49
YGL206C	-3.00	0.00	35.68	11.88
YBL105C	-3.00	0.00	41.08	13.68
YFL028C	-3.00	0.00	62.64	20.86
YAL016C-B	-3.00	0.00	71.68	23.88
YPL212C	-3.00	0.00	57.08	19.02
YOR132W	-3.00	0.00	97.18	32.38
YPL122C	-3.00	0.01	32.73	10.90
YEL043W	-3.00	0.00	44.02	14.68
YGR243W	-3.00	0.00	2336.68	779.13
YBR300C	-3.00	0.02	22.55	7.52
YDR166C	-3.00	0.02	23.10	7.70
YGR112W	-3.00	0.00	35.29	11.77
YBR024W	-3.00	0.00	73.06	24.37
YBR289W	-3.00	0.04	18.83	6.28
YIL030C	-3.00	0.01	31.65	10.56
YGL256W	-3.00	0.02	23.67	7.90
YNR023W	-3.00	0.00	38.68	12.91
YGR113W	-3.00	0.01	33.71	11.25
YML094C-A	-3.00	0.02	22.69	7.58
YFL001W	-2.99	0.01	33.31	11.12
YLR382C	-2.99	0.02	24.76	8.27
YOR270C	-2.99	0.00	69.49	23.21
YIL172C	-2.99	0.00	45.06	15.06
YOR325W	-2.99	0.01	29.24	9.77
YLR188W	-2.99	0.02	25.09	8.39
YLL057C	-2.99	0.01	26.81	8.96
YMR119W	-2.99	0.01	27.23	9.10
YCL026C-B	-2.99	0.00	438.07	146.53
YPL188W	-2.99	0.00	55.75	18.65

YFR001W	-2.99	0.00	67.22	22.49
YKR096W	-2.99	0.00	44.28	14.82
YOR123C	-2.99	0.00	135.77	45.44
YIL104C	-2.99	0.01	30.85	10.33
YHR029C	-2.99	0.00	52.66	17.64
YFR024C-A	-2.99	0.00	143.73	48.14
YLR243W	-2.99	0.00	37.70	12.63
YNR022C	-2.98	0.00	143.41	48.04
YOR005C	-2.98	0.00	37.07	12.42
YDL146W	-2.98	0.04	18.34	6.15
YOR171C	-2.98	0.00	79.06	26.50
YFR052W	-2.98	0.00	186.06	62.38
YOR260W	-2.98	0.00	55.45	18.59
YMR115W	-2.98	0.00	106.66	35.77
YNL097C-B	-2.98	0.01	26.15	8.77
YMR194C-B	-2.98	0.00	261.56	87.75
YLR396C	-2.98	0.03	21.41	7.18
YLR189C	-2.98	0.00	63.50	21.31
YJL044C	-2.98	0.02	24.72	8.29
YOL018C	-2.98	0.00	48.44	16.26
YAL031W-A	-2.98	0.00	66.05	22.18
YLR362W	-2.98	0.00	56.85	19.09
YHR121W	-2.98	0.00	85.43	28.69
YNR003C	-2.98	0.01	29.12	9.78
YPL107W	-2.98	0.00	103.96	34.91
YMR100W	-2.98	0.00	50.91	17.10
YDR203W	-2.98	0.00	54.06	18.16
YMR278W	-2.98	0.00	57.41	19.28
YOL057W	-2.98	0.02	25.73	8.64
YGL196W	-2.98	0.00	104.00	34.96
YFR028C	-2.98	0.00	37.96	12.76
YNL181W	-2.97	0.00	35.93	12.08
YMR165C	-2.97	0.00	83.03	27.92
YER059W	-2.97	0.01	27.64	9.29
YMR063W	-2.97	0.05	16.24	5.46
YPL236C	-2.97	0.00	40.80	13.73
YOL042W	-2.97	0.00	40.22	13.54
YCR017C	-2.97	0.00	68.06	22.92
YJL002C	-2.97	0.00	80.95	27.27
YOR165W	-2.97	0.00	39.34	13.26
YMR099C	-2.97	0.00	114.14	38.47
YNL329C	-2.97	0.05	17.47	5.89
YGL224C	-2.97	0.00	39.75	13.40
YPR094W	-2.97	0.00	74.36	25.07
YLL055W	-2.97	0.00	77.24	26.04
YGL207W	-2.97	0.00	61.58	20.76
YNL271C	-2.97	0.02	24.88	8.39

YGL057C	-2.97	0.00	42.03	14.17
YAL051W	-2.97	0.00	58.10	19.60
YDR473C	-2.96	0.00	66.44	22.41
YLR277C	-2.96	0.03	22.27	7.51
YHL010C	-2.96	0.01	28.67	9.67
YFL055W	-2.96	0.04	18.17	6.13
YKL091C	-2.96	0.00	114.89	38.77
YPL263C	-2.96	0.02	24.60	8.30
YEL050W-A	-2.96	0.00	109.64	37.01
YCR020C	-2.96	0.00	37.99	12.83
YOR156C	-2.96	0.02	25.07	8.47
YHR028C	-2.96	0.00	84.94	28.69
YOR258W	-2.96	0.01	32.46	10.96
YPL181W	-2.96	0.00	270.35	91.36
YHR103W	-2.96	0.00	73.58	24.87
YKR001C	-2.96	0.00	88.83	30.03
YKL011C	-2.96	0.04	19.44	6.57
YOR330C	-2.96	0.03	19.93	6.74
YOR116C	-2.96	0.01	33.25	11.25
YHR001W	-2.96	0.00	48.95	16.56
YDL132W	-2.95	0.00	40.44	13.69
YGL226C-A	-2.95	0.00	97.69	33.06
YKL007W	-2.95	0.00	153.55	51.97
YPR049C	-2.95	0.01	33.91	11.48
YDR145W	-2.95	0.00	93.35	31.61
YGR056W	-2.95	0.02	24.40	8.26
YDR387C	-2.95	0.00	40.32	13.66
YOR076C	-2.95	0.03	22.20	7.52
YOR256C	-2.95	0.00	52.80	17.89
YJL049W	-2.95	0.02	23.25	7.88
YNL165W	-2.95	0.00	61.64	20.89
YBR117C	-2.95	0.00	180.92	61.34
YDR359C	-2.95	0.04	18.08	6.13
YDL032W	-2.95	0.04	17.99	6.10
YLR071C	-2.95	0.01	26.78	9.08
YGL056C	-2.95	0.00	140.69	47.71
YBL051C	-2.95	0.00	46.24	15.68
YHR072W	-2.95	0.00	37.57	12.74
YDR311W	-2.95	0.01	33.07	11.22
YMR181C	-2.95	0.00	975.74	331.18
YML042W	-2.95	0.00	136.88	46.46
YDL206W	-2.95	0.00	37.48	12.72
YJR084W	-2.94	0.04	18.80	6.39
YLR335W	-2.94	0.00	71.35	24.23
YMR129W	-2.94	0.03	20.10	6.83
YOR161W-A	-2.94	0.00	154.49	52.49

YNL136W	-2.94	0.00	73.94	25.12
YKL135C	-2.94	0.00	45.98	15.62
YKL154W	-2.94	0.00	39.38	13.38
YCR022C	-2.94	0.01	33.56	11.40
YJL008C	-2.94	0.00	124.59	42.34
YHR034C	-2.94	0.00	55.20	18.76
YML099C	-2.94	0.02	24.58	8.35
YGL043W	-2.94	0.00	102.37	34.80
YLR253W	-2.94	0.00	65.38	22.23
YFR026C	-2.94	0.05	17.20	5.85
YGL244W	-2.94	0.00	75.11	25.54
YMR023C	-2.94	0.01	29.74	10.11
YOR138C	-2.94	0.00	91.05	30.97
YLR197W	-2.94	0.00	46.78	15.92
YDR222W	-2.94	0.00	93.38	31.78
YMR271C	-2.94	0.00	236.81	80.61
YDR436W	-2.94	0.00	60.97	20.76
YMR155W	-2.94	0.00	46.35	15.79
YDR183W	-2.94	0.01	33.33	11.35
YGR105W	-2.94	0.00	107.46	36.61
YNL264C	-2.94	0.00	120.45	41.04
YOR287C	-2.93	0.00	36.91	12.58
YOR161C	-2.93	0.00	86.52	29.49
YLR210W	-2.93	0.01	27.99	9.54
YER123W	-2.93	0.01	31.08	10.60
YIR010W	-2.93	0.01	32.46	11.07
YOR259C	-2.93	0.00	295.99	100.97
YOR361C	-2.93	0.00	61.74	21.07
YGR078C	-2.93	0.00	43.08	14.70
YMR047C	-2.93	0.01	28.54	9.74
YOR227W	-2.93	0.00	42.44	14.49
YJL020C	-2.93	0.00	94.15	32.15
YOR266W	-2.93	0.04	19.72	6.73
YAL059C-A	-2.93	0.00	47.00	16.05
YDL190C	-2.93	0.02	23.69	8.09
YKL210W	-2.93	0.00	72.36	24.72
YBR003W	-2.93	0.00	82.41	28.16
YLR128W	-2.93	0.01	33.93	11.59
YKL143W	-2.93	0.00	66.42	22.70
YNL121C	-2.92	0.00	77.27	26.42
YIR005W	-2.92	0.00	40.69	13.91
YDR535C	-2.92	0.04	19.26	6.59
YNL101W	-2.92	0.00	64.18	21.95
YPR082C	-2.92	0.00	104.77	35.84
YOR051C	-2.92	0.00	133.09	45.53
YKL195W	-2.92	0.00	221.46	75.76
YOR346W	-2.92	0.04	20.07	6.86

YPL273W	-2.92	0.01	34.32	11.74
YML013W	-2.92	0.00	54.31	18.58
YLL011W	-2.92	0.00	43.52	14.89
YPR067W	-2.92	0.00	101.34	34.68
YJR071W	-2.92	0.02	23.61	8.08
YDL176W	-2.92	0.00	42.61	14.59
YGL176C	-2.92	0.00	42.64	14.60
YBR049C	-2.92	0.00	49.44	16.93
YJL221C	-2.92	0.00	43.25	14.81
YER142C	-2.92	0.00	125.62	43.01
YHR039C	-2.92	0.00	38.02	13.02
YLR386W	-2.92	0.05	17.52	6.00
YDR393W	-2.92	0.00	40.39	13.84
YHR024C	-2.92	0.00	76.56	26.23
YKL219W	-2.92	0.01	32.68	11.20
YPL193W	-2.92	0.02	25.21	8.64
YGR143W	-2.92	0.00	133.97	45.92
YLR436C	-2.92	0.03	21.63	7.42
YOR075W	-2.92	0.00	84.99	29.14
YNL004W	-2.92	0.00	128.13	43.93
YML095C	-2.92	0.02	26.61	9.12
YLR201C	-2.92	0.00	63.33	21.72
YGL101W	-2.92	0.00	96.20	33.00
YMR254C	-2.91	0.02	25.74	8.83
YGR111W	-2.91	0.00	74.71	25.63
YGR194C	-2.91	0.00	49.85	17.10
YNL025C	-2.91	0.00	38.98	13.38
YMR172W	-2.91	0.00	45.27	15.54
YHL043W	-2.91	0.00	58.36	20.04
YMR323W	-2.91	0.00	583.97	200.55
YNL320W	-2.91	0.02	23.32	8.02
YDL030W	-2.91	0.01	31.75	10.91
YBL070C	-2.91	0.00	176.52	60.69
YPR139C	-2.91	0.02	24.93	8.57
YHR139C	-2.91	0.00	189.97	65.33
YMR064W	-2.91	0.00	63.40	21.80
YDR066C	-2.91	0.01	30.28	10.41
YKR060W	-2.91	0.01	30.62	10.54
YGL144C	-2.91	0.01	27.05	9.31
YIL005W	-2.90	0.00	50.06	17.23
YKR016W	-2.90	0.00	111.51	38.39
YPR199C	-2.90	0.00	59.14	20.36
YAR002W	-2.90	0.00	45.95	15.82
YLR132C	-2.90	0.00	36.51	12.57
YDL119C	-2.90	0.01	33.29	11.47
YLR182W	-2.90	0.01	31.15	10.73
YMR152W	-2.90	0.00	71.10	24.50

YMR221C	-2.90	0.01	30.38	10.47
YNL138W	-2.90	0.00	87.44	30.14
YIL079C	-2.90	0.00	37.04	12.77
YBL036C	-2.90	0.00	123.38	42.55
YPR071W	-2.90	0.02	25.74	8.88
YOL007C	-2.90	0.05	17.21	5.94
YDR206W	-2.90	0.02	24.73	8.53
YGL185C	-2.90	0.00	51.14	17.64
YER125W	-2.90	0.00	98.52	34.00
YLR276C	-2.90	0.02	25.03	8.64
YOL013C	-2.90	0.00	77.93	26.90
YDR394W	-2.90	0.00	245.54	84.75
YOR175C	-2.90	0.00	49.71	17.16
YMR201C	-2.90	0.00	85.15	29.40
YOL050C	-2.90	0.00	84.16	29.06
YGR013W	-2.90	0.00	79.98	27.62
YNL174W	-2.90	0.01	36.23	12.51
YER030W	-2.90	0.00	250.11	86.39
YOR368W	-2.89	0.02	25.89	8.94
YEL002C	-2.89	0.00	60.65	20.95
YDR316W	-2.89	0.00	56.54	19.54
YOR060C	-2.89	0.04	20.40	7.05
YOL051W	-2.89	0.00	50.28	17.38
YOR304W	-2.89	0.01	27.84	9.62
YGL041W-A	-2.89	0.00	125.13	43.26
YMR261C	-2.89	0.00	51.95	17.96
YMR114C	-2.89	0.00	152.19	52.62
YFR007W	-2.89	0.01	31.28	10.81
YKL124W	-2.89	0.00	58.11	20.09
YJL111W	-2.89	0.00	124.10	42.92
YBR253W	-2.89	0.00	91.71	31.73
YGL201C	-2.89	0.01	32.55	11.26
YCL056C	-2.89	0.00	124.35	43.03
YNL326C	-2.89	0.01	32.10	11.11
YIL097W	-2.89	0.00	46.45	16.08
YCL057W	-2.89	0.00	80.98	28.03
YJL101C	-2.89	0.00	141.99	49.15
YEL015W	-2.89	0.00	92.73	32.11
YBL064C	-2.89	0.00	710.35	245.98
YBL066C	-2.89	0.01	35.18	12.19
YFL013C	-2.89	0.00	77.97	27.01
YJR108W	-2.89	0.02	26.09	9.04
YDL215C	-2.89	0.00	53.34	18.48
YAL031C	-2.89	0.01	35.30	12.23
YBR015C	-2.89	0.00	72.98	25.29
YOR169C	-2.89	0.00	69.29	24.02
YHR079C	-2.88	0.03	21.82	7.56

YJL056C	-2.88	0.00	37.33	12.94
YOR354C	-2.88	0.00	45.43	15.75
YGR109W-B	-2.88	0.01	28.75	9.97
YLR022C	-2.88	0.00	51.49	17.86
YBL059C-A	-2.88	0.00	156.82	54.42
YIL108W	-2.88	0.00	87.53	30.38
YGL079W	-2.88	0.01	35.60	12.36
YPR137W	-2.88	0.00	40.85	14.19
YOL055C	-2.88	0.01	33.86	11.76
YIL177W-A	-2.88	0.01	27.60	9.59
YDL219W	-2.88	0.02	26.20	9.10
YML131W	-2.88	0.00	1024.99	356.15
YDL001W	-2.88	0.00	46.31	16.10
YHR104W	-2.88	0.00	556.06	193.32
YJR135C	-2.87	0.03	23.31	8.11
YMR138W	-2.87	0.00	50.35	17.52
YER184C	-2.87	0.03	22.56	7.85
YKL176C	-2.87	0.00	48.91	17.02
YMR092C	-2.87	0.00	67.49	23.49
YDL098C	-2.87	0.00	76.37	26.57
YOL094C	-2.87	0.02	27.01	9.40
YOR355W	-2.87	0.01	29.63	10.31
YIL021W	-2.87	0.00	87.62	30.50
YDR268W	-2.87	0.00	36.93	12.86
YFL034C-A	-2.87	0.00	76.07	26.48
YDL194W	-2.87	0.01	35.83	12.48
YGL008C	-2.87	0.00	1710.97	595.72
YDR229W	-2.87	0.00	42.55	14.81
YHR003C	-2.87	0.01	35.45	12.35
YCL004W	-2.87	0.02	24.20	8.43
YPL267W	-2.87	0.04	20.23	7.05
YDR505C	-2.87	0.00	103.16	35.95
YML032C	-2.87	0.00	85.48	29.80
YOL069W	-2.87	0.01	34.63	12.07
YDR299W	-2.87	0.02	25.39	8.86
YEL077C	-2.87	0.05	18.12	6.32
YFL009W	-2.87	0.00	62.33	21.75
YGL208W	-2.87	0.00	120.05	41.89
YDL103C	-2.86	0.04	20.14	7.04
YBR041W	-2.86	0.00	52.43	18.31
YBR108W	-2.86	0.00	129.93	45.38
YPL277C	-2.86	0.00	59.44	20.76
YOR326W	-2.86	0.05	18.14	6.34
YOR307C	-2.86	0.00	45.73	15.98
YDL221W	-2.86	0.01	28.28	9.89
YLR153C	-2.86	0.00	163.38	57.11

YOR034C	-2.86	0.01	28.80	10.07
YER048C	-2.86	0.00	235.80	82.45
YIL002W-A	-2.86	0.00	234.19	81.88
YNL119W	-2.86	0.01	29.63	10.36
YMR140W	-2.86	0.00	104.78	36.65
YML097C	-2.86	0.01	28.76	10.06
YLL056C	-2.86	0.00	443.89	155.27
YLR052W	-2.86	0.00	73.46	25.70
YML004C	-2.86	0.00	706.19	247.08
YOR033C	-2.86	0.00	46.94	16.43
YDR200C	-2.86	0.00	44.94	15.73
YML050W	-2.85	0.00	47.79	16.74
YLR190W	-2.85	0.01	30.43	10.66
YOR264W	-2.85	0.00	43.55	15.26
YDR111C	-2.85	0.02	27.20	9.53
YNR043W	-2.85	0.00	123.58	43.31
YJL097W	-2.85	0.02	26.02	9.12
YLR397C	-2.85	0.03	21.79	7.64
YDR425W	-2.85	0.01	28.24	9.90
YBR276C	-2.85	0.02	25.09	8.80
YGL227W	-2.85	0.00	39.07	13.70
YGR076C	-2.85	0.00	52.31	18.34
YKL131W	-2.85	0.00	47.83	16.77
YMR199W	-2.85	0.03	22.27	7.81
YBL005W	-2.85	0.01	35.61	12.49
YDR435C	-2.85	0.00	133.25	46.74
YDR409W	-2.85	0.02	24.25	8.51
YBR198C	-2.85	0.01	34.11	11.97
YLR238W	-2.85	0.01	35.24	12.36
YNR035C	-2.85	0.00	138.49	48.59
YER114C	-2.85	0.01	32.66	11.46
YKL038W	-2.85	0.00	50.12	17.59
YDR196C	-2.85	0.00	76.68	26.92
YIL171W-A	-2.85	0.00	92.94	32.64
YJR049C	-2.85	0.00	100.03	35.13
YER137W-A	-2.85	0.00	39.56	13.89
YHR063W-A	-2.85	0.00	169.34	59.49
YOL108C	-2.85	0.00	264.56	92.95
YLR096W	-2.85	0.03	21.02	7.39
YKR039W	-2.85	0.04	19.46	6.84
YGR197C	-2.84	0.00	62.03	21.81
YHR052W	-2.84	0.00	42.76	15.04
YIL098C	-2.84	0.00	90.21	31.73
YHR178W	-2.84	0.02	26.51	9.32
YLR083C	-2.84	0.00	42.66	15.01
YAL056W	-2.84	0.00	40.47	14.24

YGR127W	-2.84	0.00	160.92	56.63
YDL016C	-2.84	0.00	64.27	22.62
YPL043W	-2.84	0.01	32.59	11.47
YML065W	-2.84	0.03	21.35	7.51
YDR082W	-2.84	0.01	36.66	12.90
YGR150C	-2.84	0.02	27.22	9.59
YGR120C	-2.84	0.00	39.28	13.83
YMR180C	-2.84	0.00	78.76	27.74
YPR148C	-2.84	0.00	248.84	87.66
YHR036W	-2.84	0.02	23.91	8.42
YGR138C	-2.84	0.00	2497.51	879.94
YPR060C	-2.84	0.01	32.23	11.36
YJR099W	-2.84	0.00	50.91	17.94
YDR099W	-2.84	0.00	465.75	164.11
YIR001C	-2.84	0.00	79.60	28.06
YOR166C	-2.84	0.05	18.43	6.50
YPL006W	-2.84	0.01	30.89	10.89
YHR181W	-2.84	0.00	47.16	16.63
YNL108C	-2.84	0.00	79.91	28.18
YFR044C	-2.84	0.00	118.98	41.95
YHL017W	-2.84	0.00	40.74	14.37
YBR254C	-2.83	0.00	44.97	15.86
YOL021C	-2.83	0.02	25.54	9.01
YPR150W	-2.83	0.00	240.40	84.85
YLR187W	-2.83	0.00	39.27	13.86
YKL122C	-2.83	0.00	57.78	20.40
YHR031C	-2.83	0.01	32.44	11.45
YER068W	-2.83	0.00	93.75	33.09
YJL100W	-2.83	0.00	91.43	32.28
YPL243W	-2.83	0.03	23.16	8.18
YGR072W	-2.83	0.00	48.63	17.17
YJL146W	-2.83	0.00	40.27	14.22
YJL005W	-2.83	0.01	34.57	12.21
YGR274C	-2.83	0.01	31.82	11.24
YBR028C	-2.83	0.02	27.31	9.65
YNR016C	-2.83	0.00	90.59	32.02
YPR056W	-2.83	0.00	51.17	18.09
YOR014W	-2.83	0.00	91.37	32.31
YDR027C	-2.83	0.00	40.58	14.35
YKL018W	-2.83	0.01	32.07	11.34
YCR028C-A	-2.83	0.00	130.14	46.03
YDR233C	-2.83	0.00	278.95	98.68
YLL021W	-2.83	0.04	20.58	7.28
YIL075C	-2.83	0.00	201.37	71.26
YDR122W	-2.83	0.00	54.21	19.18
YGR081C	-2.83	0.00	38.52	13.63
YIL048W	-2.82	0.02	26.19	9.27

YDR197W	-2.82	0.02	25.89	9.17
YDR017C	-2.82	0.01	33.25	11.77
YER169W	-2.82	0.00	60.12	21.28
YOL072W	-2.82	0.01	30.39	10.76
YBR079C	-2.82	0.00	52.96	18.76
YJL022W	-2.82	0.02	27.82	9.86
YDR379C-A	-2.82	0.00	215.63	76.41
YNL214W	-2.82	0.00	48.05	17.03
YAL026C-A	-2.82	0.01	33.11	11.73
YLR068W	-2.82	0.00	58.09	20.59
YBR056W	-2.82	0.00	148.25	52.58
YOR090C	-2.82	0.01	35.17	12.48
YNR040W	-2.82	0.00	51.04	18.11
YOR118W	-2.82	0.00	37.78	13.41
YPR118W	-2.82	0.01	29.95	10.63
YDL100C	-2.82	0.00	186.52	66.19
YLR457C	-2.82	0.01	32.41	11.50
YIL105W-A	-2.82	0.00	177.50	63.00
YDR257C	-2.82	0.01	33.83	12.01
YDR386W	-2.82	0.02	28.15	9.99
YLR408C	-2.82	0.00	60.06	21.32
YJL054W	-2.82	0.00	108.81	38.64
YPL042C	-2.82	0.00	42.31	15.03
YJR135W-A	-2.82	0.00	73.10	25.96
YNL191W	-2.82	0.00	197.64	70.19
YJL164C	-2.82	0.00	112.06	39.80
YKR086W	-2.81	0.03	21.66	7.69
YHR131C	-2.81	0.00	61.96	22.02
YJR079W	-2.81	0.00	62.20	22.11
YMR098C	-2.81	0.00	42.90	15.25
YMR316C-B	-2.81	0.00	45.04	16.02
YNR026C	-2.81	0.04	19.66	6.99
YOR211C	-2.81	0.01	37.02	13.17
YDL029W	-2.81	0.00	116.21	41.33
YKL013C	-2.81	0.00	259.63	92.35
YGL090W	-2.81	0.00	50.16	17.84
YDR530C	-2.81	0.00	111.99	39.84
YLR274W	-2.81	0.05	18.46	6.57
YDL006W	-2.81	0.00	95.04	33.83
YJL060W	-2.81	0.00	91.07	32.42
YGL052W	-2.81	0.00	48.35	17.21
YNL090W	-2.81	0.02	26.16	9.32
YBR102C	-2.81	0.02	25.28	9.00
YOR067C	-2.81	0.02	24.35	8.67
YJL127C	-2.81	0.03	22.23	7.92
YNL219C	-2.81	0.00	45.47	16.21
YNL261W	-2.81	0.02	28.06	10.00

YJL050W	-2.81	0.01	28.89	10.30
YDL050C	-2.81	0.00	98.09	34.97
YLR262C	-2.81	0.00	56.58	20.17
YOR316C	-2.80	0.00	139.55	49.75
YGL139W	-2.80	0.01	30.88	11.01
YGL048C	-2.80	0.00	384.90	137.27
YMR190C	-2.80	0.04	21.22	7.57
YBR260C	-2.80	0.00	42.40	15.13
YJR091C	-2.80	0.00	76.72	27.37
YER033C	-2.80	0.01	37.10	13.24
YFL036W	-2.80	0.01	36.97	13.19
YMR223W	-2.80	0.05	18.58	6.63
YKL171W	-2.80	0.00	82.79	29.55
YKR020W	-2.80	0.00	99.47	35.51
YOR120W	-2.80	0.00	253.03	90.35
YNL110C	-2.80	0.00	105.31	37.61
YML068W	-2.80	0.00	40.49	14.46
YPL096C-A	-2.80	0.00	68.65	24.52
YDL097C	-2.80	0.00	375.28	134.10
YDR464W	-2.80	0.03	22.67	8.10
YHR188C	-2.80	0.00	70.79	25.30
YMR245W	-2.80	0.00	193.23	69.07
YDR403W	-2.80	0.02	25.01	8.94
YBL098W	-2.80	0.00	47.86	17.11
YKL172W	-2.80	0.00	84.57	30.24
YJR056C	-2.80	0.01	29.44	10.53
YNL012W	-2.80	0.02	24.98	8.94
YGL001C	-2.80	0.00	146.14	52.27
YGR207C	-2.80	0.00	60.93	21.80
YNL149C	-2.80	0.00	467.96	167.42
YKR012C	-2.79	0.01	29.08	10.41
YJR039W	-2.79	0.04	19.65	7.03
YMR026C	-2.79	0.00	42.40	15.18
YPL210C	-2.79	0.02	24.69	8.84
YPL011C	-2.79	0.00	39.37	14.10
YGR097W	-2.79	0.00	58.94	21.11
YLR254C	-2.79	0.00	119.31	42.75
YCR027C	-2.79	0.00	59.59	21.35
YGL067W	-2.79	0.00	38.93	13.95
YJL023C	-2.79	0.00	62.40	22.37
YML099W-A	-2.79	0.00	59.54	21.34
YMR014W	-2.79	0.01	38.01	13.63
YFR021W	-2.79	0.00	66.18	23.73
YKL211C	-2.79	0.00	60.81	21.80
YAR019C	-2.79	0.03	23.59	8.46
YDR511W	-2.79	0.00	121.46	43.56

YOR389W	-2.79	0.00	160.40	57.53
YGL250W	-2.79	0.00	68.71	24.65
YNR028W	-2.79	0.03	24.22	8.69
YOR098C	-2.79	0.00	59.42	21.33
YBR235W	-2.79	0.04	20.92	7.51
YBR149W	-2.79	0.00	280.24	100.60
YOR275C	-2.79	0.00	59.98	21.53
YCR077C	-2.78	0.00	44.34	15.92
YIR003W	-2.78	0.00	80.55	28.93
YIL126W	-2.78	0.02	28.28	10.16
YKL039W	-2.78	0.00	127.44	45.77
YER092W	-2.78	0.00	221.07	79.40
YPR084W	-2.78	0.00	55.92	20.09
YJR051W	-2.78	0.00	57.58	20.69
YLR085C	-2.78	0.00	47.86	17.20
YFL020C	-2.78	0.02	25.36	9.11
YDL165W	-2.78	0.00	66.19	23.79
YIL151C	-2.78	0.03	22.98	8.26
YNL230C	-2.78	0.00	42.58	15.31
YDR506C	-2.78	0.05	18.05	6.49
YPL165C	-2.78	0.00	68.69	24.71
YAL033W	-2.78	0.00	42.23	15.19
YOL027C	-2.78	0.00	151.86	54.65
YOL022C	-2.78	0.00	50.14	18.05
YBL028C	-2.78	0.00	82.89	29.85
YGL111W	-2.78	0.00	77.09	27.76
YLR133W	-2.78	0.00	62.25	22.42
YDR445C	-2.78	0.01	37.12	13.37
YOR059C	-2.78	0.00	148.63	53.56
YER005W	-2.78	0.00	57.86	20.85
YBR218C	-2.78	0.00	44.23	15.94
YLR001C	-2.78	0.00	42.51	15.32
YMR208W	-2.77	0.00	49.83	17.96
YDR142C	-2.77	0.00	73.67	26.55
YLR427W	-2.77	0.00	60.34	21.75
YPL092W	-2.77	0.01	38.60	13.92
YKL018C-A	-2.77	0.00	135.47	48.86
YDR295C	-2.77	0.04	20.24	7.30
YAL016C-A	-2.77	0.00	67.02	24.17
YIL027C	-2.77	0.00	49.97	18.02
YBL022C	-2.77	0.00	73.57	26.54
YKL129C	-2.77	0.00	54.43	19.64
YER162C	-2.77	0.00	75.08	27.09
YOR205C	-2.77	0.01	29.36	10.59
YNR075W	-2.77	0.00	45.95	16.58
YDR266C	-2.77	0.00	40.66	14.67
YDR485C	-2.77	0.00	58.60	21.15

YOR046C	-2.77	0.00	62.23	22.46
YKR002W	-2.77	0.00	90.71	32.75
YMR177W	-2.77	0.04	20.41	7.37
YDR117C	-2.77	0.01	36.95	13.34
YKL145W	-2.77	0.00	303.30	109.51
YPR128C	-2.77	0.01	33.65	12.15
YJL092W	-2.77	0.03	22.18	8.01
YBL107C	-2.77	0.00	133.48	48.21
YLL003W	-2.77	0.03	21.88	7.91
YCR028C	-2.77	0.00	41.42	14.97
YPL138C	-2.77	0.00	72.90	26.35
YDR186C	-2.77	0.00	148.83	53.79
YDR304C	-2.77	0.00	135.41	48.95
YLL025W	-2.76	0.04	20.58	7.45
YCL059C	-2.76	0.00	47.96	17.35
YDR442W	-2.76	0.01	33.03	11.95
YDR520C	-2.76	0.04	20.80	7.52
YIL092W	-2.76	0.04	21.77	7.87
YKL140W	-2.76	0.03	22.05	7.97
YLR363W-A	-2.76	0.00	50.32	18.20
YML077W	-2.76	0.00	47.51	17.19
YNL333W	-2.76	0.04	20.93	7.57
YOR013W	-2.76	0.01	30.54	11.05
YNL161W	-2.76	0.00	64.17	23.22
YGR238C	-2.76	0.01	38.32	13.87
YMR322C	-2.76	0.00	135.05	48.88
YKR019C	-2.76	0.01	33.86	12.26
YER041W	-2.76	0.03	23.06	8.35
YNR056C	-2.76	0.02	26.08	9.45
YJL042W	-2.76	0.00	56.05	20.30
YOR086C	-2.76	0.04	21.89	7.93
YGR092W	-2.76	0.00	42.69	15.47
YBL020W	-2.76	0.01	33.59	12.18
YGL073W	-2.76	0.00	91.24	33.07
YJL140W	-2.76	0.00	167.18	60.59
YGL133W	-2.76	0.04	21.45	7.77
YJL032W	-2.76	0.00	83.35	30.22
YIR007W	-2.76	0.03	22.73	8.24
YOR064C	-2.76	0.00	165.68	60.09
YHR017W	-2.76	0.00	103.77	37.64
YPL068C	-2.76	0.00	64.64	23.45
YEL055C	-2.76	0.05	18.41	6.68
YNR011C	-2.76	0.05	18.87	6.85
YML007W	-2.75	0.00	156.27	56.73
YNR032W	-2.75	0.00	68.35	24.82
YNR007C	-2.75	0.00	253.52	92.08
YDR265W	-2.75	0.00	81.14	29.47

YDR486C	-2.75	0.00	138.99	50.49
YDR338C	-2.75	0.00	42.23	15.35
YPL070W	-2.75	0.00	47.67	17.32
YPL152W	-2.75	0.00	57.72	20.97
YMR111C	-2.75	0.00	50.65	18.41
YPL244C	-2.75	0.00	45.52	16.55
YKR081C	-2.75	0.00	64.24	23.36
YMR172C-A	-2.75	0.00	82.69	30.07
YOL158C	-2.75	0.00	121.83	44.32
YGL247W	-2.75	0.00	49.91	18.16
YBR234C	-2.75	0.00	93.01	33.84
YLR092W	-2.75	0.00	43.43	15.80
YEL031W	-2.75	0.00	53.62	19.52
YDL051W	-2.75	0.00	76.84	27.97
YKL170W	-2.75	0.00	148.79	54.17
YBR059C	-2.75	0.00	49.60	18.06
YKL179C	-2.75	0.00	50.48	18.38
YDR330W	-2.75	0.00	107.58	39.18
YOR018W	-2.75	0.04	20.10	7.32
YDR337W	-2.75	0.00	77.09	28.08
YGL213C	-2.74	0.00	47.41	17.27
YPL207W	-2.74	0.00	67.56	24.62
YKL223W	-2.74	0.03	23.00	8.38
YJR144W	-2.74	0.00	65.55	23.89
YOR135C	-2.74	0.00	239.72	87.39
YDR514C	-2.74	0.01	34.27	12.50
YJL077W-B	-2.74	0.00	142.35	51.92
YOR388C	-2.74	0.00	243.01	88.64
YHL019C	-2.74	0.00	48.99	17.87
YML038C	-2.74	0.00	56.54	20.63
YKL166C	-2.74	0.00	56.67	20.67
YKR069W	-2.74	0.00	55.62	20.30
YMR169C	-2.74	0.00	655.51	239.21
YBR272C	-2.74	0.00	40.61	14.82
YDR395W	-2.74	0.01	32.07	11.71
YDR177W	-2.74	0.00	145.11	52.98
YGL044C	-2.74	0.00	60.64	22.15
YLR003C	-2.74	0.02	26.97	9.85
YNL247W	-2.74	0.03	22.69	8.29
YNL234W	-2.74	0.00	67.79	24.77
YLR021W	-2.74	0.00	74.61	27.26
YER175C	-2.74	0.00	57.31	20.94
YCR049C	-2.74	0.00	50.89	18.60
YLL038C	-2.74	0.03	22.64	8.27
YNR048W	-2.74	0.01	37.75	13.80
YDR221W	-2.74	0.02	26.26	9.60
YER112W	-2.74	0.00	106.17	38.81

YPL023C	-2.74	0.00	101.37	37.06
YIL146C	-2.74	0.00	64.62	23.63
YKR028W	-2.74	0.01	33.01	12.07
YBL007C	-2.73	0.00	61.70	22.56
YCR082W	-2.73	0.00	400.87	146.58
YFR022W	-2.73	0.00	469.01	171.51
YOR015W	-2.73	0.00	102.66	37.54
YOL068C	-2.73	0.00	113.94	41.67
YFR010W-A	-2.73	0.00	110.15	40.29
YMR158C-A	-2.73	0.01	37.71	13.79
YMR135W-A	-2.73	0.00	58.48	21.39
YLR275W	-2.73	0.00	93.25	34.11
YDR376W	-2.73	0.01	34.29	12.54
YPL235W	-2.73	0.00	57.20	20.93
YKR087C	-2.73	0.00	51.77	18.95
YLR390W	-2.73	0.00	100.22	36.69
YOR281C	-2.73	0.00	50.53	18.50
YGL039W	-2.73	0.00	50.66	18.54
YNL242W	-2.73	0.05	18.86	6.90
YNL039W	-2.73	0.00	100.77	36.90
YMR056C	-2.73	0.00	91.30	33.43
YGR270W	-2.73	0.00	49.08	17.98
YKL201C	-2.73	0.00	113.76	41.67
YGL246C	-2.73	0.00	47.02	17.23
YGR084C	-2.73	0.00	52.97	19.41
YHR100C	-2.73	0.00	56.49	20.70
YCR072C	-2.73	0.05	20.13	7.38
YMR269W	-2.73	0.00	54.98	20.15
YDR205W	-2.73	0.01	29.84	10.94
YKL202W	-2.73	0.00	368.74	135.19
YGR005C	-2.73	0.00	149.04	54.64
YLR135W	-2.73	0.01	33.96	12.45
YKR074W	-2.73	0.00	62.85	23.05
YGR262C	-2.73	0.00	79.90	29.30
YMR306C-A	-2.73	0.04	21.29	7.81
YOR329C	-2.73	0.00	50.97	18.70
YKL213C	-2.72	0.00	53.11	19.50
YPL141C	-2.72	0.00	56.02	20.56
YKL025C	-2.72	0.00	42.02	15.43
YMR020W	-2.72	0.00	152.91	56.14
YMR227C	-2.72	0.00	72.13	26.48
YGR264C	-2.72	0.00	42.82	15.72
YJL033W	-2.72	0.01	33.17	12.18
YDR341C	-2.72	0.00	50.40	18.51
YEL032C-A	-2.72	0.03	23.46	8.62
YGR116W	-2.72	0.01	31.96	11.74

YER138W-A	-2.72	0.00	141.46	51.97
YDR101C	-2.72	0.03	22.58	8.30
YJR120W	-2.72	0.00	288.22	105.93
YGR137W	-2.72	0.00	249.50	91.71
YDL143W	-2.72	0.00	122.11	44.90
YKL099C	-2.72	0.00	69.66	25.62
YMR033W	-2.72	0.00	44.11	16.22
YMR113W	-2.72	0.01	34.66	12.75
YHR098C	-2.72	0.01	36.22	13.33
YKL194C	-2.72	0.03	24.21	8.91
YLR450W	-2.72	0.00	44.33	16.32
YOR181W	-2.72	0.00	41.69	15.35
YKL150W	-2.72	0.00	537.23	197.76
YOL157C	-2.72	0.00	244.12	89.87
YLR247C	-2.72	0.02	29.41	10.83
YDR468C	-2.72	0.00	77.36	28.48
YBR045C	-2.72	0.01	30.43	11.20
YGR145W	-2.72	0.01	37.97	13.98
YDR365C	-2.72	0.01	35.79	13.18
YDR190C	-2.72	0.00	73.52	27.08
YOR290C	-2.72	0.02	27.50	10.13
YOR243C	-2.71	0.04	21.80	8.03
YGR186W	-2.71	0.00	111.68	41.15
YMR194W	-2.71	0.00	275.01	101.36
YDR034C	-2.71	0.01	37.21	13.72
YOR078W	-2.71	0.00	89.12	32.86
YDR079W	-2.71	0.00	182.22	67.23
YBL059W	-2.71	0.00	44.91	16.57
YHR063C	-2.71	0.00	45.40	16.75
YIL093C	-2.71	0.00	71.57	26.42
YDL135C	-2.71	0.00	101.88	37.61
YGL238W	-2.71	0.04	22.35	8.25
YMR061W	-2.71	0.00	48.07	17.75
YMR089C	-2.71	0.00	81.96	30.27
YMR029C	-2.71	0.01	33.55	12.39
YAR003W	-2.71	0.04	21.32	7.88
YER051W	-2.71	0.00	62.59	23.12
YIL010W	-2.71	0.00	113.16	41.81
YCR090C	-2.71	0.00	53.79	19.88
YOL071W	-2.70	0.00	150.56	55.67
YHR085W	-2.70	0.01	33.98	12.56
YNL336W	-2.70	0.00	75.62	27.96
YDR358W	-2.70	0.00	71.23	26.34
YDR069C	-2.70	0.02	29.80	11.02
YPR170C	-2.70	0.00	44.90	16.62
YDL007W	-2.70	0.00	295.37	109.33
YHR171W	-2.70	0.02	29.07	10.76

YKL157W	-2.70	0.00	80.03	29.63
YMR068W	-2.70	0.00	106.73	39.53
YGR042W	-2.70	0.00	74.74	27.68
YOR233W	-2.70	0.03	25.38	9.40
YJL110C	-2.70	0.02	29.27	10.84
YOL056W	-2.70	0.04	21.22	7.86
YDL202W	-2.70	0.00	57.31	21.24
YOR003W	-2.70	0.00	54.57	20.22
YKL082C	-2.70	0.00	103.11	38.22
YPL076W	-2.70	0.03	25.18	9.33
YDR223W	-2.70	0.03	23.28	8.63
YBR142W	-2.70	0.03	22.84	8.47
YPR190C	-2.70	0.01	39.79	14.76
YGR231C	-2.70	0.00	285.30	105.82
YEL052W	-2.70	0.00	61.38	22.77
YLL009C	-2.70	0.00	370.63	137.48
YMR125W	-2.70	0.03	22.88	8.49
YLR252W	-2.69	0.01	36.88	13.69
YOR134W	-2.69	0.00	206.28	76.56
YNL031C	-2.69	0.00	1292.89	479.83
YJR109C	-2.69	0.01	36.72	13.63
YDR383C	-2.69	0.02	27.89	10.35
YGL100W	-2.69	0.00	67.72	25.14
YGR157W	-2.69	0.00	113.26	42.06
YOR066W	-2.69	0.00	70.05	26.02
YKL208W	-2.69	0.01	39.77	14.77
YIL161W	-2.69	0.00	51.87	19.27
YOR115C	-2.69	0.00	58.40	21.70
YKL059C	-2.69	0.00	91.55	34.02
YIL009W	-2.69	0.02	27.43	10.20
YDR357C	-2.69	0.00	56.89	21.15
YDR262W	-2.69	0.00	456.32	169.67
YOR157C	-2.69	0.00	204.00	75.88
YDR237W	-2.69	0.00	71.38	26.56
YDR212W	-2.69	0.00	88.79	33.05
YKR070W	-2.69	0.00	52.95	19.71
YMR039C	-2.69	0.00	231.71	86.26
YBR010W	-2.69	0.00	561.43	209.04
YDR467C	-2.69	0.00	54.72	20.37
YDL116W	-2.69	0.04	21.80	8.12
YIL138C	-2.69	0.00	118.16	44.00
YGR222W	-2.68	0.01	37.86	14.10
YHR012W	-2.68	0.00	89.47	33.33
YPL160W	-2.68	0.01	32.46	12.10
YER122C	-2.68	0.00	132.66	49.45
YDR321W	-2.68	0.00	41.59	15.50
YFR052C-A	-2.68	0.01	31.15	11.61

YJL045W	-2.68	0.01	36.01	13.42
YNL155W	-2.68	0.00	252.90	94.29
YER107C	-2.68	0.01	36.27	13.52
YOL041C	-2.68	0.00	52.63	19.63
YLR193C	-2.68	0.00	251.52	93.86
YJR160C	-2.68	0.05	19.36	7.23
YBR166C	-2.68	0.00	41.91	15.64
YJL036W	-2.68	0.00	142.28	53.13
YIL127C	-2.68	0.00	77.97	29.12
YJR082C	-2.68	0.00	151.49	56.59
YDL002C	-2.68	0.00	75.48	28.20
YBR221C	-2.68	0.00	237.52	88.75
YKL006C-A	-2.68	0.00	178.41	66.69
YNL315C	-2.67	0.00	83.71	31.30
YMR027W	-2.67	0.00	167.65	62.69
YIL061C	-2.67	0.00	57.31	21.43
YOR151C	-2.67	0.00	60.24	22.53
YOR288C	-2.67	0.01	34.04	12.73
YPR187W	-2.67	0.00	120.33	45.01
YDR079C-A	-2.67	0.00	69.69	26.08
YER074W-A	-2.67	0.00	210.33	78.70
YHL006W-A	-2.67	0.05	19.16	7.17
YER126C	-2.67	0.00	53.49	20.02
YGL107C	-2.67	0.01	38.95	14.58
YGL228W	-2.67	0.00	139.51	52.22
YPL254W	-2.67	0.04	22.88	8.56
YOR016C	-2.67	0.00	64.10	24.00
YJL220W	-2.67	0.00	87.52	32.78
YMR093W	-2.67	0.01	33.18	12.43
YGL140C	-2.67	0.03	26.15	9.80
YBR244W	-2.67	0.00	50.58	18.94
YLR034C	-2.67	0.00	57.90	21.69
YDR287W	-2.67	0.00	94.20	35.30
YDR415C	-2.67	0.00	54.63	20.47
YLR324W	-2.67	0.00	114.05	42.75
YJR005C-A	-2.67	0.04	22.81	8.55
YOL122C	-2.67	0.00	44.57	16.71
YDL236W	-2.67	0.00	146.53	54.94
YHR058C	-2.67	0.00	52.22	19.58
YPL184C	-2.67	0.00	41.69	15.63
YFR011C	-2.67	0.00	74.55	27.95
YKR021W	-2.67	0.04	21.43	8.04
YOR186W	-2.67	0.01	36.16	13.57
YBR170C	-2.67	0.00	83.84	31.45
YAL036C	-2.67	0.00	47.99	18.01
YIL020C	-2.67	0.00	81.54	30.60
YNL008C	-2.67	0.00	54.62	20.49

YHR117W	-2.66	0.02	29.24	10.97
YLR361C	-2.66	0.01	31.24	11.73
YDR178W	-2.66	0.00	638.10	239.52
YPL077C	-2.66	0.01	32.03	12.02
YOL143C	-2.66	0.00	266.70	100.16
YAL027W	-2.66	0.00	44.49	16.71
YGR026W	-2.66	0.00	56.10	21.08
YGL020C	-2.66	0.00	62.03	23.30
YGR266W	-2.66	0.03	25.82	9.70
YMR280C	-2.66	0.01	40.32	15.15
YNL223W	-2.66	0.00	72.10	27.09
YER101C	-2.66	0.00	45.45	17.08
YDR264C	-2.66	0.00	81.97	30.80
YLR338W	-2.66	0.00	57.86	21.74
YOR047C	-2.66	0.00	109.29	41.07
YGR103W	-2.66	0.00	46.16	17.35
YIL115W-A	-2.66	0.00	60.36	22.69
YAL009W	-2.66	0.00	45.88	17.25
YGL259W	-2.66	0.02	29.83	11.21
YER079W	-2.66	0.00	170.07	63.95
YLR208W	-2.66	0.00	126.63	47.62
YPR088C	-2.66	0.00	109.37	41.13
YMR189W	-2.66	0.01	33.96	12.77
YDR238C	-2.66	0.00	48.61	18.28
YMR252C	-2.66	0.00	182.79	68.78
YJR034W	-2.66	0.00	75.29	28.33
YLR368W	-2.66	0.00	45.49	17.13
YBL100C	-2.66	0.00	181.37	68.29
YLR145W	-2.66	0.00	44.77	16.86
YJL131C	-2.66	0.00	67.98	25.59
YDR362C	-2.66	0.00	57.67	21.72
YNL127W	-2.66	0.03	25.72	9.69
YOR323C	-2.65	0.00	100.23	37.77
YMR133W	-2.65	0.03	24.99	9.42
YLR228C	-2.65	0.05	19.42	7.32
YEL073C	-2.65	0.00	201.60	75.99
YDL067C	-2.65	0.00	1674.71	631.35
YJR143C	-2.65	0.05	21.10	7.96
YGL219C	-2.65	0.00	169.50	63.91
YBR202W	-2.65	0.05	19.49	7.35
YLR299W	-2.65	0.00	94.10	35.49
YPR016W-A	-2.65	0.00	41.90	15.80
YMR312W	-2.65	0.01	33.15	12.51
YNL308C	-2.65	0.00	83.90	31.65
YML092C	-2.65	0.00	242.06	91.34
YOR110W	-2.65	0.00	66.84	25.23
YOR106W	-2.65	0.00	102.40	38.65

YJL167W	-2.65	0.00	201.27	75.98
YCR044C	-2.65	0.03	24.88	9.39
YLR176C	-2.65	0.05	19.73	7.45
YDL138W	-2.65	0.00	58.73	22.18
YER143W	-2.65	0.00	129.27	48.81
YGL078C	-2.65	0.00	75.55	28.54
YJR042W	-2.65	0.04	21.79	8.23
YOR231C-A	-2.65	0.01	32.58	12.31
YOR184W	-2.65	0.00	157.46	59.50
YJR059W	-2.65	0.00	130.73	49.40
YPR169W	-2.65	0.00	58.24	22.01
YCR091W	-2.65	0.01	37.88	14.32
YDR498C	-2.65	0.00	43.86	16.58
YJR068W	-2.64	0.00	62.22	23.54
YJL202C	-2.64	0.00	65.53	24.80
YNL293W	-2.64	0.00	55.28	20.92
YEL059C-A	-2.64	0.00	84.21	31.87
YNL011C	-2.64	0.00	44.46	16.83
YER136W	-2.64	0.00	118.68	44.92
YNR042W	-2.64	0.00	67.20	25.44
YOR119C	-2.64	0.00	60.12	22.76
YKL141W	-2.64	0.00	342.93	129.88
YNR038W	-2.64	0.04	23.58	8.93
YJL072C	-2.64	0.00	48.00	18.19
YJL103C	-2.64	0.00	50.32	19.07
YDL019C	-2.64	0.00	63.33	24.00
YBR179C	-2.64	0.00	57.25	21.69
YLR020C	-2.64	0.00	82.42	31.24
YPR185W	-2.64	0.04	22.05	8.36
YKL094W	-2.64	0.00	418.34	158.56
YKL020C	-2.64	0.00	54.25	20.56
YOR363C	-2.64	0.05	20.31	7.70
YNL310C	-2.64	0.00	73.62	27.92
YPL196W	-2.64	0.00	108.70	41.22
YBR226C	-2.64	0.00	55.77	21.15
YDL052C	-2.64	0.00	88.61	33.60
YER042W	-2.64	0.00	307.45	116.62
YPR191W	-2.64	0.00	862.20	327.06
YGR080W	-2.64	0.00	70.65	26.80
YBL075C	-2.63	0.00	408.08	154.89
YMR292W	-2.63	0.00	45.29	17.19
YMR080C	-2.63	0.01	33.19	12.60
YNL215W	-2.63	0.00	156.55	59.43
YMR072W	-2.63	0.00	185.81	70.58
YGR077C	-2.63	0.04	23.03	8.75
YMR109W	-2.63	0.05	20.31	7.71
YKR037C	-2.63	0.00	62.63	23.79

YKL074C	-2.63	0.00	56.30	21.39
YHR118C	-2.63	0.00	51.19	19.45
YLL049W	-2.63	0.00	44.83	17.04
YMR289W	-2.63	0.01	31.76	12.07
YGR048W	-2.63	0.00	160.95	61.17
YFR041C	-2.63	0.00	42.47	16.15
YML128C	-2.63	0.00	417.26	158.71
YPR129W	-2.63	0.00	115.45	43.93
YHR106W	-2.63	0.00	79.22	30.15
YPR036W-A	-2.63	0.00	23882.56	9092.37
YJR072C	-2.63	0.00	114.28	43.51
YCR076C	-2.63	0.00	79.68	30.34
YMR275C	-2.63	0.01	37.81	14.40
YDR292C	-2.63	0.01	39.02	14.86
YPL111W	-2.63	0.00	68.16	25.96
YML081W	-2.63	0.01	41.91	15.96
YCL048W-A	-2.63	0.04	22.90	8.72
YNL186W	-2.63	0.00	56.36	21.47
YGR095C	-2.63	0.00	68.66	26.16
YPR149W	-2.62	0.00	1129.88	430.43
YKL028W	-2.62	0.00	81.60	31.09
YDR513W	-2.62	0.00	324.19	123.53
YER186C	-2.62	0.00	73.59	28.04
YFR004W	-2.62	0.00	320.19	122.01
YEL018W	-2.62	0.00	80.06	30.52
YAR023C	-2.62	0.03	24.04	9.17
YLR251W	-2.62	0.00	59.95	22.86
YDR496C	-2.62	0.04	22.96	8.76
YOL009C	-2.62	0.01	39.56	15.09
YOL061W	-2.62	0.00	82.79	31.58
YKL139W	-2.62	0.00	51.99	19.83
YNR021W	-2.62	0.03	25.46	9.71
YBR057C	-2.62	0.00	62.67	23.92
YDL134C	-2.62	0.00	183.91	70.20
YGR275W	-2.62	0.00	156.06	59.57
YBL058W	-2.62	0.00	278.55	106.35
YMR301C	-2.62	0.02	28.86	11.02
YBR155W	-2.62	0.00	43.18	16.49
YGR106C	-2.62	0.00	116.15	44.37
YKR014C	-2.62	0.00	447.41	170.92
YHR076W	-2.62	0.00	63.24	24.16
YNL094W	-2.62	0.00	110.19	42.12
YFR025C	-2.62	0.01	34.58	13.22
YNL013C	-2.62	0.00	127.32	48.68
YDR253C	-2.62	0.00	97.66	37.34
YIL121W	-2.62	0.00	338.80	129.55
YIL050W	-2.62	0.00	120.29	46.00

YHR132W-A	-2.61	0.00	252.22	96.46
YAL043C	-2.61	0.01	36.08	13.80
YBR210W	-2.61	0.04	23.58	9.02
YBR193C	-2.61	0.00	49.60	18.98
YMR282C	-2.61	0.04	21.97	8.41
YNL228W	-2.61	0.00	72.55	27.77
YGL041C	-2.61	0.00	143.04	54.74
YNL091W	-2.61	0.00	47.37	18.13
YER115C	-2.61	0.00	63.86	24.46
YAR014C	-2.61	0.01	35.77	13.70
YAL054C	-2.61	0.00	197.79	75.78
YJL102W	-2.61	0.00	51.23	19.63
YIR034C	-2.61	0.00	303.64	116.39
YMR153W	-2.61	0.00	72.56	27.82
YMR290C	-2.61	0.01	40.76	15.63
YHR205W	-2.61	0.00	83.14	31.89
YLR360W	-2.61	0.00	53.12	20.38
YGR212W	-2.61	0.05	20.45	7.85
YML067C	-2.60	0.00	62.12	23.85
YAL015C	-2.60	0.01	32.50	12.48
YFR040W	-2.60	0.00	95.95	36.84
YCR024C	-2.60	0.00	65.36	25.10
YNL248C	-2.60	0.03	25.82	9.91
YGR104C	-2.60	0.03	25.57	9.82
YHR059W	-2.60	0.00	60.11	23.09
YOR174W	-2.60	0.00	60.46	23.23
YML019W	-2.60	0.03	27.28	10.48
YDR038C	-2.60	0.00	92.61	35.58
YOR239W	-2.60	0.00	61.17	23.50
YGL017W	-2.60	0.03	27.30	10.49
YDR143C	-2.60	0.00	51.52	19.80
YMR319C	-2.60	0.00	86.68	33.31
YBR258C	-2.60	0.00	51.93	19.97
YPR010C	-2.60	0.02	31.57	12.14
YOR357C	-2.60	0.00	96.50	37.11
YJR050W	-2.60	0.00	96.22	37.01
YJL094C	-2.60	0.00	77.43	29.79
YDR452W	-2.60	0.00	52.44	20.18
YHR081W	-2.60	0.00	204.40	78.66
YDR160W	-2.60	0.04	23.58	9.08
YDL169C	-2.60	0.00	198.49	76.39
YHR113W	-2.60	0.00	89.08	34.29
YAL028W	-2.60	0.01	34.38	13.23
YNL238W	-2.60	0.01	41.26	15.88
YNL192W	-2.60	0.00	351.14	135.18
YKL053C-A	-2.60	0.00	258.10	99.43

YML005W	-2.60	0.00	62.48	24.07
YAR027W	-2.60	0.00	179.31	69.10
YNL023C	-2.59	0.01	39.87	15.37
YMR260C	-2.59	0.00	257.58	99.30
YLR267W	-2.59	0.00	54.38	20.97
YOL067C	-2.59	0.00	81.36	31.37
YKR022C	-2.59	0.00	68.62	26.45
YBR110W	-2.59	0.00	57.65	22.23
YOR164C	-2.59	0.01	42.22	16.29
YPL009C	-2.59	0.01	38.95	15.02
YGR195W	-2.59	0.00	48.61	18.75
YCR097W	-2.59	0.00	45.28	17.49
YER133W-A	-2.59	0.00	141.23	54.55
YDL140C	-2.59	0.00	56.85	21.96
YDR494W	-2.59	0.00	115.55	44.64
YLR099C	-2.59	0.00	663.87	256.49
YCR099C	-2.59	0.03	25.61	9.90
YOR125C	-2.59	0.00	51.23	19.80
YER087C-A	-2.59	0.02	29.45	11.38
YDR192C	-2.59	0.01	42.15	16.29
YBR158W	-2.59	0.01	35.51	13.73
YMR156C	-2.59	0.01	34.34	13.27
YPR015C	-2.59	0.01	39.93	15.44
YJR154W	-2.59	0.03	25.22	9.75
YGL027C	-2.59	0.04	24.00	9.28
YDR085C	-2.59	0.00	94.42	36.51
YDL054C	-2.59	0.00	98.94	38.26
YNL016W	-2.59	0.00	103.00	39.83
YGR158C	-2.59	0.00	44.89	17.36
YCR033W	-2.59	0.01	35.57	13.76
YIL034C	-2.59	0.00	116.21	44.95
YBR212W	-2.59	0.00	88.80	34.35
YPL118W	-2.59	0.00	119.50	46.23
YDL182W	-2.58	0.00	310.33	120.05
YBR192W	-2.58	0.01	36.30	14.04
YNL270C	-2.58	0.01	34.57	13.38
YLR088W	-2.58	0.03	25.42	9.84
YNL040W	-2.58	0.03	26.79	10.37
YER063W	-2.58	0.00	191.09	73.98
YDL222C	-2.58	0.00	119.66	46.33
YLL013C	-2.58	0.01	33.34	12.91
YNL133C	-2.58	0.00	125.58	48.62
YHR170W	-2.58	0.00	67.57	26.16
YGR101W	-2.58	0.00	58.08	22.49
YDR391C	-2.58	0.00	116.95	45.30
YHR074W	-2.58	0.00	49.18	19.05
YGL019W	-2.58	0.00	135.82	52.61

YLR114C	-2.58	0.00	59.52	23.06
YNL286W	-2.58	0.01	40.28	15.60
YLR231C	-2.58	0.00	59.03	22.87
YJL179W	-2.58	0.02	29.77	11.54
YHR086W	-2.58	0.01	38.02	14.73
YOR324C	-2.58	0.00	45.06	17.47
YLR005W	-2.58	0.00	76.62	29.71
YBR251W	-2.58	0.00	62.15	24.10
YAL045C	-2.58	0.00	83.65	32.44
YGR148C	-2.58	0.00	401.59	155.78
YCR041W	-2.58	0.01	33.89	13.15
YER133W	-2.58	0.00	254.46	98.79
YBL021C	-2.58	0.00	127.71	49.60
YGL169W	-2.57	0.01	35.20	13.67
YNR064C	-2.57	0.04	22.64	8.79
YJL156C	-2.57	0.02	31.97	12.42
YDR363W-A	-2.57	0.00	440.96	171.32
YNL317W	-2.57	0.00	54.67	21.24
YOR056C	-2.57	0.00	93.56	36.37
YBR042C	-2.57	0.02	28.16	10.95
YNL150W	-2.57	0.00	443.59	172.47
YML074C	-2.57	0.00	184.18	71.62
YDL203C	-2.57	0.01	37.73	14.68
YBR267W	-2.57	0.00	69.56	27.06
YML116W	-2.57	0.00	57.58	22.40
YOR279C	-2.57	0.00	44.75	17.41
YNL323W	-2.57	0.00	73.23	28.49
YGR277C	-2.57	0.00	73.19	28.48
YGL089C	-2.57	0.04	23.36	9.09
YGR125W	-2.57	0.01	37.10	14.44
YLR125W	-2.57	0.03	26.18	10.19
YPR172W	-2.57	0.00	75.16	29.25
YML112W	-2.57	0.00	71.54	27.85
YJR112W	-2.57	0.01	34.16	13.30
YML014W	-2.57	0.01	39.19	15.26
YMR141C	-2.57	0.00	120.17	46.82
YIL007C	-2.57	0.00	98.25	38.28
YGR209C	-2.57	0.00	1019.54	397.23
YPL203W	-2.56	0.00	167.45	65.28
YHL007C	-2.56	0.02	31.56	12.31
YBL026W	-2.56	0.00	109.03	42.52
YDR204W	-2.56	0.00	82.32	32.10
YMR077C	-2.56	0.00	76.21	29.73
YPL190C	-2.56	0.00	113.99	44.46
YDR429C	-2.56	0.00	192.44	75.07
YER168C	-2.56	0.01	43.12	16.82

YBL039C	-2.56	0.05	22.25	8.68
YCL016C	-2.56	0.01	35.15	13.71
YLR346C	-2.56	0.00	849.82	331.57
YKL066W	-2.56	0.00	50.18	19.58
YGR237C	-2.56	0.00	143.22	55.89
YLR045C	-2.56	0.05	22.19	8.66
YML011C	-2.56	0.00	66.36	25.90
YBR143C	-2.56	0.00	104.40	40.76
YFL067W	-2.56	0.00	69.55	27.16
YKR088C	-2.56	0.00	54.32	21.21
YGL216W	-2.56	0.01	42.13	16.45
YEL060C	-2.56	0.00	2178.87	851.09
YLR100W	-2.56	0.00	109.06	42.61
YDL122W	-2.56	0.00	100.16	39.14
YBR022W	-2.56	0.00	52.89	20.68
YBR084W	-2.56	0.04	22.73	8.89
YAL041W	-2.56	0.02	30.12	11.78
YFL059W	-2.56	0.05	21.71	8.49
YOR219C	-2.56	0.03	27.86	10.89
YFL057C	-2.56	0.00	65.74	25.71
YHL048W	-2.56	0.05	21.94	8.58
YPL260W	-2.56	0.00	280.59	109.78
YPL101W	-2.56	0.00	75.71	29.62
YAR007C	-2.56	0.01	40.24	15.74
YMR088C	-2.56	0.00	52.90	20.70
YFL041W	-2.56	0.00	78.25	30.62
YIL020C-A	-2.55	0.00	100.39	39.31
YNL235C	-2.55	0.03	26.26	10.28
YGR178C	-2.55	0.00	92.18	36.10
YLR373C	-2.55	0.00	48.80	19.11
YML030W	-2.55	0.00	201.50	78.92
YPL051W	-2.55	0.00	66.21	25.93
YDR472W	-2.55	0.01	39.74	15.57
YOR231W	-2.55	0.00	48.37	18.95
YLR330W	-2.55	0.00	170.61	66.88
YOR172W	-2.55	0.01	38.39	15.05
YKL164C	-2.55	0.00	157.42	61.72
YOR071C	-2.55	0.01	34.40	13.49
YFR042W	-2.55	0.01	35.69	14.00
YNL258C	-2.55	0.01	34.57	13.56
YFL013W-A	-2.55	0.00	121.32	47.59
YAL021C	-2.55	0.02	29.15	11.43
YER060W	-2.55	0.00	61.76	24.23
YER182W	-2.55	0.00	171.61	67.34
YOL082W	-2.55	0.00	81.62	32.03
YLR447C	-2.55	0.00	193.46	75.92
YGL218W	-2.55	0.00	125.67	49.32

YDL124W	-2.55	0.00	1819.38	714.06
YKL151C	-2.55	0.00	287.08	112.70
YER082C	-2.55	0.02	32.91	12.92
YDL057W	-2.55	0.04	24.88	9.77
YCR069W	-2.55	0.00	178.12	69.95
YDL031W	-2.55	0.04	22.82	8.96
YGR019W	-2.55	0.00	273.59	107.46
YML114C	-2.55	0.01	37.31	14.65
YPL223C	-2.55	0.00	769.08	302.12
YGL156W	-2.54	0.00	102.33	40.21
YGR295C	-2.54	0.00	253.04	99.44
YNL037C	-2.54	0.00	353.56	138.97
YER024W	-2.54	0.00	74.00	29.09
YAL064W-B	-2.54	0.04	22.87	8.99
YBR175W	-2.54	0.04	24.00	9.44
YKL138C-A	-2.54	0.00	136.72	53.78
YGR253C	-2.54	0.00	336.82	132.50
YCR096C	-2.54	0.00	103.47	40.72
YKL193C	-2.54	0.00	71.01	27.95
YGL226W	-2.54	0.00	111.77	44.01
YNL122C	-2.54	0.00	96.28	37.93
YJL077C	-2.54	0.00	71.18	28.04
YLR038C	-2.54	0.00	641.62	252.80
YPL084W	-2.54	0.01	36.40	14.34
YLR401C	-2.54	0.01	44.61	17.58
YDR538W	-2.54	0.00	77.97	30.73
YLR270W	-2.54	0.00	307.66	121.24
YKL036C	-2.54	0.02	31.54	12.43
YLR069C	-2.54	0.00	61.90	24.40
YPL129W	-2.54	0.00	118.70	46.79
YJL132W	-2.54	0.05	21.65	8.53
YDL145C	-2.54	0.04	24.32	9.59
YGL190C	-2.54	0.00	57.92	22.84
YBR137W	-2.54	0.00	115.33	45.47
YNL259C	-2.54	0.00	213.10	84.03
YPL228W	-2.54	0.01	34.52	13.61
YJL148W	-2.54	0.00	57.06	22.51
YLR149C	-2.53	0.00	132.61	52.31
YPL093W	-2.53	0.00	48.40	19.09
YBL100W-C	-2.53	0.03	26.80	10.58
YER144C	-2.53	0.00	58.26	22.99
YMR010W	-2.53	0.00	86.32	34.07
YCL033C	-2.53	0.00	98.61	38.92
YLR246W	-2.53	0.00	72.18	28.49
YPR063C	-2.53	0.00	131.05	51.75
YOL011W	-2.53	0.00	262.96	103.85
YDR423C	-2.53	0.00	82.82	32.71

YGL137W	-2.53	0.00	57.16	22.58
YOR267C	-2.53	0.00	413.03	163.17
YDR463W	-2.53	0.00	162.98	64.39
YER166W	-2.53	0.02	31.94	12.62
YNL218W	-2.53	0.05	22.58	8.92
YOR376W-A	-2.53	0.00	56.60	22.37
YPL270W	-2.53	0.00	60.57	23.94
YDR272W	-2.53	0.00	239.15	94.53
YFR032C-A	-2.53	0.00	535.06	211.51
YDR312W	-2.53	0.02	33.23	13.14
YKL174C	-2.53	0.00	47.36	18.72
YIL063C	-2.53	0.00	125.75	49.72
YIL070C	-2.53	0.00	113.60	44.92
YOR002W	-2.53	0.02	29.94	11.84
YMR250W	-2.53	0.00	195.32	77.24
YDR537C	-2.53	0.00	81.54	32.25
YNL021W	-2.53	0.01	44.47	17.59
YIL068W-A	-2.53	0.01	40.51	16.03
YPL099C	-2.53	0.00	100.76	39.87
YDR084C	-2.53	0.00	48.63	19.25
YIL071W-A	-2.53	0.00	48.06	19.02
YLR264W	-2.53	0.00	221.58	87.71
YER098W	-2.53	0.00	101.33	40.12
YKL093W	-2.53	0.00	107.95	42.74
YHR195W	-2.53	0.00	154.42	61.15
YFL029C	-2.53	0.02	32.28	12.78
YCL052C	-2.52	0.00	119.10	47.17
YDL212W	-2.52	0.00	105.78	41.90
YOR263C	-2.52	0.03	27.09	10.73
YGL062W	-2.52	0.00	249.27	98.76
YDR302W	-2.52	0.01	37.12	14.71
YDR088C	-2.52	0.00	66.06	26.18
YHR194W	-2.52	0.04	23.56	9.34
YGL252C	-2.52	0.00	126.68	50.20
YKR067W	-2.52	0.00	50.64	20.07
YER071C	-2.52	0.01	43.28	17.15
YCL031C	-2.52	0.00	91.31	36.20
YDR439W	-2.52	0.01	36.63	14.53
YHR096C	-2.52	0.00	177.96	70.59
YDR364C	-2.52	0.00	52.15	20.69
YIL085C	-2.52	0.00	80.38	31.89
YML017W	-2.52	0.02	34.19	13.57
YLR291C	-2.52	0.00	64.19	25.47
YNL042W	-2.52	0.00	132.12	52.42
YML034W	-2.52	0.00	95.50	37.89
YNL159C	-2.52	0.00	110.10	43.69

YLR392C	-2.52	0.00	65.73	26.08
YDR334W	-2.52	0.02	33.13	13.15
YDR504C	-2.52	0.01	37.46	14.87
YKR098C	-2.52	0.00	59.51	23.63
YMR053C	-2.52	0.01	38.94	15.46
YDL181W	-2.52	0.00	503.62	199.95
YLR347W-A	-2.52	0.00	63.45	25.20
YIR006C	-2.52	0.01	41.71	16.57
YER062C	-2.52	0.00	1979.66	786.37
YLR262C-A	-2.52	0.00	244.10	96.97
YGR123C	-2.52	0.03	25.79	10.25
YOR391C	-2.52	0.00	124.57	49.50
YHR152W	-2.52	0.00	59.04	23.46
YCL012C	-2.52	0.00	244.01	96.98
YMR031C	-2.52	0.00	125.73	49.97
YLR094C	-2.52	0.00	248.59	98.82
YNL109W	-2.52	0.00	85.36	33.93
YLR221C	-2.51	0.00	82.56	32.83
YFR034C	-2.51	0.00	110.29	43.86
YML120C	-2.51	0.00	610.02	242.58
YDR031W	-2.51	0.00	122.07	48.54
YKR084C	-2.51	0.01	43.54	17.31
YML115C	-2.51	0.00	65.79	26.16
YMR313C	-2.51	0.00	77.00	30.62
YGL014C-A	-2.51	0.05	21.66	8.62
YLR223C	-2.51	0.04	23.98	9.54
YGL143C	-2.51	0.01	36.58	14.56
YGL011C	-2.51	0.00	532.45	211.93
YHR064C	-2.51	0.00	91.10	36.26
YHR114W	-2.51	0.02	33.94	13.51
YBR164C	-2.51	0.00	67.27	26.78
YJR063W	-2.51	0.00	55.23	21.99
YLR281C	-2.51	0.03	27.24	10.85
YDR161W	-2.51	0.00	68.98	27.47
YNL243W	-2.51	0.00	64.19	25.58
YOR393W	-2.51	0.01	35.38	14.10
YPL018W	-2.51	0.00	139.98	55.79
YGR201C	-2.51	0.00	346.29	138.04
YLL001W	-2.51	0.00	46.54	18.56
YPL019C	-2.51	0.01	42.13	16.80
YDL015C	-2.51	0.00	64.81	25.84
YDL084W	-2.51	0.00	120.18	47.93
YAR031W	-2.51	0.04	24.12	9.62
YMR153C-A	-2.51	0.00	96.59	38.52
YDR033W	-2.51	0.00	343.27	136.92
YDL065C	-2.51	0.00	151.96	60.62
YDL008W	-2.51	0.00	66.11	26.37

YLR244C	-2.51	0.00	233.50	93.16
YNR034W	-2.51	0.00	162.66	64.90
YBR231C	-2.51	0.00	110.54	44.11
YDR477W	-2.51	0.00	63.37	25.29
YNR006W	-2.51	0.00	99.87	39.86
YPL119C	-2.51	0.00	91.15	36.38
YJR101W	-2.51	0.00	70.45	28.12
YGR227W	-2.51	0.05	22.16	8.85
YEL056W	-2.50	0.01	42.43	16.94
YPL119C-A	-2.50	0.03	27.69	11.06
YKL012W	-2.50	0.00	74.26	29.66
YKL077W	-2.50	0.00	175.03	69.91
YDR087C	-2.50	0.02	33.40	13.34
YPR019W	-2.50	0.01	43.81	17.50
YGL002W	-2.50	0.00	107.07	42.79
YPL031C	-2.50	0.00	106.89	42.72
YLR420W	-2.50	0.00	61.04	24.40
YDR074W	-2.50	0.00	297.45	118.89
YLR337C	-2.50	0.00	93.53	37.39
YPR186C	-2.50	0.05	23.25	9.30
YOR370C	-2.50	0.00	84.88	33.93
YMR060C	-2.50	0.03	28.70	11.48
YOR382W	-2.50	0.00	1081.82	432.63
YLR072W	-2.50	0.01	44.88	17.95
YMR226C	-2.50	0.00	314.93	125.96
YMR107W	-2.50	0.00	953.10	381.26
YJL082W	-2.50	0.00	308.41	123.38
YNL231C	-2.50	0.00	605.59	242.27
YPR114W	-2.50	0.00	152.92	61.18
YMR079W	-2.50	0.00	55.98	22.40
YGL214W	-2.50	0.00	60.04	24.02
YIR009W	-2.50	0.00	49.08	19.64
YMR234W	-2.50	0.00	50.88	20.36
YPR178W	-2.50	0.00	56.34	22.56
YBR009C	-2.50	0.00	1149.48	460.23
YBR176W	-2.50	0.03	28.52	11.42
YDR202C	-2.50	0.00	69.77	27.94
YBR199W	-2.50	0.00	178.66	71.55
YLR358C	-2.50	0.00	100.26	40.16
YBL010C	-2.50	0.01	37.39	14.98
YIR038C	-2.50	0.00	155.69	62.37
YJL069C	-2.50	0.01	39.84	15.96
YJL001W	-2.50	0.00	246.09	98.61
YJL212C	-2.50	0.05	23.03	9.23
YDL080C	-2.49	0.03	28.63	11.48
YBR236C	-2.49	0.00	53.12	21.30
YOR251C	-2.49	0.00	66.59	26.70

YGR245C	-2.49	0.03	28.30	11.35
YPR103W	-2.49	0.00	234.25	93.93
YJL123C	-2.49	0.00	72.88	29.23
YGL050W	-2.49	0.00	64.67	25.94
YHR206W	-2.49	0.00	100.21	40.20
YLR195C	-2.49	0.01	44.63	17.90
YJL129C	-2.49	0.05	23.25	9.33
YLR357W	-2.49	0.01	39.69	15.92
YER140W	-2.49	0.02	33.88	13.59
YGR149W	-2.49	0.00	212.03	85.09
YDR289C	-2.49	0.00	76.73	30.80
YFL056C	-2.49	0.00	58.39	23.43
YNL047C	-2.49	0.03	26.23	10.53
YHR049C-A	-2.49	0.00	102.19	41.02
YMR091C	-2.49	0.00	69.61	27.94
YIL083C	-2.49	0.00	67.37	27.05
YCR068W	-2.49	0.00	58.55	23.51
YFR020W	-2.49	0.00	263.10	105.66
YDR345C	-2.49	0.00	8458.56	3400.44
YKL136W	-2.49	0.00	99.66	40.08
YFL017C	-2.49	0.00	70.66	28.42
YPL065W	-2.49	0.03	27.91	11.23
YGL004C	-2.49	0.01	35.35	14.22
YAL011W	-2.49	0.02	34.94	14.06
YPL222W	-2.48	0.00	112.88	45.43
YKR049C	-2.48	0.00	392.90	158.16
YCL028W	-2.48	0.00	116.33	46.83
YML091C	-2.48	0.00	47.12	18.97
YGL181W	-2.48	0.00	196.49	79.12
YLR163W-A	-2.48	0.00	81.56	32.84
YML111W	-2.48	0.05	22.24	8.96
YPL030W	-2.48	0.02	33.94	13.67
YJL053W	-2.48	0.00	72.02	29.00
YDL200C	-2.48	0.01	43.63	17.57
YMR225C	-2.48	0.00	132.51	53.41
YBR127C	-2.48	0.00	276.54	111.47
YLR268W	-2.48	0.00	91.75	36.99
YGR196C	-2.48	0.00	62.53	25.21
YPR059C	-2.48	0.01	44.73	18.04
YPR166C	-2.48	0.00	93.60	37.74
YBR242W	-2.48	0.00	86.45	34.87
YNR033W	-2.48	0.00	53.03	21.39
YBR154C	-2.48	0.00	59.47	23.99
YJL203W	-2.48	0.00	61.95	24.99
YOL097C	-2.48	0.00	47.58	19.20
YGR244C	-2.48	0.00	224.62	90.63
YNL038W	-2.48	0.01	38.73	15.63

YIL090W	-2.48	0.01	42.47	17.15
YKR100C	-2.48	0.00	112.68	45.51
YBR030W	-2.48	0.03	27.18	10.98
YOL135C	-2.48	0.00	92.04	37.18
YDL085W	-2.48	0.00	78.54	31.73
YDL144C	-2.48	0.00	53.67	21.68
YKL117W	-2.47	0.00	580.37	234.51
YDR175C	-2.47	0.00	100.26	40.52
YHR077C	-2.47	0.02	34.00	13.74
YLR312W-A	-2.47	0.00	83.03	33.56
YGL106W	-2.47	0.00	122.80	49.63
YBL060W	-2.47	0.04	24.34	9.84
YHR190W	-2.47	0.00	218.58	88.36
YKR024C	-2.47	0.05	23.17	9.37
YNL314W	-2.47	0.00	47.82	19.33
YDR173C	-2.47	0.00	64.06	25.90
YMR298W	-2.47	0.00	131.28	53.09
YOL073C	-2.47	0.00	78.21	31.63
YJL133C-A	-2.47	0.00	1865.28	754.66
YGR001C	-2.47	0.01	43.45	17.58
YML071C	-2.47	0.05	23.72	9.60
YOR353C	-2.47	0.01	45.92	18.59
YLR015W	-2.47	0.01	41.41	16.76
YNR027W	-2.47	0.02	31.38	12.70
YDL166C	-2.47	0.00	88.90	36.00
YLL050C	-2.47	0.00	361.96	146.59
YOR209C	-2.47	0.00	197.14	79.88
YOR374W	-2.47	0.00	794.91	322.10
YBR161W	-2.47	0.02	33.92	13.75
YCL032W	-2.47	0.00	50.67	20.54
YJR107W	-2.47	0.00	55.81	22.63
YPR123C	-2.47	0.00	103.24	41.86
YDL139C	-2.47	0.00	68.22	27.67
YNL022C	-2.47	0.00	69.24	28.09
YPL015C	-2.46	0.00	148.97	60.44
YML078W	-2.46	0.00	284.29	115.35
YBR095C	-2.46	0.00	79.10	32.09
YLR435W	-2.46	0.00	55.16	22.38
YBL089W	-2.46	0.02	31.27	12.69
YGR115C	-2.46	0.01	46.71	18.95
YLR146C	-2.46	0.04	24.41	9.91
YBR065C	-2.46	0.00	67.40	27.35
YML020W	-2.46	0.01	45.52	18.48
YBR288C	-2.46	0.05	23.36	9.48
YFL047W	-2.46	0.03	27.75	11.27
YPR020W	-2.46	0.00	177.78	72.20
YDL118W	-2.46	0.02	34.84	14.16

YDL230W	-2.46	0.00	133.54	54.26
YOR061W	-2.46	0.00	93.85	38.13
YER031C	-2.46	0.00	105.03	42.68
YIL107C	-2.46	0.00	60.60	24.62
YER007C-A	-2.46	0.00	58.91	23.94
YPL024W	-2.46	0.00	89.25	36.27
YJL137C	-2.46	0.00	124.12	50.46
YDR284C	-2.46	0.01	38.92	15.83
YGR132C	-2.46	0.00	334.21	135.94
YKL100C	-2.46	0.00	86.12	35.04
YKL080W	-2.46	0.00	78.32	31.86
YGR155W	-2.46	0.00	149.72	60.91
YGL093W	-2.46	0.00	49.77	20.25
YNL103W-A	-2.46	0.02	31.19	12.69
YNR010W	-2.46	0.00	79.01	32.15
YDL188C	-2.46	0.01	45.64	18.58
YDR083W	-2.46	0.00	49.15	20.02
YNR054C	-2.45	0.00	55.03	22.42
YMR150C	-2.45	0.00	59.80	24.36
YLR033W	-2.45	0.01	44.37	18.08
YMR052W	-2.45	0.00	60.00	24.45
YKL070W	-2.45	0.00	67.76	27.62
YCR024C-A	-2.45	0.00	4238.37	1728.69
YFL034W	-2.45	0.05	22.54	9.20
YLR120C	-2.45	0.00	349.56	142.64
YBL001C	-2.45	0.00	195.48	79.77
YHL034C	-2.45	0.00	336.06	137.16
YOR182C	-2.45	0.00	590.25	240.92
YJR155W	-2.45	0.00	120.66	49.25
YPR104C	-2.45	0.04	24.88	10.16
YMR054W	-2.45	0.00	74.86	30.57
YDR400W	-2.45	0.02	35.38	14.45
YDL090C	-2.45	0.02	31.77	12.97
YNL105W	-2.45	0.05	23.17	9.47
YLR295C	-2.45	0.00	470.93	192.39
YPL020C	-2.45	0.00	52.93	21.63
YHR189W	-2.45	0.01	40.92	16.72
YJL176C	-2.45	0.05	22.56	9.22
YGR016W	-2.45	0.02	31.43	12.85
YPL028W	-2.45	0.00	160.43	65.57
YLR312C	-2.45	0.00	129.41	52.90
YBR086C	-2.45	0.00	73.09	29.88
YER014W	-2.45	0.02	34.58	14.14
YLR209C	-2.45	0.00	67.47	27.59
YER090W	-2.45	0.00	67.30	27.52
YFR037C	-2.45	0.00	78.60	32.14
YCL057C-A	-2.45	0.00	444.34	181.72

YAL016W	-2.45	0.00	95.62	39.11
YDR234W	-2.44	0.00	82.41	33.71
YDL049C	-2.44	0.05	22.68	9.28
YOR070C	-2.44	0.00	51.30	20.99
YPR073C	-2.44	0.00	66.06	27.03
YHR027C	-2.44	0.00	147.74	60.45
YMR286W	-2.44	0.00	285.66	116.94
YMR233W	-2.44	0.01	46.88	19.19
YOR362C	-2.44	0.00	318.82	130.56
YEL032W	-2.44	0.01	37.46	15.34
YKL204W	-2.44	0.00	48.87	20.01
YER057C	-2.44	0.00	144.99	59.39
YOR218C	-2.44	0.03	27.29	11.18
YBL103C	-2.44	0.00	79.93	32.75
YPL071C	-2.44	0.00	131.85	54.02
YPR144C	-2.44	0.05	24.36	9.98
YNL087W	-2.44	0.04	26.65	10.93
YDR219C	-2.44	0.00	77.38	31.73
YDR139C	-2.44	0.00	183.18	75.11
YCL007C	-2.44	0.00	82.28	33.74
YLR080W	-2.44	0.01	38.59	15.83
YHR102W	-2.44	0.00	50.04	20.52
YNR047W	-2.44	0.00	70.71	29.01
YNL134C	-2.44	0.00	541.03	221.94
YBR273C	-2.44	0.00	121.50	49.85
YOR335C	-2.44	0.00	67.46	27.68
YHL009C	-2.44	0.00	51.70	21.21
YGR220C	-2.44	0.00	131.54	53.97
YDL095W	-2.44	0.00	81.28	33.36
YHR147C	-2.44	0.00	74.07	30.40
YEL045C	-2.44	0.01	47.91	19.66
YMR175W	-2.44	0.00	3236.20	1328.27
YDR188W	-2.44	0.00	203.01	83.33
YPR003C	-2.44	0.02	31.19	12.80
YJR001W	-2.44	0.02	36.14	14.84
YPL086C	-2.44	0.01	36.92	15.16
YDR260C	-2.44	0.00	53.92	22.14
YOR053W	-2.43	0.00	441.82	181.45
YNL224C	-2.43	0.01	38.15	15.67
YNL190W	-2.43	0.00	812.68	333.87
YNL050C	-2.43	0.00	74.44	30.59
YJL020W-A	-2.43	0.00	83.18	34.19
YDR267C	-2.43	0.00	51.00	20.96
YER151C	-2.43	0.00	73.44	30.19
YCL051W	-2.43	0.01	43.52	17.89
YBL050W	-2.43	0.00	238.30	97.96
YLR354C	-2.43	0.00	435.27	178.96

YOL031C	-2.43	0.00	49.98	20.55
YJL024C	-2.43	0.00	81.77	33.62
YDR510W	-2.43	0.00	560.69	230.59
YNL290W	-2.43	0.00	66.19	27.23
YAL008W	-2.43	0.00	101.28	41.66
YKL079W	-2.43	0.00	54.00	22.21
YGL083W	-2.43	0.05	24.14	9.93
YLR351C	-2.43	0.00	84.51	34.77
YKL083W	-2.43	0.00	151.47	62.32
YLL061W	-2.43	0.03	29.57	12.17
YNR032C-A	-2.43	0.00	131.97	54.31
YGL211W	-2.43	0.00	84.09	34.61
YJL065C	-2.43	0.00	91.78	37.77
YLR009W	-2.43	0.00	102.53	42.20
YDR294C	-2.43	0.00	157.66	64.89
YPR072W	-2.43	0.00	56.15	23.11
YKL146W	-2.43	0.00	132.20	54.42
YBR185C	-2.43	0.00	65.74	27.06
YEL006W	-2.43	0.00	61.15	25.18
YEL051W	-2.43	0.00	166.63	68.64
YOR041C	-2.43	0.00	99.09	40.83
YKL138C	-2.43	0.00	122.86	50.63
YMR277W	-2.43	0.02	33.75	13.91
YHR072W-A	-2.43	0.00	426.19	175.66
YJL128C	-2.43	0.00	68.65	28.30
YOL060C	-2.43	0.00	99.86	41.16
YGR215W	-2.43	0.00	129.42	53.35
YGR054W	-2.43	0.00	84.09	34.67
YOR262W	-2.42	0.00	124.35	51.30
YLR294C	-2.42	0.00	55.46	22.88
YGR213C	-2.42	0.00	65.77	27.14
YDR162C	-2.42	0.00	87.59	36.14
YMR203W	-2.42	0.00	133.08	54.95
YNR041C	-2.42	0.00	61.25	25.29
YDR251W	-2.42	0.00	96.83	39.99
YGR124W	-2.42	0.00	182.78	75.49
YKL114C	-2.42	0.00	56.36	23.28
YGL098W	-2.42	0.00	87.00	35.94
YPL176C	-2.42	0.00	74.71	30.86
YOR028C	-2.42	0.00	102.20	42.23
YOR121C	-2.42	0.00	250.34	103.47
YGR086C	-2.42	0.00	770.40	318.44
YLL051C	-2.42	0.00	62.19	25.72
YPL178W	-2.42	0.00	116.49	48.17
YAL044W-A	-2.42	0.00	104.13	43.06
YER006W	-2.42	0.00	76.66	31.71

YJR006W	-2.42	0.03	29.76	12.31
YLR403W	-2.42	0.00	68.02	28.14
YIR022W	-2.42	0.00	95.26	39.41
YDR510C-A	-2.42	0.00	559.78	231.57
YDL248W	-2.42	0.00	227.10	93.97
YLR078C	-2.42	0.00	80.12	33.15
YLR060W	-2.42	0.01	39.70	16.43
YBR012C	-2.42	0.00	72.26	29.91
YLR059C	-2.42	0.02	34.44	14.26
YKR089C	-2.42	0.00	79.23	32.81
YBR103W	-2.41	0.01	45.17	18.70
YGR041W	-2.41	0.01	41.19	17.06
YMR314W	-2.41	0.00	363.55	150.58
YDL074C	-2.41	0.00	51.72	21.42
YIL125W	-2.41	0.00	239.51	99.23
YDR100W	-2.41	0.01	44.67	18.51
YIL008W	-2.41	0.00	137.81	57.11
YGR135W	-2.41	0.00	264.84	109.76
YLR175W	-2.41	0.00	76.64	31.77
YMR258C	-2.41	0.02	32.40	13.44
YEL041W	-2.41	0.01	39.38	16.33
YNL255C	-2.41	0.00	215.55	89.41
YPR109W	-2.41	0.00	82.26	34.13
YEL063C	-2.41	0.02	33.64	13.96
YIL024C	-2.41	0.00	74.58	30.95
YNL104C	-2.41	0.00	181.12	75.19
YHR069C	-2.41	0.00	66.92	27.79
YLR091W	-2.41	0.03	29.97	12.45
YJR131W	-2.41	0.04	25.55	10.61
YMR220W	-2.41	0.00	117.13	48.67
YIL003W	-2.41	0.00	67.69	28.13
YDR475C	-2.41	0.00	172.30	71.60
YJL125C	-2.41	0.01	49.70	20.66
YGR174C	-2.41	0.00	192.53	80.03
YBR207W	-2.41	0.00	178.07	74.03
YOR185C	-2.41	0.00	229.50	95.42
YPR036W	-2.40	0.00	200.70	83.46
YPL147W	-2.40	0.01	43.37	18.04
YJL014W	-2.40	0.00	147.27	61.28
YJR133W	-2.40	0.00	132.64	55.19
YDR132C	-2.40	0.01	37.61	15.65
YNL089C	-2.40	0.05	25.25	10.51
YBR230W-A	-2.40	0.00	264.75	110.17
YAL014C	-2.40	0.00	117.71	48.99
YCR084C	-2.40	0.00	103.33	43.01
YMR038C	-2.40	0.00	203.42	84.69

YJL019W	-2.40	0.03	31.22	13.01
YNL287W	-2.40	0.01	45.13	18.80
YEL017C-A	-2.40	0.00	1470.78	612.89
YJL009W	-2.40	0.00	168.10	70.05
YBL096C	-2.40	0.00	83.27	34.70
YPR133W-A	-2.40	0.00	293.53	122.34
YJR094C	-2.40	0.00	133.26	55.54
YGR255C	-2.40	0.00	64.16	26.75
YDR381C-A	-2.40	0.00	120.00	50.03
YHR107C	-2.40	0.00	70.47	29.39
YDR247W	-2.40	0.00	540.97	225.65
YGR094W	-2.40	0.01	49.23	20.54
YDL089W	-2.40	0.01	37.74	15.74
YHL014C	-2.40	0.01	42.83	17.87
YOR155C	-2.40	0.00	61.59	25.70
YLR185W	-2.40	0.00	301.80	125.95
YNL278W	-2.40	0.02	34.81	14.53
YGL125W	-2.40	0.00	60.20	25.13
YDR460W	-2.40	0.00	95.04	39.67
YER061C	-2.40	0.00	67.94	28.36
YEL021W	-2.40	0.00	136.30	56.90
YIR002C	-2.39	0.04	25.63	10.70
YBR239C	-2.39	0.03	31.15	13.01
YDR047W	-2.39	0.00	111.05	46.38
YDR051C	-2.39	0.00	97.34	40.66
YLR025W	-2.39	0.00	285.02	119.09
YCL044C	-2.39	0.00	62.11	25.96
YLR130C	-2.39	0.00	57.19	23.90
YMR243C	-2.39	0.00	152.73	63.83
YBR018C	-2.39	0.00	61.77	25.82
YIL165C	-2.39	0.00	51.00	21.33
YHR008C	-2.39	0.00	446.57	186.74
YOL053W	-2.39	0.00	62.71	26.22
YEL016C	-2.39	0.02	35.83	14.99
YIL105C	-2.39	0.00	87.08	36.42
YNL164C	-2.39	0.00	54.88	22.95
YGL167C	-2.39	0.00	63.91	26.73
YLR198C	-2.39	0.00	76.67	32.08
YCR061W	-2.39	0.00	78.86	33.00
YIR023C-A	-2.39	0.01	43.50	18.21
YMR139W	-2.39	0.00	86.59	36.26
YMR030W	-2.39	0.00	98.60	41.29
YGR126W	-2.39	0.01	48.10	20.14
YBL099W	-2.39	0.00	373.57	156.46
YBR197C	-2.39	0.00	51.41	21.54
YPL180W	-2.39	0.01	42.03	17.61
YOL103W	-2.39	0.00	57.10	23.92

YEL018C-A	-2.39	0.00	58.70	24.60
YLR245C	-2.39	0.00	71.29	29.88
YGL183C	-2.39	0.00	107.56	45.09
YKL084W	-2.39	0.01	43.98	18.44
YMR096W	-2.38	0.00	339.87	142.52
YLR287C-A	-2.38	0.00	1057.45	443.51
YIL051C	-2.38	0.00	264.88	111.11
YLR374C	-2.38	0.00	316.82	132.92
YKL196C	-2.38	0.00	326.52	137.01
YGR017W	-2.38	0.00	183.02	76.80
YNL330C	-2.38	0.00	89.20	37.43
YJL161W	-2.38	0.01	49.00	20.57
YKR094C	-2.38	0.00	364.46	152.97
YNL147W	-2.38	0.00	158.96	66.73
YMR241W	-2.38	0.00	195.11	81.92
YPR176C	-2.38	0.00	85.14	35.75
YIL103W	-2.38	0.00	59.94	25.17
YLR344W	-2.38	0.00	291.93	122.61
YLR405W	-2.38	0.01	41.05	17.24
YBR204C	-2.38	0.00	114.15	47.98
YKR044W	-2.38	0.01	43.51	18.29
YDR225W	-2.38	0.00	990.44	416.50
YHR021C	-2.38	0.00	324.79	136.59
YLR316C	-2.38	0.02	34.10	14.34
YMR205C	-2.38	0.00	111.33	46.84
YHR111W	-2.38	0.00	70.10	29.50
YLR356W	-2.38	0.00	169.52	71.36
YOR380W	-2.38	0.02	34.35	14.46
YPL091W	-2.38	0.00	112.52	47.37
YKR101W	-2.38	0.03	28.84	12.14
YOR113W	-2.37	0.04	27.78	11.70
YOL010W	-2.37	0.00	116.42	49.03
YPL108W	-2.37	0.05	25.26	10.64
YFR051C	-2.37	0.00	82.35	34.68
YBR121C	-2.37	0.00	62.62	26.38
YBL003C	-2.37	0.00	158.58	66.79
YMR085W	-2.37	0.00	247.37	104.19
YER127W	-2.37	0.00	55.81	23.51
YDR113C	-2.37	0.00	68.59	28.90
YGL186C	-2.37	0.00	59.89	25.24
YDL178W	-2.37	0.00	51.61	21.75
YLR363C	-2.37	0.02	36.67	15.45
YOR390W	-2.37	0.02	33.90	14.29
YNR008W	-2.37	0.03	29.42	12.40
YHR049W	-2.37	0.00	260.75	109.92
YLL058W	-2.37	0.01	50.69	21.37
YGL245W	-2.37	0.00	86.60	36.51

YAR002C-A	-2.37	0.00	68.40	28.84
YER027C	-2.37	0.00	105.95	44.68
YGR163W	-2.37	0.00	82.41	34.76
YPR107C	-2.37	0.00	74.15	31.27
YPL117C	-2.37	0.00	224.19	94.56
YMR112C	-2.37	0.00	65.71	27.72
YOL139C	-2.37	0.00	204.30	86.18
YJL139C	-2.37	0.01	51.07	21.55
YIL044C	-2.37	0.00	74.45	31.41
YHR161C	-2.37	0.00	110.17	46.48
YMR059W	-2.37	0.01	48.96	20.66
YHR105W	-2.37	0.04	27.74	11.71
YDR207C	-2.37	0.03	32.39	13.67
YLR196W	-2.37	0.02	36.05	15.21
YGL220W	-2.37	0.00	144.50	61.01
YOR039W	-2.37	0.00	150.67	63.62
YLR317W	-2.37	0.03	32.13	13.57
YJL154C	-2.37	0.01	46.43	19.61
YLR370C	-2.37	0.00	213.76	90.28
YLR186W	-2.37	0.00	81.36	34.36
YER015W	-2.37	0.01	42.75	18.06
YGL221C	-2.37	0.00	86.80	36.67
YCL035C	-2.37	0.00	833.95	352.32
YMR170C	-2.37	0.00	81.16	34.29
YMR124W	-2.37	0.00	54.24	22.92
YJL184W	-2.37	0.00	98.09	41.45
YNL189W	-2.37	0.00	59.91	25.32
YGR036C	-2.37	0.01	51.09	21.59
YGL172W	-2.37	0.00	82.30	34.79
YNR049C	-2.37	0.00	110.02	46.51
YMR240C	-2.37	0.00	69.49	29.38
YDL061C	-2.37	0.00	441.48	186.65
YCR026C	-2.37	0.00	63.70	26.93
YMR196W	-2.36	0.00	92.72	39.21
YGL203C	-2.36	0.01	50.28	21.27
YJR007W	-2.36	0.00	127.88	54.09
YOR328W	-2.36	0.04	28.34	11.99
YGL109W	-2.36	0.00	89.34	37.80
YLR040C	-2.36	0.03	32.66	13.82
YHR018C	-2.36	0.00	208.45	88.20
YMR251W	-2.36	0.03	32.82	13.89
YML125C	-2.36	0.00	200.71	84.94
YDR226W	-2.36	0.00	309.95	131.17
YJR015W	-2.36	0.00	57.60	24.38
YIL162W	-2.36	0.00	209.15	88.53
YOR305W	-2.36	0.03	29.20	12.36
YJL185C	-2.36	0.00	52.51	22.23

YLR463C	-2.36	0.00	108.58	45.98
YIL055C	-2.36	0.02	35.79	15.16
YHR039C-A	-2.36	0.00	370.86	157.07
YHR020W	-2.36	0.00	55.22	23.39
YGL153W	-2.36	0.00	82.93	35.13
YGL215W	-2.36	0.00	94.02	39.83
YGL018C	-2.36	0.00	61.53	26.07
YGR236C	-2.36	0.00	1354.10	573.72
YBL076C	-2.36	0.00	63.69	26.99
YDR187C	-2.36	0.00	118.31	50.13
YCL002C	-2.36	0.02	38.76	16.42
YDL108W	-2.36	0.00	62.92	26.66
YLR152C	-2.36	0.00	101.72	43.11
YPR098C	-2.36	0.00	74.24	31.47
YML010W	-2.36	0.00	64.82	27.47
YPR110C	-2.36	0.00	100.25	42.49
YOR020W-A	-2.36	0.00	452.39	191.75
YFL018C	-2.36	0.00	242.99	103.00
YJR122W	-2.36	0.03	29.36	12.44
YAL030W	-2.36	0.00	251.09	106.47
YBR283C	-2.36	0.00	83.69	35.50
YGL184C	-2.36	0.00	66.01	28.00
YLR163C	-2.36	0.00	96.58	40.98
YPL003W	-2.36	0.02	34.77	14.76
YLR441C	-2.36	0.00	441.32	187.30
YMR237W	-2.36	0.02	34.09	14.47
YBR031W	-2.36	0.00	270.26	114.73
YML098W	-2.36	0.00	170.21	72.27
YDR293C	-2.36	0.00	124.04	52.67
YMR178W	-2.36	0.00	127.16	53.99
YOR131C	-2.36	0.00	73.70	31.29
YBR233W-A	-2.36	0.00	75.51	32.06
YLR077W	-2.35	0.03	30.11	12.78
YEL039C	-2.35	0.00	3974.36	1687.80
YBR167C	-2.35	0.00	64.28	27.30
YIR017C	-2.35	0.00	114.67	48.71
YOR339C	-2.35	0.05	26.32	11.18
YDL017W	-2.35	0.00	55.83	23.73
YNL193W	-2.35	0.00	84.56	35.95
YHR175W	-2.35	0.00	122.80	52.21
YMR235C	-2.35	0.00	94.59	40.23
YGR082W	-2.35	0.00	93.22	39.66
YPL047W	-2.35	0.00	118.32	50.34
YHR134W	-2.35	0.00	64.61	27.50
YBL015W	-2.35	0.00	484.90	206.37
YDR023W	-2.35	0.00	62.14	26.45

YGL091C	-2.35	0.00	138.34	58.89
YHR123W	-2.35	0.01	47.79	20.34
YDL115C	-2.35	0.00	174.60	74.33
YNL068C	-2.35	0.00	66.61	28.36
YOL088C	-2.35	0.02	39.12	16.66
YGR032W	-2.35	0.00	108.88	46.37
YIL045W	-2.35	0.00	122.63	52.23
YKL130C	-2.35	0.00	56.90	24.23
YCR007C	-2.35	0.00	173.81	74.03
YDR322W	-2.35	0.00	61.39	26.15
YPR100W	-2.35	0.00	279.94	119.25
YIL143C	-2.35	0.00	101.41	43.20
YMR090W	-2.35	0.00	545.87	232.57
YLR399W-A	-2.35	0.00	106.37	45.32
YCL011C	-2.35	0.00	158.08	67.36
YJL178C	-2.35	0.00	79.19	33.75
YDL025C	-2.35	0.00	122.67	52.28
YLR178C	-2.35	0.00	797.14	339.76
YBR133C	-2.35	0.04	28.89	12.31
YGR129W	-2.35	0.02	37.90	16.16
YNL131W	-2.35	0.00	200.02	85.29
YOR372C	-2.34	0.03	33.33	14.21
YDR193W	-2.34	0.02	34.29	14.63
YPL063W	-2.34	0.00	85.32	36.40
YDR152W	-2.34	0.00	131.76	56.22
YGR030C	-2.34	0.00	54.55	23.28
YPL140C	-2.34	0.01	50.25	21.44
YHR151C	-2.34	0.04	28.96	12.36
YKL088W	-2.34	0.00	120.22	51.32
YHR176W	-2.34	0.00	55.15	23.54
YJL168C	-2.34	0.03	32.53	13.89
YGR167W	-2.34	0.00	443.07	189.18
YDR348C	-2.34	0.00	107.48	45.90
YNL070W	-2.34	0.00	109.60	46.81
YML041C	-2.34	0.00	71.17	30.41
YPR161C	-2.34	0.00	57.32	24.49
YMR188C	-2.34	0.00	158.89	67.90
YDR319C	-2.34	0.00	60.11	25.69
YHR051W	-2.34	0.00	484.56	207.11
YKL051W	-2.34	0.00	199.71	85.38
YDR361C	-2.34	0.00	87.44	37.39
YNL239W	-2.34	0.00	66.53	28.45
YDR059C	-2.34	0.00	218.34	93.40
YLR232W	-2.34	0.04	29.41	12.58
YLR288C	-2.34	0.02	34.55	14.78
YBR205W	-2.34	0.00	62.62	26.79
YGL163C	-2.34	0.00	80.05	34.26

YOR320C	-2.34	0.01	41.08	17.58
YDR502C	-2.34	0.00	716.00	306.55
YDL177C	-2.34	0.00	80.59	34.51
YDR388W	-2.33	0.00	220.71	94.54
YCR011C	-2.33	0.05	25.67	11.00
YDL113C	-2.33	0.00	85.42	36.59
YBR173C	-2.33	0.00	282.96	121.23
YMR315W	-2.33	0.00	406.55	174.22
YBR053C	-2.33	0.00	107.23	45.95
YER137C	-2.33	0.01	46.70	20.02
YMR228W	-2.33	0.04	27.41	11.75
YKR011C	-2.33	0.00	106.44	45.65
YMR310C	-2.33	0.01	44.50	19.09
YJR075W	-2.33	0.00	98.10	42.09
YNL084C	-2.33	0.00	61.54	26.41
YML021C	-2.33	0.00	76.51	32.84
YBR262C	-2.33	0.00	266.15	114.25
YHR082C	-2.33	0.00	89.30	38.34
YLR429W	-2.33	0.00	69.06	29.65
YBR282W	-2.33	0.00	155.14	66.62
YMR015C	-2.33	0.03	32.44	13.93
YJR064W	-2.33	0.00	109.79	47.15
YNL002C	-2.33	0.00	160.10	68.76
YDR331W	-2.33	0.01	45.28	19.46
YKL127W	-2.33	0.03	32.84	14.11
YMR272W-A	-2.33	0.00	3287.00	1412.65
YGR073C	-2.33	0.00	55.96	24.05
YPL221W	-2.33	0.00	408.26	175.47
YOR257W	-2.33	0.00	263.02	113.07
YDR182W	-2.33	0.00	66.20	28.46
YMR263W	-2.33	0.00	112.51	48.37
YER149C	-2.33	0.00	67.41	28.99
YDR375C	-2.33	0.00	58.01	24.95
YMR052C-A	-2.33	0.01	43.94	18.90
YKR099W	-2.32	0.04	28.28	12.16
YER178W	-2.32	0.00	346.51	149.06
YNL069C	-2.32	0.00	386.91	166.44
YLR181C	-2.32	0.01	46.64	20.06
YIL112W	-2.32	0.00	55.06	23.69
YLR361C-A	-2.32	0.00	213.04	91.65
YNL152W	-2.32	0.02	35.37	15.22
YAR042W	-2.32	0.01	40.56	17.45
YKR026C	-2.32	0.01	53.00	22.81
YLR323C	-2.32	0.00	116.05	49.95
YKL184W	-2.32	0.00	72.29	31.11
YJR087W	-2.32	0.00	79.80	34.35

YIL041W	-2.32	0.00	199.87	86.03
YLR079W	-2.32	0.00	150.33	64.71
YMR040W	-2.32	0.00	121.43	52.29
YLR400W	-2.32	0.03	31.09	13.39
YLR380W	-2.32	0.00	90.55	38.99
YDR071C	-2.32	0.00	124.57	53.65
YLR406C	-2.32	0.00	221.42	95.36
YBR178W	-2.32	0.01	40.86	17.60
YDR340W	-2.32	0.00	345.65	148.89
YIL087C	-2.32	0.00	148.54	63.99
YER010C	-2.32	0.00	78.96	34.02
YKL022C	-2.32	0.01	41.79	18.01
YOR163W	-2.32	0.00	115.30	49.69
YBR107C	-2.32	0.00	79.40	34.22
YKL004W	-2.32	0.00	132.42	57.09
YIL139C	-2.32	0.04	29.71	12.81
YLR082C	-2.32	0.02	34.32	14.80
YIL009C-A	-2.32	0.03	33.42	14.41
YOL142W	-2.32	0.00	94.63	40.81
YEL058W	-2.32	0.00	139.31	60.08
YLR191W	-2.32	0.00	97.81	42.19
YLR387C	-2.32	0.00	120.37	51.92
YGR062C	-2.32	0.02	35.42	15.28
YDR120C	-2.32	0.01	49.36	21.30
YGR146C	-2.32	0.00	113.28	48.89
YOR276W	-2.32	0.00	159.43	68.81
YJL006C	-2.32	0.01	43.26	18.67
YOR221C	-2.32	0.00	83.21	35.92
YHR112C	-2.32	0.00	135.88	58.65
YMR146C	-2.32	0.00	178.96	77.25
YNL153C	-2.32	0.00	84.42	36.44
YPR138C	-2.32	0.01	42.09	18.17
YGL152C	-2.32	0.00	99.70	43.05
YDR211W	-2.32	0.01	41.96	18.13
YNR045W	-2.31	0.00	67.15	29.01
YMR147W	-2.31	0.04	27.76	11.99
YLR192C	-2.31	0.00	192.14	83.01
YOR141C	-2.31	0.01	44.44	19.21
YGR288W	-2.31	0.01	44.29	19.14
YDR347W	-2.31	0.00	148.01	63.98
YGR234W	-2.31	0.00	366.70	158.53
YJL015C	-2.31	0.00	154.50	66.79
YGR290W	-2.31	0.00	82.97	35.87
YNL029C	-2.31	0.02	38.16	16.50
YDR354W	-2.31	0.02	40.06	17.32
YDL157C	-2.31	0.00	68.63	29.68
YJR010C-A	-2.31	0.00	57.66	24.94

YGL129C	-2.31	0.00	56.92	24.62
YMR299C	-2.31	0.00	57.48	24.87
YKL026C	-2.31	0.00	309.90	134.08
YNL197C	-2.31	0.02	38.10	16.49
YDR063W	-2.31	0.00	64.19	27.78
YNL284C	-2.31	0.00	102.89	44.53
YDL131W	-2.31	0.00	175.52	75.97
YKL147C	-2.31	0.00	68.79	29.78
YER065C	-2.31	0.00	112.69	48.78
YER183C	-2.31	0.00	72.82	31.53
YDL204W	-2.31	0.00	177.56	76.87
YPL126W	-2.31	0.05	26.73	11.58
YNL168C	-2.31	0.00	55.40	24.00
YJL016W	-2.31	0.00	125.45	54.34
YDR503C	-2.31	0.02	36.93	16.00
YGR240C	-2.31	0.00	155.86	67.52
YLR051C	-2.31	0.00	87.09	37.74
YDL021W	-2.31	0.02	40.67	17.63
YIL047C	-2.31	0.00	148.88	64.53
YLR421C	-2.31	0.00	407.47	176.62
YGL049C	-2.31	0.00	67.40	29.22
YER040W	-2.31	0.03	32.50	14.09
YJL141C	-2.31	0.00	154.39	66.93
YDR052C	-2.31	0.02	40.20	17.43
YBR285W	-2.31	0.00	66.95	29.03
YER047C	-2.31	0.03	32.43	14.06
YNL167C	-2.31	0.03	33.87	14.69
YPR005C	-2.31	0.00	135.06	58.58
YDR461C-A	-2.31	0.00	172.78	74.94
YBR269C	-2.31	0.00	332.21	144.10
YIL124W	-2.31	0.00	61.03	26.47
YAL046C	-2.30	0.00	64.70	28.08
YBR217W	-2.30	0.02	36.48	15.83
YGL014W	-2.30	0.02	38.59	16.75
YIL089W	-2.30	0.05	26.49	11.50
YJR020W	-2.30	0.01	54.44	23.63
YKL162C	-2.30	0.02	36.28	15.75
YMR158W	-2.30	0.00	72.47	31.46
YMR166C	-2.30	0.03	31.43	13.64
YPL066W	-2.30	0.00	64.77	28.11
YOR286W	-2.30	0.00	201.68	87.56
YPL097W	-2.30	0.02	37.84	16.43
YKL187C	-2.30	0.00	148.36	64.44
YNL295W	-2.30	0.00	70.39	30.58
YNL027W	-2.30	0.00	156.54	68.00
YPL139C	-2.30	0.01	50.27	21.84
YNL097C	-2.30	0.00	97.81	42.49

YGL031C	-2.30	0.00	337.99	146.84
YJR117W	-2.30	0.00	68.52	29.77
YHL034W-A	-2.30	0.00	392.25	170.44
YPR163C	-2.30	0.00	121.59	52.85
YBR188C	-2.30	0.01	45.90	19.95
YCL017C	-2.30	0.00	113.82	49.48
YDR153C	-2.30	0.00	125.52	54.57
YJL122W	-2.30	0.00	83.73	36.41
YJL068C	-2.30	0.00	113.64	49.42
YPL026C	-2.30	0.00	342.64	149.07
YGR280C	-2.30	0.00	100.61	43.78
YMR149W	-2.30	0.00	78.24	34.05
YBL102W	-2.30	0.00	117.68	51.21
YER025W	-2.30	0.00	123.16	53.60
YDL048C	-2.30	0.00	615.97	268.11
YHR201C	-2.30	0.02	39.67	17.27
YMR300C	-2.30	0.00	103.87	45.24
YCR043C	-2.30	0.00	105.84	46.10
YGL231C	-2.30	0.00	110.83	48.28
YGL121C	-2.30	0.00	749.30	326.42
YLR388W	-2.30	0.00	270.84	118.00
YEL001C	-2.30	0.00	134.46	58.59
YNL103W	-2.29	0.00	92.54	40.32
YHR198C	-2.29	0.00	59.38	25.88
YBR111C	-2.29	0.00	211.89	92.35
YOR241W	-2.29	0.01	50.56	22.04
YHR207C	-2.29	0.05	26.15	11.40
YMR204C	-2.29	0.01	42.64	18.59
YOR254C	-2.29	0.02	37.99	16.56
YBR284W	-2.29	0.03	34.10	14.87
YOL155W-A	-2.29	0.01	46.35	20.21
YOR010C	-2.29	0.03	32.72	14.27
YOL113W	-2.29	0.00	65.88	28.73
YPR124W	-2.29	0.00	101.63	44.33
YGR257C	-2.29	0.00	73.99	32.27
YOR035C	-2.29	0.00	61.19	26.69
YIL006W	-2.29	0.04	30.85	13.46
YIL021C-A	-2.29	0.00	85.12	37.13
YHR150W	-2.29	0.01	44.80	19.55
YAL007C	-2.29	0.01	41.51	18.12
YNL138W-A	-2.29	0.00	122.85	53.61
YPR017C	-2.29	0.00	85.14	37.16
YGR154C	-2.29	0.02	38.82	16.94
YGL134W	-2.29	0.00	693.46	302.69
YNL195C	-2.29	0.00	238.37	104.06
YCR002C	-2.29	0.00	93.30	40.73
YDL232W	-2.29	0.00	269.73	117.76

YEL034W	-2.29	0.00	1599.97	698.65
YBR120C	-2.29	0.00	88.85	38.80
YDR172W	-2.29	0.00	86.49	37.77
YIR039C	-2.29	0.00	85.50	37.35
YBL090W	-2.29	0.00	109.62	47.89
YPR034W	-2.29	0.00	62.60	27.35
YGR252W	-2.29	0.01	46.65	20.38
YCL001W	-2.29	0.00	75.80	33.13
YGL009C	-2.29	0.00	137.45	60.06
YGR010W	-2.29	0.01	52.91	23.13
YKL034W	-2.29	0.01	42.01	18.36
YJL124C	-2.29	0.00	148.50	64.92
YGR223C	-2.29	0.00	105.01	45.93
YHR016C	-2.29	0.00	205.60	89.92
YDR116C	-2.29	0.00	90.78	39.71
YPR188C	-2.29	0.00	79.28	34.69
YLR065C	-2.28	0.03	32.13	14.06
YPL050C	-2.28	0.00	61.38	26.87
YOR006C	-2.28	0.01	46.93	20.54
YMR084W	-2.28	0.00	147.86	64.74
YKL068W-A	-2.28	0.00	305.71	133.87
YJR112W-A	-2.28	0.00	109.33	47.88
YKL010C	-2.28	0.01	49.18	21.54
YBL030C	-2.28	0.00	915.28	400.94
YDR385W	-2.28	0.00	183.45	80.36
YNL010W	-2.28	0.00	142.65	62.49
YDL208W	-2.28	0.00	132.85	58.20
YBL012C	-2.28	0.04	30.98	13.57
YBR266C	-2.28	0.00	61.70	27.03
YOL086W-A	-2.28	0.00	161.72	70.89
YKR058W	-2.28	0.00	76.01	33.32
YOL125W	-2.28	0.01	47.93	21.02
YIL078W	-2.28	0.00	86.83	38.07
YFL005W	-2.28	0.00	206.29	90.48
YDR479C	-2.28	0.00	72.81	31.94
YBR130C	-2.28	0.04	29.19	12.81
YDR006C	-2.28	0.00	57.07	25.04
YCL038C	-2.28	0.00	93.11	40.86
YOR043W	-2.28	0.00	113.51	49.82
YKR075W-A	-2.28	0.00	1282.37	562.85
YBR112C	-2.28	0.02	36.63	16.08
YML119W	-2.28	0.00	161.65	70.96
YDR179C	-2.28	0.04	31.33	13.75
YPL213W	-2.28	0.00	73.56	32.30
YBR211C	-2.28	0.01	43.72	19.20
YPL173W	-2.28	0.00	88.24	38.75
YDL209C	-2.28	0.02	40.07	17.60

YOR148C	-2.28	0.00	98.09	43.10
YHR002W	-2.28	0.00	77.32	33.97
YLR224W	-2.28	0.00	190.71	83.80
YJR060W	-2.28	0.00	66.73	29.32
YLR104W	-2.28	0.00	76.94	33.81
YKL016C	-2.27	0.00	432.50	190.12
YNL005C	-2.27	0.00	157.14	69.08
YOR042W	-2.27	0.00	172.83	75.98
YPR033C	-2.27	0.00	77.40	34.03
YMR222C	-2.27	0.00	56.91	25.02
YJR125C	-2.27	0.00	109.85	48.30
YLR109W	-2.27	0.00	3797.90	1669.96
YDR062W	-2.27	0.00	101.59	44.67
YAL025C	-2.27	0.02	38.54	16.95
YOR252W	-2.27	0.00	94.30	41.47
YOR097C	-2.27	0.00	119.94	52.76
YIL065C	-2.27	0.00	282.89	124.46
YJL121C	-2.27	0.00	91.92	40.44
YJR130C	-2.27	0.02	40.78	17.95
YNL244C	-2.27	0.00	781.83	344.04
YKL218C	-2.27	0.00	109.80	48.32
YOL038W	-2.27	0.00	250.26	110.15
YDR246W	-2.27	0.00	215.57	94.89
YGR083C	-2.27	0.01	53.57	23.58
YLR298C	-2.27	0.00	107.46	47.32
YKL023W	-2.27	0.00	147.38	64.90
YNL184C	-2.27	0.04	30.40	13.39
YKR006C	-2.27	0.00	82.09	36.16
YKR065C	-2.27	0.00	79.54	35.04
YOR304C-A	-2.27	0.02	41.77	18.40
YPR041W	-2.27	0.00	140.43	61.89
YHR009C	-2.27	0.00	188.52	83.11
YDL185W	-2.27	0.00	127.99	56.45
YOR085W	-2.27	0.01	51.37	22.66
YDR481C	-2.27	0.00	251.10	110.75
YLR105C	-2.27	0.05	28.41	12.53
YDR424C	-2.27	0.00	106.68	47.08
YHR133C	-2.27	0.01	47.93	21.15
YKL019W	-2.27	0.00	58.35	25.75
YMR253C	-2.27	0.00	101.03	44.60
YHR108W	-2.27	0.01	46.04	20.32
YPL013C	-2.27	0.00	178.31	78.71
YMR005W	-2.27	0.00	80.17	35.40
YLL041C	-2.26	0.00	553.81	244.54
YCL058W-A	-2.26	0.00	112.17	49.54
YLR180W	-2.26	0.00	577.44	255.03
YMR272C	-2.26	0.00	2362.00	1043.42

YLR117C	-2.26	0.00	71.25	31.48
YOL001W	-2.26	0.04	29.64	13.09
YPR130C	-2.26	0.00	149.20	65.94
YHR071W	-2.26	0.00	345.35	152.65
YPL281C	-2.26	0.02	37.25	16.47
YBR122C	-2.26	0.00	203.46	89.95
YDL170W	-2.26	0.00	98.12	43.38
YDR346C	-2.26	0.00	220.08	97.33
YHR200W	-2.26	0.00	374.77	165.75
YPR028W	-2.26	0.00	138.17	61.12
YDL081C	-2.26	0.00	399.50	176.72
YNL073W	-2.26	0.00	101.18	44.76
YOL036W	-2.26	0.00	119.15	52.71
YGR175C	-2.26	0.00	184.61	81.67
YNL130C	-2.26	0.01	50.12	22.17
YOR194C	-2.26	0.00	174.07	77.01
YAR035W	-2.26	0.00	85.45	37.81
YNL275W	-2.26	0.03	32.80	14.52
YOR201C	-2.26	0.00	86.79	38.41
YIL116W	-2.26	0.00	98.67	43.67
YKL064W	-2.26	0.00	72.12	31.92
YNR017W	-2.26	0.00	189.85	84.03
YJR024C	-2.26	0.01	50.12	22.19
YDR483W	-2.26	0.00	273.42	121.03
YKL156C-A	-2.26	0.00	263.39	116.60
YOR004W	-2.26	0.03	34.47	15.26
YEL050C	-2.26	0.00	67.53	29.90
YDR230W	-2.26	0.00	254.07	112.50
YNL154C	-2.26	0.00	76.83	34.03
YNL116W	-2.26	0.00	88.81	39.35
YHR078W	-2.26	0.01	49.21	21.80
YHR213W-B	-2.26	0.01	46.78	20.73
YOL054W	-2.26	0.00	90.66	40.17
YDL201W	-2.26	0.00	58.21	25.79
YDL086W	-2.26	0.00	150.67	66.77
YBL038W	-2.26	0.00	166.73	73.89
YDR061W	-2.26	0.00	101.90	45.16
YER188W	-2.26	0.00	70.58	31.29
YER145C-A	-2.26	0.00	59.14	26.22
YKL040C	-2.26	0.00	121.58	53.91
YPL094C	-2.26	0.00	80.66	35.76
YMR270C	-2.26	0.05	27.11	12.02
YNL294C	-2.25	0.00	77.97	34.58
YGL082W	-2.25	0.01	54.90	24.36
YDL226C	-2.25	0.00	58.86	26.12
YBL041W	-2.25	0.00	321.54	142.72

YDL035C	-2.25	0.03	34.77	15.43
YML016C	-2.25	0.01	45.09	20.02
YIL084C	-2.25	0.04	32.09	14.25
YNL162W	-2.25	0.00	300.40	133.43
YMR291W	-2.25	0.00	140.50	62.41
YHL021C	-2.25	0.00	445.81	198.07
YLR008C	-2.25	0.00	104.50	46.43
YDR092W	-2.25	0.00	194.42	86.39
YIL069C	-2.25	0.00	228.89	101.71
YOR232W	-2.25	0.00	176.88	78.60
YDR519W	-2.25	0.00	95.17	42.30
YPL048W	-2.25	0.00	294.73	131.02
YLR439W	-2.25	0.00	67.80	30.14
YMR173W-A	-2.25	0.00	249.80	111.06
YOL044W	-2.25	0.00	70.61	31.40
YIR017W-A	-2.25	0.00	75.63	33.63
YLR459W	-2.25	0.03	35.04	15.58
YNL096C	-2.25	0.00	146.65	65.22
YGL026C	-2.25	0.00	104.78	46.63
YGL077C	-2.25	0.00	59.24	26.36
YDR275W	-2.25	0.00	222.51	99.03
YLR101C	-2.25	0.00	89.63	39.90
YML012C-A	-2.25	0.00	71.63	31.89
YOL030W	-2.25	0.00	206.74	92.06
YJL210W	-2.24	0.00	84.49	37.64
YOL008W	-2.24	0.03	35.61	15.86
YER052C	-2.24	0.00	78.23	34.85
YAL062W	-2.24	0.00	112.57	50.15
YIL033C	-2.24	0.00	236.90	105.55
YGR021W	-2.24	0.00	105.50	47.03
YKL061W	-2.24	0.00	221.42	98.70
YMR134W	-2.24	0.00	288.45	128.59
YLR292C	-2.24	0.00	122.28	54.51
YDL133C-A	-2.24	0.00	1985.21	885.08
YLR248W	-2.24	0.00	220.99	98.55
YDL075W	-2.24	0.00	564.08	251.58
YOR089C	-2.24	0.00	473.08	211.01
YFR036W-A	-2.24	0.00	131.33	58.58
YBL068W	-2.24	0.01	51.62	23.03
YBR241C	-2.24	0.00	110.54	49.31
YFL017W-A	-2.24	0.00	102.71	45.83
YDL024C	-2.24	0.01	47.50	21.20
YKL003C	-2.24	0.00	152.25	67.94
YML031W	-2.24	0.02	41.03	18.31
YLR172C	-2.24	0.00	115.72	51.65
YFL062W	-2.24	0.05	27.19	12.13

YNR052C	-2.24	0.00	68.76	30.70
YMR062C	-2.24	0.00	133.84	59.77
YOR272W	-2.24	0.04	29.89	13.35
YGL080W	-2.24	0.00	107.73	48.11
YPR076W	-2.24	0.00	155.31	69.37
YOL006C	-2.24	0.01	52.15	23.29
YNL100W	-2.24	0.00	180.32	80.55
YOL016C	-2.24	0.00	1153.22	515.22
YHL031C	-2.24	0.00	88.32	39.47
YKR035W-A	-2.24	0.00	210.04	93.89
YDL195W	-2.24	0.02	38.77	17.33
YJR080C	-2.24	0.00	61.44	27.47
YHL004W	-2.24	0.00	76.04	34.00
YNL015W	-2.24	0.00	1199.03	536.29
YER046W	-2.24	0.00	87.99	39.36
YHR141C	-2.23	0.00	306.59	137.18
YFL030W	-2.23	0.00	189.57	84.82
YPL175W	-2.23	0.00	66.78	29.88
YBR263W	-2.23	0.00	146.97	65.78
YOR367W	-2.23	0.00	103.67	46.41
YLR347C	-2.23	0.01	47.13	21.10
YPL231W	-2.23	0.00	221.42	99.17
YML121W	-2.23	0.01	48.14	21.56
YDL068W	-2.23	0.02	41.64	18.65
YHR199C	-2.23	0.00	373.67	167.37
YLR173W	-2.23	0.01	50.86	22.78
YMR182W-A	-2.23	0.00	73.26	32.82
YDL070W	-2.23	0.00	186.17	83.41
YIL157C	-2.23	0.00	127.29	57.04
YDR236C	-2.23	0.01	54.74	24.53
YDL088C	-2.23	0.00	75.21	33.71
YPL132W	-2.23	0.01	56.60	25.37
YPR101W	-2.23	0.00	86.83	38.94
YHL019W-A	-2.23	0.00	65.27	29.27
YNL321W	-2.23	0.03	33.77	15.15
YPR004C	-2.23	0.00	129.55	58.12
YBR257W	-2.23	0.01	57.92	25.99
YPR145W	-2.23	0.00	109.33	49.06
YDR497C	-2.23	0.00	770.39	345.72
YDR296W	-2.23	0.00	142.37	63.92
YER180C	-2.23	0.02	37.97	17.05
YBR139W	-2.23	0.00	103.74	46.58
YPL116W	-2.23	0.05	27.73	12.45
YJL156W-A	-2.23	0.02	41.36	18.58
YJL134W	-2.23	0.00	82.11	36.89
YBR278W	-2.23	0.01	49.41	22.20

YBR007C	-2.23	0.02	37.87	17.02
YOR162C	-2.23	0.01	54.44	24.46
YGR099W	-2.23	0.02	41.19	18.51
YEL059W	-2.22	0.01	52.99	23.82
YOR297C	-2.22	0.01	56.56	25.42
YEL036C	-2.22	0.00	120.30	54.08
YLR048W	-2.22	0.00	263.80	118.63
YHL036W	-2.22	0.01	57.27	25.75
YKL169C	-2.22	0.00	155.79	70.06
YER002W	-2.22	0.00	218.11	98.10
YML035C	-2.22	0.05	28.53	12.83
YML080W	-2.22	0.03	34.71	15.61
YPL017C	-2.22	0.00	124.40	55.97
YNL156C	-2.22	0.00	276.27	124.30
YBR064W	-2.22	0.03	33.53	15.09
YOL130W	-2.22	0.00	75.82	34.11
YNL079C	-2.22	0.00	259.93	116.96
YLR260W	-2.22	0.01	45.47	20.47
YLR118C	-2.22	0.00	89.00	40.08
YIL164C	-2.22	0.02	44.15	19.88
YAL059W	-2.22	0.00	65.25	29.39
YER141W	-2.22	0.00	288.90	130.16
YPR106W	-2.22	0.00	74.28	33.49
YNL306W	-2.22	0.00	186.79	84.22
YBL049W	-2.22	0.00	421.82	190.21
YIL042C	-2.22	0.01	55.81	25.17
YPL183W-A	-2.22	0.00	124.21	56.03
YML022W	-2.22	0.00	73.82	33.30
YDR286C	-2.22	0.00	77.46	34.94
YLR017W	-2.22	0.00	77.39	34.92
YJL219W	-2.22	0.01	49.52	22.34
YMR035W	-2.22	0.00	85.85	38.74
YGR074W	-2.22	0.00	117.35	52.95
YDL234C	-2.22	0.00	281.29	126.93
YOR150W	-2.22	0.00	134.31	60.62
YOR159C	-2.22	0.00	123.31	55.66
YDL005C	-2.22	0.00	99.13	44.75
YHL013C	-2.22	0.01	57.65	26.03
YPL172C	-2.21	0.02	40.67	18.36
YOL083C-A	-2.21	0.00	76.72	34.65
YLR151C	-2.21	0.01	49.85	22.52
YKL048C	-2.21	0.05	29.65	13.40
YDR352W	-2.21	0.02	41.07	18.56
YLR412W	-2.21	0.03	34.38	15.54
YDL160C	-2.21	0.02	42.37	19.15
YBR084C-A	-2.21	0.00	380.92	172.21
YER014C-A	-2.21	0.01	45.57	20.60

YHL024W	-2.21	0.00	75.87	34.30
YHR135C	-2.21	0.00	122.59	55.45
YLR116W	-2.21	0.00	92.35	41.77
YKR035C	-2.21	0.00	178.53	80.75
YBR286W	-2.21	0.00	234.23	105.95
YDL241W	-2.21	0.00	242.24	109.68
YGR085C	-2.21	0.00	284.81	128.96
YDL126C	-2.21	0.00	406.10	183.91
YPL164C	-2.21	0.01	49.25	22.30
YBR256C	-2.21	0.00	129.35	58.59
YER147C	-2.21	0.01	45.19	20.47
YDL158C	-2.21	0.01	52.99	24.03
YNL032W	-2.21	0.00	105.20	47.70
YML051W	-2.21	0.00	66.43	30.13
YOR234C	-2.20	0.00	253.04	114.76
YDL086C-A	-2.20	0.00	198.42	90.00
YOR189W	-2.20	0.00	121.95	55.32
YNL277W	-2.20	0.00	178.27	80.87
YDR093W	-2.20	0.05	28.47	12.92
YDR005C	-2.20	0.00	70.24	31.89
YJL213W	-2.20	0.00	146.90	66.70
YJR014W	-2.20	0.00	153.78	69.83
YPR085C	-2.20	0.01	51.72	23.49
YLR028C	-2.20	0.00	191.33	86.89
YBR181C	-2.20	0.00	331.45	150.55
YNL099C	-2.20	0.00	120.79	54.87
YLR043C	-2.20	0.00	196.98	89.48
YDL205C	-2.20	0.03	34.77	15.80
YOR128C	-2.20	0.01	58.17	26.44
YGL005C	-2.20	0.00	78.60	35.73
YGR198W	-2.20	0.05	30.31	13.78
YER001W	-2.20	0.00	93.14	42.36
YKL033W-A	-2.20	0.00	73.77	33.56
YPR002W	-2.20	0.02	41.55	18.90
YPL186C	-2.20	0.00	173.90	79.12
YIL156W-A	-2.20	0.01	49.60	22.57
YBL046W	-2.20	0.00	83.70	38.09
YKL160W	-2.20	0.00	220.29	100.25
YDR406W	-2.20	0.00	214.02	97.40
YOR277C	-2.20	0.00	239.58	109.04
YJL093C	-2.20	0.01	53.04	24.15
YML082W	-2.20	0.01	58.90	26.81
YPR058W	-2.20	0.03	36.64	16.69
YNL071W	-2.20	0.00	200.37	91.26
YBR279W	-2.19	0.00	91.47	41.69
YGR038W	-2.19	0.00	64.07	29.21
YKR080W	-2.19	0.01	55.20	25.17

YBR213W	-2.19	0.01	56.00	25.53
YML110C	-2.19	0.00	184.92	84.33
YPL105C	-2.19	0.01	60.40	27.55
YDR532C	-2.19	0.01	46.61	21.26
R0030W	-2.19	0.00	1706.96	778.63
YIL088C	-2.19	0.00	65.82	30.02
YGR002C	-2.19	0.00	86.02	39.24
YLR399C	-2.19	0.00	110.00	50.18
YLL023C	-2.19	0.00	178.98	81.66
YDR438W	-2.19	0.02	45.60	20.81
YMR183C	-2.19	0.00	90.35	41.23
YPR167C	-2.19	0.00	95.30	43.51
YCR079W	-2.19	0.00	61.69	28.17
YOL035C	-2.19	0.00	235.26	107.43
YGL123C-A	-2.19	0.00	439.71	200.80
YBR261C	-2.19	0.00	65.00	29.68
YBR200W	-2.19	0.01	56.22	25.67
YKL133C	-2.19	0.01	48.31	22.06
YMR230W	-2.19	0.00	359.14	164.02
YKR038C	-2.19	0.00	85.07	38.86
YBL086C	-2.19	0.00	143.46	65.54
YIL046W	-2.19	0.00	320.15	146.27
YIL144W	-2.19	0.02	39.66	18.12
YBR037C	-2.19	0.00	89.23	40.80
YDR163W	-2.19	0.00	124.04	56.72
YOL112W	-2.19	0.01	59.66	27.29
YOR077W	-2.19	0.02	45.84	20.97
YLR378C	-2.19	0.00	73.92	33.81
YDR333C	-2.19	0.00	62.38	28.54
YER148W-A	-2.19	0.00	79.99	36.60
YKR051W	-2.19	0.03	38.05	17.42
YOR111W	-2.18	0.01	47.60	21.79
YBR160W	-2.18	0.00	92.12	42.16
YNL092W	-2.18	0.04	33.88	15.51
YGL105W	-2.18	0.00	129.67	59.36
YBR011C	-2.18	0.00	483.31	221.28
YGR256W	-2.18	0.00	215.88	98.85
YHR216W	-2.18	0.05	29.95	13.72
YNR053C	-2.18	0.03	38.26	17.55
YOR220W	-2.18	0.00	598.62	274.56
YDL125C	-2.18	0.00	579.99	266.05
YBR159W	-2.18	0.00	88.50	40.60
YGR020C	-2.18	0.00	303.36	139.17
YJL030W	-2.18	0.01	61.54	28.24
YDL072C	-2.18	0.00	290.09	133.13
YDL174C	-2.18	0.00	206.76	94.89
YJR011C	-2.18	0.02	43.08	19.78

YDL137W	-2.18	0.00	485.16	222.78
YDR374W-A	-2.18	0.00	132.55	60.87
YKR055W	-2.18	0.04	33.91	15.57
YOR236W	-2.18	0.01	48.00	22.05
YPR170W-B	-2.18	0.00	228.01	104.77
YEL017W	-2.18	0.01	61.82	28.41
YHR148W	-2.18	0.05	30.51	14.02
YHR032W	-2.18	0.01	55.50	25.51
YOR192C-C	-2.18	0.00	137.43	63.18
YMR095C	-2.17	0.05	30.67	14.10
YAL044C	-2.17	0.00	198.23	91.16
YPR029C	-2.17	0.02	45.77	21.05
YLR449W	-2.17	0.01	59.67	27.45
YKL041W	-2.17	0.00	183.49	84.42
YGR267C	-2.17	0.00	218.33	100.47
YBR223W-A	-2.17	0.01	48.24	22.21
YDR016C	-2.17	0.00	108.34	49.87
YMR311C	-2.17	0.00	628.24	289.31
YOR244W	-2.17	0.00	85.57	39.41
YBL077W	-2.17	0.00	186.53	85.93
YJL200C	-2.17	0.03	36.15	16.65
YHR037W	-2.17	0.00	134.58	62.02
YPL266W	-2.17	0.00	76.50	35.27
YGL068W	-2.17	0.00	133.85	61.72
YLR203C	-2.17	0.00	135.51	62.48
YHL008C	-2.17	0.00	63.75	29.40
YJL003W	-2.17	0.00	94.02	43.37
YPL080C	-2.17	0.05	29.86	13.78
YIR024C	-2.17	0.00	102.04	47.08
YJR069C	-2.17	0.02	41.45	19.12
YIL036W	-2.17	0.00	76.48	35.29
YEL037C	-2.17	0.00	315.10	145.41
YML118W	-2.17	0.02	46.92	21.65
YBR171W	-2.17	0.00	69.49	32.08
YGR232W	-2.17	0.00	118.83	54.86
YFL014W	-2.17	0.00	4347.30	2007.21
YBR089C-A	-2.17	0.00	273.48	126.27
YNL177C	-2.17	0.00	141.98	65.57
YCR095C	-2.17	0.02	41.51	19.17
YKL002W	-2.16	0.00	225.21	104.03
YLR285W	-2.16	0.01	52.08	24.06
YMR262W	-2.16	0.02	40.54	18.73
YLR138W	-2.16	0.00	69.13	31.94
YER100W	-2.16	0.00	189.49	87.55
YML058W	-2.16	0.00	1107.72	511.85
YJL127C-B	-2.16	0.00	158.88	73.43

YDR412W	-2.16	0.00	107.62	49.74
YKL192C	-2.16	0.00	322.86	149.23
YDL155W	-2.16	0.00	67.68	31.28
YMR157C	-2.16	0.00	73.25	33.87
YLR120W-A	-2.16	0.00	621.46	287.40
YDR339C	-2.16	0.00	111.93	51.76
YOL064C	-2.16	0.00	139.88	64.69
YJR076C	-2.16	0.00	108.00	49.98
YGR029W	-2.16	0.00	82.69	38.29
YHL030W-A	-2.16	0.00	77.97	36.12
YBR230C	-2.16	0.00	654.36	303.16
YGR251W	-2.16	0.00	79.26	36.72
YLR333C	-2.16	0.00	366.06	169.59
YDR329C	-2.16	0.00	151.66	70.30
YJL064W	-2.16	0.00	76.05	35.25
YOR091W	-2.16	0.00	70.81	32.83
YLR027C	-2.16	0.00	174.73	81.02
YGL072C	-2.16	0.00	146.68	68.04
YDR123C	-2.16	0.00	95.35	44.24
YKR090W	-2.16	0.03	37.14	17.23
YPL133C	-2.15	0.01	62.10	28.82
YKL120W	-2.15	0.00	81.33	37.75
YCL049C	-2.15	0.00	128.66	59.74
YLR393W	-2.15	0.05	30.91	14.35
YNL274C	-2.15	0.00	230.85	107.20
YBR104W	-2.15	0.02	42.65	19.80
YGL174W	-2.15	0.01	52.71	24.48
YHL015W	-2.15	0.00	703.48	326.80
YLR107W	-2.15	0.00	163.45	75.93
YNL176C	-2.15	0.00	66.49	30.91
YNL001W	-2.15	0.01	59.84	27.82
YHL026C	-2.15	0.00	68.65	31.93
YLL029W	-2.15	0.00	188.74	87.82
YPR057W	-2.15	0.02	44.51	20.72
YGR006W	-2.15	0.05	29.93	13.93
YKR072C	-2.15	0.00	192.57	89.64
YDL121C	-2.15	0.03	40.28	18.75
YDR469W	-2.15	0.00	65.56	30.52
YDR306C	-2.15	0.01	53.47	24.90
YJR077C	-2.15	0.00	656.05	305.74
YNL175C	-2.15	0.01	49.99	23.30
YFL045C	-2.15	0.00	126.51	58.97
YBR162W-A	-2.15	0.00	560.25	261.18
YOL146W	-2.14	0.03	37.68	17.57
YJL117W	-2.14	0.00	115.14	53.69
YHR115C	-2.14	0.00	68.85	32.11

YEL046C	-2.14	0.00	340.16	158.63
YMR120C	-2.14	0.00	127.93	59.67
YLR395C	-2.14	0.00	922.06	430.25
YPL215W	-2.14	0.00	88.35	41.23
YGL025C	-2.14	0.01	60.53	28.27
YPL001W	-2.14	0.05	32.12	15.00
YGR075C	-2.14	0.02	42.67	19.93
YIL094C	-2.14	0.00	111.14	51.91
YOR198C	-2.14	0.01	56.32	26.32
YLR285C-A	-2.14	0.00	71.47	33.40
YCR048W	-2.14	0.00	88.82	41.51
YBL002W	-2.14	0.00	220.47	103.03
YLR303W	-2.14	0.00	455.64	212.93
YNL083W	-2.14	0.02	47.73	22.30
YHR050W	-2.14	0.00	121.45	56.76
YGR102C	-2.14	0.00	312.62	146.10
YKL107W	-2.14	0.03	37.66	17.60
YML048W	-2.14	0.00	260.11	121.56
YKL065C	-2.14	0.00	399.54	186.78
YLR220W	-2.14	0.00	131.80	61.62
YHR139C-A	-2.14	0.02	46.11	21.56
YOR142W	-2.14	0.00	173.24	81.01
YPL177C	-2.14	0.00	136.57	63.87
YCL043C	-2.14	0.00	527.37	246.69
YHR042W	-2.14	0.00	111.85	52.33
YMR110C	-2.14	0.00	151.18	70.75
YDR167W	-2.14	0.00	137.10	64.17
YGL128C	-2.14	0.03	38.50	18.02
YIR025W	-2.14	0.00	74.69	34.96
YKL180W	-2.14	0.00	405.65	189.90
YDR174W	-2.14	0.00	235.96	110.46
YER119C-A	-2.14	0.05	30.97	14.50
YGL130W	-2.14	0.00	69.62	32.60
YFL023W	-2.13	0.01	54.44	25.50
YNL052W	-2.13	0.00	1344.20	629.72
YPL128C	-2.13	0.04	34.31	16.08
YMR142C	-2.13	0.00	370.06	173.44
YDL082W	-2.13	0.00	169.68	79.53
YHR089C	-2.13	0.00	116.95	54.83
YCR039C	-2.13	0.00	75.47	35.39
YMR174C	-2.13	0.00	1262.47	591.92
YEL020W-A	-2.13	0.00	260.93	122.34
YHR043C	-2.13	0.00	129.11	60.54
YKL058W	-2.13	0.00	338.82	158.89
YHR156C	-2.13	0.04	35.84	16.81
YLL019C	-2.13	0.00	185.76	87.13
YGR044C	-2.13	0.01	51.68	24.24

YNR055C	-2.13	0.01	59.04	27.71
YKR075C	-2.13	0.00	1300.98	610.70
YDR279W	-2.13	0.04	33.38	15.67
YDL197C	-2.13	0.03	37.43	17.57
YFR033C	-2.13	0.00	2779.22	1305.06
YIL074C	-2.13	0.00	91.70	43.07
YCL005W-A	-2.13	0.00	292.65	137.48
YDL059C	-2.13	0.01	57.25	26.90
YGL003C	-2.13	0.00	87.56	41.15
YER016W	-2.13	0.01	50.74	23.85
YDR450W	-2.13	0.00	428.56	201.58
YMR024W	-2.13	0.00	78.07	36.73
YLL018C	-2.13	0.00	121.56	57.20
YOR311C	-2.13	0.00	147.36	69.34
YER146W	-2.13	0.00	121.93	57.38
YNL061W	-2.12	0.02	46.16	21.73
YDL066W	-2.12	0.00	201.06	94.66
YCR083W	-2.12	0.00	237.56	111.87
YKL112W	-2.12	0.03	38.35	18.06
YOR122C	-2.12	0.00	670.10	315.60
YGL146C	-2.12	0.02	42.73	20.13
YHR005C-A	-2.12	0.00	197.20	92.93
YDR245W	-2.12	0.00	121.75	57.39
YOL049W	-2.12	0.05	33.56	15.82
YDR018C	-2.12	0.01	62.01	29.25
YPL079W	-2.12	0.00	345.90	163.16
YIL136W	-2.12	0.00	573.09	270.34
YIL142W	-2.12	0.00	147.93	69.78
YKL067W	-2.12	0.00	665.52	313.97
YHR132C	-2.12	0.00	130.34	61.49
YKL052C	-2.12	0.00	364.90	172.17
YFL022C	-2.12	0.00	74.18	35.00
YOR065W	-2.12	0.00	570.24	269.16
YBL084C	-2.12	0.03	41.91	19.79
YOR147W	-2.12	0.00	71.34	33.68
YKL207W	-2.12	0.00	135.99	64.20
YDR055W	-2.12	0.00	2423.30	1144.33
YPR024W	-2.12	0.00	124.28	58.70
YGR185C	-2.12	0.01	57.24	27.04
YHR068W	-2.12	0.00	76.16	35.98
YDL175C	-2.12	0.01	61.87	29.24
YOR145C	-2.12	0.00	199.95	94.53
YJL155C	-2.12	0.00	179.95	85.07
YML001W	-2.11	0.00	90.09	42.61
YDL009C	-2.11	0.00	247.62	117.11
YML117W	-2.11	0.00	132.08	62.48
YMR255W	-2.11	0.00	446.16	211.06

YHR166C	-2.11	0.05	31.15	14.74
YBL061C	-2.11	0.00	69.24	32.77
YGL117W	-2.11	0.00	101.42	48.03
YCR047W-A	-2.11	0.00	277.69	131.50
YDR459C	-2.11	0.05	32.75	15.51
YBL069W	-2.11	0.00	447.69	212.05
YIL109C	-2.11	0.01	62.98	29.84
YPL198W	-2.11	0.00	80.51	38.16
YHR006W	-2.11	0.00	136.77	64.82
YLL060C	-2.11	0.01	60.06	28.47
YGL115W	-2.11	0.01	64.09	30.38
YOR222W	-2.11	0.00	87.34	41.41
YHR138C	-2.11	0.00	1536.50	728.69
YER165W	-2.11	0.00	160.49	76.11
YGR169C-A	-2.11	0.00	196.60	93.25
YNL055C	-2.11	0.00	1009.82	479.10
YPL171C	-2.11	0.00	177.52	84.23
YEL029C	-2.11	0.02	46.71	22.16
YPR040W	-2.11	0.00	178.60	84.78
YDR493W	-2.11	0.02	45.27	21.49
YOR170W	-2.11	0.00	102.62	48.73
YIL133C	-2.11	0.00	199.31	94.65
YIR015W	-2.11	0.01	52.83	25.09
YDR115W	-2.11	0.00	190.33	90.39
YLR099W-A	-2.10	0.00	198.24	94.22
YDR454C	-2.10	0.00	114.57	54.45
YER046W-A	-2.10	0.03	42.88	20.38
YOR040W	-2.10	0.00	122.88	58.42
YOR197W	-2.10	0.00	262.00	124.61
YPL135W	-2.10	0.00	1812.66	862.22
YOR146W	-2.10	0.00	184.79	87.92
YPR181C	-2.10	0.00	80.76	38.42
YER074W	-2.10	0.00	336.96	160.34
YDR248C	-2.10	0.00	154.63	73.59
YNL180C	-2.10	0.00	133.86	63.71
YER019W	-2.10	0.00	84.86	40.40
YAL037W	-2.10	0.05	32.66	15.55
YGR202C	-2.10	0.00	103.79	49.42
YGL154C	-2.10	0.01	55.48	26.42
YEL003W	-2.10	0.00	71.36	33.99
YBR029C	-2.10	0.00	70.86	33.76
YGL054C	-2.10	0.00	92.27	43.98
YBL056W	-2.10	0.00	159.35	75.94
YBL057C	-2.10	0.00	107.44	51.21
YBR039W	-2.10	0.00	481.43	229.47
YBR046C	-2.10	0.00	120.50	57.45
YOL080C	-2.10	0.02	46.65	22.24

YDR070C	-2.10	0.00	754.81	360.01
YDR054C	-2.10	0.00	401.57	191.57
YKL032C	-2.10	0.00	196.91	93.94
YIL135C	-2.10	0.00	122.75	58.56
YCR018C-A	-2.10	0.00	70.40	33.59
YKL175W	-2.10	0.00	118.00	56.32
YOL070C	-2.10	0.03	42.63	20.35
YGR139W	-2.09	0.00	106.26	50.72
YMR135C	-2.09	0.00	375.40	179.23
YIL086C	-2.09	0.03	42.58	20.33
YLL027W	-2.09	0.00	311.88	148.98
YKL190W	-2.09	0.00	261.48	124.98
YMR044W	-2.09	0.00	129.48	61.94
YMR041C	-2.09	0.01	57.90	27.70
YGR122C-A	-2.09	0.00	72.98	34.92
YER088C	-2.09	0.00	152.68	73.10
YNL217W	-2.09	0.00	151.17	72.38
YKL054C	-2.09	0.00	110.70	53.01
YOR130C	-2.09	0.03	42.51	20.36
YPR061C	-2.09	0.00	142.45	68.21
YKR045C	-2.09	0.02	51.59	24.71
YGR140W	-2.09	0.02	51.35	24.60
YMR021C	-2.09	0.00	93.26	44.68
YLR359W	-2.09	0.00	100.65	48.26
YIL040W	-2.09	0.04	36.18	17.35
YOL077W-A	-2.09	0.00	494.09	236.95
YOR322C	-2.08	0.01	63.36	30.40
YPR184W	-2.08	0.00	102.56	49.21
YER009W	-2.08	0.00	150.06	72.01
YPL157W	-2.08	0.01	57.74	27.71
YML026C	-2.08	0.00	357.22	171.51
YPL142C	-2.08	0.00	560.68	269.37
YOR317W	-2.08	0.00	323.33	155.39
YOR319W	-2.08	0.00	127.70	61.38
YKL098W	-2.08	0.00	97.35	46.79
YJR019C	-2.08	0.00	79.58	38.25
YNL276C	-2.08	0.00	246.02	118.25
YEL020C-B	-2.08	0.00	137.33	66.02
YMR297W	-2.08	0.00	397.96	191.35
YBL045C	-2.08	0.00	482.54	232.06
YBR119W	-2.08	0.00	79.27	38.13
YBL078C	-2.08	0.00	609.21	293.06
YDR298C	-2.08	0.00	279.48	134.45
YOR012W	-2.08	0.05	33.76	16.25
YKL029C	-2.08	0.00	70.58	33.97
YML024W	-2.08	0.00	327.81	157.78
YPR125W	-2.08	0.00	98.96	47.65

YEL054C	-2.08	0.00	290.03	139.65
YER180C-A	-2.08	0.03	40.34	19.43
YML081C-A	-2.08	0.00	1138.67	548.51
YJL138C	-2.07	0.00	323.15	155.80
YMR073C	-2.07	0.00	72.08	34.76
YCR009C	-2.07	0.00	456.16	220.10
YBR056C-B	-2.07	0.00	2275.81	1098.25
YMR034C	-2.07	0.00	91.77	44.30
YDR208W	-2.07	0.01	59.25	28.61
YGR012W	-2.07	0.01	64.91	31.35
YJR139C	-2.07	0.00	132.66	64.10
YIR018C-A	-2.07	0.00	97.04	46.90
YDL092W	-2.07	0.00	105.68	51.08
YGL127C	-2.07	0.00	180.15	87.08
YMR316W	-2.07	0.00	536.87	259.58
YGR141W	-2.07	0.00	114.20	55.23
YJR085C	-2.07	0.00	351.41	170.00
YIR004W	-2.07	0.00	99.35	48.07
YJL012C	-2.07	0.01	56.53	27.36
YCR008W	-2.07	0.00	162.20	78.51
YDL078C	-2.07	0.00	242.46	117.37
YAR015W	-2.07	0.00	141.02	68.28
YPR043W	-2.07	0.00	748.25	362.29
YOR283W	-2.06	0.00	134.59	65.19
YOR293W	-2.06	0.00	616.58	298.71
YKL156W	-2.06	0.00	393.37	190.61
YKL142W	-2.06	0.00	433.35	210.07
YPR143W	-2.06	0.00	106.55	51.66
YGR133W	-2.06	0.00	91.74	44.49
YNL086W	-2.06	0.02	51.66	25.05
YIL004C	-2.06	0.00	109.18	52.95
YEL053W-A	-2.06	0.00	246.17	119.43
YCL067C	-2.06	0.00	75.57	36.69
YER161C	-2.06	0.00	182.08	88.40
YJL066C	-2.06	0.00	347.93	168.96
YJL026W	-2.06	0.00	85.47	41.51
YMR145C	-2.06	0.00	553.70	269.00
YOR273C	-2.06	0.00	663.44	322.36
YDL020C	-2.06	0.00	495.99	241.13
YNL240C	-2.06	0.00	95.68	46.51
YBR105C	-2.06	0.00	913.93	444.34
YOR173W	-2.06	0.00	475.58	231.29
YOL077C	-2.06	0.01	67.15	32.67
YAL023C	-2.06	0.01	58.81	28.61
YMR198W	-2.06	0.04	38.13	18.56
YPL112C	-2.05	0.01	60.85	29.61
YFR014C	-2.05	0.00	77.49	37.71

YNL078W	-2.05	0.02	52.93	25.76
YOR289W	-2.05	0.00	131.57	64.04
YDR077W	-2.05	0.00	4740.58	2307.69
YOR045W	-2.05	0.00	254.34	123.83
YER145C	-2.05	0.00	306.53	149.26
YFR039C	-2.05	0.01	69.35	33.78
YJL217W	-2.05	0.00	314.42	153.16
YJR010W	-2.05	0.00	80.14	39.04
YER056C-A	-2.05	0.00	302.45	147.36
YLR007W	-2.05	0.00	115.91	56.49
YDR533C	-2.05	0.00	211.71	103.18
YOR186C-A	-2.05	0.02	49.57	24.17
YMR136W	-2.05	0.00	292.38	142.66
YDR322C-A	-2.05	0.00	640.63	312.68
YLR301W	-2.05	0.00	112.66	54.99
YDR462W	-2.05	0.00	176.22	86.03
YOL079W	-2.05	0.05	35.17	17.18
YMR296C	-2.05	0.00	90.66	44.27
YGL199C	-2.05	0.00	95.97	46.88
YER019C-A	-2.05	0.00	297.20	145.20
YCL030C	-2.05	0.00	138.69	67.76
YGR028W	-2.05	0.00	87.63	42.83
YER058W	-2.05	0.00	94.57	46.22
YNL213C	-2.05	0.00	144.51	70.63
YPR025C	-2.05	0.00	104.34	51.00
YBR109C	-2.05	0.00	372.72	182.21
YOR140W	-2.05	0.00	94.54	46.22
YCR071C	-2.04	0.00	153.55	75.11
YKL089W	-2.04	0.05	34.34	16.81
YDR037W	-2.04	0.03	41.32	20.22
YML028W	-2.04	0.00	575.76	281.83
YLR379W	-2.04	0.03	46.31	22.67
YOR044W	-2.04	0.00	138.54	67.87
YHR187W	-2.04	0.05	35.78	17.53
YOR176W	-2.04	0.00	78.32	38.38
YPR099C	-2.04	0.00	236.69	116.06
YOR021C	-2.04	0.00	229.17	112.38
YGR172C	-2.04	0.04	39.14	19.20
YNR067C	-2.04	0.00	112.14	55.03
YPL233W	-2.04	0.04	40.51	19.88
YHR110W	-2.04	0.00	106.61	52.33
YHR163W	-2.04	0.00	106.51	52.28
YCR060W	-2.04	0.00	82.32	40.41
YML073C	-2.04	0.00	294.48	144.59
YMR276W	-2.04	0.00	325.06	159.65
YER003C	-2.04	0.01	68.00	33.40
YPL154C	-2.04	0.00	586.78	288.25

YLR355C	-2.04	0.00	277.03	136.09
YGR031W	-2.03	0.02	48.93	24.05
YCL008C	-2.03	0.04	38.68	19.01
YGR061C	-2.03	0.05	36.80	18.10
YDL047W	-2.03	0.00	310.38	152.67
YKL103C	-2.03	0.00	89.17	43.86
YJR093C	-2.03	0.00	80.23	39.46
YDR524C	-2.03	0.04	41.28	20.32
YBL027W	-2.03	0.00	511.41	251.81
YNL097W-A	-2.03	0.00	182.55	89.89
YBR001C	-2.03	0.00	112.91	55.60
YIL114C	-2.03	0.05	35.18	17.33
YJL163C	-2.03	0.01	72.29	35.61
YBL091C	-2.03	0.00	123.19	60.70
YDL106C	-2.03	0.01	66.45	32.75
YKL049C	-2.03	0.00	93.65	46.16
YML063W	-2.03	0.00	296.95	146.40
YNL076W	-2.03	0.01	66.44	32.76
YOR023C	-2.03	0.00	235.52	116.12
YKL062W	-2.03	0.00	248.55	122.55
YMR016C	-2.03	0.01	62.97	31.05
YEL024W	-2.03	0.00	833.11	410.97
YLR417W	-2.03	0.03	46.65	23.02
YLR170C	-2.03	0.00	96.10	47.42
YIL064W	-2.03	0.00	111.29	54.93
YOR310C	-2.03	0.02	53.57	26.44
YHR090C	-2.02	0.00	111.99	55.31
YOR137C	-2.02	0.01	57.19	28.25
YPL146C	-2.02	0.02	53.90	26.62
YGR130C	-2.02	0.00	97.53	48.20
YER119C	-2.02	0.01	65.86	32.55
YIL043C	-2.02	0.00	176.11	87.05
YDR500C	-2.02	0.00	348.89	172.53
YBR066C	-2.02	0.00	101.78	50.34
YDR019C	-2.02	0.02	55.66	27.53
YGL038C	-2.02	0.01	60.26	29.81
YKL081W	-2.02	0.00	93.36	46.19
YOR167C	-2.02	0.00	607.70	300.78
YCR003W	-2.02	0.03	45.98	22.76
YNL117W	-2.02	0.01	58.97	29.19
YLL018C-A	-2.02	0.00	128.57	63.67
YDR003W	-2.02	0.00	224.67	111.27
YNL046W	-2.02	0.03	42.70	21.15
YML108W	-2.02	0.00	76.13	37.71
YBL062W	-2.02	0.00	129.08	63.95
YPR011C	-2.02	0.02	55.73	27.62
YEL034C-A	-2.02	0.00	1233.54	611.38

YDL233W	-2.02	0.00	79.67	39.49
YKR047W	-2.02	0.00	387.74	192.22
YHR050W-A	-2.02	0.00	103.27	51.21
YFR049W	-2.02	0.00	298.51	148.06
YMR285C	-2.02	0.02	48.43	24.02
YDL159W	-2.02	0.02	54.62	27.09
YDR261C	-2.02	0.05	37.18	18.45
YKR046C	-2.02	0.00	695.95	345.27
YOR136W	-2.02	0.00	429.04	212.88
YPL238C	-2.01	0.00	223.56	110.96
YDL064W	-2.01	0.00	142.12	70.55
YLR372W	-2.01	0.02	51.72	25.67
YDR231C	-2.01	0.00	225.01	111.71
YJR067C	-2.01	0.01	69.60	34.56
YHR007C	-2.01	0.00	114.05	56.64
YGR031C-A	-2.01	0.03	43.62	21.67
YML052W	-2.01	0.01	72.37	35.95
YOR331C	-2.01	0.00	380.20	188.88
YER093C-A	-2.01	0.00	82.07	40.77
YCR023C	-2.01	0.00	139.57	69.40
YJL192C	-2.01	0.00	105.51	52.47
YGL168W	-2.01	0.00	135.22	67.26
YLR147C	-2.01	0.01	62.11	30.90
YKL104C	-2.01	0.00	163.00	81.10
YNL220W	-2.01	0.00	90.01	44.79
YDL213C	-2.01	0.00	88.58	44.08
YGL040C	-2.01	0.00	132.58	65.98
YAL055W	-2.01	0.01	58.69	29.21
YDR434W	-2.01	0.03	45.98	22.89
YCR087W	-2.01	0.01	57.80	28.77
YLR444C	-2.01	0.01	68.13	33.93
YMR236W	-2.01	0.00	120.16	59.84
YNL123W	-2.01	0.03	43.57	21.70
YPR127W	-2.01	0.00	231.54	115.35
YNL202W	-2.01	0.00	140.84	70.17
YLR328W	-2.01	0.00	117.54	58.56
YLL036C	-2.01	0.03	46.91	23.38
YPL249C-A	-2.01	0.00	848.01	422.60
YER091C	-2.01	0.00	368.27	183.53
YIL148W	-2.01	0.00	499.70	249.06
YML018C	-2.01	0.02	56.00	27.91
YNL003C	-2.01	0.00	129.06	64.34
YDR201W	-2.01	0.01	61.06	30.45
YDR086C	-2.00	0.00	194.20	96.88
R0040C	-2.00	0.00	2789.36	1391.61
YGR182C	-2.00	0.00	187.16	93.39

YOL058W	-2.00	0.00	129.18	64.46
YOL120C	-2.00	0.00	367.43	183.34
YDR013W	-2.00	0.03	45.42	22.67
YGR219W	-2.00	0.00	179.53	89.61
YFL039C	-2.00	0.00	489.07	244.13
YIL052C	-2.00	0.00	437.94	218.62
YPL143W	-2.00	0.00	393.82	196.62
YPR074C	-2.00	0.00	108.22	54.04
YOL002C	-2.00	0.00	287.42	143.53
YKR059W	-2.00	0.00	277.96	138.87
YCR087C-A	-2.00	0.02	56.07	28.02
YMR318C	-2.00	0.00	147.95	73.94
YJL055W	-2.00	0.00	288.58	144.27
YOR342C	-2.00	0.04	40.45	20.23
YGR009C	-2.00	0.00	149.00	74.51
YDL179W	-2.00	0.02	52.53	26.28
YLR093C	-2.00	0.00	278.95	139.56
YDR404C	-2.00	0.00	148.68	74.40
YDR343C	-2.00	0.00	1987.56	994.65
YBL011W	-2.00	0.02	51.99	26.02
YGR204W	-2.00	0.00	121.05	60.59
YPL262W	-2.00	0.00	230.12	115.23
YOL127W	-2.00	0.00	549.05	274.96
YIL152W	-2.00	0.01	66.57	33.34
YKL198C	-2.00	0.00	90.11	45.14
YKR068C	-2.00	0.00	135.34	67.81
YOR126C	-2.00	0.02	53.50	26.81
YMR008C	-1.99	0.00	398.08	199.58
YNL307C	-1.99	0.01	60.81	30.49
YMR070W	-1.99	0.01	63.92	32.05
YDR487C	-1.99	0.00	154.17	77.32
YER020W	-1.99	0.00	355.97	178.56
YHL032C	-1.99	0.00	83.43	41.85
YMR009W	-1.99	0.00	761.28	382.01
YDL193W	-1.99	0.01	71.18	35.72
YKL181W	-1.99	0.00	98.46	49.42
YBR248C	-1.99	0.03	48.22	24.21
YDR075W	-1.99	0.02	53.43	26.83
YGR027C	-1.99	0.00	608.55	305.62
YNL169C	-1.99	0.00	84.82	42.60
YPL098C	-1.99	0.00	188.77	94.81
YOL059W	-1.99	0.00	84.51	42.45
YDR090C	-1.99	0.00	95.71	48.08
YML069W	-1.99	0.01	66.23	33.28
YJL067W	-1.99	0.00	379.18	190.54
YBR146W	-1.99	0.00	133.58	67.17
YFR047C	-1.99	0.00	190.84	95.96

YDR372C	-1.99	0.00	107.32	53.98
YDL025W-A	-1.99	0.00	359.21	180.69
YNL251C	-1.99	0.04	40.07	20.16
YFL050C	-1.99	0.05	39.10	19.67
YDL120W	-1.99	0.00	155.38	78.20
YHL025W	-1.99	0.00	188.42	94.83
YLR219W	-1.99	0.00	87.49	44.04
YDR022C	-1.99	0.02	50.76	25.55
YBR264C	-1.99	0.01	69.29	34.90
YNL288W	-1.99	0.00	90.37	45.53
YER131W	-1.98	0.00	445.72	224.55
YDR169C	-1.98	0.00	87.87	44.28
YGL234W	-1.98	0.00	83.72	42.20
YLR204W	-1.98	0.00	246.09	124.07
YNR050C	-1.98	0.02	54.42	27.44
YML087C	-1.98	0.02	59.35	29.94
YPL064C	-1.98	0.00	79.97	40.34
YNL166C	-1.98	0.01	63.69	32.13
YCR052W	-1.98	0.02	57.59	29.06
YER073W	-1.98	0.00	79.73	40.23
YCR075W-A	-1.98	0.00	92.08	46.48
YGL189C	-1.98	0.00	822.41	415.26
YJR121W	-1.98	0.00	879.89	444.33
YHR057C	-1.98	0.00	220.19	111.20
YEL027W	-1.98	0.00	343.60	173.54
YER087C-B	-1.98	0.00	293.56	148.31
YHR097C	-1.98	0.00	551.73	278.76
YGR250C	-1.98	0.00	1032.24	521.68
YJR078W	-1.98	0.00	175.56	88.75
YGR235C	-1.98	0.00	215.58	109.01
YGL202W	-1.98	0.01	76.30	38.59
YPR010C-A	-1.98	0.00	832.83	421.28
YIR029W	-1.98	0.05	40.23	20.35
YBR147W	-1.98	0.02	56.44	28.56
YGL187C	-1.98	0.00	603.13	305.20
YIL156W-B	-1.98	0.00	168.32	85.18
YJL165C	-1.98	0.00	111.42	56.39
YIL060W	-1.98	0.00	86.17	43.61
YGL135W	-1.97	0.00	444.74	225.19
YDR035W	-1.97	0.00	142.54	72.18
YMR131C	-1.97	0.05	38.26	19.37
YER023W	-1.97	0.00	142.97	72.44
YDR529C	-1.97	0.00	1820.09	922.54
YNL053W	-1.97	0.01	74.07	37.55
YHL001W	-1.97	0.00	292.80	148.51
YPL251W	-1.97	0.03	47.48	24.08
YNL036W	-1.97	0.00	491.52	249.43

YNL044W	-1.97	0.00	397.88	201.95
YDR150W	-1.97	0.05	38.14	19.37
YDR354C-A	-1.97	0.02	57.26	29.08
YNL157W	-1.97	0.00	641.63	326.02
YBL087C	-1.97	0.00	245.21	124.61
YDR413C	-1.97	0.00	110.76	56.29
YIR042C	-1.97	0.03	47.04	23.92
YBR058C-A	-1.97	0.00	183.85	93.48
YFL010C	-1.97	0.00	333.48	169.61
YLR455W	-1.97	0.02	54.26	27.60
YBL029W	-1.97	0.02	53.05	26.99
YJL211C	-1.97	0.01	65.46	33.30
YPR142C	-1.97	0.01	79.84	40.61
YBR191W	-1.97	0.00	302.07	153.70
YPL271W	-1.96	0.00	1487.91	757.74
YEL075W-A	-1.96	0.01	67.55	34.42
YGR190C	-1.96	0.05	39.46	20.11
YDR148C	-1.96	0.00	371.36	189.26
YNL111C	-1.96	0.01	66.53	33.91
YMR242C	-1.96	0.00	296.44	151.11
YGL023C	-1.96	0.00	91.64	46.72
YOR224C	-1.96	0.00	84.33	43.02
YML100W	-1.96	0.00	134.67	68.71
YGL022W	-1.96	0.00	98.08	50.07
YDL087C	-1.96	0.02	54.09	27.61
YKL167C	-1.96	0.00	124.30	63.45
YOL163W	-1.96	0.05	40.93	20.90
YKL096W-A	-1.96	0.00	910.27	464.86
YLR367W	-1.96	0.00	177.96	90.90
YGR287C	-1.96	0.02	57.62	29.43
YIL077C	-1.96	0.00	218.60	111.68
YJR074W	-1.96	0.00	88.65	45.30
YDR350C	-1.96	0.03	47.98	24.52
YMR171C	-1.96	0.00	253.79	129.71
YJR114W	-1.96	0.00	177.22	90.58
YCR059C	-1.96	0.01	69.01	35.28
YJL062W-A	-1.96	0.00	365.14	186.67
YGL069C	-1.96	0.00	104.88	53.63
YLR448W	-1.96	0.00	178.95	91.53
YLR314C	-1.96	0.00	88.26	45.14
YML106W	-1.95	0.00	99.09	50.69
YER072W	-1.95	0.00	322.52	164.98
YJR016C	-1.95	0.00	132.65	67.89
YML008C	-1.95	0.00	119.24	61.03
YBL032W	-1.95	0.00	83.28	42.63
YBR091C	-1.95	0.00	91.26	46.72
YOR133W	-1.95	0.00	240.01	122.92

YCR053W	-1.95	0.01	71.84	36.80
YLL014W	-1.95	0.00	154.51	79.17
YDR471W	-1.95	0.00	235.90	120.88
YER044C	-1.95	0.00	122.71	62.88
YOR096W	-1.95	0.00	256.87	131.67
YNR015W	-1.95	0.05	40.40	20.71
YCL039W	-1.95	0.04	46.48	23.84
YNL009W	-1.95	0.03	47.97	24.62
YMR210W	-1.95	0.00	98.80	50.72
YPR141C	-1.95	0.05	39.84	20.46
YDR476C	-1.95	0.00	210.52	108.10
YKL046C	-1.95	0.00	201.64	103.55
YML101C	-1.95	0.02	61.78	31.73
YCR073W-A	-1.95	0.00	154.58	79.38
YIL142C-A	-1.95	0.01	66.03	33.92
YFL021W	-1.95	0.00	123.51	63.45
YNL170W	-1.95	0.00	112.52	57.84
YER083C	-1.94	0.01	68.15	35.05
YHR180W	-1.94	0.04	43.62	22.44
YJR025C	-1.94	0.00	124.95	64.28
YOR063W	-1.94	0.00	504.54	259.59
YJR048W	-1.94	0.00	578.03	297.46
YGL097W	-1.94	0.01	65.94	33.94
YLR061W	-1.94	0.00	211.38	108.87
YPL078C	-1.94	0.00	633.38	326.24
YJL169W	-1.94	0.04	44.06	22.70
YDR411C	-1.94	0.01	71.64	36.92
YPL179W	-1.94	0.00	123.26	63.53
YER177W	-1.94	0.00	610.88	314.89
YMR022W	-1.94	0.00	299.78	154.55
YDL013W	-1.94	0.00	110.23	56.83
YMR215W	-1.94	0.03	48.67	25.10
YKL111C	-1.94	0.00	91.54	47.21
YOR210W	-1.94	0.00	200.96	103.67
YKL023C-A	-1.94	0.01	67.97	35.07
YEL074W	-1.94	0.03	52.96	27.33
YJL063C	-1.94	0.00	130.65	67.43
YPL169C	-1.94	0.01	64.94	33.52
YKL216W	-1.94	0.00	118.25	61.10
YOR092W	-1.93	0.02	54.51	28.18
YMR206W	-1.93	0.00	130.80	67.63
YFL049W	-1.93	0.05	40.36	20.88
YPR052C	-1.93	0.00	166.93	86.40
YPL049C	-1.93	0.00	145.40	75.31
YNL185C	-1.93	0.00	127.37	65.98
YBR036C	-1.93	0.00	227.93	118.11
YNL158W	-1.93	0.00	87.18	45.17

YOR008C	-1.93	0.00	148.94	77.18
YER116C	-1.93	0.00	90.51	46.92
YGR060W	-1.93	0.00	161.72	83.85
YKL053W	-1.93	0.00	430.08	223.01
YOL140W	-1.93	0.01	72.68	37.71
YNL241C	-1.93	0.00	451.21	234.12
YJR058C	-1.93	0.00	156.99	81.46
YCR024C-B	-1.93	0.00	679.82	352.91
YNR001C	-1.93	0.00	1139.48	591.74
YGL087C	-1.93	0.00	162.01	84.14
YLR325C	-1.93	0.00	876.16	455.14
YNR020C	-1.92	0.04	44.74	23.26
YBR268W	-1.92	0.00	168.44	87.60
YPL135C-A	-1.92	0.00	1747.24	908.76
YDR389W	-1.92	0.03	52.20	27.16
YPR086W	-1.92	0.00	200.89	104.53
YDL114W-A	-1.92	0.00	87.72	45.64
YER026C	-1.92	0.00	239.75	124.77
YDL010W	-1.92	0.00	227.35	118.34
YDR001C	-1.92	0.00	321.41	167.29
YER167W	-1.92	0.03	54.54	28.40
YMR184W	-1.92	0.00	92.47	48.15
YER064C	-1.92	0.04	48.15	25.08
YER124C	-1.92	0.00	165.89	86.41
YLR029C	-1.92	0.00	446.04	232.35
YDL129W	-1.92	0.00	99.13	51.65
YGL253W	-1.92	0.00	159.58	83.17
YJL186W	-1.92	0.02	61.03	31.82
YDR526C	-1.92	0.02	60.46	31.52
YPL039W	-1.92	0.01	66.29	34.56
YPL002C	-1.92	0.01	83.55	43.57
YNL301C	-1.92	0.03	53.79	28.05
YBL025W	-1.92	0.01	79.70	41.58
YOR223W	-1.92	0.00	112.50	58.69
YEL042W	-1.92	0.01	80.15	41.81
YAR028W	-1.92	0.00	213.92	111.60
YLR026C	-1.92	0.00	101.41	52.91
YGL148W	-1.92	0.00	121.76	63.56
YER120W	-1.91	0.00	223.64	116.80
YOR312C	-1.91	0.00	319.99	167.13
YLR257W	-1.91	0.00	507.71	265.17
YNR004W	-1.91	0.01	71.07	37.12
YPL134C	-1.91	0.01	84.24	44.00
YOR274W	-1.91	0.00	109.73	57.34
YHR140W	-1.91	0.01	81.79	42.74
YBL040C	-1.91	0.02	60.34	31.53
YGR007W	-1.91	0.00	122.25	63.91

YNL322C	-1.91	0.00	293.69	153.58
YMR121C	-1.91	0.00	180.85	94.61
YER066C-A	-1.91	0.00	203.33	106.39
YPL250W-A	-1.91	0.00	981.31	513.79
YDR349C	-1.91	0.01	86.13	45.10
YGR034W	-1.91	0.00	375.53	196.64
YDL180W	-1.91	0.01	73.56	38.52
YMR266W	-1.91	0.02	59.64	31.24
YKL159C	-1.91	0.00	269.31	141.07
YPR023C	-1.91	0.00	252.19	132.11
YCR046C	-1.91	0.00	192.06	100.65
YOR246C	-1.91	0.01	85.68	44.92
YBR035C	-1.91	0.00	259.27	136.05
YMR307W	-1.91	0.00	508.50	266.88
YJL189W	-1.91	0.00	517.67	271.71
YLR058C	-1.91	0.00	353.93	185.77
YNL212W	-1.90	0.03	54.22	28.47
YIL076W	-1.90	0.01	75.67	39.74
YDR032C	-1.90	0.00	345.08	181.22
YOR383C	-1.90	0.00	1091.18	573.03
YER154W	-1.90	0.01	78.55	41.25
YPL206C	-1.90	0.00	168.35	88.41
YHR183W	-1.90	0.00	391.63	205.68
YDR277C	-1.90	0.00	384.14	201.96
YOR207C	-1.90	0.05	41.73	21.94
YMR074C	-1.90	0.00	156.47	82.29
YGR008C	-1.90	0.00	2053.56	1079.94
YHR116W	-1.90	0.00	101.31	53.29
YJL026C-A	-1.90	0.00	113.00	59.45
YPR062W	-1.90	0.00	598.74	315.00
YMR042W	-1.90	0.00	94.83	49.91
YPR069C	-1.90	0.05	41.97	22.09
YOR213C	-1.90	0.00	93.86	49.44
YBR243C	-1.90	0.04	46.67	24.59
YGR285C	-1.90	0.00	131.33	69.20
YBL072C	-1.90	0.00	548.79	289.27
YDR480W	-1.90	0.05	45.06	23.76
YGL123W	-1.90	0.00	437.85	230.92
YBR048W	-1.90	0.00	340.18	179.45
YBR126C	-1.90	0.00	559.34	295.09
YKR009C	-1.90	0.01	83.81	44.23
YJL096W	-1.89	0.00	92.77	48.96
YKR085C	-1.89	0.01	80.36	42.41
YKL069W	-1.89	0.05	43.83	23.14
YGR214W	-1.89	0.00	199.85	105.50
YBR114W	-1.89	0.00	113.01	59.68
YLR249W	-1.89	0.00	214.06	113.12

YOR332W	-1.89	0.00	476.23	251.73
YHR025W	-1.89	0.00	96.70	51.16
YML124C	-1.89	0.04	51.27	27.13
YLR179C	-1.89	0.00	605.03	320.19
YNL075W	-1.89	0.02	65.78	34.82
YDR096W	-1.89	0.01	80.17	42.44
YLR230W	-1.89	0.00	105.68	55.99
YHR182C-A	-1.89	0.00	210.22	111.38
YKR008W	-1.89	0.03	55.08	29.19
YGR181W	-1.89	0.00	145.27	77.02
YDL229W	-1.89	0.00	186.13	98.69
YJR105W	-1.89	0.00	210.53	111.65
YOR007C	-1.88	0.00	624.99	331.59
YOR158W	-1.88	0.00	94.83	50.32
YPR160C-A	-1.88	0.00	124.13	65.90
YGR064W	-1.88	0.00	155.15	82.37
YEL007W	-1.88	0.02	61.40	32.60
YDL111C	-1.88	0.03	58.40	31.01
YER117W	-1.88	0.00	449.73	238.94
YMR214W	-1.88	0.00	93.90	49.91
YBR189W	-1.88	0.00	319.53	169.85
YLL044W	-1.88	0.00	350.60	186.38
YPL225W	-1.88	0.00	859.65	457.12
YBL029C-A	-1.88	0.00	150.60	80.15
YCL009C	-1.88	0.00	257.61	137.14
YBR165W	-1.88	0.00	97.18	51.74
YPR087W	-1.88	0.00	169.24	90.14
YNL074C	-1.88	0.00	202.41	107.81
YGR023W	-1.88	0.00	199.55	106.29
YMR197C	-1.88	0.00	250.98	133.70
YJR009C	-1.88	0.00	1042.28	555.38
YJL004C	-1.88	0.01	70.80	37.74
YLR075W	-1.88	0.00	1125.46	599.94
YDR105C	-1.88	0.03	57.08	30.43
YMR256C	-1.88	0.00	1359.02	724.68
YKR048C	-1.88	0.00	340.74	181.70
YNR002C	-1.87	0.00	244.51	130.42
YJL104W	-1.87	0.00	220.65	117.74
YML088W	-1.87	0.00	111.01	59.25
YBR290W	-1.87	0.00	275.19	146.94
YKR043C	-1.87	0.00	155.94	83.28
YKL137W	-1.87	0.01	89.46	47.78
YIL014C-A	-1.87	0.01	85.21	45.52
YPL127C	-1.87	0.00	164.97	88.20
YDL136W	-1.87	0.00	430.76	230.39
YPL059W	-1.87	0.00	128.83	68.92
YLR286C	-1.87	0.00	679.25	363.55

YPR132W	-1.87	0.00	608.40	325.66
YER050C	-1.87	0.00	244.28	130.86
YHR208W	-1.87	0.00	160.04	85.78
YGR161C	-1.86	0.00	1105.59	592.86
YER094C	-1.86	0.00	435.93	233.79
YER048W-A	-1.86	0.00	250.32	134.25
YGL036W	-1.86	0.01	73.36	39.35
YER054C	-1.86	0.00	153.91	82.56
YPR133C	-1.86	0.00	127.58	68.44
YAL032C	-1.86	0.01	83.20	44.64
YPL149W	-1.86	0.00	127.33	68.33
YLR350W	-1.86	0.00	391.55	210.14
YPL222C-A	-1.86	0.00	178.28	95.69
YDL053C	-1.86	0.00	169.04	90.74
YNL200C	-1.86	0.00	218.20	117.14
YIL145C	-1.86	0.01	80.42	43.19
YOR230W	-1.86	0.00	221.27	118.84
YDR129C	-1.86	0.00	349.71	187.86
YNL305C	-1.86	0.00	360.67	193.76
YBR187W	-1.86	0.00	99.61	53.52
YDL130W	-1.86	0.00	501.88	269.82
YNL020C	-1.86	0.01	81.02	43.56
YGR024C	-1.86	0.01	72.89	39.19
YGL198W	-1.86	0.00	99.53	53.59
YBL092W	-1.86	0.00	585.81	315.49
YML085C	-1.86	0.00	132.62	71.43
YPL204W	-1.86	0.00	198.07	106.69
YJL177W	-1.86	0.00	178.27	96.04
YMR200W	-1.86	0.00	236.03	127.15
YMR281W	-1.86	0.01	84.68	45.63
YJR148W	-1.86	0.00	110.96	59.81
YGR018C	-1.86	0.00	219.73	118.44
YLR390W-A	-1.85	0.00	462.59	249.39
YGL028C	-1.85	0.00	102.95	55.51
YGR118W	-1.85	0.00	543.78	293.21
YDR194C	-1.85	0.03	57.33	30.92
YDR328C	-1.85	0.00	326.67	176.15
YNL203C	-1.85	0.00	97.46	52.57
YMR143W	-1.85	0.00	328.93	177.43
YJR070C	-1.85	0.04	52.20	28.16
YNL178W	-1.85	0.00	424.78	229.15
YPL090C	-1.85	0.00	377.84	203.92
YPL211W	-1.85	0.02	63.72	34.40
YFL038C	-1.85	0.00	514.24	277.62
YLR218C	-1.85	0.02	65.32	35.30
YKL001C	-1.85	0.00	316.77	171.19
YIR018W	-1.85	0.00	122.18	66.03

YMR003W	-1.85	0.04	52.31	28.27
YNL246W	-1.85	0.01	78.70	42.54
YLR121C	-1.85	0.00	490.02	264.95
YPR045C	-1.85	0.04	54.30	29.37
YER089C	-1.85	0.00	99.01	53.58
YDR098C	-1.85	0.01	83.63	45.26
YHR203C	-1.85	0.00	264.19	143.05
YER090C-A	-1.84	0.03	55.88	30.32
YNL081C	-1.84	0.00	209.27	113.54
YBR141W-A	-1.84	0.02	64.57	35.03
YHR019C	-1.84	0.01	95.95	52.06
YLR443W	-1.84	0.04	54.09	29.35
YNL268W	-1.84	0.00	124.85	67.74
YKL148C	-1.84	0.00	390.70	212.14
YDR313C	-1.84	0.00	152.20	82.69
YFR036W	-1.84	0.00	116.17	63.11
YNL207W	-1.84	0.03	62.05	33.71
YDR418W	-1.84	0.00	292.62	159.14
YDL173W	-1.84	0.00	190.91	103.82
YOR226C	-1.84	0.00	101.31	55.10
YJL199C	-1.84	0.02	72.43	39.39
YOR103C	-1.84	0.00	111.60	60.71
YPL247C	-1.84	0.01	92.51	50.33
YDL128W	-1.84	0.00	401.91	218.70
YNL232W	-1.84	0.00	120.01	65.33
YBR052C	-1.84	0.00	288.32	156.98
YBR265W	-1.84	0.02	67.28	36.64
YJR113C	-1.84	0.00	216.77	118.04
YIL153W	-1.84	0.00	112.80	61.47
YCR031C	-1.83	0.00	601.01	327.53
YOL039W	-1.83	0.00	383.65	209.33
YKR062W	-1.83	0.00	131.77	71.94
YML009C	-1.83	0.00	254.22	138.82
YLR256W	-1.83	0.05	49.58	27.08
YMR083W	-1.83	0.00	630.96	344.71
YPL199C	-1.83	0.00	101.67	55.55
YPR152C	-1.83	0.04	55.59	30.41
YFL021C-A	-1.83	0.01	79.61	43.56
YCR050C	-1.83	0.00	127.93	70.02
YLL045C	-1.83	0.00	357.99	195.95
YIL155C	-1.83	0.00	184.82	101.23
YOR187W	-1.83	0.00	357.49	195.81
YKL186C	-1.83	0.00	175.32	96.04
YCL018W	-1.82	0.00	172.87	94.74
YLR415C	-1.82	0.03	61.75	33.88
YDR244W	-1.82	0.00	132.69	72.80

YER099C	-1.82	0.00	111.39	61.13
YER152W-A	-1.82	0.01	97.05	53.27
YKL183W	-1.82	0.05	48.19	26.46
YLR375W	-1.82	0.00	1137.92	625.18
YPL234C	-1.82	0.00	138.81	76.27
YOR369C	-1.82	0.00	661.92	363.82
YJL048C	-1.82	0.00	491.97	270.49
YJL149W	-1.82	0.02	69.34	38.13
YBR203W	-1.82	0.01	82.50	45.39
YDL004W	-1.82	0.00	464.18	255.39
YGR239C	-1.82	0.04	57.06	31.40
YDL159C-B	-1.82	0.01	89.20	49.11
YDR373W	-1.82	0.00	117.06	64.45
YGL166W	-1.82	0.00	247.28	136.17
YLR171W	-1.82	0.03	59.08	32.54
YOR196C	-1.81	0.00	156.41	86.18
YBR132C	-1.81	0.01	80.16	44.18
YLR023C	-1.81	0.00	291.38	160.61
YGR180C	-1.81	0.00	132.84	73.23
YAL042C-A	-1.81	0.02	66.99	36.93
YPR012W	-1.81	0.04	55.95	30.86
YOL155C	-1.81	0.00	535.13	295.33
YDL198C	-1.81	0.01	100.57	55.51
YGR121C	-1.81	0.02	73.82	40.76
YLR258W	-1.81	0.00	284.57	157.13
YLR062C	-1.81	0.00	298.42	164.84
YPL237W	-1.81	0.00	223.89	123.80
YGR046W	-1.81	0.00	132.25	73.15
YDR378C	-1.81	0.00	264.60	146.35
YFL010W-A	-1.81	0.00	398.87	220.64
YDR417C	-1.81	0.00	198.85	110.02
YBR002C	-1.81	0.01	81.77	45.25
YML012W	-1.81	0.00	210.00	116.23
YOR271C	-1.81	0.04	55.68	30.82
YJL136C	-1.81	0.00	380.32	210.55
YNL245C	-1.80	0.00	110.02	60.98
YPL089C	-1.80	0.00	212.26	117.66
YHR162W	-1.80	0.00	915.98	508.11
YHR026W	-1.80	0.00	133.26	73.93
YHR032C-A	-1.80	0.01	85.77	47.59
YPL131W	-1.80	0.00	426.08	236.49
YDR432W	-1.80	0.00	786.73	436.68
YNR037C	-1.80	0.00	208.69	115.87
YJR061W	-1.80	0.00	112.29	62.37
YPL202C	-1.80	0.02	68.76	38.19
YPL224C	-1.80	0.02	70.69	39.29
YML009C-A	-1.80	0.00	131.62	73.15

YOL111C	-1.80	0.00	119.52	66.43
YJR103W	-1.80	0.01	100.73	56.00
YOL121C	-1.80	0.00	228.80	127.34
YDL110C	-1.80	0.00	804.73	447.95
YDL192W	-1.80	0.00	250.72	139.57
YBR016W	-1.80	0.00	390.45	217.41
YMR264W	-1.80	0.01	93.26	51.94
YKR007W	-1.80	0.00	138.13	76.94
YDR280W	-1.80	0.01	102.37	57.02
YGR282C	-1.79	0.00	727.92	405.64
YDR121W	-1.79	0.01	104.59	58.30
YJL079C	-1.79	0.00	126.18	70.43
YML129C	-1.79	0.00	560.33	312.79
YOL005C	-1.79	0.01	94.56	52.79
YBR249C	-1.79	0.02	78.81	44.01
YNL098C	-1.79	0.00	180.08	100.58
YPL004C	-1.79	0.00	428.20	239.28
YJR018W	-1.79	0.01	85.70	47.90
YPL087W	-1.79	0.00	312.73	174.79
YGR057C	-1.79	0.01	84.07	47.00
YLR169W	-1.79	0.01	102.58	57.36
YDL217C	-1.79	0.01	99.05	55.42
YLR339C	-1.79	0.00	278.82	156.10
YJL159W	-1.79	0.00	1851.34	1036.90
YLR174W	-1.78	0.02	76.41	42.81
YDR025W	-1.78	0.00	355.33	199.11
YJL190C	-1.78	0.00	274.53	153.87
YER152C	-1.78	0.00	145.23	81.41
YKL006W	-1.78	0.00	314.68	176.51
YOL040C	-1.78	0.00	797.55	447.42
YMR148W	-1.78	0.03	68.81	38.61
YJL191W	-1.78	0.00	158.60	89.02
YIR035C	-1.78	0.00	897.64	503.89
YNL196C	-1.78	0.03	70.80	39.76
YPL252C	-1.78	0.03	67.49	37.90
YNR046W	-1.78	0.00	121.54	68.27
YNR036C	-1.78	0.00	407.82	229.09
YER102W	-1.78	0.00	328.75	184.68
YNL114C	-1.78	0.02	83.47	46.91
YBR194W	-1.78	0.04	60.36	33.94
YGR248W	-1.78	0.00	324.29	182.43
YER086W	-1.78	0.02	84.08	47.36
YDL076C	-1.78	0.01	93.17	52.48
YER095W	-1.77	0.00	368.94	207.87
YNL263C	-1.77	0.05	57.42	32.36
YEL044W	-1.77	0.00	229.59	129.56
YJR097W	-1.77	0.03	64.11	36.19

YJR021C	-1.77	0.01	97.89	55.26
YDR064W	-1.77	0.00	419.21	236.69
YFL037W	-1.77	0.02	82.44	46.55
YER148W	-1.77	0.00	246.12	139.02
YLR299C-A	-1.77	0.00	137.70	77.78
YKR071C	-1.77	0.00	268.53	151.75
YGL122C	-1.77	0.00	246.69	139.41
YBR145W	-1.77	0.05	56.87	32.15
YPR173C	-1.77	0.01	88.83	50.27
YPR102C	-1.77	0.00	286.59	162.20
YOR139C	-1.77	0.01	89.57	50.70
YPL218W	-1.77	0.00	197.88	112.07
YNL135C	-1.77	0.00	386.12	218.68
YOL012C	-1.76	0.00	176.59	100.11
YER055C	-1.76	0.00	200.42	113.63
YGR183C	-1.76	0.00	1904.42	1080.59
YGL006W	-1.76	0.00	148.58	84.33
YDR043C	-1.76	0.00	1439.74	817.68
YDR447C	-1.76	0.00	214.13	121.66
YJR008W	-1.76	0.00	448.67	255.00
YDL191W	-1.76	0.00	472.00	268.67
YNL067W	-1.76	0.00	340.40	193.77
YDR158W	-1.76	0.00	122.39	69.69
YER069W	-1.76	0.02	78.01	44.43
YOR200W	-1.76	0.01	96.58	55.02
YHR083W	-1.76	0.01	117.78	67.11
YBR299W	-1.76	0.05	55.78	31.78
YPR075C	-1.75	0.00	322.24	183.62
YDL011C	-1.75	0.00	124.71	71.09
YEL011W	-1.75	0.00	245.93	140.20
YJR123W	-1.75	0.00	653.59	373.13
YIL022W	-1.75	0.00	186.26	106.44
YNL056W	-1.75	0.00	163.91	93.68
YPL159C	-1.75	0.00	203.90	116.75
YNL209W	-1.75	0.00	247.62	141.82
YCR047C	-1.75	0.00	254.95	146.06
YOL129W	-1.75	0.00	303.13	173.67
YBR298C	-1.75	0.00	189.85	108.78
YBR214W	-1.75	0.00	217.07	124.38
YDR377W	-1.75	0.00	503.74	288.65
YPR044C	-1.74	0.00	780.85	447.57
YJL153C	-1.74	0.00	815.06	467.42
YLR340W	-1.74	0.00	376.83	216.17
YDR130C	-1.74	0.03	69.16	39.69
YNL019C	-1.74	0.05	60.87	35.03
YOL026C	-1.74	0.01	112.51	64.75
YOR104W	-1.74	0.01	97.39	56.05

YOL159C-A	-1.74	0.03	73.90	42.53
YNL285W	-1.74	0.03	77.34	44.52
YKL065W-A	-1.74	0.01	93.25	53.73
YFL054C	-1.73	0.00	191.01	110.13
YMR316C-A	-1.73	0.00	519.17	299.57
YJR073C	-1.73	0.00	880.73	508.23
YDL045W-A	-1.73	0.00	239.19	138.14
YNL302C	-1.73	0.00	307.57	177.67
YER156C	-1.73	0.02	82.63	47.73
YDR156W	-1.73	0.00	236.59	136.71
YKL191W	-1.73	0.04	63.65	36.81
YOR358W	-1.73	0.01	120.00	69.46
YPL053C	-1.73	0.00	137.88	79.82
YBR051W	-1.73	0.03	74.30	43.02
YMR265C	-1.73	0.04	63.96	37.04
YPL081W	-1.73	0.01	121.09	70.18
YDL172C	-1.72	0.00	254.62	147.66
YJL188C	-1.72	0.00	335.91	194.88
YGL070C	-1.72	0.02	84.47	49.01
YDR525W-A	-1.72	0.00	234.64	136.16
YCL058C	-1.72	0.03	77.84	45.20
YOR375C	-1.72	0.00	334.45	194.36
YOR052C	-1.72	0.00	1313.34	763.25
YKR013W	-1.72	0.04	70.35	40.89
YBR077C	-1.72	0.00	184.16	107.05
YOR344C	-1.72	0.02	89.72	52.15
YPR183W	-1.72	0.03	73.75	42.93
YLR150W	-1.72	0.00	265.92	154.85
YNL093W	-1.72	0.00	194.39	113.22
YJL116C	-1.72	0.02	91.75	53.44
YDR140W	-1.72	0.03	80.95	47.16
YOL134C	-1.72	0.00	131.80	76.79
YNL125C	-1.72	0.01	101.57	59.18
YHL033C	-1.72	0.01	125.52	73.16
YFL048C	-1.72	0.04	66.96	39.03
YPR002C-A	-1.71	0.00	341.70	199.33
YJR145C	-1.71	0.00	320.51	186.97
YDR397C	-1.71	0.00	170.66	99.57
YKR066C	-1.71	0.00	811.57	473.50
YBR287W	-1.71	0.00	301.08	175.73
YMR191W	-1.71	0.00	299.00	174.58
YER004W	-1.71	0.00	399.76	233.66
YGR260W	-1.71	0.04	68.57	40.13
YNL113W	-1.71	0.01	114.23	66.85
YOR179C	-1.71	0.02	98.08	57.41
YIL122W	-1.71	0.01	129.08	75.59

YOR102W	-1.71	0.00	144.11	84.42
YBL091C-A	-1.71	0.01	99.45	58.28
YOR294W	-1.70	0.02	88.38	51.84
YMR202W	-1.70	0.01	123.16	72.27
YDL184C	-1.70	0.00	4966.77	2916.38
YIL059C	-1.70	0.02	91.23	53.57
YJR095W	-1.70	0.00	137.65	80.87
YGR022C	-1.70	0.00	209.98	123.44
YHR143W-A	-1.70	0.00	252.85	148.65
YPR126C	-1.70	0.00	207.79	122.18
YNL043C	-1.70	0.00	487.85	287.02
YOL133W	-1.70	0.00	295.42	173.89
YOR285W	-1.70	0.00	1705.57	1004.51
YIL154C	-1.70	0.00	160.15	94.42
YHR193C	-1.70	0.00	204.39	120.50
YKL030W	-1.69	0.02	89.93	53.09
YGL165C	-1.69	0.00	236.33	139.51
YBL043W	-1.69	0.00	631.31	373.01
YAL042W	-1.69	0.01	106.13	62.74
YKL128C	-1.69	0.04	70.20	41.52
YPR093C	-1.69	0.02	92.87	54.96
YCL034W	-1.69	0.00	139.52	82.58
YER043C	-1.69	0.00	329.64	195.10
YEL009C	-1.69	0.00	667.23	395.19
YOR099W	-1.69	0.01	134.47	79.66
YKL185W	-1.69	0.01	106.03	62.84
YDR327W	-1.69	0.00	340.85	202.19
YNL194C	-1.69	0.00	381.78	226.50
YBL018C	-1.68	0.04	75.21	44.67
YJR017C	-1.68	0.00	170.07	101.05
YMR002W	-1.68	0.00	1146.44	681.41
YOR327C	-1.68	0.00	456.89	271.68
YGR249W	-1.68	0.01	112.13	66.69
YGR192C	-1.68	0.00	2117.86	1259.78
YHR092C	-1.68	0.00	442.88	263.49
YBL055C	-1.68	0.03	80.43	47.85
YER159C	-1.68	0.00	351.81	209.59
YOR049C	-1.68	0.00	557.20	332.04
YHR122W	-1.68	0.01	113.17	67.46
YPL232W	-1.68	0.00	291.65	174.00
YHR146W	-1.68	0.00	180.28	107.57
YKR092C	-1.68	0.04	72.80	43.44
YLL043W	-1.68	0.03	84.98	50.73
YCR004C	-1.68	0.00	286.57	171.08
YAL012W	-1.67	0.00	200.30	119.73
YMR123W	-1.67	0.04	77.02	46.08

YDR381W	-1.67	0.00	177.92	106.50
YMR102C	-1.67	0.00	195.37	117.03
YKL008C	-1.67	0.02	107.84	64.61
YGL200C	-1.67	0.00	172.85	103.58
YJL174W	-1.67	0.00	247.77	148.51
YBR135W	-1.67	0.03	87.13	52.25
YLR438C-A	-1.67	0.00	172.40	103.40
YNL173C	-1.67	0.00	152.33	91.40
YPL197C	-1.67	0.00	398.18	238.94
YGL012W	-1.67	0.02	96.68	58.05
YJL171C	-1.66	0.00	583.49	350.61
YGL045W	-1.66	0.00	252.72	151.87
YLR225C	-1.66	0.01	143.28	86.11
YER163C	-1.66	0.00	187.73	112.83
YFL053W	-1.66	0.00	167.92	101.00
YBR201C-A	-1.66	0.00	155.65	93.62
YOR107W	-1.66	0.00	358.03	215.40
YPL220W	-1.66	0.00	191.88	115.46
YHL027W	-1.66	0.00	189.01	113.76
YNL066W	-1.66	0.00	189.60	114.19
YKL085W	-1.66	0.00	724.41	436.40
YHR174W	-1.66	0.00	1103.49	665.82
YHR143W	-1.66	0.00	336.63	203.14
YMR043W	-1.66	0.00	327.97	197.95
YPL088W	-1.66	0.00	306.82	185.30
YGL237C	-1.66	0.01	112.56	67.98
YLR229C	-1.65	0.00	175.43	106.19
YDL133W	-1.65	0.03	93.63	56.69
YPR153W	-1.65	0.05	72.58	43.95
YDR382W	-1.65	0.00	392.65	237.99
YDL055C	-1.65	0.00	601.78	364.94
YDR408C	-1.65	0.02	106.53	64.63
YML025C	-1.65	0.01	134.14	81.51
YDR366C	-1.64	0.00	416.08	253.01
YLR293C	-1.64	0.00	375.14	228.24
YNL080C	-1.64	0.03	87.58	53.31
YAL038W	-1.64	0.00	911.43	554.86
YJL078C	-1.64	0.01	136.31	83.02
YLR076C	-1.64	0.00	1287.32	785.73
YGL076C	-1.64	0.00	288.56	176.20
YDL014W	-1.64	0.01	147.74	90.21
YPR016C	-1.64	0.00	184.86	113.06
YPL037C	-1.63	0.00	178.88	109.50
YPL057C	-1.63	0.00	539.12	330.35
YGR268C	-1.63	0.00	214.12	131.26
YPL061W	-1.63	0.00	883.45	542.24
YDR041W	-1.63	0.00	180.02	110.52

YKL063C	-1.63	0.00	204.32	125.52
YBR025C	-1.63	0.01	128.70	79.09
YMR116C	-1.63	0.00	272.40	167.62
YHR209W	-1.62	0.04	90.92	55.99
YKL087C	-1.62	0.00	190.24	117.22
YER023C-A	-1.62	0.00	165.27	101.88
YER147C-A	-1.62	0.00	300.92	185.57
YDR007W	-1.62	0.03	96.94	59.79
YGR279C	-1.62	0.03	99.02	61.16
YGR147C	-1.62	0.00	194.65	120.25
YLL039C	-1.62	0.00	1169.89	722.89
YBR151W	-1.62	0.00	418.81	258.81
YMR216C	-1.62	0.03	95.05	58.76
YBR050C	-1.62	0.01	143.46	88.72
YDR044W	-1.62	0.00	313.48	193.96
YFR031C-A	-1.62	0.00	219.00	135.53
YHR001W-A	-1.62	0.00	985.86	610.12
R0020C	-1.61	0.00	3403.27	2112.54
YGL010W	-1.61	0.01	132.55	82.31
YGR136W	-1.61	0.00	647.67	402.39
YDL083C	-1.61	0.00	324.33	201.52
YBR004C	-1.61	0.01	149.69	93.03
YDL046W	-1.61	0.00	501.08	311.55
YKL217W	-1.61	0.00	390.76	243.08
YLR414C	-1.61	0.00	1141.03	709.84
YDL123W	-1.61	0.00	499.06	310.51
YCR036W	-1.61	0.01	148.18	92.20
YGR110W	-1.60	0.03	108.08	67.34
YBL095W	-1.60	0.00	201.68	125.73
YDR527W	-1.60	0.04	92.99	57.97
YLR056W	-1.60	0.03	104.22	65.01
YPR030W	-1.60	0.05	84.14	52.54
YKL044W	-1.60	0.03	103.47	64.64
YLR167W	-1.60	0.00	812.18	507.62
YJL052W	-1.60	0.00	1303.29	814.85
YMR307C-A	-1.60	0.00	444.72	278.54
YLR300W	-1.60	0.00	377.82	236.71
YGL147C	-1.60	0.01	160.81	100.80
YLR286W-A	-1.59	0.00	1246.64	782.11
YDR524C-B	-1.59	0.00	3419.87	2147.92
YJL143W	-1.59	0.00	383.35	240.77
YGR292W	-1.59	0.02	120.82	76.00
YMR104C	-1.59	0.00	334.90	210.70
YDR012W	-1.59	0.00	326.05	205.16
YMR295C	-1.59	0.00	996.66	627.15
YGL103W	-1.59	0.00	668.32	420.76

YER081W	-1.59	0.01	159.63	100.58
YDL228C	-1.58	0.00	604.62	381.70
YKL043W	-1.58	0.00	283.35	179.00
YDR155C	-1.58	0.00	1756.93	1109.96
YDR353W	-1.58	0.00	345.87	218.51
YGR228W	-1.58	0.02	135.60	85.89
YFL031C-A	-1.58	0.00	540.05	342.15
YNL327W	-1.58	0.03	115.01	72.87
YPR113W	-1.58	0.00	332.78	210.93
YPL056C	-1.58	0.01	149.82	94.97
YKL060C	-1.58	0.00	2668.05	1691.30
YPL229W	-1.58	0.03	112.72	71.52
YLR016C	-1.58	0.05	94.13	59.74
YHR179W	-1.57	0.00	508.45	322.96
YOR036W	-1.57	0.00	573.57	364.98
YOL126C	-1.57	0.00	211.06	134.46
YKR025W	-1.57	0.04	104.00	66.37
YGR063C	-1.57	0.00	284.06	181.32
YDR517W	-1.57	0.02	129.50	82.73
YER088W-B	-1.56	0.00	201.29	128.63
YDR072C	-1.56	0.00	338.20	216.24
YCR012W	-1.56	0.00	961.62	615.45
YAL013W	-1.56	0.05	94.96	60.80
YBR090C	-1.56	0.01	182.09	116.59
YDR297W	-1.56	0.00	561.65	359.69
YKL152C	-1.56	0.00	1181.56	757.00
YOR031W	-1.56	0.00	2181.46	1398.37
YOR202W	-1.56	0.01	176.66	113.41
YGR033C	-1.56	0.03	114.84	73.76
YBL006C	-1.56	0.01	174.78	112.30
YER034W	-1.56	0.04	110.56	71.07
YOR178C	-1.55	0.03	121.96	78.50
YIL106W	-1.55	0.01	153.83	99.11
YPL067C	-1.55	0.04	109.02	70.25
YKL035W	-1.55	0.00	312.54	201.61
YGL191W	-1.55	0.00	1284.99	829.60
YIL056W	-1.55	0.01	179.66	116.02
YER158W-A	-1.55	0.00	489.47	316.09
YLR250W	-1.54	0.01	191.52	124.20
YDR405W	-1.54	0.01	165.76	107.52
YBR068C	-1.54	0.04	116.63	75.73
YBL094C	-1.54	0.00	267.27	173.59
YDR050C	-1.54	0.00	1082.72	704.35
YBR056W-A	-1.54	0.00	2881.65	1876.43
YLR113W	-1.53	0.03	127.01	82.86
YHL020C	-1.53	0.00	221.15	144.30

YDR524W-C	-1.53	0.00	1975.86	1291.61
YIR016W	-1.53	0.03	137.32	89.85
YDR119W-A	-1.53	0.00	591.17	387.03
YER053C-A	-1.53	0.00	4577.08	3001.19
YMR036C	-1.52	0.04	117.13	76.83
YIL101C	-1.52	0.05	111.93	73.44
YKL109W	-1.52	0.00	397.68	261.17
YDR396W	-1.52	0.02	159.67	104.87
YHR010W	-1.52	0.00	350.43	230.19
YKR057W	-1.52	0.00	300.58	197.57
YPL095C	-1.52	0.00	397.78	262.14
YAL037C-B	-1.52	0.00	1195.74	788.63
YJL151C	-1.52	0.00	777.51	512.83
YMR108W	-1.51	0.05	112.19	74.06
YIR011C	-1.51	0.02	167.63	110.91
YJR094W-A	-1.51	0.00	389.43	257.68
YPR159W	-1.51	0.04	132.04	87.57
YMR071C	-1.51	0.04	131.34	87.12
YIL018W	-1.51	0.00	404.37	268.57
YBR196C	-1.50	0.00	261.37	174.01
YNL024C-A	-1.50	0.03	157.27	105.17
YPL014W	-1.49	0.00	293.05	196.61
YKL056C	-1.49	0.00	589.29	395.57
YJR104C	-1.48	0.00	2841.34	1915.31
YDR232W	-1.48	0.03	167.58	113.00
YMR294W-A	-1.48	0.00	1010.51	681.94
YAL060W	-1.48	0.00	581.81	393.47
YGR035C	-1.48	0.00	864.82	585.72
YOR247W	-1.48	0.02	189.10	128.11
YLR332W	-1.47	0.01	233.23	158.60
YDL012C	-1.47	0.00	396.34	270.06
YPR160W	-1.47	0.03	173.06	117.96
YJL196C	-1.47	0.05	138.76	94.67
YNL208W	-1.46	0.00	2774.13	1893.85
YPR035W	-1.46	0.00	574.31	392.29
YBR126W-A	-1.46	0.00	996.08	682.34
YDR258C	-1.46	0.00	310.20	212.58
YIL111W	-1.46	0.01	233.65	160.30
YGR289C	-1.45	0.04	159.63	109.73
YJR096W	-1.45	0.00	704.54	484.53
YGL102C	-1.45	0.00	705.13	485.14
YAL061W	-1.44	0.00	2080.21	1440.69
YBR005W	-1.44	0.00	917.14	636.30
YAL003W	-1.44	0.00	344.93	239.51

YBR085C-A	-1.44	0.00	5438.33	3776.65
YGL030W	-1.44	0.00	461.38	320.65
YLR327C	-1.44	0.00	6267.31	4358.05
YGL248W	-1.44	0.00	446.85	310.80
YIL053W	-1.43	0.01	307.76	215.55
YPL170W	-1.42	0.01	322.58	226.85
YKL153W	-1.42	0.00	1397.71	986.87
YDR516C	-1.42	0.04	197.22	139.36
YMR105C	-1.41	0.02	268.68	190.17
YOR204W	-1.41	0.03	219.02	155.40
YDR276C	-1.40	0.00	2619.96	1866.18
YLR264C-A	-1.40	0.02	255.40	182.22
YLR194C	-1.40	0.00	1293.52	923.01
YBR067C	-1.40	0.00	712.07	508.32
YAL034C	-1.40	0.01	382.97	273.68
YCR013C	-1.40	0.00	1263.20	902.73
YMR186W	-1.39	0.01	392.58	283.35
YBR182C	-1.38	0.04	229.22	165.61
YGL058W	-1.38	0.04	230.75	166.76
YGR161W-C	-1.38	0.00	731.48	529.00
YPR165W	-1.38	0.00	779.41	564.22
YJR115W	-1.38	0.02	331.83	241.00
YLR142W	-1.37	0.03	262.68	191.16
YFL031W	-1.37	0.00	640.31	466.82
YDR034C-A	-1.37	0.00	586.09	427.32
YBR106W	-1.37	0.00	489.57	356.99
YPL189C-A	-1.37	0.01	416.40	303.78
YBR082C	-1.37	0.01	447.93	326.92
YLL028W	-1.36	0.04	269.24	198.10
YBR177C	-1.36	0.00	652.99	481.79
YKL096W	-1.35	0.01	447.35	331.01
YBR118W	-1.35	0.00	2191.79	1623.82
YER067W	-1.35	0.00	1025.75	761.43
YKR042W	-1.35	0.01	463.82	344.71
YLR110C	-1.35	0.00	2839.03	2110.35
YHR030C	-1.34	0.05	287.32	214.17
YHR087W	-1.34	0.00	1332.26	995.03
YDR002W	-1.33	0.01	477.85	359.46
YMR122W-A	-1.30	0.00	2306.50	1773.44
YPR080W	-1.30	0.00	1597.30	1229.65
YHR052W-A	-1.29	0.00	1786.39	1380.66
YBR183W	-1.29	0.03	537.30	415.88
YJL034W	-1.29	0.05	415.19	321.38
YFR017C	-1.28	0.03	562.29	438.23
YJL152W	-1.28	0.03	554.23	432.01

YOL109W	-1.28	0.00	2250.84	1762.38
YNL160W	-1.28	0.00	6171.24	4839.01
YHR054W-A	-1.27	0.00	1772.29	1397.91
YJR045C	-1.27	0.03	696.30	549.44
YCR021C	-1.26	0.00	5175.80	4094.69
YNR034W-A	-1.26	0.00	2237.27	1775.82
YKL163W	-1.25	0.00	3682.36	2936.14
YCL040W	-1.24	0.01	1427.87	1149.62
YHR055C	-1.23	0.00	2193.50	1784.86
YOL086C	-1.23	0.01	1593.78	1298.08
YJL166W	-1.01	0.02	1865.30	1838.12
YER150W	1.07	0.00	5308.56	5685.74
YOR298C-A	1.07	0.00	1871.13	2004.18
YLR217W	1.11	0.01	315.12	349.97
YNL064C	1.13	0.00	395.31	447.57
YBR072W	1.15	0.00	7932.88	9105.09
YFR053C	1.16	0.00	648.02	750.03
YNL007C	1.18	0.00	515.41	609.96
YLR154C-H	1.20	0.00	331.81	398.02
YBR169C	1.21	0.00	317.07	384.10
YDR210W	1.22	0.00	638.37	780.08
R0010W	1.25	0.00	938.66	1169.23
YPL106C	1.26	0.00	213.46	269.75
YDR209C	1.28	0.00	417.11	535.67
YLR216C	1.28	0.00	346.35	445.02
YLL024C	1.29	0.00	352.14	454.02
YBL093C	1.32	0.00	240.17	316.69
YKR097W	1.38	0.00	124.22	171.32
YNL077W	1.41	0.00	280.63	394.47
YJL088W	1.41	0.01	66.81	94.27
YNR014W	1.41	0.00	162.71	229.68
YGL188C-A	1.43	0.05	36.50	52.20
YAL005C	1.48	0.00	1097.02	1627.63
YJL144W	1.51	0.00	1206.10	1821.59
YAL004W	1.53	0.00	927.32	1420.24
YOL047C	1.54	0.03	32.76	50.42
YLR154W-E	1.55	0.00	4951.31	7679.93
YJL218W	1.60	0.00	47.79	76.55
YGR211W	1.61	0.00	142.33	228.79
YIL117C	1.66	0.00	96.30	159.79
YGR152C	1.66	0.02	28.56	47.42
YPR192W	1.72	0.00	40.51	69.60
YGR142W	1.72	0.00	485.55	835.02
YBR101C	1.75	0.00	321.45	562.93
YDL039C	1.76	0.01	26.18	46.08
Q0130	1.95	0.02	14.68	28.57

YDR171W	2.04	0.00	844.28	1725.03
YER103W	2.31	0.00	481.70	1113.53
YBR296C	2.67	0.00	14.68	39.14
YBR072C-A	3.54	0.00	6.86	24.28
Q0275	4.11	0.05	2.02	8.30
YLR154W-C	4.96	0.00	28567.96	141560.21
YLR162W-A	5.20	0.00	30.32	157.79
YLR162W	5.45	0.00	3959.05	21561.59
Q0250	5.82	0.02	1.70	9.90
YLR154W-B	5.83	0.00	13099.48	76420.29
YLR154W-A	6.51	0.00	24428.16	158912.75
Q0045	6.60	0.00	2.11	13.96
YLR154W-F	8.13	0.00	5624.96	45756.92